



Holtec Center, 555 Lincoln Drive West, Marlton, NJ 08053

Telephone (856) 797-0900

Fax (856) 797-0909

April 20, 2000

71-9261

U.S. Nuclear Regulatory Commission
ATTN: Document Control Desk
Washington, DC 20555-0001

Subject: NRC 10 CFR 71 Certificate of Compliance No. 9261, TAC L22085
License Amendment Request 9261-1

References: 1. Holtec Project No. 5014
2. Holtec Letter to NRC dated November 24, 1999, as supplemented.


Dear Sir:


In support of the issuance of Revision 1 to 10CFR Part 71 Certificate of Compliance 9261 for the HI-STAR 100 transportation package, enclosed please find replacement pages comprising Revision 9 to the Safety Analysis Report (SAR). SAR Revision 9 reflects those proposed changes included in Reference 2 including a complete set of certificate drawings containing an appropriate level of detail for a transportation package.

We thank the SFPO for their prompt review of this amendment request and look forward to receiving the revised CoC in the near future.

Sincerely,

Approved:


Brian Gutherman, P.E.
Licensing Manager


K. P. Singh, Ph.D., P.E.
President and CEO

Document I.D.: 5014385

Enclosure: Replacement pages for HI-STAR 100 SAR, Revision 9

Cc: Ms. Marissa Bailey, USNRC, (One full SAR copy and four sets of Revision 9 replacement pages)
Dr. Stan Turner, Holtec Florida Operations Center (cover letter only)
Mr. E. W. Brach, USNRC (cover letter only)
Ms. S. Frant-Shankman, USNRC (cover letter only)

DNSSO!
Public



Holtec Center, 555 Lincoln Drive West, Marlton, NJ 08053

Telephone (856) 797-0900


Fax (856) 797-0909

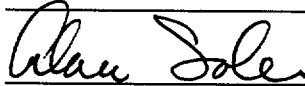
U. S. Nuclear Regulatory Commission
ATTN: Document Control Desk
Document ID: 5014385
Page 2 of 3


Cc: Mr. J. Lyons, USNRC (cover letter only)
Mr. R. Hall, USNRC (cover letter only)
Mr. M. McNamara, Holtec (cover letter only)
Mr. R. Kellar, Holtec (cover letter only)
Holtec Dry Storage Project Managers (cover letter only)
Mr. R. Moscardini, UST&D (cover letter only)
Mr. J. Singh, Omni Fabricators (cover letter only)


Technical Concurrence:

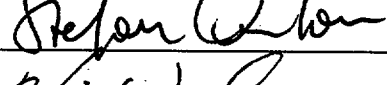
Mr. Bernard Gilligan (Configuration Control)
Dr. Alan Soler (Structural Evaluation)
Dr. Indresh Rampall (Thermal Evaluation)
Dr. Everett Redmond II (Shielding Evaluation)
Dr. Stefan Anton (Criticality Evaluation)
Mr. Kris Cummings (Containment Evaluation)
Mr. Steve Agace (Operations)
Mr. Mark Soler (Inspections and Acceptance Criteria)

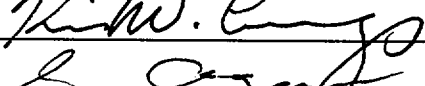


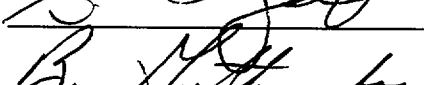














_____ for MS

Distribution (w/o encl):

Recipient

Utility

Mr. David Bland	Southern Nuclear Operating Company
Mr. Ken Phy	New York Power Authority
Mr. J. Nathan Leech	Commonwealth Edison
Dr. Max DeLong	Private Fuel Storage
Mr. Stan Miller	Vermont Yankee Nuclear Power Corporation
Mr. Bruce Patton	Pacific Gas & Electric – Diablo Canyon
Mr. Mark Smith	Pacific Gas & Electric – Humboldt Bay



Holtec Center, 555 Lincoln Drive West, Marlton, NJ 08053

Telephone (856) 797-0900

Fax (856) 797-0909

U. S. Nuclear Regulatory Commission
ATTN: Document Control Desk
Document ID: 5014385
Page 3 of 3

Distribution (w/o encl.) (continued):

Mr. Rodney Pickard	American Electric Power
Mr. David Larkin	Energy Northwest
Mr. Eric Meils	Wisconsin Electric Power Company
Mr. Paul Plante	Maine Yankee Atomic Power Company
Mr. Jeff Ellis	Southern California Edison
Mr. Darrell Williams	Entergy Operations – Arkansas Nuclear One
Mr. Joe Andrescavage	GPUN – Oyster Creek Nuclear Power Station
Mr. Ron Bowker	IES Utilities
Mr. William Swantz	Nebraska Public Power District
Mr. Chris Kudla	Entergy Operations – Millstone Unit 1 Decommissioning
Mr. Keith Waldrop	Duke Power
Mr. Matt Eyre	PECO Energy
Mr. Al Gould	Florida Power & Light
Dr. Seymour Raffety	Dairyland Power
Mr. John Sanchez	Consolidated Edison
Ms. Kathy Picciott	Niagara Mohawk
Mr. Charles Davis	Tennessee Valley Authority – Sequoyah Nuclear Plant
Mr. John Donnell	Private Fuel Storage, LLC (SWEC)

HI-STAR 100 SAR
SUMMARY OF CHANGES IN REVISION 9

Chapter 1

- a. The Holtec Design Drawings in Section 1.4 are replaced by the more appropriately detailed certificate drawings. In addition, the detailed fabrication drawings and Bill-of-Material for the damaged fuel container are removed in lieu of Figure 1.2.10.
- b. Last paragraph of Section 1.0 is revised to annotate that Revision 9 is made on a page basis.
- c. Table 1.0.1 in Section 1.0 is revised to 1) clarify that the classification of fuel as damaged is to be performed by the review of records, 2) add the Transnuclear Dresden Unit 1 damaged fuel canister to the definition of “damaged fuel container”, 3) specify that the B₄C quantity in Holtite is nominal in lieu of minimum, and 4) correct the definition of “intact fuel” to specify that dummy fuel rods must displace a volume equal to *or greater than* the original fuel rods.
- d. Subsection 1.2.1.2 is revised to clarify that material classified as Not Important to Safety may not be ASME Code material.
- e. Subsections 1.2.1.2.1 and 1.2.1.2.2 are revised to add the terms “approximately” and “nominally” to the dimensions specified.
- f. Subsection 1.2.1.2.2 is revised to 1) clarify the description of the aluminum heat conduction elements, 2) specify that the MPC is backfilled with a helium *pressure* in lieu of mass, and 3) refer to TSAR Figures 1.2.10 and 1.2.11 for the DFCs instead of design drawings.
- g. Subsection 1.2.1.4.2 is revised to specify the quantity of B₄C as nominal in lieu of minimum (2 places).
- h. Subsection 1.2.1.6 and Table 1.2.3 are revised to specify that the MPC is backfilled with a helium *pressure* in lieu of mass and to provide a lower limit on the pressure range.
- i. Incorrectly numbered Subsection 1.2.1.5 for “Design Life” is corrected to 1.2.1.10.
- j. Subsection 1.2.2 is revised to delete reference to measuring the water removed from the MPC.
- k. Subsection 1.2.3.2 is revised to correctly specify that dummy fuel rods must displace a volume equal to *or greater than* the original fuel rods.

- l. Subsection 1.2.3.4 and Tables 1.2.16 and 1.2.17 are revised to clarify that the fuel spacer lengths presented are suggested and that the user must appropriately specify the correct fuel spacer lengths.
- m. Subsections 1.2.3.6 and 1.2.3.8 are revised to address the Thoria Rod Canister and the Antimony-Beryllium neutron sources.
- n. Table 1.2.2 is revised to clarify the number of MPC models to be consistent with other licensing documents.
- o. Table 1.2.9 is revised to delete the exception for the QUAD+ assembly.
- p. Subsections 1.2.3.7 and 1.2.3.8 and Tables 1.2.10, 1.2.11, 1.2.13, 1.2.14, and 1.2.21 are revised to reflect the additional fuel characteristics added to the CoC.
- q. Table 1.2.19 is revised to conform with the CoC.
- r. Figures 1.2.10 is revised and Figures 1.2.11 and 1.2.11A are added in lieu of detailed fabrication drawings for the damaged fuel containers.
- s. Section 1.3 is revised to clarify the requirements for PT inspection of the closure ring weld if only one weld pass is required and add the ASME Code exception that only UT or multi-layer PT is to be performed on the MPC lid to shell weld (no RT).
- t. Table 1.3.2 is revised to clarify the Code exception to be consistent with the storage CoCs.
- u. Table 1.3.3 of Section 1.3 is revised to 1) delete the backing strip, alignment pin, rupture disk coupling, and rupture disk pipe, 2) specify the material of the rupture disk as "commercial", and 3) re-classify the closure bolt washer as Not Important to Safety and stainless steel.
- v. Subsection 1.4 is revised to reflect the new certificate drawings and the deletion of the DFC drawings and BOM..
- w. Table 1.B.1 in Appendix 1.B is revised to specify the Holtite specific gravity as nominal in lieu of maximum.
- x. Appendix 1.C is revised to add NEVER-SEEZ NGBT to FEL-PRO N-5000 as acceptable materials for use on the HI-STAR 100 System.

Chapter 2

- a. Table 2.0.1, under is revised to refer to Appendix 2.AO.
- b. Table 2.2.4 is revised to add dimensions used in the analytic calculations.

- c. Subsection 2.5.2.7.5 is revised to reflect a smaller pocket trunnion weld size.
- d. Subsection 2.10.1 is revised to add Appendix 2.AO to the list of Appendices.
- e. Appendix 2.L is revised to reflect the reduction in closure ring weld size to 1/8 inch.
- f. Appendix 2.O is revised to include calculations to demonstrate the adequacy of the modification to the upper fuel spacer design to accommodate certain PWR fuel assemblies (see Attachment 4, Drawing C1396, Sheet 6)
- g. Appendix 2.R is revised to analyze changes to the pocket trunnion-to-overpack weld detail.
- h. Appendix 2.AM has been revised to reflect the new, optional weld detail proposed for the overpack neutron shield enclosure panel to radial channel weld. The optional detail reduces the weld size from 7/16 inch to 3/16 inch.
- i. New Appendix 2.AO has been added to address the TN/D-1 damaged fuel canister and Thoria Rod Canister.

Chapter 3

- a. Section 3.3 text and Tables 3.3.2, 3.3.3, 3.3.5, 3.3.6, and 3.3.7 are revised in support of changes to modify/add fuel assembly array/classes to the CoC. These revisions address fuel cladding stress and temperature limits for the following fuel:

B&W 15x15 Mark B-11 (Entergy-ANO)
CE-14x14 (Millstone Unit 2)
GE 6x6 Dresden-1 Fuel (with TN Damaged Fuel Container)
Dresden Unit 1 Thoria Rod Canister
GE 7x7 (GPUN-Oyster Creek)
GE 8x8 (GPUN-Oyster Creek)
GE 8x8 QUAD+ (NYPA-Fitzpatrick)
GE 8x8 (TVA-Browns Ferry)
Seimens 9x9 SPC-5 (Entergy-Grand Gulf)

- b. Subsection 3.4.1.1.2 text and Tables 3.4.4 through 3.4.6 are revised, and new Table 3.4.34 is added in support of changes that modify/add fuel assembly array/classes in the CoC.
- c. New Subsection 3.4.1.1.18 is added to provide a discussion of Low Heat Emitting (LHE) fuel, including the TN/D-1 damaged fuel canister and the D-1 Thoria Rod Canister.

Chapter 4

- a. Section 4.0 is revised to present the leakage rate acceptance criteria in units of “atm cc/sec.”
- b. Table 4.1.1 is revised to reduce the required pressure ratings for the overpack mechanical seals, to present the leakage rate acceptance criteria in units of “atm cc/sec”, and to delete the leakage rate sensitivity for the secondary containment (MPC).
- c. Subsection 4.2.5.2 is revised to reflect the addition of thorium rods to the authorized package contents in the containment analysis.
- d. Subsections 4.2.5.7 and 4.2.5.8 are revised to correct a minor error in the MPC free gas volume used in the containment analysis and to present the leakage rate acceptance criteria in units of “atm cc/sec.”
- e. Subsection 4.2.5.9 is revised to clarify the leakage rate terminology and to present the leakage rate acceptance criteria in units of “atm cc/sec.”
- f. Table 4.2.6 is revised to correct the A_2 values for the MPC-24 and MPC-68.
- g. Tables 4.2.7 and 4.2.9 are revised to provide corrected release rates.
- h. Table 4.2.12 is revised to change the secondary capillary length (a) to 3.175 cm to conform with the text in Subsections 4.2.5.8 and 4.2.5.9.

Chapter 5

- a. Section 5.0 is revised to add text discussing the antimony-beryllium sources and Thorium Rod Canister which are being added as permissible contents to HI-STAR 100 for transport.
- b. Section 5.1 is revised to add Dresden Unit 1 antimony-beryllium neutron sources to the list of neutron sources.
- c. Subsection 5.1.1 is revised to add discussion of the Thorium Rod Canister and Dresden Unit 1 antimony-beryllium sources.
- d. Subsection 5.1.2 is revised to add two words in the discussion of 10CFR71.51.
- e. Subsection 5.2.1 is revised to change three of the reference numbers in Section 5.2.1. These were typographical errors.
- f. Subsection 5.2.5.3 is revised to add discussion about heavy metal mass.

- g. New Subsection 5.2.6 is added to discuss the source terms for the Dresden Unit 1 Thoria Rod Canister which is being added to the allowable contents for the HI-STAR 100 package.
- h. New Subsection 5.2.7 is added to discuss the source terms for the Dresden Unit 1 antimony-beryllium neutron sources which are being added to the allowable contents for the HI-STAR 100 package.
- i. Table 5.2.1 is revised to remove the partial note from the end of the table. This was a typographical error.
- j. New Tables 5.2.29 through 5.2.31 are added in support of additional Section 5.2.6.
- k. Figure 5.3.9 is revised to correct a typographical error.
- l. New Subsection 5.4.5 is added to discuss the source terms for the Dresden Unit 1 antimony-beryllium neutron sources which are being added to the allowable contents for the HI-STAR 100 package.
- m. New Subsection 5.4.6 is added to discuss the source terms for the Dresden Unit 1 Thoria Rod Canister which is being added to the allowable contents for the HI-STAR 100 package.
- n. New Table 5.4.25 is added to provide neutron source information accounting for the Sb-Be neutron source.

Chapter 6

- a. Subsection 6.1 is revised to clarify the assumptions regarding fuel stack density and pellet density.
- b. Tables 6.1.1 through 6.1.3 are revised to reflect changes to the authorized fuel contents for HI-STAR 100.

- b. Table numbers in Section 6.2 are revised as follows:

Tables 6.2.15 through 6.2.23 become Tables 6.2.16 through 6.2.24.

Tables 6.2.24 through 6.2.39 become Tables 6.2.26 through 6.2.41.

Table references in TSAR Subsections 6.2.2, 6.2.3 and 6.2.4 are updated accordingly

- c. Tables 6.2.6, 20, 21, 23, 27, 29, 30, 31, 34, 37, 38 and 41 and Appendix 6.C are revised to reflect changes to the authorized fuel contents for HI-STAR 100.

- d. Tables 6.2.15 and 6.2.25 are added to Section 6.2.
- e. Subsection 6.2.4, after the third sentence is revised to add “Two different DFC types with slightly different cross sections are considered.” At the end of the first paragraph, “for both DFC types” is added.
- f. Subsection 6.2.5 is added, together with Table 6.2.42. This subsection and table provides information about the Thoria Rod Canister.
- g. Table 6.3.4, MOX fuel specification, is revised as follows:
 - 92235 Atom-Density from 1.659E-04 to 1.719E-04
 - 92235 Wtg.-Fraction from 6.150E-03 to 6.380E-03
 - 92238 Wtg.-Fraction from 8.586E-01 to 8.584E-01
- h. Table 6.3.4, Specification for fuel in Thoria Rods is added.
- i. Subsection 6.4.4, after the first sentence is revised to add “Two different DFC types with slightly different cross sections are considered.” The third paragraph, after the first sentence is revised to add “There is no significant difference in reactivity between the two DFC types.” In Table 6.4.5, a third column is added to show results of the criticality analyses for the TN/D-1 DFC.
- j. Subsection 6.4.6 is added discussing results of the criticality analyses for the Thoria Rod Canister.
- k. Subsection 6.4.7 is added discussing the impact of sealed water rods in BWR fuel assemblies on the reactivity of the cask.
- l. Subsection 6.4.8 is added, discussing the impact of neutron sources in BWR fuel assemblies on the reactivity of the cask.
- m. Figures 6.4.1 through 6.4.8 are revised to reflect two sets of dimensions for the damaged fuel container (Holtec design and TN/D-1 design).
- n. New Figure 6.4.10 is added for the Thoria Rod Canister.

Chapter 7

- a. Section 7.0 is revised to 1) clarify vacuum drying time information for consistency with Chapter 3, 2) clarify that DFCs must be used for damaged fuel and fuel debris as defined in the CoC, but the location where the fuel is placed in the DFC is determined by the user and 3) clarify the applicability of operational requirements for an empty overpack.

- b. Subsection 7.1.1 is revised to 1) add a note clarifying the intent of the SAR operating procedures and clarifying users' responsibilities, 2) delete text referring to the need to measure the volume of water drained from the MPC for use with helium backfilling, 3) change "density" to "pressure" and 4) add clarification that root pass PT is only applicable for multi-pass welds.
- c. Subsections 7.1.2, "HI-STAR 100 System Receiving and Handling Operations"; 7.1.3, "HI-STAR 100 Overpack and MPC Receipt Inspection and Loading Preparation"; 7.1.5, "MPC Closure", 7.1.6, "Preparation for Transport"; 7.2.3, "Preparation for Unloading", and 7.3 "Preparation of an Empty Package for Transport" are revised in a number of places as shown in the attached proposed SAR revisions (Attachment 5) to incorporate editorial improvements, to reflect enhancements in the operating procedures, and as conforming changes to support the CoC change of MPC helium backfill from a density limit to a pressure limit.
- d. Procedural step 7.1.5.32 is revised to recognize the smaller closure ring welds.
- e. Tables 7.1.1 and 7.1.2 are revised to correct a number of estimated weight values.
- f. Tables 7.1.4 and 7.1.5 are revised to reflect a new description for the use of the water totalizer.
- g. Table 7.1.6 is revised to correct the numbering of the inspections items.
- h. Table 7.1.3 is revised to increase the torque requirement for the overpack vent and drain port plugs and the closure plate test port plug.
- i. Subsection 7.2.3, Step 8.b is revised to reflect a different method of gaining access to the MPC vent and drain ports prior to fuel unloading..

Chapter 8

- a. Subsection 8.1.2.1, third paragraph is revised to delete the words "in accordance with ANSI N14.6" after "lifting load." Table 8.1.2 is revised to delete "per ANSI N14.6."
- b. Subsection 8.1.2.2.1 and Table 8.1.2 are revised to allow a pneumatic test in lieu of a hydrotest and to clarify the timing for when the pressure test may be performed.
- c. Subsection 8.1.2.4 is revised to change the testing for the neutron shield enclosure vessel to require a pneumatic pressure test in lieu of a bubble test.

A soap bubble method is retained for use in finding any leaks discovered during the pneumatic test.

- d. Subsection 8.1.3.1 and Table 8.1.2 are revised to reflect a provision to perform the Containment System Fabrication Verification Leakage test any time during fabrication after the containment boundary is complete, with a preference to perform it after completion of overpack fabrication, including attachment of all intermediate shells (this provision was approved during HI-STAR storage rulemaking). In addition, a revision is made to Subsection 8.1.3.1 to allow performance of the helium retention penetration leakage test simultaneously with the containment boundary weld leakage test.
- e. Subsections 8.1.3.1 and 8.1.3.2 are revised at various places to present the helium leakage rate acceptance criterion in units of "atm cc/sec."
- f. Subsection 8.1.5.1 is revised regarding Holtite-A testing as shown in the attached proposed revised SAR pages to re-define the frequency of testing to be every manufactured lot instead of every mixed batch. In addition, clarify that the material composition test is required to confirm the amount of aluminum and hydrogen and that specific gravity testing is equivalent to the density confirmation test.
- g. Subsection 8.1.5.3 is revised to clarify the administrative control requirements governing testing of neutron absorbers.
- h. Subsection 8.1.6, first sentence is revised to replace "Each" with "The first." Conforming revisions to Table 8.1.2 are also made.
- i. Table 8.1.1 is revised to add "NF" to the list of applicable Codes.
- j. Table 8.1.3 is revised to delete the liquid penetrant test requirement for the root pass of the closure ring welds (3 places). In addition, a revision is made to Table 8.1.3 to allow magnetic particle testing as an option to liquid penetrant examination for the overpack intermediate shell welds.
- k. Reference [8.1.9] is revised to provide a more recent date for this document, which is to be used for leakage testing.

TABLE OF CONTENTS

CHAPTER 1: GENERAL INFORMATION

1.0	GENERAL INFORMATION	1.0-1
1.1	INTRODUCTION	1.1-1
1.2	PACKAGE DESCRIPTION	1.2-1
1.2.1	Packaging	1.2-1
1.2.1.1	Gross Weight	1.2-3
1.2.1.2	Materials of Construction, Dimensions and Fabrication	1.2-3
1.2.1.2.1	HI-STAR 100 Overpack	1.2-3
1.2.1.2.2	Multi-Purpose Canisters	1.2-4
1.2.1.3	Impact Limiters	1.2-7
1.2.1.4	Shielding	1.2-8
1.2.1.4.1	Boral Neutron Absorber	1.2-8
1.2.1.4.2	Holtite Neutron Shielding	1.2-10
1.2.1.4.3	Gamma Shielding Material	1.2-11
1.2.1.5	Lifting and Tie-Down Devices	1.2-12
1.2.1.6	Heat Dissipation	1.2-13
1.2.1.7	Coolants	1.2-14
1.2.1.8	Pressure Relief Systems	1.2-14
1.2.1.9	Security Seal	1.2-14
1.2.1.10	Design Life	1.2-14
1.2.2	Operational Features	1.2-15
1.2.3	Contents of Packaging	1.2-18
1.2.3.1	Determination of Design Basis Fuel	1.2-18
1.2.3.2	Design Payload for Intact Fuel	1.2-19
1.2.3.3	Design Payload for Damaged Fuel and Fuel Debris	1.2-19
1.2.3.4	Structural Payload Parameters	1.2-20
1.2.3.5	Thermal Payload Parameters	1.2-21
1.2.3.6	Radiological Payload Parameters	1.2-22
1.2.3.7	Criticality Payload Parameters	1.2-23
1.2.3.8	Summary of Design Criteria	1.2-23
1.3	DESIGN CODE APPLICABILITY	1.3-1

TABLE OF CONTENTS (continued)

1.4	GENERAL ARRANGEMENT DRAWINGS and BILLS-OF-MATERIAL	1.4-1
1.5	COMPLIANCE WITH 10CFR71	1.5-1
1.6	REFERENCES	1.6-1
Appendix 1.A:	Alloy X Description	
Appendix 1.B:	Holtite™ Material Data	
Appendix 1.C:	Miscellaneous Material Data	
Appendix 1.D:	Comment Resolution Letters	

CHAPTER 2: STRUCTURAL EVALUATION

2.1	STRUCTURAL DESIGN	2.1-1
2.1.1	Discussion	2.1-1
2.1.2	Design Criteria	2.1-5
2.1.2.1	Loading and Load Combinations	2.1-7
2.1.2.2	Allowables	2.1-12
2.1.2.3	Brittle Fracture Failure	2.1-14
2.1.2.4	Impact Limiter	2.1-17
2.1.2.5	Buckling	2.1-17
2.2	WEIGHTS AND CENTERS OF GRAVITY	2.2-1
2.3	MECHANICAL PROPERTIES OF MATERIALS	2.3-1
2.3.1	Structural Materials	2.3-1
2.3.1.1	Alloy X	2.3-1
2.3.1.2	Carbon Steel, Low-Alloy, and Nickel Alloy Steel	2.3-2
2.3.1.3	Bolting Materials	2.3-2
2.3.1.4	Weld Material	2.3-3
2.3.1.5	Impact Limiter	2.3-3
2.3.2	Nonstructural Materials	2.3-6
2.3.2.1	Neutron Shield	2.3-6
2.3.3.2	Boral™ Neutron Absorber	2.3-6
2.3.3.3	Aluminum Heat Conduction Elements	2.3-6

TABLE OF CONTENTS (continued)

2.4	GENERAL STANDARDS FOR ALL PACKAGES	2.4-1
2.4.1	Minimum Package Size	2.4-1
2.4.2	Tamperproof Feature	2.4-1
2.4.3	Positive Closure	2.4-1
2.4.4	Chemical and Galvanic Reactions	2.4-1
2.5	LIFTING AND TIE-DOWN STANDARDS	2.5-1
2.5.1	Lifting Devices	2.5-1
2.5.1.1	Overpack Trunnion Analysis	2.5-3
2.5.1.2	Stresses in the Overpack Closure Plate, Main Flange, and Baseplate During Lifting	2.5-5
2.5.1.3	MPC Lifting Analysis	2.5-7
2.5.2	Tie-Down Devices	2.5-8
2.5.2.1	Discussion	2.5-8
2.5.2.2	Equilibrium Equations to Determine the Tie-Down Forces	2.5-10
2.5.2.3	Longitudinal Loading	2.5-12
2.5.2.4	Vertical Load	2.5-14
2.5.2.5	Lateral Load	2.5-15
2.5.2.6	Numerical Results for Tie-Down Reactions	2.5-16
2.5.2.7	Structural Integrity of Pocket Trunnions	2.5-17
2.5.3	Failure of Lifting and Tie-Down Devices	2.5-25
2.5.4	Conclusion	2.5-27

TABLE OF CONTENTS (continued)

2.6	NORMAL CONDITIONS OF TRANSPORT	2.6-1
2.6.1	Heat	2.6-1
2.6.1.1	Summary of Pressures and Temperatures	2.6-1
2.6.1.2	Differential Thermal Expansion	2.6-1
2.6.1.3	Stress Calculations	2.6-4
2.6.1.3.1	MPC Stress Calculations	2.6-6
2.6.1.3.2	Overpack Stress Calculations	2.6-18
2.6.1.3.3	Fatigue Considerations	2.6-28
2.6.1.4	Comparison with Allowable Stresses	2.6-34
2.6.1.4.1	MPC and Fuel Basket and Enclosure Vessel	2.6-35
2.6.1.4.2	Overpack	2.6-38
2.6.1.4.3	Result Summary for the Normal Heat Condition of Transport	2.6-40
2.6.2	Cold	2.6-42
2.6.2.1	Differential Thermal Expansion	2.6-43
2.6.2.2	MPC Stress Analysis	2.6-44
2.6.2.3	Overpack Stress Analysis	2.6-44
2.6.3	Reduced External Pressure	2.6-49
2.6.4	Increased External Pressure	2.6-50
2.6.5	Vibration	2.6-50
2.6.6	Water Spray	2.6-50
2.6.7	Free Drop	2.6-51
2.6.8	Corner Drop	2.6-51
2.6.9	Compression	2.6-51
2.6.10	Penetration	2.6-51
2.7	HYPOTHETICAL ACCIDENT CONDITIONS	2.7-1
2.7.1	Free Drop	2.7-1

TABLE OF CONTENTS (continued)

2.7.1.1	End Drop	2.7-7
2.7.1.2	Side Drop (Load Cases F3 (Table 2.1.6), E3 (Table 2.1.7), And 3 and 11 (Table 2.1.9))	2.7-12
2.7.1.3	Corner Drop	2.7-14
2.7.1.4	Oblique Drops	2.7-21
2.7.1.5	Comparison with Allowable Stresses	2.7-24
2.7.2	Puncture	2.7-25
2.7.3	Thermal	2.7-27
2.7.3.1	Summary of Pressures and Temperatures	2.7-28
2.7.3.2	Differential Thermal Expansion	2.7-30
2.7.3.3	Stress Calculations	2.7-31
2.7.3.3.1	MPC	2.7-31
2.7.3.3.2	Overpack	2.7-33
2.7.3.3.3	Closure Bolts	2.7-34
2.7.3.3.4	Bounding Thermal Stresses During the Fire Transient	2.7-35
2.7.3.4	Comparison of Fire Accident Results with Allowable Stresses	2.7-37
2.7.4	Immersion - Fissile Material	2.7-38
2.7.5	Immersion - All Packages	2.7-39
2.7.6	Summary of Damage	2.7-39
2.8	SPECIAL FORM	2.8-1
2.9	FUEL RODS	2.9-1
2.10	MISCELLANEOUS	2.10-1
2.10.1	Appendices	2.10-1
2.10.2	Summary of 10CFR71 Compliance	2.10-3
2.11	REFERENCES	2.11-1
Appendix 2.A:	Top Flange Bolt Hole Analysis	
Appendix 2.B:	Lifting Trunnion Stress Analysis	

TABLE OF CONTENTS (continued)

Appendix 2.C:	Calculation of Transport Tie-Down Reactions
Appendix 2.D:	HI-STAR 100 Component Thermal Expansions; MPC-24
Appendix 2.E:	Deleted
Appendix 2.F:	HI-STAR 100 Component Thermal Expansions; MPC-68
Appendix 2.G:	Thermal Expansion During Fire Accident
Appendix 2.H:	Design, Testing, and Computer Simulation of the AL-STAR™ Impact Limiter
Appendix 2.I:	Overpack Protection Lip Deformation Analysis
Appendix 2.J:	Code Case N-284 Stability Calculations
Appendix 2.K:	Calculation of Dynamic Load Factors
Appendix 2.L:	Analysis of MPC Top Closure
Appendix 2.M:	Supplemental Data
Appendix 2.N:	Structural Qualification of MPC Baseplate
Appendix 2.O:	Fuel Support Spacer Strength Evaluations
Appendix 2.P:	Stress Report Locations for the Overpack
Appendix 2.Q:	Fabrication Stresses
Appendix 2.R:	Pocket Trunnion Recess Weld Analysis
Appendix 2.S:	Overpack Closure Plate Lifting Bolts
Appendix 2.T:	MPC Lid Lifting Bolts
Appendix 2.U:	Stress Analysis of Overpack Closure Bolts
Appendix 2.V:	Stress Analysis of Overpack Closure Bolts During Fire
Appendix 2.W:	Detailed Finite Element Listings for the MPC-24 Fuel Basket
Appendix 2.X:	Detailed Finite Element Listings for the MPC-24 Enclosure Vessel
Appendix 2.Y:	Deleted
Appendix 2.Z:	Deleted
Appendix 2.AA:	Detailed Finite Element Listings for the MPC-68 Fuel Basket
Appendix 2.AB:	Detailed Finite Element Listings for the MPC-68 Enclosure Vessel
Appendix 2.AC:	ANSYS Finite Element Results for the MPCs
Appendix 2.AD:	Miscellaneous Calculations
Appendix 2.AE:	ANSYS Finite Element Results for Overpack
Appendix 2.AF:	Impact Limiter Attachment Bolts
Appendix 2.AG:	Cask under Three Times Dead Load
Appendix 2.AH:	Analysis of Damaged Fuel Container
Appendix 2.AI:	HI-STAR 100 Component Thermal Expansions; MPC-24 Under Steady Cold Conditions
Appendix 2.AJ:	Deleted
Appendix 2.AK:	HI-STAR 100 Component Thermal Expansions; MPC-68 Under Steady Cold Conditions
Appendix 2.AL:	Overpack Closure Bolt Analysis - Normal Cold Conditions of Transport
Appendix 2.AM:	Stress Analysis of the HI-STAR 100 Enclosure Shell Under 30 psi Internal

TABLE OF CONTENTS (continued)

	Pressure	
Appendix 2.AN:	Pocket Trunnion Stress Analysis	
Appendix 2.AO	Analysis of Transnuclear Damaged Fuel Canister and Thoria Rod Canister	

CHAPTER 3: THERMAL EVALUATION

3.1	DISCUSSION	3.1-1
3.2	SUMMARY OF THERMAL PROPERTIES OF MATERIALS	3.2-1
3.3	TECHNICAL SPECIFICATIONS FOR COMPONENTS	3.3-1
3.3.1	Evaluation of Zircaloy Clad Fuel	3.3-1
3.3.2	Evaluation of Stainless Steel Clad Fuel	3.3-3
3.3.3	Accident Condition Cladding Temperature Limit	3.3-4
3.4	THERMAL EVALUATION FOR NORMAL CONDITIONS OF TRANSPORT	3.4-1
3.4.1	Thermal Model	3.4-1
3.4.1.1	Analytical Model - General Remarks	3.4-2
3.4.1.1.1	Overview of the Thermal Model	3.4-3
3.4.1.1.2	Fuel Region Effective Thermal Conductivity Calculation	3.4-5
3.4.1.1.3	Effective Thermal Conductivity of Sheathing/Boral/Cell Wall Sandwich	3.4-9
3.4.1.1.4	ANSYS Modeling of Basket In-Plane Conductive Heat Transport	3.4-9
3.4.1.1.5	Heat Transfer in MPC Basket Peripheral Regions	3.4-11
3.4.1.1.6	Effective Conductivity of Multilayered Intermediate Shell Region	3.4-12
3.4.1.1.7	Heat Rejection from Overpack and Impact Limiter Outside Surfaces	3.4-14
3.4.1.1.8	Determination of Solar Heat Input	3.4-15
3.4.1.1.9	Effective Thermal Conductivity of Radial	

TABLE OF CONTENTS (continued)

	Channels - Holtite Region	3.4-15
3.4.1.1.10	Effective Thermal Conductivity of the Eccentric MPC to Overpack Gap	3.4-16
3.4.1.1.11	Effective Thermal Conductivity of Flexible MPC Basket-to-Shell Aluminum Heat Conduction Elements	3.4-18
3.4.1.1.12	FLUENT Model for HI-STAR Temperature Field Computation	3.4-20
3.4.1.1.13	Effect of Fuel Cladding Crud Resistance	3.4-22
3.4.1.1.14	Maximum Time Limit During Wet Transfer	3.4-23
3.4.1.1.15	Cask Cooldown and Reflood Analysis During Fuel Unloading Operation	3.4-25
3.4.1.1.16	MPC Temperature Distribution Under Vacuum Conditions	3.4-27
3.4.1.1.17	Effects of Helium Dilution from Fuel Rod Gases	3.4-28
3.4.1.1.18	HI-STAR Temperature Field With Low Heat Emitting Fuel	3.4-30
3.4.1.2	Test Model	3.4-31
3.4.2	Maximum Temperatures Under Normal Transport Conditions	3.4-31
3.4.3	Minimum Temperatures	3.4-33
3.4.4	Maximum Internal Pressures	3.4-35
3.4.5	Maximum Thermal Stresses	3.4-35
3.4.6	Evaluation of System Performance for Normal Conditions of Transport	3.4-36
3.5	HYPOTHETICAL ACCIDENT THERMAL EVALUATION	3.5-1
3.5.1	Thermal Model	3.5-2
	3.5.1.1 Analytical Model	3.5-2
	3.5.1.2 Test Model	3.5-4
3.5.2	System Conditions and Environment	3.5-4

TABLE OF CONTENTS (continued)

3.5.3	System Temperatures	3.5-4
3.5.4	Maximum Internal Pressure	3.5-6
3.5.5	Maximum Thermal Stresses	3.5-6
3.5.6	Evaluation of System Performance for the Hypothetical Accident Thermal Conditions	3.5-6
3.6	REGULATORY COMPLIANCE	3.6-1
3.7	REFERENCES	3.7-1

CHAPTER 4: CONTAINMENT

4.0	INTRODUCTION	4.0-1
4.1	CONTAINMENT BOUNDARIES	4.1-1
4.1.1	Containment Vessel	4.1-1
4.1.2	Containment Penetrations	4.1-2
4.1.3	Seals and Welds	4.1-2
4.1.3.1	Containment Seals	4.1-2
4.1.3.2	Containment Welds	4.1-3
4.1.4	Closure	4.1-4
4.1.4.1	Primary Closure	4.1-4
4.1.4.2	Secondary Closure	4.1-4
4.1.5	Damaged Fuel Container	4.1-4
4.2	REQUIREMENTS FOR NORMAL AND HYPOTHETICAL ACCIDENT CONDITIONS OF TRANSPORT	4.2-1
4.2.1	Containment Criteria	4.2-1
4.2.2	Containment of Radioactive Material	4.2-1

TABLE OF CONTENTS (continued)

4.2.3	Pressurization of Containment Vessel	4.2-2
4.2.4	Assumptions	4.2-2
4.2.5	Analysis and Results	4.2-4
4.2.5.1	Volume in the Containment Vessel	4.2-4
4.2.5.2	Source Terms For Spent Nuclear Fuel Assemblies	4.2-5
4.2.5.3	Effective A_2 of Individual Contributors (Crud, Fines, Gases, and Volatiles)	4.2-9
4.2.5.4	Releasable Activity	4.2-10
4.2.5.5	Effective A_2 for the Total Source Term	4.2-10
4.2.5.6	Allowable Radionuclide Release Rates	4.2-10
4.2.5.7	Allowable Leakage Rates	4.2-11
4.2.5.8	Standard Leakage Rates	4.2-12
4.2.5.9	10CFR71.63(b) Plutonium Leakage Verification	4.2-13
4.2.5.10	Leak Test Sensitivity	4.2-15
4.3	REGULATORY COMPLIANCE	4.3-1
4.4	REFERENCES	4.4-1

Appendix 4.A:	Bolt and Plug Torques
Appendix 4.B:	Manufacturer Seal Information

CHAPTER 5: SHIELDING EVALUATION

5.0	INTRODUCTION	5.0-1
5.1	Discussion and Results	5.1-1
5.1.1	Normal Operations	5.1-2
5.1.2	Hypothetical Accident Conditions	5.1-4
5.2	SOURCE SPECIFICATION	5.2-1
5.2.1	Gamma Source	5.2-2
5.2.2	Neutron Source	5.2-3
5.2.3	Stainless Steel Clad Fuel Source	5.2-4

TABLE OF CONTENTS (continued)

5.2.4	Control Components	5.2-5
5.2.5	Choice of Design Basis Assembly	5.2-5
5.2.5.1	PWR Design Basis Assembly	5.2-5
5.2.5.2	BWR Design Basis Assembly	5.2-6
5.2.5.3	Decay Heat Loads	5.2-7
5.2.6	Thoria Rod Canister	5.2-8
5.2.7	Fuel Assembly Neutron Sources	5.2-8
5.3	MODEL SPECIFICATIONS	5.3-1
5.3.1	Description of the Radial and Axial Shielding Configuration	5.3-1
5.3.1.1	Fuel Configuration	5.3-3
5.3.1.2	Streaming Considerations	5.3-3
5.3.2	Regional Densities	5.3-4
5.4	SHIELDING EVALUATION	5.4-1
5.4.1	Streaming Through Radial Steel Fins and Pocket Trunnions	5.4-2
5.4.2	Damaged Fuel Post-Accident Shielding Evaluation	5.4-3
5.4.3	Mixed Oxide Fuel Evaluation	5.4-4
5.4.4	Stainless Steel Clad Fuel Evaluation	5.4-5
5.4.5	Dresden Unit 1 Antimony-Beryllium Neutron Sources	5.4-5
5.4.6	Thoria Rod Canister	5.4-7
5.5	REGULATORY COMPLIANCE	5.5-1
5.6	REFERENCES	5.6-1
Appendix 5.A:	Sample Input File for SAS2H	
Appendix 5.B:	Sample Input File for ORIGEN-S	

TABLE OF CONTENTS (continued)

Appendix 5.C: Sample Input File for MCNP

CHAPTER 6: CRITICALITY EVALUATION

6.1	DISCUSSION AND RESULTS	6.1-2
6.2	SPENT FUEL LOADING	6.2-1
6.2.1	Definition of Assembly Classes	6.2-1
6.2.2	PWR Fuel Assemblies in the MPC-24	6.2-2
6.2.3	BWR Fuel Assemblies in the MPC-68	6.2-3
6.2.4	Damaged BWR Fuel Assemblies and BWR Fuel Debris	6.2-4
6.2.5	Thoria Rod Canister	6.2-5
6.3	MODEL SPECIFICATION	6.3-1
6.3.1	Description of Calculational Model	6.3-1
6.3.2	Cask Regional Densities	6.3-2
6.4	CRITICALITY CALCULATIONS	6.4-1
6.4.1	Calculational or Experimental Method	6.4-1
6.4.2	Fuel Loading or Other Contents Loading Optimization	6.4-2
6.4.2.1	Internal and External Moderation	6.4-2
6.4.2.2	Partial Flooding	6.4-5
6.4.2.3	Clad Gap Flooding	6.4-5
6.4.2.4	Preferential Flooding	6.4-5
6.4.2.5	Hypothetical Accident Conditions of Transport	6.4-6
6.4.3	Criticality Results	6.4-6
6.4.4	Damaged Fuel Container	6.4-7

TABLE OF CONTENTS (continued)

6.4.5	Fuel Assemblies with Missing Rods	6.4-8
6.4.6	Thoria Rod Canister	6.4-8
6.4.7	Sealed Rods Replacing BWR Water Rods	6.4-9
6.4.8	Neutron Sources in Fuel Assemblies	6.4-9
6.5	CRITICALITY BENCHMARK EXPERIMENTS	6.5-1
6.6	REGULATORY COMPLIANCE	6.6-1
6.7	REFERENCES	6.7-1
Appendix 6.A:	Benchmark Calculations	
Appendix 6.B:	Distributed Enrichments in BWR Fuel	
Appendix 6.C:	Calculational Summary	
Appendix 6.D:	Sample Input Files	

CHAPTER 7: OPERATING PROCEDURES

7.0	INTRODUCTION	7.0-1
7.0.1	Technical and Safety Basis for Loading and Unloading Procedures	7.0-2
7.1	PROCEDURE FOR LOADING THE HI-STAR 100 SYSTEM IN THE SPENT FUEL POOL AND PREPARATION FOR SHIPMENT	7.1-1
7.1.1	Overview of Loading Operations	7.1-1
7.1.2	HI-STAR 100 System Receiving and Handling Operations	7.1-3
7.1.3	HI-STAR 100 Overpack and MPC Receipt Inspection and Loading Preparation	7.1-7
7.1.4	MPC Fuel Loading	7.1-12
7.1.5	MPC Closure	7.1-12
7.1.6	Preparation for Transport	7.1-24

TABLE OF CONTENTS (continued)

7.1.7	Placement of the HI-STAR 100 Overpack on the Transport Frame	7.1-27
7.2	PROCEDURE FOR UNLOADING THE HI-STAR 100 SYSTEM IN THE SPENT FUEL POOL	7.2-1
7.2.1	Overview of HI-STAR 100 System Unloading Operations	7.2-1
7.2.2	HI-STAR 100 Overpack Packaging Receipt	7.2-2
7.2.3	Preparation for Unloading	7.2-3
7.2.4	MPC Unloading	7.2-8
7.2.5	Post-Unloading Operations	7.2-8
7.3	PREPARATION OF AN EMPTY PACKAGE FOR TRANSPORT	7.3-1
7.3.1	Overview of the HI-STAR 100 System Empty Package Transport	7.3-1
7.3.2	Preparation for Empty Package Shipment	7.3-1
7.4	PROCEDURE FOR PREPARING THE HI-STAR 100 OVERPACK FOR TRANSPORT FOLLOWING A PERIOD OF STORAGE.	7.4-1
7.4.1	Overview of the HI-STAR 100 System Preparation for Transport Following a Period of Storage.	7.4-1
7.4.2	Preparation for Transport Following a Period of Storage.	7.4-1
7.5	REGULATORY COMPLIANCE	7.5-1
7.6	REFERENCES	7.6-1

CHAPTER 8: ACCEPTANCE CRITERIA AND MAINTENANCE PROGRAM

8.1	ACCEPTANCE CRITERIA	8.1-1
8.1.1	Fabrication and Nondestructive Examination (NDE)	8.1-2
8.1.1.1	MPC Lid-to-Shell Weld Volumetric Inspection	8.1-5

TABLE OF CONTENTS (continued)

8.1.2	Structural and Pressure Tests	8.1-6
8.1.2.1	Lifting Trunnions	8.1-6
8.1.2.2	Pressure Testing	8.1-7
8.1.2.3	Material Testing	8.1-8
8.1.2.4	Pneumatic Bubble Testing of the Neutron Shield Enclosure Vessel	8.1-9
8.1.3	Leakage Testing	8.1-9
8.1.3.1	HI-STAR Overpack	8.1-10
8.1.3.2	MPC Secondary Containment Boundary	8.1-11
8.1.4	Component Tests	8.1-12
8.1.4.1	Valves, Rupture Discs, and Fluid Transport Devices	8.1-12
8.1.4.2	Seals and Gaskets	8.1-12
8.1.4.3	Transport Impact Limiter	8.1-12
8.1.5	Shielding Integrity	8.1-13
8.1.5.1	Fabrication Testing and Controls	8.1-13
8.1.5.2	Shielding Effectiveness Test	8.1-14
8.1.5.3	Neutron Absorber Tests	8.1-15
8.1.6	Thermal Acceptance Test	8.1-15
8.1.7	Cask Identification	8.1-17
8.2	MAINTENANCE PROGRAM	8.2-1
8.2.1	Structural and Pressure Parts	8.2-1
8.2.2	Leakage Tests	8.2-1
8.2.3	Subsystem Maintenance	8.2-2
8.2.4	Rupture Discs	8.2-2
8.2.5	Shielding	8.2-2
8.2.6	In-Service Thermal Test	8.2-3
8.2.7	Miscellaneous	8.2-3

TABLE OF CONTENTS (continued)

8.3	Regulatory Compliance	8.3-1
8.4	References	8.4-1

LIST OF FIGURES

- 1.1.1 Pictorial View of HI-STAR 100 Packaging
- 1.1.2 HI-STAR 100 Overpack With MPC Partially Inserted
- 1.1.3 Cross Section Elevation View of MPC
- 1.1.4 Cross Section Elevation View of Overpack
- 1.2.1 Overpack Containment Boundary
- 1.2.2 Overpack Mid-Plane Cross Section
- 1.2.3 MPC-68 Cross Section View
- 1.2.4 Deleted
- 1.2.5 MPC-24 Cross Section View
- 1.2.6 MPC Lid and Port Details
- 1.2.7 HI-STAR 100 Overpack Shell Layering
- 1.2.8 HI-STAR 100 Transport Configuration
- 1.2.9a Major HI-STAR 100 Loading Operations (Sheet 1 of 3)
- 1.2.9b Major HI-STAR 100 Loading Operations (Sheet 2 of 3)
- 1.2.9c Major HI-STAR 100 Loading Operations (Sheet 3 of 3)
- 1.2.10 Holtec Damaged Fuel Container for Dresden Unit 1/Humboldt Bay SNF
- 1.2.11 TN Damaged Fuel Canister for Dresden Unit -1
- 1.2.11A TN Thoria Rod Canister for Dresden Unit-1
- 1.2.12 Acceptable Decay Heat Load Per Assembly

LIST OF FIGURES (continued)

- 1.2.13 PWR Axial Burnup Profile with Normalized Distribution
- 1.2.14 BWR Axial Burnup Profile with Normalized Distribution
- 1.2.15 HI-STAR 100 MPC With Upper and Lower Fuel Spacers
- 1.2.16a Major HI-STAR 100 Unloading Operations (Sheet 1 of 3)
- 1.2.16b Major HI-STAR 100 Unloading Operations (Sheet 2 of 3)
- 1.2.16c Major HI-STAR 100 Unloading Operations (Sheet 3 of 3)
- 1.A.1 Design Stress Intensity vs. Temperature
- 1.A.2 Tensile Strength vs. Temperature
- 1.A.3 Yield Stress vs. Temperature
- 1.A.4 Coefficient of Thermal Expansion vs. Temperature
- 1.A.5 Thermal Conductivity vs. Temperature
- 2.1.1 MPC Fuel Basket Geometry
- 2.1.2 Schematic of Closure Plate Bolted Joint
- 2.1.3 0E Drop Orientations for the MPCs
- 2.1.4 45E Drop Orientations for the MPCs
- 2.1.5 Free Body Diagram of Overpack - Internal Pressure
- 2.1.6 Free Body Diagram of Overpack - External Pressure
- 2.1.7 Free Body Diagram of Overpack - Bottom End Drop
- 2.1.8 Free Body Diagram of Overpack - Top End Drop
- 2.1.9 Free Body Diagram of Overpack - Side Drop

LIST OF FIGURES (continued)

- 2.1.10 Free Body Diagram for Bottom CG-Over-Corner Drop
- 2.1.11 Free Body Diagram for Top CG-Over-Corner Drop
- 2.1.12 Free Body Diagram for Puncture Drop Onto Bar - Side
- 2.1.13 Free Body Diagram for Puncture Drop Onto Bar - Top End
- 2.1.14 Free Body Diagram for Puncture Drop Onto Bar - Bottom End
- 2.2.1 HI-STAR 100 Datum Definition for Table 2.2.2
- 2.3.1 Cross Layered Aluminum Honeycomb
- 2.3.2 Average Crush Strength of Tested Specimens vs. Test Temperature
- 2.5.1 Transport Configuration Showing General Layout and Loads
- 2.5.2 Free Body Diagram of Overpack Showing Applied Transport Load and Tie-Down Reaction Vectors
- 2.5.3 Pocket Trunnion Recess Subject to Vertical Pressure
- 2.5.4 Normal Stress σ_z Distribution
- 2.5.5 Plot of σ_z At the Surface $Z = -3 \frac{15}{16}$ Inch
- 2.5.6 Sketch of Shear Ring Geometry & Weld Detail
- 2.5.7 Sketch of Shear Ring Showing Shear and Bearing Loading
- 2.5.8 View of Pocket Trunnion Into Pocket Showing Net Force Action on Curved Surface
- 2.5.9 View of Pocket Trunnion Showing Load Applied to Side Surface of Pocket
- 2.5.10 Geometry of Pocket Trunnion
- 2.5.11 Dimensions of Pocket Trunnion Sections

LIST OF FIGURES (continued)

- 2.6.1 Temperature Distribution for MPC Thermal Stress Analysis
- 2.6.2 Temperature Distribution for Overpack Thermal Stress Analysis
- 2.6.3 Finite Element Model of MPC-24 (Basic Model)
- 2.6.4 Deleted
- 2.6.5 Finite Element Model of MPC-68 (Basic Model)
- 2.6.6 Finite Element Model of MPC-24 (0 Degree Drop Model)
- 2.6.7 Deleted
- 2.6.8 Finite Element Model of MPC-68 (0 Degree Drop Model)
- 2.6.9 Finite Element Model of MPC-24 (45 Degree Drop Model)
- 2.6.10 Deleted
- 2.6.11 Finite Element Model of MPC-68 (45 Degree Drop Model)
- 2.6.12 MPC Thermal Load
- 2.6.13 0 Degree Side Drop of MPC
- 2.6.14 45 Degree Side Drop of MPC
- 2.6.15 Detail of Fuel Assembly Pressure Load on MPC Basket
- 2.6.16 Overpack Finite Element Model
- 2.6.17 Overpack Finite Element Model
- 2.6.18 Overpack Finite Element Model
- 2.6.19 Overpack Finite Element Model
- 2.6.20 Confinement Boundary Model Showing Temperature Data Points

LIST OF FIGURES (continued)

- 2.6.21 MPC Confinement Boundary Finite Element Grid (Exploded View)
- 2.6.22 Nodal Coupling in Overpack Finite Element Model
- 2.6.23 Overpack Internal Pressure Loading
- 2.7.1 Non-Linear Buckling Analysis for MPC-24 Displacement vs. Impact Acceleration (0E Drop)
- 2.7.2 Non-Linear Buckling Analysis for MPC-24 Displacement vs. Impact Acceleration (45E Drop)
- 2.7.3 Deleted
- 2.7.4 Deleted
- 2.7.5 Non-Linear Buckling Analysis for MPC-68 Displacement vs. Impact Acceleration (0E Drop)
- 2.7.6 Non-Linear Buckling Analysis for MPC-68 Displacement vs. Impact Acceleration (45E Drop)
- 2.7.7 Impact Limiter Loaded Areas on the Overpack
- 2.7.8 Top Lid Loading - Drop Analysis
- 2.7.9 Side View of Top Forging Showing End Loads
- 2.7.10 Baseplate Loading From Impact Limiter - Top End Drop
- 2.7.11 Loading From PC On Inner Shell
- 2.7.12 End View Showing MPC Loading On Inner Shell
- 2.7.13 Load From Impact Limiter At Support Locations - Side Drop
- 2.7.14 Oblique Drop Showing Offset Of Impact Limiter Reaction Load From Applied Inertia Loads

LIST OF FIGURES (continued)

- 2.7.15 Inner Shell Stress Intensity Distribution - "Heat" Condition - 30 Degree - Top End Impact
- 2.7.16 Intermediate Shell - Stress Intensity Distribution - "Heat" Condition - 30 Degree - Top End Impact
- 2.7.17 Localized Stress Intensity Distribution In Lid - Top End Puncture - (Deformed Shape Expanded For Clarity)
- 2.7.18 Impact Loads For Slapdown Finite Element Analysis
- 2.7.19 Free Body of MPC For Corner Drop
- 2.7.20 Free Body of MPC Lid - Impact on Shell
- 2.7.21 Free Body of MPC Lid - Impact on Top Closure
- 2.7.22 MPC-68F Closure Region
- 2.9.1 Fuel Rod Deformation; $g_1 > 0$
- 2.9.2 Fuel Rod Deformation; $g_1 = 0$
- 2.9.3 Fuel Rod Deformation; $g_1 = 0, F_2 > F_1$
- 2.9.4 Inter-Grid Strap Deformation; $F_3 > F_2$
- 2.9.5 Point Contact at Load F_4 , Maximum Bending Moment at A'
- 2.9.6 Extended Region of Contact, $F_5 > F_4$, Zero Bending Moment at A'
- 2.9.7 Free Body Diagram When Moment at A' = 0, $P_{AX} = F_3/\cos\theta$. Resisting Moment M_R At Grid Strap Not Shown
- 2.9.8 View C-C
- 2.9.9 Exaggerated Detail Showing Multiple Fuel Rods Subject to Lateral Deflection with Final Stacking of Rod Column

LIST OF FIGURES (continued)

- 2.A.1 Schematic of Closure Plate/Top Flange Interface
- 2.A.2 Free Body Diagram for the Determination of Minimum Closure Plate Bolt Preload
- 2.B.1 Sketch of Lifting Trunnion Geometry Showing Applied Load
- 2.B.2 Free Body Sketch of Lifting Trunnion Threaded Region Showing Moment Balance by Shear Stresses
- 2.C.1 Vertical and Lateral Load Distributions on Top End Saddle
- 2.D.1 Geometry of Section for Thermal Expansion Calculations
- 2.E.1 Deleted
- 2.F.1 Geometry of Section for Thermal Expansion Calculations
- 2.G.1 Deleted
- 2.H.1.1 HI-STAR 100 Package With Top and Bottom Impact Limiters
- 2.H.1.2 Drop From 9 Meters On To An Essentially Unyielding Surface (Hypothetical Accident Condition)
- 2.H.1.3 Pictorial View of AL-STAR (With a Portion Removed)
- 2.H.2.1 Pressure-Crush Strain Curve (Static Testing)
- 2.H.3.1 Illustration of the Force-Crush Model Construction Using the Example of the Side Drop Test
- 2.H.4.1 Test Fixture
- 2.H.4.2 Internal Stiffening Structure in 1/8 Scale Model
- 2.H.4.3 1/8th Scale Initial Impact Limiter Configuration - Comparison of Static Force-Crush Data from Test and Simulation - END DROP
- 2.H.4.4 1/8th Scale Initial Impact Limiter Configuration - Comparison of Static Force-Crush

LIST OF FIGURES (continued)

Data from Test and Simulation - 60 DEGREE CRUSH

- 2.H.5.1 Quarter Scale Model of Loaded MPC For Quarter Scale Drop Test Experiment
- 2.H.5.2 Overpack Quarter Scale Model (Cross Section View)
- 2.H.5.3 Overpack Quarter Scale Model (Top View)
- 2.H.5.4 Overpack Quarter Scale Model (Bottom View)
- 2.H.5.5 Accelerometer Locations for End and Side Drops
- 2.H.5.6 Accelerometer Locations for Slap Down and CGOC Drops
- 2.H.5.7 1/4 Scale HI-STAR 100 Packaging at 30 FT (9M) Prior to Side Drop
- 2.H.5.8 1/4 Scale Bottom Impact Limiter After Side Drop
- 2.H.5.9 1/4 Scale Top Impact Limiter After Side Drop
- 2.H.5.10 1/4 Scale HI-STAR 100 Packaging After Slap Down Drop
- 2.H.5.11 1/4 Scale Impact Limiter After C.G. Over Corner Drop
- 2.H.5.12 1/4 Scale HI-STAR 100 Packaging After Top End Drop
- 2.H.5.13 1/4 Scale Impact Limiter Top End Drop
- 2.H.5.14 Acceleration Raw Data for Top End Drop
- 2.H.5.15 Acceleration Data Filtered at 450 Hz for Top End Drop
- 2.H.5.15A Top End Drop, Cutoff Frequency = 450 Hz
- 2.H.5.15B Top End Drop, Cutoff Frequency = 550 Hz
- 2.H.5.15C Top End Drop, Cutoff Frequency = 1250 Hz
- 2.H.5.16 Acceleration Raw Data for C.G. Over Corner Drop

LIST OF FIGURES (continued)

- 2.H.5.17 Acceleration Data Filtered at 450 Hz for C.G. Over Corner Drop
- 2.H.5.17.A CG Over Corner, Cutoff Frequency = 450 Hz
- 2.H.5.18 Acceleration Raw Data at Bottom End During Slapdown Drop
- 2.H.5.19 Acceleration Data Filtered at 350 Hz for Slapdown Drop
- 2.H.5.19A Slapdown, Cutoff Frequency = 350 Hz
- 2.H.5.20 Acceleration Raw Data for Side Drop
- 2.H.5.21 Acceleration Data Filtered at 350 Hz for Side Drop
- 2.H.5.21A Side Drop, Cutoff Frequency = 350 Hz
- 2.H.6.1 Impact Limiter Force vs. Crush Depth ($\theta = 90$ degrees)
- 2.H.6.2 Impact Limiter Force vs. Crush Depth ($\theta = 67.5$ degrees)
- 2.H.6.3 Impact Limiter Force vs. Crush Depth ($\theta = 0$ degrees)
- 2.H.6.4 Impact Limiter Force vs. Crush Depth ($\theta = 15$ degrees)
- 2.H.6.5 Dynamic Model for Dual Impact Scenarios
- 2.H.6.6 Free-Body Diagram for Impact Scenarios
- 2.H.7.1 Static Crush Force vs. Crush Depth - Impact at 30 Degrees with Horizontal Target
- 2.H.7.2 Static Crush Force vs. Crush Depth - Impact at 45 Degrees with Horizontal Target
- 2.H.7.3 Static Crush Force vs. Crush Depth - Impact at 60 Degrees with Horizontal Target
- 2.H.10.1 1/8th Scale Impact Limiter - Crush Force vs. Crush Depth - Side Orientation
- 2.H.10.2 1/8th Scale Impact Limiter - Crush Force vs. Crush Depth - Center of Gravity Over Corner Orientation

LIST OF FIGURES (continued)

- 2.H.10.3 1/8th Scale Impact Limiter - Crush Force vs. Crush Depth - End Orientation
- 2.I.1 HI-STAR Top Forging & Protection Lip
- 2.I.2 Impact Limiter Steel Work Geometry and Loading
- 2.I.3 Deformed Limiter with Internal Stiffener Deformation
- 2.I.4 Finite Element Model
- 2.I.5 Pressure Distribution on Lip
- 2.I.6 Circumferential Variation of Pressure
- 2.I.7 Von Mises Stress
- 2.K.1 Triangular Deceleration Pulse Shape
- 2.K.2 Dynamic Load Factor for Single Degree of Freedom System - Triangular Pulse Shape, No Damping
- 2.K.3 Dynamic Model for Multi-Degree of Freedom Analysis for DLF Determination
- 2.K.4 Clamped Beam Model for Fuel Basket Panel
- 2.K.5 Dynamic Force in Lower Panel Spring vs. Time - PWR Basket, 60G Peak Value of Deceleration, Triangular Pulse, Duration 0.04 Seconds
- 2.K.6 Dynamic Force in Lower Panel Spring vs. Time - BWR Basket, 60G Peak Value of Deceleration, Triangular Pulse, Duration 0.04 Seconds
- 2.L.1 Top Closure Lid with Closure Ring Attached
- 2.L.2 Finite Element Model - Closure Ring
- 2.N.1 Finite Element Model

LIST OF FIGURES (continued)

- 2.P.1 Overpack Finite Element Model Stress Report Locations
- 2.P.2 Overpack Stress Report Location Reference Lines
- 2.Q.1 Simulation Model for Fabrication Stresses in the Overpack
- 2.Q.2 Partial Free Body Diagram of a Shell Section
- 2.R.1 Weld Group Geometry
- 2.R.2 Geometry of Load Application Point
- 2.AD.1 Freebody of Stress Distribution in the Weld and the Honeycomb Panel
- 2.AD.2 Freebody of Idealized Fuel Basket Support
- 2.AF.1 Attachment Bolt Geometry
- 2.AG.1 Finite Element Plot
- 2.AG.2 Material Stress-Strain Curve
- 2.AG.3 Path Locations for Stress Classification Plots in Figs. 2.AG.4(a)-(e)
- 2.AG.4(a) Stress Classifications at Critical Sections (psi)
- 2.AG.4(b) Stress Classifications at Critical Sections (psi)
- 2.AG.4(c) Stress Classifications at Critical Sections (psi)
- 2.AG.4(d) Stress Classifications at Critical Sections (psi)
- 2.AG.4(e) Stress Classifications at Critical Sections (psi)
- 2.AN.1 Geometry of Pocket Trunnion
- 2.AN.2 Dimensions of Pocket Trunnion Sections
- 3.3.1 Deleted

LIST OF FIGURES (continued)

- 3.4.1 Homogenization of the Storage Cell Cross-Section
- 3.4.2 MPC Cross-Section Replaced with an Equivalent Two Zone Axisymmetric Model
- 3.4.3 Natural Convection in MPC Basket Periphery Region
- 3.4.4 Neutron Shield Region Resistance Network Analogy for Effective Conductivity Calculation
- 3.4.5 Typical MPC Basket Parts in a Cross-Sectional View
- 3.4.6 Resistance Network Model of a "Box Wall-Boral-Sheathing" Sandwich
- 3.4.7 Westinghouse 17x17 OFA PWR Fuel Assembly Model
- 3.4.8 General Electric 9x9 BWR Fuel Assembly Model
- 3.4.9 Deleted
- 3.4.10 MPC-24 Basket Cross-Section ANSYS Finite Element Model
- 3.4.11 MPC-68 Basket Cross-Section ANSYS Finite Element Model
- 3.4.12 Illustration of an MPC Basket to Shell Aluminum Heat Conduction Element
- 3.4.13 Comparison of FLUENT Based Fuel Assembly Effective Conductivity Results with Published Technical Data
- 3.4.14 HI-STAR 100 System Finite Element Mesh for Thermal Analysis
- 3.4.15 Deleted
- 3.4.16 HI-STAR 100 System Normal Transport Condition Temperature Contours Plot (MPC-24 Basket)
- 3.4.17 HI-STAR 100 System Normal Transport Condition Temperature Contours Plot (MPC-68 Basket)
- 3.4.18 Deleted

LIST OF FIGURES (continued)

- 3.4.19 MPC-24 Hottest Rod Temperature Profile
- 3.4.20 MPC-68 Hottest Rod Temperature Profile
- 3.4.21 Deleted
- 3.4.22 MPC-24 Radial Temperature Profile
- 3.4.23 MPC-68 Radial Temperature Profile
- 3.4.24 HI-STAR 100 Package Control Locations Tracked in the Cooldown Event
- 3.4.25 Containment Boundary Cooldown Temperature Profiles
- 3.4.26 Multi-Layered Shells Cooldown Temperature Profiles
- 3.4.27 Overpack Forging Through Thickness Temperature Gradient During Cooldown Transient
- 3.4.28 Impact Limiters Surface Temperature Map
- 3.5.1 Location of HI-STAR 100 Package Control Points Monitored During Hypothetical Fire Accident Condition
- 3.5.2 HI-STAR 100 Package Containment Boundary Components Fire Accident Transient Temperature Response
- 3.5.3 HI-STAR 100 Package Neutron Shielding Region Fire Accident Transient Temperature Response
- 3.5.4 HI-STAR 100 Package MPC Shell and Fuel Basket Fire Accident Transient Temperature Response
- 3.5.5 Fuel Cladding Peak Axial Temperature Distribution During Post Fire Cooldown
- 3.5.6 HI-STAR Model for Transport Fire
- 3.5.7 Transport Fire Condition Containment Boundary and Layered Shells Temperature Distributions (Section A-A)

LIST OF FIGURES (continued)

- 3.5.8 Transport Fire Condition Overpack Top Forging Temperature Distributions (Section B-B)
- 3.5.9 Transport Fire Condition Overpack Top Forging Temperature Distributions (Section C-C)
- 4.1.1 HI-STAR 100 Overpack Primary Containment Boundary Components
- 4.1.2 HI-STAR 100 Closure Plate Containment Details
- 4.1.3 HI-STAR Overpack Vent and Drain Port Details
- 4.1.4 MPC-68 Secondary Containment Boundary
- 5.1.1 Cross Section Elevation View of the HI-STAR 100 System with Dose Point Locations During Normal Conditions
- 5.1.2 Cross Section Elevation View of the HI-STAR 100 System with Dose Point Locations During Accident Conditions
- 5.3.1 Deleted
- 5.3.2 HI-STAR 100 Overpack with MPC-24 Cross Sectional View as Modelled in MCNP
- 5.3.3 HI-STAR 100 Overpack with MPC-68 Cross Sectional View as Modelled in MCNP
- 5.3.4 Deleted
- 5.3.5 Cross Sectional View of an MPC-24 Basket Cell as Modeled in MCNP
- 5.3.6 Cross Sectional View of an MPC-68 Basket Cell as Modeled in MCNP
- 5.3.7 Axial Location of PWR Design Basis Fuel in the HI-STAR 100 System
- 5.3.8 Axial Location of BWR Design Basis Fuel in the HI-STAR 100 System
- 5.3.9 HI-STAR 100 Overpack with MPC-24 Cross Sectional View Showing the Thickness of the MPC Shell and Overpack as Modeled in MCNP

LIST OF FIGURES (continued)

- 5.3.10 Axial View of HI-STAR 100 Overpack and MPC with Axial Dimensions Shown as Modeled in MCNP
- 5.3.11 Cross Section Elevation View of the HI-STAR 100 System With As-Modeled Dimensions for the Impact Limiter
- 5.3.12 Cross Sectional View of Impact Limiter with As-Modeled Dimensions
- 5.4.1 Depiction of the Azimuthal Segmentation of the Overpack Used in Analyzing Neutron and Photon Streaming
- 6.2.1 Deleted
- 6.3.1 Typical Cell in the Calculation Model (Planar Cross-Section) with Representative Fuel in the MPC-24 Basket
- 6.3.2 Deleted
- 6.3.3 Typical Cell in the Calculation Model (Planar Cross-Section) with Representative Fuel in the MPC-68 Basket
- 6.3.4 Calculation Model (Planar Cross-Section) with Fuel Illustrated in One Quadrant of the MPC-24
- 6.3.5 Deleted
- 6.3.6 Calculation Model (Planar Cross-Section) with Fuel Illustrated in One Quadrant of the MPC-68
- 6.3.7 Sketch of the Calculational Model in the Axial Direction
- 6.4.1 Failed Fuel Calculation Model (Planar Cross-Section) with 6x6 Array with 4 Missing Rods in the MPC-68 Basket
- 6.4.2 Failed Fuel Calculation Model (Planar Cross-Section) with 6x6 Array with 8 Missing Rods in the MPC-68 Basket
- 6.4.3 Failed Fuel Calculation Model (Planar Cross-Section) with 6x6 Array with 12 Missing Rods in the MPC-68 Basket

LIST OF FIGURES (continued)

- 6.4.4 Failed Fuel Calculation Model (Planar Cross-Section) with 6x6 Array with 18 Missing Rods in the MPC-68 Basket
- 6.4.5 Failed Fuel Calculation Model (Planar Cross-Section) with 7x7 Array with 8 Missing Rods in the MPC-68 Basket
- 6.4.6 Failed Fuel Calculation Model (Planar Cross-Section) with 7x7 Array with 13 Missing Rods in the MPC-68 Basket
- 6.4.7 Failed Fuel Calculation Model (Planar Cross-Section) with 7x7 Array with 24 Missing Rods in the MPC-68 Basket
- 6.4.8 Failed Fuel Calculation Model (Planar Cross-Section) with Damaged Fuel Collapsed into 8x8 Array in the MPC-68 Basket
- 6.4.9 Calculated k-effective As A Function of Internal Moderator Density
- 6.4.10 Thoria Rod Canister (Planar Cross-Section) with 18 Thoria Rods in the MPC-68 Basket
- 6.A.1 MCNP4a Calculated k-eff Values for Various Values of the Spectral Index
- 6.A.2 KENO5a Calculated k-eff Values for Various Values of the Spectral Index
- 6.A.3 MCNP4a Calculated k-eff Values at Various U-235 Enrichments
- 6.A.4 KENO Calculated k-eff Values at Various U-235 Enrichments
- 6.A.5 Comparison of MCNP4a and KENO5a Calculations for Various Fuel Enrichments
- 6.A.6 Comparison of MCNP4a and KENO5a Calculations for Various Boron-10 Areal Densities
- 7.1.1 Loading Operations Flow Diagram
- 7.1.2a Major HI-STAR 100 Loading Operations (Sheet 1 of 3)
- 7.1.2b Major HI-STAR 100 Loading Operations (Sheet 2 of 3)

LIST OF FIGURES (continued)

- 7.1.2c Major HI-STAR 100 Loading Operations (Sheet 3 of 3)
- 7.1.3 Lift Yoke Engagement and Vertical HI-STAR Handling
- 7.1.4 HI-STAR Upending/Downending in the Transport Frame
- 7.1.5 HI-STAR 100 Overpack Rigging for Horizontal Handling
- 7.1.6 MPC Upending in the MPC Upending Frame
- 7.1.7 MPC Rigging for Vertical Lifts
- 7.1.8 MPC Alignment in HI-STAR
- 7.1.9 Personnel Barrier Removal and Installation
- 7.1.10 Impact Limiter Handling
- 7.1.11 HI-STAR 100 Impact Limiter and Tie-Down Bolting
- 7.1.12 MPC Lid and HI-STAR Accessory Rigging
- 7.1.13 Annulus Shield/Annulus Seal/Seal Surface Protector
- 7.1.14 Fuel Spacers
- 7.1.15 Drain Port Details
- 7.1.16 Drain Line Positioning
- 7.1.17 Annulus Overpressure System
- 7.1.18 HI-STAR 100 Lid Retention System in Exploded View
- 7.1.19 Drain Line Installation
- 7.1.20 Temporary Shield Ring

LIST OF FIGURES (continued)

- 7.1.21 MPC Vent and Drain Port RVOA Connector
- 7.1.22 Water Pump-Down for MPC Lid Welding Operations
- 7.1.23 MPC Air Displacement and Hydrostatic Testing
- 7.1.24 MPC Blowdown and Helium Injection for Leak Testing
- 7.1.25 Vacuum Drying System
- 7.1.26 Helium Backfill System
- 7.1.27 HI-STAR 100 Overpack Test Cover
- 7.1.28 HI-STAR 100 Backfill Tool
- 7.1.29 HI-STAR 100 Closure Plate Test Tool
- 7.1.30 HI-STAR Closure Plate Bolt Torquing Pattern
- 7.2.1 Unloading Operations Flow Diagram
- 7.2.2.a Major HI-STAR 100 Unloading Operations (Sheet 1 of 3)
- 7.2.2.b Major HI-STAR 100 Unloading Operations (Sheet 2 of 3)
- 7.2.2.c Major HI-STAR 100 Unloading Operations (Sheet 3 of 3)
- 7.2.3 HI-STAR Annulus Gas Sampling
- 7.2.4 MPC Gas Sampling in Preparation for Unloading
- 7.2.5 MPC Cool-Down
- 8.1.1 Deleted
- 8.1.2 Thermocouple Locations
- 8.1.3 Overpack Steam Heated Test Temperature Contours Plot

LIST OF FIGURES (continued)

- 8.1.4 Overpack Surface Temperature History During A Steam Heated Test
- 8.2.1 Temperature Measurement Locations for Periodic Thermal Test

LIST OF EFFECTIVE PAGES FOR REVISION 9

<u>Page</u>	<u>Revision</u>	<u>Page</u>	<u>Revision</u>
i	9	xxx	9
ii	9	xxxi	9
iii	9	xxxii	9
iv	9	xxxiii	9
v	9	xxxiv	9
vi	9	xxxv	9
vii	9		
viii	9		
ix	9		
x	9		
xi	9		
xii	9		
xiii	9		
xiv	9		
xv	9		
xvi	9		
xvii	9		
xviii	9		
xix	9		
xx	9		
xxi	9		
xxii	9		
xxiii	9		
xxiv	9		
xxv	9		
xxvi	9		
xxvii	9		
xxviii	9		
xxix	9		
xxx	9		
xxvi	9		
xxvii	9		
xxvi	9		
xxvii	9		
xxviii	9		
xxix	9		
xxvii	9		
xxvi	9		
xxvii	9		
xxviii	9		
xxix	9		
xxvii	9		
xxvi	9		
xxvii	9		
xxviii	9		
xxix	9		
xxvii	9		
xxvi	9		
xxvii	9		
xxviii	9		
xxix	9		

LIST OF EFFECTIVE PAGES FOR REVISION 9

Page	Revision	Page	Revision
1.0-1	9	1.2-37	9
1.0-2	9	1.2-38	9
1.0-3	9	1.2-39	9
1.0-4	9	1.2-40	9
1.0-5	9	1.2-41	9
1.0-6	7	1.2-42	9
1.0-7	7	1.2-43	9
1.0-8	7	1.2-44	9
1.0-9	7	1.2-45	9
1.0-10	7	1.2-46	9
1.1-1	7	1.2-47	9
Fig. 1.1.1	7	1.2-48	9
Fig. 1.1.2	4	1.2-49	9
Fig. 1.1.3	7	1.2-50	9
Fig. 1.1.4	7	Fig. 1.2.1	7
1.2-1	9	Fig. 1.2.2	7
1.2-2	9	Fig. 1.2.3	6
1.2-3	9	Fig. 1.2.4	7
1.2-4	9	Fig. 1.2.5	6
1.2-5	9	Fig. 1.2.6	7
1.2-6	9	Fig. 1.2.7	7
1.2-7	9	Fig. 1.2.8	7
1.2-8	9	Fig. 1.2.9a	7
1.2-9	9	Fig. 1.2.9b	7
1.2-10	9	Fig. 1.2.9c	7
1.2-11	9	Fig. 1.2.10	9
1.2-12	9	Fig. 1.2.11	9
1.2-13	9	Fig. 1.2.11A	9
1.2-14	9	Fig. 1.2.12	7
1.2-15	9	Fig. 1.2.13	4
1.2-16	9	Fig. 1.2.14	4
1.2-17	9	Fig. 1.2.15	7
1.2-18	9	Fig. 1.2.16a	7
1.2-19	9	Fig. 1.2.16b	7
1.2-20	9	Fig. 1.2.16c	7
1.2-21	9	1.3-1	9
1.2-22	9	1.3-2	9
1.2-23	9	1.3-3	9
1.2-24	9	1.3-4	9
1.2-25	9	1.3-5	9
1.2-26	9	1.3-6	9
1.2-27	9	1.3-7	9
1.2-28	9	1.3-8	9
1.2-29	9	1.3-9	9
1.2-30	9	1.3-10	9
1.2-31	9	1.3-11	9
1.2-32	9	1.3-12	9
1.2-33	9	1.3-13	9
1.2-34	9	1.3-14	9
1.2-35	9	1.3-15	9
1.2-36	9	1.4-1	9

LIST OF EFFECTIVE PAGES FOR REVISION 9

<u>Page</u>	<u>Revision</u>		<u>Page</u>	<u>Revision</u>
1.4-2	9			
1.4-3	9			
9 Drawings w/ 41 sheets	See Section 1.4			
3 Bills-of-Material w/ 6 sheets	See Section 1.4			
1.5-1	7			
1.5-2	7			
1.6-1	8			
1.6-2	8			
1.A-1	7			
1.A-2	7			
1.A-3	7			
1.A-4	7			
1.A-5	7			
1.A-6	7			
1.A-7	7			
Fig. 1.A.1	4			
Fig. 1.A.2	4			
Fig. 1.A.3	4			
Fig. 1.A.4	4			
Fig. 1.A.5	4			
1.B-1	7			
1.B-2	7			
1.B-3	9			
1.B-4	7			
1.B-5	7			
1.B-6	7			
1.B-7	7			
1.B-8	7			
1.B-9	7			
1.B-10	7			
1.B-11	7			
1.B-12	7			
1.B-13	7			
1.B-14	7			
1.B-15	7			
1.B-16	7			
1.B-17	7			
1.B-18	7			
1.B-19	7			
1.B-20	7			
1.C-1	9			
1.C-2	7			
1.C-3	7			
1.C-4	7			
1.C-5	7			
1.C-6	7			
1.C-7	7			
1.C-8	7			
App. 1.D (Total of 83 Pages)	8			

LIST OF EFFECTIVE PAGES FOR REVISION 9

<u>Page</u>	<u>Revision</u>	<u>Page</u>	<u>Revision</u>
2.0-1	8	Fig. 2.1.2	6
2.0-2	8	Fig. 2.1.3	7
2.0-3	8	Fig. 2.1.4	7
2.0-4	8	Fig. 2.1.5	4
2.0-5	9	Fig. 2.1.6	4
2.0-6	8	Fig. 2.1.7	4
2.1-1	8	Fig. 2.1.8	4
2.1-2	8	Fig. 2.1.9	4
2.1-3	8	Fig. 2.1.10	6
2.1-4	8	Fig. 2.1.11	4
2.1-5	8	Fig. 2.1.12	4
2.1-6	8	Fig. 2.1.13	4
2.1-7	8	Fig. 2.1.14	6
2.1-8	8	2.2-1	7
2.1-9	8	2.2-2	7
2.1-10	8	2.2-3	7
2.1-11	8	2.2-4	7
2.1-12	8	2.2-5	9
2.1-13	8	Fig. 2.2.1	4
2.1-14	8	2.3-1	7
2.1-15	8	2.3-2	7
2.1-16	8	2.3-3	7
2.1-17	8	2.3-4	7
2.1-18	8	2.3-5	7
2.1-19	8	2.3-6	7
2.1-20	8	2.3-7	7
2.1-21	8	2.3-8	7
2.1-22	8	2.3-9	7
2.1-23	8	2.3-10	7
2.1-24	8	2.3-11	7
2.1-25	8	2.3-12	7
2.1-26	8	Fig. 2.3.1	4
2.1-27	8	Fig. 2.3.2	7
2.1-28	8	2.4-1	7
2.1-29	8	2.4-2	7
2.1-30	8	2.4-3	7
2.1-31	8	2.4-4	7
2.1-32	8	2.4-5	7
2.1-33	8	2.4-6	7
2.1-34	8	2.4-7	7
2.1-35	8	2.5-1	8
2.1-36	8	2.5-2	8
2.1-37	8	2.5-3	8
2.1-38	8	2.5-4	8
2.1-39	8	2.5-5	8
2.1-40	8	2.5-6	8
2.1-41	8	2.5-7	8
2.1-42	8	2.5-8	8
2.1-43	8	2.5-9	8
2.1-44	8	2.5-10	8
Fig. 2.1.1	7	2.5-11	8

LIST OF EFFECTIVE PAGES FOR REVISION 9

<u>Page</u>	<u>Revision</u>	<u>Page</u>	<u>Revision</u>
2.5-12	8	2.6-23	8
2.5-13	8	2.6-24	8
2.5-14	8	2.6-25	8
2.5-15	8	2.6-26	8
2.5-16	8	2.6-27	8
2.5-17	8	2.6-28	8
2.5-18	8	2.6-29	8
2.5-19	8	2.6-30	8
2.5-20	8	2.6-31	8
2.5-21	8	2.6-32	8
2.5-22	8	2.6-33	8
2.5-23	9	2.6-34	8
2.5-24	8	2.6-35	8
2.5-25	8	2.6-36	8
2.5-26	8	2.6-37	8
2.5-27	8	2.6-38	8
2.5-28	8	2.6-39	8
2.5-29	8	2.6-40	8
Fig. 2.5.1	4	2.6-41	8
Fig. 2.5.2	4	2.6-42	8
Fig. 2.5.3	4	2.6-43	8
Fig. 2.5.4	4	2.6-44	8
Fig. 2.5.5	4	2.6-45	8
Fig. 2.5.6	6	2.6-46	8
Fig. 2.5.7	7	2.6-47	8
Fig. 2.5.8	7	2.6-48	8
Fig. 2.5.9	7	2.6-49	8
Fig. 2.5.10	8	2.6-50	8
Fig. 2.5.11	8	2.6-51	8
2.6-1	8	2.6-52	8
2.6-2	8	2.6-53	8
2.6-3	8	2.6-54	8
2.6-4	8	2.6-55	8
2.6-5	8	2.6-56	8
2.6-6	8	2.6-57	8
2.6-7	8	2.6-58	8
2.6-8	8	2.6-59	8
2.6-9	8	2.6-60	8
2.6-10	8	2.6-61	8
2.6-11	8	2.6-62	8
2.6-12	8	2.6-63	8
2.6-13	8	2.6-64	8
2.6-14	8	2.6-65	8
2.6-15	8	2.6-66	8
2.6-16	8	2.6-67	8
2.6-17	8	2.6-68	8
2.6-18	8	2.6-69	8
2.6-19	8	Fig. 2.6.1	4
2.6-20	8	Fig. 2.6.2	4
2.6-21	8	Fig. 2.6.3	6
2.6-22	8	Fig. 2.6.4	7

LIST OF EFFECTIVE PAGES FOR REVISION 9

Page	Revision	Page	Revision
Fig. 2.6.5	6	2.7-30	8
Fig. 2.6.6	6	2.7-31	8
Fig. 2.6.7	7	2.7-32	8
Fig. 2.6.8	6	2.7-33	8
Fig. 2.6.9	6	2.7-34	8
Fig. 2.6.10	7	2.7-35	8
Fig. 2.6.11	6	2.7-36	8
Fig. 2.6.12	7	2.7-37	8
Fig. 2.6.13	7	2.7-38	8
Fig. 2.6.14	7	2.7-39	8
Fig. 2.6.15	4	2.7-40	8
Fig. 2.6.16	8	2.7-41	8
Fig. 2.6.17	8	2.7-42	8
Fig. 2.6.18	8	2.7-43	8
Fig. 2.6.19	8	2.7-44	8
Fig. 2.6.19A	8	2.7-45	8
Fig. 2.6.19B	8	2.7-46	8
Fig. 2.6.19C	8	2.7-47	8
Fig. 2.6.20	7	2.7-48	8
Fig. 2.6.21	7	2.7-49	8
Fig. 2.6.22	6	2.7-50	8
Fig. 2.6.23	8	Fig. 2.7.1	6
2.7-1	8	Fig. 2.7.2	6
2.7-2	8	Fig. 2.7.3	7
2.7-3	8	Fig. 2.7.4	7
2.7-4	8	Fig. 2.7.5	6
2.7-5	8	Fig. 2.7.6	6
2.7-6	8	Fig. 2.7.7	8
2.7-7	8	Fig. 2.7.8	8
2.7-8	8	Fig. 2.7.9	8
2.7-9	8	Fig. 2.7.10	8
2.7-10	8	Fig. 2.7.11	8
2.7-11	8	Fig. 2.7.12	8
2.7-12	8	Fig. 2.7.13	8
2.7-13	8	Fig. 2.7.14	8
2.7-14	8	Fig. 2.7.15	8
2.7-15	8	Fig. 2.7.16	8
2.7-16	8	Fig. 2.7.17	8
2.7-17	8	Fig. 2.7.18	8
2.7-18	8	Fig. 2.7.19	8
2.7-19	8	Fig. 2.7.20	8
2.7-20	8	Fig. 2.7.21	8
2.7-21	8	Fig. 2.7.22	8
2.7-22	8	2.8-1	7
2.7-23	8	2.9-1	8
2.7-24	8	2.9-2	8
2.7-25	8	2.9-3	8
2.7-26	8	2.9-4	8
2.7-27	8	2.9-5	8
2.7-28	8	2.9-6	8
2.7-29	8	2.9-7	8

LIST OF EFFECTIVE PAGES FOR REVISION 9

Page	Revision	Page	Revision
2.9-8	8	2.C-2	6
2.9-9	8	2.C-3	6
2.9-10	8	2.C-4	6
2.9-11	8	2.C-5	6
2.9-12	8	2.C-6	6
2.9-13	8	2.C-7	6
2.9-14	8	2.C-8	6
2.9-15	8	2.C-9	6
2.9-16	8	2.C-10	6
2.9-17	8	2.C-11	6
2.9-18	8	2.C-12	6
2.9-19	8	2.C-13	6
Fig. 2.9.1	8	2.C-14	6
Fig. 2.9.2	8	Fig. 2.C.1	4
Fig. 2.9.3	8	2.D-1	7
Fig. 2.9.4	8	2.D-2	7
Fig. 2.9.5	8	2.D-3	7
Fig. 2.9.6	8	2.D-4	7
Fig. 2.9.7	8	2.D-5	7
Fig. 2.9.8	8	2.D-6	7
Fig. 2.9.9	8	2.D-7	7
2.10-1	8	2.D-8	7
2.10-2	8	2.D-9	7
2.10-3	9	2.D-10	7
2.10-4	9	Fig. 2.D.1	4
2.10-5	9	2.F-1	7
2.11-1	8	2.F-2	7
2.11-2	8	2.F-3	7
2.11-3	8	2.F-4	7
2.A-1	7	2.F-5	7
2.A-2	7	2.F-6	7
2.A-3	7	2.F-7	7
2.A-4	7	2.F-8	7
2.A-5	7	2.F-9	7
2.A-6	7	2.F-10	7
Fig. 2.A.1	6	Fig. 2.F.1	4
Fig. 2.A.2	4	2.G-1	7
2.B-1	8	2.G-2	7
2.B-2	8	2.G-3	7
2.B-3	8	2.G-4	7
2.B-4	8	2.G-5	7
2.B-5	8	2.G-6	7
2.B-6	8	2.G-7	7
2.B-7	8	2.G-8	7
2.B-8	8	2.G-9	7
2.B-9	8	2.G-10	7
2.B-10	8	2.H-1	8
2.B-11	8	2.H-2	8
2.B-12	8	2.H-3	8
2.B-13	8	2.H-4	8
2.C-1	6	2.H-5	8

LIST OF EFFECTIVE PAGES FOR REVISION 9

<u>Page</u>	<u>Revision</u>	<u>Page</u>	<u>Revision</u>
2.H-6	8	Fig. 2.H.5.17	7
2.H-7	8	Fig. 2.H.5.17A	8
2.H-8	8	Fig. 2.H.5.18	7
2.H-9	8	Fig. 2.H.5.19	7
2.H-10	8	Fig. 2.H.5.19A	8
2.H-11	8	Fig. 2.H.5.20	7
2.H-12	8	Fig. 2.H.5.21	7
2.H-13	8	Fig. 2.H.5.21A	8
2.H-14	8	Fig. 2.H.6.1	7
2.H-15	8	Fig. 2.H.6.2	7
2.H-16	8	Fig. 2.H.6.3	7
2.H-17	8	Fig. 2.H.6.4	7
2.H-18	8	Fig. 2.H.6.5	7
2.H-19	8	Fig. 2.H.6.6	7
2.H-20	8	Fig. 2.H.7.1	8
2.H-21	8	Fig. 2.H.7.2	8
2.H-22	8	Fig. 2.H.7.3	8
2.H-23	8	Fig. 2.H.10.1	7
2.H-24	8	Fig. 2.H.10.2	7
2.H-25	8	Fig. 2.H.10.3	7
2.H-26	8	2.I-1	7
2.H-27	8	2.I-2	7
2.H-28	8	2.I-3	7
Fig. 2.H.1	7	2.I-4	7
Fig. 2.H.2	7	2.I-5	7
Fig. 2.H.3	7	2.I-6	7
Fig. 2.H.2.1	7	2.I-7	7
Fig. 2.H.3.1	7	2.I-8	7
Fig. 2.H.4.1	7	2.I-9	7
Fig. 2.H.4.2	7	2.I-10	7
Fig. 2.H.4.3	7	2.I-11	7
Fig. 2.H.4.4	7	Fig. 2.I.1	6
Fig. 2.H.5.1	7	Fig. 2.I.2	6
Fig. 2.H.5.2	7	Fig. 2.I.3	6
Fig. 2.H.5.3	7	Fig. 2.I.4	7
Fig. 2.H.5.4	7	Fig. 2.I.5	7
Fig. 2.H.5.5	7	Fig. 2.I.6	7
Fig. 2.H.5.6	7	Fig. 2.I.7	7
Fig. 2.H.5.7	7	2.J-1	7
Fig. 2.H.5.8	7	2.J-2	7
Fig. 2.H.5.9	7	2.J-3	7
Fig. 2.H.5.10	7	2.J-4	7
Fig. 2.H.5.11	7	2.J-5	7
Fig. 2.H.5.12	7	2.J-6	7
Fig. 2.H.5.13	7	2.J-7	7
Fig. 2.H.5.14	7	2.J-8	7
Fig. 2.H.5.15	7	2.J-9	7
Fig. 2.H.5.15A	8	2.J-10	7
Fig. 2.H.5.15B	8	2.J-11	7
Fig. 2.H.5.15C	8	2.J-12	7
Fig. 2.H.5.16	7	2.J-13	7

LIST OF EFFECTIVE PAGES FOR REVISION 9

<u>Page</u>	<u>Revision</u>	<u>Page</u>	<u>Revision</u>
2.J-14	7	2.M-5	4
2.J-15	7	2.M-6	4
2.J-16	7	2.M-7	4
2.J-17	7	2.M-8	4
2.J-18	7	2.N-1	7
2.J-19	7	2.N-2	7
2.J-20	7	2.N-3	7
2.J-21	7	2.N-4	7
2.J-22	7	2.N-5	7
2.J-23	7	2.N-6	7
2.J-24	7	2.N-7	7
2.J-25	7	Fig. 2.N.1	4
2.J-26	7	2.O-1	7
2.J-27	7	2.O-2	7
2.J-28	7	2.O-3	7
2.J-29	7	2.O-4	7
2.J-30	7	2.O-5	7
2.J-31	7	2.O-6	7
2.J-32	7	2.O-7	7
2.J-33	7	2.O-8	7
2.J-34	7	2.O-9	9
2.J-35	7	2.O-10	9
2.K-1	7	2.O-11	9
2.K-2	7	2.O-12	9
2.K-3	7	2.O-13	9
2.K-4	7	2.O-14	9
2.K-5	7	2.O-15	9
2.K-6	7	2.O-16	9
2.K-7	7	2.O-17	9
2.K-8	7	2.O-18	9
2.K-9	7	2.O-19	9
2.K-10	7	2.O-20	9
Fig. 2.K.1	7	2.O-21	9
Fig. 2.K.2	7	2.O-22	9
Fig. 2.K.3	7	2.O-23	9
Fig. 2.K.4	7	2.O-24	9
Fig. 2.K.5	7	2.P-1	4
Fig. 2.K.6	7	2.P-2	4
2.L-1	8	2.P-3	4
2.L-2	8	2.P-4	4
2.L-3	8	2.P-5	4
2.L-4	8	2.P-6	4
2.L-5	8	2.P-7	4
2.L-6	8	2.P-8	4
2.L-7	8	2.P-9	4
2.L-8	9	2.P-10	4
2.L-9	9	2.P-11	4
2.M-1	4	Fig. 2.P.1	4
2.M-2	4	Fig. 2.P.2	4
2.M-3	4	2.Q-1	7
2.M-4	4	2.Q-2	7

LIST OF EFFECTIVE PAGES FOR REVISION 9

<u>Page</u>	<u>Revision</u>	<u>Page</u>	<u>Revision</u>
2.Q-3	7	2.V-2	7
Fig. 2.Q.1	7	2.V-3	7
Fig. 2.Q.2	7	2.V-4	7
2.R-1	9	2.V-5	7
2.R-2	9	2.V-6	7
2.R-3	9	2.V-7	7
2.R-4	9	2.V-8	7
2.R-5	9	2.V-9	7
2.R-6	9	2.V-10	7
2.R-7	9	2.V-11	7
2.R-8	9	2.V-12	7
2.R-9	9	2.W-1	4
Fig. 2.R.1	7	2.W-2	4
Fig. 2.R.2	7	2.W-3	4
2.T-1	7	2.W-4	4
2.T-2	7	2.W-5	4
2.T-3	7	2.W-6	4
2.T-4	7	2.W-7	4
2.T-5	7	2.W-8	4
2.S-1	7	2.W-9	4
2.S-2	7	2.W-10	4
2.S-3	7	2.W-11	4
2.S-4	7	2.W-12	4
2.S-5	7	2.W-13	4
2.S-6	7	2.W-14	4
2.U-1	7	2.W-15	4
2.U-2	7	2.W-16	4
2.U-3	7	2.W-17	4
2.U-4	7	2.W-18	4
2.U-5	7	2.W-19	4
2.U-6	7	2.W-20	4
2.U-7	7	2.W-21	4
2.U-8	7	2.W-22	4
2.U-9	7	2.W-23	4
2.U-10	7	2.W-24	4
2.U-11	7	2.W-25	4
2.U-12	7	2.W-26	4
2.U-13	7	2.X-1	4
2.U-14	7	2.X-2	4
2.U-15	7	2.X-3	4
2.U-16	7	2.X-4	4
2.U-17	7	2.X-5	4
2.U-18	7	2.X-6	4
2.U-19	7	2.X-7	4
2.U-20	7	2.X-8	4
2.U-21	7	2.X-9	4
2.U-22	7	2.X-10	4
2.U-23	7	2.X-11	4
2.U-24	6	2.X-12	4
2.U-25	6	2.X-13	4
2.V-1	7	2.X-14	4

LIST OF EFFECTIVE PAGES FOR REVISION 9

<u>Page</u>	<u>Revision</u>	<u>Page</u>	<u>Revision</u>
2.Y-1	7	2.AA-49	4
2.Z-1	7	2.AA-50	4
2.AA-1	4	2.AA-51	4
2.AA-2	4	2.AA-52	4
2.AA-3	4	2.AA-53	4
2.AA-4	4	2.AA-54	4
2.AA-5	4	2.AA-55	4
2.AA-6	4	2.AA-56	4
2.AA-7	4	2.AA-57	4
2.AA-8	4	2.AA-58	4
2.AA-9	4	2.AA-59	4
2.AA-10	4	2.AA-60	4
2.AA-11	4	2.AA-61	4
2.AA-12	4	2.AA-62	4
2.AA-13	4	2.AA-63	4
2.AA-14	4	2.AA-64	4
2.AA-14	4	2.AA-65	4
2.AA-15	4	2.AA-66	4
2.AA-16	4	2.AA-67	4
2.AA-17	4	2.AA-68	4
2.AA-18	4	2.AA-69	4
2.AA-19	4	2.AA-70	4
2.AA-20	4	2.AB-1	4
2.AA-21	4	2.AB-2	4
2.AA-22	4	2.AB-3	4
2.AA-23	4	2.AB-4	4
2.AA-24	4	2.AB-5	4
2.AA-25	4	2.AB-6	4
2.AA-26	4	2.AB-7	4
2.AA-27	4	2.AB-8	4
2.AA-28	4	2.AB-9	4
2.AA-29	4	2.AB-10	4
2.AA-30	4	2.AC-1	7
2.AA-31	4	2.AC-2	7
2.AA-32	4	2.AC-3	7
2.AA-33	4	2.AC-4	7
2.AA-34	4	2.AC-5	7
2.AA-35	4	2.AC-6	7
2.AA-36	4	2.AC-7	7
2.AA-37	4	2.AC-8	7
2.AA-38	4	2.AC-9	7
2.AA-39	4	2.AC-10	7
2.AA-40	4	2.AC-11	7
2.AA-41	4	2.AC-12	7
2.AA-42	4	2.AC-13	7
2.AA-43	4	2.AC-14	7
2.AA-44	4	2.AC-15	7
2.AA-45	4	2.AC-16	7
2.AA-46	4	2.AC-17	7
2.AA-47	4	2.AC-18	7
2.AA-48	4	2.AC-19	7

LIST OF EFFECTIVE PAGES FOR REVISION 9

<u>Page</u>	<u>Revision</u>	<u>Page</u>	<u>Revision</u>
2.AC-20	7	2.AC-71	7
2.AC-21	7	2.AC-72	7
2.AC-22	7	2.AC-73	7
2.AC-23	7	2.AC-74	7
2.AC-24	7	2.AC-75	7
2.AC-25	7	2.AC-76	7
2.AC-26	7	2.AC-77	7
2.AC-27	7	2.AC-78	7
2.AC-28	7	2.AC-79	7
2.AC-29	7	2.AC-80	7
2.AC-30	7	2.AC-81	7
2.AC-31	7	2.AC-82	7
2.AC-32	7	2.AC-83	7
2.AC-33	7	2.AC-84	7
2.AC-34	7	2.AC-85	7
2.AC-35	7	2.AC-86	7
2.AC-36	7	2.AC-87	7
2.AC-37	7	2.AC-88	7
2.AC-38	7	2.AC-89	7
2.AC-39	7	2.AC-90	7
2.AC-40	7	2.AC-91	7
2.AC-41	7	2.AC-92	7
2.AC-42	7	2.AC-93	7
2.AC-43	7	2.AC-94	7
2.AC-44	7	2.AC-95	7
2.AC-45	7	2.AC-96	7
2.AC-46	7	2.AC-97	7
2.AC-47	7	2.AC-98	7
2.AC-48	7	2.AC-99	7
2.AC-49	7	2.AC-100	7
2.AC-50	7	2.AC-101	7
2.AC-51	7	2.AC-102	7
2.AC-52	7	2.AC-103	7
2.AC-53	7	2.AC-104	7
2.AC-54	7	2.AC-105	7
2.AC-55	7	2.AC-106	7
2.AC-56	7	2.AC-107	7
2.AC-57	7	2.AC-108	7
2.AC-58	7	2.AC-109	7
2.AC-59	7	2.AC-110	7
2.AC-60	7	2.AC-111	7
2.AC-61	7	2.AC-112	7
2.AC-62	7	2.AC-113	7
2.AC-63	7	2.AC-114	7
2.AC-64	7	2.AC-115	7
2.AC-65	7	2.AC-116	7
2.AC-66	7	2.AC-117	7
2.AC-67	7	2.AC-118	7
2.AC-68	7	2.AC-170	7
2.AC-69	7	2.AC-171	7
2.AC-70	7	2.AC-172	7

LIST OF EFFECTIVE PAGES FOR REVISION 9

<u>Page</u>	<u>Revision</u>	<u>Page</u>	<u>Revision</u>
2.AC-173	7	2.AC-224	7
2.AC-174	7	2.AC-225	7
2.AC-175	7	2.AC-226	7
2.AC-176	7	2.AC-227	7
2.AC-177	7	2.AC-228	7
2.AC-178	7	2.AC-229	7
2.AC-179	7	2.AC-230	7
2.AC-180	7	2.AC-231	7
2.AC-181	7	2.AC-232	7
2.AC-182	7	2.AC-233	7
2.AC-183	7	2.AC-234	7
2.AC-184	7	2.AC-235	7
2.AC-185	7	2.AC-236	7
2.AC-186	7	2.AC-237	7
2.AC-187	7	2.AC-238	7
2.AC-188	7	2.AC-239	7
2.AC-189	7	2.AC-240	7
2.AC-190	7	2.AC-241	7
2.AC-191	7	2.AC-242	7
2.AC-192	7	2.AC-243	7
2.AC-193	7	2.AC-244	7
2.AC-194	7	2.AC-245	7
2.AC-195	7	2.AC-246	7
2.AC-196	7	2.AC-247	7
2.AC-197	7	2.AC-248	7
2.AC-198	7	2.AC-249	7
2.AC-199	7	2.AC-250	7
2.AC-200	7	2.AC-251	7
2.AC-201	7	2.AC-252	7
2.AC-202	7	2.AC-253	7
2.AC-203	7	2.AC-254	7
2.AC-204	7	2.AC-255	7
2.AC-205	7	2.AC-256	7
2.AC-206	7	2.AC-257	7
2.AC-207	7	2.AC-258	7
2.AC-208	7	2.AC-259	7
2.AC-209	7	2.AC-260	7
2.AC-210	7	2.AC-261	7
2.AC-211	7	2.AC-262	7
2.AC-212	7	2.AC-263	7
2.AC-213	7	2.AC-264	7
2.AC-214	7	2.AC-265	7
2.AC-215	7	2.AC-266	7
2.AC-216	7	2.AC-267	7
2.AC-217	7	2.AC-268	7
2.AC-218	7	2.AC-269	7
2.AC-219	7	2.AC-270	7
2.AC-220	7	2.AC-271	7
2.AC-221	7	2.AC-272	7
2.AC-222	7	2.AC-273	7
2.AC-223	7	2.AC-274	7

LIST OF EFFECTIVE PAGES FOR REVISION 9

<u>Page</u>	<u>Revision</u>	<u>Page</u>	<u>Revision</u>
2.AC-275	7	2.AC-326	7
2.AC-276	7	2.AC-327	7
2.AC-277	7	2.AC-328	7
2.AC-278	7	2.AC-329	7
2.AC-279	7	2.AC-330	7
2.AC-280	7	2.AC-331	7
2.AC-281	7	2.AC-332	7
2.AC-282	7	2.AC-333	7
2.AC-283	7	2.AC-334	7
2.AC-284	7	2.AC-335	7
2.AC-285	7	2.AC-336	7
2.AC-286	7	2.AC-337	7
2.AC-287	7	2.AC-338	7
2.AC-288	7	2.AC-339	7
2.AC-289	7	2.AC-340	7
2.AC-290	7	2.AC-341	7
2.AC-291	7	2.AC-342	7
2.AC-292	7	2.AC-343	7
2.AC-293	7	2.AC-344	7
2.AC-294	7	2.AC-345	7
2.AC-295	7	2.AC-346	7
2.AC-296	7	2.AC-347	7
2.AC-297	7	2.AC-348	7
2.AC-298	7	2.AC-349	7
2.AC-299	7	2.AC-350	7
2.AC-300	7	2.AC-351	7
2.AC-301	7	2.AC-352	7
2.AC-302	7	2.AC-353	7
2.AC-303	7	2.AC-354	7
2.AC-304	7	2.AC-355	7
2.AC-305	7	2.AC-356	7
2.AC-306	7	2.AC-357	7
2.AC-307	7	2.AC-358	7
2.AC-308	7	2.AC-359	7
2.AC-309	7	2.AC-360	7
2.AC-310	7	2.AC-361	7
2.AC-311	7	2.AC-362	7
2.AC-312	7	2.AC-363	7
2.AC-313	7	2.AC-364	7
2.AC-314	7	2.AC-365	7
2.AC-315	7	2.AC-366	7
2.AC-316	7	2.AC-367	7
2.AC-317	7	2.AC-368	7
2.AC-318	7	2.AC-369	7
2.AC-319	7	2.AC-370	7
2.AC-320	7	2.AC-371	7
2.AC-321	7	2.AC-372	7
2.AC-322	7	2.AC-373	7
2.AC-323	7	2.AC-374	7
2.AC-324	7	2.AC-375	7
2.AC-325	7	2.AC-376	7

LIST OF EFFECTIVE PAGES FOR REVISION 9

<u>Page</u>	<u>Revision</u>	<u>Page</u>	<u>Revision</u>
2.AC-377	7	Fig. 2.AD.2	7
2.AC-378	7	2.AE-1	8
2.AC-379	7	2.AE-2	8
2.AC-380	7	2.AE-3	8
2.AC-381	7	2.AE-4	7
2.AC-382	7	2.AE-5	7
2.AC-383	7	2.AE-6	7
2.AC-384	7	2.AE-7	7
2.AC-385	7	2.AE-8	7
2.AC-386	7	2.AE-9	7
2.AC-387	7	2.AE-10	7
2.AC-388	7	2.AE-11	7
2.AC-389	7	2.AE-12	7
2.AC-390	7	2.AE-13	7
2.AC-391	7	2.AE-14	7
2.AC-392	7	2.AE-15	7
2.AC-393	7	2.AE-16	7
2.AC-394	7	2.AE-17	7
2.AC-395	7	2.AE-18	7
2.AC-396	7	2.AE-19	7
2.AC-397	7	2.AE-20	7
2.AC-398	7	2.AE-21	7
2.AC-399	7	2.AE-22	7
2.AC-400	7	2.AE-23	7
2.AD-1	7	2.AE-24	7
2.AD-2	7	2.AE-25	7
2.AD-3	7	2.AE-26	7
2.AD-4	7	2.AE-27	7
2.AD-5	7	2.AE-28	7
2.AD-6	7	2.AE-29	7
2.AD-7	7	2.AE-30	7
2.AD-8	7	2.AE-31	7
2.AD-9	7	2.AE-32	7
2.AD-10	7	2.AE-33	7
2.AD-11	7	2.AE-34	7
2.AD-12	7	2.AE-35	7
2.AD-13	7	2.AE-36	7
2.AD-14	7	2.AE-37	7
2.AD-15	7	2.AE-38	7
2.AD-16	7	2.AE-39	7
2.AD-17	7	2.AE-40	7
2.AD-18	7	2.AE-41	7
2.AD-19	7	2.AE-42	7
2.AD-20	7	2.AE-43	7
2.AD-21	7	2.AE-44	7
2.AD-22	7	2.AE-45	7
2.AD-23	7	2.AE-46	7
2.AD-24	7	2.AE-47	7
2.AD-25	7	2.AE-48	7
2.AD-26	7	2.AE-49	7
Fig. 2.AD.1	6	2.AE-50	7

LIST OF EFFECTIVE PAGES FOR REVISION 9

<u>Page</u>	<u>Revision</u>	<u>Page</u>	<u>Revision</u>
2.AE-51	7	2.AE-102	8
2.AE-52	7	2.AE-103	8
2.AE-53	7	2.AE-104	8
2.AE-54	7	2.AE-105	8
2.AE-55	7	2.AE-106	8
2.AE-56	7	2.AE-107	8
2.AE-57	7	2.AE-108	8
2.AE-58	7	2.AE-109	8
2.AE-59	7	2.AE-110	8
2.AE-60	8	2.AE-111	8
2.AE-61	8	2.AE-112	8
2.AE-62	8	2.AE-113	8
2.AE-63	8	2.AE-114	8
2.AE-64	8	2.AE-115	8
2.AE-65	8	2.AE-116	8
2.AE-66	8	2.AE-117	8
2.AE-67	8	2.AE-118	8
2.AE-68	8	2.AE-119	8
2.AE-69	8	2.AE-120	8
2.AE-70	8	2.AE-121	8
2.AE-71	8	2.AE-122	8
2.AE-72	8	2.AE-123	8
2.AE-73	8	2.AE-124	8
2.AE-74	8	2.AE-125	8
2.AE-75	8	2.AE-126	8
2.AE-76	8	2.AE-127	8
2.AE-77	8	2.AE-128	8
2.AE-78	8	2.AE-129	8
2.AE-79	8	2.AE-130	8
2.AE-80	8	2.AE-131	8
2.AE-81	8	2.AE-132	8
2.AE-82	8	2.AE-133	8
2.AE-83	8	2.AE-134	8
2.AE-84	8	2.AE-135	8
2.AE-85	8	2.AE-136	8
2.AE-86	8	2.AE-137	8
2.AE-87	8	2.AE-138	8
2.AE-88	8	2.AE-139	8
2.AE-89	8	2.AE-140	8
2.AE-90	8	2.AE-141	8
2.AE-91	8	2.AE-142	8
2.AE-92	8	2.AE-143	8
2.AE-93	8	2.AE-144	8
2.AE-94	8	2.AE-145	8
2.AE-95	8	2.AE-146	8
2.AE-96	8	2.AE-147	8
2.AE-97	8	2.AE-148	8
2.AE-98	8	2.AE-149	8
2.AE-99	8	2.AE-150	8
2.AE-100	8	2.AE-151	8
2.AE-101	8	2.AE-152	8

LIST OF EFFECTIVE PAGES FOR REVISION 9

Page	Revision	Page	Revision
2.AE-153	8	Fig. 2.AG.4(b)	6
2.AE-154	8	Fig. 2.AG.4(c)	6
2.AE-155	8	Fig. 2.AG.4(d)	6
2.AE-156	8	Fig. 2.AG.4(e)	6
2.AE-157	8	2.AH-1	7
2.AE-158	8	2.AH-2	7
2.AE-159	8	2.AH-3	7
2.AE-160	8	2.AH-4	7
2.AE-161	8	2.AH-5	7
2.AE-162	8	2.AH-6	7
2.AE-163	8	2.AH-7	7
2.AE-164	8	2.AH-8	7
2.AE-165	8	2.AI-1	7
2.AE-166	8	2.AI-2	7
2.AE-167	8	2.AI-3	7
2.AE-168	8	2.AI-4	7
2.AE-169	8	2.AI-5	7
2.AE-170	8	2.AI-6	7
2.AE-171	8	2.AI-7	7
2.AE-172	8	2.AI-8	7
2.AE-173	8	2.AI-9	7
2.AF-1	7	2.AI-10	7
2.AF-2	7	2.AK-1	7
2.AF-3	7	2.AK-2	7
2.AF-4	7	2.AK-3	7
2.AF-5	7	2.AK-4	7
2.AF-6	7	2.AK-5	7
2.AF-7	7	2.AK-6	7
2.AF-8	7	2.AK-7	7
2.AF-9	7	2.AK-8	7
2.AF-10	7	2.AK-9	7
2.AF-11	7	2.AK-10	7
2.AF-12	7	2.AL-1	7
2.AF-13	7	2.AL-2	7
2.AF-14	7	2.AL-3	7
2.AF-15	7	2.AL-4	7
2.AF-16	7	2.AL-5	7
Fig. 2.AF.1	6	2.AL-6	7
2.AG-1	6	2.AL-7	7
2.AG-2	6	2.AL-8	7
2.AG-3	6	2.AL-9	7
2.AG-4	6	2.AL-10	7
2.AG-5	6	2.AL-11	7
2.AG-6	6	2.AL-12	7
2.AG-7	6	2.AM-1	7
2.AG-8	6	2.AM-2	7
2.AG-9	6	2.AM-3	7
Fig. 2.AG.1	6	2.AM-4	7
Fig. 2.AG.2	6	2.AM-5	7
Fig. 2.AG.3	6	2.AM-6	9
Fig. 2.AG.4(a)	6		

LIST OF EFFECTIVE PAGES FOR REVISION 9

<u>Page</u>	<u>Revision</u>		<u>Page</u>	<u>Revision</u>
2.AN-1	8		2.AO-1	9
2.AN-2	8		2.AO-2	9
2.AN-3	8		2.AO-3	9
2.AN-4	8		2.AO-4	9
2.AN-5	8		2.AO-5	9
2.AN-6	8		2.AO-6	9
2.AN-7	8		2.AO-7	9
2.AN-8	8		2.AO-8	9
2.AN-9	8		2.AO-9	9
2.AN-10	8		2.AO-10	9
2.AN-11	8		2.AO-11	9
2.AN-12	8			
2.AN-13	8			
Fig. 2.AN.1	8			
Fig. 2.AN.2	8			

LIST OF EFFECTIVE PAGES FOR REVISION 9

Page	Revision	Page	Revision
3.0-2	7	3.4-23	9
3.1-1	7	3.4-24	9
3.1-2	7	3.4-25	9
3.1-3	7	3.4-26	9
3.2-1	7	3.4-27	9
3.2-2	7	3.4-28	9
3.2-3	7	3.4-29	9
3.2-4	7	3.4-30	9
3.2-5	7	3.4-31	9
3.2-6	7	3.4-32	9
3.2-7	7	3.4-33	9
3.2-8	7	3.4-34	9
3.2-9	7	3.4-35	9
3.2-10	7	3.4-36	9
3.3-1	9	3.4-37	9
3.3-2	9	3.4-38	9
3.3-3	9	3.4-39	9
3.3-4	9	3.4-40	9
3.3-5	9	3.4-41	9
3.3-6	9	3.4-42	9
3.3-7	9	3.4-43	9
3.3-8	9	3.4-44	9
3.3-9	9	3.4-45	9
3.3-10	9	3.4-46	9
3.3-11	9	3.4-47	9
3.3-12	9	3.4-48	9
3.3-13	9	3.4-49	9
3.3-14	9	3.4-50	9
3.3-15	9	3.4-51	9
3.4-1	8	3.4-52	9
3.4-2	8	3.4-53	9
3.4-3	8	3.4-54	9
3.4-4	8	3.4-55	9
3.4-5	8	3.4-56	9
3.4-6	9	3.4-57	9
3.4-7	9	3.4-58	9
3.4-8	9	3.4-59	9
3.4-9	9	3.4-60	9
3.4-10	9	3.4-61	9
3.4-11	9	3.4-62	9
3.4-12	9	3.4-63	9
3.4-13	9	3.4-64	9
3.4-14	9	3.4-65	9
3.4-15	9	3.4-66	9
3.4-16	9	3.4-67	9
3.4-17	9	3.4-68	9
3.4-18	9	3.4-70	9
3.4-19	9	3.4-71	9
3.4-20	9	Fig. 3.4.1	6
3.4-21	9	Fig. 3.4.2	7
3.4-22	9	Fig. 3.4.3	7

LIST OF EFFECTIVE PAGES FOR REVISION 9

<u>Page</u>	<u>Revision</u>	<u>Page</u>	<u>Revision</u>
Fig. 3.4.4	4	3.7-3	7
Fig. 3.4.5	7		
Fig. 3.4.6	6		
Fig. 3.4.7	6		
Fig. 3.4.8	6		
Fig. 3.4.9	7		
Fig. 3.4.10	6		
Fig. 3.4.11	6		
Fig. 3.4.12	7		
Fig. 3.4.13	7		
Fig. 3.4.14	6		
Fig. 3.4.15	7		
Fig. 3.4.16	6		
Fig. 3.4.17	6		
Fig. 3.4.18	7		
Fig. 3.4.19	7		
Fig. 3.4.20	7		
Fig. 3.4.21	7		
Fig. 3.4.22	7		
Fig. 3.4.23	7		
Fig. 3.4.24	8		
Fig. 3.4.25	8		
Fig. 3.4.26	8		
Fig. 3.4.27	8		
Fig. 3.4.28	8		
3.5-1	8		
3.5-2	8		
3.5-3	8		
3.5-4	8		
3.5-5	8		
3.5-6	8		
3.5-7	8		
3.5-8	8		
3.5-9	8		
3.5-10	8		
3.5-11	8		
Fig. 3.5.1	7		
Fig. 3.5.2	5		
Fig. 3.5.3	6		
Fig. 3.5.4	6		
Fig. 3.5.5	6		
Fig. 3.5.6	7		
Fig. 3.5.7	7		
Fig. 3.5.8	7		
Fig. 3.5.9	7		
3.6-1	7		
3.6-2	7		
3.6-3	7		
3.6-4	7		
3.7-1	7		
3.7-2	7		

LIST OF EFFECTIVE PAGES FOR REVISION 9

<u>Page</u>	<u>Revision</u>	<u>Page</u>	<u>Revision</u>
4.0-1	9	4.B-1	8
4.0-2	9	4.B-2	8
4.1-1	8	4.B-3	8
4.1-2	8	4.B-4	8
4.1-3	8	4.B-5	8
4.1-4	8		
4.1-5	9		
4.1-6	9		
4.1-7	8		
Fig. 4.1.1	8		
Fig. 4.1.2	8		
Fig. 4.1.3	8		
Fig. 4.1.4	8		
4.2-1	8		
4.2-2	8		
4.2-3	8		
4.2-4	8		
4.2-5	9		
4.2-6	9		
4.2-7	9		
4.2-8	9		
4.2-9	9		
4.2-10	9		
4.2-11	9		
4.2-12	9		
4.2-13	9		
4.2-14	9		
4.2-15	9		
4.2-16	8		
4.2-17	8		
4.2-18	8		
4.2-19	8		
4.2-20	8		
4.2-21	8		
4.2-22	8		
4.2-23	8		
4.2-24	9		
4.2-25	9		
4.2-26	8		
4.2-27	9		
4.2-28	8		
4.2-29	8		
4.2-30	9		
4.2-31	8		
4.2-32	8		
4.3-1	8		
4.3-2	8		
4.4-1	8		
4.A-1	8		
4.A-2	8		
4.A-3	8		

LIST OF EFFECTIVE PAGES FOR REVISION 9

Page	Revision	Page	Revision
5.0-1	9	5.2-35	9
5.1-1	9	5.2-36	9
5.1-2	9	5.2-37	9
5.1-3	9	5.2-38	9
5.1-4	9	5.2-39	9
5.1-5	9	5.2-40	9
5.1-6	8	5.3-1	8
5.1-7	8	5.3-2	8
5.1-8	8	5.3-3	8
5.1-9	8	5.3-4	8
5.1-10	8	5.3-5	8
5.1-11	8	5.3-6	8
5.1-12	8	5.3-7	8
5.1-13	8	5.3-8	8
5.1-14	8	5.3-9	8
Fig. 5.1.1	8	Fig. 5.3.1	7
Fig. 5.1.2	6	Fig. 5.3.2	4
5.2-1	8	Fig. 5.3.3	4
5.2-2	8	Fig. 5.3.4	7
5.2-3	9	Fig. 5.3.5	7
5.2-4	8	Fig. 5.3.6	7
5.2-5	8	Fig. 5.3.7	6
5.2-6	8	Fig. 5.3.8	6
5.2-7	9	Fig. 5.3.9	9
5.2-8	9	Fig. 5.3.10	8
5.2-9	9	Fig. 5.3.11	8
5.2-10	9	Fig. 5.3.12	8
5.2-11	9	5.4-1	8
5.2-12	9	5.4-2	8
5.2-13	9	5.4-3	8
5.2-14	9	5.4-4	8
5.2-15	9	5.4-5	9
5.2-16	9	5.4-6	9
5.2-17	9	5.4-7	9
5.2-18	9	5.4-8	9
5.2-19	9	5.4-9	9
5.2-20	9	5.4-10	9
5.2-21	9	5.4-11	9
5.2-22	9	5.4-12	9
5.2-23	9	5.4-13	9
5.2-24	9	5.4-14	9
5.2-25	9	5.4-15	9
5.2-26	9	5.4-16	9
5.2-27	9	5.4-17	9
5.2-28	9	5.4-18	9
5.2-29	9	5.4-19	9
5.2-30	9	5.4-20	9
5.2-31	9	5.4-21	9
5.2-32	9	5.4-22	9
5.2-33	9	5.4-23	9
5.2-34	9	5.4-24	9

LIST OF EFFECTIVE PAGES FOR REVISION 9

<u>Page</u>	<u>Revision</u>		<u>Page</u>	<u>Revision</u>
5.4-25	9		5.C-25	7
5.4-26	9		5.C-26	7
5.4-27	9		5.C-27	7
5.4-28	9		5.C-28	7
5.4-29	9		5.C-29	7
5.4-30	9		5.C-30	7
5.4-31	9		5.C-31	7
5.4-32	9		5.C-32	7
5.4-33	9		5.C-33	7
5.4-34	9		5.C-34	7
Fig. 5.4-1	8			
5.5-1	8			
5.5-2	8			
5.5-3	8			
5.5-4	8			
5.6-1	8			
5.6-2	8			
5.A-1	7			
5.A-2	7			
5.A-3	7			
5.B-1	7			
5.B-2	7			
5.B-3	7			
5.B-4	7			
5.B-5	7			
5.B-6	7			
5.C-1	7			
5.C-2	7			
5.C-3	7			
5.C-4	7			
5.C-5	7			
5.C-6	7			
5.C-7	7			
5.C-8	7			
5.C-9	7			
5.C-10	7			
5.C-11	7			
5.C-12	7			
5.C-13	7			
5.C-14	7			
5.C-15	7			
5.C-16	7			
5.C-17	7			
5.C-18	7			
5.C-19	7			
5.C-20	7			
5.C-21	7			
5.C-22	7			
5.C-23	7			
5.C-24	7			

LIST OF EFFECTIVE PAGES FOR REVISION 9

Page	Revision	Page	Revision
6.1-1	7	6.2-41	9
6.1-2	8	6.2-42	9
6.1-3	9	6.2-43	9
6.1-4	9	6.2-44	9
6.1-5	9	6.2-45	9
6.1-6	9	6.2-46	9
6.1-7	9	6.2-47	9
6.1-8	9	6.2-48	9
6.1-9	9	6.2-49	9
6.1-10	9	6.2-50	9
6.1-11	8	6.2-51	9
6.2-1	9	6.2-52	9
6.2-2	9	6.2-53	9
6.2-3	9	6.2-54	9
6.2-4	9	6.2-55	9
6.2-5	9	6.2-56	9
6.2-6	9	6.3-1	7
6.2-7	9	6.3-2	7
6.2-8	9	6.3-3	7
6.2-9	9	6.3-4	7
6.2-10	9	6.3-5	7
6.2-11	9	6.3-6	7
6.2-12	9	6.3-7	7
6.2-13	9	6.3-8	7
6.2-14	9	6.3-9	9
6.2-15	9	6.3-10	9
6.2-16	9	Fig. 6.3.1	7
6.2-17	9	Fig. 6.3.2	7
6.2-18	9	Fig. 6.3.3	7
6.2-19	9	Fig. 6.3.4	4
6.2-20	9	Fig. 6.3.5	7
6.2-21	9	Fig. 6.3.6	4
6.2-22	9	Fig. 6.3.7	7
6.2-23	9	6.4-1	9
6.2-24	9	6.4-2	9
6.2-25	9	6.4-3	9
6.2-26	9	6.4-4	9
6.2-27	9	6.4-5	9
6.2-28	9	6.4-6	9
6.2-29	9	6.4-7	9
6.2-30	9	6.4-8	9
6.2-31	9	6.4-9	9
6.2-32	9	6.4-10	9
6.2-33	9	6.4-11	9
6.2-34	9	6.4-12	9
6.2-35	9	6.4-13	9
6.2-36	9	6.4-14	9
6.2-37	9	6.4-15	9
6.2-38	9	6.4-16	9
6.2-39	9	6.4-17	9
6.2-40	9	6.4-18	9

LIST OF EFFECTIVE PAGES FOR REVISION 9

<u>Page</u>	<u>Revision</u>	<u>Page</u>	<u>Revision</u>
Fig. 6.4.1	9	6.D-2	7
Fig. 6.4.2	9	6.D-3	7
Fig. 6.4.3	9	6.D-4	7
Fig. 6.4.4	9	6.D-5	7
Fig. 6.4.5	9	6.D-6	7
Fig. 6.4.6	9	6.D-7	7
Fig. 6.4.7	9	6.D-8	7
Fig. 6.4.8	7	6.D-9	7
Fig. 6.4.9	7	6.D-10	7
Fig. 6.4.10	9	6.D-11	7
6.5-1	7	6.D-12	7
6.6-1	7	6.D-13	7
6.7-1	8	6.D-14	7
6.7-2	7	6.D-15	7
6.A-1	7	6.D-16	7
6.A-2	7	6.D-17	7
6.A-3	7	6.D-18	7
6.A-4	7	6.D-19	7
6.A-5	7	6.D-20	7
6.A-6	7	6.D-21	7
6.A-7	7	6.D-22	7
6.A-8	7	6.D-23	7
6.A-9	7	6.D-24	7
6.A-10	7	6.D-25	7
6.A-11	7	6.D-26	7
6.A-12	7	6.D-27	7
6.A-13	7	6.D-28	7
6.A-14	7	6.D-29	7
6.A-15	7	6.D-30	7
6.A-16	7	6.D-31	7
6.A-17	7	6.D-32	7
6.A-18	7	6.D-33	7
6.A-19	7	6.D-34	7
6.A-20	7	6.D-35	7
Fig. 6.A.1	7	6.D-36	7
Fig. 6.A.2	7	6.D-37	7
Fig. 6.A.3	7	6.D-38	7
Fig. 6.A.4	7	6.D-39	7
Fig. 6.A.5	7	6.D-40	7
Fig. 6.A.6	7	6.D-41	7
6.B-1	7	6.D-42	7
6.B-2	7	6.D-43	7
6.C-1	9	6.D-44	7
6.C-2	9		
6.C-3	9		
6.C-4	9		
6.C-5	9		
6.C-6	9		
6.C-7	9		
6.C-8	9		
6.D-1	7		

LIST OF EFFECTIVE PAGES FOR REVISION 9

<u>Page</u>	<u>Revision</u>	<u>Page</u>	<u>Revision</u>
7.0-1	9	Fig. 7.1.6	7
7.0-2	9	Fig. 7.1.7	7
7.1-1	9	Fig. 7.1.8	7
7.1-2	9	Fig. 7.1.9	7
7.1-3	9	Fig. 7.1.10	7
7.1-4	9	Fig. 7.1.11	7
7.1-5	9	Fig. 7.1.12	7
7.1-6	9	Fig. 7.1.13	7
7.1-7	9	Fig. 7.1.14	7
7.1-8	9	Fig. 7.1.15	7
7.1-9	9	Fig. 7.1.16	7
7.1-10	9	Fig. 7.1.17	7
7.1-11	9	Fig. 7.1.18	7
7.1-12	9	Fig. 7.1.19	7
7.1-13	9	Fig. 7.1.20	7
7.1-14	9	Fig. 7.1.21	7
7.1-15	9	Fig. 7.1.22	7
7.1-16	9	Fig. 7.1.23	7
7.1-17	9	Fig. 7.1.24	7
7.1-18	9	Fig. 7.1.25	7
7.1-19	9	Fig. 7.1.26	7
7.1-20	9	Fig. 7.1.27	7
7.1-21	9	Fig. 7.1.28	7
7.1-22	9	Fig. 7.1.29	7
7.1-23	9	Fig. 7.1.30	7
7.1-24	9	7.2-1	9
7.1-25	9	7.2-2	9
7.1-26	9	7.2-3	9
7.1-27	9	7.2-4	9
7.1-28	9	7.2-5	9
7.1-29	9	7.2-6	9
7.1-30	9	7.2-7	9
7.1-31	9	7.2-8	9
7.1-32	9	7.2-9	9
7.1-33	9	7.2-10	9
7.1-34	9	Fig. 7.2.1	7
7.1-35	9	Fig. 7.2.2a	7
7.1-36	9	Fig. 7.2.2b	7
7.1-37	9	Fig. 7.2.2c	7
7.1-38	9	Fig. 7.2.3	7
7.1-39	9	Fig. 7.2.4	7
7.1-40	9	Fig. 7.2.5	7
7.1-41	9	7.3-1	9
		7.3-2	9
Fig. 7.1.1	7	7.3-3	9
Fig. 7.1.2a	7	7.4-1	9
Fig. 7.1.2b	7	7.4-2	9
Fig. 7.1.2c	7	7.4-3	9
Fig. 7.1.3	7	7.4-4	9
Fig. 7.1.4	7	7.5-1	8
Fig. 7.1.5	7	7.6-1	8

LIST OF EFFECTIVE PAGES FOR REVISION 9

<u>Page</u>	<u>Revision</u>	<u>Page</u>	<u>Revision</u>
8.1-1	8		
8.1-2	8		
8.1-3	8		
8.1-4	8		
8.1-5	8		
8.1-6	9		
8.1-7	9		
8.1-8	9		
8.1-9	9		
8.1-10	9		
8.1-11	9		
8.1-12	9		
8.1-13	9		
8.1-14	9		
8.1-15	9		
8.1-16	9		
8.1-17	9		
8.1-18	9		
8.1-19	9		
8.1-20	9		
8.1-21	9		
8.1-22	9		
8.1-23	9		
8.1-24	9		
8.1-25	9		
8.1-26	9		
8.1-27	9		
8.1-28	9		
8.1-29	8		
Fig. 8.1.1	7		
Fig. 8.1.2	7		
Fig. 8.1.3	7		
Fig. 8.1.4	7		
8.2-1	7		
8.2-2	7		
8.2-3	7		
8.2-4	7		
8.2-5	7		
Fig. 8.2.1	7		
8.3-1	7		
8.3-2	7		
8.4-1	9		

CHAPTER 1: GENERAL INFORMATION

1.0 GENERAL INFORMATION

This Safety Analysis Report (SAR) for Holtec International's HI-STAR 100 packaging is a compilation of information and analyses to support a United States Nuclear Regulatory Commission (NRC) licensing review as a spent nuclear fuel transportation package (Docket No. 71-9261) under requirements specified in 10CFR71 [1.0.1] and 49CFR173 [1.0.2]. This application seeks NRC approval and issuance of a Certificate of Compliance under provisions and definitions in 10CFR71, Subpart D, for the new design Model: HI-STAR 100 as an acceptable Type B(U)F-85 packaging for transport by exclusive use shipment (10CFR71.47). The HI-STAR 100 packaging complies with the requirements of 10CFR71 for a Type B(U)F-85 package. The HI-STAR 100 packaging does not have a maximum normal operating pressure (MNOP) greater than 700 kPa (100 lb/in²). The HI-STAR 100 internal design pressure is specified in Table 2.1.1 as 100 psig to calculate bounding stress values. Section 3.4 calculates the MNOP (reported in Table 3.4.15) and demonstrates that the value remains below the design value specified in Table 2.1.1. No pressure relief device is provided on the HI-STAR 100 containment boundary, as discussed in Subsection 1.2.1.8. Therefore, there is no pressure relief device that would allow the release of radioactive material under the tests specified in 10CFR71.73. Analyses which demonstrate that the HI-STAR 100 packaging complies with the requirements of Subparts E and F of 10CFR71 are provided in this SAR. Specific reference to each section of the SAR that is used to specifically address compliance to 10CFR71 is provided in Table 1.0.2. Therefore, the new HI-STAR 100 packaging to transport spent nuclear fuel should be designated B(U)F-85.

The HI-STAR 100 transport index for nuclear criticality control is zero, as an unlimited number of packages is subcritical under the procedures specified in 10CFR71.59(a). Section 6.1 provides the determination of the transport index for nuclear criticality control. The transport index based on radiation is in excess of 10 for the HI-STAR 100 Packaging with design basis fuel contents. Therefore, the HI-STAR 100 Packaging must be transported by exclusive use shipment (10CFR71.47).

The HI-STAR 100 packaging design, fabrication, assembly, and testing shall be performed in accordance with Holtec International's quality assurance program. Holtec International's quality assurance program was originally developed to meet NRC requirements delineated in 10CFR50, Appendix B, and was expanded to include provisions of 10CFR71, Subpart H, and 10CFR72, Subpart G, for structures, systems, and components designated as important to safety. NRC approval of Holtec International's quality assurance program is documented by the Quality Assurance Program Approval for Radioactive material Packages (NRC Form 311), Approval Number 0784, Docket No. 71-0784.

This report has been prepared in the format and content suggested in NRC Regulatory Guide 7.9 [1.0.3]. The purpose of this chapter is to provide a general description of the design features and transport capabilities of the HI-STAR 100 packaging including its intended use. This chapter provides a summary description of the packaging, operational features, and contents, and provides reasonable assurance that the package will meet the regulations and operating objectives. Table 1.0.1 contains a listing of the terminology and notation used in preparing this licensing application report.

This SAR was prepared prior to the issuance of the draft version of NUREG-1617 [1.0.5]. To aid NRC review, additional tables and references have been added to facilitate the location of information needed to demonstrate compliance with 10CFR71 as outlined by NUREG-1617. Table 1.0.2 provides a matrix of the 10CFR71 requirements as outlined in NUREG-1617, the format requirements of Regulatory Guide 7.9, and reference to the applicable SAR section(s) that address(es) each topic.

The HI-STAR 100 Topical Safety Analysis Report (TSAR) [1.0.6] has been submitted to the NRC for a Certificate of Compliance for HI-STAR 100 to store spent nuclear fuel at an Independent Spent Fuel Storage Installation (ISFSI) facility under requirements of 10CFR72, Subpart L [1.0.4] (Docket Number 72-1008).

Within this report, all figures, tables and references cited are identified by the double decimal system m.n.i, where m is the chapter number, n is the section number, and i is the sequential number. Thus, for example, Figure 1.1.1 is the first figure in Section 1.1 of Chapter 1 (which is the next section in this chapter).

Revision of this document to Revision 9 was made on a page level. Therefore, if any change occurs on a page or figure, the affected page or figure was updated to Revision 9.

Table 1.0.1

TERMINOLOGY AND NOTATION

ALARA is an acronym for As Low As Reasonably Achievable.

AL-STAR™ is the trademark name of the HI-STAR 100 impact limiter.

Boral is a generic term to denote an aluminum-boron carbide cermet manufactured in accordance with U.S. Patent No. 4027377. The individual material supplier may use another trade name to refer to the same product.

Boral™ means Boral manufactured by AAR Advanced Structures.

BWR is an acronym for boiling water reactor.

C.G. is an acronym for center of gravity.

Containment System Boundary means the enclosure formed by the overpack inner shell welded to a bottom plate and top flange plus the bolted closure plate with dual seals and the vent and drain port plugs with seals. It is also called the primary containment boundary when used with the inner (secondary) containment boundary of the MPC-68F.

Containment System means the HI-STAR 100 overpack which forms the containment boundary of the packaging intended to contain the radioactive material during transport.

Damaged Fuel Assembly is a fuel assembly with known or suspected cladding defects, as determined by a review of records, greater than pinhole leaks or hairline cracks, missing fuel rods that are not replaced with dummy fuel rods, or those that cannot be handled by normal means. Fuel assemblies which cannot be handled by normal means due to fuel cladding damage are considered to Fuel Debris.

Damaged Fuel Container means a specially designed enclosure for damaged fuel assemblies or fuel debris which permits gaseous and liquid media to escape while minimizing dispersal of gross solid particulates. The Damaged Fuel Container (DFC) features a lifting location which is suitable for remote handling of a loaded or unloaded DFC. DFCs authorized for use in the HI-STAR 100 System are the Holtec design or the Transnuclear Dresden Unit 1 design as shown on Figures 1.2.10 and 1.2.11.

Enclosure Vessel means the pressure vessel defined by the cylindrical shell, baseplate, port cover plates, lid, and closure ring which provides confinement for the helium gas contained within the MPC. The Enclosure Vessel (EV) and the fuel basket together constitute the multi-purpose canister. See also Helium Retention Boundary.

Table 1.0.1 (continued)

TERMINOLOGY AND NOTATION

Exclusive use means the sole use by a single consignor of a conveyance for which all initial, intermediate, and final loading and unloading are carried out in accordance with the direction of the consignor or consignee. The consignor and the carrier must ensure that loading or unloading is performed by personnel having radiological training and resources appropriate for safe handling of the consignment. The consignor must issue specific instructions, in writing, for maintenance of exclusive use shipment controls, and include them with the shipping paper information provided to the carrier by the consignor.

Fuel Basket means a honeycomb structural weldment with square openings which can accept a fuel assembly of the type for which it is designed.

Fuel Debris is fuel with known or suspected defects, such as ruptured fuel rods, severed rods, or loose fuel pellets. Fuel assemblies which cannot be handled by normal means due to fuel cladding damage are considered to be Fuel Debris.

Helium Retention Boundary or Enclosure Vessel means the enclosure formed by the MPC shell welded to the baseplate, lid, welded port cover plates, and closure ring.

HI-STAR 100 MPC means the sealed spent nuclear fuel container which consists of a honeycombed fuel basket contained in a cylindrical canister shell which is welded to a baseplate, lid with welded port cover plates and closure ring. MPC is an acronym for multi-purpose canister. There are different MPCs with different fuel basket geometries for storing PWR or BWR fuel, but all MPCs have identical exterior design dimensions.

HI-STAR 100 overpack or overpack means the cask which receives and contains the sealed multi-purpose canisters containing spent nuclear fuel. It provides the containment boundary for radioactive materials, gamma and neutron shielding, and a set each of lifting and pocket trunnions for handling.

HI-STAR 100 System or HI-STAR 100 Packaging consists of the HI-STAR 100 MPC sealed within the HI-STAR 100 overpack with impact limiters installed.

Holtite™ is a trade name denoting an approved neutron shield material for use in the HI-STAR 100 System. In this application, Holtite-A is the only approved neutron shield material.

Holtite™-A is a commercially available neutron shield material developed by Bisco, Inc., and currently sold under the trade name NS-4-FR. The neutron shield material is specified with a nominal B_4C loading of 1 weight percent. An equivalent neutron shield material with equivalent neutron shielding properties and composition, but not sold under the trade name NS-4-FR, may be used.

Table 1.0.1 (continued)

TERMINOLOGY AND NOTATION

Impact Limiter means a set of fully-enclosed energy absorbers which are attached to the top and bottom of the overpack during transport. The impact limiters are used to absorb kinetic energy resulting from normal and hypothetical accident drop conditions. The HI-STAR impact limiters are called AL-STAR.

Important to Safety (ITS) means a function or condition required to transport spent nuclear fuel safely; to prevent damage to spent nuclear fuel, and to provide reasonable assurance that spent nuclear fuel can be received, handled, packaged, transported, and retrieved without undue risk to the health and safety of the public.

Intact Fuel Assembly is defined as a fuel assembly without known or suspected cladding defects greater than pinhole leaks and hairline cracks, and which can be handled by normal means. Partial fuel assemblies, that is fuel assemblies from which fuel rods are missing, shall not be classified as Intact Fuel Assemblies unless dummy fuel rods are used to displace an amount of water greater than or equal to that displaced by the original fuel rod(s).

Maximum Normal Operating Pressure (MNOP) means the maximum gauge pressure that would develop in the containment system in a period of 1 year under the heat condition specified in 10CFR71.71(c)(1), in the absence of venting, external cooling by an ancillary system, or operational controls during transport.

Maximum Reactivity means the highest possible k -effective including bias, uncertainties, and calculational statistics evaluated for the worst-case combination of fuel basket manufacturing tolerances.

MGDS is an acronym for Mined Geological Depository System.

MPC Fuel Basket means the honeycombed composite cell structure utilized to maintain subcriticality of the spent nuclear fuel. The number and size of the storage cells depends on the type of spent nuclear fuel to be transported. Each MPC fuel basket has sheathing welded to the storage cell walls for retaining the Boral neutron absorber. Boral is a commercially-available thermal neutron poison material composed of boron carbide and aluminum.

Multi-Purpose Canister (MPC) means the sealed canister which consists of a honeycombed fuel basket for spent nuclear fuel storage, contained in a cylindrical canister shell which is welded to a baseplate, lid with welded port cover plates, and closure ring. There are different MPCs with different fuel basket geometries for storing PWR or BWR fuel, but all MPCs have identical exterior dimensions. MPC is an acronym for multi-purpose canister. The MPCs used as part of the HI-STAR 100 Packaging (Docket No. 71-9261) are identical to the MPCs evaluated in the HI-STAR 100 Storage (Docket No. 72-1008) and HI-STORM 100 Storage (72-

Table 1.0.1 (continued)

TERMINOLOGY AND NOTATION

Neutron Shielding means Holtite, a material used in the overpack to thermalize and capture neutrons emanating from the radioactive spent nuclear fuel.

Packaging means the HI-STAR 100 System consisting of a single HI-STAR 100 overpack, a set of impact limiters, and a multi-purpose canister (MPC). It excludes all lifting devices, rigging, transporters, saddle blocks, welding machines, and auxiliary equipment (such as the drying and helium backfill system) used during fuel loading operations and preparation for off-site transportation.

Package means the HI-STAR 100 System plus the licensed radioactive contents loaded for transport.

Planar-Average Initial Enrichment is the average of the distributed fuel rod initial enrichments within a given axial plane of the assembly lattice.

PWR is an acronym for pressurized water reactor.

Reactivity is used synonymously with effective multiplication factor or k-effective.

SAR is an acronym for Safety Analysis Report (10CFR71).

Secondary Containment Boundary means the outline formed by the sealed, cylindrical enclosure of the MPC-68F shell welded to a solid baseplate, a lid welded around the top circumference of the shell wall, the port coverplates welded to the lid, and the closure ring welded to the lid and shell. The secondary containment boundary of the MPC-68F provides the separate inner container for the transport of fuel debris. The MPC-68F, in conjunction with the overpack containment system boundary, to meet the double barrier requirement of 10CFR71.63(b) for plutonium shipments.

Single Failure Proof means that the handling system is designed so that a single failure will not result in the loss of the capability of the system to safely retain the load.

SNF is an acronym for spent nuclear fuel.

STP is Standard Temperature (298°K) and Pressure (1 atm) conditions.

1.2 PACKAGE DESCRIPTION

1.2.1 Packaging

The HI-STAR 100 System consists of an MPC designed for BWR or PWR spent nuclear fuel, an overpack which provides the containment boundary and a set of impact limiters which provide energy absorption capability for the normal and hypothetical accident conditions of transport. Each of these components are described below, including information with respect to component fabrication techniques and designed safety features. This discussion is supplemented with a full set of Design Drawings and Bills-of-Material in Section 1.4. Section 1.3 provides the HI-STAR 100 design code applicability and details any exceptions to the codes.

Before proceeding to present detailed physical data on HI-STAR 100, it is contextual to summarize the design attributes which set it apart from the prior generation.

There are several features in the HI-STAR 100 System design which increase its effectiveness with respect to the safe transport of spent nuclear fuel (SNF). Some of the principal features of the HI-STAR 100 System which enhance its effectiveness are:

- the honeycomb design of the MPC fuel basket
- the effective distribution of neutron and gamma shielding materials within the system
- the high heat rejection capability
- the structural robustness of the multi-shell overpack construction

The honeycomb design of the MPC fuel baskets renders the basket into a multi-flange plate weldment where all structural elements (box walls) are arrayed in two orthogonal sets of plates. Consequently, the walls of the cells are either completely co-planar (no offset) or orthogonal with each other. There is complete edge-to-edge continuity between the contiguous cells.

Among the many benefits of the honeycomb construction is the uniform distribution of the metal mass over the body of the basket (in contrast to the "box and spacer disk" construction where the support plates are localized mass points). Physical reasoning suggests that a uniformly distributed mass provides a more effective shielding barrier than can be obtained from a nonuniform (box and spacer disk) basket. In other words, the honeycomb basket is a more effective radiation attenuation device.

The complete cell-to-cell connectivity inherent in the honeycomb basket structure provides an uninterrupted heat transmission path, making the HI-STAR 100 MPC an effective heat rejection device.

The multilayer shell construction in the overpack provides a natural barrier against crack propagation in the radial direction across the overpack structure. If, during a hypothetical accident (impact) event, a crack was initiated in one layer, the crack could not propagate to the adjacent layer. Additionally, it is highly unlikely that a crack would initiate as the thinner layers are more ductile than a thicker plate.

In this Safety Analysis Report the HI-STAR 100 System design is demonstrated to have predicted responses to accident conditions which are clearly acceptable with respect to certification requirements for post-accident containment system integrity, maintenance of subcriticality margin, dose rates, and adequate heat rejection capability. Table 1.2.18 presents a summary of the HI-STAR 100 System performance against these aspects of post-accident performance at two levels. At the first level, the integrity of the MPC boundary prevents release of radioactive material or helium from the MPC, and ingress of moderator. The integrity of the MPC is demonstrated by the analysis of the response of this high quality, ASME Code, Section III, Subsection NB-designed, pressure vessel to the accident loads while in the overpack. With this demonstration of integrity, the excellent performance results listed in the second column of Table 1.2.18 constitutes an acceptable basis for certification of the HI-STAR 100 System for the safe transport of intact fuel assemblies. However, no credit is taken for this additional basis for certification of the HI-STAR 100 System for the transport of intact fuel assemblies. Credit is only taken for the additional containment boundary of the MPC-68F for the transport of fuel assemblies classified as fuel debris.

The HI-STAR 100 System provides a large margin of safety. The third column in Table 1.2.18 summarizes the performance if the MPC is postulated to suffer gross failure, essentially an open top, in the post-accident analysis. Even with this postulated failure, the performance of the HI-STAR 100 System is acceptable for the transport of intact fuel assemblies, showing a clear basis for certification and the defense-in-depth methodology incorporated into the HI-STAR 100 System.

The containment boundary of the HI-STAR 100 System is shown to satisfy the special requirement of 10CFR71.61 for irradiated nuclear fuel shipments.

To meet the requirements of 10CFR71.63(b) for plutonium shipments, which is considered applicable for the transport of fuel assemblies classified as fuel debris, double containment is provided by the containment boundary of the overpack and the secondary containment boundary of the MPC-68F serving as the separate inner container.

1.2.1.1 Gross Weight

The gross weight of the HI-STAR 100 System depends on which of the MPCs are loaded into the HI-STAR 100 overpack for shipment. Table 1.2.1 summarizes the maximum calculated component weights for the HI-STAR 100 overpack, impact limiters, and each MPC loaded to maximum capacity with design basis SNF. The maximum gross transport weight of the HI-STAR 100 Packaging is to be marked on the regulatory label plate as shown on the Design Drawings in Section 1.4.

1.2.1.2 Materials of Construction, Dimensions and Fabrication

All materials utilized to construct the HI-STAR 100 System are ASME Code materials, except the neutron shield, neutron poison, heat conduction inserts, thermal expansion foam, seals, rupture disks, aluminum honeycomb, pipe couplings and other material classified as Not Important to Safety. The specified materials of construction along with the detailed dimensions are provided in the Design Drawings and Bills-of-Material in Section 1.4.

The materials of construction and method of fabrication are further detailed in the subsections that follow. Section 1.3 provides the codes applicable to the HI-STAR 100 packaging for materials, design, fabrication, and inspection.

1.2.1.2.1 HI-STAR 100 Overpack

The HI-STAR 100 overpack is a heavy-walled steel cylindrical vessel. A single overpack design is provided which is capable of transporting each type of MPC. The inner diameter of the overpack is approximately 68-3/4 inches and the height of the internal cavity is approximately 191-1/8 inches. The overpack inner cavity is sized to accommodate the MPCs. The outer diameter of the overpack is approximately 96 inches and the height is approximately 203-1/8 inches.

Figure 1.2.1 provides a cross sectional elevation view of the overpack containment boundary. The overpack containment boundary is formed by a steel inner shell welded at the bottom to a bottom plate and, at the top, to a heavy top flange with bolted closure plate. Two concentric grooves are machined into the closure plate for the seals. The closure plate is recessed into the top flange and the bolted joint is configured to protect the closure bolts and seals in the event of a drop accident. The closure plate has a vent port which is sealed by a threaded port plug with a seal. The bottom plate has a drain port which is sealed by a threaded port plug with a seal. The containment boundary forms an internal cylindrical cavity for housing the MPC.

The outer surface of the overpack inner shell is buttressed with intermediate shells of gamma shielding which are installed in a manner to ensure a permanent state of contact between adjacent

layers. Besides serving as an effective gamma shield, these layers provide additional strength to the overpack to resist puncture or penetration. Radial channels are vertically welded to the outside surface of the outermost intermediate shell at equal intervals around the circumference. These radial channels act as fins for improved heat conduction to the overpack outer enclosure shell surface and as cavities for retaining and protecting the neutron shielding. The enclosure shell is formed by welding enclosure shell panels between each of the channels to form additional cavities. Neutron shielding material is placed into each of the radial cavity segments formed by the radial channels, the outermost intermediate shell, and the enclosure shell panels. The exterior flats of the radial channels and the enclosure shell panels form the overpack outer enclosure shell (Figure 1.2.2). Atop the outer enclosure shell, rupture disks are positioned in a recessed area. The rupture disks relieve internal pressure which may develop as a result of the fire accident and subsequent off-gassing of the neutron shield material. Within each radial channel, a layer of silicone sponge is positioned to act as a thermal expansion foam to compress as the neutron shield expands. Appendix 1.C provides material information on the thermal expansion foam. Figure 1.2.2 contains a mid-plane cross section of the overpack depicting the inner shell, intermediate shells, radial channels, outer enclosure shell, and neutron shield.

The exposed steel surfaces (except seal seating surfaces) of the overpack and the intermediate shell layers are coated to prevent corrosion. The paints applied to the overpack exposed exterior and interior surfaces are specified on the design drawings; the material data on the paint is provided in Appendix 1.C. The inner cavity of the overpack is coated with a paint appropriate to its higher temperatures and the exterior of the overpack is coated with a paint appropriate for fuel pool operations and environmental exposure. The coating applied to the intermediate shells acts as a surface preservative and is not exposed to the fuel pool or ambient environment.

Lifting trunnions are attached to the overpack top flange for lifting and rotating the cask body between vertical and horizontal positions. The lifting trunnions are located 180° apart in the sides of the top flange. Pocket trunnions are welded to the lower side of the overpack to provide a pivoting axis for rotation. The pocket trunnions are located slightly off-center to ensure proper rotation direction of the overpack. As shown in Figure 1.1.4, the trunnions do not protrude beyond the cylindrical envelope of the overpack outer enclosure shell. This feature reduces the potential for a direct impact on a trunnion in the event of an overpack side impact.

1.2.1.2.2 Multi-Purpose Canisters

The HI-STAR 100 MPCs are welded cylindrical structures with flat ends. Each MPC is an assembly consisting of a honeycombed fuel basket, a baseplate, a canister shell, a lid with vent and drain ports and cover plates, and a closure ring. The outer diameter and cylindrical height of each MPC is fixed. However, the number of spent nuclear fuel storage locations in each of the MPCs depends on the fuel assembly characteristics. As the MPCs are interchangeable, they correspondingly have identical exterior dimensions. The outer diameter of the MPC is nominally

68-3/8 inches and the length is approximately 190-1/2 inches. Figures 1.2.3-1.2.5 depict the cross sectional views of the different MPCs. Detailed Design Drawings of the MPCs are provided in Section 1.4. Key operational and design parameters for the MPCs are outlined in Tables 1.2.2 and 1.2.3.

The construction features of the PWR MPC-24 and the BWR MPC-68 are similar. However, the PWR MPC-24 canister in Figure 1.2.5, which is designed for highly enriched PWR fuel, differs in construction in one important aspect: the fuel cells are physically separated from one another by a flux trap between each cell for criticality control. All MPC baskets are formed from an array of plates welded to each other, such that a honeycomb structure is created which resembles a multi-flanged, closed-section beam in its structural characteristics.

The MPC fuel basket is positioned and supported within the MPC shell by a basket support structure welded to the inside of the MPC shell. Between the periphery of the basket, the MPC shell, and the basket supports, heat conduction elements are installed. These heat conduction elements are fabricated from thin aluminum alloy 1100 in shapes and a design which allow a snug fit in the confined spaces and ease of installation. The heat conduction elements are installed along the full length of the MPC basket, except at the drain pipe location, to create a nonstructural thermal connection which facilitates heat transfer from the basket to shell. In their operating condition, the heat conduction elements will conform to and contact the MPC shell and basket walls.

Lifting lugs attached to the inside surface of the MPC canister shell serve to permit placement of the empty MPC into the overpack. The lifting lugs also serve to axially locate the MPC lid prior to welding. These internal lifting lugs are not used to handle a loaded MPC, since the MPC lid blocks access to the lifting lugs.

The top end of the HI-STAR 100 MPC incorporates a redundant closure system. Figure 1.2.6 provides a sketch of the MPC closure details. The MPC lid is a circular plate edge-welded to the MPC shell. This lid is equipped with vent and drain ports which are utilized to remove moisture and air from the MPC and backfill the MPC with a specified pressure of inert gas (helium). The vent and drain ports are sealed closed by cover plates welded to the MPC lid before the closure ring is installed. The closure ring is a circular ring edge-welded to the MPC shell and MPC lid. The MPC lid provides sufficient rigidity to allow the entire MPC loaded with SNF to be lifted by the threaded holes in the MPC lid. Threaded insert plugs are installed to provide shielding when the threaded holes are not in use.

All MPCs are designed to handle intact and damaged SNF and fuel debris in damaged fuel containers. However, at this time only the MPC-68 is being licensed to handle intact and damaged SNF/fuel debris. The definition and design basis characteristics for damaged fuel, fuel debris and intact SNF are provided in Subsection 1.2.3.

To distinguish an MPC-68 which is to transport fuel assemblies classified as fuel debris in damaged fuel containers, the MPC shall be designated as an "MPC-68F." The MPC-68F design to transport fuel debris is similar to the MPC-68 design to transport intact fuel and damaged fuel. The sole differences in the MPC-68F is a reduction in the required ^{10}B areal density in the Boral for the transport of fuel debris, an increase in the thickness of the MPC shell in the MPC lid region, a corresponding decrease in the outer diameter of the MPC lid and closure ring, and an increase in the MPC lid to shell weld size. A reduction in the required ^{10}B areal density of the Boral is possible due to limited enrichment permitted. The modification to the MPC closure design is specified to ensure that the MPC provides the inner containment boundary for the transportation of fuel assemblies classified as fuel debris. Therefore, an MPC-68 which is to transport fuel assemblies classified as fuel debris is designated with the unique nomenclature, MPC-68F.

Intact SNF can be placed directly into the MPC-68F. Damaged SNF and fuel debris must be placed into damaged fuel containers prior to insertion into the MPC-68F. Figures 1.2.10 and 1.2.11 provide sketches of damaged fuel containers.

The MPC-68F provides the separate inner container per 10CFR71.63(b) for the HI-STAR 100 System transporting fuel classified as fuel debris to ensure double containment. The overpack containment boundary provides the primary containment boundary.

The HI-STAR MPC is constructed entirely from stainless steel alloy materials (except for the neutron absorber and aluminum heat conduction elements). No carbon steel parts are used in the design of the HI-STAR 100 MPC. Concerns regarding interaction of coated carbon steel materials and various MPC operating environments [1.2.1] are not applicable to the HI-STAR MPCs. All structural components in a HI-STAR MPC will be fabricated of Alloy X, a designation which warrants further explanation.

Alloy X is a material which should be acceptable as a Mined Geological Depository System (MGDS) waste package and which meets the thermophysical properties set forth in this document.

At this time, there is considerable uncertainty with respect to the material of construction for an MPC which would be acceptable as a waste package for the MGDS. Candidate materials being considered for acceptability by the DOE include:

- Type 316
- Type 316LN
- Type 304
- Type 304LN

The DOE material selection process is primarily driven by corrosion resistance in the potential environment of the MGDS. As the decision regarding a suitable material to meet disposal

requirements is not imminent, this application requests approval for use of any one of the four Alloy X materials.

For the MPC design and analysis, Alloy X (as defined in this application) may be one of the following materials (only a single alloy from the list of acceptable Alloy X materials may be used in the fabrication of a single MPC):

- Type 316
- Type 316LN
- Type 304
- Type 304LN

The Alloy X approach is accomplished by qualifying the MPC for all mechanical, structural, neutronic, radiological, and thermal conditions using material thermophysical properties which are the least favorable for the entire group for the analysis in question. For example, when calculating the rate of heat rejection to the outside environment, the value of thermal conductivity used is the lowest for the candidate material group. Similarly, the stress analysis calculations use the lowest value of the ASME Code allowable stress intensity for the entire group. Stated differently, we have defined a material, which is referred to as Alloy X, whose thermophysical properties, from the MPC design perspective, are the least favorable of the candidate materials group.

The evaluation of the Alloy X constituents to determine the least favorable properties is provided in Appendix 1.A.

Other alloy materials which are identified to be more suitable by the DOE for the MGDS in the future and which are also bounded by the Alloy X properties set forth in Appendix 1.A can be used in the HI-STAR 100 MPC after an amendment to this SAR is approved.

The Alloy X approach is conservative because no matter which material is ultimately utilized, the Alloy X approach guarantees that the performance of the MPC will exceed the analytical predictions contained in this document.

1.2.1.3 Impact Limiters

The HI-STAR 100 overpack is fitted with aluminum honeycomb impact limiters, termed AL-STAR™, one at each end, once the overpack is positioned and secured in the transport frame. The impact limiters ensure the inertia loadings during the normal and hypothetical accident conditions of transport are maintained below design levels. The impact limiter design is discussed further in Chapter 2 and detailed drawings are provided in Section 1.4.

1.2.1.4 Shielding

The HI-STAR 100 System is provided with shielding to minimize personnel exposure. The HI-STAR 100 System will be transported by exclusive use shipment to ensure the external radiation requirements of 10CFR71.47 are met. During transport, a personnel barrier is installed to restrict access to the overpack to protect personnel from the HI-STAR 100 exterior surface temperature in accordance with 10CFR71.43(g). The personnel barrier provides a stand-off equal to the exterior radial dimension of the impact limiters. No credit for the stand-off distance provided by the barrier is taken in the shielding analyses. Figure 1.2.8 provides a sketch of the personnel barrier being installed.

The initial attenuation of gamma and neutron radiation emitted by the radioactive spent fuel is provided by the MPC fuel basket structure built from inter-welded plates and Boral neutron poison panels attached to the fuel cell walls. The MPC canister shell, baseplate, and lid provide additional thicknesses of steel to further reduce gamma radiation and, to a smaller extent, neutron radiation at the outer MPC surfaces.

The primary HI-STAR 100 shielding is located in the overpack and consists of neutron shielding and additional layers of steel for gamma shielding. Neutron shielding is provided around the outside circumferential surface of the overpack. Gamma shielding is provided by the overpack inner, intermediate and enclosure shells with additional axial shielding provided by the bottom plate and the top closure plate. During transport, the impact limiters will provide incremental gamma shielding and provide additional distance from the radiation source at the ends of the package. An additional circular segment of neutron shielding is contained within each impact limiter to provide neutron attenuation.

1.2.1.4.1 Boral Neutron Absorber

Boral is a thermal neutron poison material composed of boron carbide and aluminum alloy 1100. Boron carbide is a compound having a high boron content in a physically stable and chemically inert form. The boron carbide contained in Boral is a fine granulated powder that conforms to ASTM C-750-80 nuclear grade Type III. The aluminum alloy 1100 is a lightweight metal with high tensile strength which is protected from corrosion by a highly resistant oxide film. The two materials, boron carbide and aluminum, are chemically compatible and ideally suited for long-term use in the radiation, thermal, and chemical environment of a nuclear reactor, spent fuel pool, or dry cask.

The documented historical applications of Boral, in environments comparable to those in spent fuel pools and fuel storage casks, dates to the early 1950s (the U.S. Atomic Energy Commission's AE-6 Water-Boiler Reactor [1.2.2]). Technical data on the material was first printed in 1949, when the report "Boral: A New Thermal Neutron Shield" was published [1.2.3]. In 1956, the first edition of the *Reactor Shielding Design Manual* [1.2.4], contains a section on Boral and its properties.

In the research and test reactors built during the 1950s and 1960s, Boral was frequently the material of choice for control blades, thermal-column shutters, and other items requiring very good thermal-neutron absorption properties. It is in these reactors that Boral has seen its longest service in environments comparable to today's applications.

Boral found other uses in the 1960s, one of which was a neutron poison material in baskets used in the shipment of irradiated, enriched fuel rods from Canada's Chalk River laboratories to Savannah River. Use of Boral in shipping containers continues, with Boral serving as the poison in many cask designs.

As indicated in Tables 1.2.4-1.2.6, Boral has been licensed by the NRC for use in numerous BWR and PWR spent fuel storage racks and has been extensively used in international nuclear installations.

Boral has been exclusively used in fuel storage applications in recent years. Its use in spent fuel pools as the neutron absorbing material can be attributed to its proven performance and several unique characteristics, such as:

- The content and placement of boron carbide provides a very high removal cross section for thermal neutrons.
- Boron carbide, in the form of fine particles, is homogeneously dispersed throughout the central layer of the Boral panels.
- The boron carbide and aluminum materials in Boral do not degrade as a result of long-term exposure to radiation.
- The neutron absorbing central layer of Boral is clad with permanently bonded surfaces of aluminum.
- Boral is stable, strong, durable, and corrosion resistant.

Boral absorbs thermal neutrons without physical change or degradation of any sort from the anticipated exposure to gamma radiation and heat. The material does not suffer loss of neutron attenuation capability when exposed to high levels of radiation dose.

Holtec International's QA Program ensures that Boral is manufactured under the control and surveillance of a Quality Assurance/Quality Control Program that conforms to the requirements of 10CFR71, Subpart H and 10CFR72, Subpart G. Holtec International has procured over 200,000 panels of Boral from AAR Advanced Structures for over 20 projects. Boral has always been purchased with a minimum ^{10}B loading requirement. Coupons extracted from production runs were tested using the "wet chemistry" procedure. The actual ^{10}B loading, out of thousands of coupons tested, has *never* been found to fall below the design specification. The size of this coupon data base is sufficient to provide confidence that all future procurements will continue

to yield Boral with full compliance with the stipulated minimum loading. Furthermore, the surveillance, coupon testing, and material tracking processes which have so effectively controlled the quality of Boral are expected to continue to yield Boral of similar quality in the future. Nevertheless, to add another layer of insurance, only 75% ^{10}B credit of the fixed neutron absorber is assumed in the criticality analysis.

1.2.1.4.2 Holtite™ Neutron Shielding

The specification for the overpack and impact limiter neutron shield material is predicated on functional performance criteria. These criteria are:

- Attenuation of neutron radiation and associated neutron capture to appropriate levels;
- Durability of the shielding material under normal conditions, in terms of thermal, chemical, mechanical, and radiation environments;
- Stability of the homogeneous nature of the shielding material matrix;
- Stability of the shielding material in mechanical or thermal accident conditions to the desired performance levels; and
- Predictability of the manufacturing process under adequate procedural control to yield an in-place neutron shield of desired function and uniformity.

Other aspects of a shielding material, such as ease of handling and prior nuclear industry use, are also considered, within the limitations of the main criteria. Final specification of a shield material is a result of optimizing the material properties with respect to the main criteria, along with the design of the shield system, to achieve the desired shielding results.

In the current submittal, Holtite-A is the only approved neutron shield material which fulfills the aforementioned criteria. Holtite-A is a poured-in-place solid borated synthetic neutron-absorbing polymer. Holtite-A is a commercially available neutron shield under the trade name NS-4-FR and is specified with a nominal B_4C loading of 1 weight percent for the HI-STAR 100 System. Appendix 1.B provides the Holtite-A material properties. Holtec has performed confirmatory qualification tests on Holtite-A under the company's QA program.

In the following, a brief summary of the performance characteristics and properties of Holtite-A is provided.

Density

The specific gravity of Holtite-A is 1.68 g/cm^3 as specified in Appendix 1.B. To conservatively bound any potential weight loss at the design temperature and any inability to reach the theoretical density, the density is reduced by 4% to 1.61 g/cm^3 . The density used for the

shielding analysis is assumed to be 1.61 g/cm³ to underestimate the shielding capabilities of the neutron shield.

Hydrogen

The weight concentration of hydrogen is 6.0%. However, all shielding analyses conservatively assume 5.9% hydrogen by weight in the calculations.

Boron Carbide

Boron carbide dispersed within Holtite-A in finely dispersed powder form is present in 1% weight concentration. Holtite-A may be specified with a B₄C content of up to 6.5 weight percent. For the HI-STAR 100 System, Holtite-A is specified with a nominal B₄C weight percent of 1%.

Design Temperature

The design temperature of Holtite-A is set at 300°F. The maximum spatial temperature of Holtite-A under all normal operating conditions must be demonstrated to be below this design temperature.

Thermal Conductivity

It is evident from Figure 1.2.2 that Holtite-A is directly in the path of heat transmission from the inside of the overpack to its outside surface. For conservatism, however, the design basis thermal conductivity of Holtite-A under heat rejection conditions is set equal to zero. The reverse condition occurs under a postulated fire event when the thermal conductivity of Holtite-A aids in the influx of heat to the stored fuel in the fuel basket. The thermal conductivity of Holtite-A is conservatively set at 1 Btu/hr-ft-°F for all fire accident analyses.

The Holtite-A neutron shielding material is stable at normal design temperatures over the long term and provides excellent shielding properties for neutrons. Technical papers provided in Appendix 1.B validate the neutron shield material's long-term stability within the design temperature and the material's ability to resist the effects of a fire accident. Holtite-A has been utilized in similar applications and has been licensed for use in a transportation cask under Docket No. 71-9235.

1.2.1.4.3 Gamma Shielding Material

For gamma shielding, HI-STAR 100 utilizes carbon steel in plate stock form. Instead of utilizing a thick forging, the gamma shield design in the HI-STAR 100 overpack borrows from the concept of layered vessels from the field of ultra-high pressure vessel technology. The shielding is made from successive layers of plate stock. The fabrication of the shell begins by rolling the inner shell plate and making the longitudinal weld seam. Each layer of the intermediate shells is constructed from two halves. The two halves of the shell are precision sheared, beveled, and

rolled to the required radii. The two halves of the second layer are wrapped around the first shell. Each shell half is positioned in its location and while applying pressure using a specially engineered fixture, the halves are tack welded. The beveled edges to be joined will be positioned to make contact or have a slight gap. The second layer is made by joining the two halves using two longitudinal welds. Successive layers are assembled in a like manner. Thus, the welding of every successive shell provides a certain inter-layer contact (Figure 1.2.7). A thick structural component radiation barrier is thus constructed with four key features, namely:

- The number of layers can be increased as necessary to realize the required design objectives.
- The layered construction is ideal to stop propagation of flaws.
- The thinner plate stock is much more ductile than heavy forgings used in other designs.
- Post-weld heat treatment is not required by the ASME Code, simplifying fabrication.

1.2.1.5 Lifting and Tie-Down Devices

The HI-STAR 100 overpack is equipped with two lifting trunnions located in the top flange. The lifting trunnions are designed in accordance with 10CFR71.45, NUREG-0612 [1.2.11], and ANSI N14.6 [1.3.3], manufactured from a high strength alloy, and are installed in threaded openings. The lifting trunnions are secured in position by a locking pad, shaped to make conformal contact with the curved overpack. Once the locking pad is bolted in position, the inner diameter is sized to restrain the trunnion from backing out. The two off-center pockets located near the overpack bottom plate are pocket trunnions.

The lifting, upending, and downending of the HI-STAR 100 System requires the use of external handling devices. A lifting yoke is utilized when the cask is to be lifted or set in a vertical orientation. Transport and rotation cradles provide rotation trunnions which interface with the pocket trunnions to provide a pivot axis. A lift yoke is connected to the lifting trunnions and the crane hook is used for upending or downending the HI-STAR 100 System by rotating on the pocket trunnions.

The HI-STAR 100 System is engineered to be mounted on a transport frame secured to the transporter bed. Figure 1.2.8 provides a sketch of the HI-STAR 100 System secured for transport. The transport frame has a trunnion which engages the pocket trunnion of the overpack to allow upending or downending. This transport frame trunnion, also, secures the lower portion of the HI-STAR 100 packaging onto the transport vehicle by restricting the motion of the package. Securing the upper portion of the HI-STAR 100 packaging onto the transport vehicle is accommodated by the saddle of the transport frame interfacing with the shear ring on the overpack top flange. The shear ring is an integral part of the overpack top flange and is simply

a raised area of the top flange. The transport frame is designed to meet the applicable requirements specified by the American Association of Railroads and to satisfy the requirements of 10CFR71.45(b)(3) the ultimate load capacity of the tie-downs shall be shown to be less than the corresponding ultimate load capacities of either the shear ring or pocket trunnion.

The top of the MPC lid is equipped with four threaded holes that allow lifting of the loaded MPC. These holes allow the loaded MPC to be raised/lowered from the HI-STAR overpack. MPC handling operations are performed using a HI-TRAC transfer cask of the HI-STORM 100 System (Docket No. 72-1014). The HI-TRAC transfer cask allows the sealed MPC loaded with spent fuel to be transferred from the HI-STORM Overpack (storage-only) to the HI-STAR Overpack, or vice versa. The threaded holes in the MPC lid are designed in accordance with NUREG-0612 and ANSI N14.6.

1.2.1.6 Heat Dissipation

The HI-STAR 100 System can safely transport SNF by maintaining the fuel cladding temperature below the design limits specified in Table 1.2.3. The temperature of the fuel cladding is dependent on the decay heat and the heat dissipation capabilities of the cask. The total heat load per MPC in this licensing application is identified in Table 1.2.3. The SNF decay heat is passively dissipated without any mechanical or forced cooling.

The HI-STAR 100 System must meet the requirements of 10CFR71.43(g) for the accessible surface temperature limit. To meet this requirement the HI-STAR 100 System is shipped as an exclusive use shipment and includes an engineered personnel barrier during transport.

The primary heat transfer mechanisms in the HI-STAR 100 System are conduction and surface radiation.

The free volume of the MPC and the annulus between the external surface of the MPC and the inside surface of the overpack containment boundary are filled with 99.995% pure helium gas during the fuel loading operations. Table 1.2.3 specifies the helium fill pressure to be placed in the MPC internal cavity. Besides providing an inert dry atmosphere for the fuel cladding, the helium also provides conductive heat transfer across any gaps between the metal surfaces inside the MPC and in the annulus between the MPC and overpack containment boundary. Metal conduction transfers the heat throughout the MPC fuel basket, through the MPC heat conduction elements and shell, through the overpack inner shell, intermediate shells, steel radial connectors and finally, to the outer neutron shield enclosure shell. The most adverse temperature profiles and thermal gradients for the HI-STAR 100 System with each of the MPCs are discussed in detail in Chapter 3.

1.2.1.7 Coolants

There are no coolants utilized in the HI-STAR 100 System. As discussed in Subsection 1.2.1.6 above, helium is sealed within the MPC internal cavity. The annulus between the MPC outer surface and overpack containment boundary is also purged and filled with helium gas.

1.2.1.8 Pressure Relief Systems

No pressure relief system is provided on the HI-STAR 100 packaging containment boundary.

The sole pressure relief device is provided in the overpack outer enclosure (Figure 1.1.4). The overpack outer enclosure contains the neutron shield material. Normal loadings will not cause the rupture disks to open. The rupture disks are installed to relieve internal pressure in the neutron shield cavities caused by the fire accident. The overpack outer enclosure is not designed as a pressure vessel. Correspondingly, the rupture disks are designed to open at relatively low pressures as stated below.

Rupture disk location	Rupture pressure, psig
Overpack outer enclosure	30

1.2.1.9 Security Seal

The HI-STAR 100 packaging provides a security seal that while intact, provides evidence that the package has not been opened by unauthorized persons. When installed the impact limiters cover all penetrations into the HI-STAR 100 packaging containment boundary. Therefore, the security seal is placed to ensure that the impact limiters are not removed which thereby ensures that the package has not been opened. As shown on Drawing 1782, in Section 1.4, a security seal is provided on one impact limiter attachment bolt of the top and bottom impact limiter. A hole is provided in the head of the bolt and the impact limiter. Lockwire shall be threaded through the hole and joined with a security seal.

1.2.1.10 Design Life

The design life of the HI-STAR 100 System is 40 years. This is accomplished by using materials of construction with a long proven history in the nuclear industry and specifying materials known to withstand their operating environments with little to no degradation. A maintenance program, as specified in Chapter 8, is also implemented to ensure the HI-STAR 100 System will exceed its design life of 40 years. The design considerations that assure the HI-STAR 100 System performs as designed throughout the service life include the following:

HI-STAR Overpack

- Exposure to Environmental Effects
- Material Degradation
- Maintenance and Inspection Provisions

MPC

- Corrosion
- Structural Fatigue Effects
- Maintenance of Helium Atmosphere
- Allowable Fuel Cladding Temperatures
- Neutron Absorber Boron Depletion

1.2.2 Operational Features

Table 1.2.7 provides the sequence of basic operations necessary to load fuel and prepare the HI-STAR 100 System for transport. The detailed sequence of steps for transportation-related loading, unloading, and handling operations is provided in Chapter 7 and is supported by the Design Drawings in Section 1.4. A summary of the loading and unloading operations is provided below. Figures 1.2.9 and 1.2.16 provide a pictorial view of the loading and unloading operations, respectively.

Loading Operations

At the start of loading operations, the overpack is configured with the closure plate removed. The lift yoke is used to position the overpack in the designated preparation area or setdown area for overpack inspection and MPC insertion. The annulus is filled with plant demineralized water and an inflatable annulus seal is installed. The inflatable seal prevents contact between spent fuel pool water and the MPC shell reducing the possibility of contaminating the outer surfaces of the MPC. The MPC is then filled with spent fuel pool water or plant demineralized water. The overpack and MPC are lowered into the spent fuel pool for fuel loading using the lift yoke. Pre-selected assemblies are loaded into the MPC and a visual verification of the assembly identification is performed.

While still underwater, a thick shielding lid (the MPC lid) is installed. The lift yoke is remotely engaged to the overpack lifting trunnions and is used to lift the overpack close to the spent fuel pool surface. As an ALARA measure, dose rates are measured on the top of the overpack and MPC prior to removal from the pool to check for activated debris on the top surface. The MPC lift bolts (securing the MPC lid to the lift yoke) are removed. As the overpack is removed from the spent fuel pool, the lift yoke and overpack are sprayed with demineralized water to help remove contamination.

The overpack is removed from the pool and placed in the designated preparation area. The top surfaces of the MPC lid and the top flange of the overpack are decontaminated. The inflatable

annulus seal is removed, and an annulus shield is installed. The annulus shield provides additional personnel shielding at the top of the annulus and also prevents small items from being dropped into the annulus. Dose rates are measured to ensure that the dose rates are within expected values. The Automated Welding System (AWS) is installed. The MPC water level is lowered slightly and the MPC lid is seal-welded using the AWS. Liquid penetrant examinations are performed on the root and final passes and ultrasonic examination is also performed on the MPC lid-to-shell weld or in place of the ultrasonic examination the weld may be inspected by multiple-pass liquid penetrant examination. The water level is raised to the top of the MPC and the weld is hydrostatically tested. Then a small volume of the water is displaced with helium gas. The helium gas is used for leakage testing. A helium leakage rate test is performed on the MPC lid confinement weld (lid-to-shell) to verify weld integrity and to ensure that the leakage rates are within acceptance criteria. The MPC water is displaced from the MPC by blowing pressurized helium or nitrogen gas into the vent port of the MPC, thus displacing the water through the drain line.

The Vacuum Drying System (VDS) is connected to the MPC and is used to remove all residual water from the MPC in a stepped evacuation process. The stepped evacuation process is used to preclude the formation of ice in the MPC and VDS lines. The internal pressure is reduced and held for a duration to ensure that all liquid water has evaporated.

Following this dryness test, the VDS is disconnected, the Helium Backfill System (HBS) is attached, and the MPC is backfilled with a predetermined amount of helium gas. The helium backfill ensures adequate heat transfer, provides an inert atmosphere for fuel cladding integrity, and provides the means of future leakage rate testing of the MPC enclosure vessel boundary welds. Cover plates are installed and seal-welded over the MPC vent and drain ports with liquid penetrant examinations performed on the root and final passes. The cover plates are helium leakage tested to confirm that they meet the established leakage rate criteria.

The MPC closure ring is then placed on the MPC, aligned, tacked in place, and seal welded, providing redundant closure of the MPC enclosure vessel closure welds. Tack welds are visually examined, and the root and final welds are inspected using the liquid penetrant examination technique to ensure weld integrity. The annulus shield is removed and the remaining water in the annulus is drained. The AWS is removed. The MPC lid and accessible areas of the top of the MPC shell are smeared for removable contamination and overpack dose rates are measured. The overpack closure plate is installed and the bolts are torqued. The overpack annulus is dried using the VDS. The overpack annulus is backfilled with helium gas for heat transfer and seal testing. Concentric metallic seals in the overpack closure plate prevent the leakage of the helium gas from the annulus and provide the containment boundary to the release of radioactive materials. The seals on the overpack vent and drain port plugs are leak tested along with the overpack closure plate inner seal. Cover plates with metallic seals are installed over the overpack vent and drain ports to provide redundant closure of the overpack penetrations. A port plug with a metallic seal is installed in the overpack closure plate test port to provide fully-redundant closure of all overpack penetrations.

The overpack is surveyed for removable contamination and downended on the transport vehicle where the impact limiters are installed, the security seals are attached, and the personnel barrier is installed. The HI-STAR 100 packaging is then ready for transport.

Unloading Operations

The HI-STAR 100 System unloading procedures describe the general actions necessary to prepare the MPC for unloading, cool the stored fuel assemblies in the MPC, flood the MPC cavity, remove the lid welds, unload the spent fuel assemblies, and recover the overpack and empty MPC. Special precautions are outlined to ensure personnel safety during the unloading operations, and to prevent the risk of MPC overpressurization and thermal shock to the stored spent fuel assemblies.

After removing the impact limiters, the overpack and MPC are positioned in the designated preparation area. At the site's discretion, a gas sample is drawn from the overpack annulus and analyzed. The gas sample provides an indication of MPC enclosure vessel performance. The annulus is depressurized, the overpack closure plate is removed, and the annulus is filled with plant demineralized water. The annulus shield is installed to protect the annulus from debris produced from the lid removal process. Similarly, overpack top surfaces are covered with a protective fire-retarding blanket.

The Weld Removal System (WRS) is positioned on the MPC lid. The MPC closure ring is core drilled over the locations of the vent and drain port cover plates. Local ventilation is established around the MPC vent port and a hot tap is attached to the vent port cover plate. The hot tap allows access to the vent port cavity to determine if the coupling is leaking at a significant rate. If the coupling is leaking, the MPC is allowed to depressurize through the hot tap. Otherwise, the vent port cover plate weld is removed, the vent port cover plate is removed, and the MPC is vented using local ventilation. The drain port cover plate weld is removed. The MPC is cooled using a closed-loop heat exchanger to reduce the MPC internal temperature to allow water flooding. Following the fuel cool-down, the MPC is flooded with water. The WRS is positioned for MPC lid-to-MPC shell weld removal. The WRS is then removed with the MPC lid left in place.

The inflatable annulus seal is installed and pressurized. The MPC lid is rigged to the lift yoke and the lift yoke is engaged to overpack lifting trunnions. The overpack is placed in the spent fuel pool and the MPC lid is removed. All fuel assemblies are returned to the spent fuel storage racks and the MPC fuel cells are vacuumed to remove any assembly debris. The overpack and MPC are returned to the designated preparation area where the MPC water is pumped back into the spent fuel pool. The annulus water is drained and the MPC and overpack are decontaminated in preparation for re-utilization.

1.2.3 Contents of Package

The HI-STAR 100 packaging is classified as a Type B package under the requirements of 10CFR71. As the HI-STAR 100 System is designed to transport spent nuclear fuel, the maximum activity of the contents requires that the HI-STAR 100 packaging be classified as Category I in accordance with Regulatory Guide 7.11 [1.2.10].

1.2.3.1 Determination of Design Basis Fuel

The HI-STAR 100 is designed to transport most types of fuel assemblies generated in the commercial U.S. nuclear industry. Boiling-water reactor (BWR) fuel assemblies have been supplied by General Electric (GE), Siemens (SPC), Exxon Nuclear, ANF, UNC, ABB Combustion Engineering, Allis-Chalmers (AC) and Gulf Atomic. Pressurized-water reactor (PWR) fuel assemblies are generally supplied by Westinghouse, Babcock & Wilcox, ANF, and ABB Combustion Engineering. ANF, Exxon, and Siemens are historically the same manufacturing company under different ownership. Within this report, SPC is used to designate fuel manufactured by ANF, Exxon, or Siemens. Publications such as Refs. [1.2.6] and [1.2.7] provide a comprehensive description of fuel discharged from U.S. reactors. A central object in the design of the HI-STAR 100 System is to ensure that a majority of SNF discharged from the U.S. reactors can be transported in one of the MPCs.

The cell openings in the fuel basket have been sized to accommodate all BWR and PWR assemblies listed in Refs. [1.2.6] and [1.2.7], except as noted below. Similarly, the cavity length of the MPC has been set at a dimension which permits transportation of most types of PWR fuel assemblies and BWR fuel assemblies with or without fuel channels. The exceptions are as follows:

- The South Texas Units 1 & 2 SNF, and CE 16x16 System 80 SNF are too long to be accommodated in the available MPC cavity length.

In addition to satisfying the cross sectional and length compatibility, the active fuel region of the SNF must be enveloped in the axial direction by the neutron absorber located in the MPC fuel basket. Alignment of the neutron absorber with the active fuel region is ensured by the use of upper and lower fuel spacers suitably designed to support the bottom and restrain the top of the fuel assembly. The spacers axially position the SNF assembly such that its active fuel region is properly aligned with the neutron absorber in the fuel basket. Figure 1.2.15 provides a pictorial representation of the fuel spacers positioning the fuel assembly active fuel region. Both the upper and lower fuel spacers are designed to perform their function under normal and hypothetical accident conditions of transport.

In summary, the geometric compatibility of the SNF with the MPC designs does not require the definition of a design basis fuel assembly. This, however, is not the case for structural, containment, shielding, thermal-hydraulic, and criticality criteria. In fact, a particular fuel type in a category (PWR or BWR) may not control the cask design in all of the above-mentioned

criteria. To ensure that no SNF listed in Refs. [1.2.6] and [1.2.7] which is geometrically admissible in the HI-STAR MPC is precluded from loading, it is necessary to determine the governing fuel specification for each analysis criteria. To make the necessary determinations, potential candidate fuel assemblies for each qualification criteria were considered. Table 1.2.8 lists the PWR fuel assemblies evaluated. These fuel assemblies were evaluated to define the governing design criteria for PWR fuel. The BWR fuel assembly designs evaluated are listed in Table 1.2.9. Tables 1.2.10 and 1.2.11 provide the fuel characteristics determined to be acceptable for transport in the HI-STAR 100 System. Table 1.2.12 lists the BWR and PWR fuel assembly designs which are found to govern for three qualification criteria, namely reactivity, shielding, and decay heat generation. Substantiating results of analyses for the governing assembly types are presented in the respective chapters dealing with the specific qualification topic. Additional information on the design basis fuel definition is presented in the following subsections.

1.2.3.2 Design Payload for Intact Fuel

Intact fuel assemblies are defined as fuel assemblies without known or suspected cladding defects greater than pinhole leaks and hairline cracks, and which can be handled by normal means. The design payload for the HI-STAR 100 System is intact zircaloy clad fuel assemblies with the characteristics listed in Table 1.2.13 or intact stainless steel clad fuel assemblies with the characteristics listed in Table 1.2.19. The placement of a single stainless steel clad fuel assembly in an MPC necessitates that all fuel assemblies (stainless steel clad or zircaloy clad) stored in that MPC meet the maximum heat generation requirements for stainless steel clad fuel specified in Table 1.2.19. Stainless steel clad fuel assemblies can only be transported in the MPC-24 and MPC-68.

Fuel assemblies with missing pins cannot be classified as intact fuel unless dummy fuel pins, which occupy a volume equal to or greater than the original fuel pins, replace the missing pins prior to loading. Any intact fuel assembly which falls within the geometric, thermal, and nuclear limits established for the design basis intact fuel assembly can be safely transported in the HI-STAR 100 System.

The fuel characteristics specified in Tables 1.2.10 and 1.2.11 have been evaluated in this SAR and are acceptable for transport in the HI-STAR 100 System.

1.2.3.3 Design Payload for Damaged Fuel and Fuel Debris

Damaged fuel assemblies are defined as fuel assemblies with known or suspected cladding defects greater than pinhole leaks and hairline cracks, missing fuel rods that are not replaced with dummy fuel rods, or those that cannot be handled by normal means; however, there shall be no loose components. No loose fuel debris is allowed with the damaged fuel assembly.

Fuel debris is defined as fuel assemblies with known or suspected defects such as ruptured fuel rods, severed fuel rods, or loose fuel pellets. Fuel assemblies which cannot be handled by normal means due to fuel cladding damage are considered to be fuel debris.

To aid in loading and unloading, damaged fuel assemblies and fuel debris will be loaded into stainless steel damaged fuel containers (DFCs) provided with 250 x 250 fine mesh screens, prior to placement in the HI-STAR 100 System. The DFC design is illustrated in Figure 2.1.10 and the Design Drawings are provided in Section 1.4. This application requests approval of Dresden Unit 1 (UO₂ rods and MOX fuel rods) and Humboldt Bay fuel arrays (Assembly Classes 6x6A, 6x6B, 6x6C, 7x7A, and 8x8A) as damaged fuel assembly contents for transport in the MPC-68 and fuel debris as contents for transport in the MPC-68F.

The design characteristics bounding Dresden Unit 1 and Humboldt Bay SNF are given in Table 1.2.14. The placement of a single damaged fuel assembly in an MPC-68 or MPC-68F, or a single fuel debris damaged fuel container in an MPC-68F necessitates that all fuel assemblies (intact, damaged, or debris) placed in that MPC meet the maximum heat generation requirements specified in Table 1.2.14.

The fuel characteristics specified in Table 1.2.14 for Dresden 1 and Humboldt Bay fuel arrays have been evaluated in this SAR and are acceptable for transport as damaged fuel or fuel debris in the HI-STAR 100 System. Because of the long cooling time, small size, and low weight of spent fuel assemblies qualified as damaged fuel or fuel debris, the DFC and its contents are bounded by the structural, thermal, and shielding analyses performed for the intact BWR design basis fuel. Separate criticality analysis of the bounding fuel assembly for the damaged fuel and fuel debris has been performed in Chapter 6.

As fuel assemblies classified as fuel debris have significant cladding damage, no cladding integrity is assumed. To meet the double containment criteria of 10CFR71.63(b) for plutonium shipments, the MPC-68F provides the secondary containment boundary (separate inner container), while the overpack provides the primary containment boundary.

The fuel characteristics specified in Table 1.2.11 for the Dresden 1 and Humboldt Bay fuel arrays (Assembly Classes 6x6A, 6x6B, 6x6C, 7x7A, and 8x8A) have been evaluated in this SAR and are acceptable for transport as damaged fuel or fuel debris in the HI-STAR 100 System after being placed in a damaged fuel container.

1.2.3.4 Structural Payload Parameters

The main physical parameters of an SNF assembly applicable to the structural evaluation are the fuel assembly length, envelope (cross sectional dimensions), and weight. These parameters, which define the mechanical and structural design, are listed in Tables 1.2.13, 1.2.14, and 1.2.19. The centers of gravity reported in Chapter 2 are based on the maximum fuel assembly weight. Upper and lower fuel spacers (as appropriate) maintain the axial position of the fuel assembly within the MPC basket and, therefore, the location of the center of gravity. The upper and lower

spacers are designed to withstand normal and accident conditions of transport. An axial clearance of approximately 2 inches is provided to account for the irradiation and thermal growth of the fuel assemblies. The suggested upper and lower fuel spacer lengths are listed in Tables 1.2.16 and 1.2.17. In order to qualify for transport in the HI-STAR 100 MPC, the SNF must satisfy the physical parameters listed in Tables 1.2.13, 1.2.14, or 1.2.19.

1.2.3.5 Thermal Payload Parameters

The principal thermal design parameter for the fuel is the peak fuel cladding temperature limit, which is a function of the maximum heat generation rate per assembly and the decay heat removal capabilities of the HI-STAR 100 System. The maximum heat generation rate per assembly for the design basis fuel assembly is based on the fuel assembly type with the highest decay heat for a given enrichment, burnup, and cooling time. This decay heat design basis fuel is listed in Table 1.2.12. Section 5.2 describes the method used to determine the design basis fuel assembly type and calculate the decay heat load.

As can be seen in Table 3.3.7, the acceptable normal condition fuel cladding temperature limit decreases with increased cooling time. Therefore, the allowable decay heat load per fuel assembly must correspondingly decrease with increased fuel assembly cooling time. For example, the maximum decay heat load for 5-year cooled zircaloy clad BWR fuel in the MPC-68 is 272W, but for 10-year cooled zircaloy clad BWR fuel, the decay heat load is limited to 245W. To ensure the allowable fuel cladding temperature limits are not exceeded, Figure 1.2.12 specifies the allowable decay heat per assembly versus cooling time for zircaloy clad fuel in each MPC type. Tables 1.2.14 and 1.2.19 provide the maximum heat generation for damaged zircaloy clad fuel assemblies and stainless steel clad fuel assemblies, respectively. Any damaged fuel assembly or fuel assembly classified as fuel debris with a decay heat load equal to or less than the maximum value specified in Table 1.2.14 is acceptable for loading into the HI-STAR 100 System. Due to the conservative thermal assessment and the long cooling time of the damaged and stainless steel clad fuel, a reduction in decay heat load is not required as the cooling time increases beyond the minimum specified.

The specified decay heat load can be attained by varying burnups and cooling times. Table 1.2.20 provides the burnup and cooling time characteristics for intact zircaloy clad fuel which meet the thermal requirements for the MPC-24 and MPC-68. Any intact zircaloy clad fuel assembly with a burnup and cooling time combination in accordance with Table 1.2.20 is thermally acceptable for transport in the MPC-24 and MPC-68. Each burnup and cooling time combination produces a decay heat equal to or below the value specified in Figure 1.2.12 for the design basis fuel assembly type.

The fuel rod cladding temperature is also affected by other factors. A governing geometry which maximizes the impedance to the transmission of heat out of the fuel rods has been defined. The governing thermal parameters to ensure that the range of SNF discussed previously are bounded by the thermal analysis discussed in detail and specified in Chapter 3. By utilizing these bounding thermal parameters, the calculated peak fuel rod cladding temperatures are

conservative for the actual spent fuel assemblies, which are apt to have a higher thermal conductivity.

Finally, the axial variation in the heat emission rate in the design basis fuel is defined based on the axial burnup distribution. For this purpose, the data provided in Refs. [1.2.8] and [1.2.9] are utilized and summarized in Table 1.2.15 and Figures 1.2.13 and 1.2.14, for reference. These distributions are representative of fuel assemblies with the design burnup levels considered. These distributions are used for analysis only, and do not provide a criteria for fuel assembly acceptability for transport in the HI-STAR 100 System.

1.2.3.6 Radiological Payload Parameters

The principal radiological design criteria are the 10CFR71.47 and 10CFR71.51 radiation dose rate and release requirements for the HI-STAR 100 System. The radiation dose rate is directly affected by the gamma and neutron source terms of the SNF assembly.

The gamma and neutron sources are separate and are affected differently by enrichment, burnup, and cool time. It is recognized that, at a given burnup, the radiological source terms increase monotonically as the initial enrichment is reduced. The shielding design basis fuel assembly is, therefore, evaluated at the maximum burnup, minimum cooling time, and a conservative enrichment corresponding to the burnup. The shielding design basis intact fuel assembly thus bounds all other intact fuel assemblies.

The design basis dose rates can be met by a variety of burnup levels and cooling times. Tables 1.2.14 and 1.2.19 provide the burnup and cooling time values which meet the radiological source term requirements for BWR damaged fuel/fuel debris and intact stainless steel clad fuel, respectively. Table 1.2.20 provides the burnup and cooling time characteristics which satisfy the radiological source term requirements for intact zircaloy clad fuel in each MPC type.

Table 1.2.15 and Figures 1.2.13 and 1.2.14 provide the axial distribution for the radiological source term for PWR and BWR fuel assemblies based on the actual burnup distribution. The axial burnup distributions are representative of fuel assemblies with the design basis burnup levels considered. These distributions are used for analysis only, and do not provide criteria for fuel assembly acceptability for transport in the HI-STAR 100 System.

Thoria rods placed in Dresden Unit 1 Thoria Rod Canisters meeting the requirements of Table 1.2.21 and Dresden Unit 1 fuel assemblies with one Antimony-Beryllium neutron source have been qualified for transport. Up to one Dresden Unit 1 Thoria Rod Canister plus any combination of damaged fuel assemblies in damaged fuel containers and intact fuel, up to a total of 68 may be transported.

1.2.3.7 Criticality Payload Parameters

As discussed earlier, the MPC-68 features a basket without flux traps. In the MPC-68 basket, there is one panel of neutron absorber between two adjacent fuel assemblies. The MPC-24 employs a construction wherein two neighboring fuel assemblies are separated by two panels of neutron absorber with a water gap between them (flux trap construction). The MPC-24 flux trap basket can accept a much higher enrichment fuel than a non-flux trap basket. The maximum initial ^{235}U enrichment for the MPC-24 is specified by the fuel array type in Table 1.2.10.

The MPC-24 Boral ^{10}B areal density is specified at a minimum loading of 0.0267 g/cm^2 . The MPC-68 Boral ^{10}B areal density is specified at a minimum loading of 0.0372 g/cm^2 . The MPC-68F Boral ^{10}B areal density is specified at a minimum loading of 0.01 g/cm^2 .

For all MPCs, the ^{10}B loading areal density used for analysis is conservatively established at 75% of the minimum ^{10}B areal density to demonstrate that the reactivity under the most adverse accumulation of tolerances and biases is less than 0.95. The reduction in ^{10}B areal density credit meets NUREG-1536 [1.2.5] which requires a 25% reduction in ^{10}B areal density credit. A large body of sampling data accumulated by Holtec from thousands of manufactured Boral panels indicates the average ^{10}B areal densities to be approximately 15% greater than the specified minimum.

1.2.3.8 Summary of Design Criteria

An intact zircaloy fuel assembly is acceptable for transport in a HI-STAR 100 System if it fulfills the following criteria.

- a. It satisfies the physical parameter characteristics listed in Tables 1.2.10 or 1.2.11, and 1.2.13.
- b. Its initial enrichment is less than that indicated by Table 1.2.13 for the MPC in which it is intended to be transported.
- c. The period from discharge is greater than or equal to the minimum cooling time listed in Table 1.2.20 for the given burnup and minimum enrichment.
- d. The average burnup of the assembly is equal to or less than the burnup specified in Table 1.2.20 for the given cooling time and minimum enrichment.

A damaged fuel assembly shall be placed in a damaged fuel container and shall meet the characteristics specified in Table 1.2.14 for transport in the MPC-68. Fuel assemblies classified as fuel debris shall be placed in a damaged fuel container and shall meet the characteristics specified in Table 1.2.14 for transport in the MPC-68F.

Stainless steel clad fuel assemblies shall meet the characteristics specified in Table 1.2.19 for transport in the MPC-24 or MPC-68.

MOX BWR fuel assemblies shall meet the requirements of Tables 1.2.13 and 1.2.14 for intact and damaged fuel/fuel debris, respectively.

No control components in PWR fuel are to be included with the fuel assembly. Only zircaloy fuel channels may be transported with the BWR fuel assemblies in the HI-STAR 100 System.

Thoria rods placed in Dresden Unit 1 Thoria Rod Canisters meeting the requirements of Table 1.2.21 and Dresden Unit 1 fuel assemblies with one Antimony-Beryllium neutron source have been qualified for transport. Up to one Dresden Unit 1 Thoria Rod Canister plus any combination of damaged fuel assemblies in damaged fuel containers and intact fuel, up to a total of 68 may be transported.

Dresden Unit 1 fuel assemblies with one Antimony-Beryllium neutron source are authorized for loading in the MPC-68 or MPC-68F.

Table 1.2.1[†]
HI-STAR 100 SYSTEM MAXIMUM WEIGHT SUMMARY

MPC WEIGHT DATA

MPC/Type	Weight Empty (lb)	Weight Loaded w/Fuel ^{††} (lb)
MPC-24	39,667	79,987
MPC-68	39,641	87,241

OVERPACK WEIGHT DATA

Weight Empty (lb)	Weight w/MPC-24 Loaded w/Fuel ^{††} (lb)	Weight w/MPC-68 Loaded w/Fuel ^{††} (lb)
153,710	233,697	240,951

IMPACT LIMITER WEIGHT DATA

Top Assembly Weight (lb)	Bottom Assembly Weight (lb)
19,187	17,231

HI-STAR 100 SYSTEM WEIGHT DATA

HI-STAR Maximum Gross Weight for Transport ^{†††}	HI-STAR Maximum Lifted Weight on Crane Hook Over Fuel Pool ^{††††} (lb.)
277,369	253,060 (249,460 lbs. on the trunnions)

[†] All weights are calculated, except the fuel assembly weight. Weights are rounded to the nearest pound.

^{††} Fuel assembly weight is the maximum weight from Table 1.2.13.

^{†††} Maximum gross weight includes overpack, MPC, fuel^{††}, and impact limiters.

^{††††} Maximum lifted weight over fuel pool includes the overpack without the closure plate (145,726 lbs.), the heaviest MPC with fuel^{††} (87,241 lbs.), the water in the MPC and overpack (16,443), the lift yoke (3,600 lbs.), and the inflatable annulus seal (50 lbs.).

Table 1.2.2
KEY SYSTEM DATA FOR HI-STAR 100

PARAMETER	VALUE (Nominal)	
Types of MPCs in this SAR	3	1 for PWR 2 for BWR
	MPC-24	Up to 24 intact zircaloy or stainless steel clad PWR fuel assemblies
	MPC-68	Up to 68 intact zircaloy or stainless steel clad BWR fuel assemblies or damaged zircaloy clad fuel assemblies in damaged fuel containers within an MPC-68
	OR MPC-68F	or Up to 4 damaged fuel containers with zircaloy clad BWR fuel debris and the complement intact or damaged zircaloy clad BWR fuel assemblies within an MPC-68F.

Table 1.2.3
KEY PARAMETERS FOR HI-STAR 100 MULTI-PURPOSE CANISTERS

PARAMETER	PWR	BWR
Unloaded MPC weight (lb)	See Table 1.2.1	See Table 1.2.1
Minimum neutron absorber ¹⁰ B loading (g/cm ²)	0.0267 (MPC-24)	0.0372 (MPC-68) 0.01 (MPC-68F)
Pre-disposal service life (years)	40	40
Design temperature, max./min. (°F)	725 ^{°†} /-40 ^{°††}	725 ^{°†} /-40 ^{°††}
Design internal pressure (psig)		
Normal Conditions	100	100
Off-normal Conditions	100	100
Accident Conditions	125	125
Total heat load, max. (kW)	20.0 (MPC-24)	18.5 (MPC-68)
Maximum permissible peak fuel cladding temperature (°F)	See Table 3.3.7 (normal conditions) 1058° (accident conditions)	See Table 3.3.7 (normal conditions) 1058° (accident conditions)
MPC internal environment Helium filled (psig)	≥ 0 psig and ≤ 22.2	≥ 0 psig and ≤ 28.5
MPC external environment/overpack internal environment Helium filled initial pressure (psig, at STP)	10	10
Maximum permissible reactivity including all uncertainties and biases	<0.95	<0.95
End closure(s)	Welded	Welded
Fuel handling	Opening compatible with standard grapples	Opening compatible with standard grapples
Heat dissipation	Passive	Passive

† Maximum normal condition design temperature for the MPC fuel basket. A complete listing of design temperatures for all components is provided in Table 2.1.2.

†† Temperature based on minimum ambient temperature (10CFR71.71(c)(2)) and no fuel decay heat load.

TABLE 1.2.4
BORAL EXPERIENCE LIST
DOMESTIC PRESSURIZED WATER REACTORS

Plant	Utility
Donald C. Cook	Indiana & Michigan Electric
Indian Point 3	New York Power Authority
Maine Yankee	Maine Yankee Atomic Power
Salem 1,2	Public Service Electric and Gas
Sequoyah 1,2	Tennessee Valley Authority
Yankee Rowe	Yankee Atomic Power
Zion 1,2	Commonwealth Edison Company
Byron 1,2	Commonwealth Edison Company
Braidwood 1,2	Commonwealth Edison Company
Three Mile Island I	GPU Nuclear
Sequoyah (rerack)	Tennessee Valley Authority
D.C. Cook (rerack)	American Electric Power
Maine Yankee	Maine Yankee Atomic Power Company
Connecticut Yankee	Northeast Utilities Service Company
Salem Units 1 & 2 (rerack)	Public Service Electric & Gas Company

Table 1.2.5
BORAL EXPERIENCE LIST
DOMESTIC BOILING WATER REACTORS

Plant	Utility
Browns Ferry 1,2,3	Tennessee Valley Authority
Brunswick 1,2	Carolina Power & Light
Clinton	Illinois Power
Dresden 2,3	Commonwealth Edison Company
Duane Arnold Energy Center	Iowa Electric Light and Power
J.A. FitzPatrick	New York Power Authority
E.I. Hatch 1,2	Georgia Power Company
Hope Creek	Public Service Electric and Gas
Humboldt Bay	Pacific Gas and Electric Company
LaCrosse	Dairyland Power
Limerick 1,2	Philadelphia Electric Company
Monticello	Northern States Power
Peachbottom 2,3	Philadelphia Electric Company
Perry 1,2	Cleveland Electric Illuminating
Pilgrim	Boston Edison Company
Susquehanna 1,2	Pennsylvania Power & Light
Vermont Yankee	Vermont Yankee Atomic Power
Hope Creek	Public Service Electric and Gas Company
Shearon Harris Pool B	Carolina Power & Light Company
Duane Arnold	Iowa Electric Light and Power
Pilgrim	Boston Edison Company
LaSalle Unit 1	Commonwealth Edison Company
Millstone Point Unit One	Northeast Utilities Service Company

Table 1.2.6

BORAL EXPERIENCE LIST
FOREIGN PLANTS

INTERNATIONAL INSTALLATIONS USING BORAL	
COUNTRY	PLANT(S)
France	12 PWR Plants
South Africa	Koeberg 1,2
Switzerland	Beznau 1,2 Gosgen
Taiwan	Chin-Shan 1,2 Kuosheng 1,2
Mexico	Laguna Verde Units 1,2
Korea	Ulchin Unit One
Brazil	Angra Unit One
United Kingdom	Sizewell B
Korea	Ulchin Unit 2

Table 1.2.7

HI-STAR 100 LOADING OPERATIONS DESCRIPTION

Site-specific handling and operating procedures will be prepared, reviewed, and approved by each owner/user.	
1	Overpack and MPC lowered into the fuel pool without closure plate and MPC lid
2	Fuel assemblies transferred to the MPC fuel basket
3	MPC lid lowered onto the MPC
4	Overpack/MPC assembly moved to the decon pit and MPC lid welded in place, examined, hydrostatically tested, and leak tested
5	MPC dewatered, vacuum dried, backfilled with helium, and the vent/drain port cover plates and closure ring welded
6	Overpack drained and external surfaces decontaminated
7	Overpack seals and closure plate installed and bolts pre-tensioned
8	Overpack cavity dried, backfilled with helium, and helium leak tested
9	HI-STAR 100 System transferred to transport bay
10	HI-STAR 100 placed onto transport saddles, tied down, impact limiters and personnel barrier installed, and package surveyed for release for transport.

Table 1.2.8

PWR FUEL ASSEMBLIES EVALUATED TO DETERMINE DESIGN BASIS SNF

Assembly Class	Array Type
B&W 15x15	All
B&W 17x17	All
CE 14x14	All
CE 16x16	All
WE 14x14	All
WE 15x15	All
WE 17x17	All
St. Lucie	All
Ft. Calhoun	All
Haddam Neck (Stainless Steel Clad)	All
San Onofre 1 (Stainless Steel Clad, except MOX)	All

Table 1.2.9

BWR FUEL ASSEMBLIES EVALUATED TO DETERMINE DESIGN BASIS SNF

Assembly Class	Array Type			
GE BWR/2-3	All 7x7	All 8x8	All 9x9	All 10x10
GE BWR/4-6	All 7x7	All 8x8	All 9x9	All 10x10
Humboldt Bay	All 6x6	All 7x7 (Zircaloy Clad)		
Dresden-1	All 6x6	All 8x8		
LaCrosse (Stainless Steel Clad)	All			

Table 1.2.10
PWR FUEL ASSEMBLY CHARACTERISTICS (note 1)

Fuel Assembly Array/Class	14x14 A	14x14 B	14x14 C	14x14 D	15x15 A
Clad Material (note 2)	Zr	Zr	Zr	SS	Zr
Design Initial U (kg/assy.) (Note 5)	≤ 407	≤ 407	≤ 425	≤ 400	≤ 464
Initial Enrichment (wt % ²³⁵ U)	≤ 4.6	≤ 4.6	≤ 4.6	≤ 4.0	≤ 4.1
No. of Fuel Rods	179	179	176	180	204
Clad O.D. (in.)	≥ 0.400	≥ 0.417	≥ 0.440	≥ 0.422	≥ 0.418
Clad I.D. (in.)	≤ 0.3514	≤ 0.3734	≤ 0.3880	≤ 0.3890	≤ 0.3660
Pellet Dia. (in.)	≤ 0.3444	≤ 0.3659	≤ 0.3805	≤ 0.3835	≤ 0.3580
Fuel Rod Pitch (in.)	0.556	0.556	0.580	0.556	0.550
Active Fuel Length (in.)	≤ 150	≤ 150	≤ 150	≤ 144	≤ 150
No. of Guide Tubes	17	17	5 (see note 3)	16	21
Guide Tube Thickness (in.)	≥ 0.017	≥ 0.017	≥ 0.038	≥ 0.0145	≥ 0.0165

- Notes:
1. All dimensions are design nominal values. Maximum and minimum dimensions are specified to bound variations in design nominal values among fuel assemblies within a given array/class.
 2. Zr designates cladding material made of Zirconium or Zirconium alloys.
 3. Each guide tube replaces four fuel rods.
 4. Description of the fuel assembly class designation is provided in Chapter 6.
 5. Design initial uranium weight is the uranium weight specified for each assembly by the fuel manufacturer or reactor user. For each PWR fuel assembly, the total uranium weight limit specified in this table may be increased up to 2.0 percent for comparison with users' fuel records to account for manufacturer's tolerances.

Table 1.2.10 (continued)
PWR FUEL ASSEMBLY CHARACTERISTICS (note 1)

Fuel Assembly Array/Class	15x15 B	15x15 C	15x15 D	15x15 E	15x15 F
Clad Material (note 2)	Zr	Zr	Zr	Zr	Zr
Design Initial U (kg/assy.) (Note 4)	≤ 464	≤ 464	≤ 475	≤ 475	≤ 475
Initial Enrichment (wt % ²³⁵ U)	≤ 4.1	≤ 4.1	≤ 4.1	≤ 4.1	≤ 4.1
No. of Fuel Rods	204	204	208	208	208
Clad O.D. (in.)	≥ 0.420	≥ 0.417	≥ 0.430	≥ 0.428	≥ 0.428
Clad I.D. (in.)	≤ 0.3736	≤ 0.3640	≤ 0.3800	≤ 0.3790	≤ 0.3820
Pellet Dia. (in.)	≤ 0.3671	≤ 0.3570	≤ 0.3735	≤ 0.3707	≤ 0.3742
Fuel Rod Pitch (in.)	0.563	0.563	0.568	0.568	0.568
Active Fuel Length (in.)	≤ 150	≤ 150	≤ 150	≤ 150	≤ 150
No. of Guide Tubes	21	21	17	17	17
Guide Tube Thickness (in.)	≥ 0.015	≥ 0.0165	≥ 0.0150	≥ 0.0140	≥ 0.0140

- Notes:
1. All Dimensions are design nominal values. Maximum and minimum dimensions are specified to bound variations in design nominal values among fuel assemblies within a given array/class.
 2. Zr designates cladding material made of Zirconium or Zirconium alloys.
 3. Description of the fuel assembly class designation is provided in Chapter 6.
 4. Design initial uranium weight is the uranium weight specified for each assembly by the fuel manufacturer or reactor user. For each PWR fuel assembly, the total uranium weight limit specified in this table may be increased up to 2.0 percent for comparison with users' fuel records to account for manufacturer's tolerances.

Table 1.2.10 (continued)
PWR FUEL ASSEMBLY CHARACTERISTICS (note 1)

Fuel Assembly Array/Class	15x15 G	15x15H	16x16 A	17x17A	17x17 B	17x17 C
Clad Material (note 2)	SS	Zr	Zr	Zr	Zr	Zr
Design Initial U (kg/assy.) (Note 5)	≤ 420	≤ 475	≤ 443	≤ 467	≤ 467	≤ 474
Initial Enrichment (wt % ²³⁵ U)	≤ 4.0	≤ 3.8	≤ 4.6	≤ 4.0	≤ 4.0	≤ 4.0
No. of Fuel Rods	204	208	236	264	264	264
Clad O.D. (in.)	≥ 0.422	≥ 0.414	≥ 0.382	≥ 0.360	≥ 0.372	≥ 0.377
Clad I.D. (in.)	≤ 0.3890	≤ 0.3700	≤ 0.3320	≤ 0.3150	≤ 0.3310	≤ 0.3330
Pellet Dia. (in.)	≤ 0.3825	≤ 0.3622	≤ 0.3255	≤ 0.3088	≤ 0.3232	≤ 0.3252
Fuel Rod Pitch (in.)	0.563	0.568	0.506	0.496	0.496	0.502
Active Fuel Length (in.)	≤ 144	≤ 150	≤ 150	≤ 150	≤ 150	≤ 150
No. of Guide Tubes	21	17	5 (note 3)	25	25	25
Guide Tube Thickness (in.)	≥ 0.0145	≥ 0.0140	≥ 0.0400	≥ 0.016	≥ 0.014	≥ 0.020

- Notes:
1. All dimensions are design nominal values. Actual uranium weights may be higher, within the manufacturer's tolerance. Maximum and minimum dimensions are specified to bound variations in design nominal values among fuel assemblies within a given array/class.
 2. Zr designates cladding material made of Zirconium or Zirconium alloys.
 3. Each guide tube replaces four fuel rods.
 4. Description of the fuel assembly class designation is provided in Chapter 6.
 5. Design initial uranium weight is the uranium weight specified for each assembly by the fuel manufacturer or reactor user. For each PWR fuel assembly, the total uranium weight limit specified in this table may be increased up to 2.0 percent for comparison with users' fuel records to account for manufacturer's tolerances.

Table 1.2.11
BWR FUEL ASSEMBLY CHARACTERISTICS (note 1)

Fuel Assembly Array/Class	6x6 A	6x6 B	6x6 C	7x7 A	7x7 B	8x8 A
Clad Material (note 2)	Zr	Zr	Zr	Zr	Zr	Zr
Design Initial U (kg/assy.) (Note 5)	≤ 110	≤ 110	≤ 110	≤ 100	≤ 195	≤ 120
Maximum Planar-Average Initial Enrichment (wt % ²³⁵ U)	≤ 2.7	≤ 2.7 for the UO ₂ rods. See Note 3 for MOX rods.	≤ 2.7	≤ 2.7	≤ 4.2	≤ 2.7
Initial Maximum Rod Enrichment (wt % ²³⁵ U)	≤ 4.0	≤ 4.0	≤ 4.0	≤ 4.0	≤ 5.0	≤ 4.0
No. of Fuel Rods	35 or 36	35 or 36 (up to 9 MOX rods)	36	49	49	63 or 64
Clad O.D. (in.)	≥ 0.5550	≥ 0.5625	≥ 0.5630	≥ 0.4860	≥ 0.5630	≥ 0.4120
Clad I.D. (in.)	≤ 0.5105	≤ 0.4945	≤ 0.4990	≤ 0.4204	≤ 0.4990	≤ 0.3620
Pellet Dia. (in.)	≤ 0.4980	≤ 0.4820	≤ 0.4880	≤ 0.4110	≤ 0.4910	≤ 0.3580
Fuel Rod Pitch (in.)	0.710	0.710	0.740	0.631	0.738	0.523
Active Fuel Length (in.)	≤ 120	≤ 120	≤ 77.5	≤ 80	≤ 150	≤ 120
No. of Water Rods (note 6)	1 or 0	1 or 0	0	0	0	1 or 0
Water Rod Thickness (in.)	> 0	> 0	N/A	N/A	N/A	N/A
Channel Thickness (in.)	≤ 0.060	≤ 0.060	≤ 0.060	≤ 0.060	≤ 0.120	≤ 0.100

- Notes:
1. Initial uranium weights and all dimensions are design nominal values. Actual uranium weights may be higher, within the manufacturer's tolerance. Maximum and minimum dimensions are specified to bound variations in design nominal values among fuel assemblies within a given array/class.
 2. Zr designates cladding material made of Zirconium or Zirconium alloys.
 3. ≤ 0.635 wt. % ²³⁵U and ≤ 1.578 wt. % total fissile plutonium (²³⁹Pu and ²⁴¹Pu), (wt. % of total fuel weight, i.e., UO₂ plus PuO₂).
 4. Description of the fuel assembly class designation is provided in Chapter 6.
 5. Design initial uranium weight is the uranium weight specified for each assembly by the fuel manufacturer or reactor user. For each BWR fuel assembly, the total uranium weight limit specified in this table may be increased up to 1.5 percent for comparison with users' fuel records to account for manufacturer's tolerances.
 6. These rods may be seal at both ends and contain Zr in lieu of water.

Table 1.2.11 (continued)
BWR FUEL ASSEMBLY CHARACTERISTICS (note 1)

Fuel Assembly Array/Class	8x8 B	8x8 C	8x8 D	8x8 E	8x8F	9x9 A
Clad Material (note 2)	Zr	Zr	Zr	Zr	Zr	Zr
Design Initial U (kg/assy.) (Note 7)	≤ 185	≤ 185	≤ 185	≤ 185	≤ 185	≤ 177
Maximum Planar-Average Initial Enrichment (wt % ²³⁵ U)	≤ 4.2	≤ 4.2	≤ 4.2	≤ 4.2	≤ 3.6	≤ 4.2
Initial Maximum Rod Enrichment (wt % ²³⁵ U)	≤ 5.0	≤ 5.0	≤ 5.0	≤ 5.0	≤ 5.0	≤ 5.0
No. of Fuel Rods	63 or 64	62	60 or 61	59	64	74/66 (note 3)
Clad O.D. (in.)	≥ 0.4840	≥ 0.4830	≥ 0.4830	≥ 0.4930	≥ 0.4576	≥ 0.4400
Clad I.D. (in.)	≤ 0.4295	≤ 0.4250	≤ 0.4230	≤ 0.4250	≤ 0.3996	≤ 0.3840
Pellet Dia. (in.)	≤ 0.4195	≤ 0.4160	≤ 0.4140	≤ 0.4160	≤ 0.3913	≤ 0.3760
Fuel Rod Pitch (in.)	≤ 0.642	≤ 0.641	0.640	0.640	≤ 0.609	0.566
Design Active Fuel Length (in.)	≤ 150	≤ 150	≤ 150	≤ 150	≤ 150	≤ 150
No. of Water Rods (note 9)	1	2	1 - 4 (note 5)	5	N/A (note 8)	2
Water Rod Thickness (in.)	≥ 0.034	> 0.00	> 0.00	≥ 0.034	≥ 0.0315	> 0.00
Channel Thickness (in.)	≤ 0.120	≤ 0.120	≤ 0.120	≤ 0.100	≤ 0.055	≤ 0.120

- Notes:
1. All dimensions are design nominal values. Actual uranium weights may be higher, within the manufacturer's tolerance. Maximum and minimum dimensions are specified to bound variations in design nominal values among fuel assemblies within a given array/class.
 2. Zr designates cladding material made of Zirconium or Zirconium alloys.
 3. This assembly class contains 74 total rods; 66 full length rods and 8 partial length rods.
 4. Square, replacing nine fuel rods.
 5. Variable.
 6. Description of the fuel assembly class designation is provided in Chapter 6.
 7. Design initial uranium weight is the uranium weight specified for each assembly by the fuel manufacturer or reactor user. For each BWR fuel assembly, the total uranium weight limit specified in this table may be increased up to 1.5 percent for comparison with users' fuel records to account for manufacturer's tolerances.
 8. This assembly is known as "QUAD+." It has four rectangular water cross-segments dividing the assembly into four quadrants.
 9. These rods may be seal at both ends and contain Zr in lieu of water.

Table 1.2.11 (continued)
BWR FUEL ASSEMBLY CHARACTERISTICS (note 1)

Fuel Assembly Array/Class	9x9 B	9x9 C	9x9 D	9x9 E (Note 7)	9x9 F (Note 7)
Clad Material (note 2)	Zr	Zr	Zr	Zr	Zr
Design Initial U (kg/assy.) (Note 5)	≤ 177	≤ 177	≤ 177	≤ 177	≤ 177
Maximum Planar-Average Initial Enrichment (wt % ²³⁵ U)	≤ 4.2	≤ 4.2	≤ 4.2	≤ 4.2	≤ 4.2
Initial Maximum Rod Enrichment (wt % ²³⁵ U)	≤ 5.0	≤ 5.0	≤ 5.0	≤ 5.0	≤ 5.0
No. of Fuel Rods	72	80	79	76	76
Clad O.D. (in.)	≥ 0.4330	≥ 0.4230	≥ 0.4240	≥ 0.4170	≥ 0.4430
Clad I.D. (in.)	≤ 0.3810	≤ 0.3640	≤ 0.3640	≤ 0.3640	≤ 0.3860
Pellet Dia. (in.)	≤ 0.3740	≤ 0.3565	≤ 0.3565	≤ 0.3530	≤ 0.3745
Fuel Rod Pitch (in.)	≤ 0.572	0.572	0.572	0.572	0.572
Design Active Fuel Length (in.)	≤ 150	≤ 150	≤ 150	≤ 150	≤ 150
No. of Water Rods (note 6)	1 (note 4)	1	2	5	5
Water Rod Thickness (in.)	> 0.00	≥ 0.020	≥ 0.0300	≥ 0.0120	≥ 0.0120
Channel Thickness (in.)	≤ 0.120	≤ 0.100	≤ 0.100	≤ 0.120	≤ 0.120

- Notes:
1. Initial uranium weights and all dimensions are design nominal values. Actual uranium weights may be higher, within the manufacturer's tolerance. Maximum and minimum dimensions are specified to bound variations in design nominal values among fuel assemblies within a given array/class.
 2. Zr designates cladding material made of Zirconium or Zirconium alloys.
 3. This assembly class contains 92 total fuel rods; 78 full length rods and 14 partial length rods.
 4. Description of the fuel assembly class designation is provided in Chapter 6.
 5. Design initial uranium weight is the uranium weight specified for each assembly by the fuel manufacturer or reactor user. For each BWR fuel assembly, the total uranium weight limit specified in this table may be increased up to 1.5 percent for comparison with users' fuel records to account for manufacturer's tolerances.
 6. These rods may be seal at both ends and contain Zr in lieu of water.
 7. For the SPC 9x9-5 fuel assembly, each fuel rod must meet either the 9x9E or 9x9F set of limits for clad O.D., clad I.D., and pellet diameter.

Table 1.2.11 (continued)
BWR FUEL ASSEMBLY CHARACTERISTICS (note 1)

Fuel Assembly Array/Class	10x10 A	10x10 B	10x10 C	10x10 D	10x10 E
Clad Material (note 2)	Zr	Zr	Zr	SS	SS
Design Initial U (kg/assy.) (Note 7)	≤ 186	≤ 186	≤ 186	≤ 125	≤ 125
Maximum Planar-Average Initial Enrichment (wt % ²³⁵ U)	≤ 4.2	≤ 4.2	≤ 4.2	≤ 4.0	≤ 4.0
Initial Maximum Rod Enrichment (wt % ²³⁵ U)	≤ 5.0	≤ 5.0	≤ 5.0	≤ 5.0	≤ 5.0
No. of Fuel Rods	92/78 (note 3)	91/83 (note 3)	96	100	96
Clad O.D. (in.)	≥ 0.4040	≥ 0.3957	≥ 0.3780	≥ 0.3960	≥ 0.3940
Clad I.D. (in.)	≤ 0.3520	≤ 0.3480	≤ 0.3294	≤ 0.3560	≤ 0.3500
Pellet Dia. (in.)	≤ 0.3455	≤ 0.3420	≤ 0.3224	≤ 0.3500	≤ 0.3430
Fuel Rod Pitch (in.)	0.510	0.510	0.488	0.565	0.557
Design Active Fuel Length (in.)	≤ 150	≤ 150	≤ 150	≤ 83	≤ 83
No. of Water Rods (note 8)	2	1 (Note 4)	5 (Note 5)	0	4
Water Rod Thickness (in.)	≥ 0.030	> 0.00	≥ 0.031	N/A	≥ 0.022
Channel Thickness (in.)	≤ 0.120	≤ 0.120	≤ 0.055	≤ 0.080	≤ 0.080

- Notes:
1. Initial uranium weights and all dimensions are design nominal values. Actual uranium weights may be higher, within the manufacturer's tolerance. Maximum and minimum dimensions are specified to bound variations in design nominal values among fuel assemblies within a given array/class.
 2. Zr designates cladding material made of Zirconium or Zirconium alloys.
 3. This assembly class contains 91 total fuel rods; 83 full length rods and 8 partial length rods.
 4. Square, replacing nine fuel rods.
 5. One diamond shaped water rod replacing the four center fuel rods and four rectangular water rods dividing the assembly into four quadrants.
 6. Description of the fuel assembly class designation is provided in Chapter 6.
 7. Design initial uranium weight is the uranium weight specified for each assembly by the fuel manufacturer or reactor user. For each BWR fuel assembly, the total uranium weight limit specified in this table may be increased up to 1.5 percent for comparison with users' fuel records to account for manufacturer's tolerances.
 8. These rods may be seal at both ends and contain Zr in lieu of water.

Table 1.2.12

DESIGN BASIS FUEL ASSEMBLY FOR EACH DESIGN CRITERION

Criterion	MPC-68	MPC-24
Reactivity	GE12/14 10x10 with Partial Length Rods (Class 10x10A)	B&W 15x15 (Class 15x15F)
Shielding (Source Term)	GE 12/14 10x10 (Class 10x10A)	B&W 15x15 (Class 15x15F)
Decay Heat	GE 12/14 10x10 (Class 10x10A)	B&W 15x15 (Class 15x15F)

Table 1.2.13
CHARACTERISTICS FOR DESIGN BASIS INTACT ZIRCALOY CLAD FUEL ASSEMBLIES

	MPC-68	MPC-24
PHYSICAL PARAMETERS:		
Max. assembly width [†] (in.)	5.85	8.54
Max. assembly length [†] (in.)	176.2	176.8
Max. assembly weight ^{††} (lb.)	700	1680
Max. active fuel length [†] (in.)	150	150
Fuel rod clad material	Zircaloy	Zircaloy
RADIOLOGICAL AND THERMAL CHARACTERISTICS:		
	MPC-68	MPC-24
Max. initial enrichment (w/o ²³⁵ U)	Table 1.2.11	Table 1.2.10
Max. heat generation (W)	Figure 1.2.12 115 (Assembly Classes 6x6A, 6x6B, 6x6C, 7x7A, 8x8A) 183.5 (Assembly Array/Class 8x8F)	Figure 1.2.12
Min. cooling time (years)	Table 1.2.20 18 (Assembly Classes 6x6A, 6x6B, 6x6C, 7x7A, 8x8A) 10 (Assembly Array/Class 8x8F)	Table 1.2.20
Max. average burnup (MWD/MTU)	Table 1.2.20 30,000 (Assembly Classes 6x6A, 6x6B, 6x6C, 7x7A, 8x8A) 27,500 (Assembly Array/Class 8x8F)	Table 1.2.20
Min. initial enrichment (w/o ²³⁵ U)	Table 1.2.20 1.8 (Assembly Classes 6x6A, 6x6B, 6x6C, 7x7A, 8x8A)	Table 1.2.20

[†] Unirradiated design dimensions are shown.

^{††} Fuel assembly weight including hardware based on DOE MPC DPS [1.1.1].

Table 1.2.14

DESIGN CHARACTERISTICS FOR DAMAGED ZIRCALOY CLAD FUEL ASSEMBLIES

	MPC-68 (Damaged Fuel)	MPC-68F (Fuel Debris)
PHYSICAL PARAMETERS:		
Max. assembly width [†] (in.)	4.7	4.7
Max. assembly length [†] (in.)	135	135
Max. assembly weight ^{††} (lb.)	400	400
Max. active fuel length [†] (in.)	120	120
Fuel rod clad material	Zircaloy	Zircaloy
Boral minimum ¹⁰ B areal density (g/cm ²)	0.0372	0.01
THERMAL CHARACTERISTICS:		
Max. heat generation (W)	115	115
Min. cooling time (yr)	18	18
RADIOLOGICAL CHARACTERISTICS:		
Max. initial enrichment (w/o ²³⁵ U)	2.7	2.7
Max. burnup (MWD/MTU)	30,000	30,000
Max. initial enrichment for MOX rods	0.635 wt.% ²³⁵ U 1.578 wt.% Total Fissile Plutonium	0.635 wt.% ²³⁵ U 1.578 wt.% Total Fissile Plutonium
Min. initial enrichment (w/o ²³⁵ U)	1.8	1.8

Note:

1. A maximum of four (4) damaged fuel containers with BWR zircaloy clad fuel debris may be stored in the MPC-68F with the remaining locations filled with undamaged or damaged fuel assemblies meeting the maximum heat generation specifications of this table.

[†] Dimensions envelop Dresden Unit 1 and Humboldt Bay SNF.

^{††} Fuel assembly weight including hardware based on DOE MPC DPS [1.1.1].

Table 1.2.15
NORMALIZED DISTRIBUTION BASED ON BURNUP PROFILE

PWR DISTRIBUTION[†]		
Interval	Axial Distance From Bottom of Active Fuel (% of Active Fuel Length)	Normalized Distribution
1	0% to 4-1/6%	0.5485
2	4-1/6% to 8-1/3%	0.8477
3	8-1/3% to 16-2/3%	1.0770
4	16-2/3% to 33-1/3%	1.1050
5	33-1/3% to 50%	1.0980
6	50% to 66-2/3%	1.0790
7	66-2/3% to 83-1/3%	1.0501
8	83-1/3% to 91-2/3%	0.9604
9	91-2/3% to 95-5/6%	0.7338
10	95-5/6% to 100%	0.4670
BWR DISTRIBUTION^{††}		
Interval	Axial Distance From Bottom of Active Fuel (% of Active Fuel Length)	Normalized Distribution
1	0% to 4-1/6%	0.2200
2	4-1/6% to 8-1/3%	0.7600
3	8-1/3% to 16-2/3%	1.0350
4	16-2/3% to 33-1/3%	1.1675
5	33-1/3% to 50%	1.1950
6	50% to 66-2/3%	1.1625
7	66-2/3% to 83-1/3%	1.0725
8	83-1/3% to 91-2/3%	0.8650
9	91-2/3% to 95-5/6%	0.6200
10	95-5/6% to 100%	0.2200

[†] Reference 1.2.8

^{††} Reference 1.2.9

Table 1.2.16

SUGGESTED PWR UPPER AND LOWER FUEL SPACER LENGTHS

Fuel Assembly Type	Assembly Length w/o C.C. [†] (in.)	Location of Active Fuel from Bottom (in.)	Max. Active Fuel Length (in.)	Upper Fuel Spacer Length (in.)	Lower Fuel Spacer Length (in.)
CE 14x14	157	4.1	137	9.5	10
CE 16x16	176.8	4.7	150	0	0
BW 15x15	165.7	8.4	141.8	6.7	4.1
W 17x17 OFA	159.8	3.7	144	8.2	8.5
W 17x17S	159.8	3.7	144	8.2	8.5
W 17x17V5H	160.1	3.7	144	7.9	8.5
W 15x15	159.8	3.7	144	8.2	8.5
W 14x14S	159.8	3.7	145.2	9.2	7.5
W 14x14 OFA	159.8	3.7	144	8.2	8.5
Ft. Calhoun	146	6.6	128	10.25	20.25
St. Lucie 2	158.2	5.2	136.7	10.25	8.05
B&W 15x15 SS	137.1	3.873	120.5	19.25	19.25
W 15x15 SS	137.1	3.7	122	19.25	19.25
W 14x14 SS	137.1	3.7	120	19.25	19.25

[†] C.C. is an abbreviation for Control Components. Fuel assemblies with control components may require shorter fuel spacers. Each user shall specify the fuel spacer lengths based on their fuel length and any control components and allowing an approximate 2-inch gap.

Table 1.2.17

SUGGESTED BWR UPPER AND LOWER FUEL SPACER LENGTHS

Fuel Assembly Type	Assembly Length (in.)	Location of Active Fuel from Bottom (in.)	Max. Active Fuel Length (in.)	Upper Fuel Spacer Length (in.)	Lower Fuel Spacer Length (in.)
GE/2-3	171.2	7.3	150	4.8	0
GE/4-6	176.2	7.3	150	0	0
Dresden 1	134.4	11.2	110	18	23.6
Humboldt Bay	95	8	79	40.5	40.5
Dresden 1 Damaged Fuel or Fuel Debris	144.5 [†]	11.2	110	17	14.5
Humboldt Bay Damaged Fuel or Fuel Debris	105.5 [†]	8	79	35.25	35.25
LaCrosse	102.5	10.5	83	37	37.5

NOTE: Each user shall specify the fuel spacer lengths based on their fuel length and allowing an approximate 2-inch gap.

[†] Fuel length includes the damaged fuel container.

Table 1.2.18

SUMMARY OF HI-STAR 100 SYSTEM POST-ACCIDENT PERFORMANCE

Aspect of Post-Accident Performance	Results with Demonstrated Integrity of MPC Enclosure Vessel	Results with Postulated Gross Failure of MPC Enclosure Vessel
Containment Boundary Integrity	The MPC enclosure vessel is leak tested to 5.0×10^{-6} std cm^3/s (helium). The overpack containment boundary is standard air leak tested to 4.3×10^{-6} std cm^3/s (helium). Both boundaries are shown to withstand all hypothetical accident conditions. Therefore, there will be no detectable release of radioactive materials.	The overpack containment boundary is leak tested to 4.3×10^{-6} std cm^3/s (helium). The overpack containment boundary is shown to withstand all hypothetical accident conditions. Therefore, the overpack containment boundary meets the accident condition leakage rates.
Maintenance of Subcritical Margins (Maximum k_{eff})	The MPC enclosure vessel is seal welded and there is no breach of the MPC. The bolted closure overpack containment boundary has been shown to prevent water immersion. Therefore, the maximum reactivity of the fuel in a dry MPC is less than 0.4.	The bolted closure overpack containment boundary has been shown to prevent water immersion. Therefore, the maximum reactivity of the fuel in a dry MPC is less than 0.4. Assuming the MPC is fully flooded with water, the reactivity is shown to be below the regulatory requirement of 0.95 including uncertainties and bias.
Adequate Shielding	The MPC enclosure vessel boundary has no effect on the dose rates of the HI-STAR 100 System.	Failure of the MPC enclosure vessel to maintain a release boundary has no effect on the dose rates of the HI-STAR 100 System.

Table 1.2.18 (continued)

SUMMARY OF HI-STAR 100 SYSTEM POST-ACCIDENT PERFORMANCE

Aspect of Post-Accident Performance	Results with Demonstrated Integrity of MPC Enclosure Vessel	Results with Postulated Gross Failure of MPC Enclosure Vessel
Adequate Heat Rejection (Peak Fuel Cladding Temperature)	The MPC enclosure vessel maintains the helium and the peak fuel cladding temperature is demonstrated to remain below 800°F in the post-fire hypothetical accident condition.	<p>Assuming the MPC internal helium fill pressure is released into the overpack containment, the pressure within the small annulus would rise to equalize with the MPC internal pressure. There would be a corresponding slight pressure decrease in the MPC enclosure vessel. The comparatively small volume of the annulus and pressure differential results in the slight pressure change. This will have a negligibly small effect on the peak fuel cladding temperature.</p> <p>The overpack containment boundary is demonstrated to withstand all hypothetical accident conditions. Therefore, there is no credible mechanism for the release of the helium.</p>

Table 1.2.19

DESIGN CHARACTERISTICS FOR STAINLESS STEEL CLAD FUEL ASSEMBLIES

	BWR MPC-68	PWR MPC-24
PHYSICAL PARAMETERS:		
Max. assembly width [†] (in.)	5.62	8.42
Max. assembly length [†] (in.)	102.5	138.8
Max. assembly weight ^{††} (lb.)	400	1421
Max. active fuel length [†] (in.)	83	122
RADIOLOGICAL AND THERMAL CHARACTERISTICS:		
Max. heat generation (W)	83	488
Min. cooling time (yr)	16	19 at 30,000 MWD/MTU 24 at 40,000 MWD/MTU
Max. initial enrichment (wt.% ²³⁵ U)	4.0	4.0
Max. burnup (MWD/MTU)	22,500	40,000
Min. initial enrichment (wt.% ²³⁵ U)	3.5	3.1

[†] Dimensions are unirradiated nominal dimensions.

^{††} Fuel assembly weight including hardware based on DOE MPC DPS [1.1.1].

Table 1.2.20

ACCEPTABLE INTACT ZIRCALOY CLAD FUEL ASSEMBLY
COOLING, AVERAGE BURNUP, AND MINIMUM ENRICHMENT

Post-Irradiation Cooling Time (years)	Assembly Burnup (MWD/MTU)	Assembly Minimum Enrichment (wt. % U-235)
MPC-24 with Non-Zircaloy In-core Grid Spacers		
≥10	≤ 24,500	≥2.3
≥12	≤ 29,500	≥2.6
≥14	≤ 34,500	≥2.9
≥15	≤ 37,500	≥3.2
MPC-24 with Zircaloy In-core Grid Spacers		
≥7	≤ 24,500	≥2.3
≥8	≤ 29,500	≥2.6
≥10	≤ 34,500	≥2.9
≥12	≤ 39,500	≥3.2
≥15	≤ 44,100	≥3.4
MPC-68		
≥8	≤ 24,500	≥2.1
≥9	≤ 29,500	≥2.4
≥12	≤ 34,500	≥2.6
≥15	≤ 39,100	≥2.9

Table 1.2.21

DESIGN CHARACTERISTICS FOR THORIA RODS IN D1 THORIA ROD CANISTERS

PARAMETER	MPC-68 or MPC-68F
Cladding Type	Zircaloy (Zr)
Composition	98.2 wt.% ThO ₂ , 1.8 wt.% UO ₂ with an enrichment of 93.5 wt. % ²³⁵ U
Number of Rods Per Thoria Canister	≤18
Decay Heat Per Thoria Canister	≤115 watts
Post-Irradiation Fuel Cooling Time and Average Burnup Per Thoria Canister	Cooling time ≥18 years and average burnup ≤16,000 MWD/MTIHM
Initial Heavy Metal Weight	≤27 kg/canister
Fuel Cladding O.D.	≥0.412 inches
Fuel Cladding I.D.	≤0.362 inches
Fuel Pellet O.D.	≤0.358 inches
Active Fuel Length	≤111 inches
Canister Weight	≤550 lbs., including Thoria Rods

**FIGURE WITHHELD AS SENSITIVE
UNCLASSIFIED INFORMATION**

*FIGURE 1.2.10; HOLTEC DAMAGED FUEL CONTAINER FOR
DRESDEN UNIT-1/ HUMBOLDT BAY SNF*

**FIGURE WITHHELD AS SENSITIVE
UNCLASSIFIED INFORMATION**

FIGURE 1.2.11; TN DAMAGED FUEL CANISTER FOR DRESDEN UNIT-1

REPORT HI-g51251

**FIGURE WITHHELD AS SENSITIVE
UNCLASSIFIED INFORMATION**

1.3 DESIGN CODE APPLICABILITY

The ASME Boiler and Pressure Vessel Code (ASME Code), 1995 Edition with Addenda through 1997 [1.3.1], is the governing code for the structural design of the HI-STAR 100 System. The ASME Code is applied to each component consistent with the function of the component. Table 1.3.3 lists each structure, system and component (SSC) of the HI-STAR 100 System which are labeled Important to Safety (ITS), along with its function and governing Code. Some components perform multiple functions and in those cases, the most restrictive Code is applied. In accordance with NUREG/CR-6407, "Classification of Transportation Packaging and Dry Spent Fuel Storage System Components" [1.3.2] and according to importance to safety, components of the HI-STAR 100 System are classified as A, B, C, or NITS (not important to safety) in Table 1.3.3.

Table 1.3.1 lists the applicable ASME Code section and paragraph for material procurement, design, fabrication and inspection of the components of the HI-STAR 100 System that are governed by the ASME Code. The ASME Code section listed in the design column is the section used to define allowable stresses for structural analyses.

Table 1.3.2 lists the exceptions to the ASME Code for the HI-STAR 100 System and the justification for those exceptions.

The MPC is classified as important to safety. The MPC structural components include the internal fuel basket and the enclosure vessel. The fuel basket is designed and fabricated as a core support structure, in accordance with the applicable requirements of Section III, Subsection NG of the ASME Code, to the maximum extent practicable, as discussed in Table 1.3.2. The enclosure vessel is designed and fabricated as a Class 1 component pressure vessel in accordance with Section III, Subsection NB of the ASME Code, to the maximum extent practicable, as discussed in Table 1.3.2. The principal exceptions are the MPC lid, vent and drain cover plates, and closure ring welds to the MPC lid and shell, as discussed in Table 1.3.2. In addition, the threaded holes in the MPC lid are designed in accordance with the requirements of ANSI N14.6 [1.3.3] for critical lifts to facilitate vertical MPC transfer.

The MPC closure welds are partial penetration welds that are structurally qualified by analysis, as presented in Chapter 2. The MPC closure ring welds are inspected by performing a liquid penetrant examination of the root pass (if more than one weld pass is required) and final weld surface, in accordance with the requirements contained in Section 7.5. The MPC lid weld may be examined by either volumetric or multi-layer liquid penetrant examination. If volumetric examination is used, it shall be the ultrasonic method and shall include a liquid penetrant examination of the root and final weld layers. If multi-layer liquid penetrant examination is used alone, at a minimum, it must include the root and final weld layers and each 3/8 inch of weld to detect critical weld flaws. The integrity of the MPC lid weld is further verified by performing a hydrostatic pressure test and a helium leak test in accordance with the requirements contained in Section 7.5.

The structural analysis of the MPC, in conjunction with the redundant closures and nondestructive examination, hydrostatic pressure testing, and helium leak testing performed during MPC fabrication and MPC closure, provides assurance of canister closure integrity in lieu of the specific weld joint requirements of the ASME Code, Section III, Subsection NB.

The HI-STAR Overpack is classified as important to safety. The HI-STAR Overpack top flange, closure plate, inner shell, and bottom plate are designed and fabricated in accordance with the requirements of ASME Code, Section III, Subsection NB, to the maximum extent practical (see Table 1.3.2). The remainder of the HI-STAR Overpack steel structure is designed and fabricated in accordance with the requirements of ASME Code, Section III, Subsection NF, to the maximum extent practical (see Table 1.3.2).

Table 1.3.1

HI-STAR 100 ASME BOILER AND PRESSURE VESSEL CODE APPLICABILITY

HI-STAR 100 Component	Material Procurement	Design	Fabrication	Inspection
Overpack containment boundary	Section II; and Section III, Subsection NB, NB-2000	Section III, Subsection NB, NB-3200	Section III, Subsection NB, NB-4000	Section III, Subsection NB, NB-5000 and Section V
Overpack intermediate shells, radial channels, outer enclosure	Section II; and Section III, Subsection NF	Section III, Subsection NF, NF-3300	Section III, Subsection NF, NF-4000	Section III, Subsection NF, NF-5360 and Section V
MPC helium retention boundary	Section II; and Section III, Subsection NB, NB-2000	Section III, Subsection NB, NB-3200	Section III, Subsection NB, NB-4000	Section III, Subsection NB, NB-5000 and Section V
MPC fuel basket	Section II; and Section III, Subsection NG, NG-2000	Section III, Subsection NG, NG-3300 and NG-3200	Section III, Subsection NG, NG-4000	Section III, Subsection NG, NG-5000 and Section V
Trunnions	Section II; and Section III, Subsection NF, NF-2000	ANSI 14.6	Section III, Subsection NF, NF-4000	ANSI 14.6 See Chapter 8
MPC Basket Supports	Section II, and Section III, Subsection NG, NG-2000	Section III, Subsection NG, NG-3300 and NG-3200	Section III, Subsection NG, NG-4000	Section III, Subsection NG, NG-5000 and Section V
Damaged Fuel Container	Section II, and Section III, Subsection NG, NG-2000	Section III, Subsection NG, NG-3300 and NG-3200	Section III, Subsection NG, NG-4000	Section III, Subsection NG, NG-5000 and Section V

Table 1.3.2

LIST OF ASME CODE EXCEPTIONS FOR HI-STAR 100 SYSTEM

Component	Reference ASME Code Section/Article	Code Requirement	Exception, Justification & Compensatory Measures
MPC	NB-1100	Statement of requirements for Code stamping of components.	MPC vessel is designed and will be fabricated in accordance with ASME Code, Section III, Subsection NB to the maximum practical extent, but Code stamping is not required.
MPC	NB-2000	Requires materials to be supplied by ASME-approved material supplier.	Materials will be supplied by Holtec approved suppliers with Certified Material Test Reports (CMTRs) in accordance with NB-2000 requirements.
MPC Lid and Closure Ring Welds	NB-4243	Full penetration welds required for Category C Joints (flat head to main shell per NB-3352.3)	MPC lid and closure ring are not full penetration welds. They are welded independently to provide a redundant seal. Additionally, a weld efficiency factor of 0.45 has been applied to the analyses of these welds.
MPC Lid-to-Shell	NB-5230	Radiographic (RT) or ultrasonic (UT) examination required	Only UT or multi-layer liquid penetrant (PT) examination is permitted. If PT alone is used, at a minimum, it will include the root and final weld layers and each approximately 3/8 inch of weld depth.

Component	Reference ASME Code Section/Article	Code Requirement	Exception, Justification & Compensatory Measures
MPC Closure Ring, Vent and Drain Cover Plate Welds	NB-5230	Radiographic (RT) or ultrasonic (UT) examination required	Root (if more than one weld pass is required) and final liquid penetrant examination to be performed in accordance with NB-5245. The MPC vent and drain cover plate welds are leak tested. The closure ring provides independent redundant closure for vent and drain cover plates.
MPC Lid Weld	NB-5230	Radiographic (RT) or ultrasonic (UT) examination required	If multi-layer liquid penetrant examination is used alone, at a minimum, it will include the root and final weld layers and each 3/8 inch of weld to detect critical weld flaws.

Table 1.3.2 (continued)

LIST OF ASME CODE EXCEPTIONS FOR HI-STAR 100 SYSTEM

Component	Reference ASME Code Section/Article	Code Requirement	Exception, Justification & Compensatory Measures
MPC Enclosure Vessel and Lid	NB-6111	All completed pressure retaining systems shall be pressure tested.	The MPC vessel is seal welded in the field following fuel assembly loading. The MPC vessel shall then be hydrostatically tested as defined in Chapter 8. Accessibility for leakage inspections preclude a Code compliant hydrostatic test. All MPC vessel welds (except closure ring and vent/drain cover plate) are inspected by RT or UT. The vent/drain cover plate welds are confirmed by helium leakage testing and liquid penetrant examination and the closure ring weld is confirmed by liquid penetrant.
MPC Enclosure Vessel	NB-7000	Vessels are required to have overpressure protection.	No overpressure protection is provided. The function of MPC vessel is as a helium retention boundary. MPC vessel is designed to withstand maximum internal pressure considering 100% fuel rod failure and maximum accident temperatures.

Table 1.3.2 (continued)

LIST OF ASME CODE EXCEPTIONS FOR HI-STAR 100 SYSTEM

Component	Reference ASME Code Section/Article	Code Requirement	Exception, Justification & Compensatory Measures
MPC Enclosure Vessel	NB-8000	States requirements for nameplates, stamping and reports per NCA-8000.	HI-STAR 100 System to be marked and identified in accordance with 10CFR71 and 10CFR72 requirements. Code stamping is not required. QA data package to be in accordance with Holtec approved QA program.
Overpack Containment Boundary	NB-1100	Statement of requirements for Code stamping of components.	Overpack containment boundary is designed, and will be fabricated in accordance with ASME Code, Section III, Subsection NB to the maximum practical extent, but Code stamping is not required.
Overpack Containment Boundary	NB-2000	Requires materials to be supplied by ASME approved Material Supplier.	Materials will be supplied by Holtec approved suppliers with CMTRs per NB-2000.
Overpack Containment Boundary	NB-7000	Vessels are required to have overpressure protection.	No overpressure protection is provided. Function of overpack vessel is as a radionuclide containment boundary under normal and hypothetical accident conditions. Overpack vessel is designed to withstand maximum internal pressure and maximum accident temperatures.

Table 1.3.2 (continued)

LIST OF ASME CODE EXCEPTIONS FOR HI-STAR 100 SYSTEM

Component	Reference ASME Code Section/Article	Code Requirement	Exception, Justification & Compensatory Measures
Overpack Containment Boundary	NB-8000	Statement of Requirements for nameplates, stamping and reports per NCA-8000.	HI-STAR 100 System to be marked and identified in accordance with 10CFR71 and 10CFR72 requirements. Code stamping is not required. QA data package to be in accordance with Holtec's approved QA program.
MPC Basket Assembly	NG-2000	Requires materials to be supplied by ASME approved Material Supplier.	Materials will be supplied by Holtec approved supplier with CMTRs in accordance with NG-2000 requirements.
MPC Basket Assembly	NG-8000	States requirements for nameplates, stamping and reports per NCA-8000.	The HI-STAR 100 System will be marked and identified in accordance with 10CFR71 and 10CFR72 requirements. No Code stamping is required. The MPC basket data package will be in conformance with Holtec's QA program.
Overpack Intermediate Shells	NF-2000	Requires materials to be supplied by ASME approved Material Supplier.	Materials will be supplied by Holtec approved supplier with CMTRs in accordance with NF-2000 requirements.
Overpack Containment Boundary	NB-2330	Defines the methods for determining the T_{NDT} for impact testing of materials.	T_{NDT} shall be defined in accordance with Regulatory Guides 7.11 and 7.12 for the containment boundary components.

TABLE 1.3.3

MATERIALS AND COMPONENTS OF THE HI-STAR 100 SYSTEM
OVERPACK ^(1,2)

Primary Function	Component ⁽³⁾	Safety Class ⁽⁴⁾	Codes/Standards (as applicable to component)	Material	Strength (ksi)	Special Surface Finish/Coating	Contact Matl. (if dissimilar)
Confinement	Inner Shell	A	ASME Section III; Subsection NB	SA203-E	Table 2.3.4	Paint inside surface with Thermaline 450. External surface to be coated with a surface preservative.	NA
Confinement	Bottom Plate	A	ASME Section III; Subsection NB	SA350-LF3	Table 2.3.4	Paint inside surface with Thermaline 450	NA
Confinement	Top Flange	A	ASME Section III; Subsection NB	SA350-LF3	Table 2.3.4	Paint inside surface with Thermaline 450. Paint outside surface with Carboline 890.	NA
Confinement	Closure Plate	A	ASME Section III; Subsection NB	SA350-LF3	Table 2.3.4	Paint inside surface with Thermaline 450. Paint outside surface with Carboline 890.	NA
Confinement	Closure Plate Bolts	A	ASME Section III; Subsection NB	SB637-N07718	Table 2.3.5	NA	NA
Confinement	Port Plug	A	Non-code	SA193-B8	Not required	NA	NA
Confinement	Port Plug Seal	A	Non-code	Alloy X750	Not required	NA	NA
Confinement	Closure Plate Seal	A	Non-code	Alloy X750	Not required	NA	NA

- Notes: 1) There are no known residuals on finished component surfaces.
 2) All welding processes used in welding the components shall be qualified in accordance with the requirements of ASME Section IX. All welds shall be made using welders qualified in accordance with ASME Section IX. Weld material shall meet the requirements of ASME Section II and the applicable Subsection of ASME Section III.
 3) Component nomenclature taken from Bill of Materials in Chapter 1.
 4) A,B and C denote important to safety classifications as described in NUREG/CR-6407. NITS stands for Not Important To Safety.

TABLE 1.3.3

MATERIALS AND COMPONENTS OF THE HI-STAR 100 SYSTEM

OVERPACK ^(1,2)

Primary Function	Component ⁽³⁾	Safety Class ⁽⁴⁾	Codes/Standards (as applicable to component)	Material	Strength (ksi)	Special Surface Finish/Coating	Contact Matl. (if dissimilar)
Confinement	Port Cover Seal	B	Non-code	Alloy X750	Not required	NA	NA
Shielding	Intermediate Shells	B	ASME Section III; Subsection NF	SA516-70	Table 2.3.2	Internal surfaces to be coated with a silicone encapsulant (Dow Corning SYLGARD 567 or equivalent) for surface preservation. Exposed areas of fifth intermediate shell to be painted with Carboline 890.	NA
Shielding	Neutron Shield	B	Non-code	Holtite-A	Not required	NA	NA
Shielding	Plugs for Drilled Holes	NITS	Non-code	SA193-B7	Not required	NA	NA
Shielding	Removeable Shear Ring	B	ASME Section III; Subsection NF	SA203-E	Table 2.3.4	Paint external surface with Carboline 890.	NA
Shielding	Pocket Trunnion Plug Plate	C	Non-code	SA240-304	Not required	NA	NA
Heat Transfer	Radial Channels	B	ASME Section III;	SA515-70	Table 2.3.3	Paint outside	NA

Notes: 1) There are no known residuals on finished component surfaces.

2) All welding processes used in welding the components shall be qualified in accordance with the requirements of ASME Section IX. All welds shall be made using welders qualified in accordance with ASME Section IX. Weld material shall meet the requirements of ASME Section II and the applicable Subsection of ASME Section III.

3) Component nomenclature taken from Bill of Materials in Chapter 1.

4) A,B and C denote important to safety classifications as described in NUREG/CR-6407. NITS stands for Not Important To Safety.

TABLE 1.3.3

MATERIALS AND COMPONENTS OF THE HI-STAR 100 SYSTEM
OVERPACK ^(1,2)

Primary Function	Component ⁽³⁾	Safety Class ⁽⁴⁾	Codes/Standards (as applicable to component)	Material	Strength (ksi)	Special Surface Finish/Coating	Contact Matl. (if dissimilar)
			Subsection NF			surface with Carboline 890.	
Structural Integrity	Pocket Trunnion	B	ASME Section III; Subsection NF	SA705-630	Table 2.3.5	NA	NA
Structural Integrity	Lifting Trunnion	A	ANSI N14.6	SB637-N07718	Table 2.3.5	NA	NA
Structural Integrity	Rupture Disk	C	Non-code	Commercial	Not required	NA	Brass-C/S
Structural Integrity	Rupture Disk Plate	C	Non-code	A569	Not required	NA	NA
Structural Integrity	Removeable Shear Ring Bolt	C	Non-code	SA193-B7	Not required	NA	NA
Structural Integrity	Thermal Expansion Foam	NITS	Non-code	Silicone Foam	Not required	NA	NA
Structural Integrity	Closure Bolt Washer	NITS	Non-code	S/S	Not required	NA	NA
Structural Integrity	Enclosure Shell Panels	B	ASME Section III; Subsection NF	SA515-70	Table 2.3.3	Paint outside surface with Carboline 890.	NA
Structural Integrity	Enclosure Shell Return	B	ASME Section III; Subsection NF	SA515-70	Table 2.3.3	Paint outside surface with Carboline 890.	NA
Structural Integrity	Port Cover	B	ASME Section III; Subsection NF	SA203E	Table 2.3.4	Paint outside surface with Carboline 890.	NA
Structural Integrity	Port Cover Bolt	C	Non-code	SA193-B7	Not required	NA	NA

Notes: 1) There are no known residuals on finished component surfaces.

2) All welding processes used in welding the components shall be qualified in accordance with the requirements of ASME Section IX. All welds shall be made using welders qualified in accordance with ASME Section IX. Weld material shall meet the requirements of ASME Section II and the applicable Subsection of ASME Section III.

3) Component nomenclature taken from Bill of Materials in Chapter 1.

4) A,B and C denote important to safety classifications as described in NUREG/CR-6407. NITS stands for Not Important To Safety.

TABLE 1.3.3

MATERIALS AND COMPONENTS OF THE HI-STAR 100 SYSTEM

OVERPACK ^(1,2)

Primary Function	Component ⁽³⁾	Safety Class ⁽⁴⁾	Codes/Standards (as applicable to component)	Material	Strength (ksi)	Special Surface Finish/Coating	Contact Matl. (if dissimilar)
Operations	Trunnion Locking Pad and End Cap Bolt	C	Non-code	SA193-B7	Not required	NA	NA
Operations	Lifting Trunnion End Cap	C	Non-code	SA516-70	Table 2.3.2	Paint exposed surfaces with Carboline 890.	NA
Operations	Lifting Trunnion Locking Pad	C	Non-code	SA516-70	Table 2.3.2	Paint exposed surfaces with Carboline 890.	NA
Operations	Nameplate	NITS	Non-code	SA240-304	Not required	NA	NA

Notes: 1) There are no known residuals on finished component surfaces.

2) All welding processes used in welding the components shall be qualified in accordance with the requirements of ASME Section IX. All welds shall be made using welders qualified in accordance with ASME Section IX. Weld material shall meet the requirements of ASME Section II and the applicable Subsection of ASME Section III.

3) Component nomenclature taken from Bill of Materials in Chapter 1.

4) A,B and C denote important to safety classifications as described in NUREG/CR-6407. NITS stands for Not Important To Safety.

TABLE 1.3.3

MATERIALS AND COMPONENTS OF THE HI-STAR 100 SYSTEM

MPC^(1,2)

Primary Function	Component ⁽³⁾	Safety Class ⁽⁴⁾	Codes/Standards (as applicable to component)	Material	Strength (ksi)	Special Surface Finish/Coating	Contact Matl. (if dissimilar)
Helium Retention	Shell	A	ASME Section III; Subsection NB	Alloy X ⁽⁵⁾	See Appendix 1.A	NA	NA
Helium Retention	Baseplate	A	ASME Section III; Subsection NB	Alloy X	See Appendix 1.A	NA	NA
Helium Retention	Lid	A	ASME Section III; Subsection NB	Alloy X	See Appendix 1.A	NA	NA
Helium Retention	Closure Ring	A	ASME Section III; Subsection NB	Alloy X	See Appendix 1.A	NA	NA
Helium Retention	Port Cover Plates	A	ASME Section III; Subsection NB	Alloy X	See Appendix 1.A	NA	NA
Criticality Control	Basket Cell Plates	A	ASME Section III; Subsection NG	Alloy X	See Appendix 1.A	NA	NA
Criticality Control	Boral	A	Non-code	NA	NA	NA	Aluminum/SS
Shielding	Drain and Vent Shield Block	C	Non-code	Alloy X	See Appendix 1.A	NA	NA
Shielding	Plugs for Drilled Holes	NITS	Non-code	Alloy X	See Appendix 1.A	NA	NA
Heat Transfer	Heat Conduction Elements	B	Non-code	Aluminum; Alloy 1100	NA	Sandblast Specified Surfaces	Aluminum/SS
Structural Integrity	Upper Fuel Spacer Column	B	ASME Section III;	Alloy X	See Appendix 1.A	NA	NA

Notes: 1) There are no known residuals on finished component surfaces.

2) All welding processes used in welding the components shall be qualified in accordance with the requirements of ASME Section IX. All welds shall be made using welders qualified in accordance with ASME Section IX. Weld material shall meet the requirements of ASME Section II and the applicable Subsection of ASME Section III.

3) Component nomenclature taken from Bill of Materials in Chapter 1.

4) A,B and C denote important to safety classifications as described in NUREG/CR-6407. NITS stands for Not Important To Safety.

5) For details on Alloy X material, see Appendix 1.A.

TABLE 1.3.3

MATERIALS AND COMPONENTS OF THE HI-STAR 100 SYSTEM

MPC ^(1,2)

Primary Function	Component ⁽³⁾	Safety Class ⁽⁴⁾	Codes/Standards (as applicable to component)	Material	Strength (ksi)	Special Surface Finish/Coating	Contact Matl. (if dissimilar)
			Subsection NG (only for stress analysis)				
Structural Integrity	Sheathing	A	Non-code	Alloy X	See Appendix 1.A	Aluminum/SS	NA
Structural Integrity	Shims	NITS	Non-code	Alloy X	See Appendix 1.A	NA	NA
Structural Integrity	Basket Supports (Angled Plates)	A	ASME Section III; Subsection NG	Alloy X	See Appendix 1.A	NA	NA
Structural Integrity	Basket Supports (Flat Plates)	B	ASME Section III; Subsection NG	Alloy X	See Appendix 1.A	NA	NA
Structural Integrity	Lift Lug	C	Non-code	Alloy X	See Appendix 1.A	NA	NA
Structural Integrity	Lift Lug Baseplate	C	Non-code	Alloy X	See Appendix 1.A	NA	NA
Structural Integrity	Upper Fuel Spacer Bolt	NITS	Non-code	A193-B8	Per ASME Section II	NA	NA
Structural Integrity	Upper Fuel Spacer End Plate	B	Non-code	Alloy X	See Appendix 1.A	NA	NA
Structural Integrity	Lower Fuel Spacer Column	B	ASME Section III; Subsection NG (only for stress analysis)	Alloy X	See Appendix 1.A	NA	NA
Structural Integrity	Lower Fuel Spacer End Plate	B	Non-code	Alloy X	See Appendix 1.A	NA	NA
Structural Integrity	Vent Shield Block Spacer	C	Non-code	Alloy X	See Appendix 1.A	NA	NA

- Notes: 1) There are no known residuals on finished component surfaces.
2) All welding processes used in welding the components shall be qualified in accordance with the requirements of ASME Section IX. All welds shall be made using welders qualified in accordance with ASME Section IX. Weld material shall meet the requirements of ASME Section II and the applicable Subsection of ASME Section III.
3) Component nomenclature taken from Bill of Materials in Chapter 1.
4) A,B and C denote important to safety classifications as described in NUREG/CR-6407. NITS stands for Not Important To Safety.
5) For details on Alloy X material, see Appendix 1.A.

TABLE 1.3.3

MATERIALS AND COMPONENTS OF THE HI-STAR 100 SYSTEM

MPC^(1,2)

Primary Function	Component ⁽³⁾	Safety Class ⁽⁴⁾	Codes/Standards (as applicable to component)	Material	Strength (ksi)	Special Surface Finish/Coating	Contact Matl. (if dissimilar)
Operations	Vent and Drain Tube	C	Non-code	304 S/S	Per ASME Section II	Thread area surface hardened	NA
Operations	Vent & Drain Cap	C	Non-code	304 S/S	Per ASME Section II	NA	NA
Operations	Vent & Drain Cap Seal Washer	NITS	Non-code	Aluminum	NA	NA	Aluminum/SS
Operations	Vent & Drain Cap Seal Washer Bolt	NITS	Non-code	Aluminum	NA	NA	NA
Operations	Reducer	NITS	Non-code	Alloy X	See Appendix 1.A	NA	NA
Operations	Drain Line	NITS	Non-code	Alloy X	See Appendix 1.A	NA	NA
Operations	Damaged Fuel Container	C	ASME Section III; Subsection NG	Primarily 304 S/S	See Appendix 1.A	NA	NA

Notes: 1) There are no known residuals on finished component surfaces.

2) All welding processes used in welding the components shall be qualified in accordance with the requirements of ASME Section IX. All welds shall be made using welders qualified in accordance with ASME Section IX. Weld material shall meet the requirements of ASME Section II and the applicable Subsection of ASME Section III.

3) Component nomenclature taken from Bill of Materials in Chapter 1.

4) A,B and C denote important to safety classifications as described in NUREG/CR-6407. NITS stands for Not Important To Safety.

5) For details on Alloy X material, see Appendix 1.A.

1.4 GENERAL ARRANGEMENT DRAWINGS and BILLS-OF-MATERIAL

The following drawings provide sufficient detail to describe the HI-STAR 100 packaging.

The classification of all components important to safety in accordance with Regulatory Guide 7.10 and NUREG/CR-6407 is provided in Table 1.3.3. Operational information, such as bolt torque and pressure-relief specifications are provided in Chapters 7 and 8. The maximum weight of the package and the maximum weight of the contents is provided in Table 1.2.1.

The following HI-STAR 100 System design drawings are provided in this section[†]:

Drawing Number/Sheet	Description	Rev.
5014-C1395 Sht 1/4	HI-STAR 100 MPC-24 Construction	1
5014-C1395 Sht 2/4	HI-STAR 100 MPC-24 Construction	1
5014-C1395 Sht 3/4	HI-STAR 100 MPC-24 Construction	1
5014-C1395 Sht 4/4	HI-STAR 100 MPC-24 Construction	1
5014-C1396 Sht 1/6	HI-STAR 100 MPC-24 Construction	1
5014-C1396 Sht 2/6	HI-STAR 100 MPC-24 Construction	1
5014-C1396 Sht 3/6	HI-STAR 100 MPC-24 Construction	1
5014-C1396 Sht 4/6	HI-STAR 100 MPC-24 Construction	1
5014-C1396 Sht 5/6	HI-STAR 100 MPC-24 Construction	0
5014-C1396 Sht 6/6	HI-STAR 100 MPC-24 Construction	1
5014-C1397 Sht 1/7	Cross Sectional View of HI-STAR 100 Overpack	2
5014-C1397 Sht 2/7	Detail of Top Flange & Bottom Plate of HI-STAR 100 Overpack	1
5014-C1397 Sht 3/7	Detail of Bolt Hole & Bolt of HI-STAR 100 Overpack	1
5014-C1397 Sht 4/7	Detail of Closure Plate Test Port and Name Plate Detail of HI-STAR 100 Overpack	1

[†] Each drawing title includes the term "CoC No. 9261, Appendix B." Rather than appending the drawings directly to the CoC, they are incorporated into the CoC by reference. The "Appendix B" will be removed from each drawing as part of its next normal revision.

Drawing Number/Sheet	Description	Rev.
5014-C1397 Sht 5/7	Detail of Lifting Trunnion & Locking Pad of HI-STAR 100 Overpack	1
5014-C1397 Sht 6/7	Detail of Shear Ring and Closure Plate Bolt Installation of HI-STAR 100 Overpack	1
5014-C1397 Sht 7/7	Detail of Shear Ring of HI-STAR 100 Overpack	1
5014-C1398 Sht 1/3	HI-STAR 100 Overpack Orientation	1
5014-C1398 Sht 2/3	Detail of Drain & Rupture Disk of HI-STAR 100 Overpack	1
5014-C1398 Sht 3/3	Detail of Vent & Port Plug of HI-STAR 100 Overpack	1
5014-C1399 Sht 1/3	Section "G" - "G" of HI-STAR 100 Overpack	1
5014-C1399 Sht 2/3	Section "X"-"X" & View "Y" of HI-STAR 100 Overpack	1
5014-C1399 Sht 3/3	Detail of Trunnion Pocket Forging of HI-STAR 100 Overpack	2
5014-C1401 Sht 1/4	HI-STAR 100 MPC-68 Construction	1
5014-C1401 Sht 2/4	HI-STAR 100 MPC-68 Construction	1
5014-C1401 Sht 3/4	HI-STAR 100 MPC-68 Construction	1
5014-C1401 Sht 4/4	HI-STAR 100 MPC-68 Construction	1
5014-C1402 Sht 1/6	HI-STAR 100 MPC-68 Construction	1
5014-C1402 Sht 2/6	HI-STAR 100 MPC-68 Construction	1
5014-C1402 Sht 3/6	HI-STAR 100 MPC-68 Construction	1
5014-C1402 Sht 4/6	HI-STAR 100 MPC-68 Construction	1
5014-C1402 Sht 5/6	HI-STAR 100 MPC-68 Construction	0
5014-C1402 Sht 6/6	HI-STAR 100 MPC-68 Construction	1
5014-C1765 Sht 1/7	HI-STAR 100 Impact Limiter	1
5014-C1765 Sht 2/7	HI-STAR 100 Bottom Impact Limiter	1
5014-C1765 Sht 3/7	HI-STAR 100 Top Impact Limiter	1
5014-C1765 Sht 4/7	HI-STAR 100 Top Impact Limiter	1

Drawing Number/Sheet	Description	Rev.
5014-C1765 Sht 5/7	HI-STAR 100 Top Impact Limiter Detail of Item #6	1
5014-C1765 Sht 6/7	HI-STAR 100 Impact Limiter Honeycomb Details	1
5014-C1765 Sht 7/7	HI-STAR 100 Bottom Impact Limiter	0
5014-C1782 Sht 1/1	HI-STAR 100 Assembly For Transport	1
BM-C1476, Sht 1/2	Bill-of-Materials for HI-STAR 100 Overpack	1
BM-C1476, Sht 2/2	Bill-of-Materials for HI-STAR 100 Overpack	2
BM-C1478, Sht 1/2	Bill-of-Materials for 24-Assembly HI-STAR 100 PWR MPC	1
BM-C1478, Sht 2/2	Bill-of-Materials for 24-Assembly HI-STAR 100 PWR MPC	1
BM-C1479, Sht 1/2	Bill-of-Materials for 68-Assembly HI-STAR 100 BWR MPC	1
BM-C1479, Sht 2/2	Bill-of-Materials for 68-Assembly HI-STAR 100 BWR MPC	1

FIGURE WITHHELD AS SENSITIVE UNCLASSIFIED INFORMATION

NOV 6-99	1	REVISED AS SHOWN	S. GEE 11-6-99	<i>N/A</i>	<i>B.G.</i>	<i>V.G.</i>
FEB. 17-99	0	FIR APPROVAL	C.Y. 2-17-99	B.G.U. 2-20-99	B.G. 2-20-99	V.G. 2-20-99
DATE	REV.	DESCRIPTION	PREP. BY:	CHECKED BY:	ENG.	Q. A.
REVISION						
<input type="checkbox"/> <input type="checkbox"/> <input type="checkbox"/> <input type="checkbox"/> <input type="checkbox"/>			EQUIPMENT DESIGN			
HOLTEC			ANALYSIS			
INTERNATIONAL			CONSULTING			
DESCRIPTION						
HI-STAR 100 MPC-24 CONSTRUCTION CoC No. 9261, APPENDIX B						
CLIENT N/A						
COMPANION DRAWINGS C1396					REV. 1	
PROJECT No. 5014				DRAWING No.		
P.O. No. N/A				C1395 SHT 1 OF 4		

FIGURE WITHHELD AS SENSITIVE UNCLASSIFIED INFORMATION

NW 6-99	1	REVISED AS SHOWN	S.GEE 11-6-99	<i>[Signature]</i>	<i>[Signature]</i>	<i>[Signature]</i>
FEB 17-99	0	FOR APPROVAL	C.Y. 2-17-99	B.G.U. 2-20-99	B.G. 2-20-99	V.G. 2-20-99
DATE	REV.	DESCRIPTION	PREP. BY:	CHECKED BY:	ENG.	Q. A.
REVISION						
<input type="checkbox"/> <input type="checkbox"/> <input type="checkbox"/> <input type="checkbox"/> <input type="checkbox"/>			EQUIPMENT DESIGN			
HOLTEC			ANALYSIS			
INTERNATIONAL			CONSULTING			
DESCRIPTION						
HI-STAR 100 MPC-24 CONSTRUCTION CoC No. 9261, APPENDIX B						
CLIENT N/A						
COMPANION DRAWINGS C1396					REV. 1	
PROJECT No. 5014				DRAWING No.		
P.O. No. N/A				C1395 SHT 2 OF 4		

FIGURE WITHHELD AS SENSITIVE UNCLASSIFIED INFORMATION

NOV 17-99	1	FOR REVISION	J.A.	<i>[Handwritten initials]</i>	<i>[Handwritten initials]</i>	<i>[Handwritten initials]</i>
FEB. 17-99	0	FOR APPROVAL	C.Y.	B.G.	B.G.	V.G.
DATE	REV.	DESCRIPTION	PREP. BY:	CHECKED BY:	ENG.	Q. A.
REVISION						
<input type="checkbox"/>	<input type="checkbox"/>	<input type="checkbox"/>	<input type="checkbox"/>	<input type="checkbox"/>	EQUIPMENT DESIGN	
HOLTEC				ANALYSIS		
INTERNATIONAL				CONSULTING		
DESCRIPTION						
HI-STAR 100 MPC-24 CONSTRUCTION CoC No. 9261, APPENDIX B						
CLIENT N/A						
COMPANION DRAWINGS C1396						REV. 1
PROJECT No. 5014				DRAWING No.		
P.O. No. N/A				C1395 SHT 3 OF 4		

FIGURE WITHHELD AS SENSITIVE UNCLASSIFIED INFORMATION

NOV. 6-99	1	REVISED AS SHOWN	S. GEE 11-6-99	<i>AW</i>	<i>W. G. WILSON</i>	<i>W. G. WILSON</i>
FEB. 17-99	0	FOR APPROVAL	C.Y. 2-17-99	B.G.D. 2-20-99	B.G. 2-20-99	V.G. 2-20-99
DATE	REV.	DESCRIPTION	PREP. BY:	CHECKED BY:	P.N.	Q. A.
REVISION						
<input type="checkbox"/> <input type="checkbox"/> <input type="checkbox"/> <input type="checkbox"/> <input type="checkbox"/>			EQUIPMENT DESIGN			
HOLTEC INTERNATIONAL			ANALYSIS CONSULTING			
DESCRIPTION						
HI-STAR 100 MPC-24 CONSTRUCTION CoC No. 9261, APPENDIX B						
CLIENT N/A						
COMPANION DRAWINGS C1396					REV. 1	
PROJECT No. 5014			DRAWING No.			
P.O. No. N/A			C1395 SHT 4 OF 4			

FIGURE WITHHELD AS SENSITIVE UNCLASSIFIED INFORMATION

NOV 6-99	1	REVISED AS SHOWN	S. GEE 11-6-99	<i>[Signature]</i>	<i>[Signature]</i>	<i>[Signature]</i>
FEB 17-99	0	FOR APPROVAL	C.Y. 2-17-99	B.G.U. 2-20-99	B.E. 2-20-99	V.G. 2-20-99
DATE	REV.	DESCRIPTION	PREP. BY:	CHECKED BY:	P.M.	Q. A.
REVISION						
<input type="checkbox"/> <input type="checkbox"/> <input type="checkbox"/> <input type="checkbox"/> <input type="checkbox"/>			EQUIPMENT DESIGN			
HOLTEC			ANALYSIS			
INTERNATIONAL			CONSULTING			
DESCRIPTION						
HI-STAR 100 MPC-24 CONSTRUCTION						
CoC No. 9261, APPENDIX B						
CLIENT N/A						
COMPANION DRAWINGS					REV.	
C1395					1	
PROJECT No. 5014				DRAWING No.		
P.O. No. N/A				C1395 SHT 1 OF 6		

FIGURE WITHHELD AS SENSITIVE UNCLASSIFIED INFORMATION

DATE	REV.	DESCRIPTION	PREP. BY:	CHECKED BY:	P. N.	Q. A.
NOV 6-99	1	REVISED AS SHOWN	S. BEE 11-6-99	<i>[Handwritten Signature]</i>	<i>[Handwritten Signature]</i>	<i>[Handwritten Signature]</i>
FEB 17-99	0	FOR APPROVAL	C.Y. 2-17-99	B.G.H. 2-20-99	B.G. 2-20-99	V.S. 2-20-99

REVISION	
<input type="checkbox"/>	EQUIPMENT DESIGN
<input type="checkbox"/>	ANALYSIS
<input type="checkbox"/>	CONSULTING
HOLTEC INTERNATIONAL	
DESCRIPTION HI-STAR 100 MPC-24 CONSTRUCTION CoC No. 9261, APPENDIX B	
CLIENT	N/A
COMPANION DRAWINGS C1395	REV. 1
PROJECT No. 5014	DRAWING No.
P.O. No. N/A	C1396 SHT 2 OF 6

FIGURE WITHHELD AS SENSITIVE UNCLASSIFIED INFORMATION

NOV 17-99	1	FOR REVISION	J.A. 10-17-99	<i>[Handwritten]</i>	<i>[Handwritten]</i>	<i>[Handwritten]</i>
FEB 17-99	0	FOR APPROVAL	C.Y. 2-17-99	B.G.	B.G.	V.G.
DATE	REV.	DESCRIPTION	PREP. BY:	CHECKED BY:	ENG.	Q. A.
REVISION						
<input type="checkbox"/>			EQUIPMENT DESIGN			
<input type="checkbox"/>			ANALYSIS			
<input type="checkbox"/>			CONSULTING			
DESCRIPTION						
HI-STAR 100 MPC-24 CONSTRUCTION CoC No. 9261, APPENDIX B						
CLIENT N/A						
COMPANION DRAWINGS C1395					REV. 1	
PROJECT No. 5014				DRAWING No.		
P.O. No. N/A				C1396 SHT 3 OF 6		

FIGURE WITHHELD AS SENSITIVE UNCLASSIFIED INFORMATION

REV 17-99	1	FOR REVISION	J.A. 10-17-99	<i>[Signature]</i> 11/19/99	<i>[Signature]</i> 11/19/99	<i>[Signature]</i> 11/19/99
REV. 17-99	0	FOR APPROVAL	C.T. 2-17-99	B.G.	B.G.	V.G.
DATE	REV.	DESCRIPTION	PREP. BY:	CHECKED BY:	ENG.	Q. A.
REVISION						
<input type="checkbox"/> <input type="checkbox"/> <input type="checkbox"/> <input type="checkbox"/> <input type="checkbox"/>						
EQUIPMENT DESIGN						
HOLTEC ANALYSIS						
INTERNATIONAL CONSULTING						
DESCRIPTION						
HI-STAR 100 MPC-24 CONSTRUCTION CoC No. 9261, APPENDIX B						
CLIENT N/A						
COMPANION DRAWINGS C1395						REV. 1
PROJECT No. 5014				DRAWING No.		
P.O. No. N/A				C1395 SET 4 OF 8		

FIGURE WITHHELD AS SENSITIVE UNCLASSIFIED INFORMATION

DATE	REV.	DESCRIPTION	PREP. BY:	CHECKED BY:	ENG.	Q. A.
FEB. 17-99	0	FIR APPROVAL	C.Y. 2-17-99	HU 2-20-99	EG 2-20-99	V.G. 2-20-99
REVISION						
		<input type="checkbox"/>	<input type="checkbox"/>	<input type="checkbox"/>	<input type="checkbox"/>	<input type="checkbox"/>
				EQUIPMENT DESIGN		
				ANALYSIS		
HOLTEC				CONSULTING		
INTERNATIONAL						
DESCRIPTION						
HI-STAR 100 MPC-24 CONSTRUCTION CoC No. 9261, APPENDIX B						
CLIENT N/A						
COMPANION DRAWINGS C1395						REV. 0
PROJECT No. 5014				DRAWING No.		
P.O. No. N/A				C1396 SHT 5 OF 6		

FIGURE WITHHELD AS SENSITIVE UNCLASSIFIED INFORMATION

NOV 6-99	1	REVISED AS SHOWN	S.GEE 11-5-99	<i>[Signature]</i>	<i>[Signature]</i>	<i>[Signature]</i>
FEB. 17-99	0	FOR APPROVAL	C.Y. 2-17-99	B.G.U. 2-20-99	B.G. 2-20-99	V.G. 2-20-99
DATE	REV.	DESCRIPTION	PREP. BY:	CHECKED BY:	P.M.	Q. A.
REVISION						
<input type="checkbox"/> <input type="checkbox"/> <input type="checkbox"/> <input type="checkbox"/> <input type="checkbox"/>						
EQUIPMENT DESIGN						
ANALYSIS						
HOLTEC INTERNATIONAL CONSULTING						
DESCRIPTION						
HI-STAR 100 MPC-24 CONSTRUCTION CoC No. 9261, APPENDIX B						
CLIENT N/A						
COMPANION DRAWINGS C1395					REV. 1	
PROJECT No. 5014				DRAWING No.		
P.O. No. N/A				C1396 SHT 6 OF 6		

FIGURE WITHHELD AS SENSITIVE UNCLASSIFIED INFORMATION

FEB. 4-2000	2	INCORPORATED ECD 1020-4	S. GEE 2-4-2000	<i>10/12/99</i>	<i>2/4/00</i>	<i>2/4/00</i>	<i>2/4/00</i>
NOV. 5-99	1	REVISED AS SHOWN	S. GEE 11-5-99	B. G. U. 11-20-99	B. G. 11-20-99	M. S. 11-20-99	
FEB. 17-99	3	FOR APPROVAL	C. Y. 2-17-99	B. G. U. 2-20-99	B. G. 2-20-99	V. G. 2-20-99	
DATE	REV.	DESCRIPTION	PREP. BY:	CHECKED BY:	P. M.	Q. A.	
REVISION							
<input type="checkbox"/> <input type="checkbox"/> <input type="checkbox"/> <input type="checkbox"/> <input type="checkbox"/>				EQUIPMENT DESIGN			
HOLTEC				ANALYSIS			
INTERNATIONAL.				CONSULTING			
DESCRIPTION							
CROSS SECTIONAL VIEW OF HI-STAR 100 OVERPACK CoC No. 9261, APPENDIX B							
CLIENT N/A							
COMPANION DRAWINGS C1398, C1399						REV. 2	
PROJECT No. 5014				DRAWING No.			
P.O. No. N/A				C1397 SH. 1 OF 7 (E.I.D. 2886)			

FIGURE WITHHELD AS SENSITIVE UNCLASSIFIED INFORMATION

NOV. 5-99	1	REVISED AS SHOWN	S. GEE 11-5-99	<i>WJH</i>	<i>WJH</i>	<i>WJH</i>	<i>WJH</i>
FEB. 17-99	0	FOR APPROVAL	C. Y. 2-17-99	B. G. U. 2-20-99	B. G. 2-20-99	V. G. 2-20-99	
DATE	REV.	DESCRIPTION	PREP. BY:	CHECKED BY:	ENG.	Q. A.	
REVISION							
<input type="checkbox"/> <input type="checkbox"/> <input type="checkbox"/> <input type="checkbox"/> <input type="checkbox"/>							
EQUIPMENT DESIGN HOLTEC INTERNATIONAL							
ANALYSIS CONSULTING							
DESCRIPTION DETAIL OF TOP FLANGE & BOTTOM PLATE OF HI-STAR 100 OVERPACK CoC No. 9261, APPENDIX B							
CLIENT N/A							
COMPANION DRAWINGS C1398, C1399						REV. 1	
PROJECT No. 5014				DRAWING No.			
P.O. No. N/A				C1397 SHT. 2 OF 7			

FIGURE WITHHELD AS SENSITIVE UNCLASSIFIED INFORMATION

NOV 5-99	1	REVISED AS SHOWN	S. GEE. 11-5-99	<i>B.H.M.</i>	<i>V.G.</i>	<i>4/10/99</i>
FEB 17-99	0	FOR APPROVAL	E. Y. 2-17-99	B. G. U. 2-20-99	B. G. 2-20-99	V. G. 2-20-99
DATE	REV.	DESCRIPTION	PREP. BY:	CHECKED BY:	P. W.	Q. A.
REVISION						
			EQUIPMENT DESIGN			
			ANALYSIS			
			CONSULTING			
DESCRIPTION						
DETAIL OF BOLT HOLE & BOLT OF HI-STAR 100 OVERPACK CoC No. 9261, APPENDIX B						
CLIENT N/A						
COMPANION DRAWINGS C1398, C1399						REV. 1
PROJECT No. 5014				DRAWING No.		
P.O. No. N/A				C1397 SHT. 3 OF 7		

FIGURE WITHHELD AS SENSITIVE UNCLASSIFIED INFORMATION

NOV 5-99	1	REVISED AS SHOWN	S. GEE 11-5-99	<i>[Handwritten]</i>	<i>[Handwritten]</i>	<i>[Handwritten]</i>
FEB 17-99	0	FOR APPROVAL	C. Y. 2-17-99	B. G. U. 2-20-99	B. G. 2-20-99	V. G. 2-20-99
DATE	REV.	DESCRIPTION	PREP. BY:	CHECKED BY:	P. N.	Q. A.
REVISION						
<input type="checkbox"/> <input type="checkbox"/> <input type="checkbox"/> <input type="checkbox"/> <input type="checkbox"/>			EQUIPMENT DESIGN			
HOLTEC			ANALYSIS			
INTERNATIONAL			CONSULTING			
DESCRIPTION						
DETAIL OF CLOSURE PLATE TEST PORT AND NAME PLATE DETAIL OF HI-STAR 100 OVERPACK CoC No. 9261, APPENDIX B						
CLIENT N/A						
COMPANION DRAWINGS C1398, C1399					REV. 1	
PROJECT No. 5014				DRAWING No.		
P.O. No. N/A				C1397 SHT. 4 OF 7		

FIGURE WITHHELD AS SENSITIVE UNCLASSIFIED INFORMATION

FEB 4-2000	1	INCORPORATED ECD 1020-4	S. GEE 2-4-2000	<i>2/11/00</i>	<i>2/11/00</i>	<i>2/11/00</i>	<i>2/11/00</i>
FEB 17-99	0	FOR APPROVAL	C. Y. 2-17-99	B. G. U. 2-20-99	B. G. 2-20-99	V. G. 2-20-99	
DATE	REV.	DESCRIPTION	PREP. BY:	CHECKED BY:	ENG.	Q. A.	
REVISION							
<input type="checkbox"/> <input type="checkbox"/> <input type="checkbox"/> <input type="checkbox"/> <input type="checkbox"/>				EQUIPMENT DESIGN			
HOLTEC				ANALYSIS			
INTERNATIONAL.				CONSULTING			
DESCRIPTION							
DETAIL OF LIFTING TRUNNION & LOCKING PAD OF HI-STAR 100 OVERPACK CoC No. 9261, APPENDIX B							
CLIENT N/A							
COMPANION DRAWINGS C1398, C1399						REV. 1	
PROJECT No. 5014				DRAWING No.			
P.O. No. N/A				C1397 SH1. 5 OF 7 (E.I.D. 2885)			

FIGURE WITHHELD AS SENSITIVE UNCLASSIFIED INFORMATION

NOV. 16-99	1	INCORPORATED ECD/ SHORT/MISC. CHANGES	S. GEE 11-16-99	<i>B.G.U.</i> 11/19/99	<i>B.G.</i> 11/19/99	<i>V.G.</i> 11/19/99	
FEB 17-99	0	FOR APPROVAL	C.Y. 2-17-99	B.G.U. 2-20-99	B.G. 2-20-99	V.G. 2-20-99	
DATE	REV.	DESCRIPTION	PREP. BY:	CHECKED BY:	ENG.	Q. A.	
REVISION							
			EQUIPMENT DESIGN				
			ANALYSIS				
			CONSULTING				
HOLTEC INTERNATIONAL							
DESCRIPTION							
DETAIL OF SHEAR RING AND CLOSURE PLATE BOLT INSTALLATION OF HI-STAR 100 OVERPACK CoC No. 9261, APPENDIX B							
CLIENT N/A							
COMPANION DRAWINGS C1398, C1399						REV. 1	
PROJECT No. 5014				DRAWING No.			
P.O. No. N/A				C1397 SHT. 6 OF 7			

FIGURE WITHHELD AS SENSITIVE UNCLASSIFIED INFORMATION

NOV 17-99	1	REVISED AS SHOWN	S. GEE 11-17-99	<i>Handwritten initials</i>	<i>Handwritten initials</i>	<i>Handwritten initials</i>	<i>Handwritten initials</i>
FEB 17-99	0	FOR APPROVAL	C. Y. 2-17-99	B. G. U. 2-20-99	B. G. 11-20-99	W. G. 11-20-99	
DATE	REV.	DESCRIPTION	PREP. BY:	CHECKED BY:	ENG.	Q. A.	
REVISION							
			EQUIPMENT DESIGN				
			ANALYSIS				
HOLTEC			CONSULTING				
INTERNATIONAL							
DESCRIPTION							
DETAIL OF SHEAR RING OF HI-STAR 100 OVERPACK CoC No. 9261, APPENDIX B							
CLIENT N/A							
COMPANION DRAWINGS C1398, C1399						REV. 1	
PROJECT No. 5014				DRAWING No.			
P.O. No. N/A				C1397 SHT. 7 OF 7			

FIGURE WITHHELD AS SENSITIVE UNCLASSIFIED INFORMATION

NOV. 17-99	1	REVISED AS SHOWN	S. GEE 11-17-99	<i>[Handwritten]</i>	<i>[Handwritten]</i>	<i>[Handwritten]</i>	<i>[Handwritten]</i>
FEB 17-99	0	FOR APPROVAL	C. Y. 2-17-99	B. G. U. 2-20-99	B. G. 2-20-99	V. G. 2-20-99	
DATE	REV.	DESCRIPTION	PREP. BY:	CHECKED BY:	ENG.	Q. A.	
REVISION							
				EQUIPMENT DESIGN			
				ANALYSIS			
				CONSULTING			
HOLTEC INTERNATIONAL							
DESCRIPTION							
HI-STAR 100 OVERPACK ORIENTATION CoC No. 9261, APPENDIX B							
CLIENT N/A							
COMPANION DRAWINGS C1397, C1399						REV. 1	
PROJECT No. 5014				DRAWING No.			
P.O. No. N/A				C1398 SHT. 1 OF 3			

FIGURE WITHHELD AS SENSITIVE UNCLASSIFIED INFORMATION

NOV 5-99	1	REVISED AS SHOWN	S. GEE 11-5-99	<i>[Signature]</i>	<i>[Signature]</i>	<i>[Signature]</i>	<i>[Signature]</i>
FEB 17-99	0	FOR APPROVAL	C. Y. 2-17-99	B. G. U. 2-20-99	B. G. 2-20-99	V. G. 2-20-99	
DATE	REV.	DESCRIPTION	PREP. BY:	CHECKED BY:	P. M.	Q. A.	
REVISION							
REVISION							
<input type="checkbox"/> <input type="checkbox"/> <input type="checkbox"/> <input type="checkbox"/> <input type="checkbox"/>							
EQUIPMENT DESIGN							
ANALYSIS							
HOLTEC INTERNATIONAL CONSULTING							
DESCRIPTION							
DETAIL OF DRAIN & RUPTURE DISK OF HI-STAR 100 OVERPACK CoC No. 9261, APPENDIX B							
CLIENT N/A							
COMPANION DRAWINGS C1397, C1399							REV. 1
PROJECT No. 5014				DRAWING No.			
P.O. No. N/A				C1398 SHT. 2 OF 3			

FIGURE WITHHELD AS SENSITIVE UNCLASSIFIED INFORMATION

NOV 5-99	1	REVISED AS SHOWN	S. GEE 11-5-99	<i>[Handwritten initials]</i>	<i>[Handwritten initials]</i>	<i>[Handwritten initials]</i>
FEB 17-99	0	FOR APPROVAL	C. Y. 2-17-99	B. G. U. 2-20-99	B. G. 2-20-99	V. G. 2-20-99
DATE	REV.	DESCRIPTION	PREP. BY:	CHECKED BY:	P. M.	Q. A.
REVISION						
<input type="checkbox"/> <input type="checkbox"/> <input type="checkbox"/> <input type="checkbox"/> <input type="checkbox"/> <input type="checkbox"/>						
EQUIPMENT DESIGN						
HOLTEC ANALYSIS						
INTERNATIONAL CONSULTING						
DESCRIPTION						
DETAIL OF VENT & PORT PLUG OF HI-STAR 100 OVERPACK CoC No. 9261, APPENDIX B						
CLIENT N/A						
COMPANION DRAWINGS						REV.
C1397, C1399						1
PROJECT No. 5014				DRAWING No.		
P.O. No. N/A				C1398 SHT. 3 OF 3		

FIGURE WITHHELD AS SENSITIVE UNCLASSIFIED INFORMATION

NOV. 5-99	1	REVISED AS SHOWN	S. GEE 11-5-99	<i>B.H.H.</i>	<i>A. D. [unclear]</i>	
FEB 18-99	0	FOR APPROVAL	C. Y. 2-18-99	B. G. U. 2-20-99	B. G. 2-20-99	V. G. 2-20-99
DATE	REV.	DESCRIPTION	PREP. BY:	CHECKED BY:	P. M.	Q. A.
REVISION						
<input type="checkbox"/> <input type="checkbox"/> <input type="checkbox"/> <input type="checkbox"/> <input type="checkbox"/>			EQUIPMENT DESIGN			
HOLTEC			ANALYSIS			
INTERNATIONAL			CONSULTING			
DESCRIPTION						
SECTION "G" - "G" OF HI-STAR 100 OVERPACK CoC No. 9261, APPENDIX B						
CLIENT N/A						
COMPANION DRAWINGS C1397, C1398					REV. 1	
PROJECT No. 5014				DRAWING No.		
P.O. No. N/A				C1399 SHT. 1 OF 3		

FIGURE WITHHELD AS SENSITIVE UNCLASSIFIED INFORMATION

NOV 5-99	1	REVISED AS SHOWN	S. GEE 11-5-99	<i>[Handwritten initials]</i>	<i>[Handwritten initials]</i>	<i>[Handwritten initials]</i>
FEB 18-99	0	FOR APPROVAL	C. Y. 2-18-99	B. G. U. 2-20-99	B. G. 2-20-99	V. G. 2-20-99
DATE	REV.	DESCRIPTION	PREP. BY:	CHECKED BY:	P. M.	Q. A.
REVISION						
			EQUIPMENT DESIGN			
			ANALYSIS			
HOLTEC			CONSULTING			
INTERNATIONAL						
DESCRIPTION						
SECTION "X"- "X" & VIEW "Y" OF HI-STAR 100 OVERPACK CoC No. 9261, APPENDIX B						
CLIENT N/A						
COMPANION DRAWINGS C1397, C1398						REV. 1
PROJECT No. 5014				DRAWING No.		
P.O. No. N/A				C1399 SHT. 2 OF 3		

FIGURE WITHHELD AS SENSITIVE UNCLASSIFIED INFORMATION

FEB. 4-2000	2	INCORPORATED ELD 1020-4	S. GEE 2-4-2000	<i>noted for 2/4/00</i>	<i>ES.</i>	<i>2/4/00</i>	<i>2/4/00</i>
NOV 5-99	1	REVISED AS SHOWN	S. GEE 11-5-99	B. G. U. 2-20-99	B. G. 2-20-99	Y. G. 2-20-99	
FEB 18-99	0	FOR APPROVAL	C. Y. 2-18-99	B. G. U. 2-20-99	B. G. 2 20 99	Y. G. 2 20 99	
DATE	REV.	DESCRIPTION	PREP. BY:	CHECKED BY:	P. N.	Q. A.	
REVISION							
				EQUIPMENT DESIGN			
				ANALYSIS			
				CONSULTING			
DESCRIPTION							
DETAIL OF TRUNNION POCKET FORGING OF HI-STAR 100 OVERPACK CoC No. 9261, APPENDIX B							
CLIENT N/A							
COMPANION DRAWINGS C1397, C1398						REV. 2	
PROJECT No. 5014				DRAWING No.			
P.O. No. N/A				C1399 SHT. 3 OF 3 (E.I.D. 2884)			

FIGURE WITHHELD AS SENSITIVE UNCLASSIFIED INFORMATION

NOV 6-99	1	REVISED AS SHOWN	S.GEE 11-6-99	<i>blu</i>	<i>11/19/99</i>	<i>11/19/99</i>	<i>11/19/99</i>
FEB 18-99	0	FOR APPROVAL	C.Y. 2-18-99	B.G.U. 2-20-99	B.G. 2-20-99	V.G. 2-20-99	
DATE	REV.	DESCRIPTION	PREP. BY:	CHECKED BY:	P.M.	Q. A.	
REVISION							
<input type="checkbox"/>	<input type="checkbox"/>	<input type="checkbox"/>	<input type="checkbox"/>	<input type="checkbox"/>	EQUIPMENT DESIGN		
HOLTEC				ANALYSIS			
INTERNATIONAL				CONSULTING			
DESCRIPTION							
HI-STAR 100 MPC-68 CONSTRUCTION CoC No 9261, APPENDIX B							
CLIENT N/A							
COMPANION DRAWINGS C1402						REV. 1	
PROJECT No. 5014				DRAWING No.			
P.O. No. N/A				C1401 SET 1 OF 4			

FIGURE WITHHELD AS SENSITIVE UNCLASSIFIED INFORMATION

NOV 6-99	1	REVISED AS SHOWN	S. GEE 11-6-99	<i>11/2/99</i>	<i>11/2/99</i>	<i>11/2/99</i>
FEB. 18-99	0	FOR REVIEW	C.Y. 2-18-99	B.G.U. 2-20-99	B.G. 2-20-99	Y.G. 2-20-99
DATE	REV.	DESCRIPTION	PREP. BY:	CHECKED BY:	P.M.	Q.A.
REVISION						
<input type="checkbox"/> <input type="checkbox"/> <input type="checkbox"/> <input type="checkbox"/> <input type="checkbox"/>						
EQUIPMENT DESIGN HOLTEC INTERNATIONAL						
ANALYSIS CONSULTING						
DESCRIPTION						
HI-STAR 100 MPC-68 CONSTRUCTION CoC No. 9261, APPENDIX B						
CLIENT N/A						
COMPANION DRAWINGS C1402					REV. 1	
PROJECT No. 5014				DRAWING No.		
P.O. No. N/A				C1401 SHT. 2 OF 4		

FIGURE WITHHELD AS SENSITIVE UNCLASSIFIED INFORMATION

NOV. 18-99	1	FOR REVIEW	J.A. 11-18-99	<i>Bike</i>	<i>B.G.</i>	<i>A.G.</i>	<i>W.S.</i>
FEB 18-99	0	FOR APPROVAL	C.Y. 2-18-99	B.G. 2-20-99	B.G. 2-20-99	V.G. 2-20-99	
DATE	REV.	DESCRIPTION	PREP. BY:	CHECKED BY:	ENG.	Q. A.	
REVISION							
				EQUIPMENT DESIGN			
				ANALYSIS			
HOLTEC				CONSULTING			
INTERNATIONAL							
DESCRIPTION							
HI-STAR 100 MPC-68 CONSTRUCTION CoC No. 9261, APPENDIX B							
CLIENT N/A							
COMPANION DRAWINGS						REV.	
C1402						1	
PROJECT No. 5014				DRAWING No.			
P.O. No. N/A				C1401 SHT 3 OF 4			

FIGURE WITHHELD AS SENSITIVE UNCLASSIFIED INFORMATION

NOV 6-99	1	REVISED AS SHOWN	S.GEE 11-6-99	<i>B/G</i>	<i>W/G</i>	<i>Y.G.</i>
FEB 18-99	0	FOR APPROVAL	C.Y. 2-18-99	B.G.U. 2-20-99	B.G. 2-20-99	Y.G. 2-20-99
DATE	REV.	DESCRIPTION	PREP- BY:	CHECKED BY:	P.M.	Q. A.
REVISION						
<input type="checkbox"/>	<input type="checkbox"/>	<input type="checkbox"/>	<input type="checkbox"/>	<input type="checkbox"/>	EQUIPMENT DESIGN	
HOLTEC			ANALYSIS			
INTERNATIONAL			CONSULTING			
DESCRIPTION						
HI-STAR 100 MPC-68 CONSTRUCTION						
CoC No. 9261, APPENDIX B						
CLIENT N/A						
COMPANION DRAWINGS						REV.
C1402						1
PROJECT No. 5014				DRAWING No.		
P.O. No. N/A				C1401 SHT 4 OF 4		

FIGURE WITHHELD AS SENSITIVE UNCLASSIFIED INFORMATION

NOV 6-99	1	REVISED AS SHOWN	S.GEE 11-6-99	<i>[Signature]</i>	<i>[Signature]</i>	
FEB 18-99	0	FOR APPROVAL	C.Y. 2-18-99	B.S.U. 2-20-99	B.G. 2-20-99	V.G. 2-20-99
DATE	REV.	DESCRIPTION	PREP. BY:	CHECKED BY:	P.M.	Q. A.
REVISION						
<input type="checkbox"/>	<input type="checkbox"/>	<input type="checkbox"/>	<input type="checkbox"/>	<input type="checkbox"/>	EQUIPMENT DESIGN	
					ANALYSIS	
					CONSULTING	
DESCRIPTION						
HI-STAR 100 MPC-68 CONSTRUCTION CoC NO. 9261, APPENDIX B						
CLIENT N/A						
COMPANION DRAWINGS C1401					REV. 1	
PROJECT No. 5014				DRAWING No.		
P.O. No. N/A				C1402 SHT 1 OF 6		

FIGURE WITHHELD AS SENSITIVE UNCLASSIFIED INFORMATION

REVISION	
<input type="checkbox"/> <input type="checkbox"/> <input type="checkbox"/> <input type="checkbox"/> <input type="checkbox"/>	EQUIPMENT DESIGN
HOLTEC	ANALYSIS
INTERNATIONAL	CONSULTING
DESCRIPTION	
HI-STAR 100 MPC-68 CONSTRUCTION CoC No. 9261, APPENDIX B	
CLIENT N/A	
COMPANION DRAWINGS	REV.
C1401	1
PROJECT No. 5014	DRAWING No.
P.O. No. N/A	C1402 SHT 2 OF 6

A

FIGURE WITHHELD AS SENSITIVE UNCLASSIFIED INFORMATION

REVISION	
<input type="checkbox"/> <input type="checkbox"/> <input type="checkbox"/> <input type="checkbox"/> <input type="checkbox"/>	EQUIPMENT DESIGN
HOLTEC INTERNATIONAL	ANALYSIS CONSULTING
DESCRIPTION HI-STAR 100 MPC-68 CONSTRUCTION CoC No. 9261, APPENDIX B	
CLIENT N/A	
COMPANION DRAWINGS C1401	REV. 1
PROJECT No. 5014	DRAWING No.
P.O. No. N/A	C1402 SET 3 OF 6

A

FIGURE WITHHELD AS SENSITIVE UNCLASSIFIED INFORMATION

REVISION	
<input type="checkbox"/> <input type="checkbox"/> <input type="checkbox"/> <input type="checkbox"/> <input type="checkbox"/>	EQUIPMENT DESIGN
HOLTEC	ANALYSIS -
INTERNATIONAL	CONSULTING -
DESCRIPTION	
HI-STAR 100 MPC-68 CONSTRUCTION CoC NO. 9261, APPENDIX B	
CLIENT N/A	
COMPANION DRAWINGS C1401	REV. 1
PROJECT No. 5014	DRAWING No.
P.O. No. N/A	C1402 SHT 4 OF 8

A

FIGURE WITHHELD AS SENSITIVE UNCLASSIFIED INFORMATION

<input type="checkbox"/> <input type="checkbox"/> <input type="checkbox"/> <input type="checkbox"/> <input type="checkbox"/>		EQUIPMENT DESIGN	
HOLTEC		ANALYSIS	
INTERNATIONAL		CONSULTING	
DESCRIPTION			
HI-STAR 100 MPC-68 CONSTRUCTION CoC NO. 9261, APPENDIX B			
CLIENT N/A			
COMPANION DRAWINGS			REV.
C1401			0
PROJECT No. 5014		DRAWING No.	
P.O. No. N/A		C1402 SET 5 OF 6	

FIGURE WITHHELD AS SENSITIVE UNCLASSIFIED INFORMATION

<input type="checkbox"/> <input type="checkbox"/> <input type="checkbox"/> <input type="checkbox"/> <input type="checkbox"/>	EQUIPMENT DESIGN
HOLTEC	ANALYSIS -
INTERNATIONAL	CONSULTING -
DESCRIPTION HI-STAR 100 MPC-68 CONSTRUCTION CoC No. 9261, APPENDIX B	
CLIENT N/A	
COMPANION DRAWINGS C1401	REV. 1
PROJECT No. 5014	DRAWING No.
P.O. No. N/A	C1402 SHT 6 OF 6

A

FIGURE WITHHELD AS SENSITIVE UNCLASSIFIED INFORMATION



CONSULT OF HOLTEC INTERNATIONAL.	
	EQUIPMENT DESIGN ANALYSIS CONSULTING
DESCRIPTION HI-STAR 100 IMPACT LIMITER CoC No. 9261, APPENDIX B	
CLIENT VARIOUS	
COMPANION DRAWINGS NONE	REV. 1
PROJECT No. 5014	DRAWING No.
P.O. No. VARIOUS	C1765 SHT. 1 OF 7

FIGURE WITHHELD AS SENSITIVE UNCLASSIFIED INFORMATION

<small>PROPERTY OF HOLTEC INTERNATIONAL</small>	
 HOLTEC INTERNATIONAL	EQUIPMENT DESIGN ANALYSIS CONSULTING
DESCRIPTION HI-STAR 100 BOTTOM IMPACT LIMITER CoC No. 9261, APPENDIX B	
CLIENT VARIOUS	
COMPANION DRAWINGS NONE	REV. 1
PROJECT No. 5014	DRAWING No.
P.O. No. VARIOUS	C1765 SHT. 2 OF 7

e:\DRAWINGS\5014\5014\IMPACT\C1765-2.R1

FIGURE WITHHELD AS SENSITIVE UNCLASSIFIED INFORMATION


 HOLTEC INTERNATIONAL	EQUIPMENT DESIGN ANALYSIS CONSULTING
DESCRIPTION HI-STAR 100 TOP IMPACT LIMITER CoC No. 9261, APPENDIX B	
CLIENT VARIOUS	
COMPANION DRAWINGS NONE	REV. 1
PROJECT No. 5014 P.O. No. VARIOUS	DRAWING No. C1765 SHT. 3 OF 7

FIGURE WITHHELD AS SENSITIVE UNCLASSIFIED INFORMATION



CONSENT OF HOLTEC INTERNATIONAL.	
	EQUIPMENT DESIGN ANALYSIS CONSULTING
DESCRIPTION HI-STAR 100 TOP IMPACT LIMITER CoC No.9261, APPENDIX B	
CLIENT VARIOUS	
COMPANION DRAWINGS NONE	REV. 1
PROJECT No.5014	DRAWING No.
P.O. No. VARIOUS	C1765 SHT. 4 OF 7

FIGURE WITHHELD AS SENSITIVE UNCLASSIFIED INFORMATION

		EQUIPMENT DESIGN	
		ANALYSIS	
		CONSULTING	
DESCRIPTION			
HI-STAR 100 TOP IMPACT LIMITER			
DETAIL OF ITEM #6			
CoC No. 9261, APPENDIX B			
CLIENT			
VARIOUS			
COMPANION DRAWINGS			REV.
NONE			1
PROJECT No. 5014		DRAWING No.	
P.O. No. VARIOUS		C1765 SHT. 5 OF 7	

e:\DRAWINGS\5014\5014\IMPACT\C1765-5.R1

FIGURE WITHHELD AS SENSITIVE UNCLASSIFIED INFORMATION


 HOLTEC INTERNATIONAL	EQUIPMENT DESIGN ANALYSIS CONSULTING
DESCRIPTION HI-STAR 100 IMPACT LIMITER HONEYCOMB DETAILS CoE No. 9261, APPENDIX B	
CLIENT VARIOUS	
COMPANION DRAWINGS NONE	REV. 1
PROJECT No. 5014 P.O. No. VARIOUS	DRAWING No. C1765 SH. 6 OF 7

FIGURE WITHHELD AS SENSITIVE UNCLASSIFIED INFORMATION

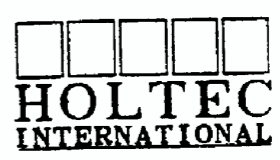
 HOLTEC INTERNATIONAL	EQUIPMENT DESIGN ANALYSIS CONSULTING
DESCRIPTION HI-STAR 100 BOTTOM IMPACT LIMITER CoC No. 9261, APPENDIX B -	
CLIENT VARIOUS	
COMPANION DRAWINGS NONE	REV. 0
PROJECT No. 5014	DRAWING No.
P.O. No. VARIOUS	C1765 SHT. 7 OF 7

FIGURE WITHHELD AS SENSITIVE UNCLASSIFIED INFORMATION

□□□□□		EQUIPMENT DESIGN	
HOLTEC		ANALYSIS	
INTERNATIONAL		CONSULTING	
DESCRIPTION			
HI-STAR 100 ASSEMBLY FOR TRANSPORT CoC No. 9261, APPENDIX B			
CLIENT N/A			
COMPANION DRAWINGS			REV.
---			1
PROJECT No. 5014		DRAWING No.	
P.O. No. N/A		C1782	

BILL OF MATERIALS FOR HI-STAR 100 OVERPACK (BM-C1476)

REF. DWGS. C1397, C1398 & C1399.

SHEET 1 OF 2

REV. NO.	PREP. BY & DATE	CHECKED BY DATE	PROJ. MANAGER & DATE	QA. MANAGER & DATE
1	S. GEE 11-18-99 INCORPORATED ECO/ SMOR/MISC CHANGES	<i>B. G.</i> 11/24/99	<i>B. G.</i> 11/24/99	<i>M. G.</i> 11/24/99
ITEM NO.	QTY.	MATERIAL	DESCRIPTION	NOMENCLATURE
1	1	SA-350 LF3	12" THK. BASE PLATE	BOTTOM PLATE
2	1	SA-203-E	2 1/2" THK. PLATE	INNER SHELL
3	20	SA-515 GRADE 70	1/2" THK. PLATE	ENCLOSURE SHELL PANELS
4	20	SA-515 GRADE 70	1/2" THK.	RADIAL CHANNELS
5	2	SA-705 630 17-4 PH OR SA-564 630 17-4 PH	FORGING	POCKET TRUNNION
6	4	SA-193 GRADE B7	SOCKET SET SCREW	CLOSURE PLATE PLUG
7	2	SB-637-N07718	BAR	LIFTING TRUNNION
8	1	SA-350 LF3	FORGING	TOP FLANGE
9	2	SA-203-E OR SA-350-LF3	1 1/2" THK.	REMOVEABLE SHEAR RING
10	1	SA-350 LF3	6" THK.	CLOSURE PLATE
11	2	SB-637-N07718	1 5/8" - 8 UN CAP SCREW	CLOSURE PLATE SHORT BOLT
12	1	SA-516 GRADE 70	1 1/4" THK. PLATE	INTERMEDIATE SHELL #1
13	1	SA-516 GRADE 70	1 1/4" THK. PLATE	INTERMEDIATE SHELL #2
14	1	SA-516 GRADE 70	1 1/4" THK. PLATE	INTERMEDIATE SHELL #3
15	1	SA-516 GRADE 70	1 1/4" THK. PLATE	INTERMEDIATE SHELL #4
16	1	SA-516 GRADE 70	1" THK. PLATE	INTERMEDIATE SHELL #5
17	2	SA-515 GRADE 70	1/2" THK. PLATE	ENCLOSURE SHELL RETURN
18	2	SA-193 GRADE B8	BAR	PORT PLUG
19	3	ALLOY X750	SPRING ENERGIZED SEAL.	PORT PLUG SEAL
20	4	SA-193 GRADE B7	SOCKET CAP SCREW	TRUNNION LOCKING PAD BOLT
21	2	SA-516 GRADE 70	1/2" THK. PLATE	LIFTING TRUNNION END CAP
22	4	SA-193 GRADE B7	BOLTS	TRUNNION END CAP BOLT
23	2	SA-516 GRADE 70	3/8" THK. PLATE	LIFTING TRUNNION LOCKING PAD
24	AS REQ.	HOLTITE - A	HOLTITE-A	NEUTRON SHIELD
25	8	SA-193 GRADE B7	SOCKET SET SCREW	REMOVEABLE SHEAR RING PLUG
26	1	COMMERCIAL	SELF ENERGIZED SEAL	CLOSURE PLATE INNER SEAL



BILL OF MATERIALS FOR HI-STAR 100 OVERPACK (BM-C1476) (E.I.D. 2883)

REF. DWGS. C1397, C1398 & C1399.

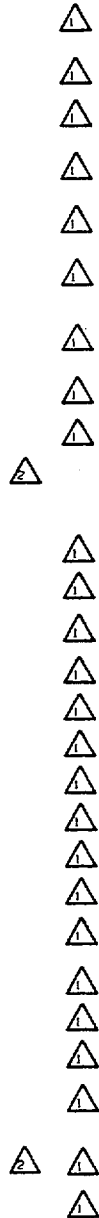
SHEET 2 OF 2

REV. NO.	PREP. BY & DATE	CHECKED BY DATE	PROJ. MANAGER & DATE	QA. MANAGER & DATE
2	S. GEE 2-4-2000 INCORPORATED ECO 1020-4	<i>note</i> BG. 2/4/00	<i>Bm</i> 2/4/00	<i>M. G.</i> 2/4/00

ITEM NO.	QTY.	MATERIAL	DESCRIPTION	NOMENCLATURE
27	1	COMMERCIAL	SELF ENERGIZED SEAL.	CLOSURE PLATE OUTER SEAL
28	2	SA-350-LF3 LR SA-203-E	1 1/2" THK. PLATE	PORT COVER
29	8	SA-193 GRADE B7	3/8 - 16 UNC SCREW	PORT COVER BOLT
30	2	ALLOY X750	SPRING ENERGIZED SEAL.	PORT COVER SEAL
31	--	---	DELETED	---
32	52	SB-637-N07718	1 5/8" - 8 UN CAP SCREW	CLOSURE PLATE LONG BOLT
33	2 (MIN.)	COMMERCIAL	RUPTURE DISK	RUPTURE DISK
34	8	SA-193 GRADE B7	3/8" - 16 UNC SCREW	REMOVEABLE SHEAR RING BOLT
35	1	SA-193 GRADE B8	7/8" Ø BAR	DRAIN PORT PLUG
36	AS REQD	SA 515 GR. 70	1/2" THK PLATE	POCKET TRUNNION SURROUND
37	AS REQD	SILICONE FOAM	TYPE HT-870 (BISCO PRODUCTS) OR EQUIVALENT	THERMAL EXPANSION FOAM
38	--	---	DELETED	---
39	2	SA-516 GRADE 70 OR A569	11 GAGE (1/8" THK.)	RUPTURE DISK PLATE
40	1	SA 240 304	14 GAGE (0.0751" THK.) SHEET	STORAGE MARKING NAME PLATE
41	1	SA 240 304	14 GAGE (0.0751" THK.) SHEET	TRANSPORTATION MARKING NAME PLATE
42	AS REQD	SA515-70	AS REQUIRED	BRIDGE
43	2	SA 240 304	11 GAGE (1/8" THK.) SHEET	POCKET TRUNNION PLUG PLATE
44	2	SA 240 304	11 GAGE (1/8" THK.) SHEET.	POCKET TRUNNION PLUG PLATE
45	2	SA 240 304	11 GAGE (1/8" THK.) SHEET.	POCKET TRUNNION PLUG PLATE
46	2	SA 240 304	11 GAGE (1/8" THK.) SHEET.	POCKET TRUNNION PLUG PLATE
47	2	SA 240 304	11 GAGE (1/8" THK.) SHEET.	POCKET TRUNNION PLUG PLATE
48	4	SA-193 GRADE B7	3/8 - 16 UNC SCREW	POCKET TRUNNION PLUG SCREW
49	54	S/S	11 GAGE (1/8" THK.) SHEET.	CLOSURE BOLT WASHER
50	40	SA-193-B7	1 3/4"-5UNC SOCKET SET SCREW	TOP FLG. LIP HOLE PLUGS
51	20	SA-193-B7	1"-8UNC SOCKET SET SCREW	TOP FLG. SIDE HOLE PLUGS
52	16	SA-193-B7	1 3/4"-8UNC SOCKET SET SCREW	BOTTOM PLATE HOLE PLUGS
53	8	SA-193-B7	2 1/2"-4UN X 2 1/2 LG SOCKET SET SCREW	THREADED PLUG
54	4	SA-193-B7	1/2-13UNC SOCKET SET SCREW	THREADED PLUG

NOTES:

- 1) ALL DIMENSIONS ARE APPROXIMATE.
- 2) HOLTITE IS A NEUTRON SHIELD MATERIAL WITH NOMINALLY 1 WT. % B₄C, 6 WT. % H, AND A DENSITY OF 1.68g/cm³.
- 3) ITEMS 12 THRU 16, MATERIAL SA-516-GR 70 IS TO BE NORMALIZED
- 4) THICKNESS OF ITEM 16 MAY VARY DEPENDING ON THICKNESSES OF ITEMS 12-15.
- 5) ITEMS 2, 12-17 MAY BE MADE FROM MORE THAN ONE PIECE.

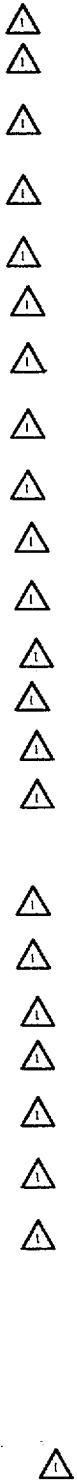


BILL OF MATERIALS FOR 24-ASSEMBLY HI-STAR 100 PWR MPC.(BM-C1478)

REF. DWG. C1395 & C1396.

SHEET 1 OF 2

REV. NO.	PREP. BY & DATE		CHECKED BY & DATE	PROJ. MANAGER & DATE	QA. MANAGER & DATE
1	S.GEE 11-3-99 REVISED AS INDICATED		<i>Ben Smith</i> 11/19/99	<i>NOVA</i> S.G. 11/19/99	<i>MLC</i> MS 11/19/99
ITEM NO.	QTY.	MATERIAL	DESCRIPTION		NOMENCLATURE
1A	2	ALLOY "X" SEE NOTE 1.	PLATE 5/16" THK.		BASKET CELL PLATE
1B	1		PLATE 5/16" THK		BASKET CELL PLATE
1C	2		PLATE 5/16" THK		BASKET CELL PLATE
1D	1		PLATE 5/16" THK		BASKET CELL PLATE
1E	1		PLATE 5/16" THK		BASKET CELL PLATE
1F	22		PLATE 5/16" THK		BASKET CELL PLATE
1G	1		PLATE 5/16" THK		BASKET CELL PLATE
1H	2		PLATE 5/16" THK		BASKET CELL PLATE
2	24	▽	PIPE 3"-SCH 80 LGTH AS REQD.		UPPER FUEL SPACER PIPE
3A (3B)	B4(12)	BORAL	.075" THK.		NEUTRON ABSORBER
4A (4B)	B4(12)	ALLOY "X" SEE NOTE 1.	.06" THK. SHEATHING		SHEATHING
5A	4		PLATE 5/16" THK		BASKET CELL PLATE
5B	4		PLATE 5/16" THK		BASKET CELL PLATE
5C	4		PLATE 1.5" APP. THK.		BASKET SUPPORT
5D	4		2 1/2" W		BASKET SUPPORT
5E	4		2" WIDE X THICKNESS AS REQD.		BASKET SUPPORT
5F	-		DELETED		---
5G	4		1 1/4" W X THICKNESS AS REQUIRED		BASKET SUPPORT SHIM
5H	---		DELETED		----
6	1		1/2" THK CYLINDER.		SHELL
7	1		BASEPLATE 2 1/2" THK		BASEPLATE
8A	22		9/32" THK. ANGLE		BASKET CELL ANGLE
8B	2		9/32" THK. CHANNEL		BASKET CELL CHANNEL
9A	1		5/16" THK. PLATE		BASKET SUPPORT
9B	2		5/16" THK. PLATE		BASKET SUPPORT
9C	1		5/16" THK. PLATE		BASKET SUPPORT
9D	AS REQD		AS REQUIRED		BASKET SUPPORT
9E	----		DELETED		---
9F	---		DELETED		---
9G	---		DELETED		---
9H	---		DELETED		---
10	4	▽	PLATE 3/4" THK.		LIFT LUG



BILL OF MATERIALS FOR 24-ASSEMBLY HI-STAR 100 PWR MPC.(BM-C1478)

REF. DWG. C1395 & C1396.

SHEET 2 OF 2

REV. NO.	PREP. BY & DATE	CHECKED BY & DATE	PROJ. MANAGER & DATE	QA. MANAGER & DATE
1	S. GEE 11-3-99 REVISED AS INDICATED	<i>B. G. Guthrie</i> 11/22/99	<i>W. G. G.</i> 11/22/95	<i>M. G. G.</i> 11/22/99
ITEM NO.	QTY.	MATERIAL	DESCRIPTION	NOMENCLATURE
11	4	ALLOY *X* SEE NOTE 1.	PLATE 3/4" THK.	LIFT LUG BASEPLATE
12	1	ALLOY *X* SEE NOTE 1.	BAR 3.75" OD.	DRAIN SHIELD BLOCK
13A	2	304 S/S	BAR 2 11/16" OD	VENT AND DRAIN TUBE
13B	2	304 S/S	BAR 2 1/4" OD	VENT AND DRAIN TUBE CAP
14	1	ALLOY *X* SEE NOTE 1.	9 1/2" THK.	MPC LID
15	1	▽	RING 3/8" THK.	MPC CLOSURE RING
16	---	----	DELETED	---
17	----	----	DELETED	----
18	AS REQD	ALLOY *X* SEE NOTE 1.	AS REQUIRED	BASKET SUPPORT SHIM
19	2	ALLOY *X* SEE NOTE 1.	PLATE 3/8" THK.	PORT COVER PLATE
20	24	A-193-B8 OR SIMILAR	3/4"-LONG LG. BOLT	UPPER FUEL SPACER BOLT
21	AS REQD	ALLOY *X* SEE NOTE 1.	3/4" X 2" X THICKNESS AS REQUIRED	LIFT LUG SHIM
22	---	---	DELETED	---
23	4	A-193-B8 OR SIMILAR	1 3/4"-SUNC SCREW	LID LIFT HOLE PLUG
24	24	ALLOY *X* SEE NOTE 1.	PLATE 3/8" THK	UPPER FUEL SPACER END PLATE
25	1 SET	ALLOY *X* SEE NOTE 1.	LENGTH, WIDTH AND THICKNESS OF SHIMS AS REQUIRED.	LID SHIM
26	1	S/S	COUPLING	COUPLING
27	AS REQD	ALLOY *X* SEE NOTE 1.	3/4" PLATE	UPPER FUEL SPACER END PLATE
28	1	ALLOY *X* SEE NOTE 1.	BAR 3.75" OD.	VENT QUICK DISCONN. CPLG.
29	4	ALLOY *X* SEE NOTE 1.	BAR 3/4" OD.	VENT SHIELD BLOCK SPACER
30	1	ALLOY *X* SEE NOTE 1.	2"-SCH 10 PIPE X 173 1/2" APPROX. LG.	DRAIN LINE
31	--	-----	DELETED	-----
32	24		6" SQ. TUBING X 1/4" WALL LENGTH AS REQ'D.	LOWER FUEL SPACER COLUMN
33A	24		PLATE 3/8" THK	LOWER FUEL SPACER END PLATE
33B	24	▽	PLATE 3/8" THK	LOWER FUEL SPACER END PLATE
35	AS REQ'D.	ALUM. ALLOY 1100 & S/S	1/8" THICK X 176 1/2" LG. ALUM. SHEET WITH S/S SPRINGS	HEAT CONDUCTION ELEMENTS
36	2	ALUMINUM	0.065" THK SHI	SEAL WASHER
37	2	S/S	1/4" DIA BAR	SEAL WASHER BOLT
38	2	ALLOY *X* SEE NOTE 1.	1/8" THK	DRAIN LINE
39	8	ALLOY *X* SEE NOTE 1.	1/8" THK	DRAIN LINE

NOTES: (FOR SHEET 1 & 2)

1. ALLOY X IS ANY OF THE FOLLOWING ACCEPTABLE STAINLESS STEEL ALLOYS: ASME TYPE 316, 316LN, 304, 304LN. THE ALLOY TO BE USED SHALL BE SPECIFIED BY THE LICENSEE.
2. MINIMUM BORAL B-10 LOADING IS 0.0267 g/cm². BORAL TO BE PASSIVATED PRIOR TO INSTALLATION.
3. ALL DIMENSIONS ARE APPROXIMATE DIMENSIONS.
4. ITEMS 30, 32, 35, 36, 37, 38, 39, 16, 18, 34 AND 35 MAY BE MADE FROM MORE THAN ONE PIECE. THE ENDS OF PIECES DO NOT NEED TO BE WELDED TOGETHER BUT THEY MUST BE FLUSH WITH EACH OTHER WHEN INSTALLED.

BILL OF MATERIALS FOR 68-ASSEMBLY HI-STAR 100 BWR MPC.(BM-C1479)

REF. DWGS. C1401 & C1402.

SHEET 1 OF 2

REV. NO.	PREP. BY & DATE	CHECKED BY DATE	PROJ. MANAGER & DATE	QA. MANAGER & DATE
1	S.GEE 11-3-99 REVISED AS INDICATED	<i>B. G. G.</i> 11/22/99	<i>B. G. G.</i> 11/22/99	<i>M. C.</i> 11/22/99
ITEM NO.	QTY.	MATERIAL	DESCRIPTION	NOMENCLATURE
1A	3	ALLOY "X" SEE NOTE 1.	PLATE 1/4" THK.	BASKET CELL PLATE
1B	4		PLATE 1/4" THK.	BASKET CELL PLATE
1C	2		PLATE 1/4" THK.	BASKET CELL PLATE
1D	2		PLATE 1/4" THK.	BASKET CELL PLATE
1E	78		PLATE 1/4" THK.	BASKET CELL PLATE
2	68	▽	3" - SCH 80 PIPE LGTH AS REGD.	LIPPER FUEL SPCCR CLUMN
3A	116	BORAL	.101" THK.	NEUTRON ABSORBER
4A	116	ALLOY "X" SEE NOTE 1.	.075" THK. SHEATHING	SHEATHING
5	8		BAR 1" WIDE X 168" LG X THICKNESS AS REQUIRED	BASKET SUPPORT SHIM
6	1		1/2" THK PLATE	SHELL
7	1		BASEPLATE 2 1/2" THK	BASEPLATE
8	8		PLATE 5/16" THK.	BASKET SUPPORT
9A	4		BAR 1" W.	BASKET SUPPORT
9B	---		DELETED	---
9C	8		2 1/2" WIDE PLATE	BASKET SUPPORT
9D	AS REGD		AS REQUIRED	BASKET SUPPORT
10	4		PLATE 3/4" THK.	LIFT LUG
11	4		PLATE 3/4" THK.	LIFT LUG BASEPLATE
12	1	▽	BAR 3.75" OD.	DRAIN SHIELD BLOCK
13A	2	304 S/S	BAR 2 11/16" OD	VENT AND DRAIN TUBE
13B	2	304 S/S	= BAR 2 1/4" OD	VENT AND DRAIN TUBE CAP
14	1	ALLOY "X" SEE NOTE 1.	10" THK. 10" THK.	MPC LID
15	1	ALLOY "X" SEE NOTE 1.	RING 3/8" THK. RING 3/8" THK.	MPC CLOSURE RING
16	---	---	DELETED	---



BILL OF MATERIALS FOR 68-ASSEMBLY HI-STAR 100 BWR MPC.(BM-C1479)

REF. DWGS. C1401 & C1402.

SHEET 2 OF 2

REV. NO.	PREP. BY & DATE	CHECKED BY DATE	PROJ. MANAGER & DATE	QA. MANAGER & DATE
1	S. GEE 11-3-99 REVISED AS INDICATED	<i>Ben Guther</i> 11/19/99	<i>nl gra</i> B.G. 11/19/99	<i>M Lee</i> ms 11/19/99
ITEM NO.	QTY.	MATERIAL	DESCRIPTION	NOMENCLATURE
17	1	ALLOY *X* SEE NOTE 1.	1" THK PLATE	SHELL (MPC-68F)
18	AS REQD	ALLOY *X* SEE NOTE 1.	AS REQUIRED	BASKET SUPPORT
19	2	ALLOY *X* SEE NOTE 1.	PLATE 3/8" THK	PORT COVER PLATE
20	68	A-193-88 OR SIMILAR	3/4"-10UNC HEX BOLT	UPPER FUEL SPACER BOLT
21	AS REQD	ALLOY *X* SEE NOTE 1.	3/4" W X 2' LG X THICKNESS AS REQUIRED	LIFT LUG SHIM
22	---	---	DELETED	---
23	4	A-193-88 OR SIMILAR	1 3/4"-5UNC SOCKET SET SCREW.	LIFT HOLE PLUG
24	68	ALLOY *X* SEE NOTE 1.	PLATE 3/8" THK	UPPER FUEL SPACER END PLATE
25	1 SET	ALLOY *X* SEE NOTE 1	LENGTH, WIDTH, THICKNESS AND QUANTITY AS REQD.	LTD SHIM
26	1	S/S	COUPLING	COUPLING
27			DELETED	
28	1	ALLOY *X* SEE NOTE 1.	BAR 3.75" OD.	VENT SHIELD BLOCK
29	4	ALLOY *X* SEE NOTE 1.	BAR .75" OD	VENT SHIELD BLOCK SPACER
30	1	ALLOY *X* SEE NOTE 1.	2"-SCH 10 PIPE X 173" APPROX.LG.	DRAIN LINE
31	--	--	DELETED	---
32	--	--	DELETED	---
33	68	ALLOY *X* SEE NOTE 1.	4" SO. TUBE X 1/4" WALL LENGTH AS REQD. (FOR SHORT FUEL ONLY)	LOWER FUEL SPACER COLUMN
34A	68	ALLOY *X* SEE NOTE 1.	3/8" THK. PLATE (FOR SHORT FUEL ONLY)	LOWER FUEL SPACER END PLATE
34B	68	ALLOY *X* SEE NOTE 1.	3/8" THK. PLATE (FOR SHORT FUEL ONLY)	LOWER FUEL SPACER END PLATE
35	-----	-----	DELETED	
36	-----	-----	DELETED	
37	AS REQD	ALUM. ALLOY 1100 & S/S	1/8" THK. ALUM. SHEET W/S/S SPRINGS.	HEAT CONDUCTION ELEMENTS
38	2	ALUMINIUM	.065" THK SHT	SEAL WASHER
39	2	S/S	1/4" DIA	SEAL WASHER BOLT
40	2	ALLOY *X* SEE NOTE 1	1/8" THK. SHEET	DRAIN LINE
41	8	ALLOY *X* SEE NOTE 1.	1/8" THK. SHEET	DRAIN LINE

NOTES: (FOR SHEET 1 & 2)

1. ALLOY X IS ANY OF THE FOLLOWING ACCEPTABLE STAINLESS STEEL ALLOYS. ASME TYPE 316, 316LN, 304, 304LN. THE ALLOY TO BE USED SHALL BE SPECIFIED BY THE LICENSEE.

2. BORAL B-10 LOADING IS 0.0372 g/cm². BORAL² TO BE PASSIVATED PRIOR TO INSTALLATION. FOR MPC-68F, MINIMUM BORAL B-10 LOADING IS 0.01 g/cm².

3. ALL DIMENSIONS ARE APPROXIMATE DIMENSIONS.

4. ITEMS 5, 8, 9A, 9C, 9D, 16, 18, AND 37 MAY BE MADE FROM MORE THAN ONE PIECE. THE ENDS OF PIECES DO NOT NEED TO BE WELDED TOGETHER BUT THEY MUST BE FLUSH WITH EACH OTHER WHEN INSTALLED.

Table 1.B.1

PROPERTIES OF HOLTITE-A NEUTRON SHIELD

PHYSICAL PROPERTIES (Reference: NAC International Brochure)	
% ATH	62 maximum (confirmed by Holtec in independent analyses)
Specific Gravity	1.68 g/cc nominal
Thermal Conductivity	0.373 Btu/hr/ft-°F
Max. Continuous Operating Temperature	300°F
Specific Heat [†]	0.39 Btu/lb-°F
Hydrogen Density	0.096 g/cc minimum (confirmed by Holtec in independent analyses)
Radiation Resistance	Excellent
Ultimate Tensile Strength	4,250 psi
Tensile elongation	0.65%
Ultimate Compression Strength	10,500 psi
Compression Yield Strength	8,780 psi
Compression Modulus	561,000 psi
CHEMICAL PROPERTIES (Nominal)	
wt% Aluminum	21.5 (confirmed by Holtec)
wt% Hydrogen	6.0 (confirmed by Holtec)
wt% Carbon	27.7
wt% Oxygen	42.8
wt% Nitrogen	2.0
wt% B ₄ C	up to 6.5 (Holtite-A uses 1% B ₄ C)

[†] BISCO Products Data from Docket M-55, NAC-STC TSAR.

Experimental Studies on Long-term Thermal Degradation of Enclosed Neutron Shielding Resin

Ryoji ASANO¹, Nagao NIOMURA²

¹Hitachi Zosen Corporation, Japan
²Ocean Cask Lease Co., Ltd, Japan

INTRODUCTION

Resins which have high Hydrogen atom content are effective for Neutron shielding and are recently used for neutron shielding material of spent fuel shipping casks. As the resins themselves are easily burned at relatively low temperature, which could be the problem during the fire test condition, mixture of resin and fire retardant which main component is a hydroxide compound is usually used as shielding material. The fire retardant prevents resin from burning by decomposing of the hydroxide compound under fire test condition.

When these resins are used for neutron shielding material of cask, their temperature rises during the transportation by decay heat of spent fuel. Therefore, thermal degradation of resin (hereafter called as "heat weight loss") at the operating temperature should be paid attention.

Furthermore, when the resin is used for neutron shielding material, there are two cases. One is to put it on the outside surface of the cask and the other is to enclose it between two layers. In former case, the heat weight loss occurs in air of which study report can be obtained. On the other hand, the latter is the reaction in the enclosed environment which study report can be seldom obtained. Therefore, the study of the heat weight loss in the enclosed environment was carried out for long term period assuming the operating time of the real cask .

TEST MATERIAL

Test material is NS-4-FR supplied by BISCO CO. LTD, U.S.A. Raw materials are epoxi resin, hardener and fire retardant. They are mixed together and hardened according to the manu-

APPENDIX 1.C: MISCELLANEOUS MATERIAL DATA
(Total of 8 Pages Including This Page)

The information provided in this appendix specifies the thermal expansion foam (silicone sponge), paint, and anti-seize lubricant properties and demonstrates their suitability for use in spent nuclear fuel storage casks. The following is a listing of the information provided.

- HT-800 Series, Silicone Sponge, Bisco Products Technical Data Sheet
- Thermaline 450, Carboline, Product Data Sheet and Application Instructions
- Carboline 890, Carboline, Product Data Sheet and Application Instructions
- FEL-PRO Technical Bulletin, N-5000 Nickel Based-Nuclear Grade Anti-Seize Lubricant

HT-870 silicone sponge is specified as a thermal expansion foam to be placed in the overpack outer enclosure with the neutron shield. Due to differing thermal expansion of the neutron shield and outer enclosure carbon steel, the silicone sponge is provided to compress and allow the neutron shield material to expand. The compression-deflection physical properties are provided for the silicone sponge.

Silicone has a long and proven history in the nuclear industry. Silicone is highly resistant to degradation as a result of radiation at the levels required for the HI-STAR 100 System. Silicone is inherently inert and stable and will not react with the metal surfaces or neutron shield material. Additionally, typical operating temperatures for silicone sponges range from -50° F to 400° F.

Thermaline 450 is specified to coat the inner cavity of the overpack and Carboline 890 is specified to coat the external surfaces of the overpack. As can be seen from the product data sheets, the paints are suitable for the design temperatures (see Table 2.2.3) and chemical environment.

Nuclear grade anti-seize lubricant, N-5000, from FEL-PRO is specified as the lubricant for the overpack closure bolts. The lubricant is formulated to have the lowest practical levels of halogens, sulfur, and heavy metals. NEVER-SEEZ NGBT provides equivalent properties to FEL-PRO N-5000 and is also acceptable for use on the HI-STAR 100 System.

HT-800 SERIES

Specification Grade
Silicone Sponge

PHYSICAL PROPERTIES

PROPERTY	SPECIFICATION			TEST METHOD
	HT-870 (Soft)	HT-800 (Medium)	HT-820 (Firm)	
Density	12 - 24 pcf	16 - 28 pcf	20 - 32 pcf	ASTM D-3574
Compression Force @ 25% Deflection	2 - 7 psi	6 - 14 psi	12 - 20 psi	ASTM D-1056
Compression Set (Maximum)	10%	10%	10%	ASTM D-1056 (Compressed 50% for 22 hrs. @ 100°C)
Water Absorption (Maximum)	10%	5%	5%	ASTM D-1056

Available Industry Specifications:

AMS-3195 (HT-800)

AMS-3196 (HT-820)

UL-94 (Limited to specific classes, densities, thicknesses and colors)

This is based on laboratory tests and should not be used for writing specifications. Each user should run independent tests to confirm material suitability for each specific application.

Bisco Products and Dow Corning neither represent nor use this material for medical device applications or for pharmaceutical end-use.

TABLE 2.0.1- MATRIX OF 10CFR71 COMPLIANCE – STRUCTURAL REVIEW (Continued)

SECTION IN NUREG-1617 AND APPLICABLE 10CFR71/REG.GUIDE (R.G.) SECTIONS	NUREG-1617/10CFR71 COMPLIANCE ITEM	LOCATION IN SAR CHAPTER 2	LOCATION OUTSIDE OF SAR CHAPTER
2.3.6 Hypothetical Accident Conditions			
10CFR71.73(c)(1)	Free Drop	2.7.1; 2.I; 2.J; 2.L; 2.N; 2.O; 2.U; 2.AC; 2.AE; 2.AF; 2.AH; 2.AO	
10CFR71.73(c)(2)	Crush	NA	NA
10CFR71.73(c)(3)	Puncture	2.7.2; 2.U	
10CFR71.73(c)(4)	Thermal	2.7.3; 2.G; 2.J; 2.L; 2.N	
10CFR71.73(c)(5)	Immersion-Fissile Material	2.7.4	NA
10CFR71.73(c)(6)	Immersion – All Material	2.7.5; 2.J	
2.3.7 Special Requirements for Irradiated Nuclear Fuel Shipments			
10CFR71.61	Elastic Stability of Containment	2.7.5; 2.J	
“	Closure Seal Region Below Yield Stress	2.AE	
2.3.8 Internal Pressure Test			
10CFR71.85(b)	Internal Pressure Test – All stresses below yield	2.6.1.4.3	8.1

TABLE 2.0.1- MATRIX OF 10CFR71 COMPLIANCE – STRUCTURAL REVIEW (Continued)

SECTION IN 10CFR71	10CFR71 COMPLIANCE ITEM	LOCATION IN SAR CHAPTER 2	LOCATION OUTSIDE OF SAR CHAPTER
Appendices			
	Supplemental Information	2.10	

† Legend for Table 2.0.1

Per the nomenclature defined in Chapter 1, the first digit refers to the chapter number, the second digit is the section number within the chapter; an alphabetic character in the second place means it is an appendix to the chapter.

NA Not Applicable for this item

Table 2.2.4

COMPONENT WEIGHTS AND DIMENSIONS FOR ANALYTIC CALCULATIONS*

Component	Weight (lbs)
MPC baseplate	3,000
MPC closure lid	10,400
MPC shell	5,900
MPC miscellaneous parts	3,700
Fuel basket	13,000
Fuel	54,000
Total MPC	90,000
Overpack baseplate	10,000
Overpack closure plate	8,000
Overpack shell	137,000
Total overpack	155,000
Total HI-STAR 100 lift weight	250,000
Impact limiters	37,000
HI-STAR with limiters	282,000
Item	Dimension (inch)
Overpack Outer Diameter	96
Overpack Length	203.125
MPC Outer Diameter	68.375
MPC Length	190.5
Overpack Inner Diameter	68.75

* Note: Analytical calculations may use weights and dimensions in Table 2.2.4 or actual weights and dimensions for conservatism in calculation of safety factors. Finite element analyses may use weights calculated based on input weight densities.

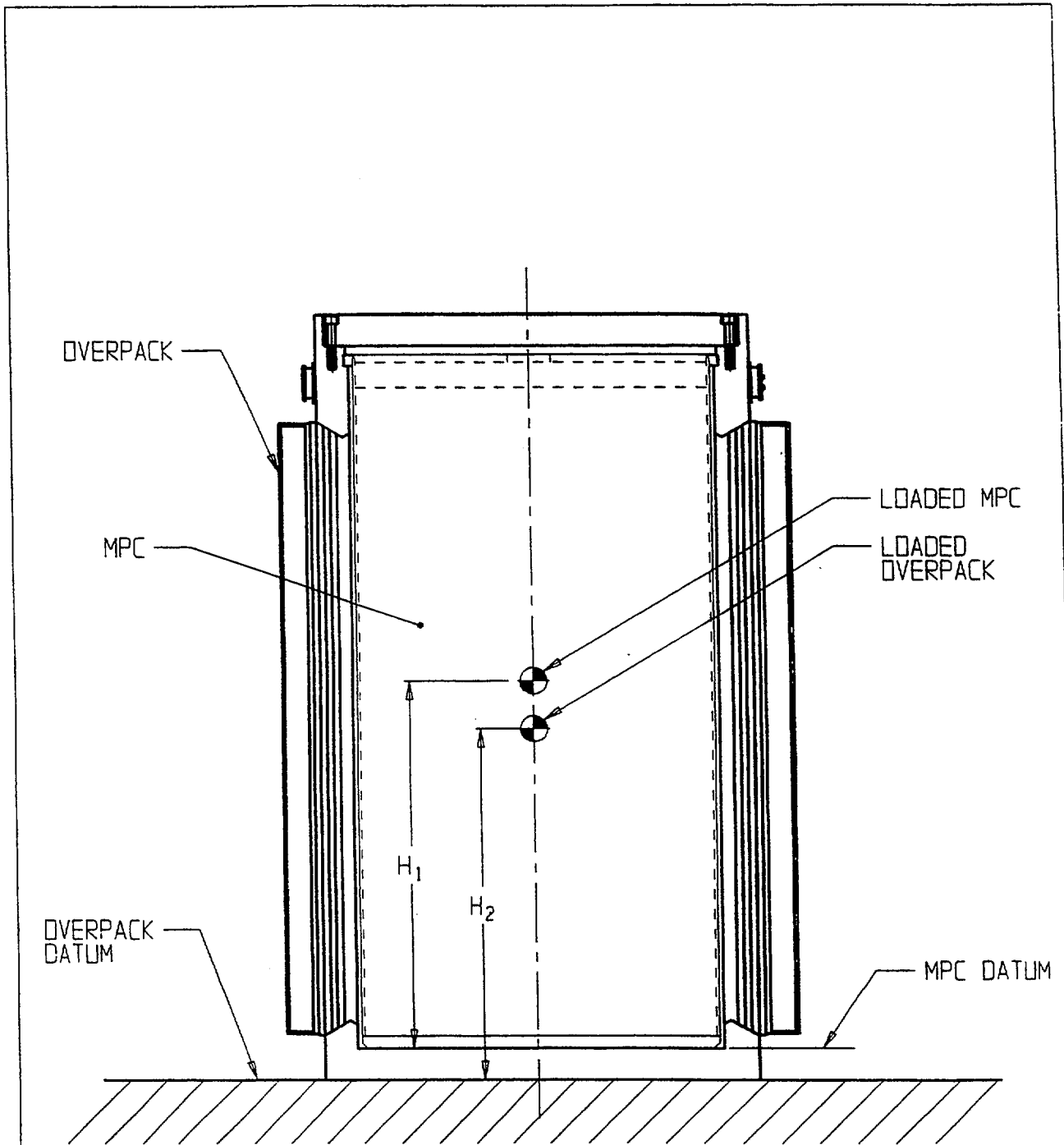


FIGURE 2.2.1; HI-STAR 100 DATUM DEFINITION FOR TABLE 2.2.2

criteria of 10CFR71.45(b). Next, since the lower trunnions are also used to provide a pivot location during upending or downending of the HI-STAR 100 loaded overpack, an evaluation of the weld group performance under the rotation operation is performed. Although this operation is, strictly speaking, not a “lifting” operation, for a conservative result, we require that the rotation trunnion weld group satisfy the strength requirements of 10CFR71.45(a). For additional conservatism, we assume in the calculation that the rotation trunnions carry 100% of the HI-STAR 100 weight during rotation, which is further magnified by a dynamic load factor of 1.15. The results from the weld analyses in Appendix 2.R are summarized in the table below:

Rotation Trunnion Weld Group Safety Factors per 10CFR71 Requirements			
Item	Required Weld Size (inch)	Available Weld Size (inch)	Safety Factor
Transport Tie-Down - 10CFR71.45(b)	3.19	4.25	1.48
Transport Rotation - 10CFR71.45(a)	0.831	4.25	5.11

Safety factors are greater than 1.0 indicating that the requirements of 10CFR71.45 are met.

2.5.2.7.6 Structural Integrity of the Top Flange Shear Ring

Longitudinal transport loads on the HI-STAR 100 System that are directed towards the forward (top end of the package) are resisted by a shear ring, integral with the top flange, which extends around the top flange over a 140 degree arc. Figure 2.5.6 shows the shear ring. The following dimensions are applicable:

$$\begin{aligned}
 R &= 41.625 \text{ in.} \\
 t &= 1.5 \text{ in.} \\
 L &= 5.0 \text{ in.}
 \end{aligned}$$

The shear ring resists the 10g longitudinal load from normal transport, designated here as, $F_{\text{long}} = 2,820,000 \text{ lb.}$, by developing a bearing pressure on the contact surface of the shear ring and then transferring the load through the available shear area. In the following, we determine the bearing and shear stresses that develop when the longitudinal load from normal transport is imposed. Figure 2.5.7 is a sketch showing the developed shear and bearing loads on the shear ring.

* Bearing stress on contact surface

The contact surface area is

$$A_s = \pi \times \left(\frac{140^\circ}{360^\circ} \right) \times [(R+t)^2 - R^2]$$
$$= \pi \times 0.389 \times [(41.625 + 1.5)^2 - 41.625^2] = 155.4 \text{ in}^2$$

Therefore, the bearing stress on the shear ring is

$$\sigma_b = \frac{F_{\text{long}}}{A_s} = \frac{2,820,000}{155.4} = 18,147 \text{ psi}$$

which is less than the yield stress of the shear ring material (SA350-LF3), $\sigma_y = 32,700$ psi. We note that the shear ring is adjacent to the intermediate shells and that Table 2.1.2 lists the appropriate temperature for the intermediate shells for normal conditions of transport as 350 degrees F; therefore, this same temperature is used to obtain the yield stress value from Table 2.3.4.

Therefore, the safety factor based on the requirements of 10CFR71.45(b) is

$$SF = 32,700/18,147 = 1.8$$

* Shear stress on shear ring interface with top flange

The transport load is transferred from the package to the rail car through the shear area afforded between the top flange and the shear ring. The total shear circumferential area for load transfer is

$$A_s = 2\pi RL \times \frac{140^\circ}{360^\circ}$$

where L is the width of the shear ring and R is the inside radius of the shear ring. From Drawing 1397, Sheet 6, we can determine L and R as

- APPENDIX 2.AE: ANSYS FINITE ELEMENT RESULTS FOR OVERPACK
- APPENDIX 2.AF: IMPACT LIMITER ATTACHMENT BOLTS
- APPENDIX 2.AG: CASK UNDER THREE TIMES DEAD LOAD
- APPENDIX 2.AH: DAMAGED FUEL CONTAINER
- APPENDIX 2.AI: HI-STAR 100 COMPONENT THERMAL EXPANSIONS; MPC-24 UNDER STEADY COLD CONDITIONS
- APPENDIX 2.AJ: DELETED
- APPENDIX 2.AK: HI-STAR 100 COMPONENT THERMAL EXPANSIONS; MPC-68 UNDER STEADY COLD CONDITIONS
- APPENDIX 2.AL: OVERPACK CLOSURE BOLT CAPACITY - NORMAL COLD CONDITION OF TRANSPORT
- APPENDIX 2.AM: STRESS ANALYSIS OF THE HI-STAR 100 ENCLOSURE VESSEL UNDER 30psi INTERNAL PRESSURE
- APPENDIX 2.AN: POCKET TRUNNION STRESS ANALYSIS
- APPENDIX 2.AO: ANALYSIS OF TRANSNUCLEAR DAMAGED FUEL CANISTER AND THORIA ROD CANISTER

2.10.2 Summary of NUREG -1617/10CFR71 Compliance

This subsection provides a “road map” of technical information to demonstrate that the SAR in compliance with the provisions of NUREG-1617 and associated referenced sections of 10CFR71 necessary to certify the HI-STAR 100 package for transport.

Description of Structural Design

The package structural design description and the contents of the application meet the requirements of 10CFR 71.31 and Regulatory Guide 7.9. Applicable sections where this is demonstrated are 1.2.1; 1.3; 1.4; and 2.1.

The codes and standards used in the package design are listed in 1.3. The use of the ASME

Boiler and Pressure Vessel Code is in compliance with NUREG/CR-6407, "Classification of Transportation Packaging and Dry Spent Fuel Storage Components".

Material Properties

There are no significant chemical, galvanic or other reactions among the packaging components, among package contents, or between the packaging components and the contents in dry or wet environment conditions. The applicable subsection where this is demonstrated is 2.4.4.

The effects of radiation on materials are considered and package containment is constructed from materials that meet the requirements of Reg. Guides 7.11 and 7.12. Applicable subsections where this is demonstrated are: 1.2.1; 2.1.2; and, 2.4.4.

Lifting and Tie-Down Standards for All Packages

Lifting and Tie-Down systems meet 10CFR 71.45 standards. The applicable section where this is demonstrated is 2.5.

General Considerations for Structural Evaluation of Packaging

The packaging structural evaluation meets the requirements of 10CFR 71.35. Applicable chapters and/or sections where this is demonstrated are: 2.5; 2.6; 2.7

Normal Conditions of Transport

The packaging structural performance under normal conditions of transport demonstrate that there will be no substantial reduction in the effectiveness of the packaging. The applicable section where this is demonstrated is 2.6.

Hypothetical Accident Conditions

The packaging structural performance under the hypothetical accident conditions demonstrates that the packaging has adequate structural integrity to satisfy the subcriticality, containment, shielding, and temperature requirements of 10CFR Part 71. The applicable section where this is demonstrated is 2.7.

Special Requirement for Irradiated Nuclear Fuel Shipments

The containment structure meets the 10CFR 71.61 requirements for irradiated nuclear fuel shipments. The applicable section where this is demonstrated is 2.7.

Internal Pressure Test

The containment structure meets the 10CFR 71.85(b) requirements for pressure test without yielding. The applicable subsection where this is demonstrated is 2.6.1.4.3.

$$LC_{\text{weld}} = 1.055 \cdot 10^6 \cdot \text{lbf}$$

The factor of safety of this load capacity, for the Level A center lift loading case (Load Case E2, Table 3.1.4 in Docket 72-1008), is determined as:

$$FS_6 := \frac{LC_{\text{weld}}}{W_{\text{lift}} + \pi \cdot P_{\text{int}} \cdot R_{\text{lid}}^2} \quad FS_6 = 2.29$$

The bounding weld load for Level D conditions is determined by multiplying the equivalent pressure load for the load case by the area of the closure plate. The bottom end drop is taken by the welds, and the top end drop is taken by bearing on the overpack closure plate.

$$L_{\text{weld}} := P_{\text{sd}} \cdot \pi \cdot (R_{\text{lid}})^2 \quad L_{\text{weld}} = 624000 \cdot \text{lbf}$$

$$MS_7 := \frac{S_d}{S_a} \cdot \frac{LC_{\text{weld}}}{L_{\text{weld}}} - 1 \quad MS_7 = 1.37$$

To further demonstrate the adequacy of the weld, its capacity is compared to a weld load that equals three times the total lifted weight. The factor of safety is

$$FS_8 := \frac{LC_{\text{weld}}}{3 \cdot W_{\text{lift}}} \quad FS_8 = 3.40$$

2.L.8.4 Fatigue Analysis of Weld

The welds will be subjected to cyclic stress each time the MPC is lifted. The force difference is equal to W_{lift} . Pressure loads are not a fatigue consideration since they remain relatively constant during normal operation. Therefore, the effective fatigue stress can be determined as follows

The fatigue factor for a single groove weld that is examined by root and final PT is $f := 4$ and the alternating stress is

The fatigue factor for a single groove weld that is examined by root and final PT is $f := 4$ and the alternating stress is

$$\sigma := \frac{\left(f \cdot \frac{W_{\text{lift}}}{2} \right)}{2 \cdot \pi \cdot R_{\text{lid}} \cdot t_{\text{weld}}} \quad \sigma = 1565 \cdot \text{psi}$$

This stress is compared to curve B in Figure I-9.2.2 of the ASME Division I Appendices per Subsection NG. This curve shows that the welds have unlimited life at this stress level.

2.L.8.5 Closure Ring Analysis

The closure ring must be capable of withstanding the application of the full MPC internal pressure, to ensure that a leak in the primary closure plate weld will be contained. This condition is modeled as an annular ring subject to the design internal pressure. A finite element analysis of a thin ring with an applied pressure is performed using the ANSYS finite element code. The thin ring is simulated by four layers of PLANE42 axisymmetric quadrilateral elements (see Figure 2.L.2). The boundary condition is conservatively set as zero displacement at node locations 1 and 2 (see Figure 2.L.2). The bottom surface is subjected to a 100 psi pressure to simulate leakage of the primary MPC weld. The maximum stress intensity in the ring (occurring at the top center point) and the resultant factor of safety for Level A conditions are determined as:

The maximum stress intensity in the ring, $SI_{\text{ring}} := 20001 \cdot \text{psi}$

The factor of safety, $FS_g := \frac{S_{\text{acr}}}{SI_{\text{ring}}} \quad FS_g = 1.405$

Since the actual support condition provides a edge fixity condition that is intermediate between a simple support and a built-in support, this result is very conservative.

The total load capacity of the closure ring weld is determined by calculating the total area of the two weld lines at radii R_i and R_o , multiplying by the allowable weld stress, and conservatively applying the specified weld efficiency.

The closure ring weld thickness, $t_{\text{crw}} := 0.125 \cdot \text{in}$ (this allows for fit-up and also provides improved ALARA considerations)

The quality factor for a single groove or a single fillet weld that is examined by PT is taken as the same value used for the MPC Top Closure-to-shell weld: $n := 0.45$

The load capacity of the ring welds is,

$$LC_{crw} := n \cdot 2 \cdot \pi \cdot \left(R_i + \frac{R_o}{\sqrt{2}} \right) \cdot t_{crw} \cdot Sa \qquad LC_{crw} = 3.164 \cdot 10^5 \cdot lbf$$

The margin of safety of these welds for the applied loading condition (design internal pressure only) is determined as:

$$MS_{10} := \frac{LC_{crw}}{\pi \cdot P_{int} \cdot (R_o^2 - R_i^2)} - 1 \qquad MS_{10} = 1.24$$

2.L.9 Conclusions

The results of the evaluations presented in this appendix demonstrate the adequacy of the MPC closure plate, closure ring and associated weldments to maintain their structural integrity during applied bounding load cases considered. Positive safety margins exist for all components examined for all load cases considered.

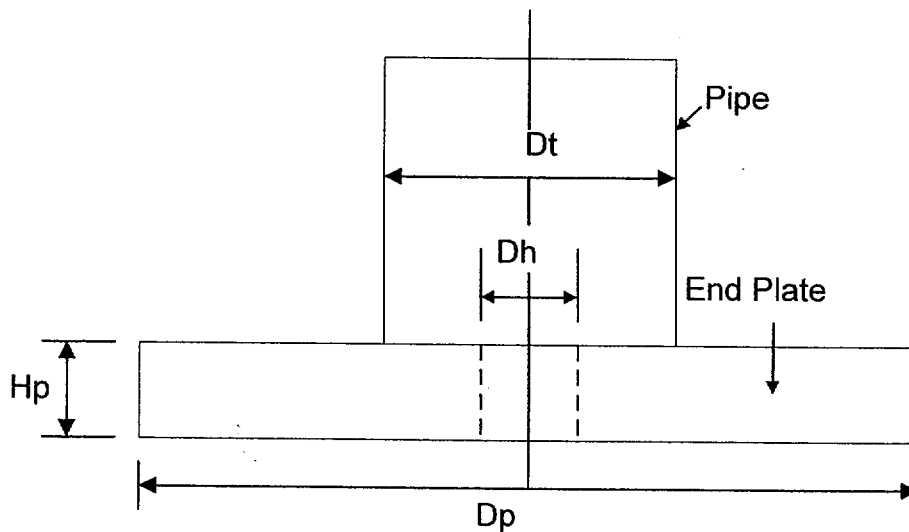
The bending stress evaluation of the closure ring conservatively assumes a simple support condition exists at the peripheral welds. The associated stress at the weld line is a radially symmetric primary shear stress that is well within Code limits if a 0.125" (min.) weld is utilized.

The closure ring has been analyzed as a continuous ring with no discontinuities around the periphery. Practical considerations in fabrication mandate that the closure ring should be constructed from two or more sections connected by a radially oriented weld. In addition, to positively preclude any interaction with the peripheral weld in the MPC lid, the radial welds connecting radial segments of the closure ring to adjacent segments should be partial penetration welds. These radial welds are not required for satisfaction of equilibrium and generate no primary state of stress in the closure ring due to their presence. Small stress adders that develop due to the local structural discontinuity at the partial penetration weld locations produce peak stresses that have no prescribed limit in the ASME Code.

Indeed, the radial weld lines are in the category of "seal" welds that are essentially required to prevent leakage but bear little stress due to lateral pressure.

2.O.4 Analysis of Upper Spacer End Plate for PWR Spacers

Some PWR fuel types are not supportable by the current upper spacer design having a simple pipe extension. To insure that all PWR fuel types are captured, an end plate having sufficient diameter is welded to the end of the pipe to extend the contact area. This section of the appendix addresses the stress analysis of the end plate to insure that it performs as desired under a handling accident that results in a direct impact of the fuel assembly onto the end plate. The configuration is shown below:



The dimensions are: (note that outer radius is taken equal to inside radius of limiting fuel assembly contact circle)

$$H_p := 0.75 \cdot \text{in} \quad D_p := 4.1 \cdot \text{in} \quad D_t := 3.5 \cdot \text{in} \quad D_h := 1 \cdot \text{in}$$

Under the postulated handling accident, the total applied load is (design basis deceleration of 60 g's):

$$P := 60 \cdot 1680 \cdot \text{lbf} \quad P = 1.008 \times 10^5 \text{ lbf}$$

This load may be applied as a line load around the outer periphery

$$q_o := \frac{P}{\pi \cdot D_p} \quad q_o = 7.826 \times 10^3 \frac{\text{lbf}}{\text{in}}$$

or it may be applied as a line load at a diameter of 1.8" (from a survey of fuel assembly types)

$$q_i := \frac{P}{\pi \cdot 1.8 \cdot \text{in}} \quad q_i = 1.783 \times 10^4 \frac{\text{lbf}}{\text{in}}$$

In either case, the shear load at the pipe connection is approximately

$$q_p := \frac{P}{\pi \cdot Dt} \quad q_p = 9.167 \times 10^3 \frac{\text{lbf}}{\text{in}}$$

At the design temperature, the ultimate strength is, (conservatively neglect any increase in ultimate strength due to strain rate effects

$$S_u := 62350 \cdot \text{psi}$$

The spacer pipe has been designed to NG, Level D requirements for axial strength and to the appropriate ASME Code requirements for gross stability. The function of the end plate is to insure that the fuel assembly impacts the spacer; the only requirement is that under an accident condition, no permanent deformation of this end plate occurs to the extent that the positioning limits of the fuel assembly is compromised. This is insured if we demonstrate that the ultimate shear capacity of the added end plate and the ultimate moment capacity of the end plate is not exceeded during the impact. Satisfaction of these stress limits will insure that no large axial movement of the assembly can occur because of the impact.

The ultimate shear capacity of the section is taken as $0.577S_u$, and the ultimate moment capacity is calculated assuming perfectly plastic behavior at the ultimate stress. Therefore, at any section of the plate the shear capacity is:

$$q_{\text{cap}} := .577 \cdot S_u \cdot Hp \quad q_{\text{cap}} = 2.698 \times 10^4 \frac{\text{lbf}}{\text{in}}$$

Comparison of this limit with the peripheral shear loads computed previously demonstrates that the end plate will not experience a gross shear failure at any section. The minimum safety factor "SF" is

$$\frac{q_{\text{cap}}}{q_i} = 1.514$$

The ultimate moment capacity is (assume rectangular distribution throuh the thickness):

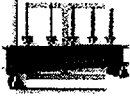
$$M_u := S_u \cdot \frac{Hp^2}{4} \quad M_u = 8.768 \times 10^3 \text{in} \cdot \frac{\text{lbf}}{\text{in}}$$

The weight of the added end plate is:

$$\text{Weight} := 0.29 \cdot \frac{\text{lbf}}{\text{in}^3} \cdot \frac{\pi}{4} \cdot Hp \cdot (Dp^2 - Dh^2) \quad \text{Weight} = 2.701 \text{ lbf}$$

The following calculations are performed to establish the maximum bending moment in the end plate based on the two extreme locations of impact load. The electronic version of Roark's Handbook (6th Edition) that is a Mathcad add-on, is used for this computation. Mathcad 2000 is used for this section of Appendix 2.O.

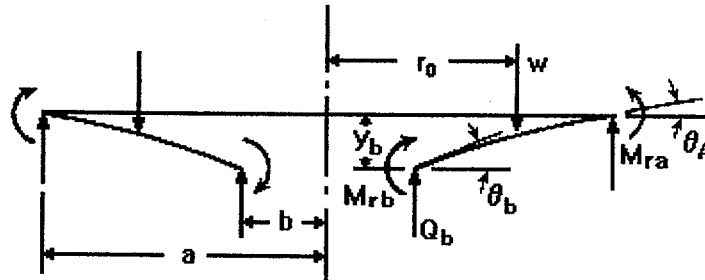
Table 24 Formulas for shear, moment and deflection of flat circular plates of constant thickness



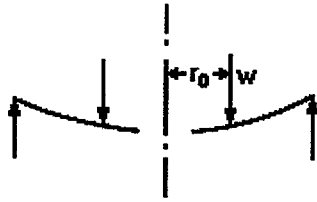
Cases 1a - 1d Annular Plate With Uniform Annular Line Load w at Radius r_0 ; Outer Edge Simply Supported

This file corresponds to Cases 1a - 1d in *Roark's Formulas for Stress and Strain*.

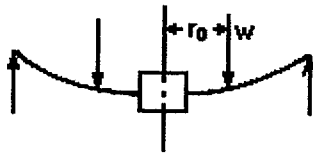
Annular plate with a uniform annular line load w at a radius r_0 .



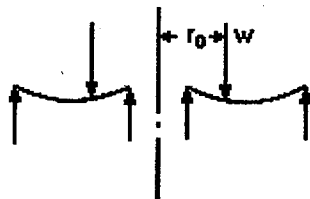
Outer edge simply supported, inner edge free



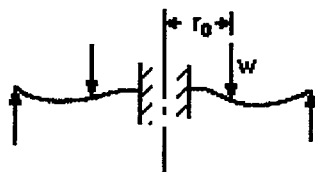
Outer edge simply supported, inner edge guided



Outer edge simply supported, inner edge simply supported



Outer edge simply supported, inner edge fixed



CASE 1A applies to the impact load at the outer periphery. The pipe diameter is the applied load location

**Enter dimensions,
properties and
loading**

Plate dimensions:

thickness: $t \equiv 0.75 \cdot \text{in}$

outer radius: $a \equiv 2.05 \cdot \text{in}$

inner radius: $b \equiv 0.5 \cdot \text{in}$

Applied unit load: $w \equiv 9167 \cdot \frac{\text{lb} \cdot \text{f}}{\text{in}}$

Modulus of elasticity: $E \equiv 24.625 \cdot 10^6 \cdot \frac{\text{lb} \cdot \text{f}}{\text{in}^2}$

Poisson's ratio: $\nu \equiv 0.3$

Radial location of applied load: $r_o \equiv .5 \cdot 3.5 \cdot \text{in}$

Constants

Shear modulus: $G \equiv \frac{E}{2 \cdot (1 + \nu)}$

D is a plate constant used in determining boundary values; it is also used in the general equations for deflection, slope, moment and shear. K_{sb} and K_{sro} are tangential shear constants used in determining the deflection due to shear:

$$D \equiv \frac{E \cdot t^3}{12 \cdot (1 - \nu^2)} \qquad D = 9.513 \times 10^5 \text{ lb} \cdot \text{f} \cdot \text{in}$$

$$K_{sro} \equiv -1.2 \cdot \frac{r_o}{a} \cdot \ln \left(\frac{a}{r_o} \right) \qquad K_{sb} \equiv K_{sro}$$

**General formulas and graphs
for deflection, slope, moment,
shear and stress as a function
of r**

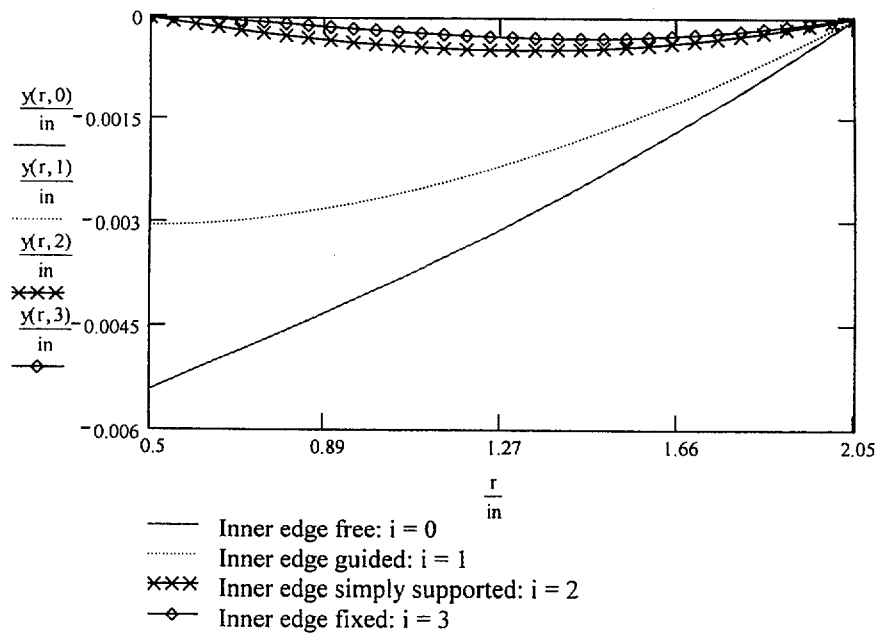
Define r, the range of the radius and i, the vector index:

$$r \equiv b, 1.1 \cdot b \dots a$$

$$i \equiv 0 \dots 3$$

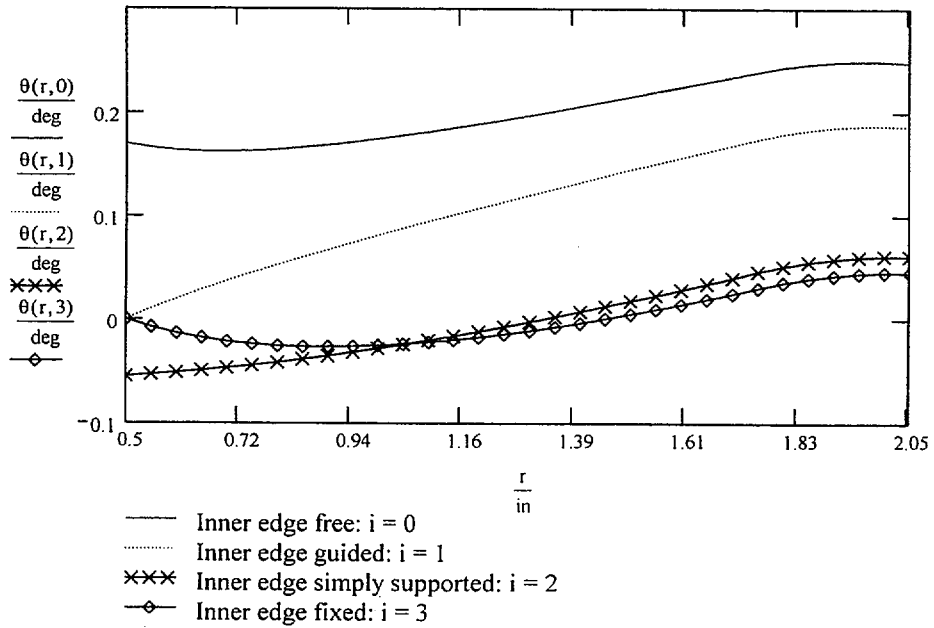
Deflection

$$y(r, i) := y_{b_i} + \theta_{b_i} \cdot r \cdot F_1(r) + M_{rb_i} \cdot \frac{r^2}{D} \cdot F_2(r) + Q_{b_i} \cdot \frac{r^3}{D} \cdot F_3(r) - w \cdot \frac{r^3}{D} \cdot G_3(r)$$



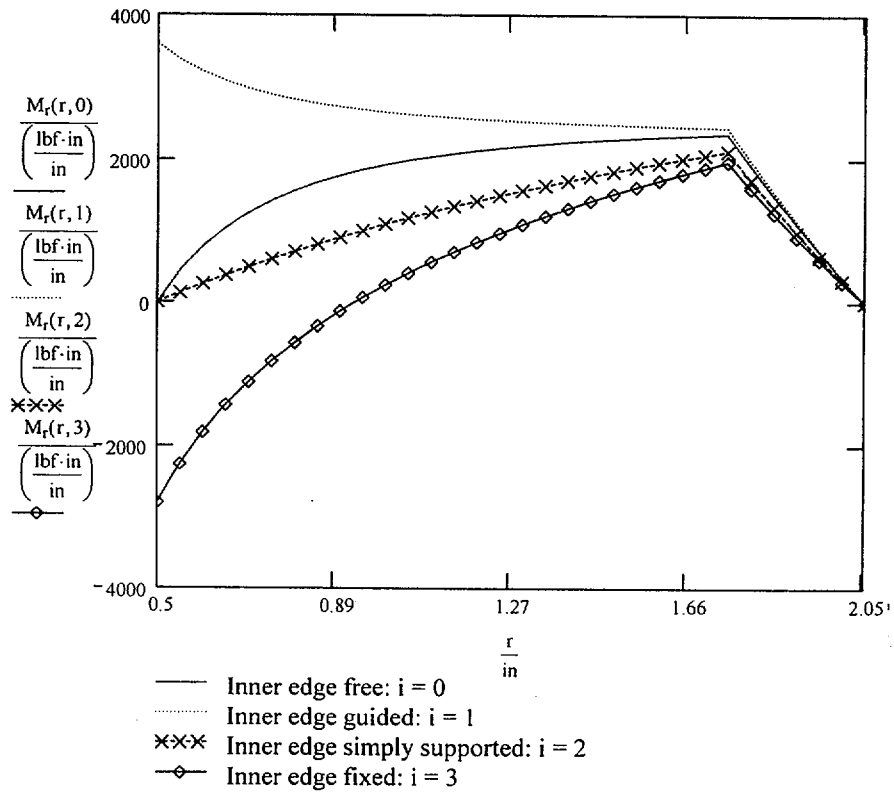
Slope

$$\theta(r,i) := \theta_{b_i} \cdot F_4(r) + M_{rb_i} \cdot \frac{r}{D} \cdot F_5(r) + Q_{b_i} \cdot \frac{r^2}{D} \cdot F_6(r) - w \cdot \frac{r^2}{D} \cdot G_6(r)$$



Radial moment

$$M_r(r, i) := \theta_{b_i} \cdot \frac{D}{r} \cdot F_7(r) + M_{rb_i} \cdot F_8(r) + Q_{b_i} \cdot r \cdot F_9(r) - w \cdot r \cdot G_9(r)$$



The following values are listed in order of inner edge:

- free (i = 0)
- guided (i = 1)
- simply supported (i = 2)
- fixed (i = 3)

Moment at points b and a (inner and outer radius):

$$\frac{M_{rb}}{\left(\frac{\text{lb}\cdot\text{in}}{\text{in}}\right)} = \begin{pmatrix} 0 \\ 3.595 \times 10^3 \\ 0 \\ -2.798 \times 10^3 \end{pmatrix} \quad \frac{M_{ra}}{\left(\frac{\text{lb}\cdot\text{in}}{\text{in}}\right)} = \begin{pmatrix} 0 \\ 0 \\ 0 \\ 0 \end{pmatrix}$$

Maximum radial moment (magnitude):

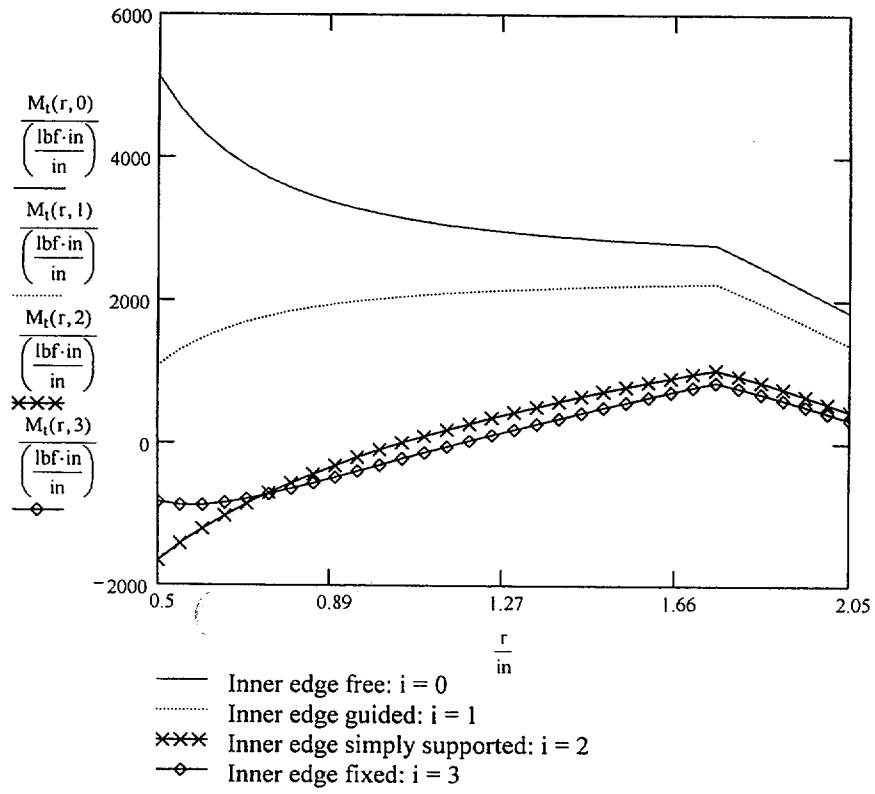
$$M_{r_{(r-b)\frac{100}{\text{in}},i}} := M_r(r, i) \quad A_{mr_i} := \max(M_r^{(i)}) \quad B_{mr_i} := \min(M_r^{(i)})$$

$$M_{r_{\max_i}} := (A_{mr_i} > -B_{mr_i}) \cdot A_{mr_i} + (A_{mr_i} \leq -B_{mr_i}) \cdot B_{mr_i}$$

$$\frac{M_{r_{\max}}}{\left(\frac{\text{lb}\cdot\text{in}}{\text{in}}\right)} = \begin{pmatrix} 2.355 \times 10^3 \\ 3.595 \times 10^3 \\ 2.115 \times 10^3 \\ -2.798 \times 10^3 \end{pmatrix}$$

Transverse moment

$$M_t(r,i) := \frac{\theta(r,i) \cdot D \cdot (1 - \nu^2)}{r} + \nu \cdot M_r(r,i)$$



The following values are listed in order of inner edge:

- free (i = 0)
- guided (i = 1)
- simply supported (i = 2)
- fixed (i = 3)

Transverse moment at points b and a (inner and outer radius) due to bending:

$\frac{M_t(b,i)}{\left(\frac{\text{lbf}\cdot\text{in}}{\text{in}}\right)} =$	$\frac{M_t(a,i)}{\left(\frac{\text{lbf}\cdot\text{in}}{\text{in}}\right)} =$
5.128·10 ³	1.828·10 ³
1.078·10 ³	1.373·10 ³
-1.661·10 ³	452.798
-839.265	334.706

Maximum tangential moment (magnitude):

$$M_{t \frac{100}{(r-b) \cdot \frac{100}{\text{in}}, i}} := M_t(r, i) \quad A_{mt_i} := \max(M_t \langle i \rangle) \quad B_{mt_i} := \min(M_t \langle i \rangle)$$

$$M_{t_{\max_i}} := (A_{mt_i} > -B_{mt_i}) \cdot A_{mt_i} + (A_{mt_i} \leq -B_{mt_i}) \cdot B_{mt_i}$$

$$\frac{M_{t_{\max}}}{\frac{\text{lbf}\cdot\text{in}}{\text{in}}} = \begin{pmatrix} 5.128 \times 10^3 \\ 2.234 \times 10^3 \\ -1.661 \times 10^3 \\ -884.013 \end{pmatrix} \quad SF := \frac{M_u}{5128 \cdot \text{lbf}} \quad SF = 1.71$$

The remainder of the document displays the general plate functions and constants used in the equations above.

$$C_1 \equiv \frac{1+v}{2} \cdot \frac{b}{a} \cdot \ln\left(\frac{a}{b}\right) + \frac{1-v}{4} \cdot \left(\frac{a}{b} - \frac{b}{a}\right)$$

$$C_7 \equiv \frac{1}{2} \cdot (1-v^2) \cdot \left(\frac{a}{b} - \frac{b}{a}\right)$$

$$C_2 \equiv \frac{1}{4} \cdot \left[1 - \left(\frac{b}{a}\right)^2 \cdot \left(1 + 2 \cdot \ln\left(\frac{a}{b}\right)\right) \right]$$

$$C_8 \equiv \frac{1}{2} \cdot \left[1 + v + (1-v) \cdot \left(\frac{b}{a}\right)^2 \right]$$

$$C_3 \equiv \frac{b}{4 \cdot a} \cdot \left[\left[\left(\frac{b}{a}\right)^2 + 1 \right] \cdot \ln\left(\frac{a}{b}\right) + \left(\frac{b}{a}\right)^2 - 1 \right]$$

$$C_9 \equiv \frac{b}{a} \cdot \left[\frac{1+v}{2} \cdot \ln\left(\frac{a}{b}\right) + \left(\frac{1-v}{4}\right) \cdot \left[1 - \left(\frac{b}{a}\right)^2 \right] \right]$$

$$C_4 \equiv \frac{1}{2} \cdot \left[(1+v) \cdot \frac{b}{a} + (1-v) \cdot \frac{a}{b} \right]$$

$$L_3 \equiv \frac{r_0}{4 \cdot a} \cdot \left[\left[\left(\frac{r_0}{a}\right)^2 + 1 \right] \cdot \ln\left(\frac{a}{r_0}\right) + \left(\frac{r_0}{a}\right)^2 - 1 \right]$$

$$C_5 \equiv \frac{1}{2} \cdot \left[1 - \left(\frac{b}{a}\right)^2 \right]$$

$$L_6 \equiv \frac{r_0}{4 \cdot a} \cdot \left[\left(\frac{r_0}{a}\right)^2 - 1 + 2 \cdot \ln\left(\frac{a}{r_0}\right) \right]$$

$$C_6 \equiv \frac{b}{4 \cdot a} \cdot \left[\left(\frac{b}{a}\right)^2 - 1 + 2 \cdot \ln\left(\frac{a}{b}\right) \right]$$

$$L_9 \equiv \frac{r_0}{a} \cdot \left[\frac{1+v}{2} \cdot \ln\left(\frac{a}{r_0}\right) + \frac{1-v}{4} \cdot \left[1 - \left(\frac{r_0}{a}\right)^2 \right] \right]$$

Boundary values due to bending:

At the inner edge of the plate:

$$Q_b \equiv \begin{bmatrix} 0 \cdot \frac{\text{lbf}}{\text{in}} \\ 0 \cdot \frac{\text{lbf}}{\text{in}} \\ w \cdot \left(\frac{C_1 \cdot L_9 - C_7 \cdot L_3}{C_1 \cdot C_9 - C_3 \cdot C_7} \right) \\ w \cdot \left(\frac{C_2 \cdot L_9 - C_8 \cdot L_3}{C_2 \cdot C_9 - C_3 \cdot C_8} \right) \end{bmatrix}$$

$$M_{rb} \equiv \begin{bmatrix} 0 \cdot \frac{\text{lbf} \cdot \text{in}}{\text{in}} \\ \frac{w \cdot a}{C_8} \cdot L_9 \\ 0 \cdot \frac{\text{lbf} \cdot \text{in}}{\text{in}} \\ -w \cdot a \cdot \left(\frac{C_3 \cdot L_9 - C_9 \cdot L_3}{C_2 \cdot C_9 - C_3 \cdot C_8} \right) \end{bmatrix}$$

$$y_b \equiv \begin{bmatrix} \frac{-w \cdot a^3}{D} \cdot \left(\frac{C_1 \cdot L_9}{C_7} - L_3 \right) \\ \frac{-w \cdot a^3}{D} \cdot \left(\frac{C_2 \cdot L_9}{C_8} - L_3 \right) \\ 0 \cdot \text{in} \\ 0 \cdot \text{in} \end{bmatrix}$$

$$\theta_b \equiv \begin{bmatrix} \frac{w \cdot a^2}{D \cdot C_7} \cdot L_9 \\ 0 \cdot \text{deg} \\ \frac{-w \cdot a^2}{D} \cdot \left(\frac{C_3 \cdot L_9 - C_9 \cdot L_3}{C_1 \cdot C_9 - C_3 \cdot C_7} \right) \\ 0 \cdot \text{deg} \end{bmatrix}$$

At the outer edge of the plate:

$$y_a \equiv \begin{pmatrix} 0 \cdot \text{in} \\ 0 \cdot \text{in} \\ 0 \cdot \text{in} \\ 0 \cdot \text{in} \end{pmatrix}$$

$$\theta_a \equiv \begin{pmatrix} \frac{w \cdot a^2}{D} \cdot \left(\frac{C_4 \cdot L_9}{C_7} - L_6 \right) \\ \frac{w \cdot a^2}{D} \cdot \left(\frac{C_5 \cdot L_9}{C_8} - L_6 \right) \\ \theta_{b_2} \cdot C_4 + Q_{b_2} \cdot \frac{a^2}{D} \cdot C_6 - \frac{w \cdot a^2}{D} \cdot L_6 \\ M_{rb_3} \cdot \frac{a}{D} \cdot C_5 + Q_{b_3} \cdot \frac{a^2}{D} \cdot C_6 - \frac{w \cdot a^2}{D} \cdot L_6 \end{pmatrix}$$

$$Q_a \equiv \begin{pmatrix} -w \cdot \frac{r_o}{a} \\ -w \cdot \frac{r_o}{a} \\ Q_{b_2} \cdot \frac{b}{a} - \frac{w \cdot r_o}{a} \\ Q_{b_3} \cdot \frac{b}{a} - \frac{w \cdot r_o}{a} \end{pmatrix}$$

$$M_{ra} \equiv \begin{pmatrix} 0 \cdot \frac{\text{lbf} \cdot \text{in}}{\text{in}} \\ 0 \cdot \frac{\text{lbf} \cdot \text{in}}{\text{in}} \\ 0 \cdot \frac{\text{lbf} \cdot \text{in}}{\text{in}} \\ 0 \cdot \frac{\text{lbf} \cdot \text{in}}{\text{in}} \end{pmatrix}$$

Due to tangential shear stresses:

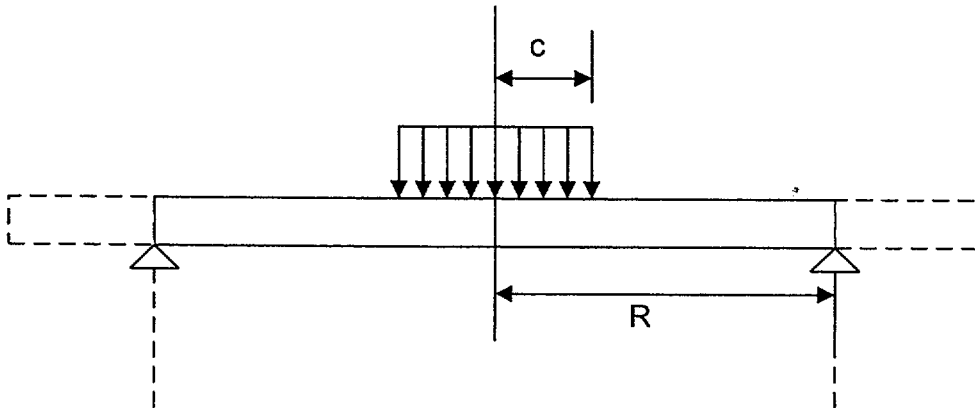
$$y_{sb} \equiv \begin{pmatrix} \frac{K_{sb} \cdot w \cdot a}{t \cdot G} \\ \frac{K_{sb} \cdot w \cdot a}{t \cdot G} \\ 0 \cdot \text{in} \\ 0 \cdot \text{in} \end{pmatrix}$$

$$y_{sro} \equiv \begin{pmatrix} \frac{K_{sro} \cdot w \cdot r_o}{t \cdot G} \\ \frac{K_{sro} \cdot w \cdot r_o}{t \cdot G} \\ 0 \cdot \text{in} \\ 0 \cdot \text{in} \end{pmatrix}$$

$$\begin{aligned}
F_1(r) &\equiv \frac{1+\nu}{2} \cdot \frac{b}{r} \cdot \ln\left(\frac{r}{b}\right) + \frac{1-\nu}{4} \cdot \left(\frac{r}{b} - \frac{b}{r}\right) & F_6(r) &\equiv \frac{b}{4 \cdot r} \cdot \left[\left(\frac{b}{r}\right)^2 - 1 + 2 \cdot \ln\left(\frac{r}{b}\right) \right] \\
F_2(r) &\equiv \frac{1}{4} \cdot \left[1 - \left(\frac{b}{r}\right)^2 \cdot \left(1 + 2 \cdot \ln\left(\frac{r}{b}\right)\right) \right] & F_7(r) &\equiv \frac{1}{2} \cdot (1-\nu^2) \cdot \left(\frac{r}{b} - \frac{b}{r}\right) \\
F_3(r) &\equiv \frac{b}{4 \cdot r} \cdot \left[\left(\frac{b}{r}\right)^2 + 1 \right] \cdot \ln\left(\frac{r}{b}\right) + \left(\frac{b}{r}\right)^2 - 1 & F_8(r) &\equiv \frac{1}{2} \cdot \left[1 + \nu + (1-\nu) \cdot \left(\frac{b}{r}\right)^2 \right] \\
F_4(r) &\equiv \frac{1}{2} \cdot \left[(1+\nu) \cdot \frac{b}{r} + (1-\nu) \cdot \frac{r}{b} \right] & F_9(r) &\equiv \frac{b}{r} \cdot \left[\frac{1+\nu}{2} \cdot \ln\left(\frac{r}{b}\right) + \frac{1-\nu}{4} \cdot \left[1 - \left(\frac{b}{r}\right)^2 \right] \right] \\
F_5(r) &\equiv \frac{1}{2} \cdot \left[1 - \left(\frac{b}{r}\right)^2 \right] \\
G_3(r) &\equiv \frac{r_0}{4 \cdot r} \cdot \left[\left(\frac{r_0}{r}\right)^2 + 1 \right] \cdot \ln\left(\frac{r}{r_0}\right) + \left(\frac{r_0}{r}\right)^2 - 1 \cdot (r > r_0) \\
G_6(r) &\equiv \frac{r_0}{4 \cdot r} \cdot \left[\left(\frac{r_0}{r}\right)^2 - 1 + 2 \cdot \ln\left(\frac{r}{r_0}\right) \right] \cdot (r > r_0) \\
G_9(r) &\equiv \frac{r_0}{r} \cdot \left[\frac{1+\nu}{2} \cdot \ln\left(\frac{r}{r_0}\right) + \frac{1-\nu}{4} \cdot \left[1 - \left(\frac{r_0}{r}\right)^2 \right] \right] \cdot (r > r_0)
\end{aligned}$$

The actual safety factor against a complete collapse of the ring like plate is much larger since unlimited large rotations will only occur when a substantial region of the plate has the circumferential moment reach capacity (this can be shown by a limit analysis solution of the plate equations).

The second impact scenario has the loading applied over a region inside the outer diameter of the pipe. To qualify this load case, we consider the plate as simply supported at the pipe diameter and conservatively neglect the overhanging portion of the pipe. Further, we assume the loading is conservatively applied as a uniform pressure over an area equal to the minimum impact diameter of 1.8". For simplicity, we neglect the inner hole in this calculation. Therefore, the limit analysis model for the second impact scenario is shown below:



Calculate effective load area at middle surface assuming a 45 degree spread of load patch

$$H_p = 0.75 \text{ in}$$

$$R := 0.5 \cdot [(3.5 - 2 \cdot 0.226) \cdot \text{in}]$$

$$P = 1.008 \times 10^5 \text{ lbf}$$

$$c := 0.5 \cdot (1.8 \cdot \text{in} + H_p)$$

Use inside radius of pipe for this calc.

$$M_u = 8.768 \times 10^3 \text{ lbf} \cdot \frac{\text{in}}{\text{in}}$$

Using a solution in the text "Introduction to Plasticity" by W. Prager, Addison Wesley, 1959, p. 61, the limit load is

$$P_{\text{lim}} := 6 \cdot \pi \cdot \frac{M_u}{\left(3 - 2 \cdot \frac{c}{R}\right)}$$

Therefore, the safety factor for this case is

$$\frac{P_{\text{lim}}}{P} = 1.236$$

Therefore it is concluded that an end plate of diameter and thickness equal to

$$D_p = 4.1 \text{ in}$$

$$H_p = 0.75 \text{ in}$$

will perform the intended load transfer and limit the movement of the fuel assembly.

APPENDIX 2.R - POCKET TRUNNION RECESS WELD ANALYSIS

2.R.1 Purpose

The purpose of this calculation is to evaluate the pocket trunnion weld stress. There are two bounding cases of interest. The first case is the analysis of the weld under the action of the calculated tie-down loads during transport. Tie-down equations of equilibrium are presented in Section 2.5, and the actual numerical calculations yielding resultant loads are carried out in Appendix 2.C. The second case of interest is an evaluation of the weld (and by implication, the cask material adjacent to the weld) under a condition where the pocket trunnions are subject to 100% of the lifted load. Although the pocket trunnions are not designated as lifting trunnions, it is recognized that they could inadvertently be subject to such loadings during cask rotation operations. Therefore, to demonstrate the conservatism in the design, the trunnion weld group is assumed subject to the total cask lifted load with an appropriate dynamic load factor and we evaluate whether the material meets the requirements of 10CFR71.45.

2.R.2 Acceptance Criteria

The requirements of CFR71.45 are applied with the calculated stress in the weld group being compared to the material yield strength. Accordingly, under the transport tie down loading, it is required to demonstrate that an acceptable margin of safety exists based on a comparison with the material yield strength. When the trunnion is considered as being subject to the bounding loads during a rotation operation, then an acceptable margin of safety must exist based on a comparison with 33% of the material yield strength.

2.R.3 Assumptions

It is assumed that the weld forces can be computed, using strength of materials theory, based on the weld being a thin line element.

It is assumed that the loads are applied at the center of the trunnion pin for the purpose of computing moment arms.

It is assumed that four intermediate shells provide strength welds.

It is assumed that loads tending to rotate the trunnion with respect to the cask body are resisted by weld forces and by direct bearing on the innermost intermediate shell.

2.R.3 Weld Group Configuration

Figure 2.R.1 shows a sketch of the weld group (view is radially inward toward the center of the overpack. X is along the longitudinal axis of the overpack, Y is vertical, and Z is radially inward. The origin of the coordinate axes is at the centroid of the weld group. Figure 2.R.2 shows a V-groove construction, but a J-groove is also an option.

2.R.4 Weld Group Data Input

The weld is analyzed as a full penetration weld. ASME Section III, Subsection NF-3324.5(f)(3)(d) is the section of the Code that sets the effective weld thickness to be used for such welds. The calculation assumes only 3/4" penetration in the innermost layer

The distance from the root of the weld to the face of the weld is

$$td := 2 \cdot 1.25 \cdot \text{in} + 0.75 \cdot \text{in} + 1 \cdot \text{in} \qquad td = 4.25 \text{ in}$$

Therefore, the effective throat thickness for calculation purposes is

$$tw := td \qquad tw = 4.25 \text{ in}$$

The length and width of the weld group for calculation purposes are

$$L := 12.375 \cdot \text{in}$$

$$w := 12 \cdot \text{in}$$

For computation of safety margins, the yield stress of the weld or adjacent base metal is required. For SA-516 Grade 70 material, at 300 degrees F operating temperature, the yield stress is:

$$\sigma_y := 33700 \cdot \text{psi}$$

2.R.5 Calculation of Weld Group Area and Moments of Inertia

Weld group property calculations follow the methodology set forth in

Omer Blodgett, Design of Welded Structures, Lincoln Arc Welding Foundation, June 1966.

The weld group is considered as a unit width line element and section properties are computed. Required properties are the area/unit throat thickness, the section modulus/unit throat thickness, and the torsional section modulus/unit throat thickness

Weld Area/unit throat thickness

$$A_{\text{weld}} := 2 \cdot L + w \qquad A_{\text{weld}} = 36.75 \text{ in}$$

The centroid of the weld group is measured from the edge of the weld group closest to the top end of the overpack.

$$x_c := \frac{(2 \cdot L \cdot .5 \cdot L)}{A_{\text{weld}}} \qquad x_c = 4.167 \text{ in}$$

Now compute the section moduli of the weld group/unit throat thickness around axes through the C.G. (S_{xx} represents the section modulus/unit throat thickness about the longitudinal x axis, for example). Following the reference (Chapter 7, Section 4, Tables 4 and 5

$$S_{xx} := L \cdot w + \frac{w^2}{6} \qquad S_{xx} = 172.5 \text{ in}^2$$

$$S_{yyt} := \frac{(2 \cdot w \cdot L + L^2)}{3} \qquad S_{yyt} = 150.047 \text{ in}^2$$

$$S_{yyb} := L^2 \cdot \frac{(2 \cdot w + L)}{3 \cdot (w + L)} \qquad S_{yyb} = 76.178 \text{ in}^2$$

The subscripts t and b denote that the property is used when computing forces/unit throat thickness on the top (positive X) section of the weld, or at the ends of the two legs (negative X).

For this trunnion analysis, the use of S_{yy} is extremely conservative since it neglects any resistance in direct compression from the bearing of the underside of the trunnion on the surface of the innermost intermediate shell. To reflect this additional resistance against trunnion rotation about the y axis, we compute the area moment of inertia of the bearing surface between the top leg of the weld and the centroid of the weld group.

$$A_{\text{comp}} := xc \cdot w \quad A_{\text{comp}} = 50.005 \text{ in}^2$$

$$I_{y\text{comp}} := A_{\text{comp}} \cdot \frac{xc^2}{2} + w \cdot \frac{xc^3}{12} \quad I_{y\text{comp}} = 506.521 \text{ in}^4$$

Appropriate adders to the calculated S_{yy} for the weld group alone, to correct for the additional resistance from direct compression on the trunnion bearing surface, are obtained by computing the appropriate section moduli increments per unit of effective throat thickness

$$DS_{yyt} := \frac{I_{y\text{comp}}}{(xc) \cdot tw} \quad DS_{yyt} = 28.601 \text{ in}^2$$

$$DS_{yyb} := \frac{I_{y\text{comp}}}{(L - xc) \cdot tw} \quad DS_{yyb} = 14.52 \text{ in}^2$$

where we have divided the computed section modulus by the weld throat length to conform to the previous definitions. Therefore, the final section moduli for computing the resistance to moments about the y axis are

$$S_{yyt} := S_{yyt} + DS_{yyt} \quad S_{yyt} = 178.647 \text{ in}^2$$

$$S_{yyb} := S_{yyb} + DS_{yyb} \quad S_{yyb} = 90.698 \text{ in}^2$$

The torsional section modulus/unit of throat thickness is

$$J_w := \frac{(w + 2 \cdot L)^3}{12} - L^2 \cdot \frac{(L + w)^2}{(w + 2 \cdot L)} \quad J_w = 1.66 \times 10^3 \text{ in}^3$$

2.R.6 Applied Loading on the Weld Group

The applied loading for any combination is three forces which are assumed to be applied at a given point in space offset from the calculated centroid of the weld. For analysis purposes, the point of application of the loads is defined relative to the extreme forward fiber of the weld group. Defining the offsets as x_o , y_o and z_o , and referencing the pocket trunnion detail drawing for dimensions and Figure 2.R.2, yields:

$$x_o := (13 - 4.25) \cdot \text{in}$$

x_o is computed as the distance from the forward edge of the weld group to the center of the pocket trunnion pin which is assumed located at the center of the half circle which defines the recess cup.

$$x_o = 8.75 \text{ in}$$

Therefore, the offset in x (longitudinal) is:

$$x_{oc} := x_o - x_c \quad x_{oc} = 4.583 \text{ in}$$

Using symmetry, y_o is determined to be:

$$y_o := 0 \cdot \text{in}$$

z_o is the distance along the local z axis from the center of the trunnion pin to the centroid of the weld group. Since four intermediate shells have strength welds, the centroid is at the mid-height of the four intermediate shells. The thicknesses of the five intermediate shells are (numbered from inside out and defined as tg_1 , tg_2 , etc.):

$$tg_1 := 0.75 \cdot \text{in}$$

$$tg_2 := 1.25 \cdot \text{in}$$

$$tg_3 := tg_2$$

$$tg_4 := tg_2$$

$$tg_5 := 1 \cdot \text{in}$$

The wall thickness of the outer enclosure plate is:

$$t_{\text{wall}} := 0.5 \cdot \text{in}$$

and the depth of the neutron absorbing material is:

$$\text{depth} := 4.4375 \cdot \text{in}$$

Therefore, the offset z_0 is computed as:

$$z_0 := \left[\text{depth} + t_{\text{wall}} + .5 \cdot (\text{tg}2 + \text{tg}3 + \text{tg}4 + \text{tg}5) - .5 \cdot (3.9375 \cdot \text{in}) \right]$$

where half the depth of the recess is used as the location of the load point.

$$z_0 = 5.344 \text{ in}$$

2.R.7 Stress Analysis for Transport Loads

The following load case is limiting for the weld qualification (refer to the summary table in Section 2.5 or the detailed calculation in Appendix 2.C).

$$F_x := 1410000 \cdot \text{lbf}$$

$$F_y := 431600 \cdot \text{lbf}$$

$$F_r := (F_x^2 + F_y^2)^{0.5}$$

$$F_r = 1.475 \times 10^6 \text{ lbf}$$

F_r is the net direct shear force acting on the weld group. The bending moments on the weld group are determined as:

$$M_x := F_y \cdot z_0 \qquad M_x = 2.306 \times 10^6 \text{ in} \cdot \text{lbf}$$

$$M_y := F_x \cdot z_0 \qquad M_y = 7.535 \times 10^6 \text{ lbf} \cdot \text{in}$$

$$M_z := F_y \cdot x_{oc} \qquad M_z = 1.978 \times 10^6 \text{ in} \cdot \text{lbf}$$

The direct shear force/unit throat thickness is determined as:

$$S_r := \frac{Fr}{A_{\text{weld}}}$$

$$S_r = 4.012 \times 10^4 \frac{\text{lbf}}{\text{in}}$$

The force/unit throat thickness at point D, which is farthest from the centroid of the weld group, due to the two bending moments is determined as:

$$S_{by} := \frac{M_x}{S_{xx}} \qquad S_{by} = 1.337 \times 10^4 \frac{\text{lbf}}{\text{in}}$$

$$S_{bx} := \frac{M_y}{S_{yyb}} \qquad S_{bx} = 8.307 \times 10^4 \frac{\text{lbf}}{\text{in}}$$

$$S_b := S_{bx} + S_{by} \qquad S_b = 9.644 \times 10^4 \frac{\text{lbf}}{\text{in}}$$

The torsional force/unit of throat thickness at point D is determined as:

$$S_t := \frac{M_z \cdot \frac{w}{2}}{J_w} \qquad S_t = 7.148 \times 10^3 \frac{\text{lbf}}{\text{in}}$$

The net force/unit of weld throat thickness is computed as a root mean square

$$S_{\text{eq}} := \left[S_b^2 + (S_r + S_t)^2 \right]^{0.5} \qquad S_{\text{eq}} = 1.074 \times 10^5 \frac{\text{lbf}}{\text{in}}$$

Dividing by the yield strength of the material yields a minimum required throat thickness

$$t_{\text{req}} := \frac{S_{\text{eq}}}{\sigma_y} \qquad t_{\text{req}} = 3.187 \text{ in}$$

and the corresponding safety factor is therefore calculated as:

$$SF := \frac{tw}{t_{req}} \quad SF = 1.333 \quad > 0.0$$

2.R.8 Stress Analysis for Rotation Loads

During cask rotation operations, a bounding load for the two pocket trunnions is the total weight of the HI-STAR 100, amplified by an appropriate inertia load factor. This could potentially occur if there is momentary slack in the lifting rig attached to the top lifting trunnions. For this case, an appropriate load set is

$$F_x := \frac{250000}{2} \cdot \text{lbf} \quad F_y := 0 \cdot \text{lbf}$$

We note that impact limiters are not installed during this operation.

A 15% dynamic load factor is incorporated into the analysis; therefore,

$$ILF := 1.15$$

Therefore, the amplified longitudinal load on each pocket trunnion is

$$F_x := ILF \cdot F_x \quad F_r := (F_x^2 + F_y^2)^{0.5}$$

$$F_r = 1.438 \times 10^5 \text{ lbf}$$

F_r is the net direct in-plane force acting on the weld group. The bending moments on the weld group are determined as:

$$M_x := F_y \cdot z_o \quad M_x = 0 \text{ in} \cdot \text{lbf}$$

$$M_y := F_x \cdot z_o \quad M_y = 7.682 \times 10^5 \text{ lbf} \cdot \text{in}$$

$$M_z := F_y \cdot x_{oc} \quad M_z = 0 \text{ in} \cdot \text{lbf}$$

The direct shear force/unit throat thickness is determined as:

$$S_r := \frac{Fr}{A_{\text{weld}}} \quad S_r = 3.912 \times 10^3 \frac{\text{lbf}}{\text{in}}$$

The force/unit throat thickness at point D, which is farthest from the centroid of the weld group, due to the two bending moments is determined as:

$$S_{by} := \frac{Mx}{S_{xx}} \quad S_{by} = 0 \text{ ft psi}$$

$$S_{bx} := \frac{My}{S_{yyb}} \quad S_{bx} = 8.469 \times 10^3 \frac{\text{lbf}}{\text{in}}$$

$$S_b := S_{bx} + S_{by} \quad S_b = 8.469 \times 10^3 \frac{\text{lbf}}{\text{in}}$$

The torsional force/unit of throat thickness at point D is determined as:

$$S_t := \frac{Mz \cdot \frac{w}{2}}{J_w} \quad S_t = 0 \frac{\text{lbf}}{\text{in}}$$

The net force/unit of weld throat thickness is computed as a root mean square

$$S_{eq} := \left[S_b^2 + (S_r + S_t)^2 \right]^{0.5} \quad S_{eq} = 9.329 \times 10^3 \frac{\text{lbf}}{\text{in}}$$

Dividing by 33% of the material yield strength to meet the limits inferred by 10CFR71.45 for cask stress during a "lifting" operation gives a minimum required throat thickness

$$t_{req} := \frac{S_{eq}}{.333 \cdot \sigma_y} \quad t_{req} = 0.831 \text{ in}$$

so that the corresponding safety margin for this case is calculated as:

$$SF := \frac{tw}{t_{req}} \quad SF = 5.112 > 0.0$$

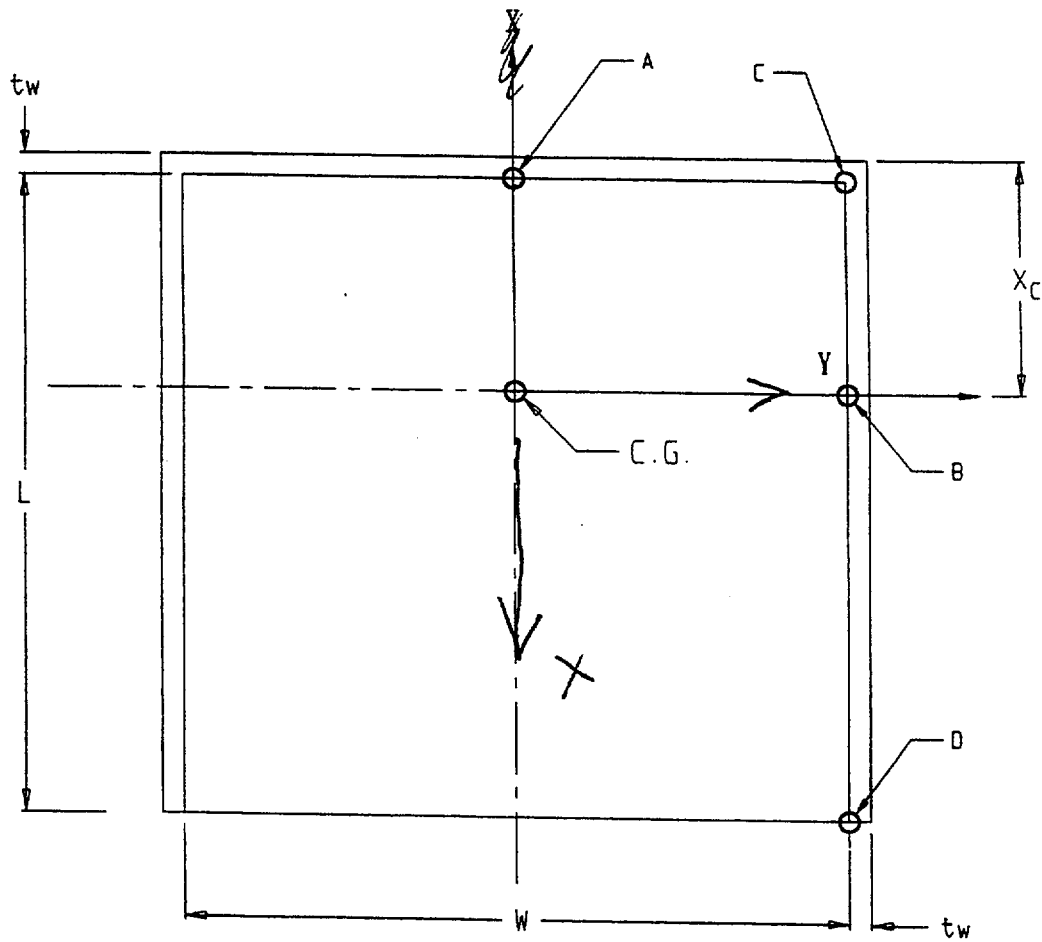


FIGURE 2.R.1; WELD GROUP GEOMETRY

$$SF := \frac{S_a}{\sigma} \quad SF = 12.296$$

(c) Enclosure Shell Flat Side Panels

These flat panels are treated as 1 inch wide beams. The actual end boundary condition is considered as an average of the simply supported and clamped conditions. This is reasonable since the groove welds most likely provide a support condition that is essentially clamped; the use of an average between pinned and clamped conditions will be conservative. The stress at the center of the panel is computed as follows:

The maximum bending moment is computed as the average of the moment for the two limiting end conditions:

$$M_{\max} := 0.5 \cdot \left(\frac{q \cdot w \cdot b_s^2}{8} + \frac{q \cdot w \cdot b_s^2}{24} \right) \quad M_{\max} = 155.039 \cdot \text{lbf} \cdot \text{in}$$

The beam section modulus is:

$$S := \frac{w \cdot t_v^2}{6} \quad S = 0.042 \cdot \text{in}^3$$

The maximum calculated bending stress is:

$$\sigma_{\max v} := \frac{M_{\max}}{S} \quad \sigma_{\max v} = 3.721 \cdot 10^3 \cdot \text{psi}$$

$$SF := \frac{S_a}{\sigma_{\max v}} \quad SF = 7.068$$

(d) Calculation of Weld Shear Stress

We consider the vertical weld between enclosure shell flat panels and the radial sectors and the circumferential weld between the enclosure shell and the enclosure shell return as representative welds for analysis. Table NF-3324.5(a)-1 in Subsection NF of the Code, requires that the allowable stress for the weld be equal to the allowable stress in the base metal. For the allowable weld stress in shear, we apply the limit given in NF-3252.2 for pure shear, namely, 60% of the tensile limit.

Model the weld as a 3/16" groove weld for calculation purposes.

$$t_{\text{weld}} := \frac{3}{16} \cdot \text{in}$$

The shear stress due to the internal pressure in the vertical flat panel weld is

$$\tau_{\text{weld}} := \frac{q \cdot 5 \cdot b_s}{t_{\text{weld}}} \qquad \tau_{\text{weld}} = 630 \text{ psi}$$

Since the allowable base metal stress for primary bending has been input earlier, we divide this value by 1.5 to obtain an allowable primary membrane stress.

$$\text{SF} := \frac{.6 \cdot \left(\frac{S_a}{1.5} \right)}{\tau_{\text{weld}}} \qquad \text{SF} = 16.698$$

For the weld around the annular ring, we note that since the unsupported strip width is less than the value used above, the weld shear stress will be even lower. Thus, the flat panel weld controls the design.

2.AM.4 Conclusion

For a 30 psi internal pressure, all safety factors are well in excess of 1.0 demonstrating that the 30 psig internal pressure is safely supported by the enclosure shell and the enclosure shell return.

Although the effect of dead weight of the neutron absorber material has not been included as an additional loading in the analysis of the enclosure shell return, it is clear from the large safety factors that structural integrity will not be compromised.

There is no credible mechanism for the pressure to exceed 30 psi under normal operating conditions in the enclosure shell sectors.

APPENDIX 2.AO - ANALYSIS OF TRANSNUCLEAR DAMAGED FUEL CANISTER AND THORIA ROD CANISTER

2.AO.1 Introduction

Some of the items at the Dresden Station that have been considered for transport in the HI-STAR 100 System are damaged fuel stored in Transnuclear damaged fuel canisters and Thoria rods that are also stored in a special canister designed by Transnuclear. Both of these canisters have been designed and have been used by ComEd to transport the damaged fuel and the Thoria rods. Despite the previous usage of these canisters, it is prudent and appropriate to provide an independent structural analysis of the major load path of these canisters prior to accepting them for inclusion as permitted items in the HI-STAR 100 MPC's. This appendix contains the necessary structural analysis of the Transnuclear damaged fuel canister and Thoria rod canister. The objective of the analysis is to demonstrate that the canisters are structurally adequate to support the loads that develop during normal lifting operations and during postulated hypothetical accident conditions.

The upper closure assembly is designed to meet the requirements of NUREG-0612 [2]. The remaining components of the canisters are governed by ASME Code Section III, Subsection NG [3]. These are the same criteria used in Appendix 2.AH to analyze the Holtec damaged fuel container for Dresden damaged fuel.

2.AO.2 Composition

This appendix was created using the Mathcad (version 8.02) software package. Mathcad uses the symbol ':=' as an assignment operator, and the equals symbol '=' retrieves values for constants or variables.

2.AO.3 References

1. Crane Manufacture's of America Association, Specifications for Electric Overhead Traveling Cranes #70.
2. NUREG-0612, Control of Heavy Loads at Nuclear Power Plants
3. ASME Boiler and Pressure Vessel Code, Section III, July 1995

2.AO.4 Assumptions

1. Buckling is not a concern during an accident since during a drop the canister will be confined by the fuel basket.
2. The strength of the weld is assumed to decrease the same as the base metal as the temperature increases.

2.AO.5 Method

Two are considered: 1) normal lifting and handling of canister, and 2) hypothetical accident drop event.

2.AO.6 Acceptance Criteria

1) Normal Handling -

a) Canister governed by ASME NG allowables:

b) Welds governed by NG and NF allowables;
quality factors taken from NG
stress limit = 0.3 Su

c) Lifting governed by NUREG-0612 allowables.

2) Drop Accident -

a) canister governed by ASME NG allowables:
shear = 0.42 Su (conservative)

b) Welds governed by NG and NF allowables;
quality factors taken from NG
stress limit = 0.42 Su

2.AO.7 Input Stress Data

The canisters is handled while still in the spent fuel pool. Therefore, its design temperature for lifting considerations is the temperature of the fuel pool water (150°F). The design temperature for accident conditions is 725°F. All dimensions are taken from the Transnuclear design drawings listed at the end of this appendix. The basic input parameters used to perform the calculations are:

Design stress intensity of SA240-304 (150°F)	$S_{m1} := 20000 \cdot \text{psi}$
Design stress intensity of SA240-304 (775°F)	$S_{m2} := 15800 \cdot \text{psi}$
Yield stress of SA240-304 (150°F)	$S_{y1} := 27500 \cdot \text{psi}$
Yield stress of SA240-304 (775°F)	$S_{y2} := 17500 \cdot \text{psi}$
Ultimate strength of SA240-304 (150°F)	$S_{u1} := 73000 \cdot \text{psi}$
Ultimate strength of SA240-304 (775°F)	$S_{u2} := 63300 \cdot \text{psi}$

Ultimate strength of weld material (150°F)

$$S_{u_w} := 70000 \text{ psi}$$

Ultimate strength of weld material (775°F)

$$S_{u_{wacc}} := S_{u_w} - (S_{u1} - S_{u2})$$

Weight of a BWR fuel assembly (D-1)

$$W_{fuel} := 400 \text{ lbf}$$

Weight of 18 Thoria Rods (Calculated by Holtec)

$$W_{thoria} := 90 \text{ lbf}$$

Bounding Weight of the damaged fuel canister (Estimated by Holtec)

$$W_{container} := 150 \text{ lbf}$$

Bounding Weight of the Thoria Rod Canister (Estimated)

$$W_{rodcan} := 300 \text{ lbf}$$

Quality factor for full penetration weld (visual inspection)

$$n := 0.5$$

Dynamic load factor for lifting

$$DLF := 1.15$$

The remaining input data is provided as needed in the calculation section

2.AO.8 Calculations for Transnuclear Damaged Fuel Canister

2.AO.8.1 Lifting Operation (Normal Condition of Storage)

The critical load case under normal conditions is the lifting operation. The key areas of concern for ASME NG analysis are the canister sleeve, the sleeve to lid frame weld, and the lid frame. All calculations performed for the lifting operation assume a dynamic load factor of 1.15 [1].

2.AO.8.1.1 Canister Sleeve

During a lift, the canister sleeve is loaded axially, and the stress state is pure tensile membrane. For the subsequent stress calculation, it is assumed that the full weight of the damaged fuel canister and the fuel assembly are supported by the sleeve. The magnitude of the load is

$$F := DLF \cdot (W_{container} + W_{fuel}) \quad F = 632 \text{ lbf}$$

From TN drawing 9317.1-120-4, the canister sleeve geometry is

$$id_{sleeve} := 4.81 \text{ in} \quad t_{sleeve} := 0.11 \text{ in}$$

The cross sectional area of the sleeve is

$$A_{sleeve} := (id_{sleeve} + 2 \cdot t_{sleeve})^2 - id_{sleeve}^2 \quad A_{sleeve} = 2.16 \text{ in}^2$$

Therefore, the tensile stress in the sleeve is

$$\sigma := \frac{F}{A_{\text{sleeve}}} \quad \sigma = 292 \text{ psi}$$

The allowable stress intensity for the primary membrane category is S_m per Subsection NG of the ASME Code. The corresponding safety margin is

$$SM := \frac{S_{m1}}{\sigma} - 1 \quad SM = 67.5$$

2.AO.8.1.2 Sleeve Welds

The top of the canister must support the amplified weight. This load is carried directly by the fillet weld that connects the lid frame to the canister sleeve. The magnitude of the load is conservatively taken as the entire amplified weight of canister plus fuel.

$$F = 632 \text{ lbf}$$

The weld thickness is $t_{\text{base}} := 0.09 \text{ in}$

The area of the weld, with proper consideration of quality factors, is

$$A_{\text{weld}} := n \cdot 4 \cdot (id_{\text{sleeve}} + 2 \cdot t_{\text{sleeve}}) \cdot 0.7071 \cdot t_{\text{base}} \quad A_{\text{weld}} = 0.64 \text{ in}^2$$

Therefore, the shear stress in the weld is

$$\tau := \frac{F}{A_{\text{weld}}} \quad \tau = 988 \text{ psi}$$

From the ASME Code the allowable weld shear stress, under normal conditions (Level A), is 30% of the ultimate strength of the base metal. The corresponding safety margin is

$$SM := \frac{0.3 \cdot S_{u1}}{\tau} - 1 \quad SM = 21.2$$

2.AO.8.1.3 Lid Frame Assembly

The Lid Frame assembly is classified as a NUREG-0612 lifting device. As such the allowable stress for design is the lesser of one-sixth of the yield stress and one-tenth of the ultimate strength.

$$\sigma_1 := \frac{S_{y1}}{6} \quad \sigma_2 := \frac{S_{u1}}{10}$$

$$\sigma_1 = 4583 \text{ psi} \quad \sigma_2 = 7300 \text{ psi}$$

For SA240-304 material the yield stress governs. $\sigma_{\text{allowable}} := \sigma_1$

The total lifted load is $F := \text{DLF} \cdot (W_{\text{container}} + W_{\text{fuel}})$ $F = 632 \text{ lbf}$

The frame thickness is obtained from Transnuclear drawing 9317.1-120-11

$$t_{\text{frame}} := 0.395 \text{ in}$$

The inside span is the same as the canister sleeve $\text{id}_{\text{sleeve}} = 4.81 \text{ in}$

The area available for direct load is

$$A_{\text{frame}} := (\text{id}_{\text{sleeve}} + 2 \cdot t_{\text{frame}})^2 - \text{id}_{\text{sleeve}}^2 \quad A_{\text{frame}} = 8.224 \text{ in}^2$$

The direct stress in the frame is

$$\sigma := \frac{F}{A_{\text{frame}}} \quad \sigma = 77 \text{ psi}$$

The safety margin is

$$\text{SM} := \frac{\sigma_{\text{allowable}}}{\sigma} - 1 \quad \text{SM} = 58.59$$

The bearing stress at the four lift locations is computed from the same drawing

$$A_{\text{bearing}} := 4 \cdot t_{\text{frame}} \cdot (2 \cdot 0.38 \text{ in}) \quad A_{\text{bearing}} = 1.201 \text{ in}^2$$

$$\sigma_{\text{bearing}} := \frac{F}{A_{\text{bearing}}} \quad \sigma_{\text{bearing}} = 526.732 \text{ psi} \quad \text{SM} := \frac{\sigma_{\text{allowable}}}{\sigma_{\text{bearing}}} - 1 \quad \text{SM} = 7.7$$

2.AO.8.2 60g End Drop (Hypothetical Accident Condition of Transport)

The critical member of the damaged fuel canister during the end drop scenario is the bottom assembly (see Transnuclear drawing 9317.1-120-5). It is subjected to direct compression due to the amplified weight of the fuel assembly and the canister. The bottom assembly is a 3.5" Schedule 40S pipe. The load due to the 60g end drop is

$$F := 60 \cdot (W_{\text{fuel}} + W_{\text{container}}) \quad F = 33000 \text{ lbf}$$

The properties of the pipe are obtained from the Ryerson Stock Catalog as

$$\text{od} := 4 \text{ in} \quad \text{id} := 3.548 \text{ in} \quad t_{\text{pipe}} := \frac{(\text{od} - \text{id})}{2} \quad t_{\text{pipe}} = 0.226 \text{ in}$$

The pipe area is

$$A_{\text{pipe}} := \frac{\pi}{4} \cdot (\text{od}^2 - \text{id}^2) \quad A_{\text{pipe}} = 2.68 \text{ in}^2$$

The stress in the member is

$$\sigma := \frac{F}{A_{\text{pipe}}} \quad \sigma = 12316 \text{ psi}$$

The allowable primary membrane stress from Subsection NG of the ASME Code, for accident conditions (Level D), is

$$\sigma_{\text{allowable}} := 2.4 \cdot S_{m2} \quad \sigma_{\text{allowable}} = 37920 \text{ psi}$$

The safety margin is

$$SM := \frac{\sigma_{\text{allowable}}}{\sigma} - 1 \quad SM = 2.1$$

To check the stability of the pipe, we conservatively compute the Euler Buckling load for a simply supported beam.

The Young's Modulus is

$$E := 27600000 \text{ psi}$$

Compute the moment of inertia as

$$I := \frac{\pi}{64} \cdot (\text{od}^4 - \text{id}^4) \quad I = 4.788 \text{ in}^4$$

$L := 22 \text{ in}$

$$P_{\text{crit}} := \pi^2 \cdot \frac{E \cdot I}{L^2} \quad P_{\text{crit}} = 2.695 \cdot 10^6 \text{ lbf}$$

The safety margin is

$$SM := \frac{P_{\text{crit}}}{F} - 1 \quad SM = 80.654$$

2.AO.8.3 Conclusion for TN Damaged Fuel Canister

The damaged fuel canister and the upper closure assembly are structurally adequate to withstand the specified normal and accident condition loads. All calculated safety margins are greater than zero.

2.AO.9 Calculations for Transnuclear Thoria Rod Canister

2.AO.9.1 Lifting Operation (Normal Condition of Storage)

The critical load case under normal conditions is the lifting operation. The key areas of concern for ASME NG analysis are the canister sleeve, the sleeve to lid frame weld, and the lid frame. All calculations performed for the lifting operation assume a dynamic load factor of 1.15.

2.AO.9.1.1 Canister Sleeve

During a lift, the canister sleeve is loaded axially, and the stress state is pure tensile membrane. For the subsequent stress calculation, it is assumed that the full weight of the Thoria rod canister and the Thoria rods are supported by the sleeve. The magnitude of the load is

$$F := DLF \cdot (W_{\text{rodcan}} + W_{\text{thoria}})$$

$$F = 449 \text{ lbf}$$

From TN drawing 9317.1-182-1, the canister sleeve geometry is

$$id_{\text{sleeve}} := 4.81 \text{ in}$$

$$t_{\text{sleeve}} := 0.11 \text{ in}$$

The cross sectional area of the sleeve is

$$A_{\text{sleeve}} := (id_{\text{sleeve}} + 2 \cdot t_{\text{sleeve}})^2 - id_{\text{sleeve}}^2$$

$$A_{\text{sleeve}} = 2.16 \text{ in}^2$$

Therefore, the tensile stress in the sleeve is

$$\sigma := \frac{F}{A_{\text{sleeve}}}$$

$$\sigma = 207 \text{ psi}$$

The allowable stress intensity for the primary membrane category is S_m per Subsection NG of the ASME Code. The corresponding safety margin is

$$SM := \frac{S_{m1}}{\sigma} - 1$$

$$SM = 95.5$$

2.AO.9.1.2 Sleeve Welds

The top of the canister must support the amplified weight. This load is carried directly by the fillet weld that connects the lid frame to the canister sleeve. The magnitude of the load is conservatively taken as the entire amplified weight of canister plus Thoria rod.

$$F = 449 \text{ lbf}$$

The weld thickness is $t_{\text{base}} := 0.09 \text{ in}$ (assumed equal to the same weld for the damaged fuel canister)

The area of the weld, with proper consideration of quality factors, is

$$A_{\text{weld}} := n \cdot 4 \cdot (id_{\text{sleeve}} + 2 \cdot t_{\text{sleeve}}) \cdot 0.7071 \cdot t_{\text{base}}$$

$$A_{\text{weld}} = 0.64 \text{ in}^2$$

Therefore, the shear stress in the weld is

$$\tau := \frac{F}{A_{\text{weld}}}$$

$$\tau = 701 \text{ psi}$$

From the ASME Code the allowable weld shear stress, under normal conditions (Level A), is 30% of the ultimate strength of the base metal. The corresponding safety margin is

$$SM := \frac{0.3 \cdot S_{u1}}{\tau} - 1$$

$$SM = 30.3$$

2.AO.9.1.3 Lid Frame Assembly

The Lid Frame assembly is classified as a NUREG-0612 lifting device. As such the allowable stress for design is the lesser of one-sixth of the yield stress and one-tenth of the ultimate strength.

$$\sigma_1 := \frac{S_{y1}}{6} \qquad \sigma_2 := \frac{S_{u1}}{10}$$

$$\sigma_1 = 4583 \text{ psi} \qquad \sigma_2 = 7300 \text{ psi}$$

For SA240-304 material the yield stress governs. $\sigma_{\text{allowable}} := \sigma_1$

The total lifted load is $F := DLF \cdot (W_{\text{rodcan}} + W_{\text{thoria}})$ $F = 449 \text{ lbf}$

The frame thickness is obtained from Transnuclear drawing 9317.1-182-8. This drawing was not available, but the TN drawing 9317.1-182-4 that included a view of the lid assembly suggests that it is identical in its structural aspects to the lid frame in the damaged fuel canister.

$$t_{\text{frame}} := 0.395 \text{ in}$$

The inside span is the same as the canister sleeve $id_{\text{sleeve}} = 4.81 \text{ in}$

The area available for direct load is

$$A_{\text{frame}} := (id_{\text{sleeve}} + 2 \cdot t_{\text{frame}})^2 - id_{\text{sleeve}}^2 \qquad A_{\text{frame}} = 8.224 \text{ in}^2$$

The direct stress in the frame is

$$\sigma := \frac{F}{A_{\text{frame}}} \qquad \sigma = 55 \text{ psi}$$

The safety margin is

$$SM := \frac{\sigma_{\text{allowable}}}{\sigma} - 1 \qquad SM = 83.04$$

The bearing stress at the four lift locations is computed from the same drawing

$$A_{\text{bearing}} := 4 \cdot t_{\text{frame}} \cdot (2 \cdot 0.38 \text{ in}) \qquad A_{\text{bearing}} = 1.201 \text{ in}^2$$

$$\sigma_{\text{bearing}} := \frac{F}{A_{\text{bearing}}} \qquad \sigma_{\text{bearing}} = 373.501 \text{ psi} \qquad SM := \frac{\sigma_{\text{allowable}}}{\sigma_{\text{bearing}}} - 1 \qquad SM = 11.27$$

2.AO.9.2 60g End Drop (Hypothetical Accident Condition of Transport)

The critical member of the damaged fuel canister during the drop scenario is the bottom assembly. Transnuclear drawing 9317.1-120-5). It is subjected to direct compression due to the amplified weight of the Thoria rods and the canister.

$$F := 60 \cdot (W_{\text{thoria}} + W_{\text{rodcan}}) \quad F = 23400 \text{ lbf}$$

The properties of the pipe are obtained from the Ryerson Stock Catalog as

$$\text{od} := 4 \text{ in} \quad \text{id} := 3.548 \text{ in} \quad t_{\text{pipe}} := \frac{(\text{od} - \text{id})}{2} \quad t_{\text{pipe}} = 0.226 \text{ in}$$

The pipe area is

$$A_{\text{pipe}} := \frac{\pi}{4} \cdot (\text{od}^2 - \text{id}^2) \quad A_{\text{pipe}} = 2.68 \text{ in}^2$$

The stress in the member is

$$\sigma := \frac{F}{A_{\text{pipe}}} \quad \sigma = 8733 \text{ psi}$$

The allowable primary membrane stress from Subsection NG of the ASME Code, for accident conditions (Level D), is

$$\sigma_{\text{allowable}} := 2.4 \cdot S_{m2} \quad \sigma_{\text{allowable}} = 37920 \text{ psi}$$

The safety margin is

$$SM := \frac{\sigma_{\text{allowable}}}{\sigma} - 1 \quad SM = 3.3$$

To check the stability of the pipe, we compute the Euler Buckling load for a simply supported beam.

The Young's Modulus is

$$E := 27600000 \text{ psi}$$

Compute the moment of inertia as

$$I := \frac{\pi}{64} \cdot (\text{od}^4 - \text{id}^4) \quad I = 4.788 \text{ in}^4$$

$L := 22 \text{ in}$

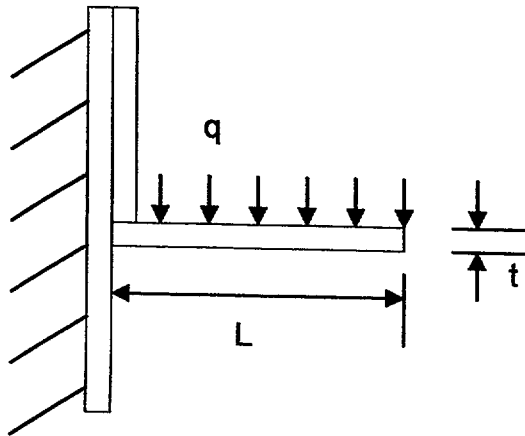
$$P_{\text{crit}} := \pi^2 \cdot \frac{E \cdot I}{L^2} \quad P_{\text{crit}} = 2.695 \cdot 10^6 \text{ lbf}$$

The safety margin is

$$SM := \frac{P_{\text{crit}}}{F} - 1 \quad SM = 114.153$$

2.AO.9.4 60g Side Drop (Hypothetical Accident Condition of Transport)

The Thoria Rod Separator Assembly is shown in TN drawings 9317.1-182-1 and 9317.1-182-3. Under the design basis side drop, we examine the consequences to one of the rod support strips acting as a cantilever strip acted upon by self-weight and the weight of one Thoria rod.



Weight of 1 rod per unit length

$$\text{length} := 113.16 \cdot \text{in}$$

$$w_{\text{rod}} := 90 \cdot \frac{\text{lbf}}{18} \cdot \frac{1}{\text{length}}$$

$$w_{\text{rod}} = 0.044 \frac{\text{lbf}}{\text{in}}$$

Weight of support per unit length (per drawing 9317.1-182-3)

$$L := 1.06 \cdot \text{in}$$

$$t := 0.11 \cdot \text{in}$$

$$w_{\text{sup}} := .29 \cdot \frac{\text{lbf}}{\text{in}^3} \cdot L \cdot t$$

$$w_{\text{sup}} = 0.034 \frac{\text{lbf}}{\text{in}}$$

Amplified load (assumed as a uniform distribution)

$$q := 60 \cdot (w_{\text{rod}} + w_{\text{sup}})$$

$$q = 4.68 \frac{\text{lbf}}{\text{in}}$$

$$\text{Moment} := \frac{q \cdot L^2}{2}$$

$$\text{Moment} = 2.629 \text{ in} \cdot \text{lbf}$$

Bending stress at the root of the cantilever beam is

$$\sigma := 6 \cdot \frac{\text{Moment}}{1 \cdot \text{in} \cdot t^2}$$

$$\sigma = 1.304 \cdot 10^3 \text{ psi}$$

Shear stress at the root of the cantilever

$$\tau := q \cdot \frac{L}{t \cdot 1 \cdot \text{in}}$$

$$\tau = 45.098 \text{ psi}$$

Large margins of safety are indicated by these stress results.

2.AO.9.5 Conclusion for TN Thoria Rod Canister

The Thoria rod canister is structurally adequate to withstand the specified normal lift and hypothetical accident condition loads. All calculated safety margins are greater than zero.

2.AO.10 General Conclusion

The analysis of the TN damaged fuel canister and the TN Thoria rod canister have demonstrated that all structural safety margins are large. We have confirmed that the TN canisters have positive safety margins for the HI-STAR 100 governing design basis loads. Therefore, the loaded TN canisters from ComEd Dresden Unit#1 can safely be carried in the HI-STAR 100 System.

2.AO.11 List of Transnuclear Drawing Numbers

9317.1-120 - 2,3,4,5,6,7,8,9,10,11,13,14,15,17,18,19,20,21,22,23

9317.1-182- 1,2,3,4,5,6

3.3 TECHNICAL SPECIFICATIONS FOR COMPONENTS

HI-STAR System materials and components which are required to be maintained within their safe operating temperature ranges to ensure their intended function are summarized in Table 3.3.1. Long-term stability and continued neutron shielding ability of the Holtite-A neutron shield material under normal transport conditions are ensured when material exposure temperatures are maintained below the maximum allowable limit. The overpack metallic seals will continue to ensure leak tightness of the closure plate, and drain and vent ports if the manufacturer's recommended design temperature limits are not exceeded. Integrity of SNF during transport requires demonstration of HI-STAR System thermal performance to maintain fuel cladding temperatures below design basis limits. Boral used in MPC baskets for criticality control (a composite material composed of B₄C and aluminum) is stable up to 1000°F for short-term and 850°F for long term dry storage[†]. However, for conservatism, a lower maximum temperature limit is imposed.

Compliance to 10CFR71 requires evaluation of hypothetical accident conditions. The inherent mechanical stability characteristics of the HI-STAR System materials and components ensure that no significant functional degradation is possible due to exposure to short-term temperature excursions outside the normal long-term temperature limits. For evaluation of the HI-STAR System's thermal performance under hypothetical accident conditions, material temperature limits for short-duration events are also provided in Table 3.3.1.

3.3.1 Evaluation of Zircaloy Clad Fuel

The PNL study [3.3.2] proposes a 1058°F fuel cladding temperature limit for zircaloy clad fuel for periods of time which are relatively short compared to typical long-term dry storage durations. Many transport only cask systems^{††} have stipulated this short-term cladding temperature limit as the design limit during transport. The HI-STAR System, however, is a dual-use (transport and storage) system. Therefore, unlike transport only cask systems, the HI-STAR can be placed in long-term storage following transport. Recognizing that the rate of cladding degradation increases at an accelerating pace with elevated temperatures, the design fuel cladding temperature limits for normal transport in the HI-STAR are specified to be the *long-term storage* temperature limits determined using the generic CSFM IDS temperature limit curves. These long-term temperature limits are a function of the fuel age at initial loading into the HI-STAR (see Table 3.3.7). This will serve to ensure that the cumulative cladding damage during transport does not substantially increase the probability of cladding failure during subsequent long-term storage conditions.

† AAR Structures Boral thermophysical test data.

†† Nuclear Assurance Corporation (NAC) UMS, Docket 71-9270.
Vectra NUHOMS MP187, Docket 71-9255.
Sierra Nuclear Corp. (SNC) TRANSTOR, Docket 71-9268.

Pacific Northwest Laboratory (PNL) has established a Commercial Spent Fuel Management (CSFM) model based on creep rupture data for zircaloy [3.3.2]. The CSFM model enables a cask designer to determine fuel-specific maximum initial peak cladding temperature limits. The CSFM Inerted Dry Storage (IDS) temperature limit curves [3.3.2] define the maximum allowable initial storage temperature at initial cladding stresses as a function of fuel age. Therefore, for SNF of a given age (decay time), the permissible peak cladding temperature is a direct function of the cladding hoop stress, which in turn depends on the radius-to-thickness ratio of the fuel rod and its internal pressure. The rod internal pressure (P_i) is calculated based upon the maximum initial fill pressures (Tables 3.3.2 and 3.3.5) with fission gas release at a conservatively bounding maximum burnup under HI-STAR System transport conditions (40,000 MWD/MTU for BWR fuel and 42,500 MWD/MTU for PWR fuel).

The free rod volumes in the third column of Tables 3.3.2 and 3.3.5 are defined as free volumes available for pressurization with rod fill gas *in each rod*. Physically, the free rod volume is the cumulative sum of the open top plenum space, the pellet-to-cladding annular space and the inter-pellet junction space. As a lower bound value of the free rod volume will lead to a conservative estimate of the cladding stress at operating temperatures, the nominal plenum space is included in the free rod volume. The plenum length for miscellaneous BWR fuel assemblies is set to 12 inches. The fission gas release fraction data is based on Regulatory Guide 1.25 (Table 3.3.4). The radius-to-thickness ratio (r^*) is determined based on rod nominal dimension values (Table 3.3.3 and 3.3.6) including the maximum cladding thickness loss due to in-reactor oxidation, as reported in another PNL study [3.3.5].

By utilizing P_i and r^* , the cladding stress for various PWR fuel types is calculated from Lamé's formula and summarized in Table 3.3.3. It can be seen from Figure 3.4.19 that the average temperature of the gas in the fuel rods, a great bulk of which is located in the top region of the SNF, is well below 300°C for the PWR fuel array types. Therefore, to compute the cladding hoop stress in a conservative manner, the ideal gas law is used to obtain the value of the in-rod gas pressure at 300°C. An inspection of cladding stress data summarized in Table 3.3.3 indicates 96.7 MPa as the bounding value of cladding stress (σ_{max}) for the PWR SNF. Corresponding fill gas data and calculations of cladding stress for the various BWR SNF types are summarized in Tables 3.3.5 and 3.3.6, respectively. It can be seen from Figure 3.4.20 that the average temperature of the gas in the fuel rods, a great bulk of which is located in the top region of the SNF, is well below 300°C for all BWR fuel array types considered in this topical report. Therefore, to compute the cladding hoop stress in a conservative manner, the ideal gas law is used to obtain the value of the in-rod gas pressure at 300°C. An inspection of the cladding stress data in Table 3.3.6 indicates that the bounding value of the cladding hoop stress for all BWR SNF types is 54.7 MPa (except for 8x8 and 6x6 GE Dresden-1, QUAD+, and 6x6 GE Humboldt Bay fuel types).

The bounding values of σ_{max} for the array of PWR and BWR SNF types are thus 96.7 MPa and 54.7 MPa, respectively (except for the 8x8 and 6x6 GE Dresden-1, QUAD+ and 6x6 GE Humboldt Bay fuel types for which the bounding value of σ_{max} is 72.5 MPa).

Several implicit assumptions in the calculation of σ_{\max} , such as neglect of the rod cavity growth due to thermal expansion, internal fill pressure, and in-core irradiation, ensure that the hoop stress value (which is the sole determinant in the establishment of permissible cladding temperature for a given cooling time) is indeed a bounding number.

The generic CSFM IDS temperature limit curves developed in the PNL study [3.3.2] are used to determine zircaloy cladding temperature limits at the conservative 300°C average rod temperature. The fuel cladding temperature limits obtained from these PNL curves ensure a low fuel rod failure probability. The calculated limits are presented, as a function of the fuel age, in Table 3.3.7.

3.3.2 Evaluation of Stainless Steel Clad Fuel

Approximately 2,200 PWR and BWR fuel assemblies stored in the United States employ stainless steel cladding. All stainless steel cladding materials are of the austenitic genre with the ASTM alloy compositions being principally type 304 and 348H. The long-term storage condition peak allowable temperature applicable for stainless steel fuel is significantly higher than that applicable to zircaloy clad fuel. A recent EPRI/PNL study [3.3.6] recommends a 430°C (806°F) peak stainless steel cladding temperature limit versus a typical 380°C (716°F) peak zircaloy cladding temperature limit. Since the peak cladding temperature limits applied to the thermal analysis are based on the zircaloy clad limit, it is readily apparent that this criterion is overly restrictive for stainless steel clad fuel. The peak clad temperature limits applied to both zircaloy and stainless steel clad fuel assemblies are provided in Table 3.3.7.

It is recognized that the peak cladding temperature of stainless fuel will differ from zircaloy clad fuel principally due to the following differences:

- i. Differences in decay heat levels
- ii. Differences in cladding emissivity
- iii. Differences in cladding conductivity
- iv. Differences in rod array dimensions

The net planar thermal resistance of the equivalent homogenized axisymmetric MPC basket containing stainless steel clad fuel is greater than the case with zircaloy clad fuel. The higher resistance arises principally from the significantly lower emissivity of stainless steel cladding. This factor is, however, offset by significantly lower design basis heat loads considered for stainless steel clad fuel. As demonstrated by examining Tables 3.4.6, 1.2.13 and 1.2.19, the percentage reduction in design basis heat duty for stainless steel fuel (at least 70% lower than zircaloy clad BWR fuel and 41% lower than zircaloy clad PWR fuel) is more pronounced than the nominal percentage decrease in MPC basket effective thermal conductivity[†] (stainless steel fueled baskets are between 9% to 13%

[†] The term "effective conductivity" of the fuel basket is defined in Section 3.4.1.

less conducting). Therefore, it is concluded that the peak cladding temperature for stainless steel clad fuel will be bounded by the zircaloy clad fuel results. Consequently, in view of significantly higher peak stainless steel cladding temperature levels recommended by the EPRI study, a separate thermal analysis to demonstrate the adequacy of stainless steel clad integrity for transport in the HI-STAR System is not necessary.

3.3.3 Accident Condition Cladding Temperature Limit

For short-term duration events (hypothetical fire accident, for example), relatively high fuel cladding temperature limits have been historically accepted by the USNRC. For example, the Safety Analysis Report of the STC transport cask (Docket No. 71-9235), recently certified by the USNRC, permits 1200°F (approximately 649°C) as the maximum value of the peak cladding temperature (T_{\max}) for transport of SNF with up to 45,000 MWD/MTU burnup. PNL test data [3.3.5], limiting itself to medium burnup levels (28,800 MWD/MTU), endorses a somewhat lower T_{\max} value ($T_{\max} = 570^{\circ}\text{C}$ or 1058°F). Based on the published industry test data, guidance in the literature, and analytical reasoning, we herein prescribe 570°C as the admissible short-term value of T_{\max} for the SNF for the relatively lower burnup levels in the HI-STAR System for transport^{††}.

A Brookhaven report written for EPRI [3.3.7] asserts that fuel cladding rupture becomes “virtually absent at stresses below about 200 MPa”. It can be readily deduced that the peak cladding stress for the limiting condition of 570°C cladding temperature will be below 200 MPa for the SNF burnup levels considered in this SAR. Recalling σ_{\max} at 96.7 MPa (Table 3.3.3) at 300°C gas temperature, the cladding circumferential stress (σ_{peak}) at 570°C is obtained by direct proportionality in absolute gas temperature:

$$\sigma_{\text{peak}} = \sigma_{\max} (570 + 273)/(300 + 273) = 142.3 \text{ MPa (approximately 20,600 psi)}$$

Therefore, short-term temperature values (T_{\max}) of 570°C for zircaloy cladding are considered safe to preclude fuel cladding failure.

The EPRI report cites experiments on fourteen irradiated Turkey Point Unit 3 rods carried out by Einziger et al.[†] in 1982 which showed no breach in cladding even after as much as 7% strain was

^{††} 40,000 MWD/MTU for BWR fuel and 45,000 MWD/MTU for PWR fuel bounds permissible maximum burnups.

[†] “High Temperature Post Irradiation Materials Performance of Spent Pressurized Water Reactor Fuel Rods under Dry Storage Conditions,” by R.E. Einziger, S.D. Atkin, D.E. Stallrecht, and V.S. Pasupathi, Nuclear Technology, 57:65-80 (1982).

accumulated at elevated temperatures lasting for 740-1,000 hours. Einziger's test data corroborates our selection of $T_{\max} = 570^{\circ}\text{C}$ as the short duration limiting temperature.

For stainless steel clad fuel, the appropriate short-term temperature limits are based on high temperature creep rupture data presented in another EPRI report by Cunningham et. al. [3.3.6, Table 5-2, page 5-2]. In this report, stainless steel cladding stress limits for 10,000 hour exposure time (in excess of one year) at elevated temperature (1000°F) is provided. This is summarized in Table 3.3.8. From this table, it is apparent that the cladding rupture stresses are significantly higher than the σ_{peak} computed above. Consequently, there is reasonable assurance that stainless steel cladding integrity is maintained by exposure at 540°C temperature for short-term conditions.

Table 3.3.1

HI-STAR SYSTEM MATERIAL TEMPERATURE LIMITS

Material	Normal Condition Temperature Limits	Accident Condition Temperature Limits
Fuel Cladding (Zircaloy and Stainless Steel)	720°F (PWR Fuel) 749°F (BWR Fuel)	1058°F (zircaloy) 1000°F (stainless steel)
Boral [†]	800°F	950°F
Overpack Closure Plate Mechanical Seals	See Table 4.1.1	See Table 4.1.1
Overpack Vent and Drain Port Plug Seals	See Table 4.1.1	See Table 4.1.1
Aluminum Alloy 5052	176°F ^{††}	1105°F ^{†††}
Holtite-A	300°F ^{††††}	N/A ^{†††††}
Aluminum Heat Conduction Elements (Alloy 1100)	725°F	950°F

[†] Based on AAR Structures Boral thermophysical test data.

^{††} AL-STAR impact limiter aluminum honeycomb test data.

^{†††} Melting range of alloy is 1105°F-1200°F [3.3.1].

^{††††} Neutron shield manufacturer's test data (Appendix 1.B).

^{†††††} For shielding analysis (Chapter 5), Holtite-A is conservatively assumed to be lost during the fire accident.

Table 3.3.2

SUMMARY OF PWR ASSEMBLY RODS INITIAL FILL GAS DATA

Assembly Type	Rods Per Assembly	Free Rod Volume (inch ³)	Fill Pressure (psig)	Maximum Fill Volume (Liters at STP [†])	
				Per Rod	Per Assembly
W 14×14 Std.	179	1.72	0-460	0.845	151.2
W 15×15 Std.	204	1.25	0-475	0.633	129.1
W 17×17 Std.	264	1.05-1.25	275-500	0.666	175.8
B&W 15×15 Mark B	208	1.308	415	0.582	121.1
B&W 17×17 Mark C	264	0.819	435	0.381	100.6
CE 14×14 Std.	164	1.693	300-450	0.814	133.5
CE 16×16 Sys 80	220	1.411	300-450	0.678	149.2
B&W-15x15 Mark B-11	208	1.260	415	0.560	116.5
CE-14x14 (MP2)	176	1.728	300-450	0.831	146.2

† STP stands for standard temperature and pressure.

Table 3.3.3
 BOUNDING VALUES OF FUEL CLADDING STRESS FOR PWR SNF

	<u>W</u> 14×14 Std.	<u>W</u> 15×15 Std.	<u>W</u> 17×17 Std.	B&W 15×15 Mark B	B&W 17×17 Mark C	CE 14×14 Std.	CE 16×16 Sys 80	B&W 15×15 Mark B-11	CE 14×14 (MP2)
Fresh Fuel Rods O.D. (inch)	0.4220	0.422	0.374	0.430	0.379	0.440	0.382	0.414	0.440
End of Life Oxidation Thickness (inch) [†]	0.0027	0.0027	0.0027	0.0027	0.0027	0.0027	0.0027	0.0027	0.0027
End of Life Rods O.D. (inch)	0.4166	0.4166	0.3686	0.4246	0.3736	0.4346	0.3766	0.4086	0.4346
Rods I.D. (inch)	0.3734	0.373	0.329	0.377	0.331	0.384	0.332	0.370	0.388
Average tube Diameter (inch)	0.3950	0.3948	0.3488	0.4008	0.3523	0.4093	0.3493	0.3893	0.4113
Wall Thickness (inch)	0.0216	0.0218	0.0198	0.0238	0.0213	0.0253	0.0223	0.0193	0.0233
Hot Volume Pressure at 300°C (MPa) ^{††}	9.77	10.67	10.08	9.62	10.87	10.01	9.61	9.76	9.67
Cladding Stress (MPa)	89.3	96.7	88.8	81.0	90.0	81.0	75.2	98.4	85.3

† PNL-4835 [3.3.5] reported maximum cladding thickness loss due to in-reactor oxidation.

†† This average rod gas temperature conservatively bounds the plenum gas temperature, which can be seen from Figure 3.4.19 is approximately 225°C. The cladding stresses reported in the bottom row of the table will be accordingly reduced by the factor of $(225+273)/(300+273)=0.87$. However, 96.7 MPa cladding stress for PWR SNF is used as the upper bound value in this SAR.

Table 3.3.4

SUMMARY OF FISSION GASES RELEASE PER ASSEMBLY[†]

Component	Release Fraction ^{††}	Release Amount (g-moles/ PWR assembly)	Release Amount (g-moles/ BWR assembly)
Tritium	0.3	0.004	0.003
⁸⁵ Kr	0.3	0.805	0.297
¹²⁹ I	0.12	0.137	0.050
¹³¹ Xe	0.10	2.664	0.985

[†] Bounding for 42,500 MWD/MTU burnup PWR assemblies and 40,000 MWD/MTU burnup BWR assemblies.

^{††} From Regulatory Guide 1.25.

Table 3.3.5

SUMMARY OF BWR ASSEMBLY RODS INITIAL GAS FILL DATA

Assembly Type	Rods Per Assembly	Free Rod Volume (inch ³)	Fill Pressure (psig)	Max. Fill Volume (Liters at STP)	
				Per Rod	Per Assy
GE 7x7 (1966)	49	2.073	0-44.1 [†]	0.126	6.17
GE 7x7 (1968)	49	2.073	0-44.1	0.126	6.17
GE 7x7R	49	1.991	0-44.1	0.121	5.93
GE 8x8	60	1.504	0-44.1	0.0915	5.49
GE 8x8R	60	1.433	0-147 ^{††}	0.240	14.4
Exxon 9x9	79	1.323	58.8-88.2 ^{†††}	0.141	11.1
6x6 GE Dresden-1	36	2.304	58.8-88.2	0.245	8.82
6x6 GE Dresden-1 MOX	36	2.286	58.8-88.2	0.243	8.75
6x6 GE Humboldt Bay	36	2.346	58.8-88.2	0.250	9.0
7x7 GE Humboldt Bay	49	1.666	58.8-88.2	0.177	8.67
8x8 GE Dresden-1	64	1.235	58.8-88.2	0.131	8.38
8x8 SPC	63	1.615	58.8-88.2	0.172	10.8
9x9 SPC w/2 water rods	79	1.248	58.8-88.2	0.133	10.5
9x9 SPC w/1 water rod	80	1.248	58.8-88.2	0.133	10.6
9x9 GE11/GE13	74	1.389	58.8-88.2	0.150	11.1
9x9 Atrium 9B SPC	72	1.366	58.8-88.2	0.145	10.4
10x10 SVEA-96	96	1.022	58.8-88.2	0.109	10.5
10x10 GE12/GE14	92	1.167	58.8-88.2	0.124	11.4
6x6 Dresden Thin Und	36	2.455	58.8-88.2	0.261	9.4
7x7 Oyster Creek	49	2.346	58.8-88.2	0.250	12.2

[†] Conservatively bounding for GE-7x7 (1966), GE-7x7 (1968), GE-7x7R and GE-8x8 (ORNL/TM-9591/V1-R1).

^{††} Conservatively bounding for GE-8x8R (ORNL/TM-9591/V1-R1 reports 3 atm).

^{†††} BWR fuel rods internal pressurization between 4 and 6 atm (PNL-4835).

Table 3.3.5 (continued)

SUMMARY OF BWR ASSEMBLY RODS INITIAL GAS FILL DATA

Assembly Type	Rods Per Assembly	Free Rod Volume (inch ³)	Fill Pressure (psig)	Max. Fill Volume (Liters at STP)	
				Per Rod	Per Assy
8x8 Oyster Creek	64	1.739	58.8-88.2	0.185	11.8
8x8 Quad [†]	64	1.201	58.8-88.2	0.128	8.2
8x8 TVA Browns Ferry	61	1.686	58.8-88.2	0.179	10.9
9x9 SPC-5	76	1.249	58.8-88.2	0.133	10.1

Table 3.3.6

BOUNDING VALUES OF FUEL CLADDING STRESS FOR BWR SNF

Fuel Type	Fresh Fuel Rod O.D. (in.)	End of Life Rod O.D. [†] (in.)	Rod I.D. (in.)	Avg. Tube Diameter (in.)	Wall Thickness (in.)	Hot Vol. Pressure at 300°C (MPa)	Cladding Stress (MPa)
GE 7×7 (1966)	0.563	0.5536	0.499	0.5263	0.0273	4.61	44.4
GE 7×7 (1968)	0.570	0.5606	0.499	0.5298	0.0308	4.61	39.6
GE 7×7R	0.563	0.5536	0.489	0.5213	0.0323	4.76	38.4
GE 8×8	0.493	0.4836	0.425	0.4543	0.0293	5.08	39.4
GE 8×8R	0.483	0.4736	0.419	0.4463	0.0273	6.68	54.7
Exxon 9×9	0.42	0.4106	0.36	0.3853	0.0253	5.08	38.7
6×6 GE Dresden-1	0.5645	0.5551	0.4945	0.5248	0.0303	6.1	52.8
6×6 MOX Dresden-1	0.5625	0.5531	0.4925	0.5228	0.0303	6.1	52.8
Humboldt Bay 6×6	0.563	0.5536	0.499	0.5263	0.0273	5.98	57.6 ^{††}
Humboldt Bay 7×7	0.486	0.4766	0.4204	0.4485	0.0281	6.13	48.9
8×8 GE Dresden-1	0.412	0.4026	0.362	0.3813	0.0203	6.29	59.1 ^{††}

[†] Excludes 0.0047 inch end of life oxidation thickness.

^{††} These fuel types are separately evaluated for peak fuel cladding temperature limits.

Table 3.3.6 (continued)

BOUNDING VALUES OF FUEL CLADDING STRESS FOR BWR SNF

Fuel Type	Fresh Fuel Rod O.D. (in.)	End of Life Rod O.D. (in.)	Rod I.D. (in.)	Avg. Tube Diameter (in.)	Wall Thickness (in.)	Hot Vol. Pressure at 300°C (MPa)	Cladding Stress (MPa)
8x8 SPC	0.484	0.4746	0.414	0.4443	0.0303	5.19	38.0
9x9 SPC w/ 2 water rods	0.424	0.4146	0.364	0.3893	0.0253	5.32	40.9
9x9 SPC w/ 1 water rod	0.423	0.4136	0.364	0.3888	0.0248	5.25	41.1
9x9 GE-11/13	0.44	0.4306	0.384	0.4073	0.0233	5.17	45.2
9x9 Atrium 9B SPC	0.433	0.4236	0.3808	0.4022	0.0214	5.32	50.0
10x10 SVEA-96	0.379	0.3696	0.3294	0.3495	0.0201	4.38	38.1
10x10 GE-12/14	0.404	0.3946	0.352	0.3733	0.0213	4.99	43.7
6x6 Dresden Thin Clad	0.5625	0.5531	0.5105	0.5318	0.0213	5.77	72.5 [†]
7x7 Oyster Creek	0.5700	0.5606	0.499	0.5298	0.0308	4.74	40.7
8x8 Oyster Creek	0.5015	0.4921	0.4295	0.4608	0.0313	4.87	35.9
8x8 Quad [†] Westinghouse	0.4576	0.4482	0.3996	0.4239	0.0243	6.42	56.0 [†]
8x8 TVA Browns Ferry	0.483	0.4736	0.423	0.4483	0.0253	5.14	45.5
9x9 SPC-5	0.417	0.4076	0.364	0.3858	0.0218	5.46	48.3

[†] These fuel types are evaluated separately for fuel cladding temperature limits.

Table 3.3.7

INITIAL PEAK CLADDING[†] TEMPERATURE LIMITS FOR TRANSPORT

Fuel Age (years)	Temperature Limits for PWR SNF (°C) [°F]	Temperature Limits for BWR ^{††} SNF (°C) [°F]	Temperature Limits for 8x8 and 6x6 Dresden-1, QUAD [†] , and 6x6 Humboldt Bay SNF ^{†††} (°C) [°F]
5	382.3 [720]	398.2 [749]	391.2 [736]
6	370.2 [698]	382.3 [720]	376.2 [709]
7	347.0 [657]	357.9 [676]	352.2 [666]
10	341.6 [647]	351.4 [665]	346.6 [656]
15	334.1 [633]	344.9 [653]	339.5 [643]

[†] These limits are conservatively applied to stainless steel clad fuel assemblies, which actually have substantially higher limits.

^{††} 8x8 and 6x6 GE Dresden-1, QUAD+, and 6x6 GE Humboldt Bay SNF, for which cladding temperature limits are evaluated separately, are excluded from this group.

^{†††} The 8x8 and 6x6 GE Dresden-1, QUAD+, and 6x6 GE Humboldt Bay fuel types are low heat emitting assemblies. The heat load for Dresden fuel is limited to 115 watts per assembly (approximately 58% lower than the design basis maximum load for BWR fuel) (183.5 Watts Quad[†] fuel). Consequently, these two assembly types are not deemed to be limiting.

Table 3.3.8

HIGH-TEMPERATURE CREEP RUPTURE DATA
FOR STAINLESS STEEL ALLOYS

Alloy	10,000 hour Rupture Stress at 1000°F (MPa)
304	170
348	275
316	210

3.4.1.1.2 Fuel Region Effective Thermal Conductivity Calculation

Thermal properties of a large number of PWR and BWR fuel assembly configurations manufactured by the major fuel suppliers (i.e., Westinghouse, CE, B&W, and GE) have been evaluated for inclusion in the HI-STAR System thermal analysis. Bounding PWR and BWR fuel assembly configurations are determined using the simplified procedure described below. This is followed by the determination of temperature-dependent properties of the bounding PWR and BWR fuel assembly configurations to be used for cask thermal analysis using a finite-volume (FLUENT) approach.

To determine which of the numerous PWR assembly types listed in Table 3.4.4 should be used in the thermal model for the MPC-24 fuel basket, we must establish which assembly has the maximum thermal resistance. The same determination must be made for the MPC-68, out of the menu of SNF types listed in Table 3.4.5. For this purpose, we utilize a simplified procedure that we describe below.

Each fuel assembly consists of a large array of fuel rods typically arranged on a square layout. Every fuel rod in this array is generating heat due to radioactive decay in the enclosed fuel pellets. There is a finite temperature difference required to transport heat from the innermost fuel rods to the storage cell walls. Heat transport within the fuel assembly is based on principles of conduction heat transfer combined with the highly conservative analytical model proposed by Wooton and Epstein [3.4.1]. The Wooton-Epstein model considers radiative heat exchange between individual fuel rod surfaces as a means to bound the hottest fuel rod cladding temperature.

Transport of heat energy within any cross section of a fuel assembly is due to a combination of radiative energy exchange and conduction through the helium gas that fills the interstices between the fuel rods in the array. With the assumption of uniform heat generation within any given horizontal cross section of a fuel assembly, the combined radiation and conduction heat transport effects result in the following heat flow equation:

$$Q = \sigma C_o F_\epsilon A [T_C^4 - T_B^4] + 13.5740 L K_{cs} [T_C - T_B]$$

where,

$$F_\epsilon = \text{Emissivity Factor} = \frac{1}{\left(\frac{1}{\epsilon_C} + \frac{1}{\epsilon_B} - 1\right)}$$

ϵ_C, ϵ_B = emissivities of fuel cladding, fuel basket (see Table 3.2.4)

C_o = Assembly Geometry Factor

$$= \frac{4N}{(N+1)^2} \text{ (when } N \text{ is odd)}$$

$$= \frac{4}{N+2} \text{ (when } N \text{ is even)}$$

- N = Number of rows or columns of rods arranged in a square array
- A = fuel assembly "box" heat transfer area
= $4 \times \text{width} \times \text{length}$ (ft²)
- L = fuel assembly length (ft)
- K_{cs} = fuel assembly constituent materials volume fraction weighted mixture conductivity (Btu/ft-hr-°F)
- T_C = hottest fuel cladding temperature (°R)
- T_B = box temperature (°R)
- Q = net radial heat transport from the assembly interior (Btu/hr)
- σ = Stefan-Boltzman Constant (0.1714×10^{-8} Btu/ft²-hr-°R⁴)

In the above heat flow equation, the first term is the Wooten-Epstein radiative heat flow contribution while the second term is the conduction heat transport contribution based on the classical solution to the temperature distribution problem inside a square shaped block with uniform heat generation [3.4.3]. The 13.574 factor in the conduction term of the equation is the shape factor for two-dimensional heat transfer in a square section. Planar fuel assembly heat transport by conduction occurs through a series of resistances formed by the interstitial helium fill gas, fuel cladding and enclosed fuel. An effective planar mixture conductivity is determined by a volume fraction weighted sum of the individual constituent materials resistances. For BWR assemblies, this formulation is applied to the region inside the fuel channel. A second conduction and radiation model is applied between the channel and the fuel basket gap. These two models are combined, in series, to yield a total effective conductivity.

The effective thermal conductivities of several representative intact PWR and BWR assemblies are presented in Tables 3.4.4 and 3.4.5. At higher temperatures (greater than 450°F), the zircaloy clad fuel assemblies with the lowest effective thermal conductivities are the Westinghouse 17×17 OFA (PWR) and the General Electric GE-11 9×9 (BWR). A discussion of fuel assembly conductivities for some of the newer 10×10 array and plant specific BWR fuel designs is presented near the end of this

subsection. Based on this *simplified* analysis, the Westinghouse 17×17 OFA PWR and GE-11 9×9 BWR fuel assemblies are determined to be the bounding configurations for analysis at design basis maximum heat loads. As discussed in Section 3.3.2, stainless clad fuel assemblies with significantly lower decay heat emission characteristics are not deemed to be bounding.

Several of the assemblies listed in Tables 3.4.5 were excluded from consideration when determining the bounding assembly because of their extremely low decay heat loads. The excluded assemblies, which were each used at a single reactor only, are physically small and have extremely low burnups and long cooling times. These factors combine to result in decay heat loads that are much lower than the design basis maximum. The excluded assemblies are:

- Dresden Unit 1 8×8
- Dresden Unit 1 6×6
- Allis-Chalmers 10×10 Stainless
- Exxon Nuclear 10×10 Stainless
- Humboldt Bay 7x7
- Quad⁺ 8x8

The Allis-Chalmers and Exxon assemblies are used only in the LaCrosse reactor of the Dairyland Power Cooperative. The design basis assembly decay heat loads for Dresden Unit 1 and LaCrosse SNF (Tables 1.2.14 and 1.2.19) are approximately 58% lower and 69% lower, respectively, than the MPC-68 design basis assembly maximum heat load (Table 1.2.13). Examining Table 3.4.5, the effective thermal conductivity of damaged Dresden Unit 1 fuel assemblies inside DFCs (the lowest of any Dresden Unit 1 assembly) and LaCrosse fuel assemblies are approximately 40% lower and 30% lower, respectively, than that of the bounding (GE-11 9×9) fuel assembly. Consequently, the fuel cladding temperatures in the HI-STAR System with Dresden Unit 1 and LaCrosse fuel assemblies (intact or damaged) will be bounded by design basis fuel cladding temperatures.

Having established the governing (most resistive) PWR and BWR SNF types, a finite-volume code is used to determine the effective conductivities in a conservative manner. Detailed conduction-radiation finite-volume models of the bounding PWR and BWR fuel assemblies are developed in the FLUENT code as shown in Figures 3.4.7 and 3.4.8, respectively. The PWR model was originally developed on the ANSYS code which enables individual rod-to-rod and rod-to-basket wall view factor calculations to be performed using that code's AUX12 processor. Limitations of radiation modeling techniques implemented in ANSYS make it difficult to take advantage of the symmetry of the fuel assembly geometry. Unacceptably long CPU time and large workspace requirements necessary for performing gray body radiation calculations for a complete fuel assembly geometry on ANSYS prompted the development of an alternate simplified model on the FLUENT code. The FLUENT model was benchmarked with the ANSYS model results for a Westinghouse 17×17 OFA fuel assembly geometry for the case of black body radiation (emissivities = 1). The FLUENT model was found to yield conservative results in comparison to the ANSYS model for the "black" surface case. The FLUENT model benchmarked in this manner is used to solve the gray body radiation

problem to provide the necessary results for determining the effective thermal conductivity of the governing PWR fuel assembly. The same modeling approach using FLUENT is then applied to the governing BWR fuel assembly and the effective conductivity of GE-11 9×9 fuel is determined.

An equivalent homogeneous material that fills the basket opening replaces the combined fuel rods-helium matrix by the following two-step procedure. In the first step, the FLUENT-based fuel assembly model is solved by applying equal heat generation per unit length to the individual fuel rods and a uniform boundary temperature along the basket cell opening inside periphery. The temperature difference between the peak cladding and boundary temperatures is used to determine an effective conductivity as described in the next step. For this purpose, we consider a two-dimensional cross section of a square shaped block of size equal to 2L and a uniform volumetric heat source (q_g) cooled at the periphery with a uniform boundary temperature. Under the assumption of constant material thermal conductivity (K), the temperature difference (ΔT) from the center of the cross section to the periphery is analytically given by [3.4.3]:

$$\Delta T = 0.29468 \frac{q_g L^2}{K}$$

This analytical formula is applied to determine the effective material conductivity from a known quantity of heat generation applied in the FLUENT model (smeared as a uniform heat source, q_g), basket opening size and ΔT calculated in the first step.

As discussed earlier, the effective fuel space conductivity is a function of the temperature coordinate. The above two step analysis is carried out for a number of reference temperatures. In this manner, the effective conductivity as a function of temperature is established.

In Table 3.4.25, 10×10 array type BWR fuel assembly effective thermal conductivity results from a simplified analysis are presented to determine the most resistive fuel assembly in this class. Using the simplified analysis procedure discussed earlier, the Atrium-10 fuel type is determined to be the most resistive in this class of fuel assemblies. A detailed finite-element model of this assembly type was developed to rigorously quantify the heat dissipation characteristics. The results of this study are presented in Table 3.4.26 and compared to the bounding BWR fuel assembly effective thermal conductivity depicted in Figure 3.4.13. The results of this study demonstrate that the bounding BWR fuel assembly effective thermal conductivity is conservative with respect to the 10×10 class of BWR assemblies. Table 3.4.34 summarizes plant specific fuel types' effective conductivities. From these analytical results, the SPC-5 is determined to be the most resistive fuel assembly in this group of fuel types. A rigorous finite element model of SPC-5 fuel assembly was developed to confirm that its in-plane heat dissipation characteristics are bounded from below by the design basis BWR fuel conductivities used in the HI-STAR thermal analysis.

Temperature-dependent effective conductivities of PWR and BWR design basis fuel assemblies (most resistive SNF types) are shown in Figure 3.4.13. The finite-volume results are also compared

to results reported from independent technical sources. From this comparison, it is readily apparent that FLUENT-based fuel assembly conductivities are conservative. The FLUENT computed values (not the published literature data) are used in the MPC thermal analysis presented in this document.

3.4.1.1.3 Effective Thermal Conductivity of Sheathing/Boral/Cell Wall Sandwich

Each MPC basket cell wall (except outer periphery MPC-68 cell walls) is manufactured with a Boral neutron absorbing plate for criticality control. Each Boral plate is sandwiched in a sheathing-to-basket wall pocket. A schematic of the “Box Wall-Boral-Sheathing” sandwich geometry of an MPC basket is illustrated in Figure 3.4.5. During fabrication, a uniformly applied normal pressure on each sheathing-Boral-cell wall sandwich prior to stitch welding of the sheathing periphery to the box wall ensures adequate surface-to-surface contact for elimination of any macroscopic air gaps. The mean coefficient of linear expansion of Boral is higher than the basket materials thermal expansion coefficients. Consequently, basket heat-up from the contained SNF will further ensure a tight fit of the Boral plate in the sheathing-to-cell wall pocket. The presence of small microscopic gaps due to less than perfect surface finish characteristics requires consideration of an interfacial contact resistance between the Boral and the box and sheathing surfaces. A conservative contact resistance resulting from a 2 mils Boral-to-pocket air gap is applied to the analysis. Note that this gap would actually be filled with helium, so this is very conservative. In other words, no credit is taken for the interfacial pressure between Boral and stainless plate/sheet stock produced by the fixturing and welding process. Furthermore, no credit is taken for the presence of helium and radiative heat exchange across the Boral-to-sheathing or Boral-to-box wall gaps.

Heat conduction properties of a composite “Box Wall-Boral-Sheathing” sandwich in the two principal basket cross sectional directions as illustrated in Figure 3.4.5 (i.e., lateral “out-of-plane” and longitudinal “in-plane”) are unequal. In the lateral direction, heat is transported across layers of sheathing, air-gap, Boral (B_4C and cladding layers) air-gap, and cell wall resistances that are in series (except for the small helium filled end regions shown in Figure 3.4.6). Heat conduction in the longitudinal direction, in contrast, is through an array of essentially parallel resistances comprised of these same layers. Resistance network models applicable to the two directions are illustrated in Figure 3.4.6. It is noted that in addition to the essentially series and parallel resistances of the composite wall layers for the “out-of-plane” and “in-plane” directions, respectively, the effect of small helium filled end regions is also included in the resistance network analogy. For the ANSYS based MPC basket thermal model, corresponding non-isotropic effective thermal conductivities in the two orthogonal directions are determined and applied in the analysis.

3.4.1.1.4 ANSYS Modeling of Basket In-Plane Conductive Heat Transport

The heat rejection capability of each MPC design (i.e., MPC-24, and MPC-68) is evaluated by developing a thermal model of the combined fuel assemblies and composite basket walls geometry on the ANSYS finite element code. The ANSYS model includes a geometric layout of the basket structure in which the “Box Wall-Boral-Sheathing” sandwich is replaced by a “homogeneous wall” with an equivalent thermal conductivity. Since the thermal conductivity of the Alloy X material is a

weakly varying function of temperature, the equivalent “homogeneous wall” must have a temperature-dependent effective conductivity. Similarly, as illustrated in Figure 3.4.6, the conductivities in the in-plane and through-thickness direction of the equivalent “homogeneous wall” are different. Finally, as discussed earlier, the fuel assemblies occupying the basket cell openings are modeled as homogeneous heat generating regions with effective temperature dependent in-plane conductivities. The methodology used to reduce the heterogeneous MPC basket - fuel assemblage to an equivalent homogeneous region with effective thermal properties is discussed in the following.

Consider a cylinder of height L and radius r_o with a uniform volumetric heat source term q_g , with insulated top and bottom faces and its cylindrical boundary maintained at a uniform temperature T_c . The maximum centerline temperature (T_h) to boundary temperature difference is readily obtained from classical one-dimensional conduction relationships (for the case of a conducting region with constant thermal conductivity K_s):

$$(T_h - T_c) = q_g r_o^2 / (4 K_s)$$

Noting that the total heat generated in the cylinder (Q_t) is $\pi r_o^2 L q_g$, the above temperature rise formula can be reduced to the following simplified form in terms of the total heat generation per unit length (Q_t/L):

$$(T_h - T_c) = (Q_t / L) / (4 \pi K_s)$$

This simple analytical approach is employed to determine an effective basket cross-sectional conductivity by applying an equivalence between the ANSYS finite element model of the basket and the analytical case. The equivalence principle employed in the HI-STAR System thermal analysis is depicted in Figure 3.4.2. The 2-dimensional ANSYS finite element model of the MPC basket is solved by applying a uniform heat generation per unit length in each basket cell region and a constant basket periphery boundary temperature, T_c' . Noting that the basket region with uniformly distributed heat sources and a constant boundary temperature is equivalent to the analytical case of a cylinder with uniform volumetric heat source discussed earlier, an effective MPC basket conductivity (K_{eff}) is readily derived from the analytical formula and the ANSYS solution leading to the following relationship:

$$K_{eff} = N (Q_f'/L) / (4 \pi [T_h' - T_c'])$$

where:

N = number of fuel assemblies

(Q_f'/L) = each fuel assembly heat generation per unit length applied in ANSYS model

T_h' = peak basket cross-section temperature from ANSYS model

Cross sectional views of the MPC basket ANSYS models are depicted in Figures 3.4.10 and 3.4.11.

Notice that many of the basket supports and all shims have been conservatively neglected in the models. This conservative geometry simplification, coupled with the conservative neglect of thermal expansion which would minimize the gaps, yields conservative gap thermal resistances. Temperature dependent equivalent thermal conductivities of the fuel region and composite basket walls, as determined from analysis procedures described earlier, are applied to the ANSYS model. The planar ANSYS conduction model is solved by applying a constant basket periphery temperature with uniform heat generation in the fuel region. Table 3.4.6 summarizes effective thermal conductivity results of each basket design obtained from the ANSYS models. *The effective calculated basket cross sectional conductivity and the effective axial direction effective conductivity are conservatively assumed to be equal in the comprehensive HI-STAR System thermal model (see Section 3.4.1.1.2).* It is recalled that the equivalent thermal conductivity values presented in Table 3.4.6 are lower bound values because, among other elements of conservatism, the effective conductivity of the most resistive SNF type (Tables 3.4.4 and 3.4.5) is used in the MPC finite-element simulations.

3.4.1.1.5 Heat Transfer in MPC Basket Peripheral Regions

Each of the MPC designs for storing PWR or BWR fuel are provided with relatively large helium filled regions formed between the relatively cooler MPC shell and hot basket peripheral panels. For a horizontally oriented cask under normal transport conditions, heat transfer in these helium-filled regions is similar to heat transfer in closed cavities under three cases listed below:

- i. differentially heated short vertical cavity
- ii. horizontal channel heated from below
- iii. horizontal channel heated from above

In a closed cavity (case i scenario), an exchange of hot and cold fluids occurs near the top and bottom ends of the cavity, resulting in a net transport of heat across the gap.

The case (ii) scenario is similar to the classical Rayleigh-Benard instability of a layer of fluid heated from below [3.4.6]. If the condition for onset of fluid motion is satisfied, then a multi-cellular natural convection pattern is formed. The flow pattern results in upward motion of heated fluid and downward motion of relatively cooler fluid from the top plate, resulting in a net transport of heat across the heated fluid channel.

The case (iii) is a special form of case (ii) with an inverted (stably stratified) temperature profile. No fluid motion is possible in this circumstance and heat transfer is thus limited to fluid (helium) conduction only.

The three possible cases of closed cavity natural convection are illustrated in Figure 3.4.3 for an MPC-68 basket geometry. Peripheral spaces labeled B and B' illustrate the case (i) scenario, the space labeled D illustrates the case (ii) scenario, and the space labeled D' illustrates the case (iii)

scenario. The basket is oriented to conservatively maximize the number of peripheral spaces having *no* fluid motion. A small alteration in the basket orientation will result in a non-zero gravity component in the x-direction which will induce case (i) type fluid motion in the D' space. The rate of natural convection heat transfer is characterized by a Rayleigh number for the cavity defined as follows:

$$R_{aL} = \frac{C_p \rho^2 g \beta \Delta T L^3}{\mu K}$$

where:

- C_p = fluid heat capacity
- ρ = average fluid density
- g = acceleration due to gravity
- β = coefficient of thermal expansion (equal to reciprocal of absolute temperature for gases)
- ΔT = temperature difference between hot and cold surfaces
- L = spacing between hot and cold surfaces
- μ = fluid viscosity
- K = fluid conductivity

Hewitt et al. [3.4.5] report Nusselt number correlations for the closed cavity natural convection cases discussed earlier. A Nusselt number equal to unity implies heat transfer by fluid conduction only. A higher than unity Nusselt number is due to the so-called "Rayleigh" effect, which monotonically rises with increasing Rayleigh number. Nusselt numbers applicable to helium filled PWR and BWR HI-STAR MPCs in the peripheral voids are provided in Table 3.4.1. These numbers are used to enhance helium conductivity *only* in the basket peripheral spaces.

3.4.1.1.6 Effective Conductivity of Multi-Layered Intermediate Shell Region

Fabrication of the layered overpack intermediate shells is discussed in Section 1.2 of this SAR. In the thermal analysis, each intermediate shell metal-to-metal interface presents an additional resistance to heat transport. The contact resistance arises from microscopic pockets of air trapped between surface irregularities of the contacting surfaces. Since air is a relatively poor conductor of heat, this results in a reduction in the ability to transport heat across the interface compared to that of the base metal.

Interfacial contact conductance depends upon three principal factors, namely: (i) base material conductivity, (ii) interfacial contact pressure, and (iii) surface finish.

Rohsenow and Hartnett [3.2.2] have reported results from experimental studies of contact conductance across air entrapped stainless steel surfaces with a typical 100 μ-inch surface finish. A minimum contact conductance of 350 Btu/ft-hr-°F is determined from extrapolation of results to zero contact pressure.

The thermal conductivity of carbon steel is about three times that of stainless steel. Thus the choice of carbon steel as the base material in a multi-layered construction significantly improves heat transport across interfaces. The fabrication process guarantees interfacial contact. Contact conductance values extrapolated to zero contact pressures are therefore conservative. The surface finish of hot-rolled carbon steel plate stock is generally in the range of 250-1000 μ-inch [3.2.1]. The process of forming hot-rolled flat plate stock to cylindrical shapes to form the intermediate shells by rolling will result in a smoother surface finish. This results from the large surface pressures exerted by the hardened roller faces that flatten out any surface irregularities.

In the HI-STAR thermal analysis, a conservatively bounding interfacial contact conductance value is determined based on the following assumptions:

1. No credit is taken for high base metal conductivity.
2. No credit is taken for interfacial contact pressure.
3. No credit is taken for a smooth surface finish resulting from rolling of hot-rolled plate stock to cylindrical shapes.
4. Contact conductance is based on a uniform 2000 μ-inch (1000 μ-inch for each surface condition) interfacial air gap at all interfaces.
5. No credit for radiation heat exchange across this hypothetical inter-surface air gap.
6. Bounding low thermal conductivity at 200°F.

These assumptions guarantee a conservative assessment of heat dissipation characteristics of the multi-layered intermediate shell region. The resistances of the five carbon steel layers along with the associated interfacial resistances are combined as resistances in series to determine an effective conductivity of this region leading to the following relationship:

$$K_{gs} = r_o \ell n \left[\frac{r_5}{r_o} \right] \left[\sum_{i=1}^5 \frac{\delta}{K_{air} r_i} + \frac{r_o \ell n \left[\frac{r_5}{r_o} \right]}{K_{cst}} \right]^{-1}$$

where (in conventional U.S. units):

K_{gs} = effective intermediate shell region thermal conductivity

r_o	=	inside radius of inner gamma shield layer
r_i	=	outer radius of i^{th} intermediate shell layer
δ	=	interfacial air gap (2000 μ -inch)
K_{air}	=	air thermal conductivity
K_{cst}	=	carbon steel thermal conductivity

3.4.1.1.7 Heat Rejection from Overpack and Impact Limiter Outside Surfaces

Jakob and Hawkins [3.2.9] recommend the following correlations for natural convection heat transfer to air from heated vertical surfaces (flat impact limiter ends) and from single horizontal cylinders (overpack and impact limiter curved surfaces):

Turbulent range:

$$h = 0.19 (\Delta T)^{1/3} \text{ (Vertical, GrPr} > 10^9 \text{)}$$

$$h = 0.18 (\Delta T)^{1/3} \text{ (Horizontal Cylinder, GrPr} > 10^9 \text{)}$$

(in conventional U.S. units)

Laminar range:

$$h = 0.29 \left(\frac{\Delta T}{L}\right)^{1/4} \text{ (Vertical, GrPr} < 10^9 \text{)}$$

$$h = 0.27 \left(\frac{\Delta T}{D}\right)^{1/4} \text{ (Horizontal Cylinder, GrPr} < 10^9 \text{)}$$

(in conventional U.S. units)

where ΔT is the temperature differential between the system exterior surface and ambient air. During normal transport conditions, the surfaces to be cooled are the impact limiter and overpack cylindrical surfaces, and the flat vertical faces of the impact limiters. The corresponding length scales for these surfaces are the impact limiter diameter, overpack diameter, and impact limiter diameter, respectively. Noting that $\text{Gr} \times \text{Pr}$ is expressed as $L^3 \Delta T Z$, where Z (from Table 3.2.7) is at least 2.6×10^5 at a conservatively high upper bound system exterior surface temperature of 340°F , it is apparent that the turbulent condition is always satisfied for ΔT in excess of a few degrees Fahrenheit. Under turbulent conditions, the more conservative heat transfer correlation for horizontal cylinders (i.e., $h = 0.18 \Delta T^{1/3}$) is utilized for thermal analyses on all exposed system surfaces.

Including both convective and radiative heat loss from the system exterior surfaces, the following relationship for surface heat flux is developed:

$$q_s = 0.18 (T_s - T_A)^{4/3} + \sigma \times \epsilon \times [(T_s + 460)^4 - (T_A + 460)^4]$$

where:

$$T_s, T_A = \text{surface, ambient temperatures } (^\circ\text{F})$$

- q_s = surface heat flux (Btu/ft²-hr)
 ϵ = surface emissivity (see Table 3.2.4)
 σ = Stefan-Boltzman Constant (0.1714×10^{-8} Btu/ft²-hr-°R⁴)

3.4.1.1.8 Determination of Solar Heat Input

The intensity of solar radiation incident on an exposed surface depends on a number of time varying parameters. The solar heat flux strongly depends upon the time of the day as well as on latitude and day of the year. Also, the presence of clouds and other atmospheric conditions (dust, haze, etc.) can significantly attenuate solar intensity levels. Rapp [3.4.2] has discussed the influence of such factors in considerable detail.

The HI-STAR System thermal analysis is based upon insolation levels specified in 10CFR71, Subpart F, which are for a 12-hour daytime period. During normal transport conditions, the HI-STAR System is cyclically subjected to solar heating during the 12-hour daytime period followed by cooling during the 12-hour nighttime. However, due to the large mass of metal and the size of the system, the inherent dynamic time lag in the temperature response is substantially larger than the 24-hour heating-cooling time period. Accordingly, the HI-STAR System cask model includes insolation at exposed surfaces averaged over a 24-hour time period. A bounding solar absorption coefficient of 1.0 is applied to cask exterior surfaces. The 10CFR71 mandated 12-hour average incident solar radiation levels are summarized in Table 3.4.7. The combined incident insolation heat flux absorbed by exposed cask surfaces and decay heat load from the MPC is rejected by natural convection and radiation to ambient air.

3.4.1.1.9 Effective Thermal Conductivity of Radial Channels - Holtite Region

In order to minimize heat transfer resistance limitations due to the poor thermal conductivity of the Holtite-A neutron shield material, a large number of thick radial channels formed from high strength and conductivity carbon steel material are embedded in the neutron shield region. These radial channels form highly conductive heat transfer paths for efficient heat removal. Each channel is welded to the outside surface of the outermost intermediate shell and at the overpack enclosure shell, thereby providing a continuous path for heat removal to the ambient environment.

The effective thermal conductivity of the composite neutron shielding and radial channels region is determined by combining the heat transfer resistance of individual components in a parallel network. In determining the heat transfer capability of this region to the outside ambient environment for normal transport conditions, *no credit is taken for conduction through the neutron shielding material*. Thus, heat transport from the outer intermediate shell surface to the overpack outer shell is conservatively based on heat transfer through the carbon steel radial channel legs alone.

Thermal conductivity of the parallel neutron shield and radial channel leg region is given by the following formula:

$$K_{ne} = \frac{K_R N_R t_R \ln \left[\frac{r_B}{r_A} \right]}{2 \pi L_R} + \frac{K_{ns} N_R t_{ns} \ln \left[\frac{r_B}{r_A} \right]}{2 \pi L_R}$$

where (in consistent U.S. units):

K_{ne}	=	effective thermal conductivity of neutron shield region
r_A	=	inner radius of neutron shielding
r_B	=	outer radius of neutron shielding
K_R	=	effective thermal conductivity of carbon steel radial channel leg
N_R	=	total number of radial channel legs (also equal number of neutron shield sections)
t_R	=	minimum (nominal) thickness of each radial channel leg
L_R	=	effective radial heat transport length through radial channel leg
K_{ns}	=	neutron shield thermal conductivity
t_{ns}	=	neutron shield circumferential thickness (between two radial channel legs)

The radial channel leg to outer intermediate shell surface weld thickness is equal to half the plate thickness. The additional weld resistance is accounted for by reducing the plate thickness in the weld region for a short radial span equal to the weld size. Conductivity of the radial carbon steel channel legs based on the full thickness for the entire radial span is correspondingly reduced. Figure 3.4.4 depicts a resistance network developed to combine the neutron shield and radial channel legs resistances to determine an effective conductivity of the neutron shield region. Note that in the resistance network analogy only the annulus region between overpack outer enclosure inner surface and intermediate shells outer surface is considered in this analysis. The effective thermal conductivity of neutron shield region is provided in Table 3.4.8.

3.4.1.1.10 Effective Thermal Conductivity of the Eccentric MPC to Overpack Gap

During horizontal shipment of the HI-STAR System under normal transport conditions, the MPC will rest on the inside surface of the overpack. In the region of line contact, the resistance to heat transfer across the gap will be negligibly small due to a vanishingly small gap thickness. The resistance to heat transfer at other regions along the periphery of the MPC will, however, increase in direct proportion to the thickness of the local gap. This variation in gap thickness can be accounted for in the thermal model by developing a relation for the total heat transferred across the gap as given below:

$$Q_E = 2 \int_0^\pi \frac{K_{He}}{g(\theta)} L R_o \Delta T d\theta$$

where:

Q_E	=	total heat transfer across the gap (Btu/hr)
K_{He}	=	helium conductivity Btu/ft-hr-°F
L	=	length of MPC (ft.)
R_o	=	MPC radius (ft.)
θ	=	angle from point of line contact
$g(\theta)$	=	variation of gap thickness with angle (ft.)
ΔT	=	temperature difference across the gap (°F)

A corresponding relationship for heat transferred across a uniform gap is given by:

$$Q_c = \frac{K_{eff}}{(R_1 - R_o)} 2\pi R_o L \Delta T$$

where R_1 is the inside radius of the overpack and K_{eff} is the effective thermal conductivity of an equivalent concentric MPC/overpack gap configuration. From these two relationships, the ratio of effective gap conductivity to helium thermal conductivity in the MPC/overpack region is shown below:

$$\frac{K_{eff}}{K_{He}} = \frac{R_1 - R_o}{\pi} \int_0^{\pi} \frac{1}{g(\theta)} d\theta$$

Based on an analysis of the geometry of a thin gap between two eccentrically positioned cylinders, the following relationship is developed for variation of the gap thickness with position:

$$g(\theta) = (R_1 - R_o)(1 - \cos \theta) + \epsilon \cos \theta$$

The above equation conservatively accounts for imperfect contact by postulating a minimum gap ϵ at the point where the two surfaces would ideally form a line of perfect contact. The relatively thin MPC shell is far more flexible than the much thicker overpack inner shell, and will ovalize to yield greater than line contact. The substantial weight of the fuel basket and contained fuel assemblies will also cause the MPC shell to conform to the overpack inner shell. An evaluation based on contact along a line would therefore be reasonable and conservative. However, a minimum gap is assumed to further increase conservatism in this calculation.

Based on an applied gap of 0.02-inch, which is conservative compared to contact along a line, the effective gap thermal conductivity determined from analytical integration [3.4.7] is in excess of 200% of the conductivity of helium gas. In the HI-STAR analysis, a conservative effective gap conductivity equal to twice the helium gas conductivity is applied to the performance evaluation.

3.4.1.1.11 Effective Thermal Conductivity of MPC Basket-to-Shell Aluminum Heat Conduction Elements

As shown in MPC Drawings 1395 and 1401, full-length heat conduction elements fabricated from aluminum alloy 1100 are placed in the large MPC basket-to-shell gaps to provide uninterrupted metal pathways to transport heat from the basket periphery to the MPC shell. Due to the high aluminum alloy 1100 thermal conductivity (about 15 times that of Alloy X), a significant rate of net heat transfer is possible along the thin plates. Figure 3.4.12 shows a mathematical idealization of a heat conduction element inserted between basket periphery panels and the MPC shell. The aluminum insert is shown to cover the MPC basket Alloy X peripheral panel and MPC shell surfaces (Regions I and III depicted in Figure 3.4.12) along the full-length of the basket. Heat transport to and from the aluminum insert is conservatively postulated to occur across a thin helium gap as shown in the figure (i.e., no credit is considered for aluminum insert to Alloy X metal-to-metal contact). Aluminum surfaces inside the hollow region are sandblasted prior to fabrication to result in a rough surface finish which has a significantly higher emissivity compared to smooth surfaces of rolled aluminum. The untreated aluminum surfaces directly facing Alloy X panels have a smooth finish to minimize contact resistance.

Net heat transfer resistance from the hot basket periphery panel to the relatively cooler MPC shell along the aluminum heat conduction element pathway is a sum of three individual resistances in regions labeled I, II, and III. In Region I, heat is transported from the basket to the aluminum insert surface directly facing the basket panel across a thin helium resistance gap. Longitudinal transport of heat (in the z direction) in the aluminum plate (in Region I) will result in an axially non-uniform temperature distribution. Longitudinal one-dimensional heat transfer in the Region I aluminum plate is analytically formulated to result in the following ordinary differential equation for the non-uniform temperature distribution:

$$t K_{Al} \frac{\partial^2 T}{\partial z^2} = - \frac{K_{He}}{h} (T_h - T) \quad \text{(Equation a)}$$

Boundary Conditions

$$\begin{aligned} \frac{\partial T}{\partial z} &= 0 \text{ at } z = 0 \\ T &= T_h \text{ at } z = P \end{aligned} \quad \text{(Equation b)}$$

where (see Figure 3.4.12):

T(z) = non-uniform aluminum metal temperature distribution

t	=	conduction element thickness
K _{Al}	=	conduction element conductivity
K _{He}	=	helium conductivity
h	=	helium gap thickness
T _h	=	hot basket temperature
T _h '	=	conduction element Region I boundary temperature at z = P
P	=	conduction element Region I length

Solution of this ordinary differential equation subject to the imposed boundary condition is:

$$(T_h - T) = (T_h - T_h') \left[\frac{e^{\frac{z}{\sqrt{\alpha}}} + e^{-\frac{z}{\sqrt{\alpha}}}}{e^{\frac{P}{\sqrt{\alpha}}} + e^{-\frac{P}{\sqrt{\alpha}}}} \right] \quad (\text{Equation c})$$

where α is a dimensional parameter equal to htK_{Al}/K_{He} . The net heat transfer (Q_I) across the Region I helium gap can be determined by the following integrated heat flux to a conduction element of length L as:

$$Q_I = \int_0^P \frac{K_{He}}{h} (T_h' - T) (L) dz \quad (\text{Equation d})$$

Substituting the analytical temperature distribution result obtained in Equation c into Equation d and then integrating, the following expression for net heat transfer is obtained:

$$Q_I = \frac{K_{He} L \sqrt{\alpha}}{h} \left(1 - \frac{1}{e^{\frac{P}{\sqrt{\alpha}}} + e^{-\frac{P}{\sqrt{\alpha}}}} \right) (T_h - T_h') \quad (\text{Equation e})$$

Based on this result, an expression for Region I resistance is obtained as shown below:

$$R_I = \frac{T_h - T_h'}{Q_I} = \frac{h}{K_{He} L \sqrt{\alpha}} \left(1 - \frac{1}{e^{\frac{P}{\sqrt{\alpha}}} + e^{-\frac{P}{\sqrt{\alpha}}}} \right)^{-1} \quad (\text{Equation f})$$

Similarly, a Region III resistance expression can be analytically determined as shown below:

$$R_{III} = \frac{(T_c' - T_c)}{Q_{III}} = \frac{h}{K_{He} L \sqrt{\alpha}} \left(1 - \frac{1}{e^{\frac{P}{\sqrt{\alpha}}} + e^{-\frac{P}{\sqrt{\alpha}}}} \right)^{-1} \quad (\text{Equation g})$$

A Region II resistance expression can be developed from the following net heat transfer equation in the vertical leg of the conduction element as shown below:

$$Q_{II} = \frac{K_{Al} L t}{W} (T_h' - T_c') \quad (\text{Equation h})$$

Hence,

$$R_{II} = \frac{T_h' - T_c'}{Q_{II}} = \frac{W}{K_{Al} L t} \quad (\text{Equation i})$$

This completes the analysis for the total thermal resistance attributable to the heat conduction elements equal to sum of the three individual resistances. The total resistance is smeared across the basket-to-MPC shell region as an effective uniform annular gap conductivity (see Figure 3.4.2). Note that heat transport along the conduction elements is an independent conduction path in parallel with conduction and radiation mechanisms in the large helium gaps. Helium conduction and radiation between the MPC basket and the MPC shell is accounted for separately in the ANSYS MPC models described earlier in this section. Therefore, the total MPC basket-to-MPC shell peripheral gaps conductivity will be the sum of the conduction elements effective conductivity and the helium conduction-radiation gap effective conductivity.

3.4.1.1.12 FLUENT Model for HI-STAR Temperature Field Computation

In the preceding subsections, the series of analytical and numerical models to define the thermal characteristics of the various elements of the HI-STAR System are presented. The thermal modeling begins with the replacement of the SNF cross section and surrounding fuel cell space by a solid lamina with an equivalent conductivity. Since radiation is an important constituent of the heat transfer process in the SNF/storage cell space and the rate of radiation heat transfer is a strong function of the surface temperatures, it is necessary to treat the equivalent lamina conductivity as a function of temperature. In fact, because of the relatively large range of temperatures which will exist in a loaded HI-STAR System under the design basis heat loads, it is necessary to include the effect of

variation in the thermal conductivity of materials with temperature throughout the system finite volume model. The presence of significant radiation effect in the storage cell spaces adds to the imperative to treat the equivalent lamina conductivity as temperature-dependent.

FLUENT finite volume simulations have been performed to establish the equivalent thermal conductivity as a function of temperature for the limiting (thermally most resistive) BWR and PWR spent fuel types. By utilizing the most limiting SNF (established through a simplified analytical process for comparing conductivities) the numerical idealization for the fuel space conductivity is ensured to be conservative for all non-limiting fuel types.

Having replaced the interior of the cell spaces by solid prismatic (square) columns possessing a temperature-dependent conductivity essentially renders the basket into a non-homogeneous three-dimensional solid where the non-homogeneity is introduced by the honeycomb basket structure. The basket panels themselves are a composite of Alloy X cell wall, Boral neutron absorber, and Alloy X sheathing metal. A conservative approach to replace this composite section with an equivalent "solid wall" is described in a preceding subsection.

In the next step, a planar section of the MPC is considered. The MPC, externally radially symmetric, contains a non-symmetric basket lamina wherein the equivalent fuel space solid squares are separated by the "equivalent" solid metal walls. The space between the basket and the MPC, called the peripheral gap, is filled with helium gas and aluminum heat conduction elements (shown in MPC Drawings 1395 and 1401). The equivalent thermal conductivity of this MPC section is computed using a finite element procedure on ANSYS, as described previously. To the "helium-conduction-radiation" based peripheral gap conductivity, the effective conductivity of aluminum conduction elements is added to obtain a combined effective conductivity. At this stage in the thermal analysis, the SNF/basket/MPC assemblage has been replaced with a two-zone (Figure 3.4.2) cylindrical solid whose thermal conductivity is a strong function of temperature.

The idealization for the overpack is considerably more straightforward. The overpack is radially symmetric except for the Holtite region (discussed in Subsection 3.4.1.1.9). The procedure to replace the multiple shell layers, Holtite-A and radial connectors with an equivalent solid utilizes classical heat conduction analogies, as described in the preceding subsections.

In the final step of the analysis, the equivalent two-zone MPC cylinder, the equivalent overpack shell, the top and bottom plates, and the impact limiters are assembled into a comprehensive finite volume model. A cross section of this axisymmetric model implemented on FLUENT is shown in Figure 3.4.14. A summary of the essential features of this model is presented in the following:

- The overpack shell is represented by 840×9 elements. The effective thermal conductivity of the overpack shell elements is set down as a function of temperature based on the analyses described earlier.

- The overpack bottom plate and bolted closure plate are modeled by 312×9 axisymmetric elements.
- The two-zone MPC “solid” is represented by 1,144×9 axisymmetric elements.
- The space between the MPC “solid” and the overpack interior space is assumed to contain helium.
- Heat input due to insolation is applied to the impact limiter surfaces and the cylindrical surface of the overpack.
- The heat generation in the MPC solid basket region is assumed to be uniform in each horizontal plane, but to vary in the axial direction to correspond to the axial burnup distribution in the active fuel region postulated in Chapter 1.

The finite volume model constructed in this manner will produce an axisymmetric temperature distribution. The peak temperature will occur near the centerline and is expected to correspond to the axial location of peak heat generation. As is shown later, the results from the finite element solution bear out these observations.

3.4.1.1.13 Effect of Fuel Cladding Crud Resistance

In this subsection, a conservatively bounding estimate of the temperature drop across a crud film adhering to a fuel rod during dry storage conditions is determined. The evaluation is performed for a BWR fuel assembly based on an upper bound crud thickness obtained from PNL-4835 report ([3.3.5], Table 3). The crud present on fuel assemblies is predominantly iron oxide mixed, with small quantities of other metals such as cobalt, nickel, chromium, etc. Consequently, the effective conductivity of the crud mixture is expected to be in the range of typical metal alloys. Metals have thermal conductivities several orders of magnitude larger than that of helium. In the interest of extreme conservatism, however, a film of helium with the same thickness replaces the crud layer. The calculation is performed in two steps. In the first step, a crud film resistance is determined based on bounding maximum crud layer thickness replaced as a helium film on the fuel rod surfaces. This is followed by a peak local cladding heat flux calculation for the smaller GE 7×7 fuel assembly postulated to emit a conservatively bounding decay heat equal to 0.5kW. The temperature drop across the crud film obtained as a product of the heat flux and crud resistance terms is determined to be less than 0.1°F. The calculations are presented below:

$$\text{Bounding Crud Thickness } (\delta) = 130\mu\text{m } (4.26 \times 10^{-4} \text{ ft})$$

(PNL-4835)

$$\text{Crud Conductivity } (K) = 0.1 \text{ Btu/ft-hr-}^\circ\text{F (conservatively assumed as helium)}$$

GE 7x7 Fuel Assembly:

Rod O.D.	=	0.563"
Active Fuel Length	=	150"
Heat Transfer Area	=	(7x7) ($\pi \times 0.563$) \times 150/144
	=	90.3 ft ²
Axial Peaking Factor	=	1.195 (Burnup distribution Table 1.2.15)
Decay Heat	=	500W (conservative assumption)

$$\text{Crud Resistance} = \frac{\delta}{K} = \frac{4.26 \times 10^{-4}}{0.1} = 4.26 \times 10^{-3} \frac{\text{ft}^2 \cdot \text{hr} \cdot ^\circ\text{F}}{\text{Btu}}$$

$$\begin{aligned} \text{Peak Heat Flux} &= \frac{(500 \times 3.417) \text{ Btu/hr}}{90.3 \text{ ft}^2} \times 1.195 \\ &= 18.92 \times 1.195 = 22.6 \frac{\text{Btu}}{\text{ft}^2 \cdot \text{hr}} \end{aligned}$$

Temperature drop (ΔT_c) across crud film:

$$\begin{aligned} &= 4.26 \times 10^{-3} \frac{\text{ft}^2 \cdot \text{hr} \cdot ^\circ\text{F}}{\text{Btu}} \times 22.6 \frac{\text{Btu}}{\text{ft}^2 \cdot \text{hr}} \\ &= 0.096^\circ\text{F} \\ &\text{(i.e., less than } 0.1^\circ\text{F)} \end{aligned}$$

Therefore, it is concluded that deposition of crud does not materially change the SNF cladding temperature.

3.4.1.1.14 Maximum Time Limit During Wet Transfer

While loading an empty HI-STAR System for transport directly from a spent fuel pool, water inside the MPC cavity is not permitted to boil. Consequently, uncontrolled pressures in the de-watering, purging, and recharging system that may result from two-phase condition, are completely avoided. This requirement is accomplished by imposing a limit on the maximum allowable time duration for fuel to be submerged in water after a loaded HI-STAR cask is removed from the pool and prior to the start of vacuum drying operations.

When the HI-STAR overpack and the loaded MPC under water-flooded conditions are removed from the pool, the combined mass of the water, the fuel, the MPC, and the overpack will absorb the decay heat emitted by the fuel assemblies. This results in a slow temperature rise of the entire system with time, starting from an initial temperature of the contents. The rate of temperature rise is limited by the thermal inertia of the HI-STAR system. To enable a bounding heat-up rate determination for

the HI-STAR system, the following conservative assumptions are imposed:

- i. Heat loss by natural convection and radiation from the exposed HI-STAR surfaces to the pool building ambient air is neglected (i.e., an adiabatic temperature rise calculation is performed).
- ii. Design Basis maximum decay heat input from the loaded fuel assemblies is imposed on the HI-STAR system.
- iii. The smallest of the *minimum* MPC cavity-free volumes between the two MPC types is considered for flooded water mass determination.
- iv. Fifty percent of the water mass in the MPC cavity is credited towards water thermal inertia evaluation.

Table 3.4.19 summarizes the weights and thermal inertias of several components in the loaded HI-STAR system. The rate of temperature rise of the HI-STAR and its contents during an adiabatic heat-up is governed by the following equation:

$$\frac{dT}{d\tau} = \frac{Q}{C_h}$$

where:

Q = decay heat load (Btu/hr) [equal to Design Basis maximum (between the two MPC types) 20.0 kW (i.e., 68,260 Btu/hr)]

C_h = combined thermal inertia of the loaded HI-STAR system (Btu/°F)

T = temperature of the contents (°F)

t = time after HI-STAR system is removed from the pool (hr)

A bounding heat-up rate for the HI-STAR system contents is determined to be equal to 2.19°F/hr. From this adiabatic rate of temperature rise estimate, the maximum allowable time duration (t_{max}) for fuel to be submerged in water is determined as follows:

$$t_{\max} = \frac{T_{\text{boil}} - T_{\text{initial}}}{dT/d\tau}$$

where:

T_{boil} = boiling temperature of water (equal to 212°F at the water surface in the MPC cavity)

T_{initial} = initial temperature of the HI-STAR contents when removed from the pool

Table 3.4.20 provides a summary of t_{max} at several initial HI-STAR contents temperatures.

As set forth in Section 7.4, in the unlikely event where the maximum allowable time provided in Table 3.4.20 is found to be insufficient to complete all wet transfer operations, a forced water circulation shall be initiated and maintained to remove the decay heat from the MPC cavity. In this case, relatively cooler water will enter via the MPC lid drain port connection and heated water will exit from the vent port. The minimum water flow rate required to maintain the MPC cavity water temperature below boiling with an adequate subcooling margin is determined as follows:

$$M_w = \frac{Q}{C_{pw}(T_{\text{max}} - T_{\text{in}})}$$

where:

M_w = minimum water flow rate (lb/hr)

C_{pw} = water heat capacity (Btu/lb-°F)

T_{max} = maximum MPC cavity water mass temperature

T_{in} = temperature of water supply to MPC

With the MPC cavity water temperature limited to 150°F, MPC inlet water maximum temperature equal to 125°F and at the design basis maximum heat load, the water flow rate is determined to be 2,731 lb/hr (5.5 gpm).

3.4.1.1.15 Cask Cooldown and Reflood Analysis During Fuel Unloading Operation

Before a loaded HI-STAR System can be unloaded (i.e., fuel removed from the MPC) the cask must be cooled from the operating temperatures and reflooded with water. Past industry experience generally supports cooldown of cask internals and fuel from hot storage conditions by direct water quenching. However, the extremely rapid cooldown rates that are typical during water injection, to which the hot cask internals and fuel cladding are subjected to, may result in uncontrolled thermal stresses and failure in the structural members. Moreover, water injection results in large amounts of steam generation and unpredictable transient two-phase flow conditions inside the MPC cavity, which may result in over-pressurization of the MPC helium retention boundary and a potentially unacceptable reduction in the safety margins to prevent criticality. To avoid potential safety concerns related to rapid cask cooldown by direct water quenching, the HI-STAR MPCs are designed to be cooled in a gradual manner, thereby eliminating thermal shock loads on the cask internals and fuel cladding.

In the unlikely event that a HI-STAR system is required to be unloaded, it will be transported back to the fuel handling building. Prior to reflooding the MPC cavity with water, a forced flow helium recirculation system with adequate flow capacity shall be operated to remove the decay heat and initiate a slow cask cooldown lasting for several days. The operating procedures in Section 7.2 provide a detailed description of the steps involved in the cask unloading. In this section, an analytical evaluation is presented to provide the basis for helium flow rates and time of forced cooling to meet the objective of eliminating thermal shock when the MPC cavity is eventually flooded with water.

Under a closed loop forced helium circulation condition, the helium gas is cooled via an external chiller, down to 100°F, and then introduced inside the MPC cavity from the drain line near the bottom baseplate. The helium gas enters the MPC basket from the bottom oversized flow holes and moves upward through the hot fuel assemblies, removing heat and cooling the MPC internals. The heated helium gas exits from the basket top and collects in the top plenum, from where it is expelled through the MPC lid vent connection to the helium recirculation and cooling system. The bulk average temperature reduction of the MPC contents as a function of time is principally dependent upon the rate of helium circulation. The temperature transient is governed by the following heat balance equation:

$$C_h \frac{dT}{dt} = Q_D - m C_p (T - T_i) - Q_c$$

Initial Condition: $T = T_0$ at $t = 0$

where:

$T =$ MPC bulk average temperature (°F)

$T_0 =$ initial MPC bulk average temperature in the HI-STAR system
(equal to 483°F [3.4.16])

$t =$ time after start of forced circulation (hr)

$Q_D =$ decay heat load (Btu/hr)
(equal to Design Basis maximum 20.0 kW (i.e., 68,260 Btu/hr))

$m =$ helium circulation rate (lb/hr)

$C_p =$ helium heat capacity (Btu/lb-°F)
(equal to 1.24 Btu/lb-°F)

Q_c = heat rejection from cask exposed surfaces to ambient (Btu/hr)
(conservatively neglected)

C_h = thermal capacity of the loaded MPC (Btu/°F)
(For a bounding upper bound 100,000 lb loaded MPC weight, and heat capacity of Alloy X equal to 0.12 Btu/lb-°F, the heat capacity is equal to 12,000 Btu/°F)

T_i = MPC helium inlet temperature (°F)

The differential equation is analytically solved, yielding the following expression for time-dependent MPC bulk temperature:

$$T(t) = \left(T_i + \frac{Q_D}{m C_p} \right) \left(1 - e^{-\frac{m C_p t}{C_h}} \right) + T_o e^{-\frac{m C_p t}{C_h}}$$

This equation is used to determine the minimum helium mass flow rate that would cool the MPC cavity down from initially hot conditions to less than 200°F. For example, to cool the MPC to less than 200°F in 72 hours would required a helium mass flow rate of 574 lb/hr (i.e., 859 SCFM).

Once the helium gas circulation has cooled the MPC internals to less than 200°F, water can be injected to the MPC without risk of boiling and the associated thermal stress concerns. Because of the relatively long cooldown period, the thermal stress contribution to the total cladding stress would be negligible, and the total stress would therefore be bounded by the normal (dry) condition. The elimination of boiling eliminates any concern of over-pressurization due to steam production.

3.4.1.1.16 MPC Temperature Distribution Under Vacuum Conditions

The initial loading of SNF in the MPC requires that the water within the MPC be drained and replaced with helium. This operation on the HI-STAR MPCs will be carried out using a conventional vacuum drying approach. In this method, removal of the last traces of residual moisture from the MPC cavity is accomplished by evacuating the MPC for a short time after draining the MPC.

Prior to the start of the MPC draining operation, both the overpack annulus and the MPC are full of water. The presence of water in the MPC ensures that the fuel cladding temperatures are lower than design basis limits by large margins. As the heat generating active fuel length is uncovered during the draining operation, the fuel and basket mass will undergo a gradual heat up from the initially cold conditions when the heated surfaces were submerged under water.

A vacuum condition steady-state analysis has been performed, for Holtec MPCs, at conservatively higher than transport design basis heat loads (22.25 kW for MPC-24 and 21.4 kW for MPC-68) to demonstrate that fuel cladding temperature limits are not exceeded. The results of this analysis, therefore, bound HI-STAR vacuum condition temperatures. The bounding analysis demonstrates that

the steady-state maximum temperatures in the vacuum condition will remain below short-term temperature limits.

3.4.1.1.17 Effects of Helium Dilution from Fuel Rod Gases

In this subsection, the generic cask transportation accident issue raised in a USNRC Spent Fuel Project Office (SFPO) staff guidance letter[†] is addressed. This issue directs cask designers to evaluate the impact of fission gas release into the canister, from a 100% fuel rods rupture accident, on the cask component temperatures and pressures. The impact is illustrated from the limiting MPC-24 design, in which the MNOP is within 10% of the design pressure.

Under a severe hypothetical accident scenario 100% of the fuel rods may rupture, releasing the rod fill gas (helium) and a portion of the gaseous fission products (³H, ⁸⁵Kr, ¹²⁹I and ¹³¹Xe). The gaseous fission products release fractions are stipulated in NUREG-1536. The released gases will mix with the MPC backfill gas and reduce its thermal conductivity. This reduction in conductivity will result in a small increase in MPC temperatures and pressures.

Appendix C of NUREG/CR-0497 [3.4.13] describes a method for calculating the effective thermal conductivity of a mixture of gases. The same method is also described by Rohsenow and Hartnett [3.2.2]. The following expression is provided by both references:

$$k_{mix} = \sum_{i=1}^n \left(\frac{k_i x_i}{x_i + \sum_{\substack{j=1 \\ j \neq i}}^n \phi_{ij} x_j} \right)$$

where:

- k_{mix} = thermal conductivity of the gas mixture (Btu/hr-ft-°F)
- n = number of gases
- k_i = thermal conductivity of gas component i (Btu/hr-ft-°F)
- x_i = mole fraction of gas component i

In the preceding equation, the term ϕ_{ij} is given by the following:

$$\phi_{ij} = \phi_{ij} \left[1 + 2.41 \frac{(M_i - M_j)(M_i - 0.142 \cdot M_j)}{(M_i + M_j)^2} \right]$$

where M_i and M_j are the molecular weights of gas components i and j , and ϕ_{ij} is:

[†] SFPO Director's Interim Staff Guidance Letter(s), W.F. Kane, (Interim Staff-Guidance-7), October 8, 1998.

$$\phi_{ij} = \frac{\left[1 + \left(\frac{k_i}{k_j} \right)^{\frac{1}{2}} \left(\frac{M_i}{M_j} \right)^{\frac{1}{4}} \right]^2}{2^{\frac{3}{2}} \left(1 + \frac{M_i}{M_j} \right)^{\frac{1}{2}}}$$

Table 3.4.30 presents a summary of the gas mixture thermal conductivity calculations for an MPC-24 containing design basis PWR fuel assemblies.

Having calculated the gas mixture thermal conductivity, the effective thermal conductivity of the design basis PWR fuel assembly is calculated using the finite-volume model described in Subsection 3.4.1.1.2. Only the helium gas conductivity is changed, all other modeling assumptions are the same. The fuel assembly effective thermal conductivity with diluted helium is compared to that with undiluted helium in Table 3.4.31.

Next, the effective thermal conductivities of the MPC fuel basket and basket periphery regions are determined as described in Subsection 3.4.1.1.4. This calculation incorporates both the diluted helium thermal conductivity and the effective thermal conductivity of the fuel assembly with diluted helium. The Rayleigh effect thermal conductivity multipliers are unchanged in this analysis. This is conservative because the released rod gases will increase the average fluid density and decrease the gas thermal conductivity, consequently increasing the Rayleigh number. The effective thermal conductivities with diluted helium are compared to those with undiluted helium in Table 3.4.31.

The MPC fuel basket and basket periphery effective thermal conductivities are input to a finite-volume model of the HI-STAR System arranged for transport. The cask system temperature distribution with diluted MPC helium is determined using the finite-volume model, as described in Subsection 3.4.1.1.12. Design basis normal environmental conditions are applied to the model and a temperature field solution obtained. Cask system temperatures with diluted MPC helium are summarized in Table 3.4.32.

The slightly higher MPC cavity temperature with MPC helium dilution will result in a small perturbation in MPC internal pressure. Based on the temperature field obtained with helium dilution, the MPC internal pressure is determined using the Ideal Gas Law. The calculated MPC internal pressure with helium dilution is presented in Table 3.4.33.

The analyses presented in this subsection are performed to determine the effect of a hypothetical rupture of all fuel rods in a HI-STAR System during a severe transportation accident. Under the extreme conditions, the MPC component temperatures and pressures are within design limits. Based

on the results of these conservative calculations, it is determined that the effects of this severe hypothetical condition do not exceed the abilities of the HI-STAR System.

3.4.1.1.18 HI-STAR Temperature Field With Low Heat Emitting Fuel

The HI-STAR 100 thermal evaluations for BWR fuel are divided in two groups of fuel assemblies proposed for storage in MPC-68. These groups are classified as Low Heat Emitting (LHE) fuel assemblies and Design Basis (DB) fuel assemblies. The LHE group of fuel assemblies are characterized by low burnup, long cooling time, and short active fuel lengths. Consequently, their heat loads are dwarfed by the DB group of fuel assemblies. The Dresden-1 (6x6 and 8x8), Quad⁺, and Humboldt Bay (7x7 and 6x6) fuel characteristics warrant their classification as LHE fuel. This fuel (except Quad⁺ is permitted to be loaded when encased in Damaged Fuel Containers (DFCs). As a result of interruption of radiation heat exchange between the fuel assembly and the fuel basket by the DFC boundary, this loading configuration is bounding for thermal evaluation. In Subsection 3.4.1.1.2, two canister designs for encasing LHE fuel are evaluated - a previously approved Holtec Design (Holtec Drawing-1783) and an existing canister in which some of the Dresden-1 fuel is currently stored (Transnuclear D-1 Canister). The most resistive fuel assembly determined by analytical evaluation is considered for thermal evaluation (see Table 3.4.5). The MPC-68 basket effective conductivity, loaded with the most resistive fuel assembly from the LHE group of fuel (encased in a canister) is provided in Table 3.4.6. To this basket, LHE fuel decay heat load is applied and a HI-STAR 100 System temperature field obtained. The low heat load burden limits the initial peak cladding temperature to 579°F, which is substantially below the temperature limit for long-cooled fuel (~643°F).

A thoria rod canister designed to hold a maximum of 20 fuel rods arrayed in a 5x4 configuration is currently stored at the Dresden-1 spent fuel pool. The fuel rods contain a mixture of enriched UO₂ and Thorium Oxide in the fuel pellets. The fuel rods were originally constituted as part of an 8x8 fuel assembly and used in the second and third cycle of Dresden-1 operation. The maximum fuel burnup of these rods is quite low (~14,400 MWD/MTU). The thoria rod canister internal design is a honeycomb structure formed from 12 g age stainless steel plates. The rods are loaded in individual square cells and are isolated from each other by the cell walls. The few number of rods (18 per assembly) and very low burnup of fuel stored in these Dresden-1 canisters render them as miniscule sources of decay heat. The canister all-metal internal honeycomb construction serves as an additional means of heat dissipation in the fuel cell space. In accordance with preferential fuel loading requirements, low burnup fuel shall be loaded toward the basket periphery (i.e., away from the hot central core of the fuel basket). All these considerations provide ample assurance that these fuel rods will be stored in a benign thermal environment and therefore remain protected during transport.

3.4.1.2 Test Model

A detailed analytical model for evaluating the thermal design of the HI-STAR System was developed using the FLUENT CFD code and the industry standard ANSYS modeling system as discussed in Subsection 3.4.1.1. Furthermore, the analysis incorporates many conservative assumptions in order to demonstrate compliance with specified temperature limits for operation with adequate margins. In view of these considerations, the HI-STAR thermal design complies with the thermal criteria set forth in the design basis for normal transport conditions. Additional experimental verification of the thermal design is therefore not required. Acceptance and periodic thermal testing for the HI-STAR System is discussed in Sections 8.1 and 8.2.

3.4.2 Maximum Temperatures Under Normal Transport Conditions

Both MPC-basket designs developed for the HI-STAR System have been analyzed to determine temperature distributions under normal transport conditions. In the HI-STAR System thermal analysis models developed on FLUENT, the overpack impact limiters are included in the finite volume geometry. However, no credit is considered for the presence of heat conducting aluminum honeycomb material. In other words, heat transmission through the ends is conservatively neglected in the analysis. The thermal results are therefore bounding with respect to impact limiter design. The MPC baskets are considered to be loaded at design-basis maximum heat load with PWR or BWR fuel assemblies, as appropriate.

As discussed in Subsection 3.4.1.1.1, the thermal analysis is performed using a submodeling process where the results of an analysis on an individual component are incorporated into the analysis of a larger set of components. Specifically, the submodeling process yields directly computed fuel temperatures from which fuel basket temperatures are indirectly calculated. This modeling process differs from previous analytical approaches wherein the basket temperatures were evaluated first and then a basket-to-cladding temperature difference calculation by Wooten-Epstein or other means provided a basis for cladding temperatures. Subsection 3.4.1.1.2 describes the calculation of an effective fuel assembly thermal conductivity for an equivalent homogenous region. It is important to note that the result of this analysis is a function for thermal conductivity versus temperature. This function for fuel thermal conductivity is then input to the fuel basket effective thermal conductivity calculation described in Subsection 3.4.1.1.4. This calculation uses a finite-element methodology, wherein each fuel cell region containing multiple finite-elements has temperature varying thermal conductivity properties. The resultant temperature varying fuel basket thermal conductivity computed by this basket-fuel composite model is then input to the fuel basket region of the FLUENT cask model.

Because the FLUENT cask model incorporates the results of the fuel basket submodel, which in turn incorporates the fuel assembly submodel, the peak temperature reported from the FLUENT model is the peak temperature in any component. In a dry storage cask, the hottest components are the fuel assemblies. It should be noted that, because the fuel assembly models described in Subsection 3.4.1.1.2 include the fuel pellets, the FLUENT calculated peak temperatures reported in Tables 3.4.10 and 3.4.11 are actually peak pellet centerline temperatures which bound the peak cladding temperatures. We conservatively assume that the peak clad temperature is equal to the peak pellet centerline temperature.

For both the 24-PWR and 68-BWR assembly MPC-basket configurations, converged temperature contours corresponding to *steady-state hot* conditions (100°F ambient, maximum design basis maximum decay heat and full insolation) are shown in Figures 3.4.16 and 3.4.17. Figures 3.4.19 and 3.4.20 show the axial temperature variation of the hottest fuel rod in the MPC-24 and MPC-68 basket designs, respectively. Figures 3.4.22 and 3.4.23 show the radial temperature profile in the MPC-24 and MPC-68 basket designs, respectively, in the horizontal plane where maximum fuel cladding temperature is indicated. Tables 3.4.10 and 3.4.11 summarize maximum calculated temperatures in different parts of the HI-STAR System at design-basis maximum decay heat loads. Tables 3.4.28 and 3.4.29 summarize the peak fuel cladding temperatures with heat loads lower than the design basis maximum. In Tables 3.4.22 and 3.4.23, maximum calculated temperatures in different parts of the HI-STAR System under *steady-state cold* conditions (-40°F ambient, maximum design basis maximum decay heat and no insolation) are summarized.

The following additional observations can be derived by inspecting the temperature field obtained from the finite element analysis:

- The maximum fuel cladding temperature is well within the PNL recommended temperature limit.
- The maximum temperature of basket structural material is well within the stipulated design temperatures.
- The maximum temperature of the Boral neutron absorber is below the material supplier's recommended limit.
- The maximum temperatures of the MPC helium retention boundary materials are well below their respective ASME Code limits.
- The maximum temperatures of the aluminum heat conduction elements are well below the stipulated design temperature limits.
- The maximum temperature of the HI-STAR containment boundary materials is well below their respective ASME Code limits.

- The neutron shielding material (Holtite-A) will not experience temperatures in excess of its qualified limit.

The above observations lead us to conclude that the temperature field in the HI-STAR System with a fully loaded MPC containing design-basis heat emitting SNF complies with all regulatory and industry thermal requirements for normal conditions of transport. In other words, the thermal environment in the HI-STAR System will be conducive to safe transport of spent nuclear fuel.

3.4.2.1 Maximum Accessible Surface Temperatures

Access to the HI-STAR overpack cylindrical surface is restricted by the use of a personnel barrier (See Holtec Drawing 1809 in Chapter 1). Therefore, the HI-STAR System surfaces accessible during normal transport are the exposed impact limiter surfaces outside the personnel barrier. In this subsection, the exposed impact limiter surface temperatures are computed by including heat transmission from the hot overpack ends through the impact limiters. A conservatively bounding analysis is performed by applying the thermal conductivity of aluminum to the encased aluminum-honeycomb material in the impact limiter shells to the normal condition thermal model discussed earlier in this chapter. In this manner heat transport to the exposed surfaces from the hot overpack is maximized and accessible surface temperatures over estimated. The maximum exposed surface temperatures of MPC-24 and MPC-68 basket designs are 142°F and 139°F respectively. In Figure 3.4.28, a color contour map of the regions of HI-STAR System less than 185°F (358°K) is depicted for the hotter MPC-24 basket design. From this map, it is apparent that the accessible (impact limiter) surface temperatures are below the 10CFR71.43(g) mandated limit by a significant margin.

3.4.3 Minimum Temperatures

As specified in 10CFR71, the minimum ambient temperature conditions for the HI-STAR System are -20°F and a cold environment at -40°F. The HI-STAR System design does not have any minimum decay heat load restrictions for transport. Therefore, under zero decay heat load in combination with no solar input conditions, the temperature distribution will be uniformly equal to the imposed minimum ambient conditions. All HI-STAR System materials of construction would satisfactorily perform their intended function in the transport mode at this minimum postulated temperature condition. Evaluations in Chapter 2 demonstrate the acceptable structural performance of the overpack and MPC steel materials at low temperature. Shielding and criticality functions of the HI-STAR System materials (Chapters 5 and 6) are unaffected by exposure to this minimum temperature.

3.4.3.1 Post Rapid Ambient Temperature Drop Overpack Cooldown Event

In this section, the thermal response of the HI-STAR overpack to a rapid ambient temperature drop is analyzed and evaluated. The ambient temperature is postulated to drop from the maximum to minimum temperature under normal condition of transport in a very short time (100°F to -40°F during a 1 hour period) and is assumed to hold steady at -40°F thereafter. The initial overpack condition prior to this rapid temperature drop corresponds to normal steady state transport with maximum design basis heat load. During this postulated cooldown event, the outer surface of the overpack will initially cool more rapidly than the bulk of metal away from the exposed surfaces. Consequently, it is expected that the through-thickness temperature gradients will increase for a period of time, reach a maximum and follow an asymptotic return to the initial steady condition through thickness temperature gradients as the overpack temperature field approaches the -40°F ambient steady condition. The results of the transient analysis reported in this sub-section verify these observations.

Noting that the state of thermal stress is influenced by changes in the overpack temperature field during the cooldown transient, a number of critical locations in the containment boundary depicted in Figure 3.4.24 are identified as pertinent to a structural integrity evaluation discussed in Subsection 2.6.2.3 of this SAR. Locations (1) and (2) are chosen to track the through-thickness temperature gradients in the overpack top forging which is directly exposed to the ambient. Locations (3) and (4) are chosen to track the overpack inner containment shell through-thickness temperature gradient in a plane of maximum heat generation (i.e. active fuel mid-height) where the heat fluxes and corresponding temperature gradients are highest. Locations (A) and (B) are similarly chosen to track the temperature differential in the multi-layered shells (outer-to-inner shells).

The normal transport condition thermal model discussed previously in this chapter is employed in the overpack cooldown transient analysis. This analysis is carried out by applying time-dependent thermal boundary conditions to the model and starting the transient solution in the FLUENT program. In the cooldown event, the ambient temperature is decreased from 100°F to -40°F in 10°F steps every 4 minutes (i.e. a total of 14 steps lasting 56 minutes). The ambient temperature is held constant thereafter. The maximum design basis heat load cask (i.e. the MPC-24 design) was selected to maximize the thermal gradients (by Fourier's Law, thermal gradient is proportional to heat flow). The overpack cooldown event is tracked by the thermal model for a period of 24 hours and results are reported in Figures 3.4.25 through 3.4.27 as discussed below.

In Figure 3.2.25, the overpack containment through-thickness temperature gradient responses are plotted. From this figure, it is evident that the exposed surface of the overpack forging (location (2)) initially cools at a faster rate than the recessed location (1). A similar but less pronounced result is observed in the multi-layered shells temperature changes depicted in Figure 3.4.26. This out-of-phase rate of cooling results in an increasing temperature gradient through the overpack metal layers. The thermal response of deeply recessed locations (3) and (4) show gradual

temperature changes that follow each other closely. In other words, while through-thickness temperature gradients in the forging are somewhat altered the overpack inner shell gradients are essentially unchanged during the cooldown period. A closer examination of the forging temperature gradient is therefore warranted.

In Figure 3.4.27, the time dependent forging through thickness temperature differential is depicted. The gradient increases to a maximum in a short time period followed by a slow return towards the starting state. In absolute terms, both the steady state and transient temperature gradients in the forging are quite modest. In the steady state the forging through thickness temperature gradient is approximately 3°F. This value reaches a maximum plateau of 7°F during the transient event (Figure 3.4.27). The incremental thermal stress arising from this short-term gradient elevation is computed and discussed in Subsection 2.6.2.3 of this SAR.

3.4.4 Maximum Internal Pressures

The MPC is initially filled with dry helium after fuel loading and prior to sealing the MPC lid port cover plates and closure ring. During normal transport conditions, the gas temperature within the MPC rises to its maximum operating temperature as determined by the thermal analysis methodology described earlier (see Subsection 3.4.1). The gas pressure inside the MPC will increase with rising temperature. The pressure rise is determined using the Ideal Gas Law which states that the absolute pressure of a fixed volume of entombed gas is proportional to its absolute temperature.

The HI-STAR Maximum Normal Operating Pressure (MNOP) is calculated for a postulated 100% fuel rod failure and the release of fill and fission gases from the rods. In Tables 3.4.13 and 3.4.14, summary calculations for determining net free volume in the MPC-24 and MPC-68 canisters are presented. Based on a 30% release of the significant radioactive gases, a 100% release of the rod fill gas, the net free volume and the initial fill gas pressure (see Table 3.3.2), the maximum MPC gas pressure for the 100% rod rupture condition is given in Table 3.4.15. The overpack containment boundary MNOP for a hypothetical MPC breach condition is bounded by the MPC pressure results reported in this table.

3.4.5 Maximum Thermal Stresses

Thermal expansion induced mechanical stresses due to imposed non-uniform temperature distributions have been determined and reported in Chapter 2. Tables 3.4.17 and 3.4.18 summarize the HI-STAR System components temperatures, under steady-state hot conditions, for structural evaluation.

Additionally, Table 3.4.24 provides a summary of MPC helium retention boundary temperatures during normal transport conditions (steady state hot). Structural evaluations in Section 2.6 reference these temperature results to demonstrate the MPC helium retention boundary integrity.

3.4.6 Evaluation of System Performance for Normal Conditions of Transport

The HI-STAR System thermal analysis is based on detailed and complete heat transfer models that properly account for radiation, conduction and natural convection modes of heat transfer. The thermal models incorporate many conservative assumptions that are listed below.

1. No credit for gap reduction between the MPC and overpack due to differential thermal expansion under hot condition is considered.
2. No credit is considered for MPC basket internal thermosiphon heat transfer. Under a perfectly horizontal transport condition, axial temperature gradients with peaking at active fuel mid-height induces buoyancy flows from both ends of the basket in each MPC cell. Buoyancy flow in shallow horizontal channels has been widely researched and reported in the technical literature [3.4.10 to 3.4.12]. An additional mode of heat transport due to thermosiphon flow within the basket cells is initiated for any cask orientation other than a perfectly horizontal condition. In practice this is a highly likely scenario. However, in the interest of conservatism, no credit is considered for this mode of heat transfer.
3. An upper bound solar absorbtivity of unity is applied to all exposed surfaces.
4. No credit considered for radiative heat transfer between the Boral neutron absorber panels and the Boral pocket walls, or for the presence of helium in the pocket gaps.
5. No credit is considered for conduction through the neutron shielding materials.
6. No credit is considered for contact between fuel assemblies and the MPC basket wall or between the MPC basket and the MPC basket supports. The fuel assemblies and MPC basket are conservatively considered to be in concentric alignment.
7. No credit considered for presence of highly conducting aluminum honeycomb material inside impact limiters.
8. The MPC basket axial conductivity is conservatively assumed to be equal to the lower basket cross sectional effective conductivity.
9. The MPC is assumed to be loaded with the SNF type which has the maximum equivalent thermal resistance of all fuel types in its category (BWR or PWR), as applicable.
10. The design basis maximum decay heat loads are used for all thermal-hydraulic analyses. For casks loaded with fuel assemblies having decay heat generation rates less than design basis, additional thermal margins of safety will exist.

11. Interfacial contact conductance of multi-layered intermediate shell contacting layers was conservatively determined to bound surface finish, contact pressure, and base metal conductivity conditions.

Temperature distribution results obtained from a conservatively developed thermal model show that maximum fuel cladding temperature limits are met with adequate margins. Margins during actual normal transport conditions are expected to be greater due to the many conservative assumptions incorporated in the analysis. The maximum local temperatures in the neutron shield and overpack seals are lower than design limits. The maximum local MPC basket temperature level is below the recommended limits for structural materials in terms of susceptibility to stress, corrosion and creep induced degradation. Furthermore, structural evaluation (Chapter 2) has demonstrated that stresses (including those induced due to imposed temperature gradients) are within ASME B&PV Code limits. Section 3.6 provides a discussion of compliance with the regulatory requirements and acceptance criteria listed in Section 3.0. As a result of the above-mentioned considerations, it is concluded that the HI-STAR thermal design is in compliance with 10CFR71 requirements for normal conditions of transport.

Table 3.4.1

CLOSED CAVITY NUSSELT NUMBER
RESULTS FOR HELIUM FILLED MPC PERIPHERAL VOIDS

Temperature (°F)	Case (i) Nusselt Number		Case (ii) Nusselt Number	
	MPC-24	MPC-68	MPC-24	MPC-68
200	6.93	4.72	5.45	3.46
450	5.44	3.71	4.09	2.58
700	4.60	3.13	3.36	2.12

Table 3.4.2

RELATIONSHIP BETWEEN HI-STAR SYSTEM REGIONS
AND MATHEMATICAL MODEL DESCRIPTIONS

<u>HI-STAR System Region</u>	<u>Mathematical Model</u>	<u>Subsections</u>
Fuel Assembly	Fuel Region Effective Thermal Conductivity	3.4.1.1.2
MPC	Effective Thermal Conductivity of Boral/Sheathing/Box Wall Sandwich	3.4.1.1.3
	Basket In-Plane Conductive Heat Transport	3.4.1.1.4
	Heat Transfer in MPC Basket Peripheral Region	3.4.1.1.5
	Effective Thermal Conductivity of MPC Basket-to-Shell Aluminum Heat Conduction Elements	3.4.1.1.11
Overpack	Effective Conductivity of Multi-Layered Intermediate Shell Region	3.4.1.1.6
	Effective Thermal Conductivity of Holtite Neutron Shielding Region	3.4.1.1.9
Ambient Environment	Heat Rejection from Overpack Exterior Surfaces	3.4.1.1.7
	Solar Heat Input	3.4.1.1.8
Assembled Cask Model	Overview of the Thermal Model	3.4.1.1.1
	Effective Conductivity of MPC to Overpack Gap	3.4.1.1.10
	FLUENT Model for HI-STAR	3.4.1.1.12

Table 3.4.3

THIS TABLE IS INTENTIONALLY DELETED.

Table 3.4.4

SUMMARY OF PWR FUEL ASSEMBLIES
EFFECTIVE THERMAL CONDUCTIVITIES

No.	Fuel	@ 200°F (Btu/ft-hr-°F)	@ 450°F (Btu/ft-hr-°F)	@ 700°F (Btu/ft-hr-°F)
1	<u>W</u> 17×17 OFA	0.182	0.277	0.402
2	<u>W</u> 17×17 Std	0.189	0.286	0.413
3	<u>W</u> 17×17 Vantage-5H	0.182	0.277	0.402
4	<u>W</u> 15×15 Std	0.191	0.294	0.430
5	<u>W</u> 14×14 Std	0.182	0.284	0.424
6	<u>W</u> 14×14 OFA	0.175	0.275	0.413
7	B&W 17×17	0.191	0.289	0.416
8	B&W 15×15	0.195	0.298	0.436
9	CE 16×16	0.183	0.281	0.411
10	CE 14×14	0.189	0.293	0.435
11	HN [†] 15×15 SS	0.180	0.265	0.370
12	<u>W</u> 14×14 SS	0.170	0.254	0.361
13	B&W 15×15 Mark B-11	0.187	0.289	0.424
14	CE 14×14 (MP2)	0.188	0.293	0.434

Note: Boldface values denote the lowest thermal conductivity in each column (excluding stainless steel clad fuel assemblies).

[†] Haddam Neck B&W or Westinghouse stainless steel clad fuel assemblies.

Table 3.4.5

SUMMARY OF BWR FUEL ASSEMBLIES EFFECTIVE THERMAL CONDUCTIVITIES

No.	Fuel	@ 200°F (Btu/ft-hr-°F)	@ 450°F (Btu/ft-hr-°F)	@ 700°F (Btu/ft-hr-°F)
1	Dresden 1 8×8†	0.119	0.201	0.319
2	Dresden 1 6×6	0.126	0.215	0.345
3	GE 7×7	0.171	0.286	0.449
4	GE 7×7R	0.171	0.286	0.449
5	GE 8×8	0.168	0.278	0.433
6	GE 8×8R	0.166	0.275	0.430
7	GE-10 8×8	0.168	0.280	0.437
8	GE-11 9×9	0.167	0.273	0.422
9	AC‡ 10×10 SS	0.152	0.222	0.309
10	Exxon 10×10 SS	0.151	0.221	0.308
11	Damaged Dresden 1 8×8 in a DFC†	0.107	0.169	0.254
12	Dresden-1 Thin Clad 6x6†	0.124	0.212	0.343
13	Humboldt Bay† -7x7	0.127	0.215	0.343
14	Damaged Dresden-1 8x8 (in TN D-1 canister)†	0.107	0.168	0.252
15	8x8 Quad† Westinghouse†	0.164	0.278	0.435

Note: Boldface values denote the lowest thermal conductivity in each column (excluding Dresden and LaCrosse clad fuel assemblies).

† Low heat emitting fuel assemblies excluded from list of fuel assemblies (zircaloy clad) evaluated to determine the most resistive SNF type.

‡ Allis-Chalmers stainless steel clad fuel assemblies.

Table 3.4.6

MPC BASKET EFFECTIVE THERMAL CONDUCTIVITY RESULTS
FROM ANSYS MODELS

Basket	@200°F (Btu/ft-hr-°F)	@450°F (Btu/ft-hr-°F)	@700°F (Btu/ft-hr-°F)
MPC-24 (Zircaloy Clad Fuel)	1.108	1.495	1.954
MPC-68 (Zircaloy Clad Fuel)	0.959	1.188	1.432
MPC-24 (Stainless Steel Clad Fuel)	0.995	1.321	1.700 ^(a)
MPC-68 (Stainless Steel Clad Fuel)	0.931	1.125	1.311 ^(b)
MPC-68 (Dresden-1 8x8 in canister)	0.861	1.055	1.242

- (a) 13% lower effective thermal conductivity than corresponding zircaloy-fueled basket
- (b) 9% lower effective thermal conductivity than corresponding zircaloy-fueled basket

Table 3.4.7

INSOLATION DATA SPECIFIED BY 10CFR71, SUBPART F

Surface Type	12-Hour Total Insolation Basis	
	(g-cal/cm ²)	(Watts/m ²)
Horizontally Transported Flat Surfaces		
- Base	None	None
- Other Surfaces	800	774.0
Non-Horizontal Flat Surfaces	200	193.5
Curved Surfaces	400	387.0

Table 3.4.8

EFFECTIVE THERMAL CONDUCTIVITY OF THE NEUTRON SHIELD/RADIAL CHANNELS REGION

Condition/Temperature (°F)	Thermal Conductivity (Btu/ft-hr-°F)
Normal Condition: 200 450 700	 1.953 1.812 1.645
Fire Condition: 200 450 700	 3.012 2.865 2.689

Table 3.4.9

THIS TABLE IS INTENTIONALLY DELETED.

Table 3.4.10

HI-STAR SYSTEM NORMAL TRANSPORT[†] MAXIMUM TEMPERATURES
(MPC-24)

	Calculated Maximum Temperature [°F]	Normal Condition Temperature Limit [°F]
Fuel Cladding	701	720
MPC Basket Centerline	667	725
MPC Basket Periphery	430	725
MPC Outer Shell Surface	315	450
MPC/Overpack Helium Gap Outer Surface	291	400
Radial Neutron Shield Inner Surface	271	300
Overpack Enclosure Shell Surface	222	350
Axial Neutron Shield	292	300
Impact Limiter Exposed Surface	121	176
Overpack Closure Plate ^{††}	163	400
Overpack Bottom Plate ^{††}	295	350

[†] Steady-state hot (100°F ambient) with maximum decay heat and insolation.

^{††} Overpack closure plate and vent/drain port plug seals normal condition design temperature is 400°F. The maximum seals temperatures are bounded by the reported closure plate and bottom plate maximum temperatures. Consequently, a large margin of safety exists to permit safe operation of seals in the overpack helium retention boundary.

Table 3.4.11

**HI-STAR SYSTEM NORMAL TRANSPORT[†] MAXIMUM TEMPERATURES
(MPC-68)**

	Calculated Maximum Temperature [°F]	Normal Condition Temperature Limit [°F]
Fuel Cladding	713	749
MPC Basket Centerline	697	725
MPC Basket Periphery	365	725
MPC Outer Shell Surface	306	450
MPC/Overpack Gap Outer Surface	282	400
Radial Neutron Shield Inner Surface	264	300
Overpack Enclosure Shell Surface	217	350
Axial Neutron Shield	255	300
Impact Limiter Exposed Surface	121	176
Overpack Closure Plate ^{††}	162	400
Overpack Bottom Plate ^{††}	256	350

[†] Steady-state hot (100°F ambient) with maximum decay heat and insolation.

^{††} Overpack closure plate and vent/drain port plug seals normal condition design temperature is 400°F. The maximum seals temperatures are bounded by the reported closure plate and bottom plate maximum temperatures. Consequently, a large margin of safety exists to permit safe operation of seals in the overpack helium retention boundary.

Table 3.4.12

THIS TABLE IS INTENTIONALLY DELETED.

Table 3.4.13

SUMMARY OF BOUNDING MINIMUM
MPC-24 FREE VOLUME CALCULATIONS

Item	Volume (ft ³)
Cavity Volume	368.3
Basket Metal Volume	47.0
Bounding Fuel Assemblies Volume	78.8
Basket Supports and Fuel Spacers Volume	6.1
Aluminum Conduction Elements [†]	5.9
Net Free Volume	230.5 (6529 liters)

[†] Bounding 1,000 lbs aluminum weight.

Table 3.4.14

SUMMARY OF BOUNDING MINIMUM
MPC-68 FREE VOLUME CALCULATIONS

Item	Volume (ft ³)
Cavity Volume	367.2
Basket Metal Volume	45.5
Bounding Fuel Assemblies Volume	93.0
Basket Supports and Fuel Spacers Volume	11.3
Aluminum Conduction Elements [†]	5.9
Net Free Volume	211.5 (5989 liters)

[†] Bounding 1,000 lbs aluminum weight.

Table 3.4.15

SUMMARY OF MAXIMUM NORMAL OPERATING PRESSURE[†]
FOR HORIZONTAL TRANSPORT CONDITIONS

Condition	Pressure (psig)	MPC Cavity Bulk Temperature (°F)
MPC-24:		
Initial Backfill (at 70°F)	28.3	483
Normal Condition	61.8	
With 100% Rods Rupture	98.9	
MPC-68:		
Initial Backfill (at 70°F)	28.5	468
Normal Condition	61.0	
With 100% Rods Rupture	89.3	

[†] Pressure analysis is based on release of 100% of the rods fill gas and 30% of the significant radioactive gases from a ruptured rod.

Table 3.4.16

THIS TABLE IS INTENTIONALLY DELETED.

Table 3.4.17

MPC-24 NORMAL HORIZONTAL TRANSPORT CONDITION
 HI-STAR SYSTEM COMPONENTS TEMPERATURE [°F] SUMMARY

	MPC Basket Axial Mid-Length	MPC Basket Axial Ends
Overpack enclosure shell	222	147
Overpack inner shell	291	163
MPC shell	315	164
Basket periphery	430	166
Basket center	667	177

Table 3.4.18

MPC-68 NORMAL HORIZONTAL TRANSPORT CONDITION
 HI-STAR SYSTEM COMPONENTS TEMPERATURE [°F] SUMMARY

	MPC Basket Axial Mid-Length	MPC Basket Axial Ends
Overpack enclosure shell	217	146
Overpack inner shell	282	161
MPC shell	306	163
Basket periphery	365	164
Basket center	697	175

Table 3.4.19

SUMMARY OF LOADED HI-STAR SYSTEM
 BOUNDING COMPONENT WEIGHTS AND THERMAL INERTIAS

Component	Weight (lbs)	Heat Capacity (Btu/lb-°F)	Thermal Inertia (Btu/°F)
Holtite-A	11,000	0.39	4,290
Carbon Steel	140,000	0.1	14,000
Alloy-X MPC (empty)	35,000	0.12	4,200
Fuel	40,000	0.056	2,240
MPC Cavity Water [†]	6,500	1.0	6,500
			31,230 (Total)

[†] Based on smallest MPC-68 cavity net free volume with 50% credit for flooded water mass.

Table 3.4.20

MAXIMUM ALLOWABLE TIME DURATION
FOR WET TRANSFER OPERATIONS

Initial Temperature (°F)	Time Duration (hr)
115	44.3
120	42.0
125	39.7
130	37.4
135	35.2
140	32.9
145	30.6
150	28.3

Table 3.4.21

THIS TABLE IS INTENTIONALLY DELETED.

Table 3.4.22

HI-STAR SYSTEM MAXIMUM TEMPERATURES [°F]
 UNDER STEADY-STATE COLD[†] CONDITIONS (MPC-24)

Fuel Cladding	620
MPC Basket Centerline	586
MPC Basket Periphery	329
MPC Outer Shell Surface	190
MPC/Overpack Gap Outer Surface	165
Radial Neutron Shield Inner Surface	141
Overpack Enclosure Shell Surface	96
Axial Neutron Shield	165
Impact Limiter Exposed Surface	-40

[†] -40°F ambient temperature with maximum decay heat and no insolation.

Table 3.4.23

HI-STAR SYSTEM MAXIMUM TEMPERATURES [°F]
 UNDER STEADY-STATE COLD[†] CONDITIONS (MPC-68)

Fuel Cladding	621
MPC Basket Centerline	605
MPC Basket Periphery	254
MPC Outer Shell Surface	178
MPC/Overpack Gap Outer Surface	153
Radial Neutron Shield Inner Surface	130
Overpack Enclosure Shell Surface	88
Axial Neutron Shield	123
Impact Limiter Exposed Surface	-40

[†] -40°F ambient temperature with maximum decay heat and no insolation.

Table 3.4.24

SUMMARY OF MPC HELIUM RETENTION BOUNDARY TEMPERATURE
DISTRIBUTION DURING NORMAL STORAGE CONDITIONS

Location	Figure 2.6.20 Designation	MPC-24 [°F]	MPC-68 [°F]
MPC Lid Inside Surface at Centerline	A	176	173
MPC Lid Outside Surface at Centerline	B	171	169
MPC Lid Inside Surface at Periphery	C	164	163
MPC Lid Outside Surface at Periphery	D	162	161
MPC Baseplate Inside Surface at Centerline	E	301	260
MPC Baseplate Outside Surface at Centerline	F	295	256
MPC Baseplate Inside Surface at Periphery	G	267	239
MPC Baseplate Outside Surface at Periphery	H	267	239
MPC Shell Maximum	I	315	306

Table 3.4.25

SUMMARY OF 10×10 ARRAY BWR FUEL ASSEMBLY TYPES
EFFECTIVE THERMAL CONDUCTIVITIES[†]

Fuel	k_{eff} at 200°F [Btu/(ft-hr-°F)]	k_{eff} at 450°F [Btu/(ft-hr-°F)]	k_{eff} at 700°F [Btu/(ft-hr-°F)]
GE-12/14	0.166	0.269	0.412
Atrium-10	0.164	0.266	0.409
SVEA-96	0.164	0.269	0.416

[†] The conductivities reported in this table are obtained by the simplified method described in the beginning of Subsection 3.4.1.1.2.

Table 3.4.26

COMPARISON OF ATRIUM-10[†] AND BOUNDING^{††} BWR FUEL ASSEMBLY
EFFECTIVE THERMAL CONDUCTIVITIES

Temperature	Atrium-10 Assembly		Bounding BWR Assembly	
	Btu/(ft-hr-°F)	W/m-K	Btu/(ft-hr-°F)	W/m-K
200	0.225	0.389	0.171	0.296
450	0.345	0.597	0.271	0.469
700	0.504	0.872	0.410	0.710

[†] The reported effective thermal conductivity has been obtained from a rigorous finite-element modeling of the Atrium-10 assembly.

^{††} The bounding BWR fuel assembly effective thermal conductivity applied in the MPC-68 basket thermal analysis.

Table 3.4.27

THIS TABLE IS INTENTIONALLY DELETED.

Table 3.4.28

MPC-24 PEAK FUEL CLADDING TEMPERATURE
AS A FUNCTION OF TOTAL HEAT LOAD

Total MPC Decay Heat Load (kW)	Peak Fuel Cladding Temperature (°F)
20.0 [†]	700.6
19.0	678.9
17.0	633.9
15.5	598.8

[†] Design Basis Maximum.

Table 3.4.29

MPC-68 PEAK FUEL CLADDING TEMPERATURE
AS A FUNCTION OF TOTAL HEAT LOAD

Total MPC Decay Heat Load (kW)	Peak Fuel Cladding Temperature (°F)
18.5 [†]	712.7
17.0	674.0
15.5	634.1

[†] Design Basis Maximum.

Table 3.4.30

SUMMARY OF THERMAL CONDUCTIVITY CALCULATIONS
FOR MPC HELIUM DILUTED BY RELEASED ROD GASES

Component Gas	Molecular Weight (g/mole)	Mole Fraction	Thermal Conductivity (Btu/hr-ft-°F)
MPC and Fuel Rod Backfill Helium	4	0.817	0.098 @ 200°F 0.129 @ 450 °F 0.158 @ 700°F
Rod Tritium	3	8.007×10^{-5}	0.119 @ 200 0.148 @ 450°F 0.177 @ 700°F
Rod Krypton	85	0.016	6.76×10^{-3} @ 200°F 8.782×10^{-3} @ 450°F 0.011 @ 700°F
Rod Xenon	131	0.160	3.987×10^{-3} @ 200°F 5.258×10^{-3} @ 450°F 6.471×10^{-3} @ 700°F
Rod Iodine	129	6.846×10^{-3}	2.496×10^{-3} @ 200°F 3.351×10^{-3} @ 450°F 4.201×10^{-3} @ 700°F
Mixture of Gases (diluted helium)	N/A	1.000	0.053 @ 200°F 0.069 @ 450°F 0.085 @ 700°F

Table 3.4.31

COMPARISON OF COMPONENT EFFECTIVE THERMAL CONDUCTIVITIES
WITH AND WITHOUT MPC HELIUM DILUTION

	Effective Thermal Conductivity (Btu/hr-ft-°F)		
	Value at 200°F	Value at 450°F	Value at 700°F
Fuel Assembly with Undiluted Helium	0.257	0.406	0.604
Fuel Assembly with Diluted Helium	0.160	0.278	0.458
MPC Fuel Basket with Undiluted Helium	1.108	1.495	1.954
MPC Fuel Basket with Diluted Helium	0.933	1.303	1.758
Basket Periphery with Undiluted Helium [†]	0.3136	0.4456	0.6459
Basket Periphery with Diluted Helium [†]	0.2286	0.3550	0.5538

† These thermal conductivity values do not include the contribution of the aluminum heat conduction elements.

Table 3.4.32

**MPC-24 HYPOTHETICAL 100% RODS RUPTURE ACCIDENT
MAXIMUM TEMPERATURES**

	Calculated Maximum Temperature (°F)	Accident Condition Temperature Limit (°F)
Fuel Cladding	743	1058
MPC Basket Centerline	709	950
MPC Basket Periphery	444	950
MPC Outer Shell Surface	314	775
MPC/Overpack Helium Gap Outer Surface	291	500
Radial Neutron Shield Inner Surface	271	N/A
Overpack Enclosure Shell Surface	222	1350
Overpack Closure Plate	176	700
Overpack Bottom Plate	296	700

Table 3.4.33

MPC-24 HYPOTHETICAL 100% RODS RUPTURE ACCIDENT PRESSURES

Calculated Accident Pressure (psig)	Accident Condition Design Pressure (psig)
102.1	125

Table 3.4.34

PLANT SPECIFIC BWR FUEL TYPES EFFECTIVE THERMAL CONDUCTIVITY*

Fuel	@200°F [Btu/ft-hr-°F]	@450°F [Btu/ft-hr-°F]	@700F° [Btu/ft-hr-°F]
Oyster Creek (7x7)	0.165	0.273	0.427
Oyster Creek (8x8)	0.162	0.266	0.413
TVA Browns Ferry (8x8)	0.160	0.264	0.411
SPC-5 (9x9)	0.149	0.245	0.380

* The conductivities reported in this table are obtained by a simplified analytical method described in Subsection 3.4.1.1.2.

CHAPTER 4: CONTAINMENT

4.0 INTRODUCTION

This chapter demonstrates the HI-STAR 100 containment boundary compliance with the permitted activity release limits specified in 10CFR71, 71.51(a)(1) and 71.51(a)(2) for both normal and hypothetical accident conditions of transport [4.0.1]. Satisfaction of the containment criteria, expressed as the leakage rate acceptance criterion (atm-cm³/sec, Helium), ensures that the HI-STAR 100 package will not exceed the specified allowable radionuclide release rates. Leakage rates are determined in accordance with the recommendations of ANSI N14.5 [4.0.2], and utilizing NUREG/CR-6487, *Containment Analysis for Type B Packages Used to Transport Various Contents* [4.0.3], Regulatory Guide 7.4, *Leakage Tests on Packages for Shipment of Radioactive Materials* [4.0.4] as content guides, and Draft NUREG-1617, *Standard Review Plan for Transportation Packages for Spent Nuclear Fuel* [4.0.5].

The HI-STAR 100 packaging allowable leakage rates established herein ensures that the requirements of 10CFR71.51 and 10CFR71.63(b) are met. The primary containment system boundary for the HI-STAR 100 packaging consists of the overpack inner shell, the bottom plate, the top flange, the top closure plate, closure bolts, the overpack vent and drain port plugs, and their respective mechanical seals. The secondary containment system boundary for a HI-STAR 100 packaging containing Dresden Unit 1 or Humboldt Bay fuel debris consists of the MPC-68F enclosure vessel including the MPC shell, the MPC bottom plate, the MPC lid, closure ring, and vent and drain port cover plates. The MPC-68F provides the separate inner container per 10CFR71.63(b) for the HI-STAR 100 System transporting fuel classified as fuel debris. The other MPC designs (MPC-24 and MPC-68) are not currently evaluated for secondary containment requirements.

Chapter 2 of this SAR shows that all primary and secondary containment boundary components are maintained within their code-allowable stress limits during all normal and hypothetical accident conditions of transport as defined in 10CFR71.71 and 10CFR71.73. Chapter 3 of this SAR shows that the peak containment component temperatures and pressures are within the design basis limits for all normal and hypothetical accident conditions of transport as defined in 10CFR71.71 and 10CFR71.73. Since both the primary and secondary containment boundaries are shown to remain intact, and the temperature and pressure design bases are not exceeded, the design basis leakage rates are not exceeded during normal or hypothetical accident conditions of transport.

The HI-STAR overpack is subjected to a containment system fabrication verification test before the first use as described in Chapter 8. The containment system fabrication verification test is performed at the factory as part of the HI-STAR 100 acceptance testing. The welds of the primary containment boundary, the closure plate inner seal, and the vent and drain port plug seals are helium leakage tested in accordance with ANSI N14.5. A containment system periodic verification test as described in Chapter 8, will be performed prior to each loaded transport. The mechanical seals of the HI-STAR 100 overpack will be replaced and retested each time the HI-STAR 100 is loaded.

The secondary containment boundary system (MPC-68F) will be subjected to the fabrication verification leakage testing at the fabrication facility as described in Chapter 8 of this SAR. Prior to transport of the MPC-68F containing fuel debris, a secondary containment boundary periodic verification leakage test will be performed as described in Chapter 8 to ensure that the measured leakage rates are below the limit specified in this chapter.

As the containment system periodic verification leakage test shall be performed on each containment boundary separately prior to each loaded transport, this test takes the place of and is performed in lieu of the assembly verification.

The MPC-68 is designed to store damaged fuel, fuel debris, or intact fuel. The sole additional requirement imposed on an MPC-68 to load fuel debris is an additional leakage rate criteria test just prior to shipment. Therefore, an MPC-68 which is to transport fuel debris will be designated to ensure the proper leakage rate test criteria is applied. To distinguish an MPC-68 which is fabricated to transport fuel debris, the MPC will be designated as an "MPC-68F".

To aid in loading and unloading, damaged fuel assemblies and fuel debris will be loaded into stainless steel DFCs prior to placement in the HI-STAR 100 System. The damaged fuel container (DFC) is shown in the Design Drawings in Section 1.4. The DFC is designed to provide SNF loose component retention and handling capabilities. The DFC consists of a smooth-walled, welded stainless steel square canister with a removable lid. The canister lid provides the means of DFC closure and handling. The DFC is provided with stainless steel wire mesh screens in the top and bottom for draining, vacuum drying and helium backfill operations. The screens are specified as a 250-by-250-mesh with an effective opening of 0.0024 inches. There are no other openings in the DFC. Chapter 1 specifies the fuel assembly characteristics for damaged fuel acceptable for loading in the MPC-68 or MPC-68F and for fuel debris acceptable for loading in the MPC-68F.

Up to four (4) DFCs containing specified fuel debris may be placed in a MPC-68F. Up to 68 damaged fuel assemblies in DFCs may be stored in an MPC-68 or MPC-68F. The quantity of fuel debris is limited to meet the off-site transportation requirements of 10CFR71, specifically, 10CFR71.63(b). Analyses provided in this chapter conservatively assume 100% of the rods of the fuel debris are breached under normal conditions of transport. Therefore, 100% of the contents of the DFCs are available for release.

Table 4.1.1

SUMMARY OF CONTAINMENT BOUNDARY DESIGN SPECIFICATIONS

Design Attribute	Design Rating	
	Primary (Overpack) 10CFR71.51	Secondary (MPC-68F) 10CFR71.63(b)
Closure Plate Mechanical Seals: ^{††} Design Temperature Pressure Rating Design Leakage Rate	1200°F 1,000 psig 1X10 ⁻⁶ cm ³ /s, Helium	N/A
Overpack Vent and Drain Port Cover Plate Mechanical Seals: ^{†,††} Design Temperature Pressure Rating Design Leakage Rate	1300°F 1,000 psig 1x10 ⁻⁶ cm ³ /sec, Helium	N/A
Overpack Vent and Drain Port Plug Mechanical Seals: ^{††} Design Temperature Pressure Rating Design Leakage Rate	1300°F 1,000 psig 1x10 ⁻⁶ cm ³ /sec, Helium	N/A
Leakage Rate Acceptance Criterion	4.3 x 10 ⁻⁶ atm cm ³ /s, He	5.0 x 10 ⁻⁶ atm cm ³ /s, He
Leakage Rate Test Sensitivity	2.15 x 10 ⁻⁶ atm cm ³ /s, He	--

† No credit is taken for the overpack vent and drain port cover plate seals as part of the containment boundary. Specifications are provided for information.

†† Per manufacturer's recommended operating limits.

4.2.5.2 Source Terms For Spent Nuclear Fuel Assemblies

In accordance with NUREG/CR-6487 [4.0.3], the following contributions are considered in determining the releasable source term for packages designed to transport irradiated fuel rods: (1) the radionuclides comprising the fuel rods, (2) the radionuclides on the surface of the fuel rods, and (3) the residual contamination on the inside surfaces of the vessel. NUREG/CR-6487 goes on to state that a radioactive aerosol can be generated inside a vessel when radioactive material from the fuel rods or from the inside surfaces of the container become airborne. The sources for the airborne material are (1) residual activity on the cask interior, (2) fission and activation-product activity associated with corrosion-deposited material (crud) on the fuel assembly surface, and (3) the radionuclides within the individual fuel rods. In accordance with NUREG/CR-6487, contamination due to residual activity on the cask interior surfaces is negligible as compared to crud deposits on the fuel rods themselves and therefore may be neglected. The source term considered for this calculation results from the spallation of crud from the fuel rods and from the fines, gases and volatiles which result from cladding breaches.

The inventory for isotopes other than ^{60}Co is calculated with the SAS2H and ORIGEN-S modules of the SCALE 4.3 system as described in Chapter 5. The inventory for the MPC-24 was conservatively based on the B&W 15x15 fuel assembly with a burnup of 40,000 MWD/MTU, 5 years of cooling time, and an enrichment of 3.4%. The inventory for the MPC-68 was based the GE 7x7 fuel assembly with a burnup of 40,000 MWD/MTU, 5 years of cooling time, and 3.0% enrichment. The inventory for the MPC-68F was based on the GE 6x6 fuel assembly with a burnup of 30,000 MWD/MTU, 18 years of cooling time, and 1.8% enrichment. Additionally, an MPC-68F was analyzed containing 67 GE 6x6 assemblies and a DFC containing 18 thorium rods. Finally, an Sb-Be source stored in one fuel rod in one assembly with 67 GE 6x6 assemblies was analyzed. The isotopes which contribute greater than 0.01% to the total curie inventory for the fuel assembly are considered in the evaluation as fines. Additionally, isotopes with A_2 values less than 1.0 in Table A-1, Appendix A, 10CFR71 are included as fines. Isotopes which contribute greater than 0.01% but which do not have an assigned A_2 value in Table A-1 are assigned an A_2 value based on the guidance in Table A-2, Appendix A, 10CFR71. Isotopes which contribute greater than 0.01% but have a radiological half life less than 10 days are neglected. Table 4.2.2 presents the isotope inventory used in the calculation.

A. Source Activity Due to Crud Spallation from Fuel Rods

The majority of the activity associated with crud is due to ^{60}Co [4.0.3]. The inventory for ^{60}Co was determined by using the crud surface activity for PWR rods (140×10^{-6} Ci/cm²) and for BWR rods (1254×10^{-6} Ci/cm²) provided in NUREG/CR-6487 [4.0.3] multiplied by the surface area per assembly (3×10^5 cm² and 1×10^5 cm² for PWR and BWR, respectively, also provided in NUREG/CR-6487).

The source terms were then decay corrected (5 years for the MPC-24 and MPC-68; 18 years for the MPC-68F) using the basic radioactive decay equation:

$$A(t) = A_0 e^{-\lambda t} \quad (4-1)$$

where:

- A(t) is activity at time t [Ci]
- A₀ is the initial activity [Ci]
- λ is the ln2/t_{1/2} (where t_{1/2} = 5.272 years for ⁶⁰Co)
- t is the time in years (5 years for the MPC-24 and MPC-68; 18 years for the MPC-68F)

The inventory for ⁶⁰Co was determined using the methodology described above with the following results:

PWR

Surface area per Assy = 3.0E+05 cm²
 140 μCi/cm² x 3.0E+05 cm² = 42.0 Ci

BWR

Surface area per Assy = 1.0E+05 cm²
 1254 μCi/cm² x 1.0E+05 cm² = 125.4 Ci

⁶⁰Co(t) = ⁶⁰Co₀ e^{-(λt)}, where λ = ln2/t_{1/2}, t = 5 years (for the MPC-24 and MPC-68), t = 18 years (MPC-68F), t_{1/2} = 5.272 years for ⁶⁰Co [4.2.4]

MPC-24

⁶⁰Co(5) = 42.0 Ci e^{-(ln 2/5.272)(5)}
⁶⁰Co(5) = 21.77 Ci

MPC-68

⁶⁰Co(5) = 125.4 Ci e^{-(ln 2/5.272)(5)}
⁶⁰Co(5) = 64.98 Ci

MPC-68F

⁶⁰Co(18) = 125.4 Ci e^{-(ln 2/5.272)(18)}
⁶⁰Co(18) = 11.76 Ci

A summary of the ⁶⁰Co inventory available for release is provided in Table 4.2.2.

The activity density that results inside the containment vessel as a result of crud spallation from spent fuel rods can be formulated as:

$$C_{\text{crud}} = \frac{f_C M_A N_A}{V} \quad (4-2)$$

where:

C_{crud} is the activity density inside the containment vessel as a result of crud spallation [Ci/cm³],
 M_A is the total crud activity inventory per assembly [Ci/assy],
 f_C is the crud spallation fraction,
 N_A is the number of assemblies, and
 V is the free volume inside the containment vessel [cm³].

NUREG/CR-6487 states that measurements have shown 15% to be a reasonable value for the percent of crud spallation for both PWR and BWR fuel rods under normal transportation conditions. For hypothetical accident conditions, it is assumed that there is 100% crud spallation [4.0.3].

B. Source Activity Due to Releases of Fines from Cladding Breaches

A breach in the cladding of a fuel rod may allow radionuclides to be released from the resulting cladding defect into the interior of the MPC. If there is a leak in the primary or secondary containment vessels, then the radioisotopes emitted from a cladding breach that were aerosolized may be entrained in the gases escaping from the package and result in a radioactive release to the environment.

NUREG/CR-6487 suggests that a bounding value of 3% of the rods develop cladding breaches during normal transportation (i.e., $f_B=0.03$). For hypothetical accident conditions, it is assumed that all of the rods develop a cladding breach (i.e., $f_B=1.0$). These values were used for both PWR and BWR fuel rods. As described in NUREG/CR-6487, roughly 0.003% of the fuel mass contained in a rod is released as fines if the cladding on the rod ruptures (i.e., $f_r=3 \times 10^{-5}$).

The calculation for normal transport conditions of an MPC-68F containing four (4) DFCs containing fuel debris assumes that for the four DFCs, 100% of the rods of the fuel debris are breached. The remaining 64 assemblies in the MPC-68F were assumed to have a 3% cladding rupture. Therefore, f_B for an MPC-68F containing fuel debris is:

$$\begin{aligned} f_B &= (0.03) \frac{64}{68} + (1.0) \frac{4}{68} \\ f_B &= 0.087 \end{aligned} \quad (4-3)$$

The activity concentration inside the containment vessel due to fines being released from cladding breaches is given by:

$$C_{\text{fines}} = \frac{f_f I_{\text{fines}} N_A f_B}{V} \quad (4-4)$$

where:

- C_{fines} is the activity concentration inside the containment vessel as a result of fines released from cladding breaches [Ci/cm³],
 f_f is the fraction of a fuel rod's mass released as fines as a result of a cladding breach ($f_f=3 \times 10^{-5}$),
 I_{fines} is the total activity inventory [Ci/assy],
 N_A is the number of assemblies,
 f_B is the fraction of rods that develop cladding breaches, and
 V is the free volume inside the containment vessel [cm³].

C. Source Activity from Gases due to Cladding Breaches

If a cladding failure occurs in a fuel rod, a large fraction of the gap fission gases will be introduced into the free volume of the system. Tritium and Krypton-85 are typically the major sources of radioactivity among the gases present [4.0.3]. NUREG/CR-6487 suggests that a bounding value of 30% of the fission product gases escape from a fuel rod as a result of a cladding breach (i.e., $f_g=0.3$).

The activity concentration due to the release of gases from a cladding breach is given by:

$$C_{\text{gases}} = \frac{f_g I_{\text{gases}} N_A f_B}{V} \quad (4-5)$$

where:

- C_{gases} is the releasable activity concentration inside the containment vessel due to gases released from cladding breaches [Ci/cm³],
 f_g is the fraction of gas that would escape from a fuel rod that developed a cladding breach,
 I_{gases} is the gas activity inventory [³H, ¹²⁹I, ⁸⁵Kr] [Ci/assy],
 N_A is the number of assemblies,
 f_B is the fraction of rods that develop cladding breaches, and
 V is the free volume inside the containment vessel [cm³].

D. Source Activity from Volatiles due to Cladding Breaches

Volatiles such as cesium, strontium, and ruthenium, can also be released from a fuel rod as a result of a cladding breach. NUREG/CR-6487 estimates that 2×10^{-4} is a conservative bounding value for the fraction of the volatiles released from a fuel rod (i.e., $f_v=2 \times 10^{-4}$).

The activity concentration due to the release of volatiles is given by:

$$C_{\text{vol}} = \frac{f_v I_{\text{vol}} N_A f_B}{V} \quad (4-6)$$

where:

- C_{vol} is the releasable activity concentration inside the containment vessel due to volatiles released from cladding breaches [Ci/cm³],
 f_v is the fraction of volatiles that would escape from a fuel rod that developed a cladding breach,
 I_{vol} is the volatile activity inventory [⁹⁰Sr, ¹³⁷Cs, ¹³⁴Cs, ¹⁰⁶Ru] [Ci/assy],
 N_A is the number of assemblies,
 f_B is the fraction of rods that develop cladding breaches, and
 V is the free volume inside the containment vessel [cm³].

E. Total Source Term for the HI-STAR 100 System

The total source term was determined by combining Equations 4-2, 4-4, 4-5, and 4-6:

$$C_{\text{total}} = C_{\text{crud}} + C_{\text{fines}} + C_{\text{gases}} + C_{\text{vol}} \quad (4-7)$$

where C_{total} has units of Ci/cm³.

Table 4.2.3 presents the total source term determined using the above methodology. Table 4.2.4 summarizes the parameters from NUREG/CR-6487 used in this analysis.

4.2.5.3 Effective A_2 of Individual Contributors (Crud, Fines, Gases, and Volatiles)

The A_2 of the individual contributions (i.e., crud, fines, gases, and volatiles) were determined in accordance with NUREG/CR-6487. As previously described, the majority of the activity due to crud is from Cobalt-60. Therefore, the A_2 value of 10.8 Ci used for crud for both PWR and BWR fuel is the same as that for Cobalt-60 found in 10CFR71, Appendix A.

In accordance with 10CFR71.51(b) the methodology presented in 10CFR71, Appendix A for mixtures of different radionuclides was used to determine the A_2 values for the gases, fines and volatiles.

$$A_2 \text{ for a mixture} = \frac{1}{\sum_{i=1}^I \frac{f(i)}{A_2(i)}} \quad (4-8)$$

Where $f(i)$ is the fraction of activity of nuclide I in the mixture and $A_2(i)$ is the appropriate A_2 value for the nuclide I .

10CFR71.51(b) also states that for Krypton-85, an effective A_2 value equal to $10 A_2$ may be used. Table 4.2.5 summarizes the effective A_2 for all individual contributors.

4.2.5.4 Releasable Activity

The releasable activity is the product of the respective activity concentrations (C_{fines} , C_{gas} , C_{crud} , and C_{vol}) and the respective MPC volume. The releasable activity of fines, volatiles, gases, and crud were determined using this methodology.

$$\text{Releasable Activity [Ci]} = \text{Activity Concentration} \left[\frac{\text{Ci}}{\text{cm}^3} \right] \times \text{Volume [cm}^3] \quad (4-9)$$

4.2.5.5 Effective A_2 for the Total Source Term

Using the releasable activity and the effective A_2 values from the individual contributors (i.e., crud, fines, gases, and volatiles), the effective A_2 for the total source term was calculated for each MPC type, for normal transportation and hypothetical accident conditions. The methodology used to determine the effective A_2 is the same as that used for a mixture, which is provided in Equation 4-8.

The results are summarized in Table 4.2.6. As stated in 4.2.5.3, the effective A_2 used for Krypton-85 is $10 A_2$ (2700 Ci).

4.2.5.6 Allowable Radionuclide Release Rates

The containment criterion for the HI-STAR 100 System under normal conditions of transport is given in 10CFR71.51(a)(1). This criterion requires that a package have a radioactive release rate less than $A_2 \times 10^{-6}$ in one hour, where A_2 is the effective A_2 for the total source term in the packaging determined in 4.2.5.5. Additionally, 10CFR71.51(b)(2) specifies that for hypothetical accident conditions, the quantity that may be released in one week is A_2 (effective A_2 for the total source term determined in 4.2.5.5).

NUREG/CR-6487 and ANSIN14.5 provides the following equations for the allowable release rates.

Release rate for normal conditions of transport:

$$R_N = L_N C_N \leq A_2 \times 2.78 \times 10^{-10} / \text{second} \quad (4-10)$$

where:

- R_N is the release rate for normal transport [Ci/s]
- L_N is the volumetric gas leakage rate [cm^3/s]
- C_N is the total source term activity concentration [Ci/cm^3]
- A_2 is the appropriate effective A_2 value [Ci].

Release rate for hypothetical accident conditions:

$$R_A = L_A C_A \leq A_2 \times 1.65 \times 10^{-6} / \text{second} \quad (4-11)$$

where:

- R_A is the release rate for hypothetical accident conditions [Ci/s]
- L_A is the volumetric gas leakage rate [cm^3/s]
- C_A is the total source term activity concentration [Ci/cm^3]
- A_2 is the appropriate effective A_2 value [Ci].

Equations 4-10 and 4-11 were used to determine the allowable radionuclide release rates for each MPC type and transport condition. The release rates are summarized in Table 4.2.7.

4.2.5.7 Allowable Leakage Rates

The allowable leakage rates at operating conditions were determined by dividing the allowable release rates by the appropriate source term activity concentration (modifying Equations 4-10 and 4-11).

$$L_N = \frac{R_N}{C_N} \quad \text{or} \quad L_A = \frac{R_A}{C_A} \quad (4-12)$$

where,

- L_N or L_A is the allowable leakage rate at the upstream pressure for normal (N) or accident (A) conditions [cm^3/s],
 R_N or R_A is the allowable release rate for normal (N) or accident (A) conditions [Ci/s], and
 C_N or C_A is the allowable release rate for normal (N) or accident (A) conditions [Ci/cm^3].

The allowable leakage rates determined using Equation 4-12 are the allowable leakage rates at the upstream pressure. Table 4.2.9 summarizes the allowable leakage rates at the upstream pressures. The most limiting allowable leakage rate presented in Table 4.2.9 ($1.93 \times 10^{-5} \text{ cm}^3/\text{s}$ under normal conditions of transport) was conservatively selected and used to determine the leakage rate acceptance criterion at average pressure using the ratio presented in Equation 4-13.

$$L_{@ P_a} = L_{@ P_u} \frac{P_u}{P_a} \quad (4-13)$$

where:

- $L_{@ P_a}$ is the allowable leakage rate at the average pressure [cm^3/s]
 $L_{@ P_u}$ is the allowable leakage rate at the upstream pressure [cm^3/s]
 P_u is the upstream pressure [ATM],
 P_a is the average pressure; $P_a = (P_u + P_d)/2$ [ATM], and
 P_d is the downstream pressure [ATM].

Substituting $1.93 \times 10^{-5} \text{ cm}^3/\text{s}$ for $L_{@ P_u}$, 7.8 ATM (the upstream pressure reported in Table 4.2.12) for P_u , and 4.4 ATM ($(P_u + P_d)/2$ where P_u and P_d are presented in Table 4.2.12) the allowable leakage rate at the average pressure is determined. The corresponding allowable leakage rate at the average pressure was $3.41 \times 10^{-5} \text{ cm}^3/\text{s}$.

4.2.5.8 Leakage Rate Acceptance Criteria

The leakage rate discussed thus far was determined at operating conditions (see normal conditions in Table 4.2.12). The following provides details of the methodology used to convert the allowable leakage rate ($3.41 \times 10^{-5} \text{ cm}^3/\text{s}$) to a leakage rate acceptance criterion at test conditions.

For conservatism, unchoked flow correlations were used as the unchoked flow correlations better approximate the true measured flow rate for the leakage rates associated with transportation packages. Using the equations for molecular and continuum flow provided in NUREG/CR-6487, the corresponding leak hole diameter was calculated by solving Equation 4-14 for D , the leak hole diameter. The capillary length required for Equation 4-14 for the primary containment was conservatively chosen as the closure plate inner seal seating width which is 0.25 cm; for the

secondary containment (MPC-68F), the capillary length was conservatively chosen to be the MPC lid closure weld thickness which is 1.25 inches thick (3.175 cm).

$$L_{@P_a} = \left[\frac{2.49 \times 10^6 D^4}{a u} + \frac{3.81 \times 10^3 D^3 \sqrt{\frac{T}{M}}}{a P_a} \right] [P_u - P_d] \quad (4-14)$$

where:

- $L_{@P_a}$ is the allowable leakage rate at the average pressure for normal and accident conditions [cm^3/s],
- a is the capillary length [cm],
- T is the temperature for normal and accident conditions [K],
- M is the gas molecular weight [g/mole] = 4.0 from ANSI N14.5, Table B1 [4.0.2],
- u is the fluid viscosity for helium [cP] from Rosenhow and Hartnett [4.2.3]
- P_u is the upstream pressure [ATM],
- D leak hole diameter [cm],
- P_d is the downstream pressure for normal and accident conditions [ATM], and
- P_a is the average pressure; $P_a = (P_u + P_d)/2$ for normal and accident conditions [ATM].

The leak hole diameter was determined by solving Equation 4-14 for 'D' where $L_{@P_a}$ is equal to $3.41 \times 10^{-5} \text{ cm}^3/\text{s}$ and using the parameters for normal conditions of transport presented in Table 4.2.12. The corresponding leak hole diameter was determined to be $3.29 \times 10^{-4} \text{ cm}$.

Using this leak hole diameter ($3.29 \times 10^{-4} \text{ cm}$), and the temperature and pressures for test conditions provided in Table 4.1.12, Equation 4-14 was solved for the leakage rate acceptance criterion ($8.20 \times 10^{-6} \text{ atm cm}^3/\text{s}$, helium) at test conditions. For additional conservatism to ensure compliance with 10CFR71.51, this leakage rate acceptance criterion ($8.20 \times 10^{-6} \text{ atm cm}^3/\text{s}$, helium) was then conservatively reduced and is presented in Table 4.1.1.

Table 4.2.12 provides additional parameters used in the analysis.

4.2.5.9 10CFR71.63(b) Plutonium Leakage Verification

The HI-STAR 100 System configured to transport fuel debris must meet the criteria of 10CFR71.63(b) for plutonium shipments. This criteria specifies that for normal conditions of transport, the separate inner container must not release plutonium as demonstrated to a sensitivity of $A_2 \times 10^{-6}$ in one hour, where A_2 is the effective A_2 for the plutonium inventory in the damaged fuel (up to four DFCs containing specified fuel debris). Additionally, 10CFR71.63(b) specifies that for hypothetical accident conditions, the separate inner container must restrict the loss of plutonium

to not more than A_2 in one week (effective A_2 for the plutonium inventory determined using the methodology described in Section 4.2.5.3).

To demonstrate compliance with this requirement, the leakage rate acceptance criterion was determined following the basic methodology described above. To determine this leakage rate, only the plutonium inventory for the GE 6x6 MOX fuel assembly was used as this inventory bounds the standard GE 6x6 fuel assembly Plutonium inventory. Table 4.2.11 contains the plutonium inventory for the MOX fuel used in this evaluation.

As discussed in 4.2.5.2, Equation 4-3 presents the methodology to determine f_B for an MPC-68F containing fuel debris. This f_B was applied in determining the source activity due to Plutonium. The calculation for normal transport conditions of an MPC-68F containing four (4) DFCs containing fuel debris assumes that for the four DFCs, 100% of the rods of the fuel debris are breached. The remaining 64 assemblies in the MPC-68F were assumed to have a 3% cladding rupture. Therefore, f_B for an MPC-68F containing fuel debris under normal conditions of transport is 0.087. The source activity due to Plutonium was determined by conservatively assuming that all of the rods develop cladding breaches during hypothetical accident conditions (i.e., $f_B=1.0$). The assumption was also made that roughly 0.003% of the plutonium is released from a fuel rod (i.e., $f_{Pu}=3 \times 10^{-5}$). Therefore, the activity concentration inside the containment vessel due to plutonium is given by:

$$C_{Pu} = \frac{f_{Pu} I_{Pu} N_A f_B}{V} \quad (4-15)$$

where:

- C_{Pu} is the activity concentration inside the containment vessel from Plutonium [Ci/cm³],
- f_{Pu} is the fraction of a fuel rod's mass released as Plutonium ($f_r = 3 \times 10^{-5}$),
- I_{Pu} is the total Plutonium inventory of one GE 6x6 MOX assembly [Ci/assy],
- N_A is the number of GE 6x6 MOX assemblies (68),
- f_B is the fraction of rods that develop cladding breaches ($f_B=0.087$ for normal conditions of transport and $f_B=1.0$ for accident conditions), and
- V is the free volume inside the containment vessel [cm³] from Table 4.2.1.

The methodology described in 4.2.5.3 for mixtures was used to calculate the effective A_2 for Plutonium (0.0297 Ci). The methodology in 4.2.5.4 was used to determine the releasable activity. The allowable radionuclide release rates were determined using the methodology presented in 4.2.5.6 and are summarized in Table 4.2.13. The allowable leakage rates at the upstream pressure were determined as discussed in 4.2.5.7 (using Equation 4-12). The allowable leakage rates are presented in Table 4.2.14. As in 4.2.5.7, the most limiting allowable leakage rate presented in Table 4.2.14 (3.77×10^{-5} cm³/s under normal conditions of transport) was conservatively selected and used

to determine the allowable leakage rate at average pressure using the ratio presented in Equation 4-13. The corresponding allowable leakage rate at average pressure was $6.68 \times 10^{-5} \text{ cm}^3/\text{s}$.

As discussed in 4.2.5.8, the allowable leakage rate at average pressure ($6.68 \times 10^{-5} \text{ cm}^3/\text{s}$) was then converted to a leakage rate acceptance criterion at test conditions using the equations for molecular and continuum flow provided in NUREG/CR-6487 (Equation 4-14). The capillary length required for Equation 4-14 for the secondary containment (MPC-68F) was conservatively chosen to be the MPC lid closure weld thickness which is assumed to be 1.25 inches thick (3.175 cm). Equation 4-14 was solved for D, the leak hole diameter ($D=7.73 \times 10^{-4} \text{ cm}$) and then using this leak hole diameter, and the temperature and pressures for test conditions (Table 4.1.12), Equation 4-14 was solved for the leakage rate acceptance criterion at test conditions ($1.88 \times 10^{-5} \text{ std cm}^3/\text{s}$, helium). For additional conservatism to ensure compliance with 10CFR71.63(b), this leakage rate acceptance criterion ($1.88 \times 10^{-5} \text{ std cm}^3/\text{s}$, helium) was conservatively reduced and is presented in Table 4.1.1.

4.2.5.10 Leak Test Sensitivity

The sensitivity for the overpack leakage test procedures is equal to one-half of the allowable leakage rate. The HI-STAR 100 containment packaging tests in Chapter 8 incorporate the appropriate leakage test procedure sensitivity. The leakage rates for the HI-STAR 100 containment packaging with its corresponding sensitivity are presented in Table 4.1.1.

Table 4.2.1

FREE GAS VOLUME OF THE PRIMARY
AND SECONDARY CONTAINMENT

MPC Type	Primary Containment Volume (overpack) (cm ³)	Secondary Containment Volume (MPC-68F) (cm ³)
MPC-24	6.69 x 10 ⁶	N/A
MPC-68	6.15 x 10 ⁶	N/A
MPC-68F	6.15 x 10 ⁶	5.99 x 10 ⁶

Table 4.2.5

INDIVIDUAL CONTRIBUTOR EFFECTIVE A₂
FOR GASES, CRUD, FINES, AND VOLATILES

MPC Type	A ₂ (Ci)
Gases	
MPC-24	2490
MPC-68	2490
MPC-68F	2440
Crud	
MPC-24	10.8
MPC-68	10.8
MPC-68F	10.8
Fines	
MPC-24	0.144
MPC-68	0.135
MPC-68F	0.070
Volatiles	
MPC-24	5.71
MPC-68	5.73
MPC-68F	5.43

Table 4.2.6

TOTAL SOURCE TERM EFFECTIVE A_2 FOR
NORMAL AND HYPOTHETICAL
ACCIDENT CONDITIONS

Normal Transport Conditions	
	Effective A_2 (Ci)
MPC-24	29.2
MPC-68	18.2
MPC-68F	14.4
Accident Conditions	
MPC-24	33.2
MPC-68	27.3
MPC-68F	14.9

Table 4.2.7

RADIONUCLIDE RELEASE RATES

	Effective A ₂ (Ci)	Allowable Release Rate (R _N or R _A) (Ci/s)
Normal Transport Conditions		
MPC-24	28.6	8.12E-09
MPC-68	17.9	5.06E-09
MPC-68F Primary Containment	14.5	4.02E-09
Accident Conditions		
MPC-24	32.5	5.47E-05
MPC-68	26.8	4.51E-05
MPC-68F Primary Containment	14.9	2.46E-05

Table 4.2.8

Table Deleted

Table 4.2.9

ALLOWABLE LEAKAGE RATES AT UPSTREAM PRESSURE

	C_{total} (Ci/cm ³)	Allowable Leakage Rate at P_u L_N or L_A (cm ³ /s)
Normal Transport Conditions		
MPC-24	1.43E-04	5.67E-05
MPC-68	2.63E-04	1.93E-05
MPC-68F Primary Containment	9.56E-05	4.20E-05
Accident Conditions		
MPC-24	4.46E-03	1.23E-02
MPC-68	5.88E-03	7.67E-03
MPC-68F Primary Containment	1.00E-03	2.45E-02

Table 4.2.10

Table Deleted

Table 4.2.11

GE 6X6 MOX FUEL
 PLUTONIUM INVENTORY
 (Ci/assembly)

Nuclide	Ci/Assy
Pu-236	4.92E-04
Pu-237	0.0
Pu-238	1.1E+03
Pu-239	3.29E+01
Pu-240	7.83E+01
Pu-241	6.15E+03
Pu-242	3.44E-01
Pu-244	0.0
Total	7.37E+03

Table 4.2.12

PARAMETERS FOR NORMAL, HYPOTHETICAL ACCIDENT
AND STANDARD CONDITIONS

Parameter	Normal (helium)	Hypothetical Accident (helium)	Standard (Test Conditions, helium)
P_u	114.7 psia (7.8 ATM)	139.7 psia (9.5 ATM)	Primary: 1.68 ATM
			Secondary: 2.0 ATM
P_d	14.7 psia (1 ATM)	14.7 psia (1 ATM)	14.7 psia (1 ATM)
T	400°C (673 K)	1058°F (843 K)	373 K
M	4 g/mol	4 g/mol	4 g/mol
u	0.0341 cP	0.0397 cP	0.0231 cP
a	Primary: 0.25 cm	Primary: 0.25 cm	Primary: 0.25 cm
	Secondary: 3.175 cm	Secondary: 3.175 cm	Secondary: 3.175 cm

CHAPTER 5: SHIELDING EVALUATION

5.0 INTRODUCTION

The shielding analysis of the HI-STAR 100 System is presented in this chapter. The HI-STAR 100 System is designed to accommodate different MPCs within one standard HI-STAR 100 overpack. The MPCs are designated as MPC-24 (24 PWR fuel assemblies) and MPC-68 (68 BWR fuel assemblies).

In addition to housing intact PWR and BWR fuel assemblies, the HI-STAR 100 System is designed to transport damaged BWR fuel assemblies and BWR fuel debris. Damaged fuel assemblies and fuel debris are defined in Subsection 1.2.3. Both damaged BWR fuel assemblies and BWR fuel debris are required to be loaded into Damaged Fuel Containers (DFCs) prior to being loaded into the MPC. DFCs containing fuel debris must be stored in the MPC-68F. DFCs containing damaged fuel assemblies may be stored in either the MPC-68 or the MPC-68F. Only the fuel assemblies in the Dresden 1 and Humboldt Bay fuel assembly classes identified in Table 1.2.9 are authorized as contents for transport in the HI-STAR 100 system as either damaged fuel or fuel debris.

The MPC-68 and MPC-68F are also capable of transporting Dresden Unit 1 antimony-beryllium neutron sources and the single Thoria rod canister which contains 18 thoria rods that were irradiated in two separate fuel assemblies.

This chapter contains the following information:

- A description of the shielding features of the HI-STAR 100 System.
- A description of the bounding source terms.
- A general description of the shielding analysis methodology.
- A description of the analysis assumptions and results for the HI-STAR 100 System.
- Analyses for each of the HI-STAR 100 Systems content conditions to show that the 10CFR71.47 radiation limits are met during normal conditions of transport and that the 10CFR71.51 dose rate limit is not exceeded following hypothetical accident conditions.
- Analyses which demonstrate that the storage of damaged fuel in the HI-STAR 100 System is bounded by the BWR intact fuel analysis during normal and hypothetical accident conditions.

5.1 DISCUSSION AND RESULTS

The principal sources of radiation in the HI-STAR 100 System are:

- Gamma radiation originating from the following sources
 1. Decay of radioactive fission products
 2. Hardware activation products generated during core operations
 3. Secondary photons from neutron capture in fissile and non-fissile nuclides

- Neutron radiation originating from the following sources
 1. Spontaneous fission
 2. α,n reactions in fuel materials
 3. Secondary neutrons produced by fission from subcritical multiplication
 4. γ,n reactions (this source is negligible)
 5. Dresden Unit 1 antimony-beryllium neutron sources

Shielding from gamma radiation is provided by the steel structure of the MPC and overpack. In order for the neutron shielding to be effective, the neutrons must be thermalized and then absorbed in a material of high neutron cross section. In the HI-STAR 100 System design, a neutron shielding material, Holtite-A, is used to thermalize the neutrons. Boron carbide, dispersed in the neutron shield, utilizes the high neutron absorption cross section of ^{10}B to absorb the thermalized neutrons.

The shielding analyses were performed with MCNP-4A [5.1.1] from Los Alamos National Laboratory. The source terms for the design basis fuels were calculated with the SAS2H and ORIGEN-S sequences from the SCALE 4.3 system [5.1.2, 5.1.3] from Oak Ridge National Laboratory. A detailed description of the MCNP models and the source term calculations are presented in Sections 5.3 and 5.2, respectively.

The design basis intact zircaloy clad fuels used in calculating the dose rates presented in this chapter are the B&W 15x15 (with zircaloy and non-zircaloy incore spacers) and the GE 7x7, for PWR and BWR fuel types, respectively. The design basis intact 6x6, damaged, and mixed oxide (MOX) fuel assemblies are the GE 6x6. Table 1.2.13 specifies the acceptable intact zircaloy clad fuel characteristics for transport. Table 1.2.14 specifies the acceptable damaged and MOX zircaloy clad fuel characteristics for transport.

The design bases intact stainless steel clad fuels are the WE 15x15 and the AC 10x10, for PWR and BWR fuel types, respectively. Table 1.2.19 specifies the acceptable fuel characteristics of stainless steel clad fuel for transport.

Table 1.2.20 specifies, in tabular form, the minimum enrichment, burnup and cooling time combinations for spent nuclear fuel that were analyzed for transport in the MPC-24 and MPC-68. Each combination provides a dose rate equal to or below the maximum values reported in this section. This table represents the fuel assembly acceptance criteria.

Table 1.2.20 was developed in a two stage process. First, the burnup and cooling time combinations that produced assembly decay heat rates equal to the thermal limits specified in Figure 1.2.12 were calculated. Second, the dose rates at the various locations were calculated for these burnup and cooling time combinations and compared to the regulatory limits. In some cases, the burnup, for a specified cooling time, had to be reduced to meet the dose rate limits. Therefore, Table 1.2.20 is based on both the maximum permissible decay heat per assembly and the regulatory dose rate limits. The burnup and cooling time combinations analyzed in this chapter are equivalent to or bound the acceptable burnup and cooling time combinations in Table 1.2.20. The dose rates from the burnup and cooling time combination which provided the highest dose rates at the midplane of the cask for each location (surface and 2 meter - normal condition, and 1 meter - hypothetical accident condition) are reported in this section. As a result, the burnup and cooling time combinations reported in this section may be different between locations. Dose rates for each combination calculated are listed in Section 5.4.

Unless otherwise stated, all dose rates reported in this chapter are average surface dose rates. The effect of radiation peaking due to azimuthal variations in the fuel loading pattern and the steel radial channels is specifically addressed in Subsection 5.4.1.

5.1.1 Normal Operations

The 10CFR71.47 external radiation requirements during normal transport operations for an exclusive use shipment are:

1. 200 mrem/hr (2 mSv/hr) on the external surface of the package.
2. 200 mrem/hr (2 mSv/hr) at any point on the outer surface of the vehicle, including the top and underside of the vehicle; or in the case of a flat-bed style vehicle, at any point on the vertical planes projected from the outer edges of the vehicle, on the upper surface of the load or enclosure, if used, and on the lower external surface of the vehicle.
3. 10 mrem/hr (0.1 mSv/hr) at any point 2 meters (80 in) from the outer lateral surfaces of the vehicle (excluding the top and underside of the vehicle); or in the case of a flat-bed style vehicle, at any point 2 meters (6.6 feet) from the vertical planes projected by the outer edges of the vehicle (excluding the top and underside of the vehicle).
4. 2 mrem/h (0.02 mSv/hr) in any normally occupied space, except that this provision does not apply to private carriers, if exposed personnel under their control wear radiation dosimetry devices in conformance with 10CFR20.1502.

The external surface of the HI-STAR 100 System during normal transportation is defined as the outer surface of the impact limiters and the outer radial surface of the overpack in the region between the impact limiters.

The HI-STAR 100 System will be transported on either a flat-bed rail car, heavy haul vehicle, or a barge. The smallest width of a transport vehicle is equivalent to the width of the impact limiters. Therefore, the vertical planes projected by the outer side edges of the transport vehicle are equivalent to the outer edge of the impact limiters. The minimum length of any transport vehicle will be 12 feet longer than the length of the overpack, with impact limiters attached. The HI-STAR 100 System will be conservatively positioned a minimum of 6 feet from either end of the transport vehicle. Therefore, the vertical planes projected from the outer edge of the ends of the vehicle will be taken as the end of the top impact limiter and 6 feet from the end of the bottom impact limiter.

Figure 5.1.1 shows the HI-STAR 100 System during normal transport conditions. The impact limiters are outlined on the figure and various dose point locations are shown on the surface of the HI-STAR 100 System. The dose values reported at the locations shown on Figure 5.1.1 are averaged over a region that is approximately 1 foot in width. Each of the dose locations on the surface of the HI-STAR 100 System has a corresponding location at 2 meters from the surface of the transport vehicle as defined above.

Tables 5.1.1 through 5.1.3 provide the maximum dose rates on the surface of the system during normal transport conditions for the MPC-24 and MPC-68 with design basis intact zircaloy clad fuel. Tables 5.1.4 through 5.1.6 list the maximum dose rates two meters from the edge of the transport vehicle during normal conditions. Section 5.4 provides a detailed list of dose rates at several cask locations for all burnup and cooling times analyzed.

Subsections 5.2.1 and 5.2.2 list the gamma and neutron sources for the design basis zircaloy clad intact, zircaloy clad damaged and MOX fuel assemblies. Since the source strengths of the damaged and MOX fuel are significantly smaller in all energy groups than the intact design basis fuel source strengths, the damaged and MOX fuel dose rates for normal conditions are bounded by the MPC-68 analysis with design basis intact fuel. Therefore, no explicit analysis of the MPC-68 with either damaged or MOX fuel for normal conditions is required to demonstrate that the MPC-68 with damaged fuel or MOX fuel will meet the normal condition regulatory requirements.

Subsection 5.2.6 lists the gamma and neutron sources from the Dresden Unit 1 Thoria rod canister and demonstrates that the Thoria rod canister is bounded by the design basis 6x6 intact fuel.

Subsection 5.4.5 demonstrates that the Dresden Unit 1 fuel assemblies containing antimony-beryllium neutron sources are bounded by the shielding analysis presented in this section.

Subsection 5.2.3 lists the gamma and neutron sources for the design basis intact stainless steel clad fuels. The dose rates from these fuels are provided in Subsection 5.4.4.

Tables 5.1.4 through 5.1.6 show that the dose rate at Dose Location #5 (the top of the HI-STAR 100 System, see Figure 5.1.1) at 2 meters from the edge of the transport vehicle is less than 2 mrem/hr. It is, therefore, recommended that the HI-STAR 100 System be positioned such that the top impact limiter is facing the normally occupied space. If this is the orientation, radiation dosimetry will not be required as long as the normally occupied space is a minimum of 2 meters from the impact limiter on the top of the HI-STAR 100 System. If a different orientation is chosen for the HI-STAR 100 System, the dose rate in the normally occupied space will have to be evaluated against the dose requirement for the normally occupied space to determine if radiation dosimetry is required.

The analyses summarized in this section demonstrate the HI-STAR 100 System's compliance with the 10CFR71.47 limits.

5.1.2 Hypothetical Accident Conditions

The 10CFR71.51 external radiation dose limit for design basis accidents is:

- The external radiation dose rate shall not exceed 1 rem/hr (10 mSv/hr) at 1 m (40 in.) from the external surface of the package.

The hypothetical accident conditions of transport have two bounding consequences which affect the shielding materials. They are the damage to the neutron shield as a result of the design basis fire and damage of the impact limiters as a result of the 30 foot drop. In a conservative fashion, the dose analysis assumes that as a result of the fire, the neutron shield is completely destroyed and replaced by a void. Additionally, the impact limiters are assumed to have been lost. These are highly conservative assumptions since some portion of the neutron shield would be expected to remain after the fire as the neutron shield material is fire retardant, and the impact limiters have been shown by 1/4-scale testing to remain attached following impact (see Appendix 2.H).

Throughout the hypothetical accident condition the axial location of the fuel will remain fixed within the MPC because of the fuel spacers or by the MPC lid and baseplate if spacers are not used. Chapter 2 provides an analysis to show that the fuel spacers do not fail under all normal and hypothetical accident conditions. Chapter 2 also shows that the inner shell, intermediate shell, radial channels, and outer enclosure shell of the overpack remain unaltered throughout the hypothetical accident conditions. Localized damage of the overpack outer enclosure shell could be experienced during the pin puncture. However, the localized deformations will have only a negligible impact on the dose rate at 1 meter from the surface.

Figure 5.1.2 shows the HI-STAR 100 System after the postulated accident. The various dose

point locations at 1 meter from the HI-STAR 100 System are shown on the figure. Tables 5.1.8 and 5.1.9 provide the maximum dose rates at 1 meter for the accident conditions.

The consequences of the hypothetical accident conditions for the MPC-68F storing either damaged or MOX (which can also be considered damaged) fuel differ slightly from those with intact fuel. For this accident condition, it is conservatively assumed that during a drop accident the damaged fuel collapses and the pellets rest in the bottom of the damaged fuel container. The analysis presented in Subsections 5.4.2 and 5.4.3 demonstrate that the damaged fuel in the post-accident condition has lower source terms (both gamma and neutron) per inch than the intact BWR design basis fuel. Therefore, the damaged fuel post-accident dose rates are bounded by the BWR intact fuel post-accident dose rates.

Analyses summarized in this section demonstrate the HI-STAR 100 System's compliance with the 10CFR71.51 radiation dose limit.

Table 5.1.1

DOSE RATES ON THE SURFACE OF THE HI-STAR 100 SYSTEM FOR NORMAL CONDITIONS
 MPC-24 WITH DESIGN BASIS ZIRCALOY CLAD FUEL WITH ZIRCALOY INCORE SPACERS
 AT WORST CASE BURNUP AND COOLING TIME
 44,500 MWD/MTU AND 15-YEAR COOLING

Dose Point [†] Location	Fuel Gammas ^{††} (mrem/hr)	Gammas from Incore Spacers (mrem/hr)	⁶⁰ Co Gammas (mrem/hr)	Neutrons (mrem/hr)	Totals (mrem/hr)
1	2.05	0.00	13.78	21.56	37.39
2	24.91	0.00	0.01	23.32	48.24
3	1.31	0.00	33.24	132.88	167.42
4	0.75	0.00	10.50	21.78	33.03
5	0.50	0.00	0.02	4.06	4.57
6	4.51	0.00	51.43	31.92	87.86
10CFR71.47 Limit					200.00

[†] Refer to Figure 5.1.1.

^{††} Gammas generated by neutron capture are included with fuel gammas.

this chapter utilizing inconel grid spacers. The BWR assembly grid spacers are zircaloy, however, some assembly designs have inconel springs in conjunction with the grid spacers. The gamma source for the BWR fuel assembly includes the activation of these springs associated with the grid spacers.

The non-fuel data listed in Table 5.2.1 was taken from References [5.2.3], [5.2.4], and [5.2.5]. The BWR masses are for an 8x8 fuel assembly. These masses are also appropriate for the 7x7 assembly since the masses of the non-fuel hardware from a 7x7 and an 8x8 are approximately the same. The masses listed are those of the steel components. The zircaloy in these regions was not included because zircaloy does not produce significant activation. These masses are larger than most other fuel assemblies from other manufacturers. This, in combination with the conservative ^{59}Co impurity level, results in a conservative estimate of the ^{60}Co activity.

The masses in Table 5.2.1 were used to calculate a ^{59}Co impurity level in the fuel material. The grams of impurity were then used in ORIGEN-S to calculate a ^{60}Co activity level for the desired burnup and decay time. The methodology used to determine the activation level was developed from Reference [5.2.2] and is described here.

1. The activity of the ^{60}Co is calculated using ORIGEN-S. The flux used in the calculation was the in-core fuel region flux at full power.
2. The activity calculated in Step 1 for the region of interest was modified by the appropriate scaling factors listed in Table 5.2.7. These scaling factors were taken from Reference [5.2.2].

Tables 5.2.8 through 5.2.10 provide the ^{60}Co activity utilized in the shielding calculations in the non-fuel regions of the assemblies for the MPC-24 and MPC-68. The design basis damaged and MOX fuel assemblies are conservatively assumed to have the same ^{60}Co source strength as the BWR intact design basis fuel. This is a conservative assumption as the design basis damaged fuel and MOX fuel are limited to a significantly lower burnup and longer cooling time than the intact design basis zircaloy clad fuel.

In addition to the two sources already mentioned, a third source arises from (n,γ) reactions in the material of the MPC and the overpack. This source of photons is properly accounted for in MCNP when a neutron calculation is performed in a coupled neutron-gamma mode.

5.2.2 Neutron Source

It is well known that the neutron source strength increases as enrichment decreases, for a constant burnup and decay time. This is due to the increase in Pu content in the fuel which increases the inventory of other transuranium nuclides such as Cm. The gamma source also varies with enrichment, although only slightly. Because of this effect and in order to obtain conservative source terms, low initial fuel enrichments were chosen for the BWR and PWR design basis fuel

assemblies as a function of burnup and cooling time. Conservatively, the minimum enrichments used to develop the source terms and dose rates presented in this chapter are specified in Table 1.2.20 as fuel assembly acceptance criteria. The minimum enrichments are also listed in Table 5.2.23 for convenience.

The neutron source calculated for the design basis intact fuel assemblies for the MPC-24 and MPC-68 and the design basis damaged fuel are listed in Tables 5.2.11 through 5.2.14 in neutrons/s. Table 5.2.17 provides the neutron source in neutrons/sec for the design basis MOX fuel assembly. ^{244}Cm accounts for approximately 96% of the total number of neutrons produced, with slightly over 2% originating from (α, n) reactions within the UO_2 fuel. The remaining 2% derive from spontaneous fission in various Pu and Cm radionuclides. In addition, any neutrons generated from subcritical multiplication, $(n, 2n)$ or similar reactions are properly accounted for in the MCNP calculation.

5.2.3 Stainless Steel Clad Fuel Source

Table 5.2.18 lists the characteristics of the design basis stainless steel clad fuel. The fuel characteristics listed in this table are the input parameters that were used in the shielding calculations described in this chapter. The active fuel length listed in the table is actually longer than the true active fuel length of 122 inches for the W15x15 and 83 inches for the A/C 10x10. Since the true active fuel length is shorter than the design basis zircaloy clad active fuel length, it would be incorrect to calculate source terms for the stainless steel fuel using the actual fuel length and compare them directly to the source terms from the zircaloy clad fuel with a longer active fuel length.

In order to eliminate the potential confusion when comparing source terms, the stainless steel clad fuel source terms were calculated with the same active fuel length as the design basis zircaloy clad fuel. Reference [5.2.3] indicates that the Cobalt-59 impurity level in steel is 800 ppm or 0.8 gm/kg and in inconel is approximately 4700 ppm or 4.7 gm/kg. In the early to mid 1980s, the fuel vendors reduced the Cobalt-59 impurity level in both inconel and steel to less than 500 ppm or 0.5 gm/kg. Prior to that, the impurity level in inconel in fuel assemblies was typically less than 1200 ppm or 1.2 gm/kg. Nevertheless, a conservative Cobalt-59 impurity level of 0.8 gm/kg was used for the stainless steel cladding and a highly conservative impurity level of 4.7 gm/kg was used for the inconel incore spacers. It is assumed that the end fitting masses of the stainless steel clad fuel are the same as the end fittings masses of the zircaloy clad fuel. Therefore, separate source terms are not provided for the end fittings of the stainless steel fuel.

Tables 5.2.19 through 5.2.22 list the neutron and gamma source strengths for the design basis stainless steel clad fuel. The gamma source strengths include the contribution from the cobalt activation in the incore spacers. Subsection 5.4.4 presents the dose rates around the HI-STAR 100 for the normal and hypothetical accident conditions for the stainless steel fuel. In the calculation of these dose rates the length of the active fuel was conservatively assumed to be 144

inches. In addition, the fuel assembly configuration used in the MCNP calculations was identical to the configuration used for the design basis fuel assemblies as described in Table 5.3.1.

5.2.4 Control Components

Control components are not permitted for transport in the HI-STAR 100 system.

5.2.5 Choice of Design Basis Assembly

The analysis presented in this chapter was performed to bound the fuel assembly classes listed in Tables 1.2.8 and 1.2.9. In order to perform a bounding analysis, a design basis fuel assembly must be chosen. Therefore, a fuel assembly from each fuel class was analyzed and a comparison of the neutrons/sec, photons/sec, and thermal power (watts) was performed. The fuel assembly which produced the highest source for a specified burnup, cooling time, and enrichment was chosen as the design basis fuel assembly. A separate design basis assembly was chosen for the MPC-24 and the MPC-68.

5.2.5.1 PWR Design Basis Assembly

Table 1.2.8 lists the PWR fuel assembly classes that were evaluated to determine the design basis PWR fuel assembly. Within each class, the fuel assembly with the highest UO_2 mass was analyzed. Since the variations of fuel assemblies within a class are very minor (pellet diameter, clad thickness, etc.), it is conservative to choose the assembly with the highest UO_2 mass. For a given class of assemblies, the one with the highest UO_2 mass will produce the highest radiation source because, for a given burnup (MWD/MTU) and enrichment, the highest UO_2 mass will have produced the most energy and therefore the most fission products.

Table 5.2.24 presents the characteristics of the fuel assemblies analyzed to determine the design basis zircaloy clad PWR fuel assembly. The fuel assembly listed for each class is the assembly with the highest UO_2 mass. The St. Lucie and Ft. Calhoun classes are not present in Table 5.2.24. These assemblies are shorter versions of the CE 16x16 and CE 14x14 assembly classes, respectively. Therefore, these assemblies are bounded by the CE 16x16 and CE 14x14 classes and were not explicitly analyzed. Since the Haddam Neck and San Onofre 1 classes are stainless steel clad fuel, these classes were analyzed separately and are discussed below. All fuel assemblies in Table 5.2.24 were analyzed at the same burnup and cooling time. The results of the comparison are provided in Table 5.2.26. These results indicate that the B&W 15x15 fuel assembly has the highest radiation source term of the zircaloy clad fuel assembly classes considered in Table 1.2.8. This fuel assembly also has the highest UO_2 mass (see Table 5.2.24) which confirms that, for a given initial enrichment, burnup, and cooling time, the assembly with the highest UO_2 mass produces the highest radiation source term.

The Haddam Neck and San Onofre 1 classes are shorter stainless steel clad versions of the WE 15x15 and WE 14x14 classes, respectively. Since these assemblies have stainless steel clad, they were analyzed separately as discussed in Subsection 5.2.3. Based on the results in Table 5.2.26, which show that the WE 15x15 assembly class has a higher source term than the WE 14x14 assembly class, the Haddam Neck, WE 15x15, fuel assembly was analyzed as the bounding PWR stainless steel clad fuel assembly.

5.2.5.2 BWR Design Basis Assembly

Table 1.2.9 lists the BWR fuel assembly classes that were evaluated to determine the design basis BWR fuel assembly. Since there are minor differences between the array types in the GE BWR/2-3 and GE BWR/4-6 assembly classes, these assembly classes were not considered individually but rather as a single class. Within that class, the array types, 7x7, 8x8, 9x9, and 10x10 were analyzed to determine the bounding BWR fuel assembly. Since the Humboldt Bay 7x7 and Dresden 1 8x8 are smaller versions of the 7x7 and 8x8 assemblies they are bounded by the 7x7 and 8x8 assemblies in the GE BWR/2-3 and GE BWR/4-6 classes. Within each array type, the fuel assembly with the highest UO₂ mass was analyzed. Since the variations of fuel assemblies within an array type are very minor, it is conservative to choose the assembly with the highest UO₂ mass. For a given array type of assemblies, the one with the highest UO₂ mass will produce the highest radiation source because, for a given burnup (MWD/MTU) and enrichment, it will have produced the most energy and therefore the most fission products. The Humboldt Bay 6x6, Dresden 1 6x6, and LaCrosse assembly classes were not considered in the determination of the bounding fuel assembly. However, these assemblies were analyzed explicitly as discussed below.

Table 5.2.25 presents the characteristics of the fuel assemblies analyzed to determine the design basis zircaloy clad BWR fuel assembly. The fuel assembly listed for each array type is the assembly that has the highest UO₂ mass. All fuel assemblies in Table 5.2.25 were analyzed at the same burnup and cooling time. The results of the comparison are provided in Table 5.2.27. These results indicate that the 7x7 fuel assembly has the highest radiation source term of the zircaloy clad fuel assembly classes considered in Table 1.2.9. This fuel assembly also has the highest UO₂ mass which confirms that, for a given initial enrichment, burnup, and cooling time, the assembly with the highest UO₂ mass produces the highest radiation source term. According to Reference [5.2.6], the last discharge of a 7x7 assembly was in 1985 and the maximum average burnup for a 7x7 during their operation was 29,000 MWD/MTU. This clearly indicates that the existing 7x7 assemblies have an average burnup and minimum cooling time that is well within the burnup and cooling time limits in Table 1.2.20. Therefore, the 7x7 assembly has never reached the burnup level analyzed in this chapter. However, in the interest of conservatism the 7x7 was chosen as the bounding fuel assembly array type.

Since the LaCrosse fuel assembly type is a stainless steel clad 10x10 assembly it was analyzed separately. The maximum burnup and minimum cooling times for this assembly are limited to

22,500 MWD/MTU and 15-year cooling as specified in Table 1.2.19. This assembly type is discussed further in Subsection 5.2.3.

The Humboldt Bay 6x6 and Dresden 1 6x6 fuel are older and shorter than the other array types analyzed and therefore are considered separately. The Dresden 1 6x6 was chosen as the design basis fuel assembly for the Humboldt Bay 6x6 and Dresden 1 6x6 fuel assembly classes because it has the higher UO₂ mass. Dresden 1 also contains a few 6x6 MOX fuel assemblies which were explicitly analyzed as well.

Reference [5.2.6] indicates that the Dresden 1 6x6 fuel assembly has a higher UO₂ mass than the Dresden 1 8x8 or the Humboldt Bay fuel (6x6 and 7x7). Therefore, the Dresden 1 6x6 fuel assembly was also chosen as the bounding assembly for damaged fuel and fuel debris for the Humboldt Bay and Dresden 1 fuel assembly classes.

Since the design basis damaged fuel assembly and the design basis intact 6x6 fuel assembly are identical, the analysis presented in Subsection 5.4.2 for the damaged fuel assembly also demonstrates the acceptability of transporting intact 6x6 fuel assemblies from the Dresden 1 and Humboldt Bay fuel assembly classes.

5.2.5.3 Decay Heat Loads

The decay heat values per assembly were calculated using the methodology described in Section 5.2. The design basis fuel assemblies, as described in Table 5.2.1, were used in the calculation of the burnup versus cooling time limits. As demonstrated in Tables 5.2.26 and 5.2.27, the design basis fuel assembly produces a higher decay heat value than the other assembly types considered. This is due to the higher heavy metal mass in the design basis fuel assemblies. Conservatively, Tables 1.2.10 and 1.2.11 limit the heavy metal mass of the design basis fuel assembly classes to a value less than the design basis value utilized in this chapter. This provides additional assurance that the decay heat values are bounding values.

As further demonstration that the decay heat values (calculated using the design basis fuel assemblies) are conservative, a comparison between these calculated decay heats and the decay heats reported in Reference [5.2.7] are presented in Table 5.2.28. This comparison is made for a burnup of 30,000 MWD/MTU and a cooling time of 5 years. The burnup was chosen based on the limited burnup data available in Reference [5.2.7].

The heavy metal mass of the non-design basis fuel assembly classes in Tables 1.2.10 and 1.2.11 are limited to the masses used in Tables 5.2.24 and 5.2.25. No margin is applied between the allowable mass and the analyzed mass of heavy metal for the non-design basis fuel assemblies. This is acceptable because additional assurance that the decay heat values for the non-design basis fuel assemblies are bounding values is obtained by using the decay heat values for the design basis fuel assemblies in determining the acceptable loading criteria for all fuel assemblies.

As mentioned above, Table 5.2.28 demonstrates the level of conservatism in applying the decay heat from the design basis fuel assembly to all fuel assemblies.

5.2.6 Thoria Rod Canister

Dresden Unit 1 has a single DFC containing 18 thoria rods which have obtained a relatively low burnup, 16,000 MWD/MTU. These rods were removed from two 8x8 fuel assemblies which contained 9 rods each. The irradiation of thorium produces an isotope which is not commonly found in depleted uranium fuel. Th-232 when irradiated produces U-233. The U-233 can undergo an (n,2n) reaction which produces U-232. The U-232 decays to produce Tl-208 which produces a 2.6 MeV gamma during Beta decay. This results in a significant source in the 2.5-3.0 MeV range which is not commonly present in depleted uranium fuel. Therefore, this single DFC container was analyzed to determine if it was bounded by the current shielding analysis.

A radiation source term was calculated for the 18 thoria rods using SAS2H and ORIGEN-S for a burnup of 16,000 MWD/MTU and a cooling time of 18 years. Table 5.2.29 describes the 8x8 fuel assembly that contains the thoria rods. Table 5.2.30 and 5.2.31 show the gamma and neutron source terms, respectively, that were calculated for the 18 thoria rods in the thoria rod canister. Comparing these source terms to the design basis 6x6 source terms for Dresden Unit 1 fuel in Tables 5.2.6 and 5.2.14 clearly indicates that the design basis source terms bound the thoria rods source terms in all neutron groups and in all gamma groups except the 2.5-3.0 MeV group. As mentioned above, the thoria rods have a significant source in this energy range due to the decay of Tl-208.

Subsection 5.4.6 provides a further discussion of the thoria rod canister and its acceptability for transport in the HI-STAR 100 System.

5.2.7 Fuel Assembly Neutron Sources

Neutron sources are used in reactors during initial startup of reactor cores. There are different types of neutron sources (e.g. californium, americium-beryllium, plutonium-beryllium, antimony-beryllium). These neutron sources are typically inserted into the water rod of a fuel assembly and are usually removable.

Dresden Unit 1 has a few antimony-beryllium neutron sources. These sources have been analyzed in Subsection 5.4.5 to demonstrate that they are acceptable for transport in the HI-STAR 100 System. Currently these are the only neutron source permitted for transport in the HI-STAR 100 System.

Table 5.2.1

DESCRIPTION OF DESIGN BASIS INTACT ZIRCALOY CLAD FUEL

	PWR	BWR
Assembly type/class	B&W 15x15	GE 7x7
Active fuel length (in.)	144	144
No. of fuel rods	208	49
Rod pitch (in.)	0.568	0.738
Cladding material	zircaloy-4	zircaloy-2
Rod diameter (in.)	0.428	0.570
Cladding thickness (in.)	0.0230	0.0355
Pellet diameter (in.)	0.3742	0.488
Pellet material	UO ₂	UO ₂
Pellet density (gm/cc)	10.412 (95% of theoretical)	10.412 (95% of theoretical)
Enrichment (w/o ²³⁵ U)	See Table 1.2.20	See Table 1.2.20
Burnup (MWD/MTU)	See Table 1.2.20	See Table 1.2.20
Cooling Time (years)	See Table 1.2.20	See Table 1.2.20
Specific power (MW/MTU)	40	30
Weight of UO ₂ (kg) [†]	562.029	225.177
Weight of U (kg) [†]	495.485	198.516

Notes:

1. The B&W 15x15 is the design basis assembly for the following fuel assembly classes listed in Table 1.2.8: B&W 15x15, B&W 17x17, CE 14x14, CE 16x16, WE 14x14, WE 15x15, WE 17x17, St. Lucie, and Ft. Calhoun.
2. The GE 7x7 is the design basis assembly for the following fuel assembly classes listed in Table 1.2.9: GE BWR/2-3, GE BWR/4-6, Humboldt Bay 7x7, and Dresden 1 8x8.

[†] Derived from parameters in this table.

Table 5.2.1 (continued)

DESCRIPTION OF DESIGN BASIS INTACT ZIRCALOY CLAD FUEL

	PWR	BWR
No. of Water Rods/Guide Tubes	17	0
Water Rod O.D. (in.)	0.53	N/A
Water Rod Thickness (in.)	0.0160	N/A
Lower End Fitting (kg)	8.16 (steel) 1.3 (inconel)	4.8 (steel)
Gas Plenum Springs (kg)	0.48428 (inconel) 0.23748 (steel)	1.1 (steel)
Gas Plenum Spacer (kg)	0.55572 (inconel) 0.27252 (steel)	N/A
Expansion Springs (kg)	N/A	0.4 (steel)
Upper End Fitting (kg)	9.28 (steel)	2.0 (steel)
Handle (kg)	N/A	0.5 (steel)
Incore Grid Spacers (kg)	4.9 (inconel) [†]	0.33 (inconel springs)

[†] This mass of inconel was used for fuel assemblies with non-zircaloy grid spacers. For fuel assemblies with zircaloy grid spacers the mass was 0.0. However, the mass of the inconel and steel in the other assembly components are identical for assemblies with zircaloy and non-zircaloy incore grid spacers.

Table 5.2.2

DESCRIPTION OF DESIGN BASIS DAMAGED ZIRCALOY CLAD FUEL

	BWR
Fuel type	GE 6x6
Active fuel length (in.)	110
No. of fuel rods	36
Rod pitch (in.)	0.694
Cladding material	zircaloy-2
Rod diameter (in.)	0.5645
Cladding thickness (in.)	0.035
Pellet diameter (in.)	0.494
Pellet material	UO ₂
Pellet density (gm/cc)	10.412 (95% of theoretical)
Enrichment (w/o ²³⁵ U)	1.8
Burnup (MWD/MTU)	30,000
Cooling Time (years)	18
Specific power (MW/MTU)	16.5
Weight of UO ₂ (kg) [†]	129.5
Weight of U (kg) [†]	114.2
Incore spacers (kg inconel)	1.07

Notes:

1. The 6x6 is the design basis damaged fuel assembly for the Humboldt Bay (all array types) and the Dresden 1 (all array types) damaged fuel assembly classes. It is also the design basis fuel assembly for the intact Humboldt Bay 6x6 and Dresden 1 6x6 fuel assembly classes.
2. This design basis damaged fuel assembly is also the design basis fuel assembly for fuel debris.

[†] Derived from parameters in this table.

Table 5.2.3
 CALCULATED MPC-24 PWR FUEL GAMMA SOURCE PER ASSEMBLY FOR DESIGN BASIS ZIRCALOY CLAD
 FUEL WITH NON-ZIRCALOY INCORE SPACERS FOR VARYING BURNUPS AND COOLING TIMES

Lower Energy	Upper Energy	24,500 MWD/MTU 10 Year Cooling		29,500 MWD/MTU 12 Year Cooling		34,500 MWD/MTU 14 Year Cooling	
		(MeV/s)	(Photons/s)	(MeV/s)	(Photons/s)	(MeV/s)	(Photons/s)
0.45	0.7	7.23E+14	1.26E+15	8.03E+14	1.40E+15	8.76E+14	1.52E+15
0.7	1.0	6.84E+13	8.05E+13	5.48E+13	6.45E+13	4.52E+13	5.32E+13
1.0	1.5	2.88E+13	2.30E+13	2.99E+13	2.39E+13	3.10E+13	2.48E+13
1.5	2.0	1.49E+12	8.54E+11	1.59E+12	9.09E+11	1.71E+12	9.77E+11
2.0	2.5	1.02E+11	4.51E+10	2.89E+10	1.29E+10	1.28E+10	5.70E+09
2.5	3.0	6.77E+09	2.46E+09	2.19E+09	7.97E+08	9.67E+08	3.52E+08
Totals		8.22E+14	1.36E+15	8.89E+14	1.49E+15	9.54E+14	1.60E+15
Lower Energy	Upper Energy	37,500 MWD/MTU 15 Year Cooling					
(MeV)	(MeV)	(MeV/s)	(Photons/s)				
0.45	0.7	9.22E+14	1.60E+15				
0.7	1.0	4.17E+13	4.91E+13				
1.0	1.5	3.15E+13	2.52E+13				
1.5	2.0	1.77E+12	1.01E+12				
2.0	2.5	1.07E+10	4.74E+09				
2.5	3.0	7.98E+08	2.90E+08				
Totals		9.97E+14	1.68E+15				

Table 5.2.4

CALCULATED MPC-24 PWR FUEL GAMMA SOURCE PER ASSEMBLY FOR DESIGN BASIS ZIRCALOY CLAD FUEL WITH ZIRCALOY INCORE SPACERS FOR VARYING BURNUPS AND COOLING TIMES

Lower Energy	Upper Energy	24,500 MWD/MTU 7 Year Cooling		29,500 MWD/MTU 8 Year Cooling		34,500 MWD/MTU 10 Year Cooling	
(MeV)	(MeV)	(MeV/s)	(Photons/s)	(MeV/s)	(Photons/s)	(MeV/s)	(Photons/s)
0.45	0.7	8.73E+14	1.52E+15	9.81E+14	1.71E+15	1.02E+15	1.78E+15
0.7	1.0	1.60E+14	1.88E+14	1.56E+14	1.83E+14	1.13E+14	1.33E+14
1.0	1.5	4.59E+13	3.67E+13	5.00E+13	4.00E+13	4.76E+13	3.81E+13
1.5	2.0	2.62E+12	1.50E+12	2.57E+12	1.47E+12	2.39E+12	1.37E+12
2.0	2.5	1.09E+12	4.84E+11	5.28E+11	2.35E+11	1.21E+11	5.37E+10
2.5	3.0	5.14E+10	1.87E+10	2.96E+10	1.08E+10	8.66E+09	3.15E+09
Totals		1.08E+15	1.74E+15	1.19E+15	1.93E+15	1.19E+15	1.95E+15
Lower Energy	Upper Energy	39,500 MWD/MTU 12 Year Cooling		44,500 MWD/MTU 15 Year Cooling			
(MeV)	(MeV)	(MeV/s)	(Photons/s)	(MeV/s)	(Photons/s)		
0.45	0.7	1.07E+15	1.87E+15	1.09E+15	1.90E+15		
0.7	1.0	8.29E+13	9.76E+13	5.27E+13	6.20E+13		
1.0	1.5	4.53E+13	3.62E+13	3.97E+13	3.18E+13		
1.5	2.0	2.37E+12	1.35E+12	2.20E+12	1.26E+12		
2.0	2.5	3.43E+10	1.52E+10	1.22E+10	5.41E+09		
2.5	3.0	2.85E+09	1.04E+09	1.10E+09	4.00E+08		
Totals		1.20E+15	2.00E+15	1.18E+15	1.99E+15		

Table 5.2.5
 CALCULATED MPC-68 BWR FUEL GAMMA SOURCE PER ASSEMBLY FOR DESIGN BASIS ZIRCALOY CLAD
 FUEL FOR VARYING BURNUPS AND COOLING TIMES

Lower Energy	Upper Energy	24,500 MWD/MTU 8 Year Cooling		29,500 MWD/MTU 9 Year Cooling		34,500 MWD/MTU 12 Year Cooling	
		(MeV/s)	(Photons/s)	(MeV/s)	(Photons/s)	(MeV/s)	(Photons/s)
0.45	0.7	3.21E+14	5.57E+14	3.64E+14	6.34E+14	3.72E+14	6.46E+14
0.7	1.0	4.54E+13	5.34E+13	4.46E+13	5.25E+13	2.60E+13	3.06E+13
1.0	1.5	1.46E+13	1.17E+13	1.63E+13	1.30E+13	1.41E+13	1.13E+13
1.5	2.0	7.68E+11	4.39E+11	8.20E+11	4.69E+11	7.45E+11	4.26E+11
2.0	2.5	1.65E+11	7.34E+10	8.09E+10	3.60E+10	1.12E+10	4.96E+09
2.5	3.0	9.32E+09	3.39E+09	5.31E+09	1.93E+09	8.97E+08	3.26E+08
Total		3.82E+14	6.23E+14	4.26E+14	7.00E+14	4.13E+14	6.89E+14
Lower Energy	Upper Energy	39,500 MWD/MTU 15 Year Cooling					
(MeV)	(MeV)	(MeV/s)	(Photons/s)				
0.45	0.7	3.84E+14	6.68E+14				
0.7	1.0	1.68E+13	1.98E+13				
1.0	1.5	1.26E+13	1.01E+13				
1.5	2.0	7.06E+11	4.04E+11				
2.0	2.5	4.20E+09	1.87E+09				
2.5	3.0	3.16E+08	1.15E+08				
Totals		4.14E+14	6.99E+14				

Table 5.2.6

CALCULATED MPC-68 and MPC-68F BWR FUEL GAMMA
SOURCE PER ASSEMBLY FOR DESIGN BASIS
ZIRCALOY CLAD DAMAGED FUEL

Lower Energy	Upper Energy	30,000 MWD/MTU 18 Year Cooling	
(MeV)	(MeV)	(MeV/s)	(Photons/s)
0.45	0.7	1.52e+14	2.65e+14
0.7	1.0	4.07e+12	4.79e+12
1.0	1.5	3.80e+12	3.04e+12
1.5	2.0	2.24e+11	1.28e+11
2.0	2.5	1.26e+9	5.58e+8
2.5	3.0	7.42e+7	2.70e+7
Totals		1.61e+14	2.73e+14

Table 5.2.7

SCALING FACTORS USED IN CALCULATING THE ^{60}Co SOURCE

Region	PWR	BWR
Handle	N/A	0.05
Top end fitting	0.1	0.1
Gas plenum spacer	0.1	N/A
Expansion springs	N/A	0.1
Gas plenum springs	0.2	0.2
Grid spacer spring	N/A	1.0
Bottom end fitting	0.2	0.15

Table 5.2.8

CALCULATED MPC-24 ⁶⁰Co SOURCE PER ASSEMBLY FOR DESIGN BASIS ZIRCALOY CLAD FUEL WITH NON-ZIRCALOY INCORE SPACERS AT VARYING BURNUPS AND COOLING TIMES

Location	24,500 MWD/MTU 10 Year Cooling (curies)	29,500 MWD/MTU 12 Year Cooling (curies)	34,500 MWD/MTU 14 Year Cooling (curies)	37,500 MWD/MTU 15 Year Cooling (curies)
Lower end fitting	83.92	72.00	60.09	54.25
Gas plenum springs	16.33	14.01	11.69	10.56
Gas plenum spacer	9.37	8.04	6.71	6.06
Expansion springs	N/A	N/A	N/A	N/A
Grid spacers	762.29	654.05	545.81	492.84
Upper end fitting	30.72	26.36	21.99	19.86
Handle	N/A	N/A	N/A	N/A

Table 5.2.9

CALCULATED MPC-24 ⁶⁰Co SOURCE PER ASSEMBLY FOR DESIGN BASIS ZIRCALOY CLAD FUEL WITH ZIRCALOY INCORE SPACERS AT VARYING BURNUPS AND COOLING TIMES

Location	24,500 MWD/MTU 7 Year Cooling (curies)	29,500 MWD/MTU 8 Year Cooling (curies)	34,500 MWD/MTU 10 Year Cooling (curies)	39,500 MWD/MTU 12 Year Cooling (curies)	44,500 MWD/MTU 15 Year Cooling (curies)
Lower end fitting	124.48	121.69	101.92	84.17	61.10
Gas plenum springs	24.22	23.68	19.83	16.38	11.89
Gas plenum spacer	13.90	13.58	11.38	9.40	6.82
Expansion springs	N/A	N/A	N/A	N/A	N/A
Grid spacers [†]	N/A	N/A	N/A	N/A	N/A
Upper end fitting	45.56	44.54	37.31	30.81	22.36
Handle	N/A	N/A	N/A	N/A	N/A

[†] These burnup and cooling times represent fuel with zircaloy grid spacers. Therefore, the cobalt activation is negligible.

Table 5.2.10

CALCULATED MPC-68 ⁶⁰CO SOURCE PER ASSEMBLY FOR DESIGN BASIS ZIRCALOY CLAD FUEL
AT VARYING BURNUPS AND COOLING TIMES

Location	24,500 MWD/MTU 8 Year Cooling (curies)	29,500 MWD/MTU 9 Year Cooling (curies)	34,500 MWD/MTU 12 Year Cooling (curies)	39,500 MWD/MTU 15 Year Cooling (curies)
Lower end fitting	34.04	30.55	24.22	17.21
Gas plenum springs	10.40	9.33	7.40	5.26
Gas plenum spacer	N/A	N/A	N/A	N/A
Expansion springs	1.89	1.70	1.35	0.96
Grid spacers	73.32	65.80	52.17	37.08
Upper end fitting	9.45	8.48	6.73	4.78
Handle	1.18	1.06	0.84	0.60

Table 5.2.11

CALCULATED MPC-24 PWR NEUTRON SOURCE PER ASSEMBLY
FOR DESIGN BASIS ZIRCALOY CLAD FUEL WITH NON-ZIRCALOY
INCORE SPACERS FOR VARYING BURNUPS AND COOLING TIMES

Lower Energy (MeV)	Upper Energy (MeV)	24,500 MWD/MTU 10 Year Cooling (Neutrons/s)	29,500 MWD/MTU 12 Year Cooling (Neutrons/s)	34,500 MWD/MTU 14 Year Cooling (Neutrons/s)	37,500 MWD/MTU 15 Year Cooling (Neutrons/s)
1.0e-01	4.0e-01	2.41E+06	3.89E+06	5.79E+06	6.56E+06
4.0e-01	9.0e-01	1.23E+07	1.99E+07	2.96E+07	3.35E+07
9.0e-01	1.4	1.14E+07	1.83E+07	2.72E+07	3.08E+07
1.4	1.85	8.46E+06	1.36E+07	2.01E+07	2.28E+07
1.85	3.0	1.52E+07	2.43E+07	3.60E+07	4.08E+07
3.0	20.0	1.35E+07	2.17E+07	3.23E+07	3.66E+07
6.43	20.0	1.18E+06	1.90E+06	2.83E+06	3.21E+06
TOTALS		6.45E+07	1.04E+08	1.54E+08	1.74E+08

Table 5.2.12

CALCULATED MPC-24 PWR NEUTRON SOURCE PER ASSEMBLY
FOR DESIGN BASIS ZIRCALOY CLAD FUEL WITH ZIRCALOY
INCORE SPACERS FOR VARYING BURNUPS AND COOLING TIMES

Lower Energy (MeV)	Upper Energy (MeV)	24,500 MWD/MTU 7 Year Cooling (Neutrons/s)	29,500 MWD/MTU 8 Year Cooling (Neutrons/s)	34,500 MWD/MTU 10 Year Cooling (Neutrons/s)	39,500 MWD/MTU 12 Year Cooling (Neutrons/s)	44,500 MWD/MTU 15 Year Cooling (Neutrons/s)
1.0e-01	4.0e-01	2.70E+06	4.52E+06	6.72E+06	9.05E+06	1.17E+07
4.0e-01	9.0e-01	1.38E+07	2.31E+07	3.43E+07	4.63E+07	5.99E+07
9.0e-01	1.4	1.27E+07	2.12E+07	3.15E+07	4.24E+07	5.49E+07
1.4	1.85	9.41E+06	1.57E+07	2.33E+07	3.14E+07	4.06E+07
1.85	3.0	1.69E+07	2.80E+07	4.15E+07	5.58E+07	7.21E+07
3.0	20.0	1.51E+07	2.51E+07	3.74E+07	5.03E+07	6.50E+07
6.43	20.0	1.32E+06	2.21E+06	3.29E+06	4.43E+06	5.74E+06
TOTALS		7.18E+07	1.20E+08	1.78E+08	2.40E+08	3.10E+08

Table 5.2.13

CALCULATED MPC-68 BWR NEUTRON SOURCE PER ASSEMBLY
 FOR DESIGN BASIS ZIRCALOY CLAD FUEL
 FOR VARYING BURNUPS AND COOLING TIMES

Lower Energy (MeV)	Upper Energy (MeV)	24,500 MWD/MTU 8 Year Cooling (Neutrons/s)	29,500 MWD/MTU 9 Year Cooling (Neutrons/s)	34,500 MWD/MTU 12 Year Cooling (Neutrons/s)	39,500 MWD/MTU 15 Year Cooling (Neutrons/s)
1.0e-01	4.0e-01	1.08E+06	1.81E+06	2.70E+06	3.48E+06
4.0e-01	9.0e-01	5.52E+06	9.23E+06	1.38E+07	1.78E+07
9.0e-01	1.4	5.08E+06	8.47E+06	1.27E+07	1.63E+07
1.4	1.85	3.77E+06	6.27E+06	9.36E+06	1.20E+07
1.85	3.0	6.75E+06	1.12E+07	1.66E+07	2.14E+07
3.0	6.43	6.04E+06	1.01E+07	1.50E+07	1.93E+07
6.43	20.0	5.29E+05	8.84E+05	1.32E+06	1.70E+06
TOTALS		2.88E+07	4.79E+07	7.15E+07	9.19E+07

Table 5.2.14

**CALCULATED MPC-68 and MPC-68F BWR NEUTRON
SOURCE PER ASSEMBLY FOR DESIGN BASIS
DAMAGED ZIRCALOY CLAD FUEL**

Lower Energy (MeV)	Upper Energy (MeV)	30,000 MWD/MTU 18 Year Cooling (Neutrons/s)
1.0e-01	4.0e-01	1.18e+6
4.0e-01	9.0e-01	6.05e+6
9.0e-01	1.4	5.55e+6
1.4	1.85	4.11e+6
1.85	3.0	7.34e+6
3.0	6.43	6.59e+6
6.43	20.0	5.79e+5
Totals		3.14e+7

Table 5.2.15

DESCRIPTION OF DESIGN BASIS ZIRCALOY CLAD MIXED OXIDE FUEL

	BWR
Fuel type	GE 6x6
Active fuel length (in.)	110
No. of fuel rods	36
Rod pitch (in.)	0.696
Cladding material	zircaloy-2
Rod diameter (in.)	0.5645
Cladding thickness (in.)	0.036
Pellet diameter (in.)	0.482
Pellet material	UO ₂ and PuUO ₂
No. of UO ₂ Rods	27
No. of PuUO ₂ Rods	9
Pellet density (gm/cc)	10.412 (95% of theoretical)
Enrichment (w/o ²³⁵ U) [†]	1.8 (UO ₂ rods) 0.711 (PuUO ₂ rods)
Burnup (MWD/MTU)	30,000
Cooling Time (years)	18
Specific power (MW/MTU)	16.5
Weight of UO ₂ , PuUO ₂ (kg) ^{††}	123.3
Weight of U,Pu (kg) ^{††}	108.7
Incore spacers (kg inconel)	1.07

[†] See Table 5.3.3 for detailed composition of PuUO₂ rods.

^{††} Derived from parameters in this table.

Table 5.2.16

CALCULATED MPC-68 BWR FUEL GAMMA SOURCE PER ASSEMBLY
FOR DESIGN BASIS ZIRCALOY CLAD MIXED OXIDE FUEL

Lower Energy (MeV)	Upper Energy (MeV)	30,000 MWD/MTU 18-Year Cooling	
		(MeV/s)	(Photons/s)
0.45	0.7	1.45e+14	2.52e+14
0.7	1.0	3.95e+12	4.65e+12
1.0	1.5	3.82e+12	3.06e+12
1.5	2.0	2.22e+11	1.27e+11
2.0	2.5	1.11e+9	4.93e+8
2.5	3.0	9.31e+7	3.39e+7
Totals		1.53e+14	2.60e+14

Table 5.2.17

CALCULATED MPC-68 BWR NEUTRON SOURCE PER ASSEMBLY
FOR DESIGN BASIS ZIRCALOY CLAD MIXED OXIDE FUEL

Lower Energy (MeV)	Upper Energy (MeV)	30,000 MWD/MTU 18-Year Cooling (Neutrons/s)
1.0e-01	4.0e-01	1.50e+6
4.0e-01	9.0e-01	7.67e+6
9.0e-01	1.4	7.09e+6
1.4	1.85	5.31e+6
1.85	3.0	9.67e+6
3.0	6.43	8.47e+6
6.43	20.0	7.33e+5
Totals		4.04e+7

Table 5.2.18
DESCRIPTION OF DESIGN BASIS INTACT STAINLESS STEEL CLAD FUEL

	PWR	BWR
Fuel type	WE 15x15	A/C 10x10
Active fuel length (in.)	144	144
No. of fuel rods	204	100
Rod pitch (in.)	0.563	0.565
Cladding material	304 SS	348H SS
Rod diameter (in.)	0.422	0.396
Cladding thickness (in.)	0.0165	0.02
Pellet diameter (in.)	0.3825	0.35
Pellet material	UO ₂	UO ₂
Pellet density (gm/cc)	10.412 (95% of theoretical)	10.412 (95% of theoretical)
Enrichment (w/o ²³⁵ U)	3.1	3.5
Burnup (MWD/MTU)	30,000 @ 19 yr (MPC-24) 40,000 @ 24 yr (MPC-24)	22,500 (MPC-68)
Cooling Time (years)	19 (MPC-24) 24 (MPC-24)	16 (MPC-68)
Specific power (MW/MTU)	37.96	29.17
No. of Water Rods	21	0
Water Rod O.D. (in.)	0.546	N/A
Water Rod Thickness (in.)	0.017	N/A
Incore spacers (kg inconel)	5.1	0.83

Notes:

1. The WE 15x15 is the design basis assembly for the following fuel assembly classes listed in Table 1.2.8: Haddam Neck and San Onofre 1.
2. The A/C 10x10 is the design basis assembly for the following fuel assembly class listed in Table 1.2.9: LaCrosse.

Table 5.2.19

CALCULATED BWR FUEL GAMMA SOURCE PER ASSEMBLY
FOR STAINLESS STEEL CLAD FUEL

Lower Energy (MeV)	Upper Energy (MeV)	22,500 MWD/MTU 16-Year Cooling	
		(MeV/s)	(Photons/s)
0.45	0.7	2.26e+14	3.94e+14
0.7	1.0	6.02e+12	7.08e+12
1.0	1.5	4.04e+13	3.23e+13
1.5	2.0	2.90e+11	1.66e+11
2.0	2.5	2.94e+9	1.31e+9
2.5	3.0	7.77e+7	2.83e+7
Totals		2.73e+14	4.33e+14

Note:

1. These source terms were calculated for a 144 inch active fuel length. The actual active fuel length is 83 inches.
2. The ⁶⁰Co activation from incore spacers is included in the 1.0-1.5 MeV energy group.

Table 5.2.20

**CALCULATED PWR FUEL GAMMA SOURCE PER ASSEMBLY
FOR STAINLESS STEEL CLAD FUEL**

Lower Energy (MeV)	Upper Energy (MeV)	30,000 MWD/MTU 19-Year Cooling		40,000 MWD/MTU 24-Year Cooling	
		(MeV/s)	(Photons/s)	(MeV/s)	(Photons/s)
0.45	0.7	6.81e+14	1.18e+15	7.97e+14	1.39e+15
0.7	1.0	1.83e+13	2.16e+13	1.70e+13	2.01e+13
1.0	1.5	1.13e+14	9.06e+13	8.24e+13	6.60e+13
1.5	2.0	1.06e+12	6.04e+11	1.12e+12	6.42e+11
2.0	2.5	7.25e+9	3.22e+9	7.42e+9	3.30e+9
2.5	3.0	3.52e+8	1.28e+8	6.43e+8	2.34e+8
Totals		8.14e+14	1.30e+15	8.98e+14	1.47e+15

Note:

1. These source terms were calculated for a 144 inch active fuel length. The actual active fuel length is 122 inches.
2. The ⁶⁰Co activation from incore spacers is included in the 1.0-1.5 MeV energy group.

Table 5.2.21

CALCULATED BWR NEUTRON SOURCE PER ASSEMBLY
FOR STAINLESS STEEL CLAD FUEL

Lower Energy (MeV)	Upper Energy (MeV)	22,500 MWD/MTU 16-Year Cooling (Neutrons/s)
1.0e-01	4.0e-01	1.81e+5
4.0e-01	9.0e-01	9.26e+5
9.0e-01	1.4	8.75e+5
1.4	1.85	6.85e+5
1.85	3.0	1.34e+6
3.0	6.43	1.08e+6
6.43	20.0	8.77e+4
Total		5.18e+6

Note:

These source terms were calculated for a 144 inch active fuel length. The actual active fuel length is 83 inches.

Table 5.2.22

CALCULATED PWR NEUTRON SOURCE PER ASSEMBLY
FOR STAINLESS STEEL CLAD FUEL

Lower Energy (MeV)	Upper Energy (MeV)	30,000 MWD/MTU 19-Year Cooling (Neutrons/s)	40,000 MWD/MTU 24-Year Cooling (Neutrons/s)
1.0e-01	4.0e-01	2.68e+6	7.07e+6
4.0e-01	9.0e-01	1.37e+7	3.61e+7
9.0e-01	1.4	1.27e+7	3.32e+7
1.4	1.85	9.50e+6	2.47e+7
1.85	3.0	1.74e+7	4.43e+7
3.0	6.43	1.52e+7	3.95e+7
6.43	20.0	1.31e+6	3.46e+6
Totals		7.24e+7	1.88e+8

Note:

These source terms were calculated for a 144 inch active fuel length. The actual active fuel length is 122 inches.

Table 5.2.23

MINIMUM ENRICHMENTS AS A FUNCTION OF BURNUP
FOR THE SHIELDING ANALYSIS

Minimum Enrichment (wt.% ²³⁵ U)	Maximum Burnup Analyzed (MWD/MTU)
MPC-24 PWR assemblies with non-zircaloy incore spacers	
2.3	24,500
2.6	29,500
2.9	34,500
3.2	37,500
MPC-24 PWR assemblies with zircaloy incore spacers	
2.3	24,500
2.6	29,500
2.9	34,500
3.2	39,500
3.4	44,500
MPC-68	
2.1	24,500
2.4	29,500
2.6	34,500
2.9	39,500

Table 5.2.24

DESCRIPTION OF EVALUATED INTACT ZIRCALOY CLAD PWR FUEL

Assembly class	WE 14×14	WE 15×15	WE 17×17	CE 14×14	CE 16×16	B&W 15×15	B&W 17×17
Active fuel length (in.)	144	144	144	144	150	144	144
No. of fuel rods	179	204	264	176	236	208	264
Rod pitch (in.)	0.556	0.563	0.496	0.580	0.5063	0.568	0.502
Cladding material	Zr-4	Zr-4	Zr-4	Zr-4	Zr-4	Zr-4	Zr-4
Rod diameter (in.)	0.422	0.422	0.374	0.440	0.382	0.428	0.377
Cladding thickness (in.)	0.0243	0.0245	0.0225	0.0280	0.0250	0.0230	0.0220
Pellet diameter (in.)	0.3659	0.366	0.3225	0.377	0.3255	0.3742	0.3252
Pellet material	UO ₂	UO ₂	UO ₂	UO ₂	UO ₂	UO ₂	UO ₂
Pellet density (gm/cc) (95% of theoretical)	10.412	10.412	10.412	10.412	10.412	10.412	10.412
Enrichment (wt.% ²³⁵ U)	3.4	3.4	3.4	3.4	3.4	3.4	3.4
Burnup (MWD/MTU)	40,000	40,000	40,000	40,000	40,000	40,000	40,000
Cooling time (years)	5	5	5	5	5	5	5
Specific power (MW/MTU)	40	40	40	40	40	40	40
Weight of UO ₂ (kg) [†]	462.451	527.327	529.848	482.706	502.609	562.029	538.757
Weight of U (kg) [†]	407.697	464.891	467.114	425.554	443.100	495.485	474.968
No. of Guide Tubes	17	21	25	5	5	17	25
Guide Tube O.D. (in.)	0.539	0.546	0.474	1.115	0.98	0.53	0.564
Guide Tube Thickness (in.)	0.0170	0.0170	0.0160	0.0400	0.0400	0.0160	0.0175

[†] Derived from parameters in this table.

Table 5.2.25

DESCRIPTION OF EVALUATED INTACT ZIRCALOY CLAD BWR FUEL

Array Type	7×7	8×8	9×9	10×10
Active fuel length (in.)	144	144	144	144
No. of fuel rods	49	63	74	92
Rod pitch (in.)	0.738	0.640	0.566	0.510
Cladding material	Zr-2	Zr-2	Zr-2	Zr-2
Rod diameter (in.)	0.570	0.493	0.440	0.404
Cladding thickness (in.)	0.0355	0.0340	0.0280	0.0260
Pellet diameter (in.)	0.488	0.416	0.376	0.345
Pellet material	UO ₂	UO ₂	UO ₂	UO ₂
Pellet density (gm/cc) (95% of theoretical)	10.412	10.412	10.412	10.412
Enrichment (wt.% ²³⁵ U)	3.0	3.0	3.0	3.0
Burnup (MWD/MTU)	40,000	40,000	40,000	40,000
Cooling time (years)	5	5	5	5
Specific power (MW/MTU)	30	30	30	30
Weight of UO ₂ (kg) [†]	225.177	210.385	201.881	211.307
Weight of U (kg) [†]	198.516	185.475	177.978	186.288
No. of Water Rods	0	1	2	2
Water Rod O.D. (in.)	n/a	0.493	0.980	0.980
Water Rod Thickness (in.)	n/a	0.0340	0.0300	0.0300

[†] Derived from parameters in this table.

Table 5.2.26

COMPARISON OF SOURCE TERMS FOR INTACT ZIRCALOY CLAD PWR FUEL
3.4 wt.% ²³⁵U - 40,000 MWD/MTU - 5 years cooling

Assembly class	WE 14x14	WE 15x15	WE 17x17	CE 14x14	CE 16x16	B&W 15x15	B&W 17x17
Neutrons/sec	2.29e+8 / 2.28e+8	2.63e+8 / 2.65e+8	2.62e+8	2.31e+8	2.34e+8	2.94e+8	2.64e+8
Photons/sec (0.45-3.0 MeV)	3.28e+15/ 3.32e+15	3.74e+15/ 3.79e+15	3.76e+15	3.39e+15	3.54e+15	4.01e+15	3.82e+15
Thermal power (watts)	926.6 / 934.9	1056 / 1068	1062	956.6	995.7	1137	1077

Note:

The WE 14x14 and WE 15x15 have both zircaloy and stainless steel guide tubes. The first value presented is for the assembly with zircaloy guide tubes and the second value is for the assembly with stainless steel guide tubes.

Table 5.2.27

COMPARISON OF SOURCE TERMS FOR INTACT ZIRCALOY CLAD BWR FUEL
 3.0 wt.% ²³⁵U - 40,000 MWD/MTU - 5 years cooling

Assembly class	7×7	8×8	9×9	10×10
Neutrons/sec	1.33e+8	1.17e+8	1.11e+8	1.22e+8
Photons/sec (0.45-3.0 MeV)	1.55e+15	1.44e+15	1.38e+15	1.46e+15
Thermal power (watts)	435.5	402.3	385.3	407.4

Table 5.2.28

COMPARISON OF CALCULATED DECAY HEATS FOR DESIGN BASIS FUEL
AND VALUES REPORTED IN THE
DOE CHARACTERISTICS DATABASE [†] FOR
30,000 MWD/MTU AND 5-YEAR COOLING

Fuel Assembly Class	Decay Heat from the DOE Database (watts/assembly)	Decay Heat from Design Basis Fuel (watts/assembly)
PWR Fuel		
B&W 15x15	752.0	827.5
B&W 17x17	732.9	827.5
CE 16x16	653.7	827.5
CE 14x14	601.3	827.5
WE 17x17	742.5	827.5
WE 15x15	762.2	827.5
WE 14x14	649.6	827.5
BWR Fuel		
7x7	310.9	315.7
8x8	296.6	315.7
9x9	275.0	315.7

Notes:

1. The PWR and BWR design basis fuels are the B&W 15x15 and the GE 7x7, respectively.
2. The decay heat values from the database include contributions from in-core material (e.g. spacer grids).
3. Information on the 10x10 was not available in the DOE database. However, based on the results in Table 5.2.27, the actual decay heat values from the 10x10 would be very similar to the values shown above for the 8x8.

[†] Reference [5.2.7].

Table 5.2.29
 DESCRIPTION OF FUEL ASSEMBLY USED TO ANNALYZE
 THORIA RODS IN THE THORIA ROD CANISTER

	BWR
Fuel type	8x8
Active fuel length (in.)	110.5
No. of UO ₂ fuel rods	55
No. of UO ₂ /ThO ₂ fuel rods	9
Rod pitch (in.)	0.523
Cladding material	zircaloy
Rod diameter (in.)	0.412
Cladding thickness (in.)	0.025
Pellet diameter (in.)	0.358
Pellet material	98.2% ThO ₂ and 1.8% UO ₂ for UO ₂ /ThO ₂ rods
Pellet density (gm/cc)	10.412
Enrichment (w/o ²³⁵ U)	93.5 in UO ₂ for UO ₂ /ThO ₂ rods and 1.8 for UO ₂ rods
Burnup (MWD/MTIHM)	16,000
Cooling Time (years)	18
Specific power (MW/MTIHM)	16.5
Weight of ThO ₂ and UO ₂ (kg) [†]	121.46
Weight of U (kg) [†]	92.29
Weight of Th (kg) [†]	14.74

[†] Derived from parameters in this table.

Table 5.2.30

CALCULATED FUEL GAMMA SOURCE FOR THORIA ROD
CANISTER CONTAINING EIGHTEEN THORIA RODS

Lower Energy (MeV)	Upper Energy (MeV)	16,000 MWD/MTIHM 18-Year Cooling	
		(MeV/s)	(Photons/s)
7.0e-01	1.0	5.79e+11	6.81e+11
1.0	1.5	3.79e+11	3.03e+11
1.5	2.0	4.25e+10	2.43e+10
2.0	2.5	4.16e+8	1.85e+8
2.5	3.0	2.31e+11	8.39e+10
Totals		1.23e+12	1.09e+12

Table 5.2.31

CALCULATED FUEL NEUTRON SOURCE FOR THORIA ROD
CANISTER CONTAINING EIGHTEEN THORIA RODS

Lower Energy (MeV)	Upper Energy (MeV)	16,000 MWD/MTIHM 18-Year Cooling (Neutrons/s)
1.0e-01	4.0e-01	5.65e+2
4.0e-01	9.0e-01	3.19e+3
9.0e-01	1.4	6.79e+3
1.4	1.85	1.05e+4
1.85	3.0	3.68e+4
3.0	6.43	1.41e+4
6.43	20.0	1.60e+2
Totals		7.21e+4

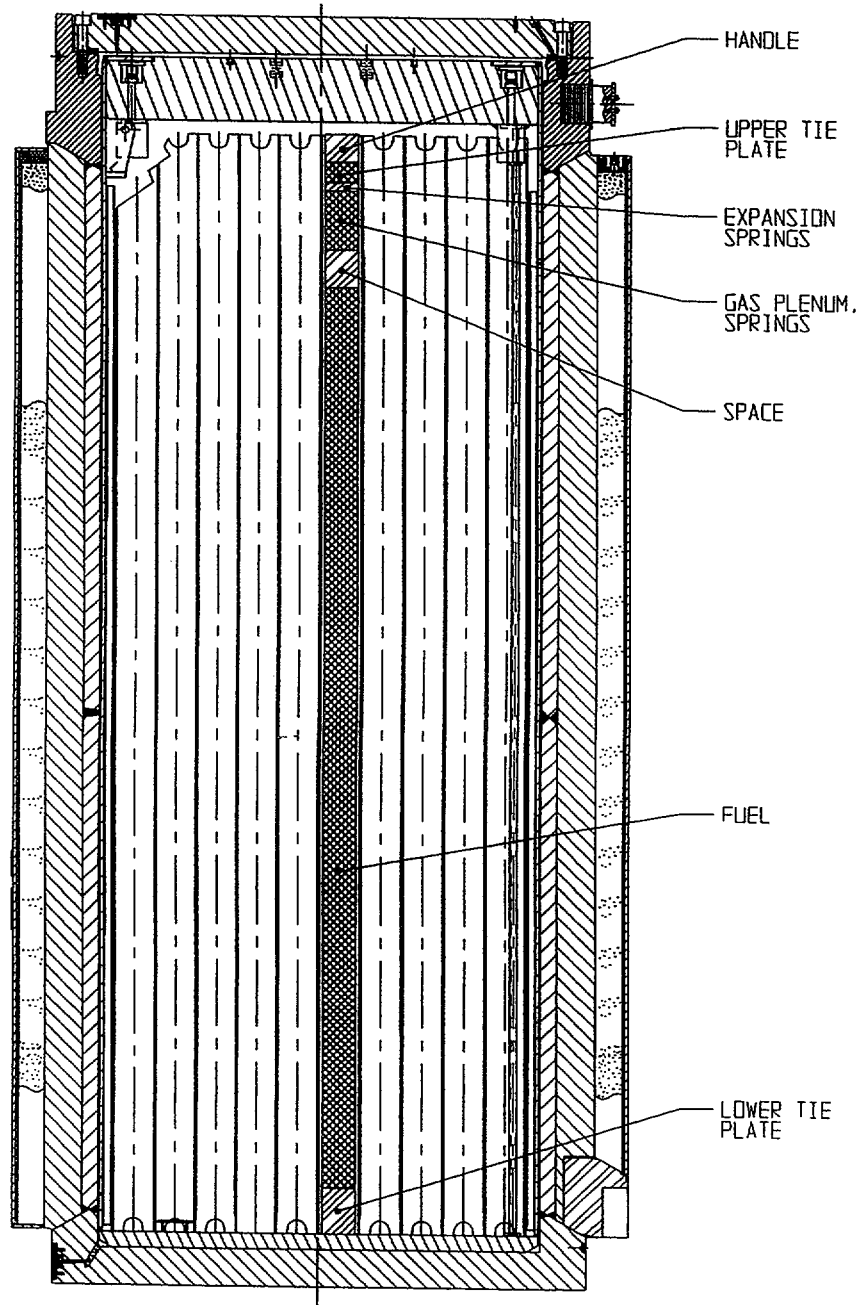


FIGURE 5.3.8; AXIAL LOCATION OF BWR DESIGN BASIS FUEL IN THE HI-STAR 100 SYSTEM

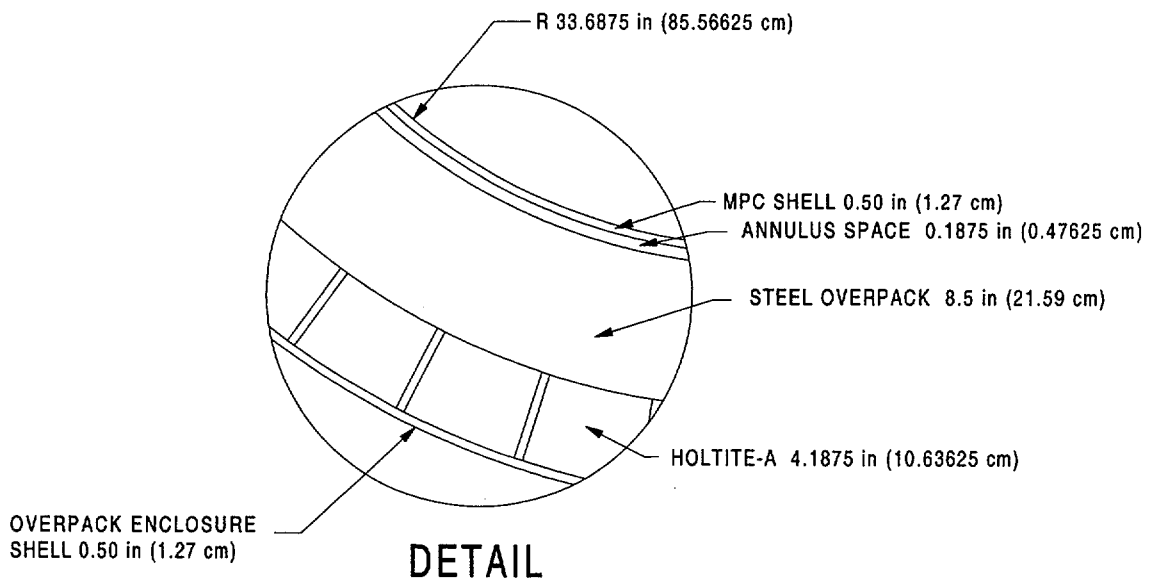
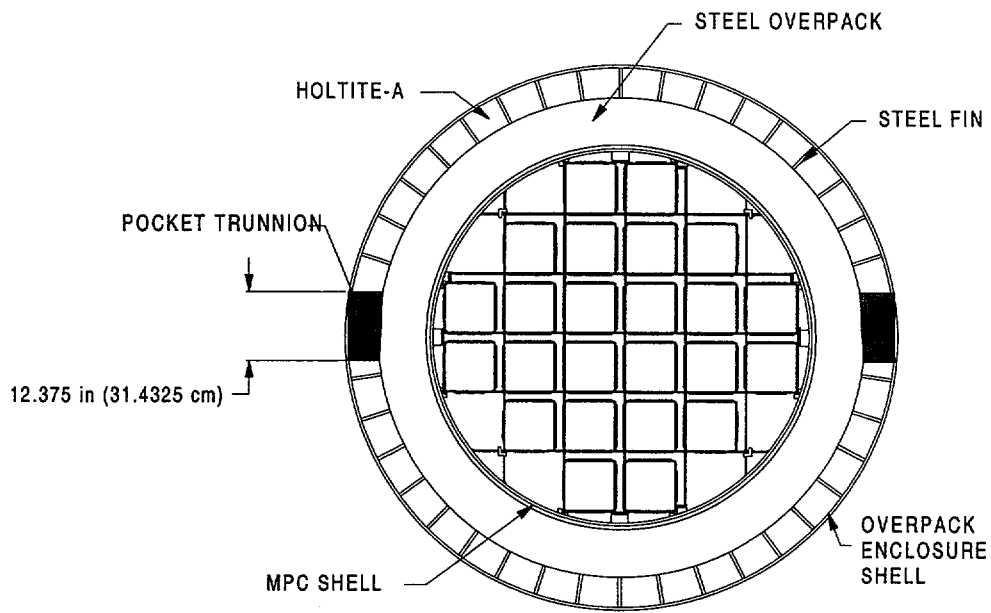


FIGURE 5.3.9; HI-STAR 100 OVERPACK WITH MPC-24 CROSS SECTIONAL VIEW SHOWING THE THICKNESS OF THE MPC SHELL AND OVERPACK AS MODELED IN MCNP

5.4.4 Stainless Steel Clad Fuel Evaluation

Tables 5.4.22 through 5.4.24 present the dose rates from the stainless steel clad fuel at various dose locations around the HI-STAR 100 overpack for the MPC-24 and the MPC-68 for normal and hypothetical accident conditions. These dose rates are below the regulatory limits indicating that these fuel assemblies are acceptable for transport.

As described in Subsection 5.2.3, the source term for the stainless steel fuel was calculated conservatively with an artificial active fuel length of 144 inches. The end fitting masses of the stainless steel clad fuel are also assumed to be identical to the end fitting masses of the zircaloy clad fuel. In addition, the fuel assembly configuration used in the MCNP calculations was identical to the configuration used for the design basis fuel assemblies as described in Table 5.3.1.

5.4.5 Dresden Unit 1 Antimony-Beryllium Neutron Sources

Dresden Unit 1 has antimony-beryllium neutron sources which are placed in the water rod location of their fuel assemblies. These sources are steel rods which contain a cylindrical antimony-beryllium source which is 77.25 inches in length. The steel rod is approximately 95 inches in length. Information obtained from Dresden Unit 1 characterizes these sources in the following manner: "About one-quarter pound of beryllium will be employed as a special neutron source material. The beryllium produces neutrons upon gamma irradiation. The gamma rays for the source at initial start-up will be provided by neutron-activated antimony (about 865 curies). The source strength is approximately $1E+8$ neutrons/second."

As stated above, beryllium produces neutrons through gamma irradiation and in this particular case antimony is used as the gamma source. The threshold gamma energy for producing neutrons from beryllium is 1.666 MeV. The outgoing neutron energy increases as the incident gamma energy increases. Sb-124, which decays by Beta decay with a half life of 60.2 days, produces a gamma of energy 1.69 MeV which is just energetic enough to produce a neutron from beryllium. Approximately 54% of the Beta decays for Sb-124 produce gammas with energies greater than or equal to 1.69 MeV. Therefore, the neutron production rate in the neutron source can be specified as $5.8E-6$ neutrons per gamma ($1E+8/865/3.7e+10/0.54$) with energy greater than 1.666 MeV or $1.16E+5$ neutrons/curie ($1E+8/865$) of Sb-124.

With the short half life of 60.2 days all of the initial Sb-124 is decayed and any Sb-124 that was produced while the neutron source was in the reactor is also decayed since these neutron sources are assumed to have the same minimum cooling time as the Dresden 1 fuel assemblies (array classes 6x6A, 6x6B, 6x6C, and 8x8A) of 18 years. Therefore, there are only two possible gamma sources which can produce neutrons from this antimony-beryllium source. The first is the gammas from the decay of fission products in the fuel assemblies in the MPC. The second

gamma source is from Sb-124 which is being produced in the MPC from neutron activation from neutrons from the decay of fission products.

MCNP calculations were performed to determine the gamma source as a result of decay gammas from fuel assemblies and Sb-124 activation. The calculations explicitly modeled the 6x6 fuel assembly described in Table 5.2.2. A single fuel rod was removed and replaced by a guide tube. In order to determine the amount of Sb-124 that is being activated from neutrons in the MPC it was necessary to estimate the amount of antimony in the neutron source. The O.D. of the source was assumed to be the I.D. of the steel rod encasing the source (0.345 in.). The length of the source is 77.25 inches. The beryllium is assumed to be annular in shape encompassing the antimony. Using the assumed O.D. of the beryllium and the mass and length, the I.D. of the beryllium was calculated to be 0.24 inches. The antimony is assumed to be a solid cylinder with an O.D. equal to the I.D. of the beryllium. These assumptions are conservative since the antimony and beryllium are probably encased in another material which would reduce the mass of antimony. A larger mass of antimony is conservative since the calculated activity of Sb-124 is directly proportional to the initial mass of antimony.

The number of gammas from fuel assemblies with energies greater than 1.666 MeV entering the 77.25 inch long neutron source was calculated to be $1.04E+8$ gammas/sec which would produce a neutron source of 603.2 neutrons/sec ($1.04E+8 * 5.8E-6$). The steady state amount of Sb-124 activated in the antimony was calculated to be 39.9 curies. This activity level would produce a neutron source of $4.63E+6$ neutrons/sec ($39.9 * 1.16E+5$) or $6.0E+4$ neutrons/sec/inch ($4.63E+6/77.25$). These calculations conservatively neglect the reduction in antimony and beryllium which would have occurred while the neutron sources were in the core and being irradiated at full reactor power.

Since this is a localized source (77.25 inches in length) it is appropriate to compare the neutron source per inch from the design basis Dresden Unit 1 fuel assembly, 6x6, containing an Sb-Be neutron source to the design basis fuel neutron source per inch. This comparison, presented in Table 5.4.25, demonstrates that a Dresden Unit 1 fuel assembly containing an Sb-Be neutron source is bounded by the design basis fuel.

As stated above, the Sb-Be source is encased in a steel rod. Therefore, the gamma source from the activation of the steel was considered assuming a burnup of 120,000 MWD/MTU which is the maximum burnup assuming the Sb-Be source was in the reactor for the entire 18 year life of Dresden Unit 1. The cooling time assumed was 18 years which is the minimum cooling time for Dresden Unit 1 fuel. The source from the steel was bounded by the design basis fuel assembly. In conclusion, transport of a Dresden Unit 1 Sb-Be neutron source in a Dresden Unit 1 fuel assembly is acceptable and bounded by the current analysis.

5.4.6 Thoria Rod Canister

Based on a comparison of the gamma spectra from Tables 5.2.30 and 5.2.6 for the thoria rod canister and design basis 6x6 fuel assembly, respectively, it is difficult to determine if the thoria rods will be bounded by the 6x6 fuel assemblies. However, it is obvious that the neutron spectra from the 6x6, Table 5.2.14, bounds the thoria rod neutron spectra, Table 5.2.31, with a significant margin. In order to demonstrate that the gamma spectrum from the single thoria rod canister is bounded by the gamma spectrum from the design basis 6x6 fuel assembly, the gamma dose rate on the outer radial surface of the overpack was estimated conservatively assuming an MPC full of thoria rod canisters. This gamma dose rate was compared to an estimate of the dose rate from an MPC full of design basis 6x6 fuel assemblies. The gamma dose rate from the 6x6 fuel was higher than the dose rate from an MPC full of thoria rod canisters. This in conjunction with the significant margin in neutron spectrum and the fact that there is only one thoria rod canister clearly demonstrates that the thoria rod canister is acceptable for transport in the MPC-68 or the MPC-68F.

Table 5.4.1

FLUX-TO-DOSE CONVERSION FACTORS
(FROM [5.4.1])

Gamma Energy (MeV)	(rem/hr)/(photon/cm ² -s)
0.01	3.96E-06
0.03	5.82E-07
0.05	2.90E-07
0.07	2.58E-07
0.1	2.83E-07
0.15	3.79E-07
0.2	5.01E-07
0.25	6.31E-07
0.3	7.59E-07
0.35	8.78E-07
0.4	9.85E-07
0.45	1.08E-06
0.5	1.17E-06
0.55	1.27E-06
0.6	1.36E-06
0.65	1.44E-06
0.7	1.52E-06
0.8	1.68E-06
1.0	1.98E-06
1.4	2.51E-06
1.8	2.99E-06
2.2	3.42E-06

Table 5.4.1 (continued)

FLUX-TO-DOSE CONVERSION FACTORS
(FROM [5.4.1])

Gamma Energy (MeV)	(rem/hr)/(photon/cm ² -s)
2.6	3.82E-06
2.8	4.01E-06
3.25	4.41E-06
3.75	4.83E-06
4.25	5.23E-06
4.75	5.60E-06
5.0	5.80E-06
5.25	6.01E-06
5.75	6.37E-06
6.25	6.74E-06
6.75	7.11E-06
7.5	7.66E-06
9.0	8.77E-06
11.0	1.03E-05
13.0	1.18E-05
15.0	1.33E-05

Table 5.4.1 (continued)

FLUX-TO-DOSE CONVERSION FACTORS
(FROM [5.4.1])

Neutron Energy (MeV)	Quality Factor	(rem/hr)/(n/cm ² -s) [†]
2.5E-8	2.0	3.67E-6
1.0E-7	2.0	3.67E-6
1.0E-6	2.0	4.46E-6
1.0E-5	2.0	4.54E-6
1.0E-4	2.0	4.18E-6
1.0E-3	2.0	3.76E-6
1.0E-2	2.5	3.56E-6
0.1	7.5	2.17E-5
0.5	11.0	9.26E-5
1.0	11.0	1.32E-4
2.5	9.0	1.25E-4
5.0	8.0	1.56E-4
7.0	7.0	1.47E-4
10.0	6.5	1.47E-4
14.0	7.5	2.08E-4
20.0	8.0	2.27E-4

[†] Includes the Quality Factor.

Table 5.4.2

DOSE RATES FROM FUEL GAMMAS[†]
DOSE LOCATION ON THE SURFACE OF THE HI-STAR 100 SYSTEM FOR NORMAL CONDITIONS
MPC-24 DESIGN BASIS ZIRCALOY CLAD FUEL WITH ZIRCALOY INCORE SPACERS
AT VARYING BURNUPS AND COOLING TIMES

Dose Point^{††} Location	24,500 MWD/MTU 7 Year Cooling (mrem/hr)	29,500 MWD/MTU 8 Year Cooling (mrem/hr)	34,500 MWD/MTU 10 Year Cooling (mrem/hr)	39,500 MWD/MTU 12 Year Cooling (mrem/hr)	44,500 MWD/MTU 15 Year Cooling (mrem/hr)
1	2.09	2.16	2.06	2.09	2.05
2	28.06	28.55	26.47	26.10	24.91
3	1.27	1.29	1.21	1.21	1.31
4	0.73	0.76	0.73	0.75	0.75
5	0.12	0.19	0.29	0.38	0.50
6	3.40	3.69	3.82	4.18	4.51

[†] Gammas generated by neutron capture and gammas from incore spacers are included with fuel gammas.

^{††} Refer to Figure 5.1.1.

Table 5.4.3

DOSE RATES FROM ⁶⁰Co GAMMAS
DOSE LOCATION ON THE SURFACE OF THE HI-STAR 100 SYSTEM FOR NORMAL CONDITIONS
MPC-24 DESIGN BASIS ZIRCALOY CLAD FUEL WITH ZIRCALOY INCORE SPACERS
AT VARYING BURNUPS AND COOLING TIMES

Dose Point[†] Location	24,500 MWD/MTU 7 Year Cooling (mrem/hr)	29,500 MWD/MTU 8 Year Cooling (mrem/hr)	34,500 MWD/MTU 10 Year Cooling (mrem/hr)	39,500 MWD/MTU 12 Year Cooling (mrem/hr)	44,500 MWD/MTU 15 Year Cooling (mrem/hr)
1	28.08	27.45	22.99	18.99	13.78
2	0.02	0.02	0.02	0.02	0.01
3	85.65	83.73	70.12	45.79	33.24
4	21.40	20.92	17.52	14.47	10.50
5	0.03	0.03	0.03	0.02	0.02
6	104.77	102.42	85.78	70.84	51.43

[†] Refer to Figure 5.1.1.

Table 5.4.4

DOSE RATES FROM NEUTRONS
DOSE LOCATION ON THE SURFACE OF THE HI-STAR 100 SYSTEM FOR NORMAL CONDITIONS
MPC-24 DESIGN BASIS ZIRCALOY CLAD FUEL WITH ZIRCALOY INCORE SPACERS
AT VARYING BURNUPS AND COOLING TIMES

Dose Point[†] Location	24,500 MWD/MTU 7 Year Cooling (mrem/hr)	29,500 MWD/MTU 8 Year Cooling (mrem/hr)	34,500 MWD/MTU 10 Year Cooling (mrem/hr)	39,500 MWD/MTU 12 Year Cooling (mrem/hr)	44,500 MWD/MTU 15 Year Cooling (mrem/hr)
1	5.00	8.34	12.39	16.67	21.56
2	5.41	9.02	13.40	18.03	23.32
3	25.04	41.75	62.02	102.73	132.88
4	5.05	8.42	12.51	16.84	21.78
5	0.94	1.57	2.33	3.14	4.06
6	7.41	12.35	18.34	24.68	31.92

[†] Refer to Figure 5.1.1.

Table 5.4.5

DOSE RATES FROM FUEL GAMMAS[†]
DOSE LOCATION ON THE SURFACE OF THE HI-STAR 100 SYSTEM FOR NORMAL CONDITIONS
MPC-68 DESIGN BASIS ZIRCALOY CLAD FUEL AT VARYING BURNUPS AND COOLING TIMES

Dose Point^{††} Location	24,500 MWD/MTU 8 Year Cooling (mrem/hr)	29,500 MWD/MTU 9 Year Cooling (mrem/hr)	34,500 MWD/MTU 12 Year Cooling (mrem/hr)	39,500 MWD/MTU 15 Year Cooling (mrem/hr)
1	2.36	2.52	2.27	2.15
2	31.67	33.47	28.46	26.62
3	0.32	0.36	0.38	0.43
4	0.33	0.36	0.34	0.33
5	0.07	0.12	0.18	0.23
6	2.30	2.75	2.99	3.28

[†] Gammas generated by neutron capture and gammas from incore spacers are included with fuel gammas.

^{††} Refer to Figure 5.1.1.

Table 5.4.6

DOSE RATES FROM ⁶⁰Co GAMMAS
DOSE LOCATION ON THE SURFACE OF THE HI-STAR 100 SYSTEM FOR NORMAL CONDITIONS
MPC-68 DESIGN BASIS ZIRCALOY CLAD FUEL AT VARYING BURNUPS AND COOLING TIMES

Dose Point[†] Location	24,500 MWD/MTU 8 Year Cooling (mrem/hr)	29,500 MWD/MTU 9 Year Cooling (mrem/hr)	34,500 MWD/MTU 12 Year Cooling (mrem/hr)	39,500 MWD/MTU 15 Year Cooling (mrem/hr)
1	26.39	23.68	18.79	13.35
2	0.01	0.01	0.01	0.01
3	96.40	86.51	63.79	45.34
4	24.41	21.90	17.37	12.34
5	0.02	0.02	0.02	0.01
6	90.75	81.44	64.57	45.90

[†] Refer to Figure 5.1.1.

Table 5.4.7

DOSE RATES FROM NEUTRONS
DOSE LOCATION ON THE SURFACE OF THE HI-STAR 100 SYSTEM FOR NORMAL CONDITIONS
MPC-68 DESIGN BASIS ZIRCALOY CLAD FUEL AT VARYING BURNUPS AND COOLING TIMES

Dose Point[†] Location	24,500 MWD/MTU 8 Year Cooling (mrem/hr)	29,500 MWD/MTU 9 Year Cooling (mrem/hr)	34,500 MWD/MTU 12 Year Cooling (mrem/hr)	39,500 MWD/MTU 15 Year Cooling (mrem/hr)
1	5.48	9.12	13.60	17.50
2	6.58	10.95	17.72	22.79
3	13.84	23.04	43.46	55.89
4	2.80	4.66	6.95	8.94
5	0.55	0.91	1.36	1.75
6	7.98	13.29	19.83	25.50

[†] Refer to Figure 5.1.1.

Table 5.4.8

TOTAL DOSE RATES
DOSE LOCATION ON THE SURFACE OF THE HI-STAR 100 SYSTEM FOR NORMAL CONDITIONS
MPC-24 DESIGN BASIS ZIRCALOY CLAD FUEL WITH ZIRCALOY INCORE SPACERS
AT VARYING BURNUPS AND COOLING TIMES

Dose Point[†] Location	24,500 MWD/MTU 7 Year Cooling (mrem/hr)	29,500 MWD/MTU 8 Year Cooling (mrem/hr)	34,500 MWD/MTU 10 Year Cooling (mrem/hr)	39,500 MWD/MTU 12 Year Cooling (mrem/hr)	44,500 MWD/MTU 15 Year Cooling (mrem/hr)
1	35.17	37.95	37.44	37.74	37.39
2	33.49	37.60	39.89	44.15	48.24
3	111.96	126.77	133.36	149.73	167.42
4	27.18	30.10	30.76	32.05	33.03
5	1.09	1.80	2.65	3.55	4.57
6	115.58	118.46	107.94	99.71	87.86
10CFR71.47 Limit	200.00	200.00	200.00	200.00	200.00

[†] Refer to Figure 5.1.1.

Table 5.4.9

TOTAL DOSE RATES
DOSE LOCATION ON THE SURFACE OF THE HI-STAR 100 SYSTEM FOR NORMAL CONDITIONS
MPC-68 DESIGN BASIS ZIRCALOY CLAD FUEL AT VARYING BURNUPS AND COOLING TIMES

Dose Point[†] Location	24,500 MWD/MTU 8 Year Cooling (mrem/hr)	29,500 MWD/MTU 9 Year Cooling (mrem/hr)	34,500 MWD/MTU 12 Year Cooling (mrem/hr)	39,500 MWD/MTU 15 Year Cooling (mrem/hr)
1	34.23	35.32	34.65	32.99
2	38.26	44.43	46.20	49.42
3	110.56	109.91	107.62	101.67
4	27.53	26.92	24.66	21.62
5	0.64	1.05	1.56	1.99
6	101.03	97.48	87.39	74.68
10CFR71.47 Limit	200.00	200.00	200.00	200.00

[†] Refer to Figure 5.1.1.

Table 5.4.10

TOTAL DOSE RATES
DOSE LOCATION AT TWO METERS FOR NORMAL CONDITIONS
MPC-24 DESIGN BASIS ZIRCALOY CLAD FUEL WITH ZIRCALOY INCORE SPACERS
AT VARYING BURNUPS AND COOLING TIMES

Dose Point[†] Location	24,500 MWD/MTU 7 Year Cooling (mrem/hr)	29,500 MWD/MTU 8 Year Cooling (mrem/hr)	34,500 MWD/MTU 10 Year Cooling (mrem/hr)	39,500 MWD/MTU 12 Year Cooling (mrem/hr)	44,500 MWD/MTU 15 Year Cooling (mrem/hr)
1	6.91	7.41	7.30	7.44	7.45
2	8.11	8.69	8.64	9.01	9.29
3	6.53	7.00	6.89	7.01	7.00
4	6.24	6.75	6.72	6.89	6.96
5	0.12	0.19	0.28	0.37	0.47
6	9.39	9.38	8.20	7.20	5.89
10CFR71.47 Limit	10.00	10.00	10.00	10.00	10.00

[†] Refer to Figure 5.1.1.

Table 5.4.11

TOTAL DOSE RATES
DOSE LOCATION AT TWO METERS FOR NORMAL CONDITIONS
MPC-68 DESIGN BASIS ZIRCALOY CLAD FUEL AT VARYING BURNUPS AND COOLING TIMES

Dose Point[†] Location	24,500 MWD/MTU 8 Year Cooling (mrem/hr)	29,500 MWD/MTU 9 Year Cooling (mrem/hr)	34,500 MWD/MTU 12 Year Cooling (mrem/hr)	39,500 MWD/MTU 15 Year Cooling (mrem/hr)
1	6.57	7.04	6.92	6.80
2	8.01	8.92	8.78	8.90
3	6.09	6.22	5.82	5.38
4	5.77	5.86	5.47	5.02
5	0.07	0.11	0.16	0.21
6	8.38	7.80	6.59	5.19
10CFR71.47 Limit	10.00	10.00	10.00	10.00

[†] Refer to Figure 5.1.1.

Table 5.4.12

**TOTAL DOSE RATES
DOSE LOCATION AT ONE METER FOR ACCIDENT CONDITIONS
MPC-24 DESIGN BASIS ZIRCALOY CLAD FUEL WITH ZIRCALOY INCORE SPACERS
AT VARYING BURNUPS AND COOLING TIMES**

Dose Point[†] Location	24,500 MWD/MTU 7 Year Cooling (mrem/hr)	29,500 MWD/MTU 8 Year Cooling (mrem/hr)	34,500 MWD/MTU 10 Year Cooling (mrem/hr)	39,500 MWD/MTU 12 Year Cooling (mrem/hr)	44,500 MWD/MTU 15 Year Cooling (mrem/hr)
1	76.86	98.98	120.33	144.25	170.56
2	144.84	217.78	302.20	393.66	497.08
3	51.17	67.08	82.95	100.58	120.08
4	37.46	49.10	60.70	73.56	87.79
5	4.34	7.07	10.35	13.82	17.79
6	623.93	630.03	559.32	500.23	419.18
10CFR71.51 Limit	1000.00	1000.00	1000.00	1000.00	1000.00

[†] Refer to Figure 5.1.2.

Table 5.4.13

**TOTAL DOSE RATES
DOSE LOCATION AT ONE METER FOR ACCIDENT CONDITIONS
MPC-68 DESIGN BASIS, ZIRCALOY CLAD FUEL AT VARYING BURNUPS AND COOLING TIMES**

Dose Point[†] Location	24,500 MWD/MTU 8 Year Cooling (mrem/hr)	29,500 MWD/MTU 9 Year Cooling (mrem/hr)	34,500 MWD/MTU 12 Year Cooling (mrem/hr)	39,500 MWD/MTU 15 Year Cooling (mrem/hr)
1	82.33	108.40	137.13	160.98
2	180.07	276.37	387.36	485.19
3	45.31	58.28	72.49	84.05
4	34.78	43.57	53.02	60.52
5	2.42	3.92	5.76	7.35
6	564.34	530.51	455.73	367.87
10CFR71.51 Limit	1000.00	1000.00	1000.00	1000.00

[†] Refer to Figure 5.1.2.

Table 5.4.14

**PEAK-TO-AVERAGE RATIOS FOR THE DOSE COMPONENTS
AT VARIOUS LOCATIONS**

Location	Fuel Gammas	Gammas from Neutrons	⁶⁰Co Gammas	Neutron
MPC-24				
Surface				
Pocket Trunnion	0.081	0.262	0.075	6.695
2	0.713	0.955	0.407	2.362
3	1.317	1.011	1.005	1.177
2 meter				
Pocket Trunnion	1.109	1.232	1.059	0.809
2	1.034	0.974	1.086	0.990
MPC-68				
Surface				
Pocket Trunnion	0.070	0.432	0.074	7.340
2	0.737	0.977	1.123	2.284
3	0.908	0.816	1.217	0.940
2 meter				
Pocket Trunnion	1.121	0.982	1.144	1.171
2	1.070	0.939	1.146	0.950

Table 5.4.15

DOSE RATES FOR NORMAL CONDITIONS SHOWING THE
EFFECT OF PEAKING

Dose Point [†] Location	Fuel Gammas (mrem/hr)	Gammas from Neutrons (mrem/hr)	⁶⁰ Co Gammas (mrem/hr)	Neutrons (mrem/hr)	Total (mrem/hr)
MPC-24					
Surface 44,500 MWD/MTU 15-Year Cooling					
Pocket Trunnion	0.16	0.40	1.91	102.56	105.03
2	13.00	6.38	0.00	55.08	74.46
3	0.72	0.77	33.40	156.37	191.26
2 meter 24,500 MWD/MTU 10-Year Cooling					
Pocket Trunnion	4.28	0.15	2.34	0.64	7.41
2	7.89	0.19	0.86	0.78	9.72
MPC-68					
Surface 27,500 MWD/MTU 9-Year Cooling					
Pocket Trunnion	0.27	0.29	2.19	50.16	52.91
2	22.18	3.29	0.01	25.01	50.49
3	0.13	0.14	97.91	27.37	125.55
2 meter 27,500 MWD/MTU 9-Year Cooling					
Pocket Trunnion	3.55	0.30	2.28	1.95	8.08
2	6.33	0.44	0.82	1.73	9.32

[†] Refer to Figure 5.1.1.

Table 5.4.16

DOSE RATES FROM FUEL GAMMAS[†]
DOSE LOCATION ON THE SURFACE OF THE HI-STAR 100 SYSTEM FOR NORMAL CONDITIONS
MPC-24 DESIGN BASIS ZIRCALOY CLAD FUEL WITH NON-ZIRCALOY INCORE SPACERS
AT VARYING BURNUPS AND COOLING TIMES

Dose Point^{††} Location	24,500 MWD/MTU 10 Year Cooling (mrem/hr)	29,500 MWD/MTU 12 Year Cooling (mrem/hr)	34,500 MWD/MTU 14 Year Cooling (mrem/hr)	37,500 MWD/MTU 15 Year Cooling (mrem/hr)
1	2.82	2.68	2.59	2.54
2	37.51	34.31	32.74	31.93
3	1.46	1.40	1.31	1.32
4	0.95	0.91	0.89	0.88
5	0.11	0.17	0.25	0.28
6	4.26	4.27	4.42	4.45

[†] Gammas generated by neutron capture and gammas from incore spacers are included with fuel gammas.

^{††} Refer to Figure 5.1.1.

Table 5.4.17

DOSE RATES FROM ⁶⁰Co GAMMAS
DOSE LOCATION ON THE SURFACE OF THE HI-STAR 100 SYSTEM FOR NORMAL CONDITIONS
MPC-24 DESIGN BASIS ZIRCALOY CLAD FUEL WITH NON-ZIRCALOY INCORE SPACERS
AT VARYING BURNUPS AND COOLING TIMES

Dose Point[†] Location	24,500 MWD/MTU 10 Year Cooling (mrem/hr)	29,500 MWD/MTU 12 Year Cooling (mrem/hr)	34,500 MWD/MTU 14 Year Cooling (mrem/hr)	37,500 MWD/MTU 15 Year Cooling (mrem/hr)
1	18.93	16.24	13.55	12.24
2	0.05	0.01	0.01	0.01
3	57.74	49.54	32.69	29.51
4	14.42	12.38	10.33	9.33
5	0.02	0.02	0.02	0.02
6	70.63	60.60	50.57	45.66

[†] Refer to Figure 5.1.1.

Table 5.4.18

DOSE RATES FROM NEUTRONS
DOSE LOCATION ON THE SURFACE OF THE HI-STAR 100 SYSTEM FOR NORMAL CONDITIONS
MPC-24 DESIGN BASIS ZIRCALOY CLAD FUEL WITH NON-ZIRCALOY INCORE SPACERS
AT VARYING BURNUPS AND COOLING TIMES

Dose Point[†] Location	24,500 MWD/MTU 10 Year Cooling (mrem/hr)	29,500 MWD/MTU 12 Year Cooling (mrem/hr)	34,500 MWD/MTU 14 Year Cooling (mrem/hr)	37,500 MWD/MTU 15 Year Cooling (mrem/hr)
1	4.49	7.21	10.70	12.13
2	4.07	7.81	11.58	13.13
3	22.50	36.12	65.94	74.78
4	4.54	7.29	10.81	12.25
5	0.85	1.36	2.02	2.29
6	6.66	10.68	15.85	17.97

[†] Refer to Figure 5.1.1.

Table 5.4.19

TOTAL DOSE RATES
DOSE LOCATION ON THE SURFACE OF THE HI-STAR 100 SYSTEM FOR NORMAL CONDITIONS
MPC-24 DESIGN BASIS ZIRCALOY CLAD FUEL WITH NON-ZIRCALOY INCORE SPACERS
AT VARYING BURNUPS AND COOLING TIMES

Dose Point[†] Location	24,500 MWD/MTU 10 Year Cooling (mrem/hr)	29,500 MWD/MTU 12 Year Cooling (mrem/hr)	34,500 MWD/MTU 14 Year Cooling (mrem/hr)	37,500 MWD/MTU 15 Year Cooling (mrem/hr)
1	26.25	26.14	26.84	26.91
2	41.63	42.12	44.33	45.06
3	81.70	87.06	99.94	105.61
4	19.91	20.57	22.03	22.46
5	0.97	1.55	2.28	2.58
6	81.55	75.56	70.83	68.09
10CFR71.47 Limit	200.00	200.00	200.00	200.00

[†] Refer to Figure 5.1.1.

Table 5.4.20

TOTAL DOSE RATES
DOSE LOCATION AT TWO METERS FOR NORMAL CONDITIONS
MPC-24 DESIGN BASIS ZIRCALOY CLAD FUEL WITH NON-ZIRCALOY INCORE SPACERS
AT VARYING BURNUPS AND COOLING TIMES

Dose Point[†] Location	24,500 MWD/MTU 10 Year Cooling (mrem/hr)	29,500 MWD/MTU 12 Year Cooling (mrem/hr)	34,500 MWD/MTU 14 Year Cooling (mrem/hr)	37,500 MWD/MTU 15 Year Cooling (mrem/hr)
1	6.42	6.32	6.39	6.37
2	9.40	9.23	9.30	9.28
3	5.89	5.80	5.87	5.86
4	5.47	5.44	5.58	5.60
5	0.10	0.16	0.24	0.27
6	6.55	5.85	5.22	4.90
10CFR71.47 Limit	10.00	10.00	10.00	10.00

[†] Refer to Figure 5.1.1.

Table 5.4.21

TOTAL DOSE RATES
DOSE LOCATION AT ONE METER FOR ACCIDENT CONDITIONS
MPC-24 DESIGN BASIS ZIRCALOY CLAD FUEL WITH NON-ZIRCALOY INCORE SPACERS
AT VARYING BURNUPS AND COOLING TIMES

Dose Point[†] Location	24,500 MWD/MTU 10 Year Cooling (mrem/hr)	29,500 MWD/MTU 12 Year Cooling (mrem/hr)	34,500 MWD/MTU 14 Year Cooling (mrem/hr)	37,500 MWD/MTU 15 Year Cooling (mrem/hr)
1	63.62	78.18	98.10	105.98
2	144.48	200.19	273.11	302.89
3	43.10	53.85	68.42	74.22
4	30.93	38.84	49.53	53.79
5	3.85	6.05	8.89	10.05
6	438.40	396.68	359.52	339.81
10CFR71.51 Limit	1000.00	1000.00	1000.00	1000.00

[†] Refer to Figure 5.1.2.

Table 5.4.22

DOSE RATES FOR
MPC-68 DESIGN BASIS STAINLESS STEEL CLAD FUEL
22,500 MWD/MTU AND 16-YEAR COOLING

Dose Point [†] Location	Fuel Gammas ^{††} (mrem/hr)	⁶⁰ Co Gammas (mrem/hr)	Neutrons (mrem/hr)	Totals (mrem/hr)
Dose Location at Surface for Normal Condition				
1	2.92	9.19	0.99	13.10
2	39.26	0.00	1.20	40.46
3	0.33	33.55	2.52	36.40
4	0.37	8.50	0.51	9.38
5	0.01	0.01	0.10	0.12
6	2.32	31.59	1.46	35.37
10CFR71.47 Limit				200.00
Dose Location at Two Meters for Normal Condition				
1	3.45	1.00	0.17	4.62
2	7.68	0.27	0.20	8.15
3	2.26	1.28	0.11	3.65
4	1.69	1.33	0.11	3.13
5	0.00	0.00	0.01	0.01
6	0.26	2.73	0.06	3.05
10CFR71.47 Limit				10.00
Dose Location at One Meter for Accident Condition				
1	9.41	10.90	7.94	28.25
2	46.41	0.23	26.02	72.66
3	3.52	6.97	4.08	14.57
4	2.10	6.03	2.87	11.00
5	0.02	0.05	0.41	0.48
6	11.57	182.92	5.42	199.91
10CFR71.51 Limit				1000.00

[†] Refer to Figures 5.1.1 and 5.1.2.

^{††} Gammas generated by neutron capture and gammas from incore spacers are included with fuel gammas.

Table 5.4.23

DOSE RATES FOR
MPC-24 DESIGN BASIS STAINLESS STEEL CLAD FUEL
30,000 MWD/MTU AND 19-YEAR COOLING

Dose Point [†] Location	Fuel Gammas ^{††} (mrem/hr)	⁶⁰ Co Gammas (mrem/hr)	Neutrons (mrem/hr)	Totals (mrem/hr)
Dose Location at Surface for Normal Condition				
1	3.02	6.23	5.05	14.30
2	39.57	0.02	4.57	44.16
3	1.38	15.03	31.13	47.54
4	1.01	4.75	5.10	10.86
5	0.12	0.01	0.95	1.08
6	4.57	23.26	7.49	35.32
10CFR71.47 Limit				200.00
Dose Location at Two Meters for Normal Condition				
1	3.42	0.81	0.83	5.06
2	8.24	0.26	0.89	9.39
3	2.86	0.81	0.80	4.47
4	2.33	0.82	0.86	4.01
5	0.01	0.00	0.10	0.11
6	0.44	1.92	0.32	2.68
10CFR71.47 Limit				10.00
Dose Location at One Meter for Accident Condition				
1	8.78	8.02	34.69	51.49
2	47.52	0.27	110.45	158.24
3	6.48	4.90	24.80	36.18
4	3.50	3.76	18.17	25.43
5	0.03	0.05	4.12	4.20
6	23.76	128.53	28.78	181.07
10CFR71.51 Limit				1000.00

[†] Refer to Figures 5.1.1 and 5.1.2.

^{††} Gammas generated by neutron capture and gammas from incore spacers are included with fuel gammas.

Table 5.4.24

DOSE RATES FOR
MPC-24 DESIGN BASIS STAINLESS STEEL CLAD FUEL
40,000 MWD/MTU AND 24-YEAR COOLING

Dose Point [†] Location	Fuel Gammas ^{††} (mrem/hr)	⁶⁰ Co Gammas (mrem/hr)	Neutrons (mrem/hr)	Totals (mrem/hr)
Dose Location at Surface for Normal Condition				
1	2.58	6.52	13.11	22.21
2	32.07	0.01	14.19	46.27
3	1.36	15.72	80.81	97.89
4	0.89	4.97	13.24	19.10
5	0.30	0.01	2.47	2.78
6	4.58	24.33	19.42	48.33
10CFR71.47 Limit				200.00
Dose Location at Two Meters for Normal Condition				
1	2.81	0.84	2.16	5.81
2	6.65	0.27	2.30	9.22
3	2.35	0.85	2.09	5.29
4	1.92	0.86	2.24	5.02
5	0.02	0.01	0.26	0.29
6	0.37	2.00	0.83	3.20
10CFR71.47 Limit				10.00
Dose Location at One Meter for Accident Condition				
1	6.80	8.39	90.10	105.29
2	36.58	0.28	286.87	323.73
3	5.00	5.13	64.39	74.52
4	2.72	3.94	47.18	53.84
5	0.05	0.05	10.71	10.81
6	18.30	134.43	74.69	227.42
10CFR71.51 Limit				1000.00

[†] Refer to Figures 5.1.1 and 5.1.2.

^{††} Gammas generated by neutron capture and gammas from incore spacers are included with fuel gammas.

Table 5.4.25

COMPARISON OF NEUTRON SOURCE PER INCH PER SECOND FOR
DESIGN BASIS 7X7 FUEL AND DESIGN BASIS DRESDEN UNIT 1 FUEL

Assembly	Active fuel length (inch)	Neutrons per sec per inch	Neutrons per sec per inch with Sb-Be source	Reference for neutrons per sec per inch
7x7 design basis	144	6.38E+5	N/A	Table 5.2.13 39.5 GWD/MTU and 15 year cooling
6x6 design basis	110	2.85e+5	3.45E+5	Table 5.2.14
6x6 design basis MOX	110	3.67E+5	4.27E+5	Table 5.2.17

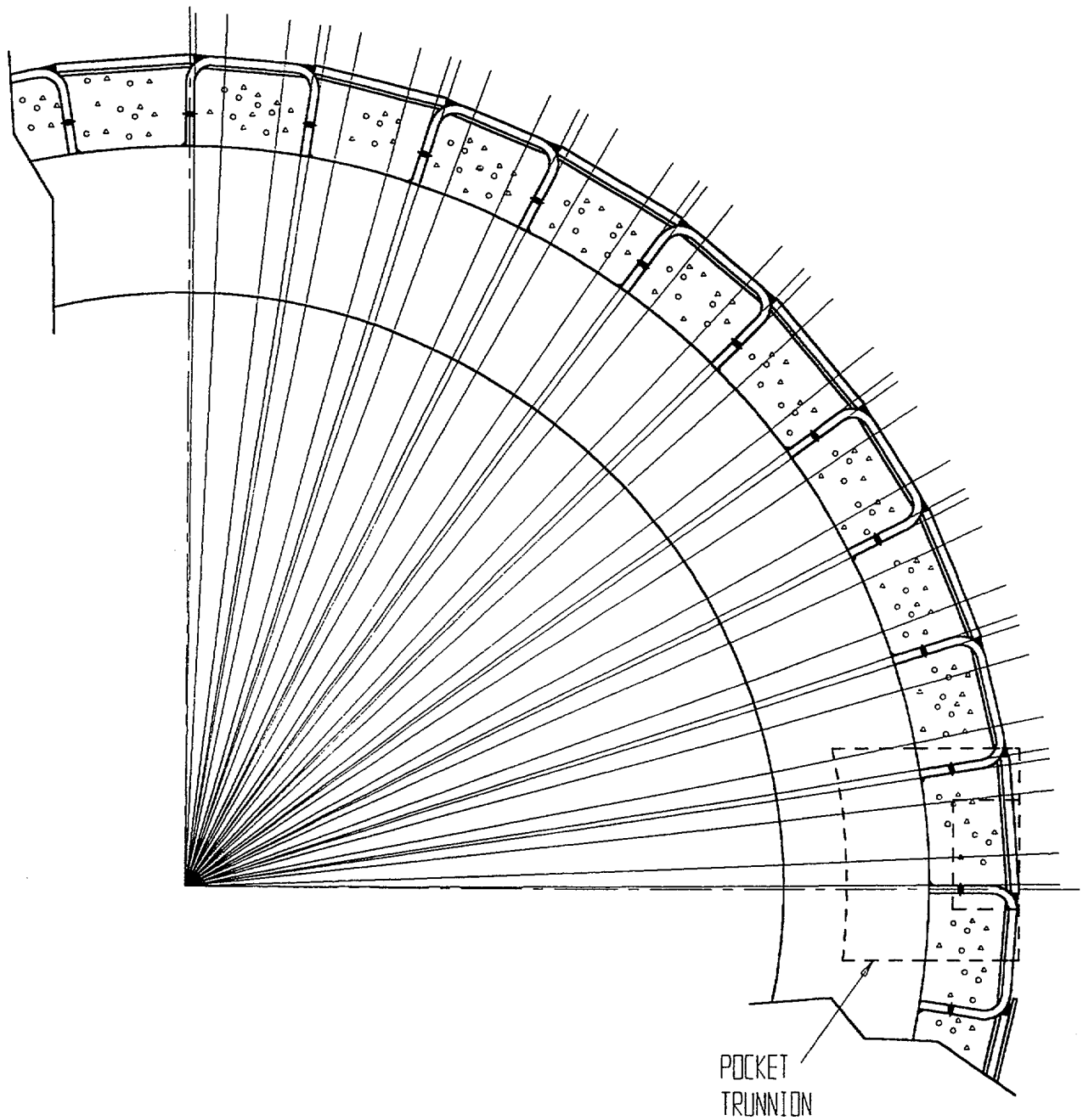


FIGURE 5.4.1; DEPICTION OF THE AZIMUTHAL SEGMENTATION OF THE OVERPACK USED IN ANALYZING NEUTRON AND PHOTON STREAMING

The following two interchangeable basket designs are available for use in the HI-STAR 100 System:

- a 24-cell basket (MPC-24), designed for intact PWR fuel assemblies with a specified maximum enrichment.
- a 68-cell basket (MPC-68), designed for both intact and damaged BWR fuel assemblies with a specified maximum planar-average enrichment. Additionally, a variation in the MPC-68, designated MPC-68F, is designed for damaged BWR fuel assemblies and BWR fuel debris with a specified maximum planar-average enrichment.

During the normal conditions of transport, the HI-STAR 100 System is dry (no moderator), and thus, the reactivity is very low ($k_{\text{eff}} < 0.40$). However, the HI-STAR 100 System for loading and unloading operations, as well as for the hypothetical accident conditions, is flooded, and thus, represents the limiting case in terms of reactivity. The calculational models for these conditions conservatively include: full flooding with ordinary water, corresponding to the highest reactivity, and the worst case (most conservative) combination of manufacturing and fabrication tolerances.

Confirmation of the criticality safety of the HI-STAR 100 Systems under flooded conditions, when filled with fuel of the maximum permissible reactivity for which they are designed, was accomplished with the three-dimensional Monte Carlo code MCNP4a [6.1.4]. Independent confirmatory calculations were made with NITAWL-KENO5a from the SCALE-4.3 package. KENO5a [6.1.5] calculations used the 238-group SCALE cross-section library in association with the NITAWL-II program [6.1.6], which adjusts the uranium-238 cross sections to compensate for resonance self-shielding effects. The Dancoff factors required by NITAWL-II were calculated with the CELLDAN code [6.1.13], which includes the SUPERDAN code [6.1.7] as a subroutine. K-factors for one-sided statistical tolerance limits with 95% probability at the 95% confidence level were obtained from the National Bureau of Standards (now NIST) Handbook 91 [6.1.8].

CASMO-3, a two-dimensional transport theory code [6.1.9-6.1.12] for fuel assemblies, was used to assess the incremental reactivity effects due to manufacturing tolerances. The CASMO-3 calculations identify those tolerances that cause a positive reactivity effect, enabling the Monte Carlo code input to define the worst case (most conservative) conditions. CASMO-3 was not used for quantitative information, but only to qualitatively indicate the direction and approximate magnitude of the reactivity effects of the manufacturing tolerances.

Benchmark calculations were made to compare the primary code packages (MCNP4a and KENO5a) with experimental data, using critical experiments selected to encompass, insofar as practical, the design parameters of the HI-STAR 100 System. The most important parameters are

(1) the enrichment, (2) the water-gap size (MPC-24) or cell spacing (MPC-68), and (3) the ^{10}B loading of the neutron absorber panels. Benchmark calculations are presented in Appendix 6.A.

Applicable codes, standards, and regulations, or pertinent sections thereof, include the following:

- U.S. Code of Federal Regulations, "Packaging and Transportation of Radioactive Materials," Title 10, Part 71.
- NUREG-1617, "Standard Review Plan for Transportation Packages for Spent Nuclear Fuel – Draft Report for Comment," USNRC, Washington D.C., March 1998.
- U.S. Code of Federal Regulations, "Prevention of Criticality in Fuel Storage and Handling," Title 10, Part 50, Appendix A, General Design Criterion 62.
- USNRC Standard Review Plan, NUREG-0800, Section 9.1.2, Spent Fuel Storage, Rev. 3, July 1981.

To assure the true reactivity will always be less than the calculated reactivity, the following conservative assumptions were made:

- The MPCs are assumed to contain the most reactive fresh fuel authorized to be loaded into a specific basket design.
- No credit for fuel burnup is assumed, either in depleting the quantity of fissile nuclides or in producing fission product poisons.
- The criticality analyses assume 75% of the manufacturer's minimum Boron-10 content for the Boral neutron absorber.
- The fuel stack density is assumed to be 96% of theoretical (10.522 g/cm^3) for all criticality analyses. The fuel stack density is approximately equal to 98% of the pellet density. Therefore, while the pellet density of some fuels might be slightly greater than 96% of theoretical, the actual stack density will still be less.
- No credit is taken for the ^{234}U and ^{236}U in the fuel.
- When flooded, the moderator is assumed to be water at a temperature corresponding to the highest reactivity within the expected operating range (i.e., water density of 1.000 g/cc).

- Neutron absorption in minor structural members and heat conduction elements is neglected, i.e., spacer grids, basket supports, and aluminum heat conduction elements are replaced by water.
- The worst hypothetical combination of tolerances (most conservative values within the range of acceptable values), as identified in Section 6.3, is assumed.
- When flooded, the fuel rod pellet-to-clad gap regions are assumed to be flooded.
- Planar-averaged enrichments are assumed for BWR fuel. (Analyses are presented in Appendix 6.B to demonstrate that the use of planar-average enrichments produces conservative results.)
- Fuel-related burnable neutron absorbers, such as the Gadolinia normally used in BWR fuel and IFBA normally used in PWR fuel, are neglected.
- For evaluation of the bias, all benchmark calculations that result in a k_{eff} greater than 1.0 are conservatively truncated to 1.0000.
- For fuel assemblies that contain low-enriched axial blankets, the governing enrichment is that of the highest planar average, and the blankets are not included in determining the average enrichment.
- For intact fuel assemblies, as defined in Chapter 1, missing fuel rods must be replaced with dummy rods that displace a volume of water that is equal to, or larger than, that displaced by the original rods.

Results of the design basis criticality safety calculations for single unreflected, internally flooded casks (limiting cases) are listed in Tables 6.1.1 through 6.1.3, conservatively evaluated for the worst combination of manufacturing tolerances (as identified in Section 6.3), and including the calculational bias, uncertainties, and calculational statistics. For each of the MPC designs and fuel assembly classes[†], Tables 6.1.1 through 6.1.3 list the bounding maximum k_{eff} value and the associated maximum allowable enrichment, as required by 10CFR71.33(b)(2). The maximum enrichment acceptance criteria are defined in Chapter 1. Maximum k_{eff} values for each of the candidate fuel assemblies and basket configurations, that are bounded by those listed in Tables

† For each array size (e.g., 6x6, 7x7, 14x14, etc.), the fuel assemblies have been subdivided into a number of assembly classes, where an assembly class is defined in terms of the (1) number of fuel rods; (2) pitch; (3) number and location of guide tubes (PWR) or water rods (BWR); and (4) cladding material. The assembly classes for BWR and PWR fuel are defined in Section 6.2.

6.1.1 through 6.1.3, are given in Section 6.2. Calculations for fully reflected casks and for array configurations with various internal and external moderator densities and various cask-to-cask spacings showed negligible reactivity increases and are discussed in Section 6.4.

A table listing the maximum k_{eff} (including bias, uncertainties, and calculational statistics), calculated k_{eff} , standard deviation, and energy of the average lethargy causing fission (EALF) for each of the candidate fuel assemblies and basket configurations is provided in Appendix 6.C. These results confirm that the maximum k_{eff} values for the HI-STAR 100 System are below the limiting design criteria ($k_{\text{eff}} < 0.95$) when fully flooded and loaded with any of the candidate fuel assemblies and basket configurations. Analyses for the various conditions of flooding that support the conclusion that the fully flooded condition corresponds to the highest reactivity, and thus is most limiting, are presented in Section 6.4. The capability of the MPC-68F to safely accommodate Dresden-1 and Humboldt Bay damaged fuel (fuel assembly classes 6x6A, 6x6B, 6x6C, 7x7A, and 8x8A) is demonstrated in Subsection 6.4.4.

Hypothetical accident conditions of transport have also been evaluated and no hypothetical accident has been identified that would result in exceeding the design criteria limit on reactivity. For an infinite array of HI-STAR 100 Systems under flooded conditions, the physical separation between overpacks and the steel radiation shielding are each adequate to preclude any significant neutronic coupling between casks in an array configuration. Therefore, the transportation index based on criticality control is zero (0). Calculations are presented in Section 6.4 confirming this conclusion.

Calculational results, which address the following conditions:

- A single package, under the conditions of 10 CFR 71.55(b), (d), and (e);
- An array of undamaged packages, under the conditions of 10 CFR 71.59(a)(1); and
- An array of damaged packages, under the conditions of 10 CFR 71.59(a)(2)

are summarized in Table 6.1.4. These results demonstrate that the HI-STAR 100 System is in full compliance with 10CFR71 (71.55(b), (d), and (e) and 71.59(a)(1) and (a)(2)).

Table 6.1.1

BOUNDED MAXIMUM k_{eff} VALUES FOR EACH ASSEMBLY CLASS IN THE MPC-24

Fuel Assembly Class	Maximum Allowable Enrichment (wt% ^{235}U)	Maximum [†] k_{eff}
14x14A	4.6	0.9383
14x14B	4.6	0.9323
14x14C	4.6	0.9400
14x14D	4.0	0.8576
15x15A	4.1	0.9301
15x15B	4.1	0.9473
15x15C	4.1	0.9444
15x15D	4.1	0.9440
15x15E	4.1	0.9475
15x15F	4.1	0.9478 ^{††}
15x15G	4.0	0.8986
15x15H	3.8	0.9411
16x16A	4.6	0.9383
17x17A	4.0	0.9452
17x17B	4.0	0.9436
17x17C	4.0	0.9427

Note: These calculations are for single unreflected, fully flooded casks. However, comparable reactivities were obtained for fully reflected casks and for arrays of casks.

† The term "maximum k_{eff} " as used here, and elsewhere in this document, means the highest possible k-effective, including bias, uncertainties, and calculational statistics, evaluated for the worst case combination of manufacturing tolerances.

†† KENO5a verification calculation resulted in a maximum k_{eff} of 0.9466.

Table 6.1.2

BOUNDING MAXIMUM k_{eff} VALUES FOR EACH ASSEMBLY CLASS IN THE MPC-68

Fuel Assembly Class	Maximum Allowable Planar-Average Enrichment (wt% ^{235}U)	Maximum [†] k_{eff}
6x6A	2.7 ^{††}	0.7888 ^{†††}
6x6B [‡]	2.7 ^{††}	0.7824 ^{†††}
6x6C	2.7 ^{††}	0.8021 ^{†††}
7x7A	2.7 ^{††}	0.7974 ^{†††}
7x7B	4.2	0.9386
8x8A	2.7 ^{††}	0.7697 ^{†††}
8x8B	4.2	0.9416
8x8C	4.2	0.9425
8x8D	4.2	0.9403
8x8E	4.2	0.9312
8x8F	3.6	0.9153

Note: These calculations are for single unreflected, fully flooded casks. However, comparable reactivities were obtained for fully reflected casks and for arrays of casks.

- † The term "maximum k_{eff} " as used here, and elsewhere in this document, means the highest possible k-effective, including bias, uncertainties, and calculational statistics, evaluated for the worst case combination of manufacturing tolerances.
- †† This calculation was performed for 3.0% planar-average enrichment, however, the authorized contents are limited to maximum planar-average enrichment of 2.7%. Therefore, the listed maximum k_{eff} value is conservative.
- ††† This calculation was performed for a ^{10}B loading of 0.0067 g/cm², which is 75% of a minimum ^{10}B loading of 0.0089 g/cm². The minimum ^{10}B loading in the MPC-68 is 0.0372 g/cm². Therefore, the listed maximum k_{eff} value is conservative.
- ‡ Assemblies in this class contain both MOX and UO₂ pins. The composition of the MOX fuel pins is given in Table 6.3.4. The maximum allowable planar-average enrichment for the MOX pins is given in the specification of authorized contents, Chapter 1.

Table 6.1.2 (continued)

BOUNDING MAXIMUM k_{eff} VALUES FOR EACH ASSEMBLY CLASS IN THE MPC-68

Fuel Assembly Class	Maximum Allowable Planar-Average Enrichment (wt% ^{235}U)	Maximum [†] k_{eff}
9x9A	4.2	0.9417
9x9B	4.2	0.9422
9x9C	4.2	0.9395
9x9D	4.2	0.9394
9x9E	4.1	0.9424
9x9F	4.1	0.9424
10x10A	4.2	0.9457 ^{††}
10x10B	4.2	0.9436
10x10C	4.2	0.9021
10x10D	4.0	0.9376
10x10E	4.0	0.9185

Note: These calculations are for single unreflected, fully flooded casks. However, comparable reactivities were obtained for fully reflected casks and for arrays of casks.

† The term "maximum k_{eff} " as used here, and elsewhere in this document, means the highest possible k-effective, including bias, uncertainties, and calculational statistics, evaluated for the worst case combination of manufacturing tolerances.

†† KENO5a verification calculation resulted in a maximum k_{eff} of 0.9453.

Table 6.1.3

BOUNDING MAXIMUM k_{eff} VALUES FOR EACH ASSEMBLY CLASS IN THE MPC-68F

Fuel Assembly Class	Maximum Allowable Planar-Average Enrichment (wt% ^{235}U)	Maximum [†] k_{eff}
6x6A	2.7 ^{††}	0.7888
6x6B ^{†††}	2.7	0.7824
6x6C	2.7	0.8021
7x7A	2.7	0.7974
8x8A	2.7	0.7685

Note:

1. These calculations are for single unreflected, fully flooded casks. However, comparable reactivities were obtained for fully reflected casks and for arrays of casks.
2. These calculations were performed for a ^{10}B loading of 0.0067 g/cm^2 , which is 75% of a minimum ^{10}B loading of 0.0089 g/cm^2 . The minimum ^{10}B loading in the MPC-68F is 0.010 g/cm^2 . Therefore, the listed maximum k_{eff} values are conservative.

† The term "maximum k_{eff} " as used here, and elsewhere in this document, means the highest possible k-effective, including bias, uncertainties, and calculational statistics, evaluated for the worst case combination of manufacturing tolerances.

†† These calculations were performed for 3.0% planar-average enrichment, however, the authorized contents are limited to a maximum planar-average enrichment of 2.7%. Therefore, the listed maximum k_{eff} values are conservative.

††† Assemblies in this class contain both MOX and UO_2 pins. The composition of the MOX fuel pins is given in Table 6.3.4. The maximum allowable planar-average enrichment for the MOX pins is given in the specification of authorized contents, Chapter 1.

6.2 SPENT FUEL LOADING

Specifications for the BWR and PWR fuel assemblies that were analyzed in this criticality evaluation are given in Tables 6.2.1 and 6.2.2, respectively. For the BWR fuel characteristics, the number and dimensions for the water rods are the actual number and dimensions. For the PWR fuel characteristics, the actual number and dimensions of the control rod guide tubes and thimbles are used. Table 6.2.1 lists 56 unique BWR assemblies while Table 6.2.2 lists 41 unique PWR assemblies, all of which were explicitly analyzed for this evaluation. Examination of Tables 6.2.1 and 6.2.2 reveals that there are a large number of minor variations in fuel assembly dimensions.

Due to the large number of minor variations in fuel assembly dimensions, the use of explicit dimensions in defining the authorized contents could limit the applicability of the HI-STAR 100 System. To resolve this limitation, bounding criticality analyses are presented in this section for a number of defined fuel assembly classes for both fuel types (PWR and BWR). The results of the bounding criticality analyses justify using bounding fuel dimensions for defining the authorized contents.

6.2.1 Definition of Assembly Classes

For each array size (e.g., 6x6, 7x7, 15x15, etc.), the fuel assemblies have been subdivided into a number of defined classes, where a class is defined in terms of the (1) number of fuel rods; (2) pitch; (3) number and locations of guide tubes (PWR) or water rods (BWR); and (4) cladding material. The assembly classes for BWR and PWR fuel are defined in Tables 6.2.1 and 6.2.2, respectively. It should be noted that these assembly classes are unique to this evaluation and are not known to be consistent with any class designations in the open literature.

For each assembly class, calculations have been performed for all of the dimensional variations for which data is available (i.e., all data in Tables 6.2.1 and 6.2.2). These calculations demonstrate that the maximum reactivity corresponds to:

- maximum active fuel length,
- maximum fuel pellet diameter,
- minimum cladding outside diameter (OD),
- maximum cladding inside diameter (ID),
- minimum guide tube/water rod thickness, and
- maximum channel thickness (for BWR assemblies only).

Therefore, for each assembly class, a bounding assembly was defined based on the above characteristics and a calculation for the bounding assembly was performed to demonstrate compliance with the regulatory requirement of $k_{\text{eff}} < 0.95$. In some assembly classes this

bounding assembly corresponds directly to one of the actual (real) assemblies; while in most assembly classes, the bounding assembly is artificial (i.e., based on bounding dimensions from more than one of the actual assemblies). In classes where the bounding assembly is artificial, the reactivity of the actual (real) assemblies is typically much less than that of the bounding assembly; thereby providing additional conservatism. As a result of these analyses, the authorized contents (Chapter 1) are defined in terms of the bounding assembly parameters for each class.

To demonstrate that the aforementioned characteristics are bounding, a parametric study was performed for a reference BWR assembly, designated herein as 8x8C04 (identified generally as a GE8x8R). The results of this study are shown in Table 6.2.3, and verify the positive reactivity effect associated with (1) increasing the pellet diameter, (2) maximizing the cladding ID (while maintaining a constant cladding OD), (3) minimizing the cladding OD (while maintaining a constant cladding ID), (4) decreasing the water rod thickness, (5) artificially replacing the Zircaloy water rod tubes with water, and (6) maximizing the channel thickness. These results, and the many that follow, justify the approach for using bounding dimensions for defining the authorized contents. Where margins permit, the Zircaloy water rod tubes (BWR assemblies) are artificially replaced by water in the bounding cases to remove the requirement for water rod thickness from the specification of authorized contents.

As mentioned, the bounding approach used in these analyses often results in a maximum k_{eff} value for a given class of assemblies that is much greater than the reactivity of any of the actual (real) assemblies within the class, and yet, is still below the 0.95 regulatory limit.

6.2.2 PWR Fuel Assemblies in the MPC-24

For PWR fuel assemblies (specifications listed in Table 6.2.2) the 15x15F01 fuel assembly at 4.1% enrichment has the highest reactivity (maximum k_{eff} of 0.9478). The 17x17A01 assembly (otherwise known as a Westinghouse 17x17 OFA) has a similar reactivity (see Table 6.2.16) and was used throughout this criticality evaluation as a reference PWR assembly. The 17x17A01 assembly is a representative PWR fuel assembly in terms of design and reactivity and is useful for the reactivity studies presented in Sections 6.3 and 6.4. Calculations for the various PWR fuel assemblies in the MPC-24 are summarized in Tables 6.2.4 through 6.2.19 for the fully flooded condition.

Tables 6.2.4 through 6.2.19 show the maximum k_{eff} values for the assembly classes that are acceptable for storage in the MPC-24. All maximum k_{eff} values include the bias, uncertainties, and calculational statistics, evaluated for the worst combination of manufacturing tolerances. All calculations for the MPC-24 were performed for a ^{10}B loading of 0.020 g/cm^2 , which is 75% of the minimum loading, 0.0267 g/cm^2 , specified on BM-1478, Bill of Materials for 24-Assembly HI-STAR 100 PWR MPC, in Section 1.4. The maximum allowable enrichment in the MPC-24 varies from 4.0 to 4.6 wt% ^{235}U , depending on the assembly class, and is defined in Tables 6.2.4

through 6.2.19. It should be noted that the maximum allowable enrichment does not vary within an assembly class. Table 6.1.1 summarizes the maximum allowable enrichments for each of the assembly classes that are acceptable for storage in the MPC-24.

Tables 6.2.4 through 6.2.19 are formatted with the assembly class information in the top row, the unique assembly designations, dimensions, and k_{eff} values in the following rows above the bold double lines, and the bounding dimensions selected to define the authorized contents and corresponding bounding k_{eff} values in the final rows. Where the bounding assembly corresponds directly to one of the actual assemblies, the fuel assembly designation is listed in the bottom row in parentheses (e.g., Table 6.2.4). Otherwise, the bounding assembly is given a unique designation. For an assembly class that contains only a single assembly (e.g., 14x14D, see Table 6.2.7), the authorized contents dimensions are based on the assembly dimensions from that single assembly. All of the maximum k_{eff} values corresponding to the selected bounding dimensions are greater than or equal to those for the actual assembly dimensions and are below the 0.95 regulatory limit.

6.2.3 BWR Fuel Assemblies in the MPC-68

For BWR fuel assemblies (specifications listed in Table 6.2.1) the artificial bounding assembly for the 10x10A assembly class at 4.2% enrichment has the highest reactivity (maximum k_{eff} of 0.9457). Calculations for the various BWR fuel assemblies in the MPC-68 are summarized in Tables 6.2.20 through 6.2.36 for the fully flooded condition. In all cases, the gadolinia (Gd_2O_3) normally incorporated in BWR fuel was conservatively neglected.

For calculations involving BWR assemblies, the use of a uniform (planar-average) enrichment, as opposed to the distributed enrichments normally used in BWR fuel, produces conservative results. Calculations confirming this statement are presented in Appendix 6.B for several representative BWR fuel assembly designs. These calculations justify the specification of planar-average enrichments to define acceptability of BWR fuel for loading into the MPC-68.

Tables 6.2.20 through 6.2.36 show the maximum k_{eff} values for assembly classes that are acceptable for storage in the MPC-68. All maximum k_{eff} values include the bias, uncertainties, and calculational statistics, evaluated for the worst combination of manufacturing tolerances. With the exception of assembly classes 6x6A, 6x6B, 6x6C, 7x7A, and 8x8A, which will be discussed in Section 6.2.4, all calculations for the MPC-68 were performed with a ^{10}B loading of 0.0279 g/cm^2 , which is 75% of the minimum loading, 0.0372 g/cm^2 , specified on BM-1479, Bill of Materials for 68-Assembly HI-STAR 100 BWR MPC, in Section 1.4. Calculations for assembly classes 6x6A, 6x6B, 6x6C, 7x7A, and 8x8A were conservatively performed with a ^{10}B loading of 0.0067 g/cm^2 . The maximum allowable enrichment in the MPC-68 varies from 2.7 to 4.2 wt% ^{235}U , depending on the assembly class. It should be noted that the maximum allowable enrichment does not vary within an assembly class. Table 6.1.2 summarizes the maximum allowable enrichments for all assembly classes that are acceptable for storage in the MPC-68.

Tables 6.2.20 through 6.2.36 are formatted with the assembly class information in the top row, the unique assembly designations, dimensions, and k_{eff} values in the following rows above the bold double lines, and the bounding dimensions selected to define the authorized contents and corresponding bounding k_{eff} values in the final rows. Where an assembly class contains only a single assembly (e.g., 8x8E, see Table 6.2.24), the authorized contents dimensions are based on the assembly dimensions from that single assembly. For assembly classes that are suspected to contain assemblies with thicker channels (e.g., 120 mils), bounding calculations are also performed to qualify the thicker channels (e.g. 7x7B, see Table 6.2.20). All of the maximum k_{eff} values corresponding to the selected bounding dimensions are shown to be greater than or equal to those for the actual assembly dimensions and are below the 0.95 regulatory limit.

For assembly classes that contain partial length rods (i.e., 9x9A, 10x10A, and 10x10B), calculations were performed for the actual (real) assembly configuration and for the axial segments (assumed to be full length) with and without the partial length rods. In all cases, the axial segment with only the full length rods present (where the partial length rods are absent) is bounding. Therefore, the bounding maximum k_{eff} values reported for assembly classes that contain partial length rods bound the reactivity regardless of the active fuel length of the partial length rods. As a result, the specification of authorized contents has no minimum requirement for the active fuel length of the partial length rods.

For BWR fuel assembly classes where margins permit, the Zircaloy water rod tubes are artificially replaced by water in the bounding cases to remove the requirement for water rod thickness from the specification of authorized contents. For these cases, the bounding water rod thickness is listed as zero.

As mentioned, the highest observed maximum k_{eff} value is 0.9457, corresponding to the artificial bounding assembly in the 10x10A assembly class. This assembly has the following bounding characteristics: (1) the partial length rods are assumed to be zero length (most reactive configuration); (2) the channel is assumed to be 120 mils thick; and (3) the active fuel length of the full length rods is 155 inches. Therefore, the maximum reactivity value is bounding compared to any of the real BWR assemblies listed.

6.2.4 Damaged BWR Fuel Assemblies and BWR Fuel Debris

In addition to storing intact PWR and BWR fuel assemblies, the HI-STAR 100 System is designed to store damaged BWR fuel assemblies and BWR fuel debris. Damaged fuel assemblies and fuel debris are defined in Chapter 1. Both damaged BWR fuel assemblies and BWR fuel debris are required to be loaded into Damaged Fuel Containers (DFCs) prior to being loaded into the MPC. Two different DFC types with slightly different cross sections are considered. DFCs containing fuel debris must be stored in the MPC-68F. DFCs containing damaged fuel assemblies may be stored in either the MPC-68 or MPC-68F. The criticality evaluation of various possible damaged conditions of the fuel is presented in Subsection 6.4.4 for both DFC types.

Tables 6.2.37 through 6.2.41 show the maximum k_{eff} values for the six assembly classes that may be stored as damaged fuel or fuel debris. All maximum k_{eff} values include the bias, uncertainties, and calculational statistics, evaluated for the worst combination of manufacturing tolerances. All calculations were performed for a ^{10}B loading of 0.0067 g/cm^2 , which is 75% of a minimum loading, 0.0089 g/cm^2 . However, because the practical manufacturing lower limit for minimum ^{10}B loading is 0.01 g/cm^2 , the minimum ^{10}B loading of 0.01 g/cm^2 is specified on BM-1479, Bill of Materials for 68-Assembly HI-STAR 100 BWR MPC, in Section 1.4, for the MPC-68F. As an additional level of conservatism in the analyses, the calculations were performed for an enrichment of 3.0 wt% ^{235}U , while the maximum allowable enrichment for these assembly classes is limited to 2.7 wt% ^{235}U in the specification of authorized contents. Therefore, the maximum k_{eff} values for damaged BWR fuel assemblies and fuel debris are conservative. Calculations for the various BWR fuel assemblies in the MPC-68F are summarized in Tables 6.2.37 through 6.2.41 for the fully flooded condition.

For the assemblies that may be stored as damaged fuel or fuel debris, the 6x6C01 assembly at 3.0 wt% ^{235}U enrichment has the highest reactivity (maximum k_{eff} of 0.8021). Considering all of the conservatism built into this analysis (e.g., higher than allowed enrichment and lower than actual ^{10}B loading), the actual reactivity will be lower.

Because the analysis for the damaged BWR fuel assemblies and fuel debris was performed for a minimum ^{10}B loading of 0.0089 g/cm^2 , which conservatively bounds damaged BWR fuel assemblies in a standard MPC-68 with a minimum ^{10}B loading of 0.0372 g/cm^2 , damaged BWR fuel assemblies may also be stored in the standard MPC-68. However, fuel debris is limited to the MPC-68F by the specification of authorized contents in Chapter 1.

Tables 6.2.37 through 6.2.41 are formatted with the assembly class information in the top row, the unique assembly designations, dimensions, and k_{eff} values in the following rows above the bold double lines, and the bounding dimensions selected to define the authorized contents and corresponding bounding k_{eff} values in the final rows. Where an assembly class contains only a single assembly (e.g., 6x6C, see Table 6.2.39), the authorized contents dimensions are based on the assembly dimensions from that single assembly. All of the maximum k_{eff} values corresponding to the selected bounding dimensions are greater than or equal to those for the actual assembly dimensions and are well below the 0.95 regulatory limit.

6.2.5 Thoria Rod Canister

Additionally, the HI-STAR 100 System is designed to store a Thoria Rod Canister in the MPC68 or MPC68F. The canister is similar to a DFC and contains 18 intact Thoria Rods placed in a separator assembly. The reactivity of the canister in the MPC68 or MPC68F is very low compared to the reactivity of the approved fuel assemblies (The ^{235}U content of these rods corresponds to UO_2 rods with an initial enrichment of approximately 1.7 wt% ^{235}U). It is therefore permissible to store the Thoria Rod Canister together with any other approved content

in a MPC68 or MPC68F. Specifications of the canister and the Thoria Rods that are used in the criticality evaluation are given in Table 6.2.42. The criticality evaluation is presented in Subsection 6.4.6.

Table 6.2.1 (page 1 of 6)
 BWR FUEL CHARACTERISTICS AND ASSEMBLY CLASS DEFINITIONS
 (all dimensions are in inches)

Fuel Assembly Designation	Clad Material	Pitch	Number of Fuel Rods	Cladding OD	Cladding Thickness	Pellet Diameter	Active Fuel Length	Number of Water Rods	Water Rod OD	Water Rod ID	Channel Thickness	Channel ID
6x6A Assembly Class												
6x6A01	Zr	0.694	36	0.5645	0.0350	0.4940	110.0	0	n/a	n/a	0.060	4.290
6x6A02	Zr	0.694	36	0.5645	0.0360	0.4820	110.0	0	n/a	n/a	0.060	4.290
6x6A03	Zr	0.694	36	0.5645	0.0350	0.4820	110.0	0	n/a	n/a	0.060	4.290
6x6A04	Zr	0.694	36	0.5550	0.0350	0.4820	110.0	0	n/a	n/a	0.060	4.290
6x6A05	Zr	0.696	36	0.5625	0.0350	0.4820	110.0	0	n/a	n/a	0.060	4.290
6x6A06	Zr	0.696	35	0.5625	0.0350	0.4820	110.0	1	0.0	0.0	0.060	4.290
6x6A07	Zr	0.700	36	0.5555	0.03525	0.4780	110.0	0	n/a	n/a	0.060	4.290
6x6A08	Zr	0.710	36	0.5625	0.0260	0.4980	110.0	0	n/a	n/a	0.060	4.290
6x6B (MOX) Assembly Class												
6x6B01	Zr	0.694	36	0.5645	0.0350	0.4820	110.0	0	n/a	n/a	0.060	4.290
6x6B02	Zr	0.694	36	0.5625	0.0350	0.4820	110.0	0	n/a	n/a	0.060	4.290
6x6B03	Zr	0.696	36	0.5625	0.0350	0.4820	110.0	0	n/a	n/a	0.060	4.290
6x6B04	Zr	0.696	35	0.5625	0.0350	0.4820	110.0	1	0.0	0.0	0.060	4.290
6x6B05	Zr	0.710	35	0.5625	0.0350	0.4820	110.0	1	0.0	0.0	0.060	4.290
6x6C Assembly Class												
6x6C01	Zr	0.740	36	0.5630	0.0320	0.4880	77.5	0	n/a	n/a	0.060	4.542
7x7A Assembly Class												
7x7A01	Zr	0.631	49	0.4860	0.0328	0.4110	80	0	n/a	n/a	0.060	4.542

Table 6.2.1 (page 2 of 6)
 BWR FUEL CHARACTERISTICS AND ASSEMBLY CLASS DEFINITIONS
 (all dimensions are in inches)

Fuel Assembly Designation	Clad Material	Pitch	Number of Fuel Rods	Cladding OD	Cladding Thickness	Pellet Diameter	Active Fuel Length	Number of Water Rods	Water Rod OD	Water Rod ID	Channel Thickness	Channel ID
7x7B Assembly Class												
7x7B01	Zr	0.738	49	0.5630	0.0320	0.4870	150	0	n/a	n/a	0.080	5.278
7x7B02	Zr	0.738	49	0.5630	0.0370	0.4770	150	0	n/a	n/a	0.102	5.291
7x7B03	Zr	0.738	49	0.5630	0.0370	0.4770	150	0	n/a	n/a	0.080	5.278
7x7B04	Zr	0.738	49	0.5700	0.0355	0.4880	150	0	n/a	n/a	0.080	5.278
7x7B05	Zr	0.738	49	0.5630	0.0340	0.4775	150	0	n/a	n/a	0.080	5.278
7x7B06	Zr	0.738	49	0.5700	0.0355	0.4910	150	0	n/a	n/a	0.080	5.278
8x8A Assembly Class												
8x8A01	Zr	0.523	64	0.4120	0.0250	0.3580	110	0	n/a	n/a	0.100	4.290
8x8A02	Zr	0.523	63	0.4120	0.0250	0.3580	120	0	n/a	n/a	0.100	4.290

Table 6.2.1 (page 3 of 6)
 BWR FUEL CHARACTERISTICS AND ASSEMBLY CLASS DEFINITIONS
 (all dimensions are in inches)

Fuel Assembly Designation	Clad Material	Pitch	Number of Fuel Rods	Cladding OD	Cladding Thickness	Pellet Diameter	Active Fuel Length	Number of Water Rods	Water Rod OD	Water Rod ID	Channel Thickness	Channel ID
8x8B Assembly Class												
8x8B01	Zr	0.641	63	0.4840	0.0350	0.4050	150	1	0.484	0.414	0.100	5.278
8x8B02	Zr	0.636	63	0.4840	0.0350	0.4050	150	1	0.484	0.414	0.100	5.278
8x8B03	Zr	0.640	63	0.4930	0.0340	0.4160	150	1	0.493	0.425	0.100	5.278
8x8B04	Zr	0.642	64	0.5015	0.0360	0.4195	150	0	n/a	n/a	0.100	5.278
8x8C Assembly Class												
8x8C01	Zr	0.641	62	0.4840	0.0350	0.4050	150	2	0.484	0.414	0.100	5.278
8x8C02	Zr	0.640	62	0.4830	0.0320	0.4100	150	2	0.591	0.531	0.000	no channel
8x8C03	Zr	0.640	62	0.4830	0.0320	0.4100	150	2	0.591	0.531	0.080	5.278
8x8C04	Zr	0.640	62	0.4830	0.0320	0.4100	150	2	0.591	0.531	0.100	5.278
8x8C05	Zr	0.640	62	0.4830	0.0320	0.4100	150	2	0.591	0.531	0.120	5.278
8x8C06	Zr	0.640	62	0.4830	0.0320	0.4110	150	2	0.591	0.531	0.100	5.278
8x8C07	Zr	0.640	62	0.4830	0.0340	0.4100	150	2	0.591	0.531	0.100	5.278
8x8C08	Zr	0.640	62	0.4830	0.0320	0.4100	150	2	0.493	0.425	0.100	5.278
8x8C09	Zr	0.640	62	0.4930	0.0340	0.4160	150	2	0.493	0.425	0.100	5.278
8x8C10	Zr	0.640	62	0.4830	0.0340	0.4100	150	2	0.591	0.531	0.120	5.278
8x8C11	Zr	0.640	62	0.4830	0.0340	0.4100	150	2	0.591	0.531	0.120	5.215
8x8C12	Zr	0.636	62	0.4830	0.0320	0.4110	150	2	0.591	0.531	0.120	5.215

Table 6.2.1 (page 4 of 6)
 BWR FUEL CHARACTERISTICS AND ASSEMBLY CLASS DEFINITIONS
 (all dimensions are in inches)

Fuel Assembly Designation	Clad Material	Pitch	Number of Fuel Rods	Cladding OD	Cladding Thickness	Pellet Diameter	Active Fuel Length	Number of Water Rods	Water Rod OD	Water Rod ID	Channel Thickness	Channel ID
8x8D Assembly Class												
8x8D01	Zr	0.640	60	0.4830	0.0320	0.4110	150	2 large/ 2 small	0.591/ 0.483	0.531/ 0.433	0.100	5.278
8x8D02	Zr	0.640	60	0.4830	0.0320	0.4110	150	4	0.591	0.531	0.100	5.278
8x8D03	Zr	0.640	60	0.4830	0.0320	0.4110	150	4	0.483	0.433	0.100	5.278
8x8D04	Zr	0.640	60	0.4830	0.0320	0.4110	150	1	1.34	1.26	0.100	5.278
8x8D05	Zr	0.640	60	0.4830	0.0320	0.4100	150	1	1.34	1.26	0.100	5.278
8x8D06	Zr	0.640	60	0.4830	0.0320	0.4110	150	1	1.34	1.26	0.120	5.278
8x8D07	Zr	0.640	60	0.4830	0.0320	0.4110	150	1	1.34	1.26	0.080	5.278
8x8D08	Zr	0.640	61	0.4830	0.0300	0.4140	150	3	0.591	0.531	0.080	5.278
8x8E Assembly Class												
8x8E01	Zr	0.640	59	0.4930	0.0340	0.4160	150	5	0.493	0.425	0.100	5.278
8x8F Assembly Class												
8x8F01	Zr	0.609	64	0.4576	0.0290	0.3913	150	4 [†]	0.291 [†]	0.228 [†]	0.055	5.390
9x9A Assembly Class												
9x9A01	Zr	0.566	74	0.4400	0.0280	0.3760	150	2	0.98	0.92	0.100	5.278
9x9A02	Zr	0.566	66	0.4400	0.0280	0.3760	150	2	0.98	0.92	0.100	5.278
9x9A03	Zr	0.566	74/66	0.4400	0.0280	0.3760	150/90	2	0.98	0.92	0.100	5.278
9x9A04	Zr	0.566	74/66	0.4400	0.0280	0.3760	150/90	2	0.98	0.92	0.120	5.278

[†] Four rectangular water cross segments dividing the assembly into four quadrants

Table 6.2.1 (page 5 of 6)
 BWR FUEL CHARACTERISTICS AND ASSEMBLY CLASS DEFINITIONS
 (all dimensions are in inches)

Fuel Assembly Designation	Clad Material	Pitch	Number of Fuel Rods	Cladding OD	Cladding Thickness	Pellet Diameter	Active Fuel Length	Number of Water Rods	Water Rod OD	Water Rod ID	Channel Thickness	Channel ID
9x9B Assembly Class												
9x9B01	Zr	0.569	72	0.4330	0.0262	0.3737	150	1	1.516	1.459	0.100	5.278
9x9B02	Zr	0.569	72	0.4330	0.0260	0.3737	150	1	1.516	1.459	0.100	5.278
9x9B03	Zr	0.572	72	0.4330	0.0260	0.3737	150	1	1.516	1.459	0.100	5.278
9x9C Assembly Class												
9x9C01	Zr	0.572	80	0.4230	0.0295	0.3565	150	1	0.512	0.472	0.100	5.278
9x9D Assembly Class												
9x9D01	Zr	0.572	79	0.4240	0.0300	0.3565	150	2	0.424	0.364	0.100	5.278
9x9E Assembly Class [†]												
9x9E01	Zr	0.572	76	0.4170	0.0265	0.3530	150	5	0.546	0.522	0.120	5.215
9x9E02	Zr	0.572	48 28	0.4170 0.4430	0.0265 0.0285	0.3530 0.3745	150	5	0.546	0.522	0.120	5.215
9x9F Assembly Class [†]												
9x9F01	Zr	0.572	76	0.4430	0.0285	0.3745	150	5	0.546	0.522	0.120	5.215
9x9F02	Zr	0.572	48 28	0.4170 0.4430	0.0265 0.0285	0.3530 0.3745	150	5	0.546	0.522	0.120	5.215

[†] The 9x9E and 9x9F fuel assembly classes represent a single fuel type containing fuel rods with different dimensions (SPC 9x9-5). In addition to the actual configuration (9x9E02 and 9x9F02), the 9x9E class contains a hypothetical assembly with only small fuel rods (9x9E01), and the 9x9F class contains a hypothetical assembly with only large rods (9x9F01). This was done in order to simplify the specification of this assembly in the CoC.

Table 6.2.1 (page 6 of 6)
 BWR FUEL CHARACTERISTICS AND ASSEMBLY CLASS DEFINITIONS
 (all dimensions are in inches)

Fuel Assembly Designation	Clad Material	Pitch	Number of Fuel Rods	Cladding OD	Cladding Thickness	Pellet Diameter	Active Fuel Length	Number of Water Rods	Water Rod OD	Water Rod ID	Channel Thickness	Channel ID
10x10A Assembly Class												
10x10A01	Zr	0.510	92	0.4040	0.0260	0.3450	155	2	0.980	0.920	0.100	5.278
10x10A02	Zr	0.510	78	0.4040	0.0260	0.3450	155	2	0.980	0.920	0.100	5.278
10x10A03	Zr	0.510	92/78	0.4040	0.0260	0.3450	155/90	2	0.980	0.920	0.100	5.278
10x10B Assembly Class												
10x10B01	Zr	0.510	91	0.3957	0.0239	0.3413	155	1	1.378	1.321	0.100	5.278
10x10B02	Zr	0.510	83	0.3957	0.0239	0.3413	155	1	1.378	1.321	0.100	5.278
10x10B03	Zr	0.510	91/83	0.3957	0.0239	0.3413	155/90	1	1.378	1.321	0.100	5.278
10x10C Assembly Class												
10x10C01	Zr	0.488	96	0.3780	0.0243	0.3224	150	5	1.227	1.165	0.055	5.457
10x10D Assembly Class												
10x10D01	SS	0.565	100	0.3960	0.0200	0.3500	83	0	n/a	n/a	0.08	5.663
10x10E Assembly Class												
10x10E01	SS	0.557	96	0.3940	0.0220	0.3430	83	4	0.3940	0.3500	0.08	5.663

Table 6.2.2 (page 1 of 3)
PWR FUEL CHARACTERISTICS AND ASSEMBLY CLASS DEFINITIONS
(all dimensions are in inches)

Fuel Assembly Designation	Clad Material	Pitch	Number of Fuel Rods	Cladding OD	Cladding Thickness	Pellet Diameter	Active Fuel Length	Number of Guide Tubes	Guide Tube OD	Guide Tube ID	Guide Tube Thickness
14x14A Assembly Class											
14x14A01	Zr	0.556	179	0.400	0.0243	0.3444	150	17	0.527	0.493	0.0170
14x14A02	Zr	0.556	179	0.400	0.0243	0.3444	150	17	0.528	0.490	0.0190
14x14A03	Zr	0.556	179	0.400	0.0243	0.3444	150	17	0.526	0.492	0.0170
14x14B Assembly Class											
14x14B01	Zr	0.556	179	0.422	0.0243	0.3659	150	17	0.539	0.505	0.0170
14x14B02	Zr	0.556	179	0.417	0.0295	0.3505	150	17	0.541	0.507	0.0170
14x14B03	Zr	0.556	179	0.424	0.0300	0.3565	150	17	0.541	0.507	0.0170
14x14B04	Zr	0.556	179	0.426	0.0310	0.3565	150	17	0.541	0.507	0.0170
14x14C Assembly Class											
14x14C01	Zr	0.580	176	0.440	0.0280	0.3765	150	5	1.115	1.035	0.0400
14x14C02	Zr	0.580	176	0.440	0.0280	0.3770	150	5	1.115	1.035	0.0400
14x14C03	Zr	0.580	176	0.440	0.0260	0.3805	150	5	1.111	1.035	0.0380
14x14D Assembly Class											
14x14D01	SS	0.556	180	0.422	0.0165	0.3835	144	16	0.543	0.514	0.0145
15x15A Assembly Class											
15x15A01	Zr	0.550	204	0.418	0.0260	0.3580	150	5	0.533	0.500	0.0165

Table 6.2.2 (page 2 of 3)
PWR FUEL CHARACTERISTICS AND ASSEMBLY CLASS DEFINITIONS
(all dimensions are in inches)

Fuel Assembly Designation	Clad Material	Pitch	Number of Fuel Rods	Cladding OD	Cladding Thickness	Pellet Diameter	Active Fuel Length	Number of Guide Tubes	Guide Tube OD	Guide Tube ID	Guide Tube Thickness
15x15B Assembly Class											
15x15B01	Zr	0.563	204	0.422	0.0245	0.3660	150	21	0.533	0.499	0.0170
15x15B02	Zr	0.563	204	0.422	0.0245	0.3660	150	21	0.546	0.512	0.0170
15x15B03	Zr	0.563	204	0.422	0.0243	0.3660	150	21	0.533	0.499	0.0170
15x15B04	Zr	0.563	204	0.422	0.0243	0.3659	150	21	0.545	0.515	0.0150
15x15B05	Zr	0.563	204	0.422	0.0242	0.3659	150	21	0.545	0.515	0.0150
15x15B06	Zr	0.563	204	0.420	0.0240	0.3671	150	21	0.544	0.514	0.0150
15x15C Assembly Class											
15x15C01	Zr	0.563	204	0.424	0.0300	0.3570	150	21	0.544	0.493	0.0255
15x15C02	Zr	0.563	204	0.424	0.0300	0.3570	150	21	0.544	0.511	0.0165
15x15C03	Zr	0.563	204	0.424	0.0300	0.3565	150	21	0.544	0.511	0.0165
15x15C04	Zr	0.563	204	0.417	0.0300	0.3565	150	21	0.544	0.511	0.0165
15x15D Assembly Class											
15x15D01	Zr	0.568	208	0.430	0.0265	0.3690	150	17	0.530	0.498	0.0160
15x15D02	Zr	0.568	208	0.430	0.0265	0.3686	150	17	0.530	0.498	0.0160
15x15D03	Zr	0.568	208	0.430	0.0265	0.3700	150	17	0.530	0.499	0.0155
15x15D04	Zr	0.568	208	0.430	0.0250	0.3735	150	17	0.530	0.500	0.0150
15x15E Assembly Class											
15x15E01	Zr	0.568	208	0.428	0.0245	0.3707	150	17	0.528	0.500	0.0140
15x15F Assembly Class											
15x15F01	Zr	0.568	208	0.428	0.0230	0.3742	150	17	0.528	0.500	0.0140

Table 6.2.2 (page 3 of 3)
PWR FUEL CHARACTERISTICS AND ASSEMBLY CLASS DEFINITIONS
(all dimensions are in inches)

Fuel Assembly Designation	Clad Material	Pitch	Number of Fuel Rods	Cladding OD	Cladding Thickness	Pellet Diameter	Active Fuel Length	Number of Guide Tubes	Guide Tube OD	Guide Tube ID	Guide Tube Thickness
15x15G Assembly Class											
15x15G01	SS	0.563	204	0.422	0.0165	0.3825	144	21	0.543	0.514	0.0145
15x15H Assembly Class											
15x15H01	Zr	0.568	208	0.414	0.0220	0.3622	150	17	0.528	0.500	0.0140
16x16A Assembly Class											
16x16A01	Zr	0.506	236	0.382	0.0250	0.3255	150	5	0.980	0.900	0.0400
16x16A02	Zr	0.506	236	0.382	0.0250	0.3250	150	5	0.980	0.900	0.0400
17x17A Assembly Class											
17x17A01	Zr	0.496	264	0.360	0.0225	0.3088	144	25	0.474	0.442	0.0160
17x17A02	Zr	0.496	264	0.360	0.0225	0.3088	150	25	0.474	0.442	0.0160
17x17A03	Zr	0.496	264	0.360	0.0250	0.3030	150	25	0.480	0.448	0.0160
17x17B Assembly Class											
17x17B01	Zr	0.496	264	0.374	0.0225	0.3225	150	25	0.482	0.450	0.0160
17x17B02	Zr	0.496	264	0.374	0.0225	0.3225	150	25	0.474	0.442	0.0160
17x17B03	Zr	0.496	264	0.376	0.0240	0.3215	150	25	0.480	0.448	0.0160
17x17B04	Zr	0.496	264	0.372	0.0205	0.3232	150	25	0.427	0.399	0.0140
17x17B05	Zr	0.496	264	0.374	0.0240	0.3195	150	25	0.482	0.450	0.0160
17x17B06	Zr	0.496	264	0.372	0.0205	0.3232	150	25	0.480	0.452	0.0140
17x17C Assembly Class											
17x17C01	Zr	0.502	264	0.379	0.0240	0.3232	150	25	0.472	0.432	0.0200
17x17C02	Zr	0.502	264	0.377	0.0220	0.3252	150	25	0.472	0.432	0.0200

Table 6.2.3
 REACTIVITY EFFECT OF ASSEMBLY PARAMETER VARIATIONS
 (all dimensions are in inches)

Fuel Assembly/ Parameter Variation	reactivity effect	calculated k_{eff}	standard deviation	cladding OD	cladding ID	cladding thickness	pellet OD	water rod thickness	channel thickness
8x8C04 (GE8x8R)	reference	0.9307	0.0007	0.483	0.419	0.032	0.410	0.030	0.100
increase pellet OD (+0.001)	+0.0005	0.9312	0.0007	0.483	0.419	0.032	0.411	0.030	0.100
decrease pellet OD (-0.001)	-0.0008	0.9299	0.0009	0.483	0.419	0.032	0.409	0.030	0.100
increase clad ID (+0.004)	+0.0027	0.9334	0.0007	0.483	0.423	0.030	0.410	0.030	0.100
decrease clad ID (-0.004)	-0.0034	0.9273	0.0007	0.483	0.415	0.034	0.410	0.030	0.100
increase clad OD (+0.004)	-0.0041	0.9266	0.0008	0.487	0.419	0.034	0.410	0.030	0.100
decrease clad OD (-0.004)	+0.0023	0.9330	0.0007	0.479	0.419	0.030	0.410	0.030	0.100
increase water rod thickness (+0.015)	-0.0019	0.9288	0.0008	0.483	0.419	0.032	0.410	0.045	0.100
decrease water rod thickness (-0.015)	+0.0001	0.9308	0.0008	0.483	0.419	0.032	0.410	0.015	0.100
remove water rods (i.e., replace the water rod tubes with water)	+0.0021	0.9328	0.0008	0.483	0.419	0.032	0.410	0.000	0.100
remove channel	-0.0039	0.9268	0.0009	0.483	0.419	0.032	0.410	0.030	0.000
increase channel thickness (+0.020)	+0.0005	0.9312	0.0007	0.483	0.419	0.032	0.410	0.030	0.120

Table 6.2.4
 MAXIMUM K_{EFF} VALUES FOR THE 14X14A ASSEMBLY CLASS IN THE MPC-24
 (all dimensions are in inches)

14x14A (4.6% Enrichment, Boral ^{10}B minimum loading of 0.02 g/cm ²)									
179 fuel rods, 17 guide tubes, pitch=0.556, Zr clad									
Fuel Assembly Designation	maximum k_{eff}	calculated k_{eff}	standard deviation	cladding OD	cladding ID	cladding thickness	pellet OD	fuel length	guide tube thickness
14x14A01	0.9378	0.9332	0.0010	0.400	0.3514	0.0243	0.3444	150	0.017
14x14A02	0.9374	0.9328	0.0009	0.400	0.3514	0.0243	0.3444	150	0.019
14x14A03	0.9383	0.9340	0.0008	0.400	0.3514	0.0243	0.3444	150	0.017
Dimensions Listed for Authorized Contents				0.400 (min.)	0.3514 (max.)		0.3444 (max.)	150 (max.)	0.017 (min.)
bounding dimensions (14x14A03)	0.9383	0.9340	0.0008	0.400	0.3514	0.0243	0.3444	150	0.017

Table 6.2.5
 MAXIMUM K_{EFF} VALUES FOR THE 14X14B ASSEMBLY CLASS IN THE MPC-24
 (all dimensions are in inches)

14x14B (4.6% Enrichment, Boral ^{10}B minimum loading of 0.02 g/cm ²)									
179 fuel rods, 17 guide tubes, pitch=0.556, Zr clad									
Fuel Assembly Designation	maximum k_{eff}	calculated k_{eff}	standard deviation	cladding OD	cladding ID	cladding thickness	pellet OD	fuel length	guide tube thickness
14x14B01	0.9268	0.9225	0.0008	0.422	0.3734	0.0243	0.3659	150	0.017
14x14B02	0.9243	0.9200	0.0008	0.417	0.3580	0.0295	0.3505	150	0.017
14x14B03	0.9196	0.9152	0.0009	0.424	0.3640	0.0300	0.3565	150	0.017
14x14B04	0.9163	0.9118	0.0009	0.426	0.3640	0.0310	0.3565	150	0.017
Dimensions Listed for Authorized Contents				0.417 (min.)	0.3734 (max.)		0.3659 (max.)	150 (max.)	0.017 (min.)
bounding dimensions (B14x14B01)	0.9323	0.9280	0.0008	0.417	0.3734	0.0218	0.3659	150	0.017

Table 6.2.6
 MAXIMUM K_{EFF} VALUES FOR THE 14X14C ASSEMBLY CLASS IN THE MPC-24
 (all dimensions are in inches)

14x14C (4.6% Enrichment, Boral ^{10}B minimum loading of 0.02 g/cm ²)									
176 fuel rods, 5 guide tubes, pitch=0.580, Zr clad									
Fuel Assembly Designation	maximum k_{eff}	calculated k_{eff}	standard deviation	cladding OD	cladding ID	cladding thickness	pellet OD	fuel length	guide tube thickness
14x14C01	0.9361	0.9317	0.0009	0.440	0.3840	0.0280	0.3765	150	0.040
14x14C02	0.9355	0.9312	0.0008	0.440	0.3840	0.0280	0.3770	150	0.040
14x14C03	0.9400	0.9357	0.0008	0.440	0.3880	0.0260	0.3805	150	0.038
Dimensions Listed for Authorized Contents				0.440 (min.)	0.3880 (max.)		0.3805 (max.)	150 (max.)	0.038 (min.)
bounding dimensions (14x14C01)	0.9400	0.9357	0.0008	0.440	0.3880	0.0260	0.3805	150	0.038

Table 6.2.7
 MAXIMUM K_{EFF} VALUES FOR THE 14X14D ASSEMBLY CLASS IN THE MPC-24
 (all dimensions are in inches)

14x14D (4.0% Enrichment, Boral ^{10}B minimum loading of 0.02 g/cm ²)									
180 fuel rods, 16 guide tubes, pitch=0.556, SS clad									
Fuel Assembly Designation	maximum k_{eff}	calculated k_{eff}	standard deviation	cladding OD	cladding ID	cladding thickness	pellet OD	fuel length	guide tube thickness
14x14D01	0.8576	0.8536	0.0007	0.422	0.3890	0.0165	0.3835	144	0.0145
Dimensions Listed for Authorized Contents				0.422 (min.)	0.3890 (max.)		0.3835 (max.)	144 (max.)	0.0145 (min.)

Table 6.2.8
 MAXIMUM K_{EFF} VALUES FOR THE 15X15A ASSEMBLY CLASS IN THE MPC-24
 (all dimensions are in inches)

15x15A (4.1% Enrichment, Boral ^{10}B minimum loading of 0.02 g/cm ²)									
204 fuel rods, 5 guide tubes, pitch=0.550, Zr clad									
Fuel Assembly Designation	maximum k_{eff}	calculated k_{eff}	standard deviation	cladding OD	cladding ID	cladding thickness	pellet OD	fuel length	guide tube thickness
15x15A01	0.9301	0.9259	0.0008	0.418	0.3660	0.0260	0.3580	150	0.0165
Dimensions Listed for Authorized Contents				0.418 (min.)	0.3660 (max.)		0.3580 (max.)	150 (max.)	0.0165 (min.)

Table 6.2.9
 MAXIMUM K_{EFF} VALUES FOR THE 15X15B ASSEMBLY CLASS IN THE MPC-24
 (all dimensions are in inches)

15x15B (4.1% Enrichment, Boral ^{10}B minimum loading of 0.02 g/cm ²)									
204 fuel rods, 21 guide tubes, pitch=0.563, Zr clad									
Fuel Assembly Designation	maximum k_{eff}	calculated k_{eff}	standard deviation	cladding OD	cladding ID	cladding thickness	pellet OD	fuel length	guide tube thickness
15x15B01	0.9427	0.9384	0.0008	0.422	0.3730	0.0245	0.3660	150	0.017
15x15B02	0.9441	0.9396	0.0009	0.422	0.3730	0.0245	0.3660	150	0.017
15x15B03	0.9462	0.9420	0.0008	0.422	0.3734	0.0243	0.3660	150	0.017
15x15B04	0.9452	0.9407	0.0009	0.422	0.3734	0.0243	0.3659	150	0.015
15x15B05	0.9473	0.9431	0.0008	0.422	0.3736	0.0242	0.3659	150	0.015
15x15B06	0.9448	0.9404	0.0008	0.420	0.3720	0.0240	0.3671	150	0.015
Dimensions Listed for Authorized Contents				0.420 (min.)	0.3736 (max.)		0.3671 (max.)	150 (max.)	0.015 (min.)
bounding dimensions (B15x15B01)	0.9471 [†]	0.9428	0.0008	0.420	0.3736	0.0232	0.3671	150	0.015

[†] The k_{eff} value listed for the 15x15B05 case is slightly higher than that for the case with the bounding dimensions. However, the difference (0.0002) is well within the statistical uncertainties, and thus, the two values are statistically equivalent (within 1σ). Therefore, the 0.9473 value is listed in Table 6.1.1 as the maximum.

Table 6.2.10
 MAXIMUM K_{EFF} VALUES FOR THE 15X15C ASSEMBLY CLASS IN THE MPC-24
 (all dimensions are in inches)

15x15C (4.1% Enrichment, Boral ^{10}B minimum loading of 0.02 g/cm ²)									
204 fuel rods, 21 guide tubes, pitch=0.563, Zr clad									
Fuel Assembly Designation	maximum k_{eff}	calculated k_{eff}	standard deviation	cladding OD	cladding ID	cladding thickness	pellet OD	fuel length	guide tube thickness
15x15C01	0.9332	0.9290	0.0007	0.424	0.3640	0.0300	0.3570	150	0.0255
15x15C02	0.9373	0.9330	0.0008	0.424	0.3640	0.0300	0.3570	150	0.0165
15x15C03	0.9377	0.9335	0.0007	0.424	0.3640	0.0300	0.3565	150	0.0165
15x15C04	0.9378	0.9338	0.0007	0.417	0.3570	0.0300	0.3565	150	0.0165
Dimensions Listed for Authorized Contents				0.417 (min.)	0.3640 (max.)		0.3570 (max.)	150 (max.)	0.0165 (min.)
bounding dimensions (B15x15C01)	0.9444	0.9401	0.0008	0.417	0.3640	0.0265	0.3570	150	0.0165

Table 6.2.11
 MAXIMUM K_{EFF} VALUES FOR THE 15X15D ASSEMBLY CLASS IN THE MPC-24
 (all dimensions are in inches)

15x15D (4.1% Enrichment, Boral ^{10}B minimum loading of 0.02 g/cm ²)									
208 fuel rods, 17 guide tubes, pitch=0.568, Zr clad									
Fuel Assembly Designation	maximum k_{eff}	calculated k_{eff}	standard deviation	cladding OD	cladding ID	cladding thickness	pellet OD	fuel length	guide tube thickness
15x15D01	0.9423	0.9380	0.0008	0.430	0.3770	0.0265	0.3690	150	0.0160
15x15D02	0.9430	0.9386	0.0009	0.430	0.3770	0.0265	0.3686	150	0.0160
15x15D03	0.9419	0.9375	0.0009	0.430	0.3770	0.0265	0.3700	150	0.0155
15x15D04	0.9440	0.9398	0.0007	0.430	0.3800	0.0250	0.3735	150	0.0150
Dimensions Listed for Authorized Contents				0.430 (min.)	0.3800 (max.)		0.3735 (max.)	150 (max.)	0.0150 (min.)
bounding dimensions (15x15D04)	0.9440	0.9398	0.0007	0.430	0.3800	0.0250	0.3735	150	0.0150

Table 6.2.12
 MAXIMUM K_{EFF} VALUES FOR THE 15X15E ASSEMBLY CLASS IN THE MPC-24
 (all dimensions are in inches)

15x15E (4.1% Enrichment, Boral ^{10}B minimum loading of 0.02 g/cm ²)									
208 fuel rods, 17 guide tubes, pitch=0.568, Zr clad									
Fuel Assembly Designation	maximum k_{eff}	calculated k_{eff}	standard deviation	cladding OD	cladding ID	cladding thickness	pellet OD	fuel length	guide tube thickness
15x15E01	0.9475	0.9433	0.0007	0.428	0.3790	0.0245	0.3707	150	0.0140
Dimensions Listed for Authorized Contents				0.428 (min.)	0.3790 (max.)		0.3707 (max.)	150 (max.)	0.0140 (min.)

Table 6.2.13
 MAXIMUM K_{EFF} VALUES FOR THE 15X15F ASSEMBLY CLASS IN THE MPC-24
 (all dimensions are in inches)

15x15F (4.1% Enrichment, Boral ^{10}B minimum loading of 0.02 g/cm ²)									
208 fuel rods, 17 guide tubes, pitch=0.568, Zr clad									
Fuel Assembly Designation	maximum k_{eff}	calculated k_{eff}	standard deviation	cladding OD	cladding ID	cladding thickness	pellet OD	fuel length	guide tube thickness
15x15F01	0.9478 [†]	0.9436	0.0008	0.428	0.3820	0.0230	0.3742	150	0.0140
Dimensions Listed for Authorized Contents				0.428 (min.)	0.3820 (max.)		0.3742 (max.)	150 (max.)	0.0140 (min.)

[†] KENO5a verification calculation resulted in a maximum k_{eff} of 0.9466.

Table 6.2.14
 MAXIMUM K_{EFF} VALUES FOR THE 15X15G ASSEMBLY CLASS IN THE MPC-24
 (all dimensions are in inches)

15x15G (4.0% Enrichment, Boral ^{10}B minimum loading of 0.02 g/cm ²)									
204 fuel rods, 21 guide tubes, pitch=0.563, SS clad									
Fuel Assembly Designation	maximum k_{eff}	calculated k_{eff}	standard deviation	cladding OD	cladding ID	cladding thickness	pellet OD	fuel length	guide tube thickness
15x15G01	0.8986	0.8943	0.0008	0.422	0.3890	0.0165	0.3825	144	0.0145
Dimensions Listed for Authorized Contents				0.422 (min.)	0.3890 (max.)		0.3825 (max.)	144 (max.)	0.0145 (min.)

Table 6.2.15
 MAXIMUM K_{EFF} VALUES FOR THE 15X15H ASSEMBLY CLASS IN THE MPC-24
 (all dimensions are in inches)

15x15H (3.8% Enrichment, Boral ^{10}B minimum loading of 0.02 g/cm ²)									
208 fuel rods, 17 guide tubes, pitch=0.568, Zr clad									
Fuel Assembly Designation	maximum k_{eff}	calculated k_{eff}	standard deviation	cladding OD	cladding ID	cladding thickness	pellet OD	fuel length	guide tube thickness
15x15H01	0.9411	0.9368	0.0008	0.414	0.3700	0.0220	0.3622	150	0.0140
Dimensions Listed for Authorized Contents				0.414 (min.)	0.3700 (max.)		0.3622 (max.)	150 (max.)	0.0140 (min.)

Table 6.2.16
 MAXIMUM K_{EFF} VALUES FOR THE 16X16A ASSEMBLY CLASS IN THE MPC-24
 (all dimensions are in inches)

16x16A (4.6% Enrichment, Boral ^{10}B minimum loading of 0.02 g/cm ²)									
236 fuel rods, 5 guide tubes, pitch=0.506, Zr clad									
Fuel Assembly Designation	maximum k_{eff}	calculated k_{eff}	standard deviation	cladding OD	cladding ID	cladding thickness	pellet OD	fuel length	guide tube thickness
16x16A01	0.9383	0.9339	0.0009	0.382	0.3320	0.0250	0.3255	150	0.0400
16x16A02	0.9371	0.9328	0.0008	0.382	0.3320	0.0250	0.3250	150	0.0400
Dimensions Listed for Authorized Contents				0.382 (min.)	0.3320 (max.)		0.3255 (max.)	150 (max.)	0.0400 (min.)
bounding dimensions (16x16A01)	0.9383	0.9339	0.0009	0.382	0.3320	0.0250	0.3255	150	0.0400

Table 6.2.17
 MAXIMUM K_{eff} VALUES FOR THE 17X17A ASSEMBLY CLASS IN THE MPC-24
 (all dimensions are in inches)

17x17A (4.0% Enrichment, Boral ^{10}B minimum loading of 0.02 g/cm ²)									
264 fuel rods, 25 guide tubes, pitch=0.496, Zr clad									
Fuel Assembly Designation	maximum k_{eff}	calculated k_{eff}	standard deviation	cladding OD	cladding ID	cladding thickness	pellet OD	fuel length	guide tube thickness
17x17A01	0.9449	0.9400	0.0011	0.360	0.3150	0.0225	0.3088	144	0.016
17x17A02	0.9452 [†]	0.9408	0.0008	0.360	0.3150	0.0225	0.3088	150	0.016
17x17A03	0.9406	0.9364	0.0008	0.360	0.3100	0.0250	0.3030	150	0.016
Dimensions Listed for Authorized Contents				0.360 (min.)	0.3150 (max.)		0.3088 (max.)	150 (max.)	0.016 (min.)
bounding dimensions (17x17A02)	0.9452	0.9408	0.0008	0.360	0.3150	0.0225	0.3088	150	0.016

[†] KENO5a verification calculation resulted in a maximum k_{eff} of 0.9434.

Table 6.2.18
 MAXIMUM K_{EFF} VALUES FOR THE 17X17B ASSEMBLY CLASS IN THE MPC-24
 (all dimensions are in inches)

17x17B (4.0% Enrichment, Boral ^{10}B minimum loading of 0.02 g/cm ²)									
264 fuel rods, 25 guide tubes, pitch=0.496, Zr clad									
Fuel Assembly Designation	maximum k_{eff}	calculated k_{eff}	standard deviation	cladding OD	cladding ID	cladding thickness	pellet OD	fuel length	guide tube thickness
17x17B01	0.9377	0.9335	0.0008	0.374	0.3290	0.0225	0.3225	150	0.016
17x17B02	0.9379	0.9337	0.0008	0.374	0.3290	0.0225	0.3225	150	0.016
17x17B03	0.9330	0.9288	0.0008	0.376	0.3280	0.0240	0.3215	150	0.016
17x17B04	0.9407	0.9365	0.0007	0.372	0.3310	0.0205	0.3232	150	0.014
17x17B05	0.9349	0.9305	0.0009	0.374	0.3260	0.0240	0.3195	150	0.016
17x17B06	0.9436	0.9393	0.0008	0.372	0.3310	0.0205	0.3232	150	0.014
Dimensions Listed for Authorized Contents				0.372 (min.)	0.3310 (max.)		0.3232 (max.)	150 (max.)	0.014 (min.)
bounding dimensions (17x17B06)	0.9436	0.9393	0.0008	0.372	0.3310	0.0205	0.3232	150	0.014

Table 6.2.19
 MAXIMUM K_{EFF} VALUES FOR THE 17X17C ASSEMBLY CLASS IN THE MPC-24
 (all dimensions are in inches)

17x17C (4.0% Enrichment, Boral ^{10}B minimum loading of 0.02 g/cm ²)									
264 fuel rods, 25 guide tubes, pitch=0.502, Zr clad									
Fuel Assembly Designation	maximum k_{eff}	calculated k_{eff}	standard deviation	cladding OD	cladding ID	cladding thickness	pellet OD	fuel length	guide tube thickness
17x17C01	0.9383	0.9339	0.0008	0.379	0.3310	0.0240	0.3232	150	0.020
17x17C02	0.9427	0.9384	0.0008	0.377	0.3330	0.0220	0.3252	150	0.020
Dimensions Listed for Authorized Contents				0.377 (min.)	0.3330 (max.)		0.3252 (max.)	150 (max.)	0.020 (min.)
bounding dimensions (17x17C02)	0.9427	0.9384	0.0008	0.377	0.3330	0.0220	0.3252	150	0.020

Table 6.2.20
 MAXIMUM K_{EFF} VALUES FOR THE 7X7B ASSEMBLY CLASS IN THE MPC-68
 (all dimensions are in inches)

7x7B (4.2% Enrichment, Boral ^{10}B minimum loading of 0.0279 g/cm ²)										
49 fuel rods, 0 water rods, pitch=0.738, Zr clad										
Fuel Assembly Designation	maximum k_{eff}	calculated k_{eff}	standard deviation	cladding OD	cladding ID	cladding thickness	pellet OD	fuel length	water rod thickness	channel thickness
7x7B01	0.9372	0.9330	0.0007	0.5630	0.4990	0.0320	0.4870	150	n/a	0.080
7x7B02	0.9301	0.9260	0.0007	0.5630	0.4890	0.0370	0.4770	150	n/a	0.102
7x7B03	0.9313	0.9271	0.0008	0.5630	0.4890	0.0370	0.4770	150	n/a	0.080
7x7B04	0.9311	0.9270	0.0007	0.5700	0.4990	0.0355	0.4880	150	n/a	0.080
7x7B05	0.9350	0.9306	0.0008	0.5630	0.4950	0.0340	0.4775	150	n/a	0.080
7x7B06	0.9298	0.9260	0.0006	0.5700	0.4990	0.0355	0.4910	150	n/a	0.080
Dimensions Listed for Authorized Contents				0.5630 (min.)	0.4990 (max.)		0.4910 (max.)	150 (max.)	n/a	0.120 (max.)
bounding dimensions (B7x7B01)	0.9375	0.9332	0.0008	0.5630	0.4990	0.0320	0.4910	150	n/a	0.102
bounding dimensions with 120 mil channel (B7x7B02)	0.9386	0.9344	0.0007	0.5630	0.4990	0.0320	0.4910	150	n/a	0.120

Table 6.2.21
 MAXIMUM K_{EFF} VALUES FOR THE 8X8B ASSEMBLY CLASS IN THE MPC-68
 (all dimensions are in inches)

8x8B (4.2% Enrichment, Boral ^{10}B minimum loading of 0.0279 g/cm ²)												
63 or 64 fuel rods, 1 or 0 water rods, pitch [†] = 0.636-0.642, Zr clad												
Fuel Assembly Designation	maximum k_{eff}	calculated k_{eff}	standard deviation	Fuel rods	pitch	cladding OD	cladding ID	cladding thickness	pellet OD	fuel length	water rod thickness	channel thickness
8x8B01	0.9310	0.9265	0.0009	63	0.641	0.4840	0.4140	0.0350	0.4050	150	0.035	0.100
8x8B02	0.9227	0.9185	0.0007	63	0.636	0.4840	0.4140	0.0350	0.4050	150	0.035	0.100
8x8B03	0.9299	0.9257	0.0008	63	0.640	0.4930	0.4250	0.0340	0.4160	150	0.034	0.100
8x8B04	0.9236	0.9194	0.0008	64	0.642	0.5015	0.4295	0.0360	0.4195	150	n/a	0.100
Dimensions Listed for Authorized Contents				63 or 64	0.636-0.642	0.4840 (min.)	0.4295 (max.)		0.4195 (max.)	150 (max.)	0.034	0.120 (max.)
bounding (pitch=0.636) (B8x8B01)	0.9346	0.9301	0.0009	63	0.636	0.4840	0.4295	0.02725	0.4195	150	0.034	0.120
bounding (pitch=0.640) (B8x8B02)	0.9385	0.9343	0.0008	63	0.640	0.4840	0.4295	0.02725	0.4195	150	0.034	0.120
bounding (pitch=0.641) (B8x8B03)	0.9416	0.9375	0.0007	63	0.642	0.4840	0.4295	0.02725	0.4195	150	0.034	0.120

[†] This assembly class was analyzed and qualified for a small variation in the pitch and a variation in the number of fuel and water rods.

Table 6.2.22
 MAXIMUM K_{EFF} VALUES FOR THE 8X8C ASSEMBLY CLASS IN THE MPC-68
 (all dimensions are in inches)

8x8C (4.2% Enrichment, Boral ^{10}B minimum loading of 0.0279 g/cm ²)											
62 fuel rods, 2 water rods, pitch [†] = 0.636-0.641, Zr clad											
Fuel Assembly Designation	maximum k_{eff}	calculated k_{eff}	standard deviation	pitch	cladding OD	cladding ID	cladding thickness	pellet OD	fuel length	water rod thickness	channel thickness
8x8C01	0.9315	0.9273	0.0007	0.641	0.4840	0.4140	0.0350	0.4050	150	0.035	0.100
8x8C02	0.9313	0.9268	0.0009	0.640	0.4830	0.4190	0.0320	0.4100	150	0.030	0.000
8x8C03	0.9329	0.9286	0.0008	0.640	0.4830	0.4190	0.0320	0.4100	150	0.030	0.800
8x8C04	0.9348 ^{††}	0.9307	0.0007	0.640	0.4830	0.4190	0.0320	0.4100	150	0.030	0.100
8x8C05	0.9353	0.9312	0.0007	0.640	0.4830	0.4190	0.0320	0.4100	150	0.030	0.120
8x8C06	0.9353	0.9312	0.0007	0.640	0.4830	0.4190	0.0320	0.4110	150	0.030	0.100
8x8C07	0.9314	0.9273	0.0007	0.640	0.4830	0.4150	0.0340	0.4100	150	0.030	0.100
8x8C08	0.9339	0.9298	0.0007	0.640	0.4830	0.4190	0.0320	0.4100	150	0.034	0.100
8x8C09	0.9301	0.9260	0.0007	0.640	0.4930	0.4250	0.0340	0.4160	150	0.034	0.100
8x8C10	0.9317	0.9275	0.0008	0.640	0.4830	0.4150	0.0340	0.4100	150	0.030	0.120
8x8C11	0.9328	0.9287	0.0007	0.640	0.4830	0.4150	0.0340	0.4100	150	0.030	0.120
8x8C12	0.9285	0.9242	0.0008	0.636	0.4830	0.4190	0.0320	0.4110	150	0.030	0.120
Dimensions Listed for Authorized Contents				0.636-0.641	0.4830 (min.)	0.4250 (max.)		0.4160 (max.)	150 (max.)	0.000 (min.)	0.120 (max.)
bounding (pitch=0.636) (B8x8C01)	0.9357	0.9313	0.0009	0.636	0.4830	0.4250	0.0290	0.4160	150	0.000	0.120
bounding (pitch=0.640) (B8x8C02)	0.9425	0.9384	0.0007	0.640	0.4830	0.4250	0.0290	0.4160	150	0.000	0.120
bounding (pitch=0.641) (B8x8C03)	0.9418	0.9375	0.0008	0.641	0.4830	0.4250	0.0290	0.4160	150	0.000	0.120

[†] This assembly class was analyzed and qualified for a small variation in the pitch.

^{††} KENO5a verification calculation resulted in a maximum k_{eff} of 0.9343.

Table 6.2.23
 MAXIMUM K_{EFF} VALUES FOR THE 8X8D ASSEMBLY CLASS IN THE MPC-68
 (all dimensions are in inches)

8x8D (4.2% Enrichment, Boral ^{10}B minimum loading of 0.0279 g/cm ²)										
60 fuel rods, 1-4 water rods [†] , pitch=0.640, Zr clad										
Fuel Assembly Designation	maximum k_{eff}	calculated k_{eff}	standard deviation	cladding OD	cladding ID	cladding thickness	pellet OD	fuel length	water rod thickness	channel thickness
8x8D01	0.9342	0.9302	0.0006	0.4830	0.4190	0.0320	0.4110	150	0.03/0.025	0.100
8x8D02	0.9325	0.9284	0.0007	0.4830	0.4190	0.0320	0.4110	150	0.030	0.100
8x8D03	0.9351	0.9309	0.0008	0.4830	0.4190	0.0320	0.4110	150	0.025	0.100
8x8D04	0.9338	0.9296	0.0007	0.4830	0.4190	0.0320	0.4110	150	0.040	0.100
8x8D05	0.9339	0.9294	0.0009	0.4830	0.4190	0.0320	0.4100	150	0.040	0.100
8x8D06	0.9365	0.9324	0.0007	0.4830	0.4190	0.0320	0.4110	150	0.040	0.120
8x8D07	0.9341	0.9297	0.0009	0.4830	0.4190	0.0320	0.4110	150	0.040	0.080
8x8D08	0.9376	0.9332	0.0009	0.4830	0.4230	0.0300	0.4140	150	0.030	0.080
Dimensions Listed for Authorized Contents				0.4830 (min.)	0.4230 (max.)		0.4140 (max.)	150 (max.)	0.000 (min.)	0.120 (max.)
bounding dimensions (B8x8D01)	0.9403	0.9363	0.0007	0.4830	0.4230	0.0300	0.4140	150	0.000	0.120

[†] Fuel assemblies 8x8D01 through 8x8D03 have 4 water rods that are similar in size to the fuel rods, while assemblies 8x8D04 through 8x8D07 have 1 large water rod that takes the place of the 4 water rods. Fuel assembly 8x8D08 contains 3 water rods that are similar in size to the fuel rods.

Table 6.2.24
 MAXIMUM K_{EFF} VALUES FOR THE 8X8E ASSEMBLY CLASS IN THE MPC-68
 (all dimensions are in inches)

8x8E (4.2% Enrichment, Boral ^{10}B minimum loading of 0.0279 g/cm ²)										
59 fuel rods, 5 water rods, pitch=0.640, Zr clad										
Fuel Assembly Designation	maximum k_{eff}	calculated k_{eff}	standard deviation	cladding OD	cladding ID	cladding thickness	pellet OD	fuel length	water rod thickness	channel thickness
8x8E01	0.9312	0.9270	0.0008	0.4930	0.4250	0.0340	0.4160	150	0.034	0.100
Dimensions Listed for Authorized Contents				0.4930 (min.)	0.4250 (max.)		0.4160 (max.)	150 (max.)	0.034 (min.)	0.100 (max.)

Table 6.2.25
 MAXIMUM K_{EFF} VALUES FOR THE 8X8F ASSEMBLY CLASS IN THE MPC-68
 (all dimensions are in inches)

8x8F (3.6% Enrichment, Boral ^{10}B minimum loading of 0.0279 g/cm ²)										
64 fuel rods, 4 rectangular water cross segments dividing the assembly into four quadrants, pitch=0.609, Zr clad										
Fuel Assembly Designation	maximum k_{eff}	calculated k_{eff}	standard deviation	cladding OD	cladding ID	cladding thickness	pellet OD	fuel length	water rod thickness	channel thickness
8x8F01	0.9153	0.9111	0.0007	0.4576	0.3996	0.0290	0.3913	150	0.0315	0.055
Dimensions Listed for Authorized Contents				0.4576 (min.)	0.3996 (max.)		0.3913 (max.)	150 (max.)	0.0315 (min.)	0.055 (max.)

Table 6.2.26
 MAXIMUM K_{EFF} VALUES FOR THE 9X9A ASSEMBLY CLASS IN THE MPC-68
 (all dimensions are in inches)

9x9A (4.2% Enrichment, Boral ^{10}B minimum loading of 0.0279 g/cm ²)										
74/66 fuel rods [†] , 2 water rods, pitch=0.566, Zr clad										
Fuel Assembly Designation	maximum k_{eff}	calculated k_{eff}	standard deviation	cladding OD	cladding ID	cladding thickness	pellet OD	fuel length	water rod thickness	channel thickness
9x9A01 (axial segment with all rods)	0.9353	0.9310	0.0008	0.4400	0.3840	0.0280	0.3760	150	0.030	0.100
9x9A02 (axial segment with only the full length rods)	0.9388	0.9345	0.0008	0.4400	0.3840	0.0280	0.3760	150	0.030	0.100
9x9A03 (actual three-dimensional representation of all rods)	0.9351	0.9310	0.0007	0.4400	0.3840	0.0280	0.3760	150/90	0.030	0.100
9x9A04 (axial segment with only the full length rods)	0.9396	0.9355	0.0007	0.4400	0.3840	0.0280	0.3760	150	0.030	0.120
Dimensions Listed for Authorized Contents				0.4400 (min.)	0.3840 (max.)		0.3760 (max.)	150 (max.)	0.000 (min.)	0.120 (max.)
bounding dimensions (axial segment with only the full length rods) (B9x9A01)	0.9417	0.9374	0.0008	0.4400	0.3840	0.0280	0.3760	150	0.000	0.120

[†] This assembly class contains 66 full length rods and 8 partial length rods. In order to eliminate a requirement on the length of the partial length rods, separate calculations were performed for the axial segments with and without the partial length rods.

Table 6.2.27
 MAXIMUM K_{EFF} VALUES FOR THE 9X9B ASSEMBLY CLASS IN THE MPC-68
 (all dimensions are in inches)

9x9B (4.2% Enrichment, Boral ^{10}B minimum loading of 0.0279 g/cm ²)											
72 fuel rods, 1 water rod (square, replacing 9 fuel rods), pitch=0.569 to 0.572 [†] , Zr clad											
Fuel Assembly Designation	maximum k_{eff}	calculated k_{eff}	standard deviation	pitch	cladding OD	cladding ID	cladding thickness	pellet OD	fuel length	water rod thickness	channel thickness
9x9B01	0.9368	0.9326	0.0007	0.569	0.4330	0.3807	0.0262	0.3737	150	0.0285	0.100
9x9B02	0.9377	0.9334	0.0008	0.569	0.4330	0.3810	0.0260	0.3737	150	0.0285	0.100
9x9B03	0.9416	0.9373	0.0008	0.572	0.4330	0.3810	0.0260	0.3737	150	0.0285	0.100
Dimensions Listed for Authorized Contents				0.572	0.4330 (min.)	0.3810 (max.)		0.3740 (max.)	150 (max.)	0.000 (min.)	0.120 (max.)
bounding dimensions (B9x9B01)	0.9422	0.9380	0.0007	0.572	0.4330	0.3810	0.0260	0.3740 ^{††}	150	0.000	0.120

[†] This assembly class was analyzed and qualified for a small variation in the pitch.

^{††} This value was conservatively defined to be larger than any of the actual pellet diameters.

Table 6.2.28
 MAXIMUM K_{EFF} VALUES FOR THE 9X9C ASSEMBLY CLASS IN THE MPC-68
 (all dimensions are in inches)

9x9C (4.2% Enrichment, Boral ^{10}B minimum loading of 0.0279 g/cm ²)										
80 fuel rods, 1 water rods, pitch=0.572, Zr clad										
Fuel Assembly Designation	maximum k_{eff}	calculated k_{eff}	standard deviation	cladding OD	cladding ID	cladding thickness	pellet OD	fuel length	water rod thickness	channel thickness
9x9C01	0.9395	0.9352	0.0008	0.4230	0.3640	0.0295	0.3565	150	0.020	0.100
Dimensions Listed for Authorized Contents				0.4230 (min.)	0.3640 (max.)		0.3565 (max.)	150 (max.)	0.020 (min.)	0.100 (max.)

Table 6.2.29
 MAXIMUM K_{EFF} VALUES FOR THE 9X9D ASSEMBLY CLASS IN THE MPC-68
 (all dimensions are in inches)

9x9D (4.2% Enrichment, Boral ^{10}B minimum loading of 0.0279 g/cm^2)										
79 fuel rods, 2 water rods, pitch=0.572, Zr clad										
Fuel Assembly Designation	maximum k_{eff}	calculated k_{eff}	standard deviation	cladding OD	cladding ID	cladding thickness	pellet OD	fuel length	water rod thickness	channel thickness
9x9D01	0.9394	0.9350	0.0009	0.4240	0.3640	0.0300	0.3565	150	0.0300	0.100
Dimensions Listed for Authorized Contents				0.4240 (min.)	0.3640 (max.)		0.3565 (max.)	150 (max.)	0.0300 (min.)	0.100 (max.)

Table 6.2.30
 MAXIMUM K_{EFF} VALUES FOR THE 9X9E ASSEMBLY CLASS IN THE MPC-68
 (all dimensions are in inches)

9x9E (4.1% Enrichment, Boral ^{10}B minimum loading of 0.0279 g/cm ²)										
76 fuel rods, 5 water rods, pitch=0.572, Zr clad										
Fuel Assembly Designation	maximum k_{eff}	calculated k_{eff}	standard deviation	cladding OD	cladding ID	cladding thickness	pellet OD	fuel length	water rod thickness	channel thickness
9x9E01	0.9402	0.9359	0.0008	0.4170	0.3640	0.0265	0.3530	150	0.0120	0.120
9x9E02	0.9424	0.9380	0.0008	0.4170 0.4430	0.3640 0.3860	0.0265 0.0285	0.3530 0.3745	150	0.0120	0.120
Dimensions Listed for Authorized Contents [†]				0.4170 (min.)	0.3640 (max.)		0.3530 (max.)	150 (max.)	0.0120 (min.)	0.120 (max.)
bounding dimensions (9x9E02)	0.9424	0.9380	0.0008	0.4170 0.4430	0.3640 0.3860	0.0265 0.0285	0.3530 0.3745	150	0.0120	0.120

[†] This fuel assembly, also known as SPC 9x9-5, contains fuel rods with different cladding and pellet diameters which do not bound each other. To be consistent in the way fuel assemblies are listed for Authorized Contents, two assembly classes (9x9E and 9x9F) are required to specify this assembly. Each class contains the actual geometry (9x9E02 and 9x9F02), as well as a hypothetical geometry with either all small rods (9x9E01) or all large rods (9x9F01). The Authorized Content lists the small rod dimensions for class 9x9E and the large rod dimensions for class 9x9F, and a note that both classes are used to qualify the assembly. The analyses demonstrate that all configurations, including the actual geometry, are acceptable.

Table 6.2.31
 MAXIMUM K_{EFF} VALUES FOR THE 9X9F ASSEMBLY CLASS IN THE MPC-68
 (all dimensions are in inches)

9x9F (4.1% Enrichment, Boral ^{10}B minimum loading of 0.0279 g/cm ²)										
76 fuel rods, 5 water rods, pitch=0.572, Zr clad										
Fuel Assembly Designation	maximum k_{eff}	calculated k_{eff}	standard deviation	cladding OD	cladding ID	cladding thickness	pellet OD	fuel length	water rod thickness	channel thickness
9x9F01	0.9369	0.9326	0.0007	0.4430	0.3860	0.0285	0.3745	150	0.0120	0.120
9x9F02	0.9424	0.9380	0.0008	0.4170 0.4430	0.3640 0.3860	0.0265 0.0285	0.3530 0.3745	150	0.0120	0.120
Dimensions Listed for Authorized Contents [†]				0.4430 (min.)	0.3860 (max.)		0.3745 (max.)	150 (max.)	0.0120 (min.)	0.120 (max.)
bounding dimensions (9x9F02)	0.9424	0.9380	0.0008	0.4170 0.4430	0.3640 0.3860	0.0265 0.0285	0.3530 0.3745	150	0.0120	0.120

[†] This fuel assembly, also known as SPC 9x9-5, contains fuel rods with different cladding and pellet diameters which do not bound each other. To be consistent in the way fuel assemblies are listed for Authorized Contents, two assembly classes (9x9E and 9x9F) are required to specify this assembly. Each class contains the actual geometry (9x9E02 and 9x9F02), as well as a hypothetical geometry with either all small rods (9x9E01) or all large rods (9x9F01). The Authorized Content lists the small rod dimensions for class 9x9E and the large rod dimensions for class 9x9F, and a note that both classes are used to qualify the assembly. The analyses demonstrate that all configurations, including the actual geometry, are acceptable.

Table 6.2.32
 MAXIMUM K_{EFF} VALUES FOR THE 10X10A ASSEMBLY CLASS IN THE MPC-68
 (all dimensions are in inches)

10x10A (4.2% Enrichment, Boral ^{10}B minimum loading of 0.0279 g/cm ²)										
92/78 fuel rods [†] , 2 water rods, pitch=0.510, Zr clad										
Fuel Assembly Designation	maximum k_{eff}	calculated k_{eff}	standard deviation	cladding OD	cladding ID	cladding thickness	pellet OD	fuel length	water rod thickness	channel thickness
10x10A01 (axial segment with all rods)	0.9377	0.9335	0.0008	0.4040	0.3520	0.0260	0.3450	155	0.030	0.100
10x10A02 (axial segment with only the full length rods)	0.9426	0.9386	0.0007	0.4040	0.3520	0.0260	0.3450	155	0.030	0.100
10x10A03 (actual three-dimensional representation of all rods)	0.9396	0.9356	0.0007	0.4040	0.3520	0.0260	0.3450	155/90	0.030	0.100
Dimensions Listed for Authorized Contents				0.4040 (min.)	0.3520 (max.)		0.3455 (max.)	150 ^{††} (max.)	0.030 (min.)	0.120 (max.)
bounding dimensions (axial segment with only the full length rods) (B10x10A01)	0.9457 ^{†††}	0.9414	0.0008	0.4040	0.3520	0.0260	0.3455 [‡]	155	0.030	0.120

[†] This assembly class contains 78 full-length rods and 14 partial-length rods. In order to eliminate the requirement on the length of the partial length rods, separate calculations were performed for axial segments with and without the partial length rods.

^{††} Although the analysis qualifies this assembly for a maximum active fuel length of 155 inches, the specification for authorized contents limits the active fuel length to 150 inches. This is due to the fact that the Boral panels are 156 inches in length.

^{†††} KENO5a verification calculation resulted in a maximum k_{eff} of 0.9453.

[‡] This value was conservatively defined to be larger than any of the actual pellet diameters.

Table 6.2.33
 MAXIMUM K_{EFF} VALUES FOR THE 10X10B ASSEMBLY CLASS IN THE MPC-68
 (all dimensions are in inches)

10x10B (4.2% Enrichment, Boral ^{10}B minimum loading of 0.0279 g/cm ²)										
91/83 fuel rods [†] , 1 water rods (square, replacing 9 fuel rods), pitch=0.510, Zr clad										
Fuel Assembly Designation	maximum k_{eff}	calculated k_{eff}	standard deviation	cladding OD	cladding ID	cladding thickness	pellet OD	fuel length	water rod thickness	channel thickness
10x10B01 (axial segment with all rods)	0.9384	0.9341	0.0008	0.3957	0.3480	0.0239	0.3413	155	0.0285	0.100
10x10B02 (axial segment with only the full length rods)	0.9416	0.9373	0.0008	0.3957	0.3480	0.0239	0.3413	155	0.0285	0.100
10x10B03 (actual three-dimensional representation of all rods)	0.9375	0.9334	0.0007	0.3957	0.3480	0.0239	0.3413	155/90	0.0285	0.100
Dimensions Listed for Authorized Contents				0.3957 (min.)	0.3480 (max.)		0.3420 (max.)	150 ^{††} (max.)	0.000 (min.)	0.120 (max.)
bounding dimensions (axial segment with only the full length rods) (B10x10B01)	0.9436	0.9395	0.0007	0.3957	0.3480	0.0239	0.3420 ^{†††}	155	0.000	0.120

[†] This assembly class contains 83 full length rods and 8 partial length rods. In order to eliminate a requirement on the length of the partial length rods, separate calculations were performed for the axial segments with and without the partial length rods.

^{††} Although the analysis qualifies this assembly for a maximum active fuel length of 155 inches, the specification for authorized contents limits the active fuel length to 150 inches. This is due to the fact that the Boral panels are 156 inches in length.

^{†††} This value was conservatively defined to be larger than any of the actual pellet diameters.

Table 6.2.34
 MAXIMUM K_{EFF} VALUES FOR THE 10X10C ASSEMBLY CLASS IN THE MPC-68
 (all dimensions are in inches)

10x10C (4.2% Enrichment, Boral ^{10}B minimum loading of 0.0279 g/cm ²)										
96 fuel rods, 5 water rods (1 center diamond and 4 rectangular), pitch=0.488, Zr clad										
Fuel Assembly Designation	maximum k_{eff}	calculated k_{eff}	standard deviation	cladding OD	cladding ID	cladding thickness	pellet OD	fuel length	water rod thickness	channel thickness
10x10C01	0.9021	0.8980	0.0007	0.3780	0.3294	0.0243	0.3224	150	0.031	0.055
Dimensions Listed for Authorized Contents				0.3780 (min.)	0.3294 (max.)		0.3224 (max.)	150 (max.)	0.031 (min.)	0.055 (max.)

Table 6.2.35
 MAXIMUM K_{EFF} VALUES FOR THE 10X10D ASSEMBLY CLASS IN THE MPC-68
 (all dimensions are in inches)

10x10D (4.0% Enrichment, Boral ^{10}B minimum loading of 0.0279 g/cm ³)										
100 fuel rods, 0 water rods, pitch=0.565, SS clad										
Fuel Assembly Designation	maximum k_{eff}	calculated k_{eff}	standard deviation	cladding OD	cladding ID	cladding thickness	pellet OD	fuel length	water rod thickness	channel thickness
10x10D01	0.9376	0.9333	0.0008	0.3960	0.3560	0.0200	0.350	83	n/a	0.080
Dimensions Listed for Authorized Contents				0.3960 (min.)	0.3560 (max.)		0.350 (max.)	83 (max.)	n/a	0.080 (max.)

Table 6.2.36
 MAXIMUM K_{EFF} VALUES FOR THE 10X10E ASSEMBLY CLASS IN THE MPC-68
 (all dimensions are in inches)

10x10E (4.0% Enrichment, Boral ^{10}B minimum loading of 0.0279 g/cm ²)										
96 fuel rods, 4 water rods, pitch=0.557, SS clad										
Fuel Assembly Designation	maximum k_{eff}	calculated k_{eff}	standard deviation	cladding OD	cladding ID	cladding thickness	pellet OD	fuel length	water rod thickness	channel thickness
10x10E01	0.9185	0.9144	0.0007	0.3940	0.3500	0.0220	0.3430	83	0.022	0.080
Dimensions Listed for Authorized Contents				0.3940 (min.)	0.3500 (max.)		0.3430 (max.)	83 (max.)	0.022 (min.)	0.080 (max.)

Table 6.2.37
 MAXIMUM K_{EFF} VALUES FOR THE 6X6A ASSEMBLY CLASS IN THE MPC-68F
 (all dimensions are in inches)

6x6A (3.0% Enrichment [†] , Boral ¹⁰ B minimum loading of 0.0067 g/cm ²)												
35 or 36 fuel rods ^{††} , 1 or 0 water rods ^{††} , pitch=0.694 to 0.710 ^{††} , Zr clad												
Fuel Assembly Designation	maximum k_{eff}	calculated k_{eff}	standard deviation	pitch	fuel rods	cladding OD	cladding ID	cladding thickness	pellet OD	fuel length	water rod thickness	channel thickness
6x6A01	0.7539	0.7498	0.0007	0.694	36	0.5645	0.4945	0.0350	0.4940	110	n/a	0.060
6x6A02	0.7517	0.7476	0.0007	0.694	36	0.5645	0.4925	0.0360	0.4820	110	n/a	0.060
6x6A03	0.7545	0.7501	0.0008	0.694	36	0.5645	0.4945	0.0350	0.4820	110	n/a	0.060
6x6A04	0.7537	0.7494	0.0008	0.694	36	0.5550	0.4850	0.0350	0.4820	110	n/a	0.060
6x6A05	0.7555	0.7512	0.0008	0.696	36	0.5625	0.4925	0.0350	0.4820	110	n/a	0.060
6x6A06	0.7618	0.7576	0.0008	0.696	35	0.5625	0.4925	0.0350	0.4820	110	0.0	0.060
6x6A07	0.7588	0.7550	0.0007	0.700	36	0.5555	0.4850	0.03525	0.4780	110	n/a	0.060
6x6A08	0.7808	0.7766	0.0007	0.710	36	0.5625	0.5105	0.0260	0.4980	110	n/a	0.060
Dimensions Listed for Authorized Contents				0.710 (max.)	35 or 36	0.5550 (min.)	0.5105 (max.)	0.02225	0.4980 (max.)	120 (max.)	0.0	0.060 (max.)
bounding dimensions (B6x6A01)	0.7727	0.7685	0.0007	0.694	35	0.5550	0.5105	0.02225	0.4980	120	0.0	0.060
bounding dimensions (B6x6A02)	0.7782	0.7738	0.0008	0.700	35	0.5550	0.5105	0.02225	0.4980	120	0.0	0.060
bounding dimensions (B6x6A03)	0.7888	0.7846	0.0007	0.710	35	0.5550	0.5105	0.02225	0.4980	120	0.0	0.060

[†] Although the calculations were performed for 3.0%, the enrichment is limited in the specification for authorized contents to 2.7%.

^{††} This assembly class was analyzed and qualified for a small variation in the pitch and a variation in the number of fuel and water rods.

Table 6.2.38
 MAXIMUM K_{EFF} VALUES FOR THE 6X6B ASSEMBLY CLASS IN THE MPC-68F
 (all dimensions are in inches)

6x6B (3.0% Enrichment [†] , Boral ¹⁰ B minimum loading of 0.0067 g/cm ²)												
35 or 36 fuel rods ^{††} (up to 9 MOX rods), 1 or 0 water rods ^{††} , pitch=0.694 to 0.710 ^{††} , Zr clad												
Fuel Assembly Designation	maximum k_{eff}	calculated k_{eff}	standard deviation	pitch	fuel rods	cladding OD	cladding ID	cladding thickness	pellet OD	fuel length	water rod thickness	channel thickness
6x6B01	0.7604	0.7563	0.0007	0.694	36	0.5645	0.4945	0.0350	0.4820	110	n/a	0.060
6x6B02	0.7618	0.7577	0.0007	0.694	36	0.5625	0.4925	0.0350	0.4820	110	n/a	0.060
6x6B03	0.7619	0.7578	0.0007	0.696	36	0.5625	0.4925	0.0350	0.4820	110	n/a	0.060
6x6B04	0.7686	0.7644	0.0008	0.696	35	0.5625	0.4925	0.0350	0.4820	110	0.0	0.060
6x6B05	0.7824	0.7785	0.0006	0.710	35	0.5625	0.4925	0.0350	0.4820	110	0.0	0.060
Dimensions Listed for Authorized Contents				0.710 (max.)	35 or 36	0.5625 (min.)	0.4945 (max.)		0.4820 (max.)	120 (max.)	0.0	0.060 (max.)
bounding dimensions (B6x6B01)	0.7822 ^{†††}	0.7783	0.0007	0.710	35	0.5625	0.4945	0.0340	0.4820	120	0.0	0.060

Note:

1. These assemblies contain up to 9 MOX pins. The composition of the MOX fuel pins is given in Table 6.3.4.

[†] The ²³⁵U enrichment of the MOX and UO₂ pins is assumed to be 0.711% and 3.0%, respectively.

^{††} This assembly class was analyzed and qualified for a small variation in the pitch and a variation in the number of fuel and water rods.

^{†††} The k_{eff} value listed for the 6x6B05 case is slightly higher than that for the case with the bounding dimensions. However, the difference (0.0002) is well within the statistical uncertainties, and thus, the two values are statistically equivalent (within 1 σ). Therefore, the 0.7824 value is listed in Tables 6.1.2 and 6.1.3 as the maximum.

Table 6.2.39
 MAXIMUM K_{EFF} VALUES FOR THE 6X6C ASSEMBLY CLASS IN THE MPC-68F
 (all dimensions are in inches)

6x6C (3.0% Enrichment [†] , Boral ¹⁰ B minimum loading of 0.0067 g/cm ²)										
36 fuel rods, 0 water rods, pitch=0.740, Zr clad										
Fuel Assembly Designation	maximum k_{eff}	calculated k_{eff}	standard deviation	cladding OD	cladding ID	cladding thickness	pellet OD	fuel length	water rod thickness	channel thickness
6x6C01	0.8021	0.7980	0.0007	0.5630	0.4990	0.0320	0.4880	77.5	n/a	0.060
Dimensions Listed for Authorized Contents				0.5630 (min.)	0.4990 (max.)		0.4880 (max.)	77.5 (max.)	n/a	0.060 (max.)

[†] Although the calculations were performed for 3.0%, the enrichment is limited in the specification for authorized contents to 2.7%.

Table 6.2.40
 MAXIMUM K_{EFF} VALUES FOR THE 7X7A ASSEMBLY CLASS IN THE MPC-68F
 (all dimensions are in inches)

7x7A (3.0% Enrichment [†] , Boral ¹⁰ B minimum loading of 0.0067 g/cm ²)										
49 fuel rods, 0 water rods, pitch=0.631, Zr clad										
Fuel Assembly Designation	maximum k_{eff}	calculated k_{eff}	standard deviation	cladding OD	cladding ID	cladding thickness	pellet OD	fuel length	water rod thickness	channel thickness
7x7A01	0.7974	0.7932	0.0008	0.4860	0.4204	0.0328	0.4110	80	n/a	0.060
Dimensions Listed for Authorized Contents				0.4860 (min.)	0.4204 (max.)		0.4110 (max.)	80 (max.)	n/a	0.060 (max.)

[†] Although the calculations were performed for 3.0%, the enrichment is limited in the specification for authorized contents to 2.7%.

Table 6.2.41
 MAXIMUM K_{EFF} VALUES FOR THE 8X8A ASSEMBLY CLASS IN THE MPC-68F
 (all dimensions are in inches)

8x8A (3.0% Enrichment [†] , Boral ¹⁰ B minimum loading of 0.0067 g/cm ²)											
63 or 64 fuel rods ^{††} , 0 water rods, pitch=0.523, Zr clad											
Fuel Assembly Designation	maximum k_{eff}	calculated k_{eff}	standard deviation	fuel rods	cladding OD	cladding ID	cladding thickness	pellet OD	fuel length	water rod thickness	channel thickness
8x8A01	0.7685	0.7644	0.0007	64	0.4120	0.3620	0.0250	0.3580	110	n/a	0.100
8x8A02	0.7697	0.7656	0.0007	63	0.4120	0.3620	0.0250	0.3580	120	n/a	0.100
Dimensions Listed for Authorized Contents				63	0.4120 (min.)	0.3620 (max.)		0.3580 (max.)	110 (max.)	n/a	0.100 (max.)
bounding dimensions (8x8A02)	0.7697	0.7656	0.0007	63	0.4120	0.3620	0.0250	0.3580	120	n/a	0.100

[†] Although the calculations were performed for 3.0%, the enrichment is limited in the specification for authorized contents to 2.7%.

^{††} This assembly class was analyzed and qualified for a variation in the number of fuel rods.

Table 6.2.42

SPECIFICATION OF THE THORIA ROD CANISTER AND THE THORIA RODS

Canister ID	4.81"
Canister Wall Thickness	0.11"
Separator Assembly Plates Thickness	0.11"
Cladding OD	0.412"
Cladding ID	0.362"
Pellet OD	0.358"
Active Length	110.5"
Fuel Composition	1.8% UO ₂ and 98.2% ThO ₂
Initial Enrichment	93.5 wt% ²³⁵ U for 1.8% of the fuel
Maximum k _{eff}	0.1813
Calculated k _{eff}	0.1779
Standard Deviation	0.0004

Table 6.3.4 (continued)

COMPOSITION OF THE MAJOR COMPONENTS OF THE HI-STAR 100 SYSTEM

MPC-68		
UO₂ 4.2% ENRICHMENT, DENSITY (g/cc) = 10.522		
Nuclide	Atom-Density	Wgt. Fraction
8016	4.697E-02	1.185E-01
92235	9.983E-04	3.702E-02
92238	2.248E-02	8.445E-01
UO₂ 3.0% ENRICHMENT, DENSITY (g/cc) = 10.522		
Nuclide	Atom-Density	Wgt. Fraction
8016	4.695E-02	1.185E-01
92235	7.127E-04	2.644E-02
92238	2.276E-02	8.550E-01
MOX FUEL[†], DENSITY (g/cc) = 10.522		
Nuclide	Atom-Density	Wgt. Fraction
8016	4.714E-02	1.190E-01
92235	1.719E-04	6.380E-03
92238	2.285E-02	8.584E-01
94239	3.876E-04	1.461E-02
94240	9.177E-06	3.400E-04
94241	3.247E-05	1.240E-03
94242	2.118E-06	7.000E-05

[†] The Pu-238, which is an absorber, was conservatively neglected in the MOX description for analysis purposes.

Table 6.3.4 (continued)

COMPOSITION OF THE MAJOR COMPONENTS OF THE HI-STAR 100 SYSTEM

BORAL (0.0279 g ¹⁰B/cm sq), DENSITY (g/cc) = 2.660		
Nuclide	Atom-Density	Wgt. Fraction
5010	8.071E-03	5.089E-02
5011	3.255E-02	2.257E-01
6012	1.015E-02	7.675E-02
13027	3.805E-02	6.467E-01
FUEL IN THORIA RODS, DENSITY (g/cc) = 10.522		
Nuclide	Atom-Density	Wgt. Fraction
8016	4.798E-02	1.212E-01
92235	4.001E-04	1.484E-02
92238	2.742E-05	1.030E-03
90232	2.357E-02	8.630E-01

6.4 CRITICALITY CALCULATIONS

6.4.1 Calculational or Experimental Method

The principal method for the criticality analysis is the general three-dimensional continuous energy Monte Carlo N-Particle code MCNP4a [6.1.4] developed at the Los Alamos National Laboratory. MCNP4a was selected because it has been extensively used and verified and has all of the necessary features for this analysis. MCNP4a calculations used continuous energy cross-section data based on ENDF/B-V, as distributed with the code [6.1.4]. Independent verification calculations were performed with NITAWL-KENO5a [6.1.5], which is a three-dimensional multigroup Monte Carlo code developed at the Oak Ridge National Laboratory. The KENO5a calculations used the 238-group cross-section library, which is based on ENDF/B-V data and is distributed as part of the SCALE-4.3 package [6.4.1], in association with the NITAWL-II program [6.1.6], which adjusts the uranium-238 cross sections to compensate for resonance self-shielding effects. The Dancoff factors required by NITAWL-II were calculated with the CELLDAN code [6.1.13], which includes the SUPERDAN code [6.1.7] as a subroutine.

The convergence of a Monte Carlo criticality problem is sensitive to the following parameters: (1) number of histories per cycle, (2) the number of cycles skipped before averaging, (3) the total number of cycles and (4) the initial source distribution. The MCNP4a criticality output contains a great deal of useful information that may be used to determine the acceptability of the problem convergence. This information was used in parametric studies to develop appropriate values for the aforementioned criticality parameters to be used in the criticality calculations for this submittal. Based on these studies, a minimum of 5,000 histories were simulated per cycle, a minimum of 20 cycles were skipped before averaging, a minimum of 100 cycles were accumulated, and the initial source was specified as uniform over the fueled regions (assemblies). Further, the output was examined to ensure that each calculation achieved acceptable convergence. These parameters represent an acceptable compromise between calculational precision and computational time. Appendix 6.D provides sample input files for each of the MPC baskets in the HI-STAR 100 System.

CASMO-3 [6.1.9-6.1.12] was used for determining the small incremental reactivity effects of manufacturing tolerances. Although CASMO-3 has been extensively benchmarked, these calculations are used only to establish direction of reactivity uncertainties due to manufacturing tolerances (and their magnitude). This allows the MCNP4a calculational model to use the worst combination of manufacturing tolerances. Table 6.3.1 shows results of the CASMO-3 calculations.

6.4.2 Fuel Loading or Other Contents Loading Optimization

The basket designs are intended to safely accommodate the candidate fuel assemblies with enrichments indicated in Tables 6.1.1 and 6.1.2. The calculations were based on the assumption that the HI-STAR 100 System was fully flooded with water. In all cases, the calculations include bias and calculational uncertainties, as well as the reactivity effects of manufacturing tolerances, determined by assuming the worst case geometry.

Nominally, the fuel assemblies would be centrally positioned in each MPC basket cell. However, the consequence of eccentric positioning was also evaluated and found to be negligible. To simulate eccentric positioning (and possible closer approach to the thick steel shield), calculations were made analytically decreasing the inner radius of the steel until it was 1 cm away[†] from the nearest fuel. Results showed a minor increase in reactivity of 0.0026 Δk maximum (MPC-68) which implies that the effect of eccentric location of fuel will be negligible at the actual reflector spacing.

6.4.2.1 Internal and External Moderation

As required by 10CFR71.55, calculations in this section demonstrate that the HI-STAR 100 System remains subcritical for all credible conditions of moderation.

With a neutron absorber present (i.e., the Boral sheets on the steel walls of the storage compartments), the phenomenon of a peak in reactivity at a hypothetical low moderator density (sometimes called "optimum" moderation) does not occur to any significant extent. In a definitive study, Cano, et al. [6.4.2] has demonstrated that the phenomenon of a peak in reactivity at low moderator densities does not occur when strong neutron absorbing material is present or in the absence of large water spaces between fuel assemblies in storage. Nevertheless, calculations for a single reflected cask and for infinite arrays of casks were made to confirm that the phenomenon does not occur with low density water inside or outside the HI-STAR 100 Systems.

6.4.2.1.1 Single Package Evaluation

10CFR71.55 (b), (d), and (e) require the HI-STAR 100 System to be subcritical when surrounded by water providing external moderation to the most reactive credible extent and with internal moderation present to such an extent as to cause maximum reactivity. In accordance with these

[†] PNL critical experiments have shown a small positive reactivity effect of thick steel reflectors, with the maximum effect at 1 cm distance from the fuel. In the cask designs, the fuel is mechanically prohibited from being positioned at a 1 cm spacing from the overpack steel.

regulations, calculations for the two MPC designs in a square array with internal and external moderators of various densities are shown in Table 6.4.1. These calculations assumed 60 cm spacing between cask surfaces, with the neutron shield (Holtite-A) absent in accordance with the requirements of 10CFR71.55(e) for hypothetical accidents conditions. For comparison purposes, a calculation for a single unreflected cask (Case 1) is also included in Table 6.4.1. At 100% external moderator density, Case 2 corresponds to a single fully-flooded cask, fully reflected by water. Figure 6.4.9 plots calculated k_{eff} values ($\pm 2\sigma$) as a function of internal moderator density for both MPC designs with 100% external moderator density (i.e., full water reflection).

Results listed in Table 6.4.1 and plotted in Figure 6.4.9 support the following conclusions:

- For each type of MPC, the calculated k_{eff} for a fully-flooded cask is independent of the external moderator (the small variations in the listed values are due to statistical uncertainties which are inherent to the calculational method (Monte Carlo)), and
- For each type of MPC, reducing the internal moderation results in a monotonic reduction in reactivity, with no evidence of any optimum moderation. Thus, the fully flooded condition corresponds to the highest reactivity, and the phenomenon of optimum low-density moderation does not occur and is not applicable to the HI-STAR 100 System.
- The maximum k_{eff} results for each of the MPC designs are below the regulatory criticality safety limit ($k_{\text{eff}} < 0.95$), and thus, these results demonstrate that the HI-STAR 100 System meets the requirements of 10CFR71.55.

To satisfy the requirement of 10CFR71.55(b)(3), calculations were performed with close full reflection of the containment system (which corresponds to the 2.5 inch thick inner shell of the overpack) by water on all sides. These calculations were performed with the most reactive assembly from the most reactive assembly class in each of the MPC designs and are summarized in Table 6.4.9. Similar to the calculations presented in Table 6.4.1, these calculations were performed for an infinite square array with 60 cm spacing between containment surfaces (i.e., inner shells).

Therefore, in accordance with 10CFR71.35, this evaluation demonstrates that a single HI-STAR 100 System satisfies the criticality safety requirements for the normal conditions of transport (10CFR71.43(f), 10CFR71.51(a)(1), 10CFR71.55(b) and 10CFR71.55(d)) and the hypothetical accident conditions of transport (10CFR71.55(e)).

6.4.2.1.2 Evaluation of Package Arrays

In terms of reactivity, the normal conditions of transport (i.e., no internal or external moderation) are bounded by the hypothetical accident conditions of transport. Therefore, the calculations in

this section evaluate arrays of HI-STAR 100 Systems under hypothetical accident conditions (i.e, internal and external moderation by water to the most reactive credible extent and no neutron shield present).

In accordance with 10CFR71.59 requirements, calculations were performed to simulate an infinite three-dimensional square array of internally fully-flooded (highest reactivity) casks with varying cask spacing and external moderation density. The MPC-24 was used for this analysis. The maximum k_{eff} results of these calculations are listed in Table 6.4.2 and confirm that the individual casks in a square-pitched array are independent of external moderation and cask spacing. The maximum value listed in Table 6.4.2 is 0.9453, which is statistically equivalent (within one standard deviation) to the reference value (0.9449 shown in Table 6.4.1) for a single unreflected fully flooded cask.

To further investigate the reactivity effects of array configurations, calculations were also performed to simulate an infinite three-dimensional hexagonal (triangular-pitched) array of internally fully-flooded (highest reactivity) MPC-24 casks with varying cask spacing and external moderation density. The maximum k_{eff} results of these calculations are listed in Table 6.4.3 and confirm that the individual casks in a hexagonal (triangular pitched) array are effectively independent of external moderation and cask spacing. The maximum value listed in Table 6.4.3 is 0.9455, which is statistically equivalent (within one standard deviation) to the reference value (0.9449 shown in Table 6.4.1) for a single unreflected fully flooded cask.

To assure that internal moderation does not result in increased reactivity, hexagonal array calculations were also performed for 10% internal moderator with 10% and 100% external moderation for varying cask spacing. Maximum k_{eff} results are summarized in Table 6.4.4 and confirm the very low values of k_{eff} for low values of internal moderation.

The results presented thus far indicate that neutronic interaction between casks is not enhanced by the neighboring casks or the water between the neighboring casks, and thus, the most reactive arrangement of casks corresponds to a tightly packed array with the cask surfaces touching. Therefore, calculations were performed for an infinite hexagonal (triangular pitched) array of touching casks (neglecting the Holtite-A neutron shield). These calculations were performed for both MPC designs, in the internally flooded (highest reactivity) and internally dry conditions, with and without external flooding. The results of these calculations are listed in Table 6.4.5. For each of the MPC designs, the maximum k_{eff} values are shown to be statistically equivalent (within one standard deviation) to that of a single internally flooded unreflected cask and are below the regulatory limit of 0.95. Therefore, the transportation index for criticality control is zero because an infinite number of HI-STAR 100 casks will remain subcritical ($k_{\text{eff}} < 0.95$) under both normal and hypothetical accident conditions of transport. This analysis demonstrates that the HI-STAR 100 System is in full compliance with 10CFR71.35 and 10CFR71.59. To further demonstrate that the transport index for criticality control is zero, these infinite array calculations

were repeated with the most reactive assembly from the most reactive assembly class in each of the MPC designs. The results are listed in Table 6.1.4 and support the conclusion that the HI-STAR 100 System specifically meets the requirements of 10CFR71.59(a)(2).

The thick steel wall of the overpack is more than sufficient to preclude neutron coupling between casks, consistent with the findings of Cano, et al. Neglecting the Holtite-A neutron shielding in the calculational model provides further assurance of conservatism in the calculations.

6.4.2.2 Partial Flooding

To demonstrate that the HI-STAR 100 System would remain subcritical if water were to leak into the containment system, as required by 10CFR71.55, calculations in this section address partial flooding in the HI-STAR 100 System and demonstrate that the fully flooded condition is the most reactive.

The reactivity changes during the flooding process were evaluated in both the vertical and horizontal positions for all MPC designs. For these calculations, the cask is partially filled (at various levels) with full density (1.0 g/cc) water and the remainder of the cask is filled with steam consisting of ordinary water at partial density (0.002 g/cc). Results of these calculations are shown in Table 6.4.6. In all cases, the reactivity increases monotonically as the water level rises, confirming that the most reactive condition is fully flooded.

6.4.2.3 Clad Gap Flooding

The reactivity effect of flooding the fuel rod pellet-to-clad gap regions, in the fully flooded condition, has been investigated. Table 6.4.7 presents maximum k_{eff} values that demonstrate the positive reactivity effect associated with flooding the pellet-to-clad gap regions. These results confirm that it is conservative to assume that the pellet-to-clad gap regions are flooded. For all cases that involve flooding, the pellet-to-clad gap regions are assumed to be flooded.

6.4.2.4 Preferential Flooding

Preferential or uneven flooding within the HI-STAR 100 System was not evaluated because such a condition is not credible for any of the MPC basket designs loaded in the HI-STAR 100 System. Preferential flooding of any of the MPC fuel basket designs is not possible because flow holes are present on all four walls of each basket cell and on the two flux trap walls at both the top and bottom of the MPC basket. The flow holes are sized to ensure that they cannot be blocked by crud deposits. Because the fuel cladding temperatures remain below their design limits (as demonstrated in Chapter 3) and the inertial loading remains below 63g's (Section 2.9), the cladding remains intact. For damaged BWR fuel assemblies and BWR fuel debris, the assemblies or debris are pre-loaded into stainless steel Damaged Fuel Containers fitted with 250

micron fine mesh screens which prevent damaged fuel assemblies or fuel debris from blocking the basket flow holes. Therefore, the flow holes cannot be blocked and the MPC fuel baskets cannot be preferentially flooded.

6.4.2.5 Hypothetical Accidents Conditions of Transport

The analyses presented in Section 2.7 of Chapter 2 and Section 3.5 of Chapter 3 demonstrate that the damage resulting from the hypothetical accident conditions of transport are limited to a loss of the neutron shield material as a result of the hypothetical fire accident. Because the criticality analyses do not take credit for the neutron shield material (Holtite-A), this condition has no effect on the criticality analyses.

As reported in Table 2.7.1, the minimum factor of safety for the MPC-24 as a result of the hypothetical accident conditions of transport are 1.17 against the Level D allowables for Subsection NG, Section III of the ASME Code. Therefore, because the maximum box wall stresses are well within the ASME Level D allowables, the flux-trap gap change will be insignificant compared to the characteristic dimension of the flux trap.

In summary, the hypothetical transport accidents have no adverse effect on the geometric form of the package contents important to criticality safety, and thus, are limited to the effects on internal and external moderation evaluated in Subsection 6.4.2.1.

6.4.3 Criticality Results

Results of the criticality safety calculations for the condition of flooding with water to the most reactive credible extent are presented in Section 6.2 and summarized in Section 6.1. These data, along with the analysis in Subsection 6.4.2.1, confirm that for each of the candidate fuel assemblies and basket configurations the effective multiplication factor (k_{eff}), including all biases and uncertainties at a 95-percent confidence level, do not exceed 0.95 under all credible normal and hypothetical accident conditions of transport. Therefore, compliance with 10CFR71.55 for single packages and 10CFR71.59 for package arrays in both normal and hypothetical accident conditions of transport is demonstrated for all of the fuel assembly classes and basket configurations listed in Tables 6.1.1 through 6.1.3. A table listing the maximum k_{eff} (including bias, uncertainties, and calculational statistics), calculated k_{eff} , standard deviation, and energy of the average lethargy causing fission (EALF) for each of the candidate fuel assemblies and basket configurations is provided in Appendix 6.C

Additional calculations (CASMO-3) at elevated temperatures confirm that the temperature coefficients of reactivity are negative as shown in Table 6.3.1. This confirms that the calculations for the storage baskets are conservative.

In calculating the maximum reactivity, the analysis used the following equation:

$$k_{eff}^{max} = k_c + K_c \sigma_c + Bias + \sigma_B$$

where:

- ⇒ k_c is the calculated k_{eff} under the worst combination of tolerances;
- ⇒ K_c is the K multiplier for a one-sided statistical tolerance limit with 95% probability at the 95% confidence level [6.1.8]. Each final k_{eff} value calculated by MCNP4a (or KENO5a) is the result of averaging 100 (or more) cycle k_{eff} values, and thus, is based on a sample size of 100. The K multiplier corresponding to a sample size of 100 is 1.93. However, for this analysis a value of 2.00 was assumed for the K multiplier, which is larger (more conservative) than the value corresponding to a sample size of 100;
- ⇒ σ_c is the standard deviation of the calculated k_{eff} , as determined by the computer code (MCNP4a or KENO5a);
- ⇒ **Bias** is the systematic error in the calculations (code dependent) determined by comparison with critical experiments in Appendix 6.A; and
- ⇒ σ_B is the standard error of the bias (which includes the K multiplier for 95% probability at the 95% confidence level; see Appendix 6.A).

Appendix 6.A presents the critical experiment benchmarking and the derivation of the bias and standard error of the bias (95% probability at the 95% confidence level).

6.4.4 Damaged Fuel Container

Both damaged BWR fuel assemblies and BWR fuel debris are required to be loaded into Damaged Fuel Containers (DFCs) prior to being loaded into the MPC. Two different DFC types with slightly different cross sections are analyzed. DFCs containing fuel debris must be stored in the MPC-68F. DFCs containing damaged fuel assemblies may be stored in either the MPC-68 or MPC-68F. Evaluation of the capability of storing damaged fuel and fuel debris (loaded in DFCs) is limited to very low reactivity fuel in the MPC-68F. Because the MPC-68 has a higher specified ^{10}B loading, the evaluation of the MPC-68F conservatively bounds the storage of damaged BWR fuel assemblies in a standard MPC-68. Although the maximum planar-average enrichment of the damaged fuel is limited to 2.7% ^{235}U as specified in Chapter 1, analyses have been made for three possible scenarios, conservatively assuming fuel^{††} of 3.0% enrichment. The scenarios considered included the following:

1. Lost or missing fuel rods, calculated for various numbers of missing rods in order to determine the maximum reactivity. The configurations assumed for analysis are

^{††} 6x6A01 and 7x7A01 fuel assemblies were used as representative assemblies.

- illustrated in Figures 6.4.1 through 6.4.7.
2. Broken fuel assembly with the upper segments falling into the lower segment creating a close-packed array (described as a 8x8 array). For conservatism, the array analytically retained the same length as the original fuel assemblies in this analysis. This configuration is illustrated in Figure 6.4.8.
 3. Fuel pellets lost from the assembly and forming powdered fuel dispersed through a volume equivalent to the height of the original fuel. (Flow channel and clad material assumed to disappear).

Results of the analyses, shown in Table 6.4.8, confirm that, in all cases, the maximum reactivity is well below the regulatory limit. There is no significant difference in reactivity between the two DFC types. Collapsed fuel reactivity (simulating fuel debris) is low because of the reduced moderation. Dispersed powdered fuel results in low reactivity because of the increase in ^{238}U neutron capture (higher effective resonance integral for ^{238}U absorption).

The loss of fuel rods results in a small increase in reactivity (i.e., rods assumed to collapse, leaving a smaller number of rods still intact). The peak reactivity occurs for 8 missing rods, and a smaller (or larger) number of intact rods will have a lower reactivity, as indicated in Table 6.4.8.

The analyses performed and summarized in Table 6.4.8 provides the relative magnitude of the effects on the reactivity. This information in combination with the maximum k_{eff} values listed in Table 6.1.3 and the conservatism in the analyses, demonstrate that the maximum k_{eff} of the damaged fuel in the most adverse post-accident condition will remain well below the regulatory requirement of $k_{\text{eff}} < 0.95$.

Appendix 6.D provides sample input files for the damaged fuel analysis.

6.4.5 Fuel Assemblies with Missing Rods

For fuel assemblies that are qualified for damaged fuel storage, missing and/or damaged fuel rods are acceptable. However, for fuel assemblies to meet the limitations of intact fuel assembly storage, missing fuel rods must be replaced with dummy rods that displace a volume of water that is equal to, or larger than, that displaced by the original rods.

6.4.6 Thoria Rod Canister

The Thoria Rod Canister is similar to a DFC with an internal separator assembly containing 18 intact fuel rods. The configuration is illustrated in Figure 6.4.10. The k_{eff} value for an MPC-68F filled with Thoria Rod Canisters is calculated to be 0.1813. This low reactivity is attributed to the relatively low content in ^{235}U (equivalent to UO_2 fuel with an enrichment of approximately 1.7

wt% ^{235}U), the large spacing between the rods (the pitch is approximately 1", the cladding OD is 0.412") and the absorption in the separator assembly. Together with the maximum k_{eff} values listed in Tables 6.1.2 and 6.1.3 this result demonstrates, that the k_{eff} for a Thoria Rod Canister loaded into the MPC68 or the MPC68F together with other approved fuel assemblies or DFCs will remain well below the regulatory requirement of $k_{\text{eff}} < 0.95$.

6.4.7 Sealed Rods Replacing BWR Water Rods

Some BWR fuel assemblies contain sealed rods filled with a non-fissile instead of water rods. Compared to the configuration with water rods, the configuration with sealed rods has a reduced amount of moderator, while the amount of fissile material is maintained. Thus, the reactivity of the configuration with sealed rods will be lower compared to the configuration with water rods. Any configuration containing sealed rods instead of water rods is therefore bounded by the analysis for the configuration with water rods and no further analysis is required to demonstrate the acceptability. Therefore, for all BWR fuel assemblies analyzed, it is permissible that water rods are replaced by sealed rods filled with a non-fissile material.

6.4.8 Neutron Sources in Fuel Assemblies

Fuel assemblies containing start-up neutron sources are permitted for storage in the HI-STAR 100 System. The reactivity of a fuel assembly is not affected by the presence of a neutron source (other than by the presence of the material of the source, which is discussed later). This is true because in a system with a k_{eff} less than 1.0, any given neutron population at any time, regardless of its origin or size, will decrease over time. Therefore, a neutron source of any strength will not increase reactivity, but only the neutron flux in a system, and no additional criticality analyses are required. Sources are inserted as rods into fuel assemblies, i.e. they replace either a fuel rod or water rod (moderator). Therefore, the insertion of the material of the source into a fuel assembly will not lead to an increase of reactivity either.

Table 6.4.1

MAXIMUM REACTIVITIES WITH REDUCED WATER DENSITIES FOR CASK ARRAYS[†]

Case Number	Water Density		MCNP4a Maximum k_{eff} ^{††}	
	Internal	External	MPC-24 (17x17A01 @ 4.0%)	MPC-68 (8x8C04 @ 4.2%)
1	100%	single cask	0.9449	0.9348
2	100%	100%	0.9434	0.9339
3	100%	70%	0.9465	0.9339
4	100%	50%	0.9444	0.9347
5	100%	20%	0.9439	0.9338
6	100%	10%	0.9424	0.9336
7	100%	5%	0.9446	0.9333
8	100%	0%	0.9457	0.9338
9	70%	0%	0.8497	0.8488
10	50%	0%	0.7632	0.7631
11	20%	0%	0.5787	0.5797
12	10%	0%	0.5012	0.5139
13	5%	0%	0.4629	0.4763
14	10%	100%	0.4839	0.4946

[†] For an infinite square array of casks with 60 cm spacing between cask surfaces.

^{††} Maximum k_{eff} includes the bias, uncertainties, and calculational statistics, evaluated for the worst case combination of manufacturing tolerances.

Table 6.4.2

REACTIVITY EFFECTS OF SPACING AND WATER MODERATOR DENSITY FOR
 SQUARE ARRAYS OF MPC-24 CASKS
 (17x17A01 @ 4.0% E)

Cask-to-Cask External Spacing (cm)					
External Moderator Density (%)	2	10	20	40	60
5	0.9444	0.9443	0.9436	0.9441	0.9446
10	0.9447	0.9434	0.9440	0.9447	0.9424
20	0.9453	0.9442	0.9440	0.9439	0.9439
50	0.9436	0.9434	0.9444	0.9444	0.9444
100	0.9452	0.9443	0.9434	0.9434	0.9434

Note:

1. All values are maximum k_{eff} which include the bias, uncertainties, and calculational statistics, evaluated for the worst case combination of manufacturing tolerances.

Table 6.4.3

REACTIVITY EFFECTS OF SPACING AND WATER MODERATOR DENSITY FOR
 HEXAGONAL (TRIANGULAR-PITCHED) ARRAYS OF MPC-24 CASKS
 (17x17A01 @ 4.0% E)

Cask-to-Cask External Spacing (cm)					
External Moderator Density (%)	2	10	20	40	60
5	0.9426	0.9439	0.9430	0.9434	0.9455
10	0.9439	0.9425	0.9438	0.9446	0.9438
20	0.9449	0.9452	0.9446	0.9445	0.9440
50	0.9433	0.9440	0.9435	0.9439	0.9439
100	0.9433	0.9423	0.9431	0.9431	0.9431

Note:

1. All values are maximum k_{eff} which include the bias, uncertainties, and calculational statistics, evaluated for the worst case combination of manufacturing tolerances.

Table 6.4.4

REACTIVITY EFFECTS OF SPACING AND EXTERNAL MODERATOR DENSITY FOR HEXAGONAL (TRIANGULAR-PITCHED) ARRAYS OF MPC-24 CASKS (17x17A01 @ 4.0% E) INTERNALLY FLOODED WITH WATER OF 10% FULL DENSITY

Cask-to-Cask External Spacing (cm)					
External Moderator Density (%)	2	10	20	40	60
10	0.4752	0.4752	0.4739	0.4732	0.4728
100	0.4730	0.4728	0.4738	0.4727	0.4727

Note:

1. All values are maximum k_{eff} which include the bias, uncertainties, and calculational statistics, evaluated for the worst case combination of manufacturing tolerances.

Table 6.4.5

CALCULATIONS FOR HEXAGONAL (TRIANGULAR-PITCHED) ARRAYS OF
TOUCHING CASKS

MPC-24 (17x17A01 @ 4.0% ENRICHMENT)		
Internal Moderation (%)	External Moderation (%)	Maximum k_{eff}
0	0	0.3579
0	100	0.3433
100	0	0.9426
100	100	0.9441
MPC-68 (8x8C04 @ 4.2% ENRICHMENT)		
Internal Moderation (%)	External Moderation (%)	Maximum k_{eff}
0	0	0.4036
0	100	0.3716
100	0	0.9351
100	100	0.9340

Note:

1. All values are maximum k_{eff} which include bias, uncertainties, and calculational statistics, evaluated for the worst case combination of manufacturing tolerances.

Table 6.4.6

REACTIVITY EFFECTS OF PARTIAL CASK FLOODING

MPC-24 (17x17A01 @ 4.0% ENRICHMENT)			
Flooded Condition (% Full)	Vertical Orientation	Flooded Condition (% Full)	Horizontal Orientation
25	0.9219	25	0.9119
50	0.9397	50	0.9321
75	0.9443	75	0.9423
100	0.9449	100	0.9449
MPC-68 (8x8C04 @ 4.2% ENRICHMENT)			
Flooded Condition (% Full)	Vertical Orientation	Flooded Condition (% Full)	Horizontal Orientation
25	0.9132	23.5	0.8586
50	0.9307	50	0.9088
75	0.9312	76.5	0.9275
100	0.9348	100	0.9348

Notes:

1. All values are maximum k_{eff} which include bias, uncertainties, and calculational statistics, evaluated for the worst case combination of manufacturing tolerances.

Table 6.4.7

REACTIVITY EFFECT OF FLOODING THE PELLETT-TO-CLAD GAP

Pellet-to-Clad Condition	MPC-24 17x17A01 4.0% Enrichment	MPC-68 8x8C04 4.2% Enrichment
dry	0.9404	0.9279
flooded	0.9449	0.9348

Notes:

1. All values are maximum k_{eff} which includes bias, uncertainties, and calculational statistics, evaluated for the worst case combination of manufacturing tolerances.

Table 6.4.8

MAXIMUM k_{eff} VALUES[†] IN THE DAMAGED FUEL CONTAINER

Condition	MCNP4a Maximum ^{††} k_{eff}	
	DFC Dimensions: ID 4.93" THK. 0.12"	DFC Dimensions:ID 4.81" THK. 0.11"
<u>6x6 Fuel Assembly</u>		
6x6 Intact Fuel	0.7086	0.7016
w/32 Rods Standing	0.7183	0.7117
w/28 Rods Standing	0.7315	0.7241
w/24 Rods Standing	0.7086	0.7010
w/18 Rods Standing	0.6524	0.6453
Collapsed to 8x8 array	0.7845	0.7857
Dispersed Powder	0.7628	0.7440
<u>7x7 Fuel Assembly</u>		
7x7 Intact Fuel	0.7463	0.7393
w/41 Rods Standing	0.7529	0.7481
w/36 Rods Standing	0.7487	0.7444
w/25 Rods Standing	0.6718	0.6644

[†] These calculations were performed with a planar-average enrichment of 3.0% and a ¹⁰B loading of 0.0067 g/cm², which is 75% of a minimum ¹⁰B loading of 0.0089 g/cm². The minimum ¹⁰B loading in the MPC-68F is 0.010 g/cm². Therefore, the listed maximum k_{eff} values are conservative.

^{††} Maximum k_{eff} includes bias, uncertainties, and calculational statistics, evaluated for the worst case combination of manufacturing tolerances.

Table 6.4.9

MAXIMUM k_{eff} VALUES FOR THE MOST REACTIVE ASSEMBLY FROM THE MOST REACTIVE ASSEMBLY CLASS IN EACH OF THE MPCs WITH FULL WATER REFLECTION ON THE SURFACE OF THE CONTAINMENT BOUNDARY

Case	Maximum k_{eff}
MPC-24 (15x15F01 @ 4.1%)	0.9476
MPC-68 (B10x10A01 @ 4.2%)	0.9442
MPC-68F (6x6C01 @ 3.0%)	0.8033

Note:

1. Maximum k_{eff} values include bias, uncertainties, and calculational statistics, evaluated for the worst case combination of manufacturing tolerances.

FIGURE WITHHELD AS SENSITIVE
UNCLASSIFIED INFORMATION

FIGURE 6.4.1; FAILED FUEL CALCULATION MODEL (PLANAR CROSS-SECTION)
WITH 6X6 ARRAY WITH 4 MISSING RODS IN THE MPC-68 BASKET
(SEE CHAPTER 1 FOR TRUE BASKET DIMENSIONS)

**FIGURE WITHHELD AS SENSITIVE
UNCLASSIFIED INFORMATION**

**FIGURE 6.4.2; FAILED FUEL CALCULATION MODEL (PLANAR CROSS-SECTION)
WITH 6X6 ARRAY WITH 8 MISSING RODS IN THE MPC-68 BASKET
(SEE CHAPTER 1 FOR TRUE BASKET DIMENSIONS)**

FIGURE WITHHELD AS
SENSITIVE UNCLASSIFIED
INFORMATION

FIGURE 6.4.3; FAILED FUEL CALCULATION MODEL (PLANAR CROSS-SECTION)
WITH 6X6 ARRAY WITH 12 MISSING RODS IN THE MPC-68 BASKET
(SEE CHAPTER 1 FOR TRUE BASKET DIMENSIONS)

FIGURE WITHHELD AS SENSITIVE
UNCLASSIFIED INFORMATION

FIGURE 6.4.4; FAILED FUEL CALCULATION MODEL (PLANAR CROSS-SECTION)
WITH 6X6 ARRAY WITH 18 MISSING RODS IN THE MPC-68 BASKET
(SEE CHAPTER 1 FOR TRUE BASKET DIMENSIONS)

FIGURE WITHHELD AS SENSITIVE
UNCLASSIFIED INFORMATION

FIGURE 6.4.5; FAILED FUEL CALCULATION MODEL (PLANAR CROSS-SECTION)
WITH 7X7 ARRAY WITH 8 MISSING RODS IN THE MPC-68 BASKET
(SEE CHAPTER 1 FOR TRUE BASKET DIMENSIONS)

FIGURE WITHHELD AS SENSITIVE
UNCLASSIFIED INFORMATION

FIGURE 6.4.6; FAILED FUEL CALCULATION MODEL (PLANAR CROSS-SECTION)
WITH 7X7 ARRAY WITH 13 MISSING RODS IN THE MPC-68 BASKET
(SEE CHAPTER 1 FOR TRUE BASKET DIMENSIONS)

FIGURE WITHHELD AS SENSITIVE
UNCLASSIFIED INFORMATION

FIGURE 6.4.7; FAILED FUEL CALCULATION MODEL (PLANAR CROSS-SECTION)
WITH 7X7 ARRAY WITH 24 MISSING RODS IN THE MPC-68 BASKET
(SEE CHAPTER 1 FOR TRUE BASKET DIMENSIONS)

FIGURE WITHHELD AS SENSITIVE
UNCLASSIFIED INFORMATION

FIGURE 6.4.8; FAILED FUEL CALCULATION MODEL (PLANAR CROSS-SECTION)
WITH DAMAGED FUEL COLLAPSED INTO 8X8 ARRAY IN THE MPC-68 BASKET
(SEE CHAPTER 1 FOR TRUE BASKET DIMENSIONS)

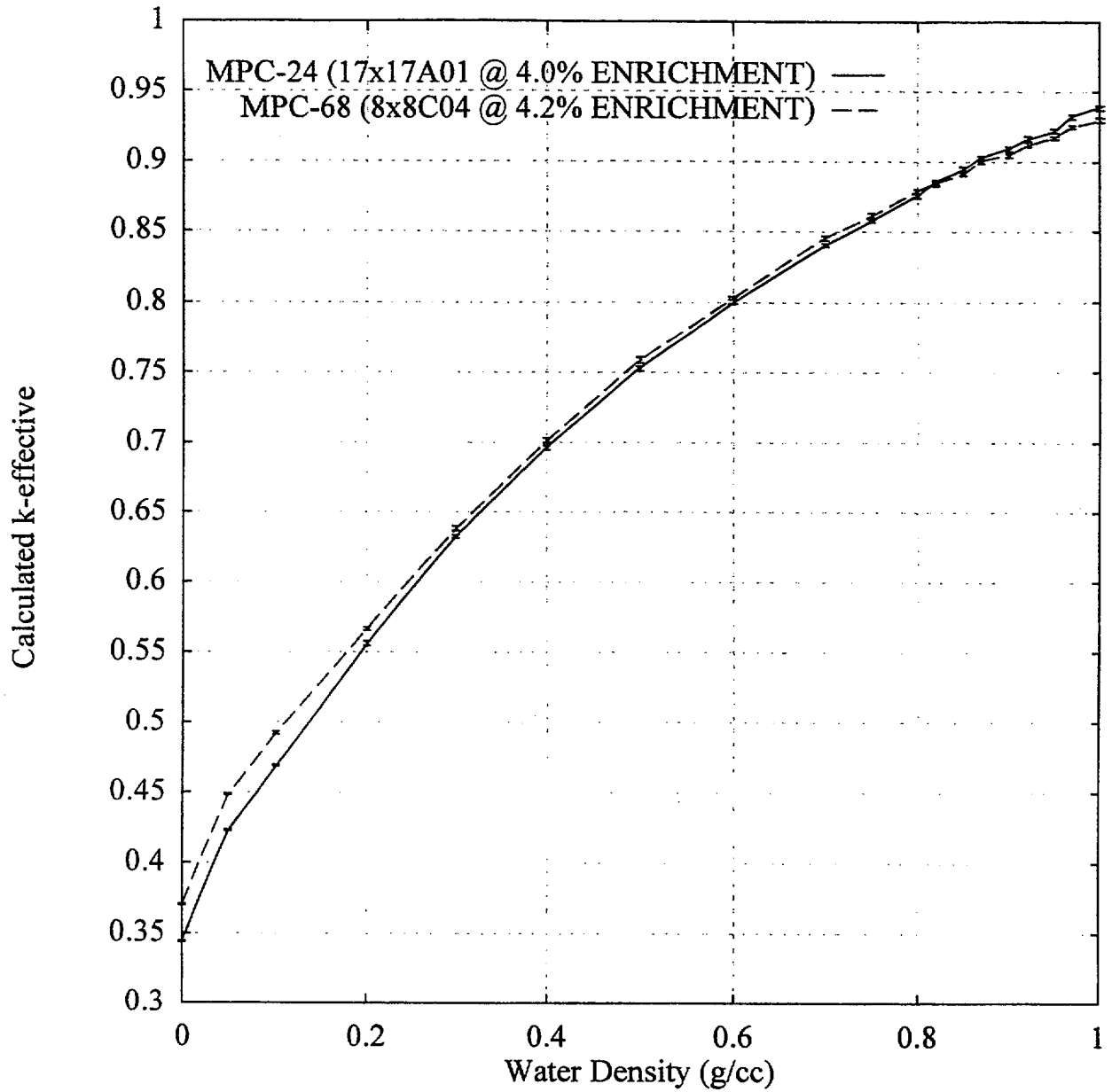


FIGURE 6.4.9; CALCULATED K-EFFECTIVE AS A FUNCTION OF INTERNAL MODERATOR DENSITY (note: error bars represent 2σ statistical uncertainty)

**FIGURE WITHHELD AS SENSITIVE
UNCLASSIFIED INFORMATION**

APPENDIX 6.C: CALCULATIONAL SUMMARY

The following table lists the maximum k_{eff} (including bias, uncertainties, and calculational statistics), MCNP calculated k_{eff} , standard deviation, and energy of average lethargy causing fission (EALF) for each of the candidate fuel types and basket configurations.

Table 6.C.1
 CALCULATIONAL SUMMARY FOR ALL CANDIDATE FUEL TYPES
 AND BASKET CONFIGURATIONS

MPC-24				
Fuel Assembly Designation	Maximum k_{eff}	Calculated k_{eff}	Std. Dev. (1-sigma)	EALF (eV)
14x14A01	0.9378	0.9332	0.0010	0.2147
14x14A02	0.9374	0.9328	0.0009	0.2137
14x14A03	0.9383	0.9340	0.0008	0.2125
14x14B01	0.9268	0.9225	0.0008	0.2788
14x14B02	0.9243	0.9200	0.0008	0.2398
14x14B03	0.9196	0.9152	0.0009	0.2598
14x14B04	0.9163	0.9118	0.0009	0.2631
B14x14B01	0.9323	0.9280	0.0008	0.2730
14x14C01	0.9361	0.9317	0.0009	0.2821
14x14C02	0.9355	0.9312	0.0008	0.2842
14x14C03	0.9400	0.9357	0.0008	0.2900
14x14D01	0.8576	0.8536	0.0007	0.3414
15x15A01	0.9301	0.9259	0.0008	0.2660
15x15B01	0.9427	0.9384	0.0008	0.2704
15C15B02	0.9441	0.9396	0.0009	0.2711
15x15B03	0.9462	0.9420	0.0008	0.2708
15x15B04	0.9452	0.9407	0.0009	0.2692
15x15B05	0.9473	0.9431	0.0008	0.2693
15x15B06	0.9448	0.9404	0.0008	0.2732
B15x15B01	0.9471	0.9428	0.0008	0.2722
15x15C01	0.9332	0.9290	0.0007	0.2563

Table 6.C.1 (continued)
 CALCULATIONAL SUMMARY FOR ALL CANDIDATE FUEL TYPES
 AND BASKET CONFIGURATIONS

MPC-24				
Fuel Assembly Designation	Maximum k_{eff}	Calculated k_{eff}	Std. Dev. (1-sigma)	EALF (eV)
15x15C02	0.9373	0.9330	0.0008	0.2536
15x15C03	0.9377	0.9335	0.0007	0.2525
15x15C04	0.9378	0.9338	0.0007	0.2499
B15x15C01	0.9444	0.9401	0.0008	0.2456
15x15D01	0.9423	0.9380	0.0008	0.2916
15x15D02	0.9430	0.9386	0.0009	0.2900
15x15D03	0.9419	0.9375	0.0009	0.2966
15x15D04	0.9440	0.9398	0.0007	0.3052
15x15E01	0.9475	0.9433	0.0007	0.2916
15x15F01	0.9478	0.9436	0.0008	0.3006
15x15G01	0.8986	0.8943	0.0008	0.3459
15x15H01	0.9411	0.9368	0.0008	0.2425
16x16A01	0.9383	0.9339	0.0009	0.2786
16x16A02	0.9371	0.9328	0.0008	0.2768
17x17A01	0.9449	0.9400	0.0011	0.2198
17x17A02	0.9452	0.9408	0.0008	0.2205
17x17A03	0.9406	0.9364	0.0008	0.2082
17x17B01	0.9377	0.9335	0.0008	0.2697
17x17B02	0.9379	0.9337	0.0008	0.2710
17x17B03	0.9330	0.9288	0.0008	0.2714
17x17B04	0.9407	0.9365	0.0007	0.2666
17x17B05	0.9349	0.9305	0.0009	0.2629

Table 6.C.1 (continued)
 CALCULATIONAL SUMMARY FOR ALL CANDIDATE FUEL TYPES
 AND BASKET CONFIGURATIONS

MPC-24				
Fuel Assembly Designation	Maximum k_{eff}	Calculated k_{eff}	Std. Dev. (1-sigma)	EALF (eV)
17x17B06	0.9436	0.9393	0.0008	0.2657
17x17C01	0.9383	0.9339	0.0008	0.2683
17x17C02	0.9427	0.9384	0.0008	0.2703

MPC-68				
Fuel Assembly Designation	Maximum k_{eff}	Calculated k_{eff}	Std. Dev. (1-sigma)	EALF (eV)
6x6A01	0.7539	0.7498	0.0007	0.2754
6x6A02	0.7517	0.7476	0.0007	0.2510
6x6A03	0.7545	0.7501	0.0008	0.2494
6x6A04	0.7537	0.7494	0.0008	0.2494
6x6A05	0.7555	0.7512	0.0008	0.2470
6x6A06	0.7618	0.7576	0.0008	0.2298
6x6A07	0.7588	0.7550	0.0005	0.2360
6x6A08	0.7808	0.7766	0.0007	0.2527
B6x6A01	0.7888	0.7846	0.0007	0.2310
6x6B01	0.7604	0.7563	0.0007	0.2461
6x6B02	0.7618	0.7577	0.0006	0.2450
6x6B03	0.7619	0.7578	0.0007	0.2439
6x6B04	0.7686	0.7644	0.0008	0.2286
6x6B05	0.7824	0.7785	0.0006	0.2184
B6x6B01	0.7822	0.7783	0.0006	0.2190

Table 6.C.1 (continued)
 CALCULATIONAL SUMMARY FOR ALL CANDIDATE FUEL TYPES
 AND BASKET CONFIGURATIONS

MPC-68				
Fuel Assembly Designation	Maximum k_{eff}	Calculated k_{eff}	Std. Dev. (1-sigma)	EALF (eV)
6x6C01	0.8021	0.7980	0.0007	0.2139
7x7A01	0.7973	0.7930	0.0008	0.2015
7x7B01	0.9372	0.9330	0.0007	0.3658
7x7B02	0.9301	0.9260	0.0007	0.3524
7x7B03	0.9313	0.9271	0.0008	0.3438
7x7B04	0.9311	0.9270	0.0007	0.3816
7x7B05	0.9350	0.9306	0.0008	0.3382
7x7B06	0.9298	0.9260	0.0006	0.3957
B7x7B01	0.9375	0.9332	0.0008	0.3887
B7x7B02	0.9386	0.9344	0.0007	0.3983
8x8A01	0.7685	0.7644	0.0007	0.2227
8x8A02	0.7697	0.7656	0.0007	0.2158
8x8B01	0.9310	0.9265	0.0009	0.2935
8x8B02	0.9227	0.9185	0.0007	0.2993
8x8B03	0.9299	0.9257	0.0008	0.3319
8x8B04	0.9236	0.9194	0.0008	0.3700
B8x8B01	0.9346	0.9301	0.0009	0.3389
B8x8B02	0.9385	0.9343	0.0008	0.3329
B8x8B03	0.9416	0.9375	0.0007	0.3293
8x8C01	0.9315	0.9273	0.0007	0.2822
8x8C02	0.9313	0.9268	0.0009	0.2716
8x8C03	0.9329	0.9286	0.0008	0.2877

Table 6.C.1 (continued)
 CALCULATIONAL SUMMARY FOR ALL CANDIDATE FUEL TYPES
 AND BASKET CONFIGURATIONS

MPC-68				
Fuel Assembly Designation	Maximum k_{eff}	Calculated k_{eff}	Std. Dev. (1-sigma)	EALF (eV)
8x8C04	0.9348	0.9307	0.0007	0.2915
8x8C05	0.9353	0.9312	0.0007	0.2971
8x8C06	0.9353	0.9312	0.0007	0.2944
8x8C07	0.9314	0.9273	0.0007	0.2972
8x8C08	0.9339	0.9298	0.0007	0.2915
8x8C09	0.9301	0.9260	0.0007	0.3183
8x8C10	0.9317	0.9275	0.0008	0.3018
8x8C11	0.9328	0.9287	0.0007	0.3001
8x8C12	0.9285	0.9242	0.0008	0.3062
B8x8C01	0.9357	0.9313	0.0009	0.3141
B8x8C02	0.9425	0.9384	0.0007	0.3081
B8x8C03	0.9418	0.9375	0.0008	0.3056
8x8D01	0.9342	0.9302	0.0006	0.2733
8x8D02	0.9325	0.9284	0.0007	0.2750
8x8D03	0.9351	0.9309	0.0008	0.2731
8x8D04	0.9338	0.9296	0.0007	0.2727
8x8D05	0.9339	0.9294	0.0009	0.2700
8x8D06	0.9365	0.9324	0.0007	0.2777
8x8D07	0.9341	0.9297	0.0009	0.2694
8x8D08	0.9376	0.9332	0.0009	0.2841
B8x8D01	0.9403	0.9363	0.0007	0.2778
8x8E01	0.9312	0.9270	0.0008	0.2831

Table 6.C.1 (continued)
 CALCULATIONAL SUMMARY FOR ALL CANDIDATE FUEL TYPES
 AND BASKET CONFIGURATIONS

MPC-68				
Fuel Assembly Designation	Maximum k_{eff}	Calculated k_{eff}	Std. Dev. (1-sigma)	EALF (eV)
8x8F01	0.9153	0.9111	0.0007	0.2143
9x9A01	0.9353	0.9310	0.0008	0.2875
9x9A02	0.9388	0.9345	0.0008	0.2228
9x9A03	0.9351	0.9310	0.0007	0.2837
9x9A04	0.9396	0.9355	0.0007	0.2262
B9x9A01	0.9417	0.9374	0.0008	0.2236
9x9B01	0.9368	0.9326	0.0007	0.2561
9x9B02	0.9377	0.9334	0.0008	0.2547
9x9B03	0.9416	0.9373	0.0008	0.2517
B9x9B01	0.9422	0.9380	0.0007	0.2501
9x9C01	0.9395	0.9352	0.0008	0.2698
9x9D01	0.9394	0.9350	0.0009	0.2625
9x9E01	0.9402	0.9359	0.0008	0.2249
9x9E02	0.9424	0.9380	0.0008	0.2088
9x9F01	0.9369	0.9326	0.0008	0.2954
9x9F02	0.9424	0.9380	0.0008	0.2088
10x10A01	0.9377	0.9335	0.0008	0.3170
10x10A02	0.9426	0.9386	0.0007	0.2159
10x10A03	0.9396	0.9356	0.0007	0.3169
B10x10A01	0.9457	0.9414	0.0008	0.2212
10x10B01	0.9384	0.9341	0.0008	0.2881
10x10B02	0.9416	0.9373	0.0008	0.2333

Table 6.C.1 (continued)
 CALCULATIONAL SUMMARY FOR ALL CANDIDATE FUEL TYPES
 AND BASKET CONFIGURATIONS

MPC-68				
Fuel Assembly Designation	Maximum k_{eff}	Calculated k_{eff}	Std. Dev. (1-sigma)	EALF (eV)
10x10B03	0.9375	0.9334	0.0007	0.2856
B10x10B01	0.9436	0.9395	0.0007	0.2366
10x10C01	0.9021	0.8980	0.0007	0.2610
10x10D01	0.9376	0.9333	0.0008	0.3355
10x10E01	0.9185	0.9144	0.0007	0.2936

Note: Maximum k_{eff} = Calculated k_{eff} + $K_c \times \sigma_c$ + Bias + σ_B
 where:

- K_c = 2.0
- σ_c = Std. Dev. (1-sigma)
- Bias = 0.0021
- σ_B = 0.0006

See Subsection 6.4.3 for further explanation.

CHAPTER 7: OPERATING PROCEDURES

7.0 INTRODUCTION

This chapter outlines the procedures for loading, preparation for shipment, unloading, and preparation for empty cask shipment of the HI-STAR 100 System in accordance with 10CFR71 [7.0.1]. The procedures provided in this chapter are prescriptive in that they provide the basis and general guidance for plant personnel in preparing detailed written site-specific loading, handling, and unloading procedures. Users may add or delete steps in their site-specific implementation procedures provided the intent of these guidelines is met. Section 7.1 provides the guidance for loading the HI-STAR 100 System in the spent fuel pool. Section 7.2 provides the guidance for unloading the HI-STAR 100 System in the spent fuel pool. Section 7.3 provides the guidance for the preparation of the empty HI-STAR 100 for transport. Section 7.4 provides guidance for preparing the HI-STAR 100 Overpack for transport following a period of storage. Equipment specific operating details such as Vacuum Drying System valve manipulation and onsite transporter operation will be provided to users based on the specific equipment selected by the users and the configuration of the site.

Licensees (Users) will utilize the procedures provided in this chapter, the conditions of the Certificate of Compliance, equipment-specific operating instructions, and plant working procedures and apply them to develop the site-specific written loading, handling, unloading and storage procedures. The procedures contained herein describe acceptable methods for performing HI-STAR 100 loading and unloading operations. Users may alter these procedures to allow operations to be performed in parallel or out of sequence as long as the general intent of the procedure is met. In the figures following each section, acceptable configurations of rigging, piping, equipment and instrumentation are shown. Users may select alternate equipment, configurations and methodology to accommodate their specific needs. Any deviations to the rigging should be approved by the user's load handling authority.

The loading and unloading procedures in Section 7.1 and 7.2 can also be appropriately revised into written site-specific procedures to allow dry loading and unloading of the system in a hot cell or other remote handling facility. The Dry Transfer Facility (DTF) loading and unloading procedures are essentially the same with respect to loading and vacuum drying, inerting, and leakage testing of the MPC. Section 7.4 provides a synopsis of the regulatory requirements for the HI-STAR 100 package. The dry transfer facility shall develop the appropriate site-specific procedures as part of the DTF facility license.

Tables 7.1.1 and 7.1.2, respectively provide the handling weights for each of the HI-STAR 100 System major components and the loads to be lifted during the operation of the HI-STAR 100 System. Table 7.1.3 provides the HI-STAR 100 System bolt torque and sequencing requirements. Table 7.1.4 provides an operational description of the HI-STAR 100 System ancillary equipment and its safety designation. Fuel assembly selection and verification shall be performed by the licensee in accordance with written, approved procedures which ensure that only SNF assemblies authorized in the Certificate of Compliance are loaded into the HI-STAR 100 System.

Users will be required to develop or modify existing programs and procedures to account for the transport operation of the HI-STAR 100 and future potential storage at an ISFSI. Written procedures will be required to be developed or modified to account for such things as nondestructive examination (NDE) of the MPC welds, handling and storage of items and components identified as Important to Safety, heavy load handling, specialized instrument calibration, special nuclear material accountability, fuel handling procedures, training, equipment and process qualifications. Users shall implement controls to ensure that the lifted weights do not exceed the HI-STAR 100 trunnion design limits. Users shall implement controls to monitor the time limit from the removal of the HI-STAR 100 from the spent fuel pool to the commencement of MPC draining to prevent boiling. Chapter 3 of this SAR provides examples of time limits based on representative spent fuel pool temperatures and design basis heat loads. Users shall also implement controls to ensure that the HI-STAR 100 overpack cannot be subjected to a fire in excess of design limits during loading operations.

Table 7.1.5 summarizes the instrumentation necessary to load and unload the HI-STAR 100 System. Tables 7.1.6 and 7.1.7 provide sample receipt inspection checklists for the HI-STAR 100 overpack and the MPC, respectively. Users shall develop site-specific receipt inspection checklists, as required. Fuel handling, including the handling of fuel assemblies in the Damaged Fuel Container (DFC) shall be performed in accordance with written site-specific procedures. Damaged fuel and fuel debris, as defined in the CoC, shall be loaded in DFCs.

7.0.1 Technical and Safety Basis for Loading and Unloading Procedures

The procedures herein (7.1 through 7.3) are developed for the loading, unloading, and empty (after initial transport) transport of the HI-STAR 100 System. The activities involved in loading of spent fuel in a canister system, if not carefully performed, may present personnel hazards and radiological impact. The design of the HI-STAR 100 System, including these procedures and the ancillary equipment to minimize risks and mitigate consequences of potential events. The primary objective is to reduce the risk of occurrence and/or to mitigate the consequences of the event. The procedures contain Notes, Warnings, and Cautions to notify the operators to upcoming situations and provide additional information as needed. The Notes, Warnings and Cautions are purposely bolded and boxed, and immediately precede the applicable steps.

In the event of an extreme abnormal condition (e.g., cask drop or tip-over event) the user shall have appropriate procedural guidance to respond to the situation. As a minimum, the procedures shall address establishing emergency action levels, implementation of emergency action program, establishment of personnel exclusion zones, monitoring of radiological conditions, actions to mitigate or prevent the release of radioactive materials, and recovery planning and execution.

7.1 PROCEDURE FOR LOADING THE HI-STAR 100 SYSTEM IN THE SPENT FUEL POOL AND PREPARATION FOR SHIPMENT

7.1.1 Overview of Loading Operations

The HI-STAR 100 System is used to load and transport spent fuel. Specific steps are performed to prepare the HI-STAR 100 System for fuel loading, to load the fuel, to prepare the system for transport and to ship the HI-STAR 100 System. The HI-STAR 100 overpack may be transported off-site using a rail car or a specially designed heavy haul trailer, or any other load handling equipment designed for such applications. Users shall develop detailed written procedures to control on-site transport operations. Section 7.1.2 provides the general procedures for handling of the HI-STAR 100 overpack and MPC.

Figure 7.1.1 shows a flow diagram of the HI-STAR 100 System loading operations. Figure 7.1.2 illustrates some of the major HI-STAR 100 System loading operations. The HI-STAR 100 overpack and empty MPC may arrive together or separately. The procedures provided assume that these components arrive separately. If the HI-STAR 100 overpack and MPC arrive together, certain steps of the procedure may be omitted.

Note:

The procedures describe plant facilities, functions, and processes in general terms. Each site is different with regard to layout, organization and nomenclature. Users shall interpret the nomenclature used herein to suit their particular site, organization, and methods of operation.

Refer to the boxes of Figure 7.1.2 for the following description. The HI-STAR 100 overpack is received and the personnel barrier is removed. Receipt inspection and radiological surveys are performed. The impact limiters are removed and the HI-STAR 100 overpack is upended. At the start of loading operations, an empty MPC is upended (Box 1). The empty MPC is raised and inserted into the HI-STAR 100 overpack (Box 2). The annulus is filled with plant demineralized water and the MPC is filled with either spent fuel pool water or plant demineralized water (Box 3). An inflatable seal is installed in the annulus between the MPC and the HI-STAR 100 overpack to prevent spent fuel pool water from contaminating the exterior surface of the MPC. The HI-STAR 100 overpack and the MPC are then raised and lowered into the spent fuel pool for fuel loading using the lift yoke (Box 4). Pre-selected assemblies are loaded into the MPC and a visual verification of the assembly identification is performed (Box 5).

While still underwater, a thick shielded lid (the MPC lid) is installed using either slings attached to the lift yoke or the lid retention system (Box 6). The lift yoke remotely engages to the HI-STAR 100 overpack lifting trunnions to lift the HI-STAR 100 overpack and loaded MPC close to the spent fuel pool surface (Box 7). When radiation dose rate measurements confirm that it is safe to remove the HI-STAR 100 overpack from the spent fuel pool, the cask is removed from the spent fuel pool. If the lid retention system is being used, the HI-STAR 100 overpack closure plate bolts are installed to the lid retention disk to secure the MPC lid for the transfer to the cask preparation area. The lift yoke and HI-STAR 100 overpack are sprayed with demineralized water to help remove contamination as they are removed from the spent fuel pool.

The HI-STAR 100 overpack is placed in the designated preparation area and the lift yoke and lid retention system retention disk are removed. The next phase of decontamination is then performed. The top surfaces of the MPC lid and the upper flange of the HI-STAR 100 overpack are decontaminated. The Temporary Shield Ring (if utilized) is installed and filled with water. The inflatable annulus seal is removed, and the annulus shield is installed. The Temporary Shield Ring provides additional personnel shielding around the top of the HI-STAR 100 overpack during MPC closure operations. The annulus shield provides additional personnel shielding at the top of the annulus and also prevents small items from being dropped into the annulus. Dose rates are measured at the MPC lid and around the mid-height circumference of the HI-STAR 100 overpack to establish appropriate radiological control.

The MPC water level is lowered slightly, the MPC is vented, and the MPC lid is seal welded using the Automated Welding System (Box 8). Visual examinations are performed on the tack welds. Liquid penetrant examinations are performed on the root and final passes. A volumetric examination is performed on the MPC welds to ensure that the completed weld is satisfactory. As an alternative to volumetric examination of the MPC lid-to-shell weld, a multi-layer PT is performed including one intermediate examination after approximately every three-eighth inch of weld depth. The water level is raised to the top of the MPC and a hydrostatic test is performed on the MPC Lid-to-Shell welds to verify structural integrity. A small amount of water is displaced with helium gas for leakage testing. A leakage rate test is performed on the MPC lid-to-shell weld to verify weld integrity and to ensure that leakage rates are within acceptance criteria.

The MPC water is displaced from the MPC by blowdown of the water using pressurized helium or nitrogen gas introduced into the vent port of the MPC thus displacing the water through the drain line. The Vacuum Drying System is connected to the MPC and is used to remove all liquid water from the MPC in a stepped evacuation process (Box 9). A stepped evacuation process is used to preclude the formation of ice in the MPC and Vacuum Drying System. The internal pressure is reduced to below 3 torr and held for 30 minutes to ensure that all liquid water is removed.

Following the dryness test, the vacuum drying system is disconnected, the Helium Backfill System is connected, and the MPC is backfilled with a predetermined pressure of helium gas. The helium backfill ensures adequate heat transfer during transport, and provides the means of future leakage rate testing of the MPC confinement boundary welds for future storage. Cover plates are installed and seal welded over the MPC vent and drain ports and liquid penetrant examinations are performed on the root (for multi-pass welds) and final passes (Box 10). The cover plates are leakage tested to confirm that they meet the established leakage rate criteria.

The MPC closure ring is then placed on the MPC and dose rates are measured at the MPC lid to ensure that the dose rates are within expected values. The closure ring is aligned, tacked in place and seal welded providing redundant closure of the MPC confinement boundary closure welds. Tack welds are visually examined, and the root (for multi-pass welds) and final welds are inspected using the liquid penetrant examination technique to ensure weld integrity.

The annulus shield is removed and the remaining water in the annulus is drained. The Temporary Shield Ring is drained and removed. The MPC lid and accessible areas at the top of the MPC shell are smeared for removable contamination. The HI-STAR 100 overpack closure plate is installed (Box 11) and the bolts are torqued. The HI-STAR 100 overpack annulus is dried and backfilled with helium gas. The HI-STAR 100 overpack mechanical seals are leakage tested to assure they will provide long-term retention of the annulus helium. The HI-STAR 100 overpack vent and drain port cover plates are installed. The HI-STAR 100 overpack is surveyed for removable contamination.

The HI-STAR 100 overpack is moved to the transport location. The HI-STAR 100 is dunnaged on the transport frame. An inspection for signs of impaired condition is performed. Contamination surveys are performed. The HI-STAR 100 overpack is placed on the transport device, the tie-down and impact limiters are installed and a shielding effectiveness test is performed to ensure that the HI-STAR 100 shielding has been manufactured and is functioning as designed. Radiation levels are verified to be within acceptable limits. The assembled package is given a final inspection to verify that all conditions for transport have been met (e.g., all mechanical seals have been installed and tested, rupture disks are intact, installed and not covered. The carrier is provided with the appropriate paperwork and the receiver is notified of the impending shipment) and the personnel barrier is installed (Box 12). The package is then labeled, placarded and released for transport.

7.1.2 HI-STAR 100 System Receiving and Handling Operations:

Note:

The HI-STAR 100 overpack may be received and handled in several different configurations and may be transported on-site in a horizontal or vertical orientation. This section provides general guidance for the HI-STAR 100 overpack and MPC rigging and handling. Site-specific procedures shall specify the required operational sequences based on the cask handling configuration and limitations at the sites.

Note:

Steps 1 through 4 describe the handling operations using a lift yoke. Specialty rigging may be substituted if the lift complies with NUREG-0612 [7.1.1].

1. Vertical Handling of the HI-STAR 100 overpack:

Note:

Prior to performing any lifting operation, the removable shear ring segments under the two lifting trunnions must be removed.

Caution:

Users shall maintain controls to ensure that heights to which the loaded HI-STAR 100 is lifted outside the fuel building are limited to ensure that the structural integrity of the MPC and overpack is not compromised should the overpack be dropped. This also assumes the on-site surfaces over which the loaded overpack will be transported have been designed and constructed consistent with the analysis assumptions provided in the HI-STAR 100 Topical Safety Analysis Report [7.1.2].

- a. Verify that the lift yoke load test certifications are current.
- b. Visually inspect the lift yoke and the lifting trunnions for gouges, cracks, deformation or other indications of damage.
- c. Engage the lift yoke to the lifting trunnions. See Figure 7.1.3.
- d. Apply lifting tension to the lift yoke and verify proper engagement of the lift yoke.

Note:

Refer to the site's heavy load handling procedures for lift height, load path, floor loading and other applicable load handling requirements.

- e. Raise the HI-STAR 100 overpack and position it accordingly.

2. Upending of the HI-STAR 100 overpack in the transport frame:

Warning:

Personnel shall remain clear of the unshielded bottom of the loaded overpack. Users shall coordinate operations to keep the bottom cover installed to the maximum extent practicable whenever when the loaded overpack is downended.

- a. Position the HI-STAR 100 overpack under the lifting device. Refer to Step 1, above.
- b. Verify that the lift yoke load test certifications are current.
- c. Visually inspect the lift yoke and the lifting trunnions for gouges, cracks, deformation or other indications of damage.
- d. Place a light layer of Fel-Pro Chemical Products, N-5000, Nuclear Grade Lubricant (or equivalent) on the cask trunnions and the palms of the lift yoke.
- e. Engage the lift yoke to the lifting trunnions. See Figure 7.1.3.
- f. Apply lifting tension to the lift yoke and verify proper engagement of the lift yoke.
- g. Slowly rotate the HI-STAR 100 overpack to the vertical position keeping all rigging as close to vertical as practicable. See Figure 7.1.4.

- h. Lift the pocket trunnions clear of the transport frame rotation trunnions.
 - i. Position the HI-STAR 100 overpack per site direction.
3. Downending of the HI-STAR 100 overpack in the transport frame:
- a. Position the transport frame under the lifting device.
 - b. Verify that the lift yoke load test certifications are current.
 - c. Visually inspect the lift yoke and the lifting trunnions for gouges, cracks, deformation or other indications of damage.
 - d. Place a light layer of Fel-Pro Chemical Products, N-5000, Nuclear Grade Lubricant (or equivalent) on the cask trunnions and the palms of the lift yoke.
 - e. Place a light layer of Fel-Pro Chemical Products, N-5000, Nuclear Grade Lubricant (or equivalent) in the inside surfaces of the cask rotation trunnion pockets and the corresponding surfaces of the transport frame.
 - f. Engage the lift yoke to the lifting trunnions. See Figure 7.1.3.
 - g. Apply lifting tension to the lift yoke and verify proper lift yoke engagement.
 - h. Position the pocket trunnions to receive the transport frame rotation trunnions. See Figure 7.1.4.
 - i. Slowly rotate the HI-STAR 100 overpack to the horizontal position keeping all rigging as close to vertical as practicable.
 - j. Disengage the lift yoke.

Warning:

Personnel shall remain clear of the unshielded bottom of the loaded overpack. Users shall coordinate operations to keep the bottom cover installed to the maximum extent practicable whenever when the loaded overpack is downended.

- k. If necessary for radiation shielding, install the overpack bottom cover. Rigging points are provided. See Figure 7.1.4.
4. Horizontal Handling of the HI-STAR 100 overpack in the transport frame:
- a. Secure the transport frame for HI-STAR 100 downending.
 - b. Downend the HI-STAR 100 overpack on the transport frame per Step 3, if necessary.

- c. Inspect the transport frame lift rigging in accordance with site approved rigging procedures.
- d. Position the transport frame accordingly.

5. Empty MPC Installation in the HI-STAR 100 overpack:

Note:
To avoid side loading the MPC lift lugs, the MPC must be upended in the MPC Upending Frame (or equivalent). See Figure 7.1.6.

- a. If necessary, remove any MPC shipping covers and rinse off any road dirt with water. Be sure to remove any foreign objects from the MPC internals.
- b. Upend the MPC as follows:
 - 1. Visually inspect the MPC Upending Frame for gouges, cracks, deformation or other indications of damage.
 - 2. Install the MPC on the Upending Frame. Make sure that the banding straps are secure around the MPC shell. See Figure 7.1.6.

Warning:
The Upending Frame rigging bars are equipped with cleats that prevent the slings from sliding along the bar. The slings must be placed to the outside of the cleats to prevent an out-of-balance condition. The Upending Frame rigging points are labeled.

- 3. Inspect the Upending Frame slings in accordance with the site's lifting equipment inspection procedures. Rig the slings around the bar in a choker configuration to the outside of the cleats. See Figure 7.1.6.
- 4. Attach the MPC upper end slings of the Upending Frame to the main overhead lifting device. Attach the bottom-end slings to a secondary lifting device (or a chain fall attached to the primary lifting device).
- 5. Raise the MPC in the Upending Frame.

Warning:
The Upending Frame corner should be kept close to the ground during the upending process.

- 6. Slowly lift the upper end of the Upending Frame while lowering the bottom end of the Upending Frame.
- 7. When the MPC approaches the vertical orientation, release the tension on the lower slings.
- 8. Place the MPC in a vertical orientation on a level surface.
- 9. Disconnect the MPC straps and disconnect the rigging.

- c. Install the MPC in the HI-STAR 100 overpack as follows:
 1. Install the four point lift sling to the lift lugs inside the MPC. See Figure 7.1.7.

Caution:
Be careful not to damage the seal seating surface during MPC installation.

2. Raise and place the MPC inside the HI-STAR 100 overpack.

Note:
An alignment punch mark is provided on the HI-STAR 100 overpack and the top edge of the MPC. Similar marks are provided on the MPC lid and closure ring. See Figure 7.1.8.

3. Rotate the MPC so the alignment marks agree and seat the MPC inside the HI-STAR 100 overpack. Disconnect the MPC rigging or the MPC lift rig.

7.1.3 HI-STAR 100 Overpack and MPC Receipt Inspection and Loading Preparation

1. Recover the shipping documentation from the carrier.
 - a. If necessary, recover the keys to the personnel barrier locks from the carrier.
 - b. Record the impact limiter security seal serial numbers and verify that they match the corresponding shipping documentation, as applicable.
 - c. Perform a receipt radiation and contamination survey in accordance with 49CFR173.443 [7.1.3] and 10CFR20.1906 [7.1.4].
2. If necessary, remove the personnel barrier as follows:

Note:
The personnel barrier is a ventilated enclosure cage that fits over the main body of the HI-STAR 100 overpack. The personnel barrier is designed to restrict personnel accessibility to the potentially hot surfaces of the HI-STAR 100 overpack. The personnel barrier in conjunction with the impact limiters restrict accessibility to all surfaces of the HI-STAR 100 overpack during transport. The personnel barrier is equipped with locks to prevent unauthorized access.

- a. Remove the locks securing the personnel barrier and remove the personnel barrier. Lifting points and a small bridle sling is provided. See Figure 7.1.9.
- b. Remove the pins securing the personnel barrier to the transport frame.
- c. Rig the personnel barrier to the lifting device as shown on Figure 7.1.9.
- d. Remove the personnel barrier.

- e. Perform a partial visual inspection of the overpack surfaces to verify that there is no outward indication that would suggest impaired condition of the overpack in accordance with 10CFR71.87(b) [7.0.1]. Identify any significant indications to the cognizant individual for evaluation and resolution and record on the receiving documentation.

3. If necessary, remove the impact limiters as follows:

Note:

To prevent damage to the impact limiters the impact limiter handling frame must be used to remove, install, handle and store the impact limiters.

- a. Clip the security seal wires and remove the security seals and wires.
- b. Attach the impact limiter handling frame as shown on Figure 7.1.10. The rigging arms secure the impact limiter and maintain it at the proper orientation during rigging.

Caution:

The slings should be preloaded to the impact limiter weight plus the weight of the impact limiter handling frame prior to removal of the impact limiter bolts. (See Table 7.1.1) This will prevent damage to the HI-STAR 100 overpack and impact limiter from excessive lift pressure during removal.

- c. Using a load measuring device, apply the correct lift load. See Table 7.1.1 for weights.
- d. Remove the bolts securing the impact limiter to the overpack. See Figure 7.1.11.
- e. Remove the impact limiter and store the impact limiter and bolts in a site-approved location.
- f. Repeat Steps 3.c. through 3.e. for the other impact limiter.
- g. Remove the alignment pins from the bottom of the HI-STAR 100 overpack. See Figure 7.1.11.
- h. Complete the visual inspection to verify that there is no outward indication that would suggest impaired condition of the overpack. (10CFR71.87(b)) [7.0.1]. Identify any significant indications to the cognizant individual for evaluation and resolution.
- i. Verify that the HI-STAR 100 overpack neutron shield rupture discs are installed, intact and not covered by tape or other covering.

ALARA Note:

A bottom protective cover may be attached to the HI-STAR 100 overpack bottom or placed in the designated preparation area or spent fuel pool. This will help prevent imbedding contaminated particles in the HI-STAR 100 overpack bottom surface and ease the decontamination effort.

4. Place the HI-STAR 100 overpack in the cask receiving area.
5. If necessary, remove the buttress plate bolts and remove the buttress plate. See Figure 7.1.11. See Figure 7.1.12 for rigging. Store these components in a site-approved storage location.
6. If necessary, remove the HI-STAR 100 overpack closure plate by removing the closure plate bolts and using the dedicated lift sling. See Figure 7.1.12 for rigging.
 - a. Place the closure plate on cribbing that protects the seal seating surfaces and allows access for seal replacement.
 - b. Store the closure plate and bolts in a site-approved location.
 - c. Install the seal surface protector on the HI-STAR 100 overpack seal seating surface. See Figure 7.1.13.
7. Install the MPC inside the HI-STAR 100 overpack as follows:
 - a. Rinse off any MPC road dirt with water. Inspect all cavity locations for foreign objects. Remove any foreign objects.
 - b. At the site's discretion, perform an MPC receipt inspection and cleanliness inspection in accordance with a site-specific inspection checklist.
 - c. Place the HI-STAR 100 overpack in the designated preparation area.

Note:

Upper fuel spacers are fuel-type specific. Not all fuel types require fuel spacers. See Figure 7.1.14. Upper Fuel spacers may be loaded any time prior to placement of the MPC lid in the spent fuel pool for installation in the MPC.

8. Install the upper fuel spacers in the MPC lid as follows:

Warning:

Never work under a suspended load.

- a. Position the MPC lid on supports to allow access to the underside of the MPC lid.
- b. Thread the fuel spacers into the holes provided on the underside of the MPC lid. See Figure 7.1.14 and Table 7.1.3 for torque requirements.

- c. Install threaded plugs in the MPC lid where and when spacers will not be installed, if necessary. See Table 7.1.3 for torque requirements.

9. At the user's discretion, perform an MPC lid and closure ring fit test:

Note:

It will be necessary to perform the MPC installation and inspection in a location that has sufficient crane clearance to perform the operation.

- a. Visually inspect the MPC lid rigging (See Figure 7.1.12).
- b. Raise the MPC lid such that the drain line can be installed. Install the drain line to the underside of the MPC lid. See Figure 7.1.15.
- c. Align the MPC lid and lift yoke so the drain line will be positioned in the MPC drain location. See Figure 7.1.16. Install the MPC lid. Verify that the MPC lid fit and weld prep are in accordance with the approved design drawings.

ALARA Note:

The closure ring is installed by hand. No tools are required.

- d. Install the closure ring.
- e. Verify that closure ring fit and weld prep are in accordance with the approved design drawings.
- f. Remove the closure ring and the MPC lid. Disconnect the drain line. Store these components in an approved plant storage location.

Note:

Fuel spacers are fuel-type specific. Not all fuel types require fuel spacers. Lower fuel spacers are set in the MPC cells manually. No restraining devices are used. Fuel spacers may be loaded any time prior to insertion of the fuel assemblies in the MPC.

10. Install lower fuel spacers in the MPC (if required for the fuel type). See Figure 7.1.14.

11. Fill the MPC and annulus as follows:

Caution:

Do not use any sharp tools or instruments to install the inflatable seal. Some air in the inflatable seal helps in the installation.

- a. Remove the HI-STAR 100 overpack drain port cover and port plug and install the drain connector. Store the drain port cover plate and port plug in an approved storage location.
- b. Fill the annulus with plant demineralized water to just below the inflatable seal seating surface.

- c. Manually insert the inflatable annulus seal around the MPC. See Figure 7.1.13.
- d. Ensure that the seal is uniformly positioned in the annulus area.
- e. Inflate the seal to between 30 and 35 psig or as directed by the manufacturer.
- f. Visually inspect the seal to ensure that it is properly seated in the annulus. Deflate, adjust and inflate the seal as necessary. Replace the seal as necessary.

ALARA Note:

Waterproof tape placed over empty bolt holes, and bolt plugs may reduce the time required for decontamination.

12. At the user's discretion, install the HI-STAR 100 overpack closure plate bolt plugs and/or apply waterproof tape over any empty bolt holes.

ALARA Note:

Keeping the water level below the top of the MPC prevents splashing during handling.

13. Fill the MPC with either demineralized water or spent fuel pool water to approximately 12 inches below the top of the MPC shell.
14. Place the HI-STAR 100 overpack in the spent fuel pool as follows:

ALARA Note:

The Annulus Overpressure System is used to provide further protection against MPC external shell contamination during in-pool operations. The Annulus Overpressure System is equipped with double-locking quick disconnects to prevent inadvertent draining. The reservoir valve must be closed to ensure that the annulus is not inadvertently drained through the Annulus Overpressure System when the cask is raised above the level of the annulus reservoir.

- a. If used, fill the Annulus Overpressure System lines and reservoir with demineralized water and close the reservoir valve. Attach the Annulus Overpressure System to the HI-STAR 100 overpack via the quick disconnect. See Figure 7.1.17.
- b. Engage the lift yoke to the HI-STAR 100 overpack lifting trunnions and position the HI-STAR 100 overpack over the cask loading area with the basket aligned to the orientation of the spent fuel racks.

ALARA Note:

Wetting the components that enter the spent fuel pool may reduce the amount of decontamination work to be performed later.

- c. Wet the surfaces of the HI-STAR 100 overpack and lift yoke with plant demineralized water while slowly lowering the HI-STAR 100 overpack into the spent fuel pool.

- d. When the top of the HI-STAR 100 overpack reaches the elevation of the reservoir, open the Annulus Overpressure System reservoir valve. Maintain the reservoir water level at approximately 3/4 full the entire time the cask is in the spent fuel pool.
- e. Place the HI-STAR 100 overpack on the floor of the cask loading area and disengage the lift yoke. Visually verify that the lift yoke is fully disengaged. Remove the lift yoke from the spent fuel pool while spraying the crane cables and yoke with plant demineralized water.

7.1.4 MPC Fuel Loading

Note:

An underwater camera or other suitable viewing device may be used for monitoring underwater operations.

1. Perform a fuel assembly selection verification using plant fuel records to ensure that only fuel assemblies that meet all the conditions for loading as specified in the Certificate of Compliance have been selected for loading into the MPC.
2. Load the pre-selected fuel assemblies into the MPC in accordance with the approved fuel loading pattern.
3. Perform a post-loading visual verification of the assembly identification to confirm that the serial numbers match the approved fuel loading pattern.

7.1.5 MPC Closure

Note:

The user may elect to use the optional Lid Retention System (See Figure 7.1.18) to assist in the installation of the MPC lid and attachment of the lift yoke, and to provide the means to secure the MPC lid in the event of a drop or tip-over accident during loaded cask handling operations outside of the spent fuel pool. The user is responsible for evaluating the additional weight imposed on the cask, lift yoke, crane and floor prior to use to ensure that its use does not exceed the crane capacity, heavy loads handling restrictions, or 250,000 pounds. See Tables 7.1.1 and 7.1.2.

1. Visually inspect the MPC lid rigging or Lid Retention System in accordance with site-approved rigging procedures. Attach the MPC lid to the lift yoke so that MPC lid, drain line and trunnions will be in relative alignment. Raise the MPC lid and adjust the rigging so the MPC lid hangs level as necessary.
2. Install the drain line to the underside of the MPC lid. See Figure 7.1.15.
3. Align the MPC lid and lift yoke so the drain line will be positioned in the MPC drain location and the cask trunnions will also engage. See Figure 7.1.16 and 7.1.19.

ALARA Note:

Wetting the components that enter the spent fuel pool may reduce the amount of decontamination work to be performed later.

4. Slowly lower the MPC lid into the pool and insert the drain line into the drain access location and visually verify that the drain line is correctly oriented. See Figure 7.1.16.
5. Lower the MPC lid while monitoring for any hang-up of the drain line. If the drain line becomes kinked or disfigured for any reason, remove the MPC lid and replace the drain line.

Note:

The upper surface of the MPC lid will seat approximately flush with the top edge of the MPC shell when properly installed.

6. Seat the MPC lid in the MPC and visually verify that the lid is properly installed.
7. Engage the lift yoke to the HI-STAR 100 overpack lifting trunnions.
8. Apply a slight tension to the lift yoke and visually verify proper engagement of the lift yoke to the lifting trunnions.

ALARA Note:

Activated debris may have settled on the top face of the HI-STAR 100 overpack and MPC during fuel loading. The cask top surface should be kept under water until a preliminary dose rate scan clears the cask for removal.

9. Raise the HI-STAR 100 overpack until the MPC lid is just below the surface of the spent fuel pool. Survey the area above the cask lid to check for hot particles. Raise and flush the upper surface of the HI-STAR 100 overpack and MPC with the plant demineralized water hoses as necessary to remove any activated particles from the HI-STAR 100 overpack or the MPC lid.
10. Visually verify that the MPC lid is properly seated. Lower the HI-STAR 100 overpack, reinstall the MPC lid, and repeat Step 9, as necessary.
11. If the Lid Retention System is used, inspect the closure plate bolts for general condition. Replace worn or damaged bolts with new bolts.
12. Install the Lid Retention System bolts if the Lid Retention System is used.

Warning:

Cask removal from the spent fuel pool is the heaviest lift that occurs during HI-STAR 100 loading operations. The HI-STAR 100 trunnions must not be subjected to lifted loads in excess of 250,000 lbs. . Users must ensure that plant-specific lifting equipment is qualified to lift the expected load. Users may elect to pump a measured quantity of water from the MPC prior to removing the HI-STAR 100 from the spent fuel pool. See Table 7.1.1 and 7.1.2 for weight information.

13. If necessary for lifted weight conditions, pump a measured amount of water from the MPC. See Figure 7.1.22 and Tables 7.1.1 and 7.1.2.
14. Continue to raise the HI-STAR 100 overpack under the direction of the plant's radiological control personnel. Continue rinsing the surfaces with demineralized water. When the top of the HI-STAR 100 overpack reaches the approximate elevation as the reservoir, close the Annulus Overpressure System reservoir valve. See Figure 7.1.17.

Caution:

Users are required to take necessary actions to prevent boiling of the water in the MPC. This may be accomplished by performing a site-specific analysis to identify a time limitation to ensure that water boiling will not occur in the MPC prior to the initiation of draining operations. Chapter 3 of this SAR provides some sample time limits for the time to initiation of draining for various spent fuel pool water temperatures using design basis heat loads. These time limits may be adopted if the user chooses not to perform a site-specific analysis. If time limitations are imposed, users shall have appropriate procedures and equipment to take action if time limits are approached or exceeded. One course of action involves initiating an MPC water flush for a certain duration and flow rate. Any site-specific analysis shall identify the methods to respond should it become likely that the imposed time limit could be exceeded.

ALARA Note:

To reduce decontamination time, the surfaces of the HI-STAR 100 overpack and lift yoke should be kept wet until decontamination begins.

15. Remove the HI-STAR 100 overpack from the spent fuel pool while spraying the surfaces with plant demineralized water. Record the time.

ALARA Note:

Decontamination of the HI-STAR 100 overpack bottom should be performed using pole-mounted cleaning devices.

16. Decontaminate the HI-STAR 100 overpack bottom and perform a contamination survey of the HI-STAR 100 overpack bottom. Remove the bottom protective cover, if used.
17. If used, disconnect the Annulus Overpressure System from the HI-STAR 100 overpack via the quick disconnect. See Figure 7.1.17.
18. Set the HI-STAR 100 overpack in the designated cask preparation area.

19. Disconnect the lifting slings or Lid Retention System (if used) from the MPC lid and disengage the lift yoke. Decontaminate and store these items in an approved storage location.

Warning:

MPC lid dose rates are measured to ensure that dose rates are within expected values. Dose rates exceeding the 429 mrem/hour could indicate that fuel assemblies not meeting the specifications in the CoC have been loaded.

- a. Measure the dose rates at the MPC lid and verify that the combined gamma and neutron dose rate is below 429 mrem/hour.
20. Perform decontamination of the HI-STAR 100 overpack.
21. Prepare the MPC for MPC lid welding as follows:

ALARA Note:

The Temporary Shield Ring is installed by hand, no tools are required.

- a. Decontaminate the area around the HI-STAR 100 overpack top flange and install the Temporary Shield Ring, (if used). See Figure 7.1.20.
- b. Fill the Temporary Shield Ring with water (if used).
- c. Carefully decontaminate the MPC lid top surface and the shell area above the inflatable annulus seal.
- d. Deflate and remove the annulus seal.

ALARA Note:

The water in the HI-STAR 100 overpack-to-MPC annulus provides personnel shielding. The level should be checked periodically and refilled accordingly.

22. Attach the drain line to the HI-STAR 100 overpack drain port connector and lower the annulus water level approximately 6 inches.

ALARA Note:

The MPC exterior shell survey is performed to evaluate the performance of the inflatable annulus seal. Indications of contamination could require the MPC to be unloaded. Removable contamination on the exterior surfaces of the Overpack and accessible portions of the MPC shall each not exceed:

- a. 2200 dpm/100 cm² from beta and gamma sources; and
- b. 220 dpm/100 cm² from alpha sources.

- a. Survey the MPC lid top surfaces and the accessible areas of the top two inches of the MPC shell.

ALARA Note:

The annulus shield is used to prevent objects from being dropped into the annulus and helps reduce dose rates directly above the annulus region. The annulus shield is hand installed and requires no tools.

23. Install the annulus shield. See Figure 7.1.13.

24. Prepare for MPC lid welding as follows:

Note:

The following steps use two identical Removable Valve Operating Assemblies (RVOAs) (See Figure 7.1.21) to engage the MPC vent and drain ports. The MPC vent and drain ports are equipped with metal-to-metal seals to minimize leakage during vacuum drying, and to withstand the long-term effects of temperature and radiation. The RVOAs allow the vent and drain ports to be operated like valves and prevent the need to hot tap into the penetrations during unloading operations. The RVOAs are purposely not installed until the cask is removed from the spent fuel pool to reduce the amount of decontamination.

Note:

The vent and drain ports are opened by pushing the RVOA handle down to engage the square nut on the cap and turning the handle fully in the counter-clockwise direction. The handle will not turn once the port is fully open. Similarly, the vent and drain ports are closed by turning the handle fully in the clockwise direction. The ports are closed when the handle cannot be turned further.

- a. Clean the vent and drain ports to remove any dirt. Install the RVOAs (See Figure 7.1.21) to the vent and drain ports leaving caps open.

ALARA Warning:

Personnel should remain clear of the drain lines any time water is being pumped or purged from the MPC. Assembly crud, suspended in the water, may create a radiation hazard to workers. Controlling the amount of water pumped from the MPC prior to welding keeps the fuel assembly cladding covered with water yet still allows room for thermal expansion.

- b. Attach the water pump to the drain port (See Figure 7.1.22) and pump between 50 and 120 gallons to the spent fuel pool or liquid radwaste system. The water level is lowered to keep moisture away from the weld region.
- c. Disconnect the water pump.

25. Weld the MPC lid as follows:

ALARA Warning:

Grinding of MPC welds may create the potential for contamination. All grinding activities shall be performed under the direction of radiation protection personnel.

Note:

The vacuum source may help improve the weld quality by keeping moist air from condensing on the MPC lid weld area. The vacuum source can be supplied from a wet/dry vacuum cleaner or small vacuum pump.

- a. Attach a vacuum source to the vent port (if used) or inert the gas space under the MPC lid.

ALARA Warning:

It may be necessary to rotate or reposition the MPC lid slightly to achieve uniform weld gap and lid alignment. A punch mark is located on the outer edge of the MPC lid and shell. These marks are aligned with the alignment mark on the top edge of the HI-STAR 100 overpack (See Figure 7.1.8). If necessary, the MPC lid lift should be performed using a hand operated chain fall to closely control the lift to allow rotation and repositioning by hand. If the chain fall is hung from the crane hook, the crane should be tagged out of service to prevent inadvertent use during this operation. Continuous radiation monitoring is recommended.

- b. If necessary center the lid in the MPC shell using a hand-operated chain fall.

Note:

The MPC is equipped with lid shims that serve to close the gap in the joint for MPC lid closure weld.

- c. As necessary, install the MPC lid shims around the MPC lid to make the weld gap uniform.

ALARA Note:

The optional AWS Baseplate shield is used to further reduce the dose rates to the operators working around the top cask surfaces.

- d. Install the Automated Welding System baseplate shield (if used). See Figure 7.1.12 for rigging.
- e. Install the Automated Welding System Robot (if used). See Figure 7.1.12 for rigging.
- f. Tack weld the MPC lid.
- g. Visually inspect the tack welds.
- h. Lay the root weld.

Note:

The Lid-to-Shell weld may be examined by either volumetric examination (UT) or multi-layer liquid penetrant examination. If volumetric examination is used, it shall be the ultrasonic method and shall include a liquid penetrant (PT) of the root and final weld layers. If PT alone is used, at a minimum, it must include the root and final weld layers and one intermediate PT after approximately every 3/8 inch weld depth.

For all liquid penetrant examinations in this procedure, ASME Boiler and Pressure Vessel Code, Section V, Article 6 provides the liquid penetrant examination methods. The acceptance standards for liquid penetrant examination shall be in accordance with ASME Boiler and Pressure Vessel Code, Section III, Subsection NB, Article NB-5350 as specified on the Design Drawings. ASME Code, Section III, Subsection NB, Article NB-4450 provides acceptable requirements for weld repair. NDE personnel shall be qualified per the requirements of Section III and V of the Code or site-specific program.

Volumetric examination of the MPC Lid-to-Shell weld by ultrasonic test methods are defined in ASME Boiler and Pressure Vessel Code, Section V, Article 5 and 2 respectively. The acceptance standards for UT examination are per Section III, Subsection NB, Article NB-5332 for UT as defined on the Design Drawings. NDE personnel shall be qualified per the requirements of Section III and V of the Code or site-specific program.

- i. Disconnect the vacuum source from the vent port (if used).
- j. Perform a liquid penetrant examination of the weld root.
- k. Complete the MPC lid welding, performing at least one intermediate layer liquid penetrant examination after approximately every 3/8 inch weld depth.
- l. Perform a liquid penetrant examination on the MPC lid final pass and UT (if required).

26. Perform hydrostatic and MPC leakage rate testing as follows:

ALARA Note:

The leakage rates are determined before the MPC is drained for ALARA reasons. A weld repair is a lower dose activity if water remains inside the MPC.

- a. Attach the drain line to the vent port and route the drain line to the spent fuel pool or the plant liquid radwaste system. See Figure 7.1.23 for the hydrostatic test arrangement.

ALARA Warning:

Water flowing from the MPC may carry activated particles and fuel particles. Apply appropriate ALARA practices around the drain line.

- b. Fill the MPC with either spent fuel pool water or plant demineralized water until water is observed flowing out of the vent port drain hose.

- c. Perform a hydrostatic test of the MPC as follows:
 - 1. Close the drain valve and pressurize the MPC to 125 +5/-0 psig.
 - 2. Close the inlet valve and monitor the pressure for a minimum of 10 minutes. The pressure shall not drop during the performance of the test.
 - 3. Following the 10-minute hold period, visually examine the MPC lid-to-shell weld for leakage of water. The acceptance criteria is no observable water leakage.
- d. Release the MPC internal pressure, disconnect the water fill line and drain line from the vent and drain port RVOAs leaving the vent and drain port caps open.
 - 1. Repeat Step 25.1
- e. Attach a regulated helium supply (pressure set to 10+10/-0 psig) to the vent port and attach the drain line to the drain port as shown on Figure 7.1.24.
- f. Verify the correct pressure (pressure set to 10+10/-0 psig) on the helium supply and open the helium supply valve. Drain approximately 5 to 10 gallons.
- g. Close the drain port valve and pressurize the MPC to 10+10/-0 psig helium.
- h. Close the vent port.

Note:

The leakage detector may detect residual helium in the atmosphere. If the leakage tests detects a leak, the area should be flushed with nitrogen or compressed air and the location should be retested.

- i. Perform a helium sniffer probe leakage rate test of the MPC lid-to shell weld in accordance with the Mass Spectrometer Leak Detector (MSLD) manufacturer's instructions and ANSI N14.5 [7.1.5]. The MPC Helium Leak Rate shall be $\leq 5.0E-6$ std cc/sec (He) with a minimum test sensitivity less than $2.5E-6$ std cc/sec (He).
- j. Repair any weld defects in accordance with the site's approved weld repair procedures. Reperform the Ultrasonic, Liquid Penetrant, Hydrostatic and Helium Leakage tests if weld repair is performed.

27. Drain the MPC as follows:

ALARA Warning:

Dose rates will rise as water is drained from the MPC. Continuous dose rate monitoring is recommended.

- a. Attach a regulated helium or nitrogen supply (pressure set to 25+5/-0 psig) to the vent port.
- b. Attach a drain line to the drain port shown on Figure 7.1.24.
- c. Verify the correct pressure (pressure set to 25+5/-0) on the gas supply.
- d. Open the gas supply valve and record the time at the start of MPC draindown.

Note:

An optional warming pad may be placed under the HI-STAR 100 Overpack to replace the heat lost during the evaporation process of vacuum drying. This may be used at the user's discretion for older and colder fuel assemblies to reduce vacuum drying times.

- e. Start the warming pad, if used.
- f. Blow the water out of the MPC until water ceases to flow out of the drain line. Shut the gas supply valve.
- g. Disconnect the gas supply line from the MPC.
- h. Disconnect the drain line from the MPC.

28. Vacuum Dry the MPC as follows:

Note:

Vacuum drying is performed to remove moisture and oxidizing gasses from the MPC. This ensures a suitable environment for long-term storage of spent fuel assemblies and ensures that the MPC pressure remains within design limits. The vacuum drying process reduces the MPC internal pressure in stages. Dropping the internal pressure too quickly may cause the formation of ice in the fittings. Ice formation could result in incomplete removal of moisture from the MPC. The vacuum stages are intermediate steps and should be considered approximate values.

- a. Attach the Vacuum Drying System (VDS) to the vent and drain port RVOAs. See Figure 7.1.25.

Note:

The Vacuum Drying System may be configured with an optional fore-line condenser to increase vacuum pump efficiency. Water may need to be periodically drained. The volume of condensed water should be measured and added to the water volume measured during MPC draining.

- b. Reduce the MPC pressure to approximately 100 torr and throttle the VDS suction valve to maintain this pressure for approximately 15 minutes.
- c. Reduce the MPC pressure to approximately 70 torr and throttle the VDS suction valve to maintain this pressure for approximately 15 minutes.
- d. Reduce the MPC pressure to approximately 50 torr and throttle the VDS suction valve to maintain this pressure for approximately 15 minutes.
- e. Reduce the MPC pressure to approximately 30 torr and throttle the VDS suction valve to maintain this pressure for approximately 15 minutes.

Note:

The Vacuum Drying System pressure will remain at about 30 torr until most of the liquid water has been removed from the MPC.

- f. When the MPC pressure begins to drop (without any operator action), completely open the VDS suction valve and reduce the MPC pressure to below 3 torr.
- g. Shut the VDS valves and verify a stable MPC pressure on the vacuum gage.

Note:

The MPC pressure may rise due to the presence of water in the MPC. The dryness test may need to be repeated several times until all the water has been removed. Leaks in the Vacuum Drying System, damage to the vacuum pump, and improper vacuum gauge calibration may cause repeated failure of the dryness verification test. These conditions should be checked as part of the corrective actions if repeated failure of the dryness verification test is occurring.

- h. Perform the MPC dryness verification test. The MPC cavity shall hold stable vacuum drying pressure of ≤ 3 torr for ≥ 30 minutes.
- i. Close the vent and drain port valves.
- j. Disconnect the VDS from the MPC.
- k. Stop the warming pad, if used.
- l. Close the drain port RVOA cap and remove the drain port RVOA.

29. Backfill the MPC as follows:

Note:

Helium backfill requires 99.995% (minimum) purity.

- a. Set the helium bottle regulator pressure to 70+5/-0 psig.
- b. Purge the Helium Backfill System to remove oxygen from the lines.

- c. Attach the Helium Backfill System (HBS) to the vent port as shown on Figure 8.1.23 and open the vent port.
- d. Slowly open the helium supply valve while monitoring the pressure rise in the MPC.

Note:

If helium bottles need to be replaced, the bottle valve needs to be closed and the entire regulator assembly transferred to the new bottle.

- e. Carefully backfill the MPC to between 0 (atmospheric) and 30 psig.
- f. Disconnect the HBS from the MPC.
- g. Close the vent port RVOA and disconnect the vent port RVOA.

30. Weld the vent and drain port cover plates as follows:

- a. Wipe the inside area of the vent and drain port recesses to dry and clean the surfaces.
- b. Place the cover plate over the vent port recess.
- c. Raise the edge of the cover plate and insert the nozzle of the helium supply into the vent port recess to displace the oxygen with helium.

Note:

Helium gas is required to be injected into the port recesses to ensure that the leakage test is valid.

- d. Displace the air in the recess using the helium nozzle and immediately close the cover plate.
- e. Tack weld the cover plate.
- f. Visually inspect the tack welds.
- g. Weld the root pass on the vent port cover plate.

Note:

ASME Boiler and Pressure Vessel Code [7.1.6], Section V, Article 6 provides the liquid penetrant inspection methods. The acceptance standards for liquid penetrant examination shall be in accordance with ASME Boiler and Pressure Vessel Code, Section III, Subsection NB, Article NB-5350 as specified on the Design Drawings. ASME Code, Section III, Subsection NB, Article NB-4450 provides acceptable requirements for weld repair. NDE personnel shall be qualified per the requirements of Section V of the Code or site-specific program.

- h. Perform a liquid penetrant examination on the vent port cover plate root weld.
- i. Complete the vent port cover plate welding.

Note:

ASME Boiler and Pressure Vessel Code [7.1.6], Section V, Article 6 provides the liquid penetrant inspection methods. The acceptance standards for liquid penetrant examination shall be in accordance with ASME Boiler and Pressure Vessel Code, Section III, Subsection NB, Article NB-5350 as specified on the Design Drawings. ASME Code, Section III, Subsection NB, Article NB-4450 provides acceptable requirements for weld repair. NDE personnel shall be qualified per the requirements of Section V of the Code or site-specific program.

- j. Perform a liquid penetrant examination on the vent port cover weld.
- k. Repeat Steps 30.a through 30.j for the drain port cover plate.

31. Perform a leakage test of the MPC vent and drain port cover plates as follows:

Note:

The leakage detector may detect residual helium in the atmosphere from the helium injection process. If the leakage tests detects a leak, the area should be blown clear with compressed air or nitrogen and the location should be retested.

- a. Flush the area around the vent and drain cover plates with compressed air or nitrogen to remove any residual helium gas.
- b. Perform a helium leakage rate test of vent and drain cover plate welds in accordance with the Mass Spectrometer Leak Detector (MSLD) manufacturer's instructions and ANSI N14.5 [7.1.5]. The MPC Helium Leak Rate shall be $\leq 5.0E-6$ std cc/sec (He) with a minimum test sensitivity less than $2.5E-6$ std cc/sec (He).
- c. Repair any weld defects in accordance with the site's approved code weld repair procedures. Repperform the leakage test as required.

32. Weld the MPC closure ring as follows:

ALARA Note:

The closure ring is installed by hand. No tools are required. The closure ring may be provided as a complete ring or in two halves. In the case of the single ring, no radial connecting welds are needed.

- a. Install and align the closure ring. See Figure 7.1.8.
- b. Tack weld the closure ring to the MPC shell and the MPC lid.
- c. Visually inspect the tack welds.
- d. Lay the root weld between the closure ring and the MPC shell if necessary.

- e. Lay the root weld between the closure ring and the MPC lid if necessary.
- f. Lay the root weld connecting the two closure ring segments, if necessary.

Note:

ASME Boiler and Pressure Vessel Code [7.1.6], Section V, Article 6 provides the liquid penetrant inspection methods. The acceptance standards for liquid penetrant examination shall be in accordance with ASME Boiler and Pressure Vessel Code, Section III, Subsection NB, Article NB-5350 as specified on the Design Drawings. ASME Code, Section III, Subsection NB, Article NB-4450 provides acceptable requirements for weld repair. NDE personnel shall be qualified per the requirements of Section V of the Code or site-specific program.

- g. Perform a liquid penetrant examination on the closure ring root welds.
- h. Complete the closure ring welding.

Note:

ASME Boiler and Pressure Vessel Code [7.1.6], Section V, Article 6 provides the liquid penetrant inspection methods. The acceptance standards for liquid penetrant examination are contained in the ASME Boiler and Pressure Vessel Code, Section III, Subsection NB, Article NB-5350. ASME Code, Section III, Subsection NB, Article NB-4450 provides acceptable requirements for weld repair. NDE personnel shall be qualified per the requirements of Section V of the Code or site-specific program.

- i. Perform a liquid penetrant examination on the closure ring final weld.
- j. Remove the Automated Welding System.
- k. If necessary, remove the AWS baseplate shield. See Figure 7.1.12 for rigging.

7.1.6 Preparation for Transport

1. Remove the annulus shield and seal surface protector and store it in an approved plant storage location

ALARA Warning:

Dose rates will rise around the top of the annulus as water is drained from the annulus. Apply appropriate ALARA practices.

2. Attach a drain line to the HI-STAR 100 overpack drain connector and drain the remaining water from the annulus to the spent fuel pool or the plant liquid radwaste system (See Figure 7.1.17).
3. Install the overpack closure plate as follows:
 - a. Remove any waterproof tape or bolt plugs used for contamination mitigation.
 - b. Clean the closure plate seal seating surface and the HI-STAR 100 overpack seal seating surface and install new overpack closure plate mechanical seals.

- c. Remove the test port plug and store it in a site-approved location. Discard any used metallic seals.

Note:

Care should be taken to protect the seal seating surface from scratches, nicks or dents.

- d. Install the closure plate (see Figure 7.1.12). Disconnect the closure plate lifting eyes and install the bolt hole plugs in the empty bolt holes (See Table 7.1.3 for torque requirements).
 - e. Install and torque the closure plate bolts. See Table 7.1.3 for torque requirements.
 - f. Remove the vent port cover plate and remove the port plug and seal. Discard any used mechanical seals.
4. Dry the overpack annulus as follows:
- a. Disconnect the drain connector from the overpack.
 - b. Install the drain port plug with a new seal and torque the plug. See Table 7.1.3 for torque requirements. Discard any used metallic seals.

Note:

Preliminary annulus vacuum drying may be performed using the test cover to improve flow rates and reduce vacuum drying time. Dryness testing and helium backfill shall use the backfill tool.

- c. Load the backfill tool with the HI-STAR 100 overpack vent port plug and the vent port with a new plug seal. Attach the backfill tool to the HI-STAR 100 overpack vent port with the plug removed. See Figure 7.1.28. See Table 7.1.3 for torque requirements.
- d. Evacuate the HI-STAR 100 overpack pressure to approximately 100 torr and hold the pressure for approximately 15 minutes.
- e. Evacuate the HI-STAR 100 overpack pressure to approximately 50 torr and hold the pressure for approximately 15 minutes.
- f. Evacuate the HI-STAR 100 overpack pressure to approximately 30 torr and hold the pressure for approximately 15 minutes.
- g. Throttle the VDS suction valves to maintain about 30 torr and hold the pressure for approximately 15 minutes.

Note:

The Vacuum Drying System pressure will remain at about 30 torr until most of the liquid

water has been removed from the overpack.

- h. Continue to operate the Vacuum Drying System at about 30 torr while monitoring the HI-STAR 100 overpack pressure.
- i. When the HI-STAR 100 overpack pressure begins to drop (without any operator action), completely open the Vacuum Drying System suction valve and reduce the HI-STAR 100 overpack pressure to below 3 torr.

Note:

The annulus pressure may rise due to the presence of water in the HI-STAR 100 overpack. The dryness test may need to be repeated several times until all the water has been removed. Leaks in the Vacuum Drying System, damage to the vacuum pump, and improper vacuum gauge calibration may cause repeated failure of the dryness verification test. These conditions should be checked as part of the corrective actions if repeated failure of the dryness verification test is occurring.

- j. Perform a HI-STAR 100 overpack Annulus Dryness Verification. The overpack annulus shall hold stable vacuum drying pressure of ≤ 3 torr for ≥ 30 minutes.
5. If necessary, perform a leakage test of the MPC-68F as follows:
- a. Evacuate the annulus per the MSLD manufacturer's instructions and isolate the vacuum pump from the overpack test cover.
 - b. Perform a leakage rate test of MPC-68F per the MSLD manufacturer's instructions. The overpack Helium Leak Rate shall be $\leq 5.0E-6$ std cc/sec (He) with a minimum test sensitivity less than $2.5E-6$ std cc/sec (He).
6. Backfill, and leakage test the overpack as follows:
- a. Attach the helium supply to the backfill tool.
 - b. Verify the correct pressure on the helium supply (pressure set to $10+4/-0$ psig) and open the helium supply valve.
 - c. Backfill the HI-STAR 100 overpack annulus to ≥ 10 psig and ≤ 14 psig.
 - d. Install the overpack vent port plug and torque. See Table 7.1.3 for torque requirements.
 - e. Disconnect the overpack backfill tool from the vent port.
 - f. Flush the overpack vent port recess with compressed air to remove any standing helium gas.
 - g. Install the overpack test cover to the overpack vent port as shown on Figure 7.1.27. See Table 7.1.3 for torque requirements.

- h. Evacuate the test cavity per the MSLD manufacturer's instructions and isolate the vacuum pump from the overpack test cover.
 - i. Perform a leakage rate test of overpack vent port plug per the MSLD manufacturer's instructions. The overpack Helium Leak Rate shall be $\leq 4.3E-6$ std cc/sec (He) with a minimum test sensitivity less than $2.15E-6$ std cc/sec (He).
 - j. Remove the overpack test cover and install a new metallic seal on the overpack vent port cover plate. Discard any used metallic seals.
 - k. Install the vent port cover plate and torque the bolts. See Table 7.1.3 for torque requirements.
 - l. Repeat Steps 6.f through 6.k for the overpack drain port.
7. Leak test the overpack closure plate inner mechanical seal as follows:
- a. Attach the closure plate test tool to the closure plate test port with the and MSLD attached. See Figure 7.1.29. See Table 7.1.3 for torque requirements.
 - b. Evacuate the closure plate test port tool and closure plate inter-seal area per the MSLD manufacturer's instructions.
 - c. Perform a leakage rate test of overpack closure plate inner mechanical seal in accordance with the MSLD manufacturer's instructions. The overpack Helium Leak Rate shall be $\leq 4.3E-6$ std cc/sec (He) with a minimum test sensitivity less than $2.15E-6$ std cc/sec (He).
 - d. Remove the closure plate test tool from the test port and install the test port plug with a new mechanical seal. See Table 7.1.3 for torque requirements. Discard any used metallic seals.
8. Drain the Temporary Shield Ring (Figure 7.1.20), if used. Remove the ring segments and store them in an approved plant storage location.

ALARA Warning:

For ALARA reasons, decontamination of the overpack bottom shall be performed using pole-mounted cleaning tools or other remote leaning devices.

ALARA Warning:

If the overpack is to be downended on the transport frame, the bottom shield should be installed quickly. Personnel should remain clear of the bottom of the unshielded overpack.

7.1.7 Placement of the HI-STAR 100 Overpack on the Transport Frame

- 1. Position the transport frame under the overhead lifting device.

2. Install the HI-STAR 100 overpack buttress plate on the HI-STAR 100 overpack. See Figure 7.1.11 and 7.1.12 for rigging. See Table 7.1.3 for torque requirements.
3. Downend the HI-STAR 100 overpack in the transport frame. See Section 7.1.2.
4. Install the removable shear ring segments. See Table 7.1.3 for torque requirements.
5. Perform a final inspection of the HI-STAR 100 overpack as follows:

ALARA Warning:

Dose rates around the unshielded bottom end of the HI-STAR 100 overpack may be higher than other locations around the overpack. Workers should exercise appropriate ALARA controls when working around the bottom end of the HI-STAR 100 overpack.

Note:

Prior to shipment of the HI-STAR 100 package, the accessible external surfaces of the HI-STAR 100 packaging (HI-STAR 100 overpack, impact limiters, personnel barrier, tie-down, transport frame and transport vehicle) shall be surveyed for removable radiological contamination and show less than 2200 dpm/100 cm² from beta and gamma emitting sources, and 220 dpm/100 cm² from alpha emitting sources.

- a. Perform a final decontamination of the HI-STAR 100 overpack, and survey for removable contamination.
 - b. Perform a visual inspection of the HI-STAR 100 overpack to verify that there are no outward visual indications of impaired physical condition. Identify any significant indications to the cognizant individual for evaluation and resolution and record on the shipping documentation.
 - c. Verify that the HI-STAR 100 overpack neutron shield rupture discs are installed, intact and not covered by tape or other covering.
6. Install the tie-down over the HI-STAR 100 overpack and secure the tie-down bolts. See Table 7.1.3 for torque requirements.
 7. Install the impact limiters as follows:
 - a. Install the alignment pins in the bottom of the HI-STAR 100 overpack. See Figure 7.1.11. See Table 7.1.3 for torque requirements.
 - b. Using the impact limiter handling frame, raise and position the impact limiter over the end of HI-STAR 100. See Figure 7.1.10.
 - c. Install the impact limiter bolts. See Table 7.1.3 for torque requirements.
 - d. Repeat for the other impact limiter.

Note:

The impact limiters cover all the HI-STAR 100 penetrations. The security seals are used to provide tamper detection.

- e. Install a security seal (one each) through the threaded hole in the top and bottom impact limiter bolts. Record the security seal number on the shipping documentation.
 - f. Perform final radiation surveys of the package surfaces per 10CFR71.47 [7.0.1] and SAR Section 8.1.5.2 and 49CFR173.443 [7.1.3]. Record the results on the shipping documentation.
8. Install the personnel barrier as follows:
- a. Rig the personnel barrier as shown in Figure 7.1.9 and position the personnel barrier over the frame.
 - b. Remove the personnel barrier rigging and install the personnel barrier locks.
 - c. Transfer the personnel barrier keys to the carrier.
9. Perform a final check to ensure that the package is ready for release as follows:
- a. Verify that required radiation survey results are properly documented on the shipping documentation.
 - b. Perform a HI-STAR 100 overpack surface temperature check. The accessible surfaces of the HI-STAR 100 Package (impact limiters and personnel barrier) shall not exceed 185 °F when measured in the shade in still air.
 - c. Verify that all required leakage testing has been performed and the acceptance criteria has been met and document the results on the shipping documentation.
 - d. Verify that the receiver has been notified of the impending shipment and that the receiver has the appropriate procedures and equipment is available to safely receive and handle the HI-STAR 100 System (10CFR20.1906(e)) [7.1.4].
 - e. Verify that the carrier has the written instructions and a list of appropriate contacts for notification of accidents or delays.
 - f. Verify that the carrier has written instructions that the shipment is to be Exclusive Use in accordance with 49CFR172.443 [7.1.3].
 - g. Verify that route approvals and notification to appropriate agencies have been completed.

- h. Verify that the appropriate labels have been applied in accordance with 49CFR172.403.
 - i. Verify that the appropriate placards have been applied in accordance with 49CFR172.500.
 - j. Verify that all required information is recorded on the shipping documentation.
10. Release the HI-STAR 100 System for transport.

Table 7.1.1

HI-STAR 100 SYSTEM COMPONENT AND HANDLING WEIGHTS

Component	Weight (lbs)		Case Applicability †			
	MPC-24	MPC-68	1	2	3	4
Empty HI-STAR Overpack (without Closure Plate)	145,726	145,726	1	1	1	1
HI-STAR Closure Plate (without rigging)	7,984	7,984		1	1	1
Empty MPC (without Lid or Closure Ring)	29,075	28,502	1	1	1	1
MPC Lid (without Fuel Spacers or Drain Line)	9677	10,194	1	1	1	1
MPC Closure Ring	145	145		1	1	1
MPC Lower Fuel Spacers ^{††}	401	258	1	1	1	1
MPC Upper Fuel Spacers ^{††}	144	315	1	1	1	1
MPC Drain Line	50	50	1	1	1	1
Fuel (Design Basis)	36,360	42,092	1	1	1	1
Non Fuel Components	3,960	5,440				
Damaged Fuel Container (Dresden 1)	0	150				
Damaged Fuel Container (Humboldt Bay)	0	120				
MPC Water ^{†††} (with Fuel in MPC)	17,630	16,957	1			
Annulus Water	280	280	1			
HI-STAR Lift Yoke (with slings)	3600	3600	1	1		
Annulus Seal	50	50	1			
Lid Retention System	2300	2300				
Transport Frame	9000	9000			1	
Temporary Shield Ring	2500	2500				
Automated Welding System Baseplate Shield	2000	2000				
Automated Welding System Robot	1900	1900				
Top Impact Limiter (without Buttress Plate)	16,667	16,667			1	1
Bottom Impact Limiter	17,231	17,231			1	1
Impact Limiter Handling Frame	1980	1980				
Buttress Plate	2520	2520			1	1
Tie-Down	995	995			1	
Personnel Barrier	1500	1500			1	

† See Table 7.1.2.

†† The fuel spacers referenced in this table are for the heaviest fuel assembly for each MPC. This yields the maximum weight of fuel assemblies and spacers.

††† Varies by fuel type and loading configuration. Users may opt to pump some water from the MPC prior to removal from the spent fuel pool to reduce the overall lifted weight.

TABLE 7.1.2
 MAXIMUM HANDLING WEIGHTS
 HI-STAR 100 SYSTEM

Caution:

The maximum weight supported by the HI-STAR 100 overpack lifting trunnions (not including the lift yoke) cannot exceed 250,000 lbs. Users should determine their specific handling weights based on the MPC contents and the expected handling modes.

Note:

The weight of the fuel spacers and the damaged fuel container are less than the weight of the design basis fuel assembly for each MPC and are therefore not included in the maximum handling weight calculations.

Case No.	Load Handling Evolution	Weight (lbs)	
		MPC-24	MPC-68
1	Loaded HI-STAR Removal from Spent Fuel Pool	242,993	248,024
2	Loaded HI-STAR During Movement through Hatchway	233,162	238,866
3	Weight on Transport Vehicle	277,475	283,179
4	Gross HI-STAR 100 Package Weight	265,980	271,684

Table 7.1.3
HI-STAR 100 SYSTEM TORQUE REQUIREMENTS

Fastener	Torque (ft-lbs)	Pattern
Overpack Closure Plate Bolts ^{†, ††}	First Pass – Hand Tight Second Pass – Wrench Tight Third Pass – 860+25/-25 Fourth Pass – 1725+50/-50 Final Pass - 2895+90/-90	Figure 7.1.30
Overpack Vent and Drain Port Cover Plate Bolts ^{††}	12+2/-0	X-pattern
Overpack Vent and Drain Port Plugs	45+5/-0	None
Closure Plate Test Port Plug	45+5/-0	None
Backfill Tool Test Cover Bolts ^{††}	16+2/-0	X-pattern
Shear Ring Segments	22+2/-0	None
Overpack Bottom Cover Bolts	200+20/-0	None
Pocket Trunnion Plugs	Hand Tight	None
Threaded Fuel Spacers	Hand Tight	None
MPC Lid Threaded Plugs	Hand Tight	None
Impact Limiter Alignment Pin	Hand Tight	None
Top Impact Limiter Attachment Bolt	256+10/-0	None
Bottom Impact Limiter Attachment Bolt	1500+45/-0	None
Buttress Plate Bolts	150+10/-0	None
Tie-Down Bolts	250+20/-0	None
Transport Frame Bolts	250+20/-0	None

† Detorquing shall be performed by turning the bolts counter-clockwise in 1/3 turn +/- 30 degrees increments per pass according to Figure 7.1.30 for three passes. The bolts may then be removed.

†† Bolts shall be cleaned and inspected for damage or excessive wear (replaced if necessary) and coated with a light layer of Fel-Pro Chemical Products, N-5000, Nuclear Grade Lubricant (or equivalent).

Table 7.1.4
HI-STAR 100 SYSTEM ANCILLARY EQUIPMENT OPERATIONAL DESCRIPTION

Equipment	Important To Safety Classification	Reference Figure	Description
Annulus Overpressure System (optional)	Not Important To Safety	7.1.17	The Annulus Overpressure System is used for supplemental protection against spent fuel pool water contamination of the external MPC shell and baseplate surfaces by providing a slight annulus overpressure. The Annulus Overpressure System consists of the quick disconnects water reservoir, reservoir valve and annulus connector hoses. User is responsible for supplying demineralized water to the location of the Annulus Overpressure System.
Annulus Shield (optional)	Not Important To Safety	7.1.13	A segmented solid shield that is placed at the top of the annulus to provide supplemental shielding to the operators performing cask loading and closure operations. Shield segments are installed by hand, no crane or tools required.
Automated Welding System (optional)	Not Important To Safety	7.1.2b	Used for remote welding of the MPC lid, vent and drain port cover plates and the MPC closure ring. The AWS consists of the robot, wire feed system, torch system, weld power supply and gas lines.
AWS Baseplate Shield (optional)	Not Important To Safety	7.1.2b	The AWS baseplate shield provides supplemental shielding to the operators during the cask closure operations.
Backfill Tool	Not Important to Safety	7.1.28	Used to dry, backfill the HI-STAR 100 annulus and install the HI-STAR 100 overpack vent and drain port plugs. The backfill tool uses the same bolts as the HI-STAR 100 overpack vent and drain cover plates.
Blowdown Supply System	Not Important To Safety	7.1.24	Gas hose with pressure gauge, regulator used for blowdown of the MPC.
Closure Plate Test Tool	Not Important to Safety	7.1.29	Used to helium leakage test the HI-STAR 100 overpack Closure Plate inner mechanical seal.
Cool-Down System	Not Important To Safety	7.2.5	The Cool-Down System is a closed-loop forced ventilation cooling system used to gas-cool the MPC fuel assemblies down to a temperature water can be introduced without the risk of thermally shocking the fuel assemblies or flashing the water, causing uncontrolled pressure transients. The Cool-Down System is attached between the MPC drain and vent ports. The CDS consists of the piping, blower, heat exchanger, valves, instrumentation, and connectors. The CDS is used only for unloading operations.
Drain Connector	Not Important To Safety	7.1.17	Used for draining the annulus water following cask closure operations. The Drain Connector consists of the connector pipe valve, and quick disconnect for adapting to the Annulus Overpressure System.

Table 7.1.4 (Continued)
HI-STAR 100 SYSTEM ANCILLARY EQUIPMENT OPERATIONAL DESCRIPTION

Equipment	Important To Safety Classification	Reference Figure	Description
Four Legged Sling and Lifting Rings	Not Important To Safety (controlled under the user's rigging equipment program)	7.1.12	Used for rigging the HI-STAR 100 overpack upper shield lid, MPC lid, Automated Welding System Baseplate shield, and Automated Welding System Baseplate Shield. Consists of a four legged sling, lifting rings, shackles and a main lift link.
Helium Backfill System	Not Important To Safety	7.1.26	Used for helium backfilling of the MPC. System consists of the gas lines, mass flow monitor, integrator, and valved quick disconnect.
Hydrostatic Test System	Not Important to Safety	7.1.23	Used to hydrostatically test the MPC primary welds. The hydrostatic test system consists of the gauges, piping, pressure protection system piping and connectors.
Impact Limiter Handling Frame	Not Important to Safety	7.1.10	The impact limiter handling frame is used for installing, removing, handling and storing the impact limiters. The impact limiter handling frame consists of the handling frame and rigging.
Impact Limiters	Important to Safety	7.1.11	The impact limiters are used to limit the HI-STAR 100 decelerations to less than 60 g during postulated transportation accidents. The impact limiters consist of the top and bottom impact limiter and the connecting fasteners.
Inflatable Annulus Seal	Not Important To Safety	7.1.13	Used to prevent spent fuel pool water from contaminating the external MPC shell and baseplate surfaces during in-pool operations.
Lid Retention System (optional)	User designated	7.1.18	The Lid Retention System provides three functions; it guides the MPC lid into place during underwater installation, establishes lift yoke alignment with the HI-STAR 100 overpack trunnions, and locks the MPC lid in place during cask handling operations between the pool and decontamination pad. The device consists of the retention disk, alignment pins, lift yoke connector links and lift yoke attachment bolts.
Lift Yoke	User designated	7.1.3	Used for HI-STAR 100 overpack cask handling when used in conjunction with the overhead crane. The lift yoke consists of the lift yoke assembly and crane hook engagement pin(s). The lift yoke is a modular design that allows inspection, disassembly, maintenance and replacement of components.
MPC Fill Pump System (optional)	Not Important To Safety	Not shown	Large pump used for filling the MPC with spent fuel pool water prior to cask insertion into the spent fuel pool. Also used for emptying of the MPC for unloading operations.
MPC Upending Frame	Not Important to Safety	7.1.6	A welded steel frame used to evenly support the MPC during upending operations. The frame consists of the main frame, MPC support saddles, two rigging bars, wrap around-straps, and strap attachment lugs.

Table 7.1.4 (Continued)
 HI-STAR 100 SYSTEM ANCILLARY EQUIPMENT OPERATIONAL DESCRIPTION

Equipment	Important To Safety Classification	Reference Figure	Description
MSLD (Helium Leakage Detector)	Not Important To Safety	Not shown	Used for helium leakage testing of the MPC closure welds.
MSLD Calibration Sources	Not Important To Safety	Not shown	Traceable leakage sources for periodic calibration of the MSLD.
Overpack Bottom Cover (optional)	Not Important to Safety	Not shown	A cup-shaped shield used to reduce dose rates around the HI-STAR 100 overpack bottom end when operated in the horizontal orientation.
Overpack Test Cover	Not Important to Safety	7.1.27	Used to helium leakage test the HI-STAR 100 overpack vent and drain port plug seals.
Personnel Barrier	Not Important to Safety	7.1.9	The personnel barrier is a ventilated enclosure cage that fits over the main body of the HI-STAR 100 overpack. The personnel barrier is designed to restrict personnel accessibility to the potentially hot surfaces of the HI-STAR 100 overpack. The personnel barrier in conjunction with the impact limiters restrict accessibility to all surfaces of the HI-STAR 100 overpack during transport. The personnel barrier is equipped with locks to prevent unauthorized access. The personnel barrier is equipped with a four-legged bridle sling used for installation and removal.
Seal Surface Protector (optional)	Not Important to Safety	7.1.13	Used to protect the HI-STAR 100 overpack mechanical seal seating surface during loading and MPC closure operations.
Small Water Pump (optional)	Not Important To Safety	7.1.22	Used for lowering the MPC water level prior to lid welding. The small water pump consists of the pump, hose and connector fittings.
Temporary Shield Ring (optional)	Not Important To Safety	7.1.20	A water-filled segmented tank that fits on the cask neutron shield around the upper forging and provides supplemental shielding to personnel performing cask loading and closure operations. Shield segments are installed by hand, no tools are required.
Threaded Inserts	Not Important To Safety	Not shown	Used to fill the empty threaded holes in the HI-STAR 100 overpack and MPC.
Tie-Down	Not Important to Safety	7.1.11	The tie-down is a horse-shoe shaped collar that secures the HI-STAR 100 top end to the transport frame. The tie-down is secured by multiple bolts.
Transport Frame	Not Important To Safety	7.1.6	A welded steel frame used to support the HI-STAR 100 overpack during on-site movement and upending/downending operations. The frame consists of the rotation trunnions, main frame beams and front saddle.

Table 7.1.4 (Continued)
HI-STAR 100 SYSTEM ANCILLARY EQUIPMENT OPERATIONAL DESCRIPTION

Equipment	Important To Safety Classification	Reference Figure	Description
Transport Vehicle	Not Important to Safety	Not Shown	Any flatbed rail car, heavy haul trailer or other vice used to transport the loaded HI-STAR 100 overpack.
Vacuum Drying System	Not Important To Safety	7.1.25	Used for removal of residual moisture from the MPC and HI-STAR 100 Overpack annulus following water draining. Used for evacuation of the MPC to support backfilling operations. Used to support test volume samples for MPC unloading operations. The VDS consists of the vacuum pump, piping, skid, gauges, valves, inlet filter, flexible hoses, connectors, control system.
Vacuum Drying System Fore-Line Condenser (optional)	Not Important to Safety	Not Shown	Optional item used to improve the Vacuum Drying System pump efficiency. The condenser removes water from the vacuum stream prior to the vacuum pump.
Vent and Drain RVOAs (optional)	Not Important To Safety	7.1.21	Used to drain, dry, inert and fill the MPC through the vent and drain ports. The vent and drain RVOAs allow the vent and drain ports to be operated like valves and prevent the need to hot tap into the penetrations during unloading operation.
Warming Pad (optional)	Not Important to Safety	Not Shown	Used to improve vacuum drying time for older and colder fuel assemblies. The pad consists of the heater pad, heater, circulation pump, expansion tank, hoses and fittings. Other configurations are acceptable.
Water Totalizers	Not Important To Safety	7.1.22 and 7.1.24	Used for water pump-down prior to lid welding operations and water removal for MPC helium leakage testing.
Weld Removal System (optional)	Not Important To Safety	7.2.2b	Semi-automated weld removal system used for removal of the MPC to shell weld, MPC to closure ring weld and closure ring to MPC shell weld. The WRS mechanically removes the welds using a high-speed cutter.

Table 7.1.5
 HI-STAR 100 SYSTEM INSTRUMENTATION SUMMARY FOR LOADING AND
 UNLOADING OPERATIONS†

Note:

The following list summarizes the instruments identified in the procedures for cask loading and unloading operations. Alternate instruments are acceptable as long as they can perform appropriate measurements.

Instrument	Function
Dose Rate Monitors/Survey Equipment	Monitors dose rate and contamination levels and ensures proper function of shielding. Ensures assembly debris is not inadvertently removed from the spent fuel pool during overpack removal.
Flow Rate Monitor	Monitors the air flow rate during assembly cool-down.
Helium Mass Flow Monitor	Determines the amount of helium introduced into the MPC during backfilling operations. Includes integrator.
Helium Mass Spectrometer Leak Detector (MSLD)	Ensures leakage rates of welds are within acceptance criteria.
Helium Pressure Gauges	Ensures correct helium backfill pressure during backfilling operation.
Volumetric Testing Rig	Used to assess the integrity of the MPC lid-to-shell weld.
Pressure Gauge	Ensures correct helium pressure during fuel cool-down operations.
Hydrostatic Test Pressure Gauge	Used for hydrostatic testing of MPC lid-to-shell weld.
Temperature Gauge	Monitors the state of fuel cool-down prior to MPC flooding.
Temperature Probe	For fuel cool-down operations
Vacuum Gauges	Used for vacuum drying operations and to prepare an MPC evacuated sample bottle for MPC gas sampling for unloading operations.
Water Pressure Gauge	Used for performance of the MPC Hydrostatic Test.
Water Totalizer	Used for water pump-down prior to lid welding operations and water removal for MPC helium leakage testing.

† All instruments require calibration. See figures at the end of this section for additional instruments, controllers and piping diagrams.

Table 7.1.6
HI-STAR 100 OVERPACK SAMPLE INSPECTION CHECKLIST

Note:

This checklist provides the basis for establishing a site-specific inspection checklist for the HI-STAR 100 overpack. Specific findings shall be brought to the attention of the appropriate site organizations for assessment, evaluation and potential corrective action prior to use.

HI-STAR 100 Overpack Closure Plate:

1. Lifting rings shall be inspected for general condition and date of required load test certification.
2. The test port shall be inspected for dirt and debris, hole blockage, thread condition, presence or availability of the port plug and replacement mechanical seals.
3. The mechanical seal grooves shall be inspected for cleanliness, dents, scratches and gouges and the presence or availability of replacement mechanical seals.
4. The painted surfaces shall be inspected for corrosion and chipped, cracked or blistered paint.
5. All closure plate surfaces shall be relatively free of dents, scratches, gouges or other damage.
6. The vent port plug shall be inspected for thread condition, and sealing surface condition (scratches, gouges).
7. Overpack vent port shall be inspected for presence or availability of port plugs, hole blockage, plug seal seating surface condition.
8. Overpack vent port cover plate shall be inspected for cleanliness, scratches, dents, and gouges, availability of retention bolts, availability of replacement mechanical seals.

HI-STAR 100 Overpack Main Body:

1. The impact limiter attachment bolt holes shall be inspected for dirt and debris and thread condition.
2. The mechanical seal seating surface shall be inspected for cleanliness, scratches, and dents or gouges.
3. The drain port plug shall be inspected for thread condition, and sealing surface condition (scratches, gouges).
4. The closure plate bolt holes shall be inspected for dirt, debris and thread damage.
5. Painted surfaces shall be inspected for corrosion and chipped, cracked or blistered paint.
6. Trunnions shall be inspected for deformation, cracks, thread damage, end plate damage, corrosion, excessive galling, damage to the locking plate, presence or availability of locking plate and end plate retention bolts.

Table 7.1.6
HI-STAR 100 OVERPACK SAMPLE INSPECTION CHECKLIST
(continued)

7. Pocket trunnion recesses shall be inspected for indications of over stressing (i.e., cracks, deformation, excessive wear).
8. Overpack drain port cover plate shall be inspected for cleanliness, scratches, dents, and gouges, availability of retention bolts, availability of replacement mechanical seals.
9. Overpack drain port shall be inspected for presence or availability of port plug, availability of replacement mechanical seals, hole blockage, plug seal seating surface condition.
10. Annulus inflatable seal groove shall be inspected for cleanliness, scratches, dents, gouges, sharp corners, burrs or any other condition that may damage the inflatable seal.
11. The overpack rupture disks shall be inspected for presence or availability and the top surface of the disk shall be visually inspected for holes, cracks, tears or breakage.
12. The nameplate shall be inspected for presence and general condition.
13. The removable shear ring shall be inspected for fit and thread condition.

Table 7.1.7
MPC SAMPLE INSPECTION CHECKLIST

Note:

This checklist provides the basis for establishing a site-specific inspection checklist for MPC. Specific findings shall be brought to the attention of the appropriate site organizations for assessment, evaluation and potential corrective action prior to use.

MPC Lid and Closure Ring:

1. The MPC lid and closure ring surfaces shall be relatively free of dents, gouges or other shipping damage.
2. The drain line shall be inspected for straightness, thread condition, and blockage.
3. Upper fuel spacers (if used) shall be inspected for availability and general condition. Plugs shall be available for non-used spacer locations.
4. Lower fuel spacers (if used) shall be inspected for availability and general condition.
5. Drain and vent port cover plates shall be inspected for availability and general condition.
6. Serial numbers shall be inspected for readability.

MPC Main Body:

1. All visible MPC body surfaces shall be inspected for dents, gouges or other shipping damage.
2. Fuel cell openings shall be inspected for debris, dents and general condition.
3. Lift lugs shall be inspected for general condition.
4. Verify proper MPC basket type for contents.

7.2 PROCEDURE FOR UNLOADING THE HI-STAR 100 SYSTEM IN THE SPENT FUEL POOL

7.2.1 Overview of HI-STAR 100 System Unloading Operations

ALARA Note:

The procedure described below uses the Weld Removal System, a remotely operated system that mechanically removes the welds. Users may opt to remove some or all of the welds using hand operated equipment. The decision should be based on dose rates, accessibility, degree of weld removal, and available tooling and equipment.

The HI-STAR 100 System unloading procedures describe the general actions necessary to prepare the MPC for unloading, cool the stored fuel assemblies in the MPC, flood the MPC cavity, remove the lid welds, unload the spent fuel assemblies, and recover the HI-STAR 100 overpack and empty MPC. These procedures are only used to respond to extreme abnormal events. Special precautions are outlined to ensure personnel safety during the unloading operations, and to prevent the risk of MPC over-pressurization and thermal shock to the stored spent fuel assemblies. Figure 7.2.1 shows a flow diagram of the HI-STAR 100 overpack unloading operations. Figure 7.2.2 illustrates the major HI-STAR 100 overpack unloading operations.

Refer to the boxes of Figure 7.2.2 for the following description. The HI-STAR 100 overpack is received from the carrier, inspected and surveyed. The personnel barrier is removed and the impact limiters and tie-down are removed. The HI-STAR 100 overpack is upended and returned to the fuel building (Box 1). The HI-STAR 100 overpack vent port cover plate is removed and a gas sample is drawn from the HI-STAR 100 overpack annulus to determine the condition of the MPC confinement boundary. The annulus is depressurized and the HI-STAR 100 overpack closure plate is removed (Box 2). The Temporary Shield Ring is installed on the HI-STAR 100 overpack upper section. The Temporary Shield Ring and annulus are filled with plant demineralized water. The annulus shield is installed to protect the annulus from debris produced from the lid removal process. The MPC closure ring above the vent and drain ports and the vent and drain port cover plates are core-drilled and removed to access the vent and drain ports. (Box 3). The design of the vent and drain ports use metal-to-metal seals that prevent rapid decompression of the MPC and subsequent spread of contamination during unloading. The vent RVOA is attached to the vent port and an evacuated sample bottle is connected. The vent port is slightly opened to allow the sample bottle to obtain a gas sample from inside the MPC. A gas sample is performed to assess the condition of the fuel assembly cladding. The MPC is cooled using a closed-loop heat exchanger to reduce the MPC internal temperature to allow water flooding (Box 4). The cool-down process gradually reduces the cladding temperature to a point where the MPC may be flooded with water without thermally shocking the fuel assemblies or over-pressurizing the MPC from the formation of steam. Following the fuel cool-down, the MPC is filled with water at a specified rate (Box 5). The Weld Removal System then removes the MPC lid to MPC shell weld. The Weld Removal System is removed with the MPC lid left in place (Box 6).

The top surfaces of the HI-STAR 100 overpack and MPC are cleared of metal shavings. The inflatable annulus seal is installed and pressurized. The MPC lid is rigged to the lift yoke or lid retention system and the lift yoke is engaged to the HI-STAR 100 overpack lifting trunnions. The HI-STAR 100 overpack is placed in the spent fuel pool and the MPC lid is removed (Box 7). All fuel assemblies are returned to the spent fuel storage racks and the MPC fuel cells are vacuumed to remove any assembly debris and crud (Box 8). The HI-STAR 100 overpack and MPC are returned to the designated preparation area (Box 9) where the MPC water is pumped back into the spent fuel pool, liquid radwaste system or other approved location. The annulus water is drained and the MPC and overpack are decontaminated (Box 10 and 11).

7.2.2 HI-STAR 100 Overpack Packaging Receipt

1. Recover the shipping documentation from the carrier along with the keys to the personnel barrier locks.
2. Remove the personnel barrier (See Figure 7.1.9) and perform a partial visual inspection of the HI-STAR 100 overpack to verify that there are no outward visual indications of impaired physical conditions. Identify any significant indications to the cognizant individual for evaluation and resolution.

ALARA Warning:

Dose rates around the unshielded bottom end of the HI-STAR 100 overpack may be higher than other locations around the overpack. Workers should exercise appropriate ALARA controls when working around the bottom end of the HI-STAR 100 overpack.

3. Remove the impact limiters as follows:
 - a. Record the impact limiter security seal serial numbers and verify that they match the corresponding shipping documentation, as applicable.
 - b. Clip the security seal wires and remove the security seals and wires.
 - c. Attach the impact limiter handling frame as shown on Figure 7.1.10.

Caution:

The slings should be preloaded to the impact limiter weight plus the weight of the impact limiter handling frame prior to removal of the impact limiter bolts. (See Table 7.1.1) This will prevent movement of the impact limiter and damage to the bolts from excessive lift pressure during bolt removal.

- d. Using the load cell, apply the correct lift load. See Table 7.1.1.
- e. Remove the bolts securing the impact limiter to the overpack. See Figure 7.1.11.
- f. Remove the impact limiter and store the impact limiter in a site-approved location.

- g. Repeat Steps 3.c. through 3.f. for the other impact limiter.
4. Complete the HI-STAR 100 overpack visual inspection to verify that there are no outward visual indications of impaired physical conditions. Identify any significant indications to the cognizant individual for evaluation and resolution.

Note:

On receipt of the loaded or empty HI-STAR 100 packaging, the accessible external surfaces of the HI-STAR 100 packaging (HI-STAR 100 overpack, impact limiters, personnel barrier, tie-down, transport frame and transport vehicle) shall be surveyed for removable radiological contamination and show less than 2200 dpm/100 cm² from beta and gamma emitting sources, and 220 dpm/100 cm² from alpha emitting sources.

5. Perform a radiation survey and removable contamination survey. Record the results on the shipping documentation.
6. Verify that the HI-STAR 100 overpack neutron shield rupture discs are installed and intact. Identify any non-conformances to the cognizant individual for evaluation and resolution.
7. If necessary, upend the HI-STAR 100 overpack in accordance with Section 7.1.2.
8. Transfer the HI-STAR 100 overpack to the fuel building.
9. Remove the buttress plate. See Figure 7.1.11 and 7.1.12.
10. Place the HI-STAR 100 overpack in the designated preparation area.

7.2.3 Preparation for Unloading

ALARA Warning:

Gas sampling is performed to assess the condition of the MPC confinement boundary. If a leak is discovered in the MPC boundary, the user's Radiation Control organization may require special actions to vent the HI-STAR 100.

1. Perform annulus gas sampling as follows:
 - a. Remove the overpack vent port cover plate and attach the backfill tool with a sample bottle attached. See Figure 7.2.3. Store the cover plate in a site-approved location.
 - b. Using a vacuum pump, evacuate the sample bottle and backfill tool.
 - c. Slowly open the vent port plug and gather a gas sample from the annulus. Reinstall the HI-STAR 100 overpack vent port plug.
 - d. Evaluate the gas sample and determine the condition of the MPC confinement boundary.

2. If the confinement boundary is intact (i.e., no radioactive gas is measured) then vent the overpack annulus by removing the overpack vent port seal plug (using the backfill tool). Otherwise vent the annulus gas in accordance with instructions from Radiation Protection.
3. Remove the closure plate bolts. See Table 7.1.3 for detorquing requirements. Store the closure plate bolts in a site-approved location.
4. Remove the overpack closure plate. See Figure 7.1.12 for rigging. Store the closure plate on cribbing to protect the seal seating surfaces.
5. Install the HI-STAR 100 overpack Seal Surface Protector (See Figure 7.1.13).

Warning:

Annulus fill water may flash to steam due to high MPC shell temperatures. Water addition should be performed in a slow and controlled manner.

6. Remove the HI-STAR 100 overpack drain port cover and port plug and install the drain connector. Store the drain port cover plate and port plug in an approved storage location.
7. Slowly fill the annulus area with plant demineralized water to approximately 4 inches below the top of the MPC shell and install the annulus shield. The annulus shield reduces the dose around the annulus area and prevents debris from entering the annulus during MPC lid weld removal operations. See Figure 7.1.13.
8. Remove the MPC closure welds as follows:

ALARA Note:

The following procedures describe weld removal using the Weld Removal System. The Weld Removal System removes the welds with a high speed machine tool head. A vacuum head is attached to remove a majority of the metal shavings. Other methods of opening the MPC are acceptable.

ALARA Warning:

Weld removal may create an airborne radiation condition. Weld removal must be performed under the direction of the user's Radiation Protection organization.

- a. Install bolt plugs and/or waterproof tape on the closure plate bolt holes.
 - b. Install the Weld Removal System on the MPC lid and core drill through the closure ring and vent and drain port cover plate welds.
9. Access the vent and drain ports.
 - a.
 10. Remove the vent port cover plate weld and remove the vent port cover plate.

ALARA Note:

The MPC vent and drain ports are equipped with metal-to-metal seals to minimize leakage and withstand the long-term effects of temperature and radiation. The vent and drain port design prevents the need to hot tap into the penetrations during unloading operation and eliminate the risk of a pressurized release of gas from the MPC.

11. Take an MPC gas sample as follows:
 - a. Attach the RVOA to the vent port (See Figure 7.1.21).
 - b. Attach a sample bottle to the vent port RVOA as shown on Figure 7.2.4.
 - c. Using the Vacuum Drying System, evacuate the RVOA and Sample Bottle.
 - d. Slowly open the vent port cap using the RVOA and gather a gas sample from the MPC internal atmosphere.
 - e. Close the vent port cap and disconnect the sample bottle.

ALARA Note:

The gas sample analysis is performed to determine the condition of the fuel cladding in the MPC. The gas sample may indicate that fuel with damaged cladding is present in the MPC. The results of the gas sample test may affect personnel protection and how the gas is processed during MPC depressurization.

- f. Turn the sample bottle over to the site's Radiation Protection or Chemistry Department for analysis.
 - g. Install the RVOA in the drain port.
12. Perform Fuel Assembly Cool-Down as follows:
 - a. Configure the Cool-Down System as shown on Figure 7.2.5.
 - b. Verify that the helium gas pressure regulator is set to less than 100 psig.
 - c. Open the helium gas supply valve to purge the gas lines of air.

Note:

The coolant flow direction is into the drain port and out of the vent port.

- d. Confirm the heat exchanger coolant flow direction.
 - e. If necessary, slowly open the helium supply valve and increase the Cool-Down System pressure to MPC pressure. Close the helium supply valve.
 - f. Start the gas coolers.
 - g. Open the vent and drain port caps using the RVOAs.

- h. Start the blower and monitor the gas exit temperature. Continue the fuel cool-down operations until the gas exit temperature is $\leq 200^{\circ}$ F. These conditions shall be met prior to initiation of MPC re-flooding operations.

Note:

Water filling should commence immediately after the completion of fuel cool-down operations to minimize prevent fuel assembly heat-up. Prepare the water fill and vent lines in advance of water filling.

- i. Prepare the MPC fill and vent lines as shown on Figure 7.1.23. Route the vent port line several feet below the spent fuel pool surface or to the radwaste gas facility. Turn off the blower and disconnect the gas lines to the vent and drain port RVOAs. Attach the vent line to the MPC vent port and slowly open the vent line valve to depressurize the MPC.
 - j. Attach the water fill line to the MPC drain port and slowly open the water supply valve and establish a pressure less than 90 psi. Fill the MPC until bubbling from the vent line has terminated. Close the water supply valve on completion.
 - k. Disconnect both lines from the drain and vent ports leaving the drain port cap open to allow for thermal expansion of the water during MPC lid weld removal.
 - l. Remove the closure ring-to-MPC shell weld and the MPC lid-to-shell weld using the Weld Removal System and remove the Weld Removal System. See Figure 7.1.12 for rigging.
 - m. Vacuum the top surfaces of the MPC and the HI-STAR 100 overpack to remove any metal shavings.
13. Install the inflatable annulus seal as follows:

Caution:

Do not use any sharp tools or instruments to install the inflatable seal.

- a. Remove the annulus shield.
 - b. Manually insert the inflatable seal around the MPC. See Figure 7.1.13.
 - c. Ensure that the seal is uniformly positioned in the annulus area.
 - d. Inflate the seal between 30 and 35 psig or as directed by the manufacturer.
 - e. Visually inspect the seal to ensure that it is properly seated in the annulus. Deflate, adjust and inflate the seal as necessary.
14. Place HI-STAR 100 overpack in the spent fuel pool as follows:

- a. Engage the lift yoke to the HI-STAR 100 overpack lifting trunnions, remove the MPC lid lifting threaded inserts and attach the MPC lid slings or Lid Retention System to the MPC lid.
- b. If the Lid Retention System is used, inspect the lid bolts for general condition. Replace worn or damaged bolts with new bolts.
- c. Install the Lid Retention System bolts if the Lid Retention System is used.

ALARA Note:

The Annulus Overpressure System is used to provide additional protection against MPC external shell contamination during in-pool operations. The Annulus Overpressure System is equipped with double locking quick disconnects to prevent inadvertent draining. The reservoir valve must be closed to ensure that the annulus is not inadvertently drained through the Annulus Overpressure System when the cask is raised above the level of the annulus reservoir.

- d. If used, fill the Annulus Overpressure System lines and reservoir with demineralized water and close the reservoir valve. Attach the Annulus Overpressure System to the HI-STAR 100 overpack via the quick disconnect. See Figure 7.1.17.

Warning:

Cask placement in the spent fuel pool is the heaviest lift that occurs during the HI-STAR 100 unloading operations. The HI-STAR 100 trunnions must not be subjected to lifted loads in excess of 250,000 lbs. Users must ensure that plant-specific lifting equipment is qualified to lift the expected load. Users may elect to pump a measured quantity of water from the MPC prior to placement of the HI-STAR 100 in the spent fuel pool. See Table 7.1.1 and 7.1.2 for weight information.

- e. Position the HI-STAR 100 overpack over the cask loading area with the basket aligned to the orientation of the spent fuel racks.

ALARA Note:

Wetting the components that enter the spent fuel pool may reduce the amount of decontamination work to be performed later.

- f. Wet the surfaces of the HI-STAR 100 overpack and lift yoke with plant demineralized water while slowly lowering the HI-STAR 100 overpack into the spent fuel pool.
- g. When the top of the HI-STAR 100 overpack reaches the approximate elevation of the reservoir, open the Annulus Overpressure System reservoir valve. Maintain the reservoir water level at approximately 3/4 full the entire time the cask is in the spent fuel pool.
- h. If the Lid Retention System is used, remove the lid retention bolts when the top of the HI-STAR 100 overpack is accessible from the operating floor.

- i. Place the HI-STAR 100 overpack on the floor of the cask loading area and disengage the lift yoke. Visually verify that the lift yoke is fully disengaged.

Note:

An underwater camera or other suitable viewing device may be used for monitoring the underwater operations.

- j. Apply slight tension to the lift yoke and visually verify proper disengagement of the lift yoke from the trunnions.
- k. Remove the lift yoke, MPC lid and drain line from the pool in accordance with directions from the site's Radiation Protection personnel. Spray the equipment with demineralized water as they are removed from the pool.

Warning:

The MPC lid and unloaded MPC may contain residual contamination. All work done on the unloaded MPC should be carefully monitored and performed.

- l. Disconnect the drain line from the MPC lid.
- m. Store the MPC lid components in an approved location. Disengage the lift yoke from MPC lid. Remove any upper fuel spacers using the same process as was used in the installation.
- n. Disconnect the Lid Retention System if used.

7.2.4 MPC Unloading

1. Remove the spent fuel assemblies from the MPC using applicable site procedures.
2. Vacuum the cells of the MPC to remove any debris or corrosion products.
3. Inspect the open cells for presence of any remaining items. Remove them as appropriate.

7.2.5 Post-Unloading Operations

1. Remove the HI-STAR 100 overpack and the unloaded MPC from the spent fuel pool as follows:
 - a. Engage the lift yoke to the top trunnions.
 - b. Apply slight tension to the lift yoke and visually verify proper engagement of the lift yoke to the trunnions.
 - c. Raise the HI-STAR 100 overpack until the HI-STAR 100 overpack flange is at the surface of the spent fuel pool.

ALARA Warning:

Activated debris may have settled on the top face of the HI-STAR 100 overpack during fuel unloading.

- d. Measure the dose rates at the top of the HI-STAR 100 overpack in accordance with plant radiological procedures and flush or wash the top surfaces to remove any highly-radioactive particles.
- e. Raise the top of the HI-STAR 100 overpack and MPC to the level of the spent fuel pool deck.
- f. Close the Annulus Overpressure System reservoir valve if the Annulus Overpressure System was used.
- g. Using a water pump, lower the water level in the MPC approximately 12 inches to prevent splashing during cask movement.

ALARA Note:

To reduce contamination of the HI-STAR 100 overpack, the surfaces of the HI-STAR 100 overpack and lift yoke should be kept wet until decontamination can begin.

- h. Remove the HI-STAR 100 overpack from the spent fuel pool while spraying the surfaces with plant demineralized water.
 - i. Disconnect the Annulus Overpressure System from the HI-STAR 100 overpack via the quick disconnect. Drain the Annulus Overpressure System lines and reservoir.
 - j. Place the HI-STAR 100 overpack in the designated preparation area.
 - k. Disengage the lift yoke.
 - l. Perform decontamination on the HI-STAR 100 overpack and the lift yoke.
2. Carefully decontaminate the area above the inflatable seal. Deflate, remove, and store the seal in an approved plant storage location.
 3. Using a water pump, pump the remaining water in the MPC to the spent fuel pool or liquid radwaste system.
 4. Drain the water in the annulus.
 5. Remove the MPC from the HI-STAR 100 overpack and decontaminate the MPC as necessary.
 6. Decontaminate the HI-STAR 100 overpack.

7. Remove any bolt plugs, seal surface protector and/or waterproof tape from the HI-STAR 100 overpack top bolt holes.
8. Move the HI-STAR 100 overpack and MPC for further inspection, corrective actions, or disposal as necessary.

7.3 PREPARATION OF AN EMPTY PACKAGE FOR TRANSPORT

7.3.1 Overview of the HI-STAR 100 System Empty Package Transport

The operations for preparing an empty package (previously used) for transport are similar to those required for transporting the loaded package with several exceptions. The closure plate is installed and the bolts are torqued. The HI-STAR 100 overpack is downended on the transport frame and the tie-down is installed. A survey for removable contamination is performed to verify that the removable contamination on the internal and external surfaces of the HI-STAR 100 overpack are ALARA and that the limits of 49CFR173.428 [7.1.3] and 10CFR71.87(i) [7.0.1] are met. At the User's discretion, impact limiters are installed and the personnel barrier is installed and locked. The procedures provided herein describe the installation of the impact limiters and personnel barrier. These steps may be omitted as needed.

7.3.2 Preparation for Empty Package Shipment

1. Install the closure plate as follows:

Note:
For empty shipments of the HI-STAR 100 overpack, used metallic seals may be reused.

- a. Remove the Seal Surface Protector from the HI-STAR 100 overpack if necessary.
 - b. Perform a contamination survey of the top accessible 12-inches of the HI-STAR 100 Overpack inside surface in accordance with 49CFR173.421(a)(3) [7.1.3]. Verify that the non-fixed contamination levels do not exceed 220,000 dpm/100 cm² from beta and gamma radiation and 22,000 pm/100 cm² from alpha.
 - c. Verify that the HI-STAR 100 Overpack is empty and contains less than 15 gm U-235 in accordance with 49CFR173.421(a)(5) [7.3.1].
 - d. Raise and install the closure plate on the HI-STAR 100 overpack. See Figure 7.1.12 for rigging.
 - e. Install and torque the closure plate bolts. See Table 7.1.3 for torque requirements.
 - f. If necessary, install the vent and drain coverplates.
2. Position the HI-STAR 100 overpack on the transport frame as follows:
 - a. Install the HI-STAR 100 overpack buttress plate on the HI-STAR 100 overpack. See Figure 7.1.11 and 7.1.12 for rigging. See Table 7.1.3 for torque requirements.
 - b. Downend the HI-STAR 100 overpack in the transport frame. See Section 7.1.2.
 - c. Install the removable shear ring segments. See Table 7.1.3 for torque requirements.

3. Perform a final inspection of the HI-STAR 100 overpack as follows:

Note:

Prior to shipment of the HI-STAR 100 package, the accessible external surfaces of the HI-STAR 100 packaging (HI-STAR 100 overpack, impact limiters, personnel barrier, tie-down, transport frame and transport vehicle) shall be surveyed for removable radiological contamination in accordance with 49CFR173.443(a) [7.1.3] and show less than 2200 dpm/100 cm² from beta and gamma emitting sources, and 220 dpm/100 cm² from alpha emitting sources.

- a. Perform a final survey for removable contamination. Record the results on the shipping documentation.
 - b. Perform a radiation survey of the HI-STAR 100 Overpack and confirm that the radiation levels on any external surface of the overpack do not exceed 0.5 mrem/hour in accordance with 49CFR173.421(a)(2) [7.1.3].
 - c. Perform a visual inspection of the HI-STAR 100 overpack to verify that there are no outward visual indications of impaired physical condition and that the package is securely closed in accordance with 49CFR173.428(b) [7.1.3]. Identify any significant indications to the cognizant individual for evaluation and resolution and record on the shipping documentation.
 - d. Verify that the HI-STAR 100 overpack neutron shield rupture discs are installed, intact and not covered by tape or other covering.
4. Install the tie-down over the HI-STAR 100 overpack and secure the tie-down bolts. See Table 7.1.3 for torque requirements.
5. If necessary, Install the impact limiters as follows:
- a. Install the alignment pins in the bottom of the HI-STAR 100 overpack. See Figure 7.1.11. See Table 7.1.3 for torque requirements.
 - b. Using the impact limiter handling frame, raise and position the impact limiter over the end of HI-STAR 100. See Figure 7.1.10.
 - c. Install the impact limiter bolts. See Table 7.1.3 for torque requirements.
 - d. Repeat for the other impact limiter.

Note:

The impact limiters cover all the HI-STAR 100 penetrations. The security seals are used to provide tamper detection.

- e. Install a security seal (one each) through the threaded hole in the top and bottom impact limiter bolts. Record the security seal number on the shipping documentation.

- f. Perform final radiation surveys of the package surfaces per 10CFR71.47 [7.0.1] and SAR Section 8.1.5.2 and 49CFR173.428(a)(2) [7.1.3].
6. Install the personnel barrier as follows:
 - a. Rig the personnel barrier as shown in Figure 7.1.9 and position the personnel barrier over the frame.
 - b. Remove the personnel barrier rigging and install the personnel barrier locks.
 - c. Transfer the personnel barrier keys to the carrier.
7. Perform a final check to ensure that the package is ready for release as follows:
 - a. Verify that the receiver has been notified of the impending shipment.
 - b. Verify that any labels previously applied in conformance with Subpart E of 49CFR172 [7.1.3] have been removed, obliterated, or covered and the "Empty" label prescribed in 49CFR172.450 [7.1.3] is affixed to the packaging in accordance with 49CFR173.428(d) [7.1.3].
 - c. Verify that the package for shipment is prepared in accordance with 49CFR173.422 [7.1.3]
 - d. Verify that all required information is recorded on the shipping documentation.
8. Release the HI-STAR 100 System for transport.

7.4 PROCEDURE FOR PREPARING THE HI-STAR 100 OVERPACK FOR TRANSPORT FOLLOWING A PERIOD OF STORAGE

7.4.1 Overview of the HI-STAR 100 System Preparation for Transport Following a Period of Storage

The operations for preparing the loaded HI-STAR 100 Overpack for transport following a period of storage (in excess of one year from the date of completion of HI-STAR 100 Overpack mechanical seal leakage testing) are identical to the later portion of operations required for normal transport of the package as summarized herein. The cask is positioned and the closure plate test port plug, HI-STAR 100 Overpack vent port cover and drain port cover plates are removed. The MSLD is attached and the mechanical seal leakage test is repeated as described in Section 7.1.6. Following successful completion of the leakage tests the closure plate plug and vent and drain port cover plates are reinstalled with new seals. The package is prepared for transport as described in Section 7.1.6.

For the MPC-68F, The HI-STAR 100 overpack vent port cover plate is removed and a gas sample is drawn from the HI-STAR 100 overpack annulus to determine the condition of the MPC confinement boundary. The annulus is vented (as described in Section 7.2.3), evacuated and backfilled with nitrogen gas several times to clear residual helium from the annulus space. The MPC-68F is then leakage tested as described in Section 7.1.6. Following the leakage test of the MPC-68F, the HI-STAR 100 Overpack is prepared for transport as described in Section 7.1.6.

7.4.2 Preparation for Transport Following a Period of Storage

1. Position the HI-STAR 100 Overpack from leakage testing.

Note:

Leakage testing for transport is only required for packages whose metallic seals have not been leakage tested within the last 12 months (in excess of one year from the date of completion of HI-STAR 100 Overpack mechanical seal leakage testing). Step 2 is only required for the MPC-68F. Skip this step if not applicable.

2. If necessary, perform a leakage test of the MPC-68F as follows:
 - a. Sample the annulus gas as follows:
 1. Remove the overpack vent port cover plate and attach the backfill tool with a sample bottle attached. See Figure 7.2.3. Store the cover plate in a site-approved location.
 2. Using a vacuum pump, evacuate the sample bottle and backfill tool.
 3. Slowly open the vent port plug and gather a gas sample from the annulus. Reinstall the HI-STAR 100 overpack vent port plug.

- b. Evaluate the gas sample and determine the condition of the MPC confinement boundary.
- c. If the confinement boundary is intact (i.e., no radioactive gas is measured) then vent the overpack annulus by removing the overpack vent port seal plug (using the backfill tool). Otherwise vent the annulus gas in accordance with instructions from Radiation Protection.
- d. Flush the annulus and perform leakage testing of the MPC-68F as follows:
 1. Install the overpack test cover to the overpack vent port as shown on Figure 7.1.27. See Table 7.1.3 for torque requirements.
 2. Evacuate the annulus to below 5 torr and break the vacuum allowing air to fill the annulus space. Repeat this process several times to remove residual helium from the annulus space.
 3. Evacuate the annulus per the MSLD manufacturer's instructions and isolate the vacuum pump from the overpack test cover.
 4. Perform a leakage rate test of MPC-68F per the MSLD manufacturer's instructions. The overpack Helium Leak Rate shall be $\leq 5.0E-6$ std cc/sec (He) with a minimum test sensitivity less than $2.5E-6$ std cc/sec (He).
 5. Disconnect the overpack test cover.
 6. Remove the closure plate test port plug. Discard any used metallic seals.
- e. Dry and backfill the overpack annulus as follows:
 1. Load the backfill tool with the HI-STAR 100 overpack vent port plug and the vent port with a new plug seal. Attach the backfill tool to the HI-STAR 100 overpack vent port with the plug removed. See Figure 7.1.28. See Table 7.1.3 for torque requirements.
 2. Attach the Vacuum Drying System to the backfill tool and reduce the HI-STAR 100 overpack pressure to below 3 torr.

Note:

The annulus pressure may rise due to the presence of water in the HI-STAR 100 overpack. The dryness test may need to be repeated several times until all the water has been removed. Leaks in the Vacuum Drying System, damage to the vacuum pump, and improper vacuum gauge calibration may cause repeated failure of the dryness verification test. These conditions should be checked as part of the corrective actions if repeated failure of the dryness verification test is occurring.

3. Perform a HI-STAR 100 overpack Annulus Dryness Verification. The overpack annulus shall hold stable vacuum drying pressure of ≤ 3 torr for ≥ 30 minutes.
 4. Attach the helium supply to the backfill tool.
 5. Verify the correct pressure on the helium supply (pressure set to $10 \pm 4/0$ psig) and open the helium supply valve.
 6. Backfill the HI-STAR 100 overpack annulus to ≥ 10 psig and ≤ 14 psig.
 7. Install the overpack vent port plug and torque. See Table 7.1.3 for torque requirements.
 8. Disconnect the overpack backfill tool from the vent port.
 9. Flush the overpack vent port recess with compressed air to remove any standing helium gas.
3. Leak test the HI-STAR 100 Overpack vent and drain port plug mechanical seals as follows:
- a. Install the overpack test cover to the overpack vent port as shown on Figure 7.1.27. See Table 7.1.3 for torque requirements.
 - b. Evacuate the test cavity per the MSLD manufacturer's instructions and isolate the vacuum pump from the overpack test cover.
 - c. Perform a leakage rate test of overpack vent port plug per the MSLD manufacturer's instructions. The overpack Helium Leak Rate shall be $\leq 4.3E-6$ std cc/sec (He) with a minimum test sensitivity less than $2.15E-6$ std cc/sec (He).
 - d. Remove the overpack test cover and install a new metallic seal on the overpack vent port cover plate. Discard any used metallic seals.
 - e. Install the vent port cover plate and torque the bolts. See Table 7.1.3 for torque requirements.
 - f. Repeat Steps a through e for the overpack drain port.
4. Leak test the overpack closure plate inner mechanical seal as follows:
- a. Attach the closure plate test tool to the closure plate test port with the and MSLD attached. See Figure 7.1.29. See Table 7.1.3 for torque requirements.
 - b. Evacuate the closure plate test port tool and closure plate inter-seal area per the MSLD manufacturer's instructions.

- c. Perform a leakage rate test of overpack closure plate inner mechanical seal in accordance with the MSLD manufacturer's instructions. The overpack Helium Leak Rate shall be $\leq 4.3E-6$ std cc/sec (He) with a minimum test sensitivity less than $2.15E-6$ std cc/sec (He).
 - d. Remove the closure plate test tool from the test port and install the test port plug with a new mechanical seal. See Table 7.1.3 for torque requirements. Discard any used metallic seals.
5. Verify that the HI-STAR 100 overpack dose rates are within the acceptance requirements listed above.
6. Continue cask loading and preparation for transport as described in Section 7.1.7.

8.1.1.1 MPC Lid-to-Shell Weld Volumetric Inspection

1. The MPC lid-to-shell (LTS) weld (the confinement boundary closure per 10CFR72, and secondary containment (inner container) boundary per 10CFR71 for the MPC-68F) shall be volumetrically or multi-layer liquid penetrant examined following completion of field welding. If volumetric examination is used, the ultrasonic test (UT) method shall be employed. Ultrasonic techniques (including, as appropriate, Time-of-Flight Diffraction, Focussed Phased Array, and conventional pulse-echo) shall be supplemented, as necessary, to ensure substantially complete coverage of the examination volume.
2. If volumetric examination is used, then a liquid penetrant (PT) examination of the root and final pass of the LTS weld shall be performed and unacceptable indications shall be documented, repaired and re-examined.
3. If a volumetric examination is not used, a multi-layer PT examination shall be employed. The multi-layer PT must, at a minimum, include the root and final weld layers and one intermediate PT after each approximately 3/8 inch weld depth has been completed. The 3/8-inch weld depth corresponds to the maximum allowable flaw size.
4. It is recognized that welding of the LTS weld may result in indications in the root pass that are not detected by the root pass PT. The overall minimum thickness of the LTS weld has been increased by 0.125 inch such that it is not necessary to take structural credit for the root pass on the Design Drawings in Chapter 1 (actual weld to be 0.75 inch). A 0.625-inch J-groove weld was assumed in the structural analyses in Chapter 2.
5. For either UT or PT, the maximum undetectable flaw size must be demonstrated to be less than the critical flaw size. The critical flaw size must be determined in accordance with ASME Section XI methods. The critical flaw size shall not cause the primary stress limits of NB-3000 to be exceeded. The inspection process, including findings (indications) shall be made a permanent part of the user's records by video, photographic, or other means which provide an equivalent retrievable record of weld integrity. The video or photographic records should be taken during the final interpretation period described in ASME Section V, Article 6, T-676. The inspection of the weld shall be performed by qualified personnel and shall meet the acceptance requirements of ASME Section III, NB-5350 for PT and NB-5332 for UT.
6. Evaluation of any indications shall include consideration of any active flaw mechanisms. However, cyclic loading on the LTS weld is not significant, so fatigue will not be a factor. The LTS weld is protected from the external environment by the closure ring and the root of the LTS weld is dry and inert (He atmosphere), so stress corrosion cracking is not a concern for the LTS weld.

7. The volumetric or multi-layer PT examination of the LTS weld, in conjunction with other examinations which will be performed on this weld (PT of root and final pass, hydrostatic test, and helium leakage test); the use of the ASME Code Section III acceptance criteria; and the additional weld material added to account for potential defects in the root pass of the weld, in total, provide reasonable assurance that the LTS weld is sound and will perform its secondary containment boundary function under all loading conditions. The volumetric (or multi-layer PT) examination and evaluation of indications provides reasonable assurance that leakage of the weld or structural failure under normal or hypothetical accident conditions of transport will not occur.

8.1.2 Structural and Pressure Tests

8.1.2.1 Lifting Trunnions

Two trunnions (located near the top of the HI-STAR overpack) are provided for vertical lifting and handling of the HI-STAR 100 Package without the impact limiters installed. The trunnions are designed and shall be inspected and tested in accordance with ANSI N14.6 [8.1.5]. The trunnions are fabricated using a high-strength and high-ductility material (see Chapter 1). The trunnions contain no welded components. The maximum design lifting load of 250,000 pounds for the HI-STAR 100 Package will occur during the removal of the HI-STAR overpack from the spent fuel pool after the MPC has been loaded, flooded with water, and the MPC lid is installed. The high material ductility, absence of materials vulnerable to brittle fracture, excellent stress margins, and a carefully engineered design to eliminate local stress risers in the highly-stressed regions (during lift operations) ensure that the lifting trunnions will work reliably. However, pursuant to the defense-in-depth approach of NUREG-0612 [8.1.6], acceptance criteria for the lifting trunnions have been established in conjunction with other considerations applicable to heavy load handling.

Section 5 of NUREG-0612 calls for measures to "provide an adequate defense-in-depth for handling of heavy loads...". The NUREG-0612 guidelines cite four major causes of load handling accidents, of which rigging failure (including trunnion failure) is one:

- i. operator errors
- ii. rigging failure
- iii. lack of adequate inspection
- iv. inadequate procedures

The cask loading and handling operations program shall ensure maximum emphasis to minimize the potential of load drop accidents by implementing measures to eliminate shortcomings in all aspects of the operation including the four aforementioned areas.

In order to ensure that the lifting trunnions do not have any hidden material flaws, the trunnions shall be tested at 300% of the maximum design (service) lifting load. The load (750,000 lbs) shall be applied for a minimum of 10 minutes to the pair of lifting trunnions. The accessible parts of the trunnions (areas outside the HI-STAR overpack), and the local HI-STAR 100 cask

areas shall then be visually examined to verify no deformation, distortion, or cracking has occurred. Any evidence of deformation, distortion or cracking of the trunnion or adjacent HI-STAR 100 cask areas shall require replacement of the trunnion and/or repair of the HI-STAR 100 cask. Following any replacements and/or repair, the load testing shall be re-performed and the components re-examined in accordance with the original procedure and acceptance criteria. Testing shall be performed in accordance with written and approved procedures. Certified material test reports verifying trunnion material mechanical properties meet ASME Code Section II requirements provide further verification of the trunnion load capabilities. Test results shall be documented and shall become part of the final quality documentation package.

The acceptance testing of the trunnions in the manner described above provide reasonable assurance that a handling accidents will not occur due to trunnion failure.

8.1.2.2 Pressure Testing

8.1.2.2.1 HI-STAR 100 Containment Boundary

The containment boundary of the HI-STAR Package shall be hydrostatically or pneumatically pressure tested to 150 psig +10,-0 psig, in accordance with the requirements of the ASME Code Section III, Subsection NB, Article NB-6000. The test pressure of 150 psig is 150% of the Maximum Normal Operating Pressure (established per 10CFR71.85(b) requirements). This bounds the ASME Code Section III requirement (NB-6221) for hydrostatic testing to 125% of the design pressure (100 psig). The test shall be performed in accordance with written and approved procedures. The written and approved test procedure shall clearly define the test equipment arrangement.

The overpack pressure test may be performed at any time during fabrication after the containment boundary is complete. Preferably, the pressure test should be performed after overpack fabrication is complete, including attachment of the intermediate shells. The HI-STAR overpack shall be assembled for this test with the closure plate mechanical seal (only one required) or temporary test seal installed. Closure bolts shall be installed and torqued to a value less than or equal to the value specified in Chapter 7.

The calibrated test pressure gage installed on the overpack shall have an upper limit of approximately twice that of the test pressure. The test pressure shall be maintained for ten minutes. During this time period, the pressure gauge reading shall not fall below 150 psig. At the end of ten minutes, and while the pressure is being maintained at a minimum of 150 psig, the overpack shall be observed for leakage. In particular, the closure plate-to-top forging joint (the only credible leakage point) shall be examined. If a leak is discovered, the overpack shall be emptied and an evaluation shall be performed to determine the cause of the leakage. Repairs and retest shall be performed until the pressure test acceptance criterion is met.

Note: If failure of the pressure retest occurs after initial repairs are completed, a nonconformance report shall be issued and root cause and corrective action shall be addressed before further repairs and retest are performed.

After completion of the pressure testing, the overpack closure plate shall be removed and the internal surfaces shall be visually examined for cracking or deformation. Any evidence of cracking or deformation shall be cause for rejection or repair and retest, as applicable. The overpack shall be required to be pressure tested until the examinations are found to be acceptable.

Test results shall be documented and shall become part of the final quality documentation package.

8.1.2.2.2 MPC Secondary Containment Boundary

Hydrostatic testing of the MPC secondary containment boundary shall be performed in accordance with the requirements of the ASME Code Section III, Subsection NB, Article NB-6000, when field welding of the MPC lid-to-shell weld is completed. The hydrostatic pressure for the test shall be 125 +5,-0 psig, which is 125% of the design pressure of 100 psig. The MPC vent and drain ports are used for pressurizing the MPC cavity. The loading procedures in Chapter 7 define the test equipment arrangement. The calibrated test pressure gage installed on the MPC pressure boundary shall have an upper limit of approximately twice that of the test pressure. Following completion of the 10-minute hold period at the hydrostatic test pressure, and while maintaining a minimum test pressure of 125 psig, the surface of the MPC lid-to-shell weld shall be visually examined for leakage and then re-examined by liquid penetrant examination performed in accordance with ASME Code Section V, Article 6, with acceptance criteria per ASME Code Section III, Subsection NB, Article NB-5350. Any unacceptable areas shall require repair in accordance with the ASME Code Section III, Subsection NB, Article NB-4450. Any evidence of cracking or deformation shall be cause for rejection, or repair and retest, as applicable. The performance and sequence of the test is described in Section 7.1 (loading procedures).

If a leak is discovered, the test pressure shall be reduced, the MPC cavity water level lowered, the MPC cavity vented (to the pool or the licensee's off-gas system), and the weld shall be examined to determine the cause of the leakage and/or cracking. Repairs to the weld shall be performed in accordance with approved written procedures prepared in accordance with the ASME Code Section III, Subsection NB, NB-4450.

The MPC pressure boundary hydrostatic test shall be repeated until all visual and dye penetrant examinations are found to be acceptable. Test results shall be documented and shall be maintained as part of the loaded MPC quality documentation package.

8.1.2.3 Materials Testing

The majority of materials used in the HI-STAR overpack are ferritic steels. ASME Code Section III and Regulatory Guides 7.11 [8.1.7] and 7.12 [8.1.8] require that certain materials be tested in order to assure that these materials are not subject to brittle fracture failures.

Each plate or forging for the HI-STAR 100 Package containment boundary (overpack inner shell, bottom plate, top flange, and closure plate) shall be required to be drop weight tested in accordance with the requirements of Regulatory Guides 7.11 and 7.12, as applicable. Additionally, per the ASME Code Section III, Subsection NB, Article NB-2300, Charpy V-notch testing shall be performed on these materials. Weld material used in welding the containment boundary shall be Charpy V-notch tested in accordance with ASME Section III, Subsection NB, Articles NB-2300 and NB-2430.

Noncontainment portions of the overpack, as required, shall be Charpy V-notch tested in accordance with ASME Section III, Subsection NF, Articles NF-2300, and NF-2430. The noncontainment materials to be tested include the intermediate shells, overpack port cover plates, and applicable weld materials.

Tables 2.1.22 and 2.1.23 provide the test temperatures or T_{NDT} , and test requirements to be used when performing the testing specified above.

Test results shall be documented and shall become part of the final quality documentation record package.

8.1.2.4 Pneumatic Testing of the Neutron Shield Enclosure Vessel

A pneumatic pressure test of the neutron shield enclosure vessel shall be performed following final closure welding of the enclosure shell returns and enclosure panels. The pneumatic test pressure shall be 37.5+2.5,-0 psig, which is 125 percent of the rupture disc relief set pressure. The test shall be performed in accordance with approved written procedures.

During the test, the two rupture discs on the neutron shield enclosure vessel shall be removed. One of the rupture disc threaded connections is used for connection of the air pressure line and the other rupture disc connection will be used for connection of the pressure gauge.

Following the introduction of pressurized air into the neutron shield enclosure vessel, a 15 minute pressure hold time is required. If the neutron shield enclosure vessel fails to hold pressure, an approved soap bubble solution shall be applied to determine the location of the leak. The leak shall be repaired using weld repair procedures prepared in accordance with the ASME Code Section III, Subsection NF, Article NF-4450. The pneumatic pressure test shall be re-performed until no pressure loss is observed.

Test results shall be documented and shall become part of the final quality documentation package.

8.1.3 Leakage Testing

Leakage testing shall be performed in accordance with the requirements of ANSI N14.5 [8.1.9]. Testing shall be performed in accordance with written and approved procedures.

8.1.3.1 HI-STAR Overpack

A Containment System Fabrication Verification Leakage test of the welded structure shall be performed at any time after the containment boundary fabrication is complete. Preferably, this test should be performed at the completion of overpack fabrication, after all intermediate shells have been attached. The leakage test instrumentation shall have a minimum test sensitivity of 2.15×10^{-6} atm cm³/s (helium). Containment boundary welds shall have indicated leakage rates not exceeding 4.3×10^{-6} atm cm³/s (helium). If a leakage rate exceeding the acceptance criterion is detected, the area of leakage shall be determined using the sniffer probe method or other means, and the area shall be repaired per ASME Code Section III, Subsection NB, NB-4450 requirements. Following repair and appropriate NDE, the leakage testing shall be re-performed until the test acceptance criterion is satisfied.

Note: If failure of the leakage rate retest occurs after initial repairs are completed, a nonconformance report shall be issued and root cause and corrective action shall be addressed before further repairs and retest are performed.

At the completion of overpack fabrication, helium leakage through the helium retention penetrations (consisting of the inner mechanical seal between the closure plate and the top flange and the vent and drain port plug seals) shall be demonstrated to not exceed the leakage rate of 4.3×10^{-6} atm cm³/sec (helium) at a minimum test sensitivity of 2.15×10^{-6} atm cm³/sec (helium). This may be performed simultaneously with the Containment System Fabrication Verification Leakage test or may be performed separately using the methods described in the paragraph below.

At the completion of fabrication, a Containment System Fabrication Verification Leakage test shall be performed on the HI-STAR overpack closures. Helium leakage through the containment penetrations (consisting of the inner mechanical seal between the closure plate and top flange, and the vent and drain port plug seals) shall be demonstrated to not exceed a leakage rate of 4.3×10^{-6} atm cm³/s (helium) at a minimum test sensitivity of 2.15×10^{-6} atm cm³/s (helium).

The leakage testing is performed by evacuating and backfilling the overpack with helium gas to an appropriate pressure.. A helium Mass Spectrometer Leak Detector (MSLD) with a minimum calibrated sensitivity of 2.15×10^{-6} atm cm³/s (helium) shall be used in parallel with a vacuum pump and a test cover (see Chapter 7 for details) designed for testing the penetration seals. Starting with the vent or drain port plug, the test cover is connected. The cavity on the external side of the port plug is evacuated and the vacuum pump is valved out. The MSLD detector measures the leakage rate of helium into the test cavity.. If the leakage rate exceeds a leakage rate of 4.3×10^{-6} atm cm³/s (helium), the test chamber is vented and removed. The corresponding plug seal is removed, seal seating surfaces are inspected and cleaned, and the plug with a new seal is reinstalled and torqued to the required value. The test process is then repeated until the seal leakage rate is successfully achieved. The same process is repeated for the remaining overpack vent or drain port. The process is used for the closure plate seals except the closure plate test tool (see Chapter 7 for details) Is used in lieu of the test cover.

If the total measured leakage rate for all tested penetrations does not exceed 4.6×10^{-6} atm cm^3/sec , the leakage tests are successful. If the total leakage rate exceeds 4.6×10^{-6} atm cm^3/sec , an evaluation should be performed to determine the cause of the leakage, repairs made as necessary, and the overpack must be re-tested until the total leakage rate is within the required acceptance criterion. Leak testing results for the HI-STAR overpack shall become part of the quality record documentation record package.

8.1.3.2 MPC Secondary Containment Boundary

Upon the completion of welding the MPC shell to the baseplate, a confinement boundary weld leakage test shall be performed using a helium MSLD as described in Chapter 9 of the HI-STAR TSAR [8.1.4]. The pressure boundary welds of the MPC canisters shall have indicated leakage rates not exceeding 5×10^{-6} atm cm^3/s (helium). If leakage rates exceeding the test criteria are detected, then the area of leakage shall be determined and the area repaired per ASME Code Section III, Subsection NB, NB-4450, requirements. Re-testing of the MPC shall be performed until the leakage rate acceptance criterion is met.

Note: If failure of the leakage rate retest occurs after initial repairs are completed, a nonconformance report shall be issued and root cause and corrective action shall be addressed before further repairs and retest are performed.

Leakage testing of the field welded MPC lid-to-shell weld shall be performed following completion of the MPC hydrostatic test performed per Subsection 8.1.2.2.2. Leakage testing of the vent and drain port cover plate welds shall be performed after welding of the cover plates and subsequent NDE. The description and procedures for these field tests are provided in Section 7.1.

All leak testing results for the MPC shall be documented and shall become part of the quality record documentation package.

Prior to the transport of an MPC-68F containing fuel debris in the HI-STAR 100 Package, a Containment Fabrication Verification Leakage Test shall be performed on the secondary containment boundary of the MPC-68F. The test is performed with the MPC-68F loaded into the HI-STAR overpack. The HI-STAR overpack annulus is sampled to inspect for radioactive material and then evacuated to an appropriate vacuum condition. The HI-STAR overpack annulus is then isolated from the vacuum pump. Following an appropriate isolation period, the HI-STAR overpack annulus atmosphere is sampled for helium leakage from the MPC-68F. The test is considered acceptable if the detected leakage from the MPC does not exceed 5×10^{-6} atm cm^3/s (helium). If the acceptance criterion is not met, transport of the MPC-68F is not authorized. Corrective actions from re-testing, up to and including off-loading of the MPC, shall be taken until the leakage rate acceptance criterion is met.

8.1.4 Component Tests

8.1.4.1 Valves, Rupture Discs, and Fluid Transport Devices

There are no fluid transport devices associated with the HI-STAR 100 Package. The only valve-like components in the HI-STAR 100 Package are the specially designed caps installed in the MPC lid for the drain and vent ports. These caps are recessed inside the MPC lid and covered by the fully-welded vent and drain port cover plates. No credit is taken for the caps' ability to confine helium or radioactivity. After completion of drying and backfill operations, the drain and vent port cover plates are welded in place on the MPC lid and are leak tested to verify the MPC secondary containment (MPC-68F) boundary.

The vent and drain ports in the HI-STAR overpack are accessed through port plugs specially designed for removal and installation using connector tools. The tools are described and presented in figures in Chapter 7.

There are two rupture discs installed in the upper ledge surface of the neutron shield enclosure vessel of the HI-STAR overpack. These rupture discs are provided for venting purposes under hypothetical fire accident conditions in which vapor formation from neutron shielding material degradation may occur. The rupture discs are designed to relieve at 30 psig (± 5 psig). Each manufactured lot of rupture discs shall be sample tested to verify their point of rupture. The sample test program shall be documented and the test results shall become part of the quality record documentation package.

8.1.4.2 Seals and Gaskets

Two concentric mechanical seals are provided on the HI-STAR overpack closure plate to provide containment boundary sealing. Mechanical seals are also used on the overpack vent and drain port plugs of the HI-STAR overpack containment boundary. Each primary seal is individually leak tested in accordance with Subsection 8.1.3.1. prior to the HI-STAR 100 Package's first use and during each loading operation. An independent and redundant seal is provided for each penetration (e.g., closure plate, port cover plates, and closure plate test plug). No containment credit is taken for these redundant seals and they are not leakage tested. Details on these seals are provided in Chapter 4.

8.1.4.3 Transport Impact Limiter

The removable HI-STAR transport impact limiters consist of aluminum honeycomb crush material arranged around a carbon steel structure and enclosed by a stainless steel shell. The Design Drawings and Bills-of-Material in Chapter 1 specify the crush strength of the aluminum honeycomb materials for each zone of the impact limiter. For manufacturing purposes, verification of the impact limiter material is accomplished by performance of a crush test of sample blocks of aluminum honeycomb material for each large block manufactured. The verification tests are performed by the aluminum honeycomb supplier in accordance with approved procedures. The certified test results shall be submitted to Holtec International with

each shipment. The honeycomb material crush strength for each block (nominal $\pm 7\%$) shall be as specified on the Design Drawings in Section 1.4.

All welds on the HI-STAR impact limiter shall be visually examined in accordance with the ASME Code, Section V, Article 9, with acceptance criteria per ASME Section III, Subsection NF, Article NF-5360.

8.1.5 Shielding Integrity

The HI-STAR 100 System has three specifically designed shields for neutron and gamma ray attenuation. For gamma shielding, there are successive carbon steel intermediate shells attached onto the outer surface of the overpack inner shell. The details of the manufacturing process are discussed in Chapter 1. Holtite-A neutron shielding is provided in the outer enclosure of the overpack. Additional neutron attenuation is provided by the encased Boral neutron absorber attached to the fuel basket cell surfaces inside the MPCs. Test requirements for each of the three shielding items are described below.

8.1.5.1 Fabrication Testing and Controls

Holtite-A:

Neutron shield properties of Holtite-A are provided in Chapter 1. Each manufactured lot of neutron shield material shall be tested to verify that the material composition (aluminum and hydrogen), boron concentration, and neutron shield density (or specific gravity) meet the requirements specified in Chapter 1. A manufactured lot is defined as the total amount of material used to make any number of mixed batches comprised of constituent ingredients from the same lot/batch identification numbers supplied by the constituent manufacturer. Testing shall be performed in accordance with written and approved procedures and/or standards. Material composition, boron concentration, and density (or specific gravity) data for each manufactured lot of neutron shield material shall become part of the quality record documentation package.

The installation of the neutron shielding material shall be performed in accordance with written, approved, and qualified procedures. The procedures shall ensure that mix ratios and mixing methods are controlled in order to achieve proper material composition, boron concentration and distribution, and that pours are controlled in order to prevent gaps or voids from occurring in the material. Samples of each lot of neutron shield material shall be maintained by Holtec International as part of the quality record documentation package.

Steel:

The steel plates utilized in the construction of the HI-STAR 100 Package shall be dimensionally inspected to assure compliance with the Design Drawings in Section 1.4.

The total measured thickness of the inner shell plus intermediate shells shall be nominally 8.5 inches over the total surface area of the overpack shell. The top flange, closure plate, and

bottom plate of the overpack shall be measured to confirm their thicknesses meet Design Drawing requirements of Section 1.4. Measurements shall be performed in accordance with written and approved procedures. The measurement locations and measurement results shall be documented. Measurements shall be made through a combination of receipt inspection thickness measurements on individual plates and actual measurements taken prior to welding the forgings and shells. Any area found to be under the specified minimum thickness shall be repaired in accordance with applicable ASME Code requirements.

No additional gamma shield testing of the HI-STAR 100 Package is required. A shielding effectiveness test as described in Subsection 8.1.5.2 shall be performed on each fabricated HI-STAR 100 Package after the first fuel loading.

General for Shield Materials:

1. Test results shall be documented and become part of the quality documentation package.
2. Dimensional inspections of the cavities containing poured neutron shielding materials shall assure that the amount of shielding material specified in the design documents is incorporated into the fabricated item.

8.1.5.2 Shielding Effectiveness Tests

Users shall implement procedures which verify the integrity of the Holtite-A neutron shield once for each overpack. Neutron shield integrity shall be verified via measurements either at first use or with a check source using, at a maximum, a 6x6 inch test grid over the entire surface of the neutron shield, including the impact limiters.

Following the first fuel loading of each HI-STAR 100 Package, a shielding effectiveness test shall be performed at the loading facility site to verify the effectiveness of the gamma and neutron shields. This test shall be performed after the HI-STAR 100 Package has been loaded with fuel, drained, sealed, and backfilled with helium.

The neutron and gamma shielding effectiveness tests shall be performed using written and approved procedures. Calibrated neutron and gamma dose meters shall be used to measure the actual neutron and gamma dose rates at the surface of the HI-STAR overpack. Measurements shall be taken at three cross sectional planes and at four points along each plane's circumference. Additionally, four measurements shall be taken at the top of the overpack closure plate. Dose rate measurements shall be documented and become part of the quality documentation package. The average results from each sectional plane shall be compared to the design basis limits for surface dose rates established in Chapter 5. The test is considered acceptable if the actual dose readings are less than the predicted dose rates for the location measured. If dose rates are higher than the predicted design basis dose rates, the HI-STAR 100 Package shall not be placed into transport service until the discrepancy is adequately resolved. See Chapter 7 for details on test performance and dose rate measurement locations.

8.1.5.3 Neutron Absorber Tests

After manufacturing, a statistical sample of each lot of Boral shall be tested using wet chemistry and/or neutron attenuation techniques to verify a minimum ^{10}B content at the ends of the panel. Any panel in which ^{10}B loading is less than the minimum allowed per the Design Drawings and Bills-of-Material shall be rejected.

Tests shall be performed using written and approved procedures. Results shall be documented and become part of the HI-STAR 100 Package quality records documentation package.

Installation of Boral panels into the fuel basket shall be performed in accordance with written and approved procedures (or shop travelers). Travelers and/or quality control procedures shall be in place to assure each required cell wall of the MPC basket contains a Boral panel in accordance with the Design Drawings in Chapter 1. These quality control processes, in conjunction with Boral manufacturing testing, provide the necessary assurances that the Boral will perform its intended function. The criticality design for the HI-STAR 100 System is based on favorable geometry and fixed neutron poisons. The inert helium environment inside the MPC cavity where the Boral is located ensures that the poisons will remain effective for the life of the canister. Given the design and service conditions, there are no credible means to lose the fixed neutron poisons. Therefore, no additional testing is required to ensure the Boral is present and in proper condition per 10 CFR 71.87(g).

8.1.6 Thermal Acceptance Test

The first fabricated HI-STAR overpack shall be tested to confirm its heat transfer capability. The test shall be conducted after the radial channels, enclosure shell panels, and neutron shield material have been installed and all inside and outside surfaces are painted per the Design Drawings in Section 1.4. A test cover plate shall be used to seal the overpack cavity. Testing shall be performed in accordance with written and approved procedures.

Steam heating of the overpack cavity surfaces is the preferred method for this test instead of electric heating. There are several advantages with steam heated testing as listed below:

- (i) Uniform cavity surface temperatures are readily achieved as a result of high steam condensation heat transfer coefficient (about $2,000 \text{ Btu/ft}^2 \text{ hr}^{-\circ}\text{F}$ compared to about $1 \text{ Btu/ft}^2 \text{ hr}^{-\circ}\text{F}$ for air) coupled with the steam's uniform distribution throughout the cavity.
- (ii) A reliable constant temperature source (steam at atmospheric pressure condenses at 212° F compared to variable heater surface temperatures in excess of $1,000^{\circ} \text{ F}$) eliminates concerns of overpack cavity surface overheating.
- (iii) Interpretation of isothermal test data is not susceptible to errors associated with electric heating systems due to heat input measurement uncertainties, leakage of heat from electrical cables, thermocouple wires, overpack lid, bottom baseplate, etc.

- (iv) The test setup is simple requiring only a steam inlet source and drain compared to numerous power measurement and control instruments, switchgear and safety interlocks required to operate an electric heater assembly.

Twelve (12) calibrated thermocouples shall be installed on the external walls of the overpack as shown in Figure 8.1.2. Three calibrated thermocouples shall be installed on the internal walls of the overpack in locations to be determined by procedure. Additional temperature sensors shall be used to monitor ambient temperature, steam supply temperature, and condensate drain temperature. The thermocouples shall be attached to strip chart recorders or other similar mechanism to allow for continuous monitoring and recording of temperatures during the test. Instrumentation shall be installed to monitor overpack cavity internal pressure.

After the thermocouples have been installed, dry steam will be introduced through an opening in the test cover plate previously installed on the overpack and the test initiated. Temperatures of the thermocouples, plus ambient, steam supply, and condensate drain temperature shall be recorded at hourly intervals until thermal equilibrium is reached. Appropriate criteria defining when thermal equilibrium is achieved shall be determined based on a variety of potential ambient test conditions and incorporated into the test procedure. In general, thermal equilibrium is expected approximately 12 hours after the start of steam heating. Air will be purged from the overpack cavity via venting during the heatup cycle. During the test, the steam condensate flowing out of the overpack drain shall be collected and the mass of the condensate measured with a precision weighing instrument.

Once thermal equilibrium is established, the final ambient, steam supply, and condensate drain temperatures and temperatures at each of the thermocouples shall be recorded. The strip charts, hand-written logs, or other similar readout shall be marked to show the point when thermal equilibrium was established and final test measurements were recorded. The final test readings along with the hourly data inputs and strip charts (or other similar mechanism) shall become part of the quality records documentation package for the HI-STAR 100 Package.

The heat rejection capability of the overpack at test conditions shall be computed using the following formula:

$$Q_{hm} = (h_1 - h_2) m_c \quad (8-1)$$

Where: Q_{hm} = Heat rejection rate of the overpack (Btu/hr)

h_1 = Enthalpy of steam entering the overpack cavity (Btu/lbm)

h_2 = Enthalpy of condensate leaving the overpack cavity (Btu/lbm)

m_c = Average rate of condensate flow measured during thermal equilibrium conditions (lbm/hr)

Based on the HI-STAR 100 overpack thermal model, a design basis minimum heat rejection capacity (Q_{hd}) shall be computed at the measured test conditions (i.e., steam temperature in the

overpack cavity and ambient air temperature). The thermal test shall be considered acceptable if the measured heat rejection capability is greater than the design basis minimum heat rejection capacity ($Q_{hm} > Q_{hd}$).

The summary of reference ambient inputs that define the thermal test environment are provided in Table 8.1.4. In Figure 8.1.3, a steady-state temperature contour plot of a steam heated overpack is provided based on the thermal analysis methodology described in SAR Chapter 3. Transient heating of the overpack is also determined to establish the time required to approach (within 2° F) the equilibrium temperatures. The surface temperature plot shown in Figure 8.1.4 demonstrates that a 12-hour steam heating time is adequate to closely approach the equilibrium condition.

If the acceptance criteria above are not met, then the HI-STAR 100 Package shall not be accepted until the root cause is determined, appropriate corrective actions are completed, and the overpack is re-tested with acceptable results.

Test results shall be documented and shall become part of the quality record documentation package.

8.1.7 Cask Identification

Each HI-STAR 100 Package shall be provided with unique identification plates with appropriate markings per 10CFR71.85(c) and 10CFR72.236(k) as shown in the Design Drawings in Section 1.4. The identification plates shall not be installed until each HI-STAR 100 Package component has completed the fabrication acceptance test program and been accepted by authorized Holtec International personnel. A unique identifying serial number shall also be stamped on the MPC to provide traceability back to the MPC specific quality records documentation package.

Table 8.1.1

MPC INSPECTION AND TEST ACCEPTANCE CRITERIA

Function	Fabrication	Pre-operation	Maintenance and Operations
<p>Visual Inspection and Nondestructive Examination (NDE)</p>	<p>a) Examination of MPC components per ASME Code Section III, Subsections NB, NF, and NG, as defined on design drawings, per NB-5300, NF-5300, and NG-5300, as applicable.</p> <p>b) A dimensional inspection of the internal basket assembly and canister shall be performed to verify compliance with design requirements.</p> <p>c) A dimensional inspection of the MPC lid and MPC closure ring shall be performed prior to inserting into the canister shell to verify compliance with design requirements.</p> <p>d) NDE of weldments are defined on the design drawings using standard American Welding Society NDE symbols and/or notations.</p> <p>e) Cleanliness of the MPC shall be verified upon completion of fabrication.</p> <p>f) The packaging of the MPC at the completion of fabrication shall be verified prior to shipment.</p>	<p>a) The MPC shall be visually inspected prior to placement in service at the licensee's facility.</p> <p>b) MPC protection at the licensee's facility shall be verified.</p> <p>c) MPC cleanliness and exclusion of foreign material shall be verified prior to placing in the spent fuel pool.</p>	<p>a) None.</p>

Table 8.1.1 (continued)

MPC INSPECTION AND TEST ACCEPTANCE CRITERIA

Function	Fabrication	Pre-operation	Maintenance and Operations
Structural	<p>a) Assembly and welding of MPC components shall be performed per ASME Code Section IX and III, Subsections NB, NF, and NG, as applicable.</p> <p>b) Materials analysis (steel, Boron, etc.), shall be performed and records shall be kept in a manner commensurate with "important to safety" classifications.</p>	<p>a) None.</p>	<p>a) An ultrasonic (UT) examination or multi-layer liquid penetrant (PT) examination of the MPC lid-to-shell weld shall be performed per ASME Section V, Article 5 (or ASME Section V, Article 2). Acceptance criteria for the examination are defined in Subsection 8.1.1.1 and in the Design Drawings.</p> <p>b) ASME Code NB-6000 hydrostatic test shall be performed after MPC closure welding. Acceptance criteria are defined in Subsection 8.1.2.2.2.</p>
Leak Tests	<p>a) Helium leak rate testing shall be performed on all MPC pressure boundary shop welds.</p>	<p>a) None.</p>	<p>a) Helium leak rate testing shall be performed on MPC lid-to-shell, and vent and drain ports-to-MPC lid field welds after closure welding. Acceptance criteria are defined in Subsection 8.1.3.2.</p> <p>b) A Containment System Fabrication Verification Leakage Test shall be performed on the MPC-68F prior to the transport of the HI-STAR 100 Package containing fuel debris. Acceptance criteria are defined in Subsection 8.1.3.2.</p>

Table 8.1.1 (continued)

MPC INSPECTION AND TEST ACCEPTANCE CRITERIA

Function	Fabrication	Pre-operation	Maintenance and Operations
Criticality Safety	<p>a) The boron content shall be verified at the time of neutron absorber material manufacture.</p> <p>b) The installation of Boral panels into MPC basket plates shall be verified by inspection.</p>	a) None.	a) None.
Shielding Integrity	<p>a) Material compliance shall be verified through CMTRs.</p> <p>b) Dimensional verification of MPC lid thickness shall be performed.</p>	a) None.	a) None.
Thermal Acceptance	a) None.	a) None.	a) None.
Fit-Up Tests	<p>a) Fit-up of the following components is to be tested during fabrication.</p> <ul style="list-style-type: none"> - MPC lid - vent/drain port coverplates - MPC closure ring <p>b) A gauge test of all basket fuel compartments.</p>	<p>a) Fit-up of the following components is to be verified during pre-operation.</p> <ul style="list-style-type: none"> - MPC lid - MPC closure ring - vent/drain coverplates 	a) None.
Canister Identification Inspections	a) Verification of identification marking applied at completion of fabrication.	a) Identification marking shall be checked for legibility during pre-operation.	a) None.

Table 8.1.2
HI-STAR OVERPACK
INSPECTION AND TEST ACCEPTANCE CRITERIA

Function	Fabrication	Pre-operation	Maintenance and Operations
<p>Visual Inspection and Nondestructive Examination (NDE)</p>	<p>a) Examination of the HI-STAR overpack shall be performed per ASME Code, Subsection NB, NB-5300 for containment boundary components, and Subsection NF, NF-5300 for non-containment boundary components.</p> <p>b) A dimensional inspection of the overpack internal cavity, external dimensions, and closure plate shall be performed to verify compliance with design requirements.</p> <p>c) The HI-STAR overpack shall be visually examined in accordance with the ASME Code Section V, Article 9, to verify that the overpack is free of cracks, pinholes, uncontrolled voids, or other defects that could significantly reduce its effectiveness.</p> <p>d) NDE of weldments shall be defined on design drawings using standard American Welding Society NDE symbols and/or notations.</p> <p>e) Cleanliness of the HI-STAR overpack shall be verified upon completion of fabrication.</p> <p>f) Packaging of the HI-STAR overpack at the completion of fabrication shall be verified prior to shipment.</p> <p>g) Examination of the AL-STAR impact limiters shall be performed per ASME Code, Subsection NF, NF-5300.</p>	<p>a) The HI-STAR overpack shall be visually inspected prior to placement in service at the licensee's facility.</p> <p>b) HI-STAR overpack protection at the licensee's facility shall be verified.</p> <p>c) HI-STAR overpack cleanliness and exclusion of foreign material shall be verified prior to use.</p>	<p>a) Inspect overpack cavity and accessible external surfaces prior to each fuel loading.</p> <p>b) Visually inspect impact limiters for damage and compliance to drawing requirements prior to each transport.</p>

Table 8.1.2 (continued)
 HI-STAR OVERPACK
 INSPECTION AND TEST ACCEPTANCE CRITERIA

Function	Fabrication	Pre-operation	Maintenance and Operations
Structural	a) Assembly and welding of HI-STAR overpack components shall be performed per ASME Code, Subsection NB and NF, as applicable. b) Verification of structural materials shall be performed through receipt inspection and review of certified material test reports (CMTRs) obtained in accordance with the item's quality classification category. c) A load test of the lifting trunnions shall be performed during fabrication. d) A pressure test of the containment boundary in accordance with ASME Code Section III, Subsection NB-6000 and 10CFR71.85(b) shall be performed. e) A pneumatic pressure test of the neutron shield enclosure shall be performed during fabrication.	a) None.	a) The rupture discs on the neutron shield vessel shall be replaced every 5 years.

Table 8.1.2 (continued)

HI-STAR OVERPACK
INSPECTION AND TEST ACCEPTANCE CRITERIA

Function	Fabrication	Pre-operation	Maintenance and Operations
Leak Tests	<p>a) Containment Fabrication Verification Leakage rate testing of the HI-STAR containment boundary welds shall be performed in accordance with ANSI N14.5.</p> <p>b) A Containment System Fabrication Verification Leakage rate test shall be performed on all HI-STAR overpack containment boundary mechanical seal boundaries in accordance with ANSI N14.5 at the completion of fabrication.</p>	<p>a) None.</p>	<p>a) Containment System Periodic Verification Leakage Test of the HI-STAR 100 Package shall be performed prior to each loaded transport (if not previously tested within 12 months).</p> <p>b) Containment System Fabrication Verification Leakage Test of the HI-STAR 100 Package shall be performed after the third use.</p>
Criticality Safety	<p>a) None.</p>	<p>a) None.</p>	<p>a) None.</p>
Shielding Integrity	<p>a) Material verifications (Holtite-A, shell plates, etc.), shall be performed in accordance with the item's quality category. The required material certifications shall be obtained.</p> <p>b) The placement of Holtite-A shall be controlled through written special process procedures.</p>	<p>a) None.</p>	<p>a) A shielding effectiveness test shall be performed after the first fuel loading and reperformed every five years while in service.</p> <p>b) Verify the integrity of the Holtite-A neutron shield once at first use or with a check source.</p>

Table 8.1.2 (continued)

HI-STAR OVERPACK
INSPECTION AND TEST ACCEPTANCE CRITERIA

Function	Fabrication	Pre-operation	Maintenance and Operation
Thermal Acceptance	a) A thermal acceptance test is performed at completion of fabrication of the first HI-STAR overpack to confirm the heat transfer capabilities.	a) None.	a) An in-service thermal test shall be performed every five years during transport operations, or prior to transport if period exceeds five years from previous test. Acceptance criteria are defined in Subsection 8.2.6.
Cask Identification Inspection	a) Identification plates shall be installed on the HI-STAR overpack at completion of the acceptance test program.	a) The identification plates shall be checked prior to loading.	a) The identification plates shall be periodically inspected per licensee procedures and shall be repaired or replaced if damaged.
Fit-Up Tests	a) Fit-up tests of HI-STAR 100 Package components (closure plates, port plugs, cover plates impact limiters (if available)), shall be performed during fabrication.	a) Fit-up test of the HI-STAR overpack lifting trunnions with the lifting yoke shall be performed. b) Fit-up test of the HI-STAR overpack rotation trunnions with the transport frame shall be performed. c) Fit-up test of the MPC into the HI-STAR overpack shall be performed prior to loading.	a) Fit-up of all removable components shall be verified during each loading operation.

Table 8.1.3
HI-STAR 100 NDE REQUIREMENTS

MPC			
Weld Location	NDE Requirement	Applicable Code	Acceptance Criteria (Applicable Code)
Shell longitudinal seam	RT	ASME Section V, Article 2 (RT)	RT: ASME Section III, Subsection NB, Article NB-5320
	PT (surface)	ASME Section V, Article 6 (PT)	PT: ASME Section III, Subsection NB, Article NB-5350
Shell circumferential seam	RT	ASME Section V, Article 2 (RT)	RT: ASME Section III, Subsection NB, Article NB-5320
	PT (surface)	ASME Section V, Article 6 (PT)	PT: ASME Section III, Subsection NB, Article NB-5350
Baseplate-to-shell	RT or UT	ASME Section V, Article 2 (RT) ASME Section V, Article 5 (UT)	RT: ASME Section III, Subsection NB, Article NB-5320 UT: ASME Section III, Subsection NB, Article NB-5330
	PT (surface)	ASME Section V, Article 6 (PT)	PT: ASME Section III, Subsection NB, Article NB-5350

Table 8.1.3 (continued)
 HI-STAR 100 NDE REQUIREMENTS

MPC

Weld Location	NDE Requirement	Applicable Code	Acceptance Criteria (Applicable Code)
Lid-to-shell	PT (root and final pass) and multi-layer PT (if UT is not performed). PT (surface following hydrostatic test) UT (if multi-layer PT is not performed)	ASME Section V, Article 6 (PT) ASME Section V, Article 5 (UT)	PT: ASME Section III, Subsection NB, Article NB-5350 UT: ASME Section III, Subsection NB, Article NB-5332
Closure ring-to-shell	PT (final pass)	ASME Section V, Article 6 (PT)	PT: ASME Section III, Subsection NB, Article NB-5350
Closure ring-to-lid	PT (final pass)	ASME Section V, Article 6 (PT)	PT: ASME Section III, Subsection NB, Article NB-5350
Closure ring radial welds	PT (final pass)	ASME Section V, Article 6 (PT)	PT: ASME Section III, Subsection NB, Article NB-5350
Port cover plates-to-lid	PT (root and final pass)	ASME Section V, Article 6 (PT)	PT: ASME Section III, Subsection NB, Article NB-5350
Lift lug and lift lug baseplate	PT (surface)	ASME Section V, Article 6 (PT)	PT: ASME Section III, Subsection NG, Article NG-5350

Table 8.1.3 (continued)
 HI-STAR 100 NDE REQUIREMENTS

HI-STAR OVERPACK			
Weld Location	NDE Requirement	Applicable Code	Acceptance Criteria (Applicable Code)
Inner shell-to-top flange	RT	ASME Section V, Article 2 (RT)	RT: ASME Section III, Subsection NB, Article NB-5320
	MT or PT (surface)	ASME Section V, Article 7 (MT)	MT: ASME Section III, Subsection NB, Article NB-5340
		ASME Section V, Article 6 (PT)	PT: ASME Section III, Subsection NB, Article NB-5350
Inner shell-to-bottom plate	RT	ASME Section V, Article 2 (RT)	RT: ASME Section III, Subsection NB, Article NB-5320
	MT or PT (surface)	ASME Section V, Article 7 (MT)	MT: ASME Section III, Subsection NB, Article NB-5340
		ASME Section V, Article 6 (PT)	PT: ASME Section III, Subsection NB, Article NB-5350
Inner shell longitudinal seam	RT	ASME Section V, Article 2 (RT)	RT: ASME Section III, Subsection NB, Article NB-5320
	MT or PT (surface)	ASME Section V, Article 7 (MT)	MT: ASME Section III, Subsection NB, Article NB-5340
		ASME Section V, Article 6 (PT)	PT: ASME Section III, Subsection NB, Article NB-5350

Table 8.1.3 (continued)

HI-STAR 100 NDE REQUIREMENTS

HI-STAR OVERPACK

Weld Location	NDE Requirement	Applicable Code	Acceptance Criteria (Applicable Code)
Inner shell circumferential seam	RT MT or PT (surface)	ASME Section V, Article 2 (RT) ASME Section V, Article 7 (MT) ASME Section V, Article 6 (PT)	RT: ASME Section III, Subsection NB, Article NB-5320 MT: ASME Section III, Subsection NB, Article NB-5340 PT: ASME Section III, Subsection NB, Article NB-5350
Intermediate shell welds (as noted on Design Drawings)	MT or PT (surface)	ASME Section V, Article 6 (PT) ASME Section V, Article 7 (MT)	PT: ASME Section III, Subsection NF, Article NF-5350 MT: ASME Section III, Subsection NF, Article NF-5340

8.4 REFERENCES

- [8.0.1] U.S. Code of Federal Regulations, Title 10, "Energy", Part 71, "Packaging and Transportation of Radioactive Materials."
- [8.1.1] Holtec International Quality Assurance Manual, current revision.
- [8.1.2] American Society of Mechanical Engineers, "Boiler and Pressure Vessel Code," Sections II, III, V, IX, and XI, 1995 Edition with 1996 and 1997 Addenda.
- [8.1.3] American Society for Nondestructive Testing, "Personnel Qualification and Certification in Nondestructive Testing," Recommended Practice No. SNT-TC-1A, December 1992.
- [8.1.4] HI-STAR 100 Topical Safety Analysis Report, Holtec Report No. HI-941184, current revision.
- [8.1.5] American National Standards Institute, Institute for Nuclear Materials Management, "American National Standard for Radioactive Materials - Special Lifting Devices for Shipping Containers Weighing 10,000 Pounds (4500 kilograms) or More", ANSI N14.6, September 1993.
- [8.1.6] NUREG-0612, "Control of Heavy Loads at Nuclear Power Plants", U.S. Nuclear Regulatory Commission, Washington, D.C., July 1980.
- [8.1.7] U.S. Nuclear Regulatory Commission, "Fracture Toughness Criteria of Base Material for Ferritic Steel Shipping Cask Containment Vessels with a Maximum Wall Thickness of 4 Inches (0.1m)," Regulatory Guide 7.11, June 1991.
- [8.1.8] U.S. Nuclear Regulatory Commission, "Fracture Toughness Criteria of Base Material for Ferritic Steel Shipping Cask Containment Vessels with a Wall Thickness Greater than 4 Inches (0.1m) But Not Exceeding 12 Inches (0.3m)," Regulatory Guide 7.12, June 1991.
- [8.1.9] American National Standards Institute, Institute for Nuclear Materials Management, "American National Standard for Radioactive Materials Leakage Tests on Packages for Shipment", ANSI N14.5, 1997.